frontiers | Research Topics

Liver cancer awareness month current progress and future prospects on advances in primary liver cancer investigation and treatment

2023

Edited by
Francisco Tustumi, Fabricio Ferreira Coelho, Wellington Andraus, Marina Alessandra Pereira and Rodrigo Xavier Das Neves

Published in
Frontiers in Oncology

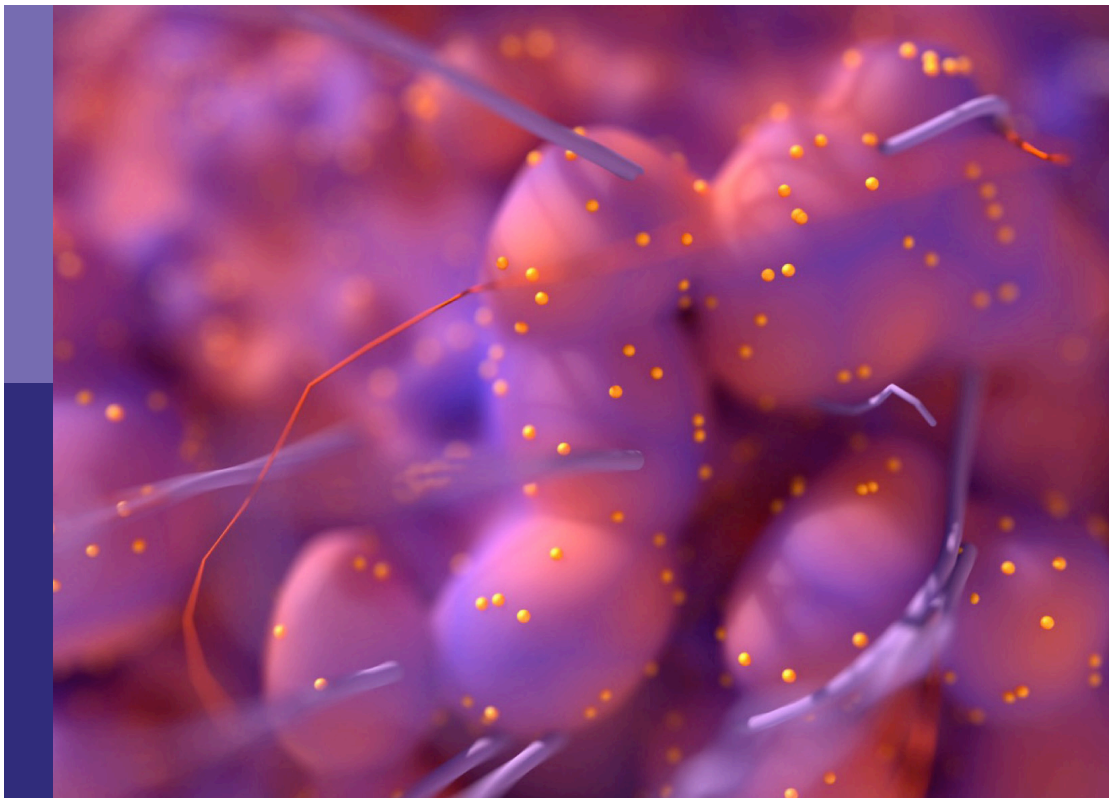

ISSN 1664-8714
ISBN 978-2-8325-5154-7
DOI 10.3389/978-2-8325-5154-7

About Frontiers

Frontiers is more than just an open access publisher of scholarly articles: it is a pioneering approach to the world of academia, radically improving the way scholarly research is managed. The grand vision of Frontiers is a world where all people have an equal opportunity to seek, share and generate knowledge. Frontiers provides immediate and permanent online open access to all its publications, but this alone is not enough to realize our grand goals.

Frontiers journal series

The Frontiers journal series is a multi-tier and interdisciplinary set of open-access, online journals, promising a paradigm shift from the current review, selection and dissemination processes in academic publishing. All Frontiers journals are driven by researchers for researchers; therefore, they constitute a service to the scholarly community. At the same time, the *Frontiers journal series* operates on a revolutionary invention, the tiered publishing system, initially addressing specific communities of scholars, and gradually climbing up to broader public understanding, thus serving the interests of the lay society, too.

Dedication to quality

Each Frontiers article is a landmark of the highest quality, thanks to genuinely collaborative interactions between authors and review editors, who include some of the world's best academicians. Research must be certified by peers before entering a stream of knowledge that may eventually reach the public - and shape society; therefore, Frontiers only applies the most rigorous and unbiased reviews. Frontiers revolutionizes research publishing by freely delivering the most outstanding research, evaluated with no bias from both the academic and social point of view. By applying the most advanced information technologies, Frontiers is catapulting scholarly publishing into a new generation.

What are Frontiers Research Topics?

Frontiers Research Topics are very popular trademarks of the *Frontiers journals series*: they are collections of at least ten articles, all centered on a particular subject. With their unique mix of varied contributions from Original Research to Review Articles, Frontiers Research Topics unify the most influential researchers, the latest key findings and historical advances in a hot research area.

Find out more on how to host your own Frontiers Research Topic or contribute to one as an author by contacting the Frontiers editorial office: frontiersin.org/about/contact

Liver cancer awareness month 2023: Current progress and future prospects on advances in primary liver cancer investigation and treatment

Topic editors

Francisco Tustumi — University of São Paulo, Brazil
Fabricio Ferreira Coelho — University of São Paulo, Brazil
Wellington Andraus — University of São Paulo, Brazil
Marina Alessandra Pereira — Universidade de São Paulo, Brazil
Rodrigo Xavier Das Neves — National Cancer Institute (NIH), United States

Citation

Tustumi, F., Coelho, F. F., Andraus, W., Pereira, M. A., Xavier Das Neves, R., eds. (2024). *Liver cancer awareness month 2023: Current progress and future prospects on advances in primary liver cancer investigation and treatment*. Lausanne: Frontiers Media SA. doi: 10.3389/978-2-8325-5154-7

Table of contents

frontiers | Frontiers in Oncology

TYPE Editorial
PUBLISHED 01 July 2024
DOI 10.3389/fonc.2024.1453709

OPEN ACCESS

EDITED AND REVIEWED BY
Liang Qiao,
The University of Sydney, Australia

*CORRESPONDENCE
Francisco Tustumi
franciscotustumi@gmail.com

RECEIVED 23 June 2024
ACCEPTED 24 June 2024
PUBLISHED 01 July 2024

CITATION
Tustumi F, Xavier das Neves R, Pereira MA, Coelho FF and Andraus W (2024) Editorial: Liver cancer awareness month 2023: current progress and future prospects on advances in primary liver cancer investigation and treatment.
Front. Oncol. 14:1453709.
doi: 10.3389/fonc.2024.1453709

Editorial: Liver cancer awareness month 2023: current progress and future prospects on advances in primary liver cancer investigation and treatment

Francisco Tustumi[1,2]*, Rodrigo Xavier das Neves[3], Marina Alessandra Pereira[4], Fabricio Ferreira Coelho[1] and Wellington Andraus[1]

[1]Department of Gastroenterology, Universidade de São Paulo, Sao Paulo, SP, Brazil, [2]Department of Surgery, Hospital Israelita Albert Einstein, Sao Paulo, SP, Brazil, [3]National Cancer Institute, Center for Cancer Research, Bethesda, MD, United States, [4]Department of Gastroenterology, Instituto do Cancer do Estado de São Paulo, Sao Paulo, SP, Brazil

KEYWORDS

liver neoplasms, hepatocellular carcinoma, cholangiocarcinoma, hepatectomy, liver cancer

Editorial on the Research Topic
Liver cancer awareness month 2023: current progress and future prospects on advances in primary liver cancer investigation and treatment

Introduction

October is Liver Cancer Awareness Month, and at Frontiers in Oncology, we highlighted recent discoveries in the field and raised awareness about the importance of early diagnosis, multidisciplinary management, and technological innovation in supporting liver cancer treatment. Primary liver cancer presents a significant global health challenge. Liver cancer poses substantial morbidity and mortality rates. Wang et al. reported a crude incidence of liver cancer of around 26/100,000 and a mortality of 22/100,000 for the year 2020. The leading primary liver cancers comprise hepatocellular carcinoma (HCC) and cholangiocarcinoma, while other neoplasms, such as primary hepatic adenosquamous carcinoma, are rare [Ai et al.] (1).

This Research Topic focuses on the latest advancements in investigating and treating primary liver cancer, providing insights into cutting-edge approaches that shape the field and improve patient outcomes (see Figure 1).

Carcinogenesis

Chronic liver disease and viral hepatitis, especially hepatitis B, work as preneoplastic conditions due to the increased risk for primary liver cancer transformation. Guo et al.

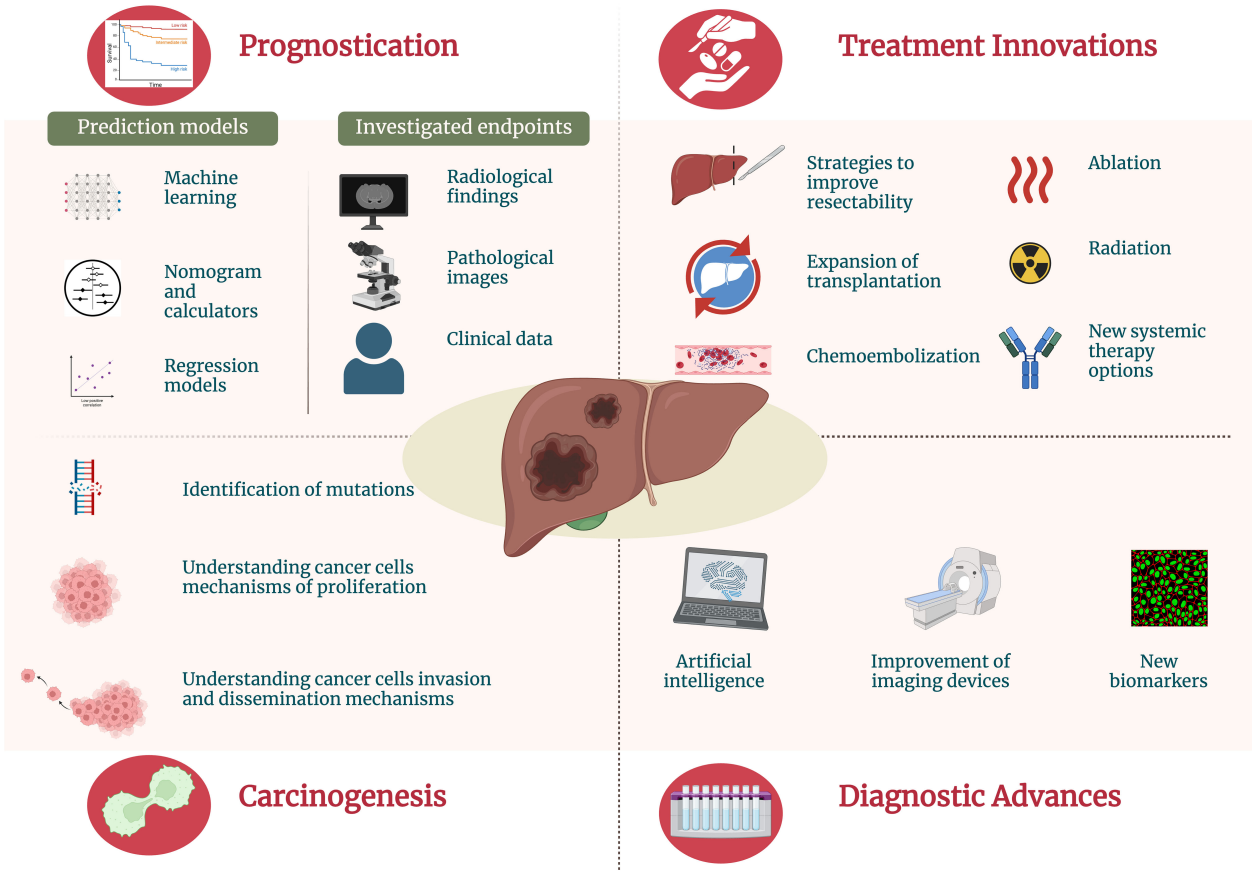

FIGURE 1
Current advances and innovations for primary liver cancer management.

identified the variables age, sex, antiviral therapy history, hepatitis B antigen, alcohol drinking history, and serum alpha-fetoprotein levels as risk factors for cancer HCC development in patients with cirrhosis. Recent advances in the carcinogenesis of primary liver cancer help us understand how risk factors can lead to cancer development and progression (2). By knowing these pathways, it is possible to interfere in crucial steps of carcinogenesis, reducing the risk for cancer development and working as a target for new cancer therapies. Continuous liver damage and regeneration lead to cellular mutations and malignant transformation. Recent molecular investigations have identified several key pathways involved in cancer development for hepatocellular carcinoma and cholangiocarcinoma, including the Wnt/β-catenin, PI3K/AKT, and MAPK signaling pathways, which play critical roles in cell proliferation, survival, and apoptosis (3, 4). Other factors, such as excessive alcohol consumption and exposure to toxins, also play critical roles in liver carcinogenesis by direct DNA damage. Recent molecular studies have highlighted the importance of epigenetic changes, such as DNA methylation and histone modification, in the development and progression of HCC (5).

Understanding these risk factors and the associated molecular pathways is crucial for developing targeted prevention and early detection strategies in high-risk populations, as well as for identifying potential therapeutic targets for treating HCC.

Prognostication

Prognostication in oncology is a dynamic area of research that aims to refine our understanding of disease progression and patient outcomes. Prognostication refers to the process of predicting the likely course and outcome of the disease (6). It involves using predictive models to assess prognostic variables, such as the type and stage of cancer, tumor characteristics, patient health status, and endpoints, such as response to treatment and survival rates. This information is crucial for guiding treatment decisions, setting realistic expectations, and planning follow-up care. Accurate prognostication helps healthcare providers tailor interventions to individual patients, ultimately aiming to improve outcomes and quality of life. In fact, the main scores for liver function (which heavily influences liver cancer treatment), such as Child-Pugh and Model for End-Stage Liver Disease, are based on prognostic indicators of survival (7, 8). Prognostic calculators or nomograms are helpful because they can be easily used in clinical practice. Tian et al. performed a retrospective analysis of HCC patients. The authors used regression models to construct a predictive nomogram based on the following independent prognostic indicators of disease-free survival: major resection, albumin, microvascular invasion, laparoscopic surgery, blood loss, bilirubin, and pleural effusion. A study by Sun et al. estimated the

tumor burden based on the sum of tumor numbers and maximum diameters. Their results highlight how tumor burden influences progression patterns and survival outcomes in patients under sorafenib treatment, emphasizing the need for tailored treatment strategies. Tan et al. built a novel immune classification based on the immune infiltration within the tumor microenvironment using pathological images to predict early HCC recurrence, offering a valuable tool for identifying high-risk patients.

However, scores based only on regression models can be limited since they only comply with a handful number of clinical or laboratory variables. This Research Topic is especially relevant since liver conditions comprise multifactorial prognostic variables. In this sense, lately, the use of artificial intelligence has boosted the predictive capability for estimating liver cancer prognostication. A machine learning approach for personalized prognostic assessment further enhances our ability to predict patient outcomes and tailor treatments accordingly. Zhang et al. created a multi-level prognostic risk model for HCC. Their models exhibited a high performance in predicting patient response to therapy.

Diagnostic advances

Early and accurate diagnosis of primary liver cancer is crucial for effective treatment. Innovations in diagnostic methods are improving our ability to detect primary liver cancer at earlier stages. The diagnosis of liver neoplasms frequently relies heavily on imaging tests. Using serum markers, such as alpha-fetoprotein (AFP), is helpful to increase the accuracy of liver cancer diagnosis. However, some tumors do not express AFP, puzzling liver cancer diagnosis. In this sense, serum interleukin-41 has emerged as a novel serum marker for diagnosing AFP-negative HCC [Li et al.]. In addition, interleukin-41 can also serve as a prognostic marker for HCC.

The construction of diagnostic models using machine learning has also shown promise in enhancing the accuracy of HCC progression detection. Jiang et al. utilized machine learning techniques to construct diagnostic models for HCC across different stages of the disease progression. Fu et al. also used machine learning to improve the diagnostic accuracy for preoperative differentiation between xanthogranulomatous cholecystitis and gallbladder carcinoma.

Advanced imaging techniques are revolutionizing not only liver cancer diagnosis but also staging. Pretreatment determination of vascular invasion is crucial in primary liver cancer since it impacts a patient's prognosis and highly influences treatment. Pan et al. evaluated perfusion indexes and spectral parameters to diagnose portal vein tumor thrombus. Yu et al., using a deep learning approach, created models to enhance preoperative diagnosis of microvascular invasion through domain-adaptation fusion of multi-phase CT images.

Treatment innovations

Treatment options for primary liver cancer are rapidly evolving, with a focus on personalized and multimodal approaches. While the transplantation is well-established for HCC, the use of transplantation for other primary liver cancers is not well-studied. However, recent studies have shown promising results for transplantation in cholangiocarcinoma, expanding the current indications for liver transplant [Andraus et al.] (9).

With the latest advances in liver surgery and postoperative care, liver resection has also expanded, and tumors once considered unresectable, nowadays are being treated with curative intention. Martinino et al., in a systematic review, found that liver resection for HCC presents similar long-term survival than transplantation if an appropriate patient selection is performed.

Currently, there is still debate about the best approach for HCC with tumor thrombus, but it seems that surgical alternatives (liver resection or transplantation), if feasible, have better outcomes (10). However, other treatment strategies should be considered for patients who are not candidates for surgery. Leung et al. evaluated multimodal strategies for advanced hepatocellular carcinoma with portal vein tumor thrombus. The authors found that the hepatic arterial infusion chemotherapy of fluorouracil, leucovorin, and oxaliplatin, with or without sorafenib, demonstrated superior survival rates than alternative treatments.

Thermal tumor ablation is a minimally invasive locoregional therapy that eradicates tumors by applying heat to eliminate malignant cells. This technique comprises radiofrequency ablation and microwave ablation (11). These techniques might be challenging to apply in certain difficult locations within the liver, such as proximity to other organs, such as the gastrointestinal tract, diaphragm, or gallbladder, due to the risk of internal bleeding or iatrogenic injury (12). In these cases, the application of hydrodissection in microwave ablation can be helpful, by separating the tumor from nearby health tissues, with a success of over 90% [Song et al.].

A systematic review and meta-analysis [Dong et al.] compared repeat hepatectomy and thermal ablation therapy for recurrent HCC. The authors found that this approach was related to fewer complications due to the less invasiveness of thermal ablation. However, the overall survival and the recurrence-free survival were higher for those treated with repeated hepatectomy. Consequently, the reduced complication rate of thermal ablation allows for quicker patient recovery and shorter hospital stays, making it a potentially safer option for individuals who cannot tolerate major surgery.

For those HCC patients who are not candidates for surgery, treatment strategies are usually based on systemic therapies. Tyrosine kinase inhibitors such as sorafenib or lenvatinib are the most common drugs used in these patients. However, currently, multimodal therapeutic strategies are being studied (13). Combining traditional treatments with newer agents showcases the potential for synergistic therapeutic effects. Chen et al., in a retrospective controlled study, compared transarterial chemoembolization in monotherapy *versus* transarterial chemoembolization associated with anlotinib, a novel oral multi-kinase inhibitor. The group treated with anlotinib showed higher survival rates.

In the last decade, target therapy and precision medicine have revolutionized HCC management. Han et al. in a multicenter,

propensity-score-matched study, compared atezolizumab-bevacizumab *versus* lenvatinib in HCC. The authors found that the combination atezolizumab-bevacizumab is a promising treatment strategy for advanced HCC, with better overall survival than lenvatinib. Jiang et al. described their treatment strategy for advanced HCC using hepatic arterial infusion chemotherapy with immunotherapy.

Conclusion

This Research Topic provided a comprehensive overview of recent advancements in investigating and treating primary liver cancer. Recent advances in the knowledge of primary liver cancer carcinogenesis, prognostication, diagnosis, and treatment are essential aspects for improving liver cancer patient care.

Author contributions

FT: Conceptualization, Writing – original draft. RX: Investigation, Validation, Visualization, Writing – review & editing. MP: Data curation, Visualization, Writing – review & editing. FC: Supervision, Writing – review & editing. WA: Supervision, Writing – review & editing.

Conflict of interest

The authors declare that the research was conducted in the absence of any commercial or financial relationships that could be construed as a potential conflict of interest.

The author(s) declared that they were an editorial board member of Frontiers, at the time of submission. This had no impact on the peer review process and the final decision.

Publisher's note

References

1. Petrick JL, McGlynn KA. The changing epidemiology of primary liver cancer. *Curr Epidemiol Rep*. (2019) 6:104–11. doi: 10.1007/s40471-019-00188-3

2. Fishbein A, Hammock BD, Serhan CN, Panigrahy D. Carcinogenesis: Failure of resolution of inflammation? *Pharmacol Ther*. (2021) 218:107670. doi: 10.1016/j.pharmthera.2020.107670

3. Andraus W, Tustumi F, de Meira Junior JD, Pinheiro RSN, Waisberg DR, Lopes LD, et al. Molecular profile of intrahepatic cholangiocarcinoma. *Int J Mol Sci*. (2023) 25:461. doi: 10.3390/ijms25010461

4. Lee JS. The mutational landscape of hepatocellular carcinoma. *Clin Mol Hepatol*. (2015) 21:220–9. doi: 10.3350/cmh.2015.21.3.220

5. Gonçalves E, Gonçalves-Reis M, Pereira-Leal JB, Cardoso J. DNA methylation fingerprint of hepatocellular carcinoma from tissue and liquid biopsies. *Sci Rep*. (2022) 12:11512. doi: 10.1038/s41598-022-15058-0

6. Hui D, Paiva CE, Del Fabbro EG, Steer C, Naberhuis J, van de Wetering M, et al. Prognostication in advanced cancer: update and directions for future research. *Support Care Cancer*. (2019) 27:1973–84. doi: 10.1007/s00520-019-04727-y

7. Calderon-Martinez E, Landazuri-Navas S, Vilchez E, Cantu-Hernandez R, Mosquera-Moscoso J, Encalada S, et al. Prognostic scores and survival rates by etiology of hepatocellular carcinoma: A review. *J Clin Med Res*. (2023) 15:200–7. doi: 10.14740/jocmr4902

8. Malinchoc M, Kamath PS, Gordon FD, Peine CJ, Rank J, ter Borg PC. A model to predict poor survival in patients undergoing transjugular intrahepatic portosystemic shunts. *Hepatology*. (2000) 31:864–71. doi: 10.1053/he.2000.5852

9. Andraus W, Tustumi F, Santana AC, Pinheiro RSN, Waisberg DR, Lopes LD, et al. Liver transplantation as an alternative for the treatment of perihilar cholangiocarcinoma: A critical review. *Hepatobiliary Pancreat Dis Int*. (2024) 23:139–45. doi: 10.1016/j.hbpd.2024.01.003

10. Tustumi F, Coelho FF, de Paiva Magalhães D, Júnior SS, Jeismann VB, Fonseca GM, et al. Treatment of hepatocellular carcinoma with macroscopic vascular invasion: A systematic review and network meta-analysis. *Transplant Rev (Orlando)*. (2023) 37:100763. doi: 10.1016/j.trre.2023.100763

11. Minami Y, Aoki T, Hagiwara S, Kudo M. Tips for preparing and practicing thermal ablation therapy of hepatocellular carcinoma. *Cancers (Basel)*. (2023) 15:4763. doi: 10.3390/cancers15194763

12. Ozen M, Raissi D. Current perspectives on microwave ablation of liver lesions in difficult locations. *J Clin Imaging Sci*. (2022) 12:61. doi: 10.25259/JCIS_126_2022

13. Llovet JM, Castet F, Heikenwalder M, Maini MK, Mazzaferro V, Pinato DJ, et al. Immunotherapies for hepatocellular carcinoma. *Nat Rev Clin Oncol*. (2022) 19:151–72. doi: 10.1038/s41571-021-00573-2

frontiers | Frontiers in Oncology

TYPE Original Research
PUBLISHED 16 November 2023
DOI 10.3389/fonc.2023.1298757

OPEN ACCESS

EDITED BY
Francisco Tustumi,
University of São Paulo, Brazil

REVIEWED BY
Tiago Siqueira,
Albert Einstein Israelite Hospital, Brazil
Eric Nakamura,
University of São Paulo, Brazil

*CORRESPONDENCE
Meng Wu
rmwumeng@nbu.edu.cn

RECEIVED 22 September 2023
ACCEPTED 02 November 2023
PUBLISHED 16 November 2023

CITATION
Song Y, Wu M, Zhou R, Zhao P and Mao D (2023) Application and evaluation of hydrodissection in microwave ablation of liver tumours in difficult locations. *Front. Oncol.* 13:1298757. doi: 10.3389/fonc.2023.1298757

Application and evaluation of hydrodissection in microwave ablation of liver tumours in difficult locations

Yuan Song, Meng Wu*, Ruhai Zhou, Ping Zhao and Dan Mao

Department of Ultrasound, The Affiliated People's Hospital of Ningbo University, Ningbo, Zhejiang, China

Objective: To investigate the safety and mid-term outcomes of hydrodissection-assisted microwave ablation (MWA) of hepatocellular carcinoma (HCC) in various difficult locations.

Methods: A total of 131 HCC patients who underwent ultrasound-guided MWA from March 2017 to March 2019 were included. Following ultrasound examination, patients with tumors at difficult locations were treated with hydrodissection-assisted MWA (hydrodissection group), while those with tumors at conventional locations received MWA (control group). Both groups were compared concerning baseline characteristics, ablation parameters, complete ablation rates, and complication rates. Kaplan-Meier curves analyzed local tumor progression and overall survival, with stratified analysis for different difficult locations (adjacent to gastrointestinal tract, diaphragm, and subcapsular tumors). Additionally, Cox regression analyses were conducted to assess the impact of different difficult locations on these outcomes.

Results: Complete ablation rates were similar between the hydrodissection and control groups (91.4% *vs.* 95.2%, P>0.05). Postoperative complications occurred in three patients, including liver abscess and biliary injury. No significant differences in major or minor complication rates were found between the groups (P>0.05). Local tumor progression was detected in 11 patients (8.4%) at the end of the follow-up period. Neither cumulative local tumor progression rate (P=0.757) nor overall survival rate (P=0.468) differed significantly between the groups. Stratified analysis showed no effect of tumor location difficulty on cumulative local tumor progression or overall survival. Tumor number and size served as independent predictors for overall survival, while minimal ablation margin ≤ 5mm independently predicted local tumor progression. In contrast, the tumor location was not statistically significant. Sensitivity analyses corroborated the robustness of the models.

Conclusion: Hydrodissection-assisted MWA for HCC in various difficult locations demonstrated safe and effective, with complete ablation and mid-term outcomes comparable to those for tumors in conventional locations.

KEYWORDS

hepatocellular carcinoma, hydrodissection, microwave ablation, difficult location, ultrasound

Introduction

Hepatocellular carcinoma (HCC), the sixth most common global neoplasia, is associated with a remarkably high mortality rate. Liver transplantation and surgical resection have been established as the gold-standard therapeutic approaches for hepatic tumors. However, over 75% of patients are precluded from surgery due to inadequate hepatic functional reserve, multifocality, advanced disease, or comorbidities (1, 2). Ablation therapy, particularly microwave ablation (MWA), has thus become an alternative for certain HCC patients, displaying benefits such as a wider ablation zone, shorter duration, and less heat-sink effect, favoring tumors over 3 cm or near major vessels (3–5).

Despite the evident advantages of MWA, previous studies have shown inferior outcomes in primary liver cancer cases involving difficult locations when treated with MWA (6, 7). In an effort to circumvent thermal damage to neighboring organs, ablations near the gastrointestinal tract, diaphragm, gallbladder, and kidneys frequently fail to achieve comprehensive treatment, thereby increasing the risk of residual malignancy and locoregional metastasis. Additionally, the incidence of complications such as intraperitoneal bleeding, gastrointestinal injury, and tract seeding tends to be higher in these areas (8, 9).

Recent studies have shown that hydrodissection can physically separate tumor lesions from adjacent tissues in patients with liver tumors in difficult locations, achieving optimal ablation margins and protecting nearby organs (10, 11). Hydrodissection is an established thermal protection method in percutaneous thermal ablation. It involves the injection of fluid between the lesion and adjacent vital structures, which reduces the risk of thermal damage and minimizes postoperative complications. Studies conducted by Xiaoyin et al. (12) have validated the safety and efficacy of hydrodissection-assisted MWA in the treatment of thyroid nodules, emphasizing its utility when anatomical structures are closely intertwined. In the context of liver tumors, particularly those located adjacent to vital structures, hydrodissection has been similarly recognized for its significance. Garnon et al. (13) illustrated the application of this technique in percutaneous thermal ablation of sub-cardiac hepatic tumors, demonstrating its pivotal role in enhancing procedural safety by maintaining a protective barrier between the ablation zone and adjacent vital tissues.

Although some studies have evaluated hydrodissection in hepatic malignancy ablation, most have focused on a particular challenging position, with limited analysis of effectiveness across various difficult locations or the impact on patient prognosis (14–16). Therefore, this study retrospectively analyzed the clinical data of patients with liver tumors in different difficult locations treated with hydrodissection-assisted MWA, and compared it with patients with liver tumors in conventional locations. The aim was to investigate the effectiveness and mid-term outcomes of ablation in various difficult tumor locations.

Materials and methods

Patients

This retrospective analysis included patients who received thermal ablation for HCC from March 2017 to March 2019. All patients had a confirmed diagnosis of HCC by the combination of radiological and pathological criteria. Inclusion criteria were as follows (1): patients who were either not suitable for or refused hepatic resection, with either solitary tumors ≤7cm or multiple tumors (up to 3) ≤3cm in maximum diameter (2); absence of tumor thrombus in the main portal or inferior vena cava (3); hepatic function status of Child-Pugh Class A or B (4); ultrasound revealed the presence of an appropriate route for puncture and ablation. Exclusion criteria included (1): extrahepatic diseases or distant metastasis (2); platelet count less than 50×10^9/L, with uncorrectable coagulation dysfunction (3); incomplete patient data. Tumors in difficult locations are defined as those where at least one tumor is located less than 5mm from the liver capsule, diaphragm, or gastrointestinal tract as confirmed by contrast-enhanced CT or MRI. Ethical approval for this study was granted by the ethics review committee of the institution (YY2023035). Informed consent was waived owing to the retrospective nature of this research.

Clinical baseline data

Demographic data and clinical parameters, including age, gender, Child-Pugh classification, presence or absence of cirrhosis, previous treatments, tumor dimensions, tumor number, and Alpha-fetoprotein (AFP) levels, were collected by reviewing electronic medical records.

Preoperative examination

A full clinical assessment was performed, which encompassed complete blood count, clotting analysis, hepatic and renal function,

and serum tumor markers. Ultrasound was used to assess the lesion site, size, number, and relation to important structures. Additionally, the distribution of blood flow in and around the tumor was observed to determine the puncture pathway of the MWA needle. The selection of the anesthesia type was dependent on the location, number, and size of the tumor. Ablation strategies were decided by three interventional radiologists with over 10 years of experience. Ultrasound images of liver tumors in difficult locations are shown in Figure 1.

Hydrodissection technique

Under the guidance of ultrasound (Philips EPIQ 7), an 18-G PTC puncture needle (Hakko, Tokyo, Japan) was inserted between the liver capsule and parietal peritoneum or adjacent structures, and the needle core was then removed. A small amount of 0.9% saline was gradually infused through the cannula to separate the liver from the surrounding tissue. When injection resistance was absent and ultrasound indicated clear separation, the guidewire was inserted and the puncture needle was withdrawn. The catheter sheath was subsequently introduced over the guidewire, and a continuous 0.9% saline infusion was maintained through a connected infusion system until successful separation was confirmed (>0.5cm between tumor and surrounding structures).

Ablation procedures

Percutaneous MWA procedures were performed under general anesthesia. All patients underwent ablation using a MWA system (KY-2000, Kangyou Medical Instruments, Nanjing, China), equipped with a 2450 MHz microwave generator and a 15G water-cooling ablation needle. Based on preoperative planning, the 18G electrode needle was inserted into the tumor via ultrasound guidance. Puncture routes for tumors in conventional locations were designed to avoid lungs, large blood vessels, gallbladder, and other organs. Depending on tumor size, ablation was either single-point (for diameters ≤3cm) or multi-point (for diameters >3cm), executed at 40-60 W for a duration of 3-8 minutes. The ablation was deemed complete when the high-echoic area under ultrasound covered the entire tumor volume and an additional 0.5 cm of adjacent hepatic parenchyma. If the ablation area was found insufficient, the needle was repositioned. For tumors in difficult locations, hydrodissection was implemented during ablation. The hyper-echogenicity areas induced by ablation in tumors near the liver surface were continuously monitored with ultrasound, and the needle depth was adjusted if the area exceeded the liver capsule to prevent repeat ablation at the same puncture site. Contrast-enhanced ultrasound (CEUS) was performed immediately after MWA to evaluate the ablation area (Figure 2). For tumors adjacent to the gastrointestinal tract, the needle trajectory was designed to be parallel or distant from visceral organs as much as possible. Post-operatively, these patients were subjected to a 48-hour fast and were administered antacids, antibiotics, and somatostatin to reduce the risk of complications such as gallbladder or gastric perforation.

Follow-up and effectiveness assessment

Perioperative and follow-up evaluations were conducted on patients, and the ablation parameters, complete ablation rate, complication incidence, local tumor progression, and overall survival were analyzed in the two groups. The initial follow-up was scheduled one month after the MWA, during which coagulation parameters, serum tumor markers, and liver function were reassessed. Meanwhile, ablation margins were assessed based on contrast-enhanced CT scans conducted preoperatively and one month postoperatively. The largest diameter of the non-contrast-enhancing zone was measured in axial, coronal, or sagittal planes one month after the operation. For ablation margins, distances to adjacent anatomical landmarks were documented on both sets of scans. The margin at each landmark was determined by subtracting the preoperative from the postoperative distance, based on a method described by Wang et al. (17). The smallest resulting value was deemed the minimal ablation margin. Subsequent follow-ups were scheduled every three months with imaging and serum assessments. Complete ablation was defined as the absence of enhancement within the ablation zone on contrast-enhanced CT, MRI, or CEUS one month post-operation (18). Patients with complete ablation underwent subsequent follow-ups to evaluate the rate of local tumor progression. Residual tumors post-ablation (characterized by irregular enhancement around the ablation lesion) were treated with a secondary ablation or interventional embolization. Major complications were life-threatening, resulted in significant morbidity and disability, or prolonged hospital stay (19). Minor complications were self-limiting, necessitating no additional treatment. Local tumor

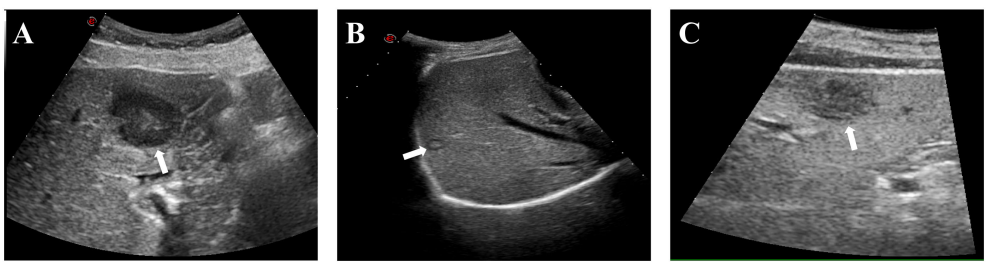

FIGURE 1
Typical ultrasound images of patients with liver tumors at difficult locations. **(A)** Liver tumor adjacent to the gastrointestinal tract (white arrow); **(B)** Liver tumor adjacent to the diaphragm (white arrow); **(C)** Liver subcapsular tumor (white arrow).

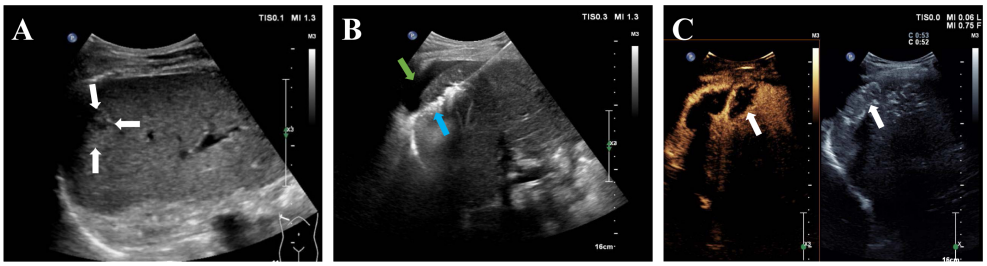

FIGURE 2
A 68-year-old man with hepatocellular carcinoma before and after MWA. **(A)** Ultrasound image showed a 1.6-cm hepatocellular carcinoma in the subcapsular region of the liver (white arrow).; **(B)** After the saline injection hydrodissection (green arrow), the electrode needle was inserted into the tumor under ultrasound guidance (blue arrow); **(C)** Postoperative CEUS showed no enhancement in the whole ablation area (white arrow).

progression was identified as the appearance of tumor foci at the edge of a sufficiently ablated zone, confirmed at least once through contrast-enhanced imaging during the post-procedure follow-up period (20). Overall survival was calculated from the day of ablation to the date of death or the final follow-up.

Statistical analysis

Statistical analyses were conducted using SPSS 22.0 software (IBM, NY, USA) and Medcalc 15.2 software (MedCalc, Ostend, Belgium). Normal distribution measurements were expressed as mean ± standard deviation, while skewed distributions were presented as median (range). Comparisons between groups were performed by independent samples t-test or the Mann-Whitney test. Categorical data were expressed as a number (percentage), and the chi-square test or Fisher's exact test was used to compare the data between the two groups. The Kaplan-Meier curves were plotted to assess local tumor progression and cumulative survival rates in both groups, and stratified analysis was conducted for tumors in different difficult locations. Univariate and multivariate Cox regression analyses were further performed to evaluate the impact of difficult tumor location on local tumor progression and overall survival, corroborated by Bootstrap resampling with 1000 replicates for sensitivity analysis. A p-value less than 0.05 was considered statistically significant.

Results

Comparison of clinical data

Based on the usage of the hydrodissection during MWA, patients were categorized into hydrodissection group and control group. Sixty-six patients with tumors in difficult locations underwent hydrodissection-assisted MWA, including 28 cases (42.4%) near the gastrointestinal tract, 21 cases (31.8%) near the diaphragm, and 17 cases (25.8%) as subcapsular liver tumors. The remaining 65 patients with conventional tumors received MWA and served as the control group. The patient selection flowchart was shown in Figure 3.

The baseline characteristics of the included patients were displayed in Table 1. A total of 131 patients (176 lesions) underwent MWA, with an average age of 58.6 ± 9.8 years. Most patients were male, rated as Child-Pugh grade A, with histories of hepatitis virus infection. In the hydrodissection group, 74 out of 93 lesions were treated with hydrodissection-assisted MWA, while the remaining 19 lesions received MWA alone. In the control group, all 83 lesions were subjected to MWA. Among the hydrodissection group, 18 individuals (27.3%) had multiple lesions, and the maximum tumor diameter exceeded 3 cm in 25 patients (37.9%). In the control group, 15 patients (23.1%) presented with multiple lesions, and 22 patients (33.9%) had a maximum tumor diameter >3 cm. No statistically significant difference was observed in the baseline characteristics between the two groups (P>0.05).

Ablation parameters and outcomes

In this study, 131 patients underwent a total of 140 ablation procedures, with a technical success rate of 100%, and the average number of treatments was 1.5 ± 0.51. Single ablation treatment was performed on 119 patients (90.8%), while 12 patients (9.2%) required repeated ablation. In the 74 lesions treated with hydrodissection-assisted MWA, saline injection separation was successful in 100% of cases, with an average fluid volume of 723.8 ± 240.5 ml. Although the hydrodissection group experienced a slight increase in ablation time, ablation frequency, and ablation duration compared to the control group, these differences were not statistically significant(P>0.05). No significant difference was observed between the hydrodissection group and the control group in terms of the number of antenna insertions (P>0.05). Initial follow-up revealed that the average ablation zone sizes in the control group were (4.62 ± 0.86) cm, compared to (4.60 ± 0.72) cm in the hydrodissection group (P>0.05). The hydrodissection group showed similar ablation zone sizes across tumor locations adjacent to the gastrointestinal tract (4.67 ± 0.62 cm), adjacent to the diaphragm (4.36 ± 0.76 cm), and subcapsular tumors (4.78 ± 0.74 cm), with no statistical significance among these subgroups (P>0.05). The proportion of patients with a minimal ablation margin of ≤5 mm was 32.3% in the control group and 41.1% in the hydrodissection group. Within the hydrodissection group, the proportions were 42.9% for tumors adjacent to the gastrointestinal tract, 42.9% for those adjacent to the diaphragm, and 35.3% for subcapsular tumors. These differences were not statistically significant (P>0.05). Data from the

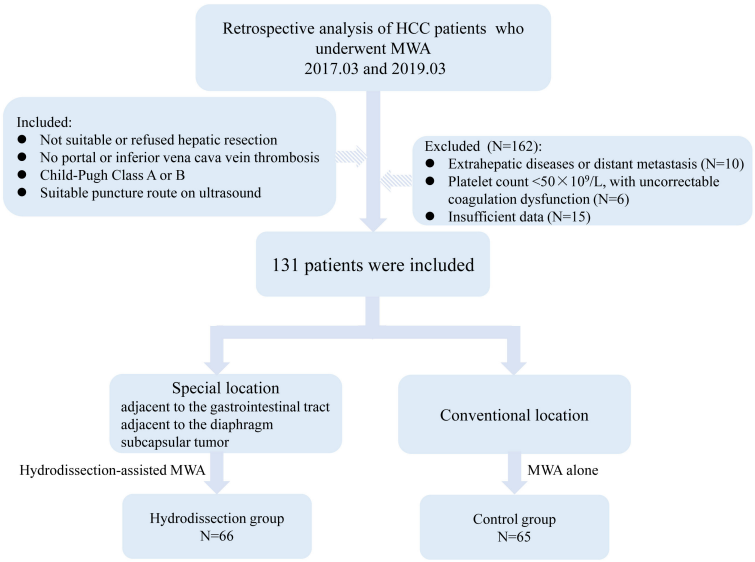

FIGURE 3
Flow diagram of the included patients.

hydrodissection group indicated a complete ablation rate of 91.4% in the hydrodissection group, which was similar to the control group, with no statistical significance (P>0.05). Further analysis demonstrated that the complete ablation rates for lesions adjacent to the gastrointestinal tract (92.3%), adjacent to the diaphragm (90.0%), and subcapsular liver tumors (91.7%) were not statistically different compared to the control group (P>0.05). Moreover, there was no statistical significance in the differences among the three categories (P>0.05), as shown in Table 2.

Post-ablation complications

Severe complications occurred in 3 of 131 patients (2.3%), comprising two hepatic abscesses and one biliary injury. These patients improved after percutaneous drainage and anti-infection treatment. The major complication rate was 3.0% for the hydrodissection group and 1.5% for the control group, with no significant difference in hepatic abscess or biliary injury (all P>0.05). Minor complications included abdominal pain, fever, gastrointestinal symptoms, minimal pleural effusion in one patient, transient hepatic function abnormality in three patients, and two asymptomatic bilomas, all of which experienced rapid remission after treatment. There was no statistically significant difference in the incidence of various minor complications between the two groups (all P>0.05). Details of the major and minor complications were presented in Table 3.

Local tumour progression and survival

Patients with complete ablation were followed for 36 months to assess local tumor progression rates and overall survival in both groups. Local tumor progression was observed in 11 patients (8.4%), including 6 in the hydrodissection group and 5 in the control group. The 1-, 2-, and 3-year cumulative local tumor progression rates for the hydrodissection group were 3.0%, 6.1%, and 9.1%, respectively, compared to 1.5%, 4.6%, and 7.7% for the control group, with no significant difference (P=0.757, Figure 4A). The 1-, 2-, and 3-year overall survival rates for the hydrodissection group were 95.5%, 87.9%, and 78.8%, respectively, while those for the control group were 96.9%, 92.3%, and 83.1%, showing no statistical significance between the two groups (P=0.468, Figure 4B).

Stratified analysis of difficult locations

The prognosis of tumors in three difficult locations (adjacent to the gastrointestinal tract, adjacent to the diaphragm, and liver subcapsular) was assessed through stratified analysis of cumulative local tumor progression rates and overall survival rates. Kaplan-Meier survival curves revealed no statistical differences in cumulative local tumor progression rates for tumors adjacent to the gastrointestinal tract (P=0.596, Figure 5A), adjacent to the diaphragm (P=0.779, Figure 5B), and liver subcapsular tumors (P=0.778, Figure 5C), compared with the control group. Subsequent analysis for internal comparison among these locations showed no significant differences (P=0.843, Figure 5D).

Similarly, the analysis of overall survival rates revealed no statistical differences when compared with the control group for tumors adjacent to the gastrointestinal tract (P=0.297, Figure 6A), adjacent to the diaphragm (P=0.420, Figure 6B), and subcapsular tumors (P=0.598, Figure 6C). No statistical significance was found among the three difficult locations (P=0.516, Figure 6D).

Univariate and multivariate analysis

Univariate Cox regression analysis (Table 4) revealed significant predictors for overall survival: tumor number (HR=3.066, P=0.009),

TABLE 1 Demographic data and tumor characteristics of the two groups.

	Hydrodissection group	Control group	P
Patients	66	65	
Age, years	58.2 ± 11.0	59.1 ± 8.5	0.597
Gender, n(%)			
Male	47(71.2)	43(66.2)	0.575
Female	19(28.8)	22(33.8)	
History of hepatitis virus infection, n(%)			
Yes	52(78.8)	48(73.8)	0.543
No	14(21.2)	17(26.2)	
Liver cirrhosis, n(%)			
Yes	38(57.6)	42(64.6)	0.475
No	28(42.4)	23(35.4)	
Tumor number, n(%)			
Single	48(72.7)	50(76.9)	0.688
Multiple	18(27.3)	15(23.1)	
Child-Pugh class, n(%)			
A	55(83.3)	53(81.5)	0.822
B	11(16.7)	12(18.5)	
Tumor size, n(%)			
≤3 cm	41(62.1)	43(66.2)	0.886
3~5 cm	19(28.8)	17(26.2)	
>5 cm	6(9.1)	5(7.7)	
AFP level, n(%)			
Positive	50(75.8)	46(70.8)	0.558
Negative	16(24.2)	19(29.2)	
History of intervention, n(%)			
Yes	20(30.3)	18(27.7)	0.848
No	46(69.7)	47(72.3)	
History of hepatectomy, n(%)			
Yes	6(9.1)	9(13.8)	0.425
No	60(90.9)	56(86.2)	

AFP, Alpha-fetoprotein.

Child-Pugh score (HR=4.025, P=0.001), tumor size (HR=4.845, P<0.001), and minimal ablation margin ≤ 5mm (HR=0.296, P=0.004). Age (HR=1.065, p=0.034) and minimal ablation margin ≤ 5mm (HR=0.142, P=0.003) were significant for local tumor progression. In the multivariate model (Table 5), tumor number (HR=3.268, P=0.024) and tumor size (HR=4.473, P=0.008) were independent factors affecting overall survival, while minimal ablation margin ≤5mm (HR=0.207, P=0.025) was an independent predictor of local tumor progression. However, the anatomical location of the tumor did not exhibit a statistically significant relationship with either overall survival or local tumor progression (P>0.05).

Sensitivity analyses employing Bootstrap resampling techniques were executed to validate the multivariate Cox regression models for both overall survival and local tumor progression. These analyses confirmed the robustness of the models, indicating that all variables, including difficult locations, consistently maintained their respective roles in influencing both overall survival and local tumor progression.

Discussion

With improvements in ablation technology, ultrasound-guided MWA in liver tumor treatment has become more prevalent, as supported by several studies that affirm its efficacy and safety. Successful ablation of liver tumors was found to be dependent on the ability of the ablation range to cover at least 5-10 mm of the lesion and its surrounding tissue, where an adequate ablation safety margin was correlated with a lower rate of local tumor progression (21, 22). However, the further application of MWA was limited by the incomplete ablation of some liver tumors due to insufficient safety distance with structures such as the diaphragm, gastrointestinal tract, and gallbladder. To minimize thermal damage to adjacent tissues during the treatment of liver tumors in difficult locations, the clinical use of hydrodissection technology to assist in ablation was initiated.

Despite studies affirming the utility of hydrodissection for liver tumors in difficult locations, few have explored mid-term clinical outcomes for multiple such tumors (23, 24). Recent studies by Li et al. (25) investigated liver tumors near the gastrointestinal tract, while Makovich et al. (26) focused on hepatocellular carcinoma ablation near vessels and below the diaphragm. In this study, a comparison was conducted between difficult and conventional locations liver tumors in terms of short-term effects and mid-term survival rates. Ultrasound-guided percutaneous MWA with hydrodissection was identified as a safe and effective treatment for hepatocellular carcinoma in difficult locations, achieving consistent local control across different positions.

Hydrodissection is an effective technique involving the use of saline to expand the extrahepatic space, thereby forming a thermal barrier between the ablation zone of the tumor and adjacent vital organs. This method not only facilitates the desired ablation effect on liver tumors that were previously challenging to fully eradicate but also minimizes unintentional thermal injury to nearby organs, reducing the incidence of postoperative complications (27). Several animal experiments have indicated that the application of hydrodissection can decrease damage to the diaphragm, stomach, and lungs, and substantially alleviate pain (28, 29). Similar results were reported by Park et al. (30), where patients with liver tumors experienced a significant reduction in pain within 24 hours following hydrodissection-assisted ablation, and the use of morphine during the perioperative period was also notably reduced.

Ultrasound-guided hydrodissection has been increasingly utilized in the ablation of liver, kidney, thyroid, and mediastinal tumors. Liu et al. (31) reported no significant difference in tumor progression or

TABLE 2 Outcome of MWA in the hydrodissection and control group.

Variates	No. of patients	Ablation time (min)	Power (watts)	No. of ablation sessions	No. insertions	Ablation zone size (cm)	Minimal ablation margin ≤5 mm (%)	Complete ablation (%)
Control group	65	10.9 ± 3.56	51.5 ± 2.35	1.4 ± 0.49	2.4 ± 1.13	4.62 ± 0.86	32.3	95.2
Hydrodissection group	66	13.6 ± 4.27	53.4 ± 2.91	1.7 ± 0.50	2.5 ± 1.19	4.60 ± 0.72	41.1	91.4
Adjacent to the gastrointestinal tract	28	13.6 ± 4.27	52.9 ± 2.91	1.6 ± 0.50	2.6 ± 1.19	4.67 ± 0.62	42.9	92.3
Adjacent to the diaphragm	21	12.9 ± 4.29	53.6 ± 2.93	1.8 ± 0.51	2.5 ± 1.20	4.36 ± 0.76	42.9	90.0
Subcapsular tumor	17	14.6 ± 4.31	53.8 ± 2.94	1.6 ± 0.51	2.2 ± 1.22	4.78 ± 0.74	35.3	91.7

MWA, microwave ablation.

postoperative complications between hydrodissection-assisted MWA and MWA alone for subcapsular hepatocellular carcinoma and colorectal liver metastases. In another study, Cheng et al. (32) retrospectively evaluated the effective local control and renal protection in hydrodissection-assisted percutaneous MWA of renal cell carcinoma adjacent to the intestines. In treating various liver tumors in difficult locations, this study found a slight increase in ablation time, number and power, but no significant difference compared to conventional locations, with a rate exceeding 90%. A 100% isolation success rate indicated ease of operation and substantial clinical utility. Initial follow-up in the present study underscores that the minimal ablation margins were statistically comparable between the hydrodissection and control groups, even when tumors were located adjacent to critical structures like the gastrointestinal tract or diaphragm. These findings are in agreement with those reported by Kim et al. (33), further substantiating the utility of hydrodissection in hepatic ablation procedures. Moreover, the results revealed no significant difference in the complete ablation rates between liver tumors at various difficult locations, suggesting hydrodissection's broad applicability to these tumors.

TABLE 3 Comparison of complication rate between hydrodissection and control group.

	Hydrodissection group	Control group	P
Patients	66	65	—
Major complications, *n*(%)			
Liver abscess	2 (3.0)	0	0.496
Biliary injury	0	1 (1.5)	0.496
Minor complications, *n*(%)			
Abdominal pain	7 (10.6)	5 (7.7)	0.763
Fever	6 (9.1)	4 (6.2)	0.527
Gastrointestinal symptoms	3 (4.5)	5 (7.7)	0.492
Minimal pleural effusion	0	1 (1.5)	0.496
Transient liver dysfunction	1 (1.5)	2 (3.1)	0.619
Asymptomatic biloma	0	2 (3.1)	0.244

Consistent with findings by Johnson et al. (34), the present study found a low incidence of serious complications in HCC treated with MWA. Three patients encountered severe complications, namely liver abscess and biliary injury. The occurrence of the liver abscess was associated with factors such as tumor size and location, whereas biliary injury was related to thermal effects and changes in biliary blood supply. No statistical difference was detected in severe complication rates between hydrodissection and control groups, and no instances of intestinal or gallbladder perforation were observed, suggesting that hydrodissection-assisted MWA is a safe and feasible approach for liver tumors in difficult locations. The frequency of minor complications was higher, including abdominal pain and gastrointestinal symptoms, possibly linked to average tumor diameter and position. Increased body temperature may result from reabsorption of necrotic tissue, and patients near the diaphragm may experience abdominal and shoulder pain, while subcapsular tumors were more likely to cause hepatic region pain.

A comprehensive follow-up analysis was conducted to compare the mid-term outcomes of two groups of patients. The findings indicated no significant difference in cumulative local tumor progression rates or overall survival rates between the hydrodissection group and the control group during the follow-up period. In an initial study evaluating the efficacy of radiofrequency ablation in 138 HCC patients in high-risk locations, Hsieh et al. (35) reported a 2-year local tumor progression rate of 22.2% in those who did not undergo artificial ascites and pleural effusion instillation. Moreover, the study also found that the instillation of artificial fluids was associated with improved overall survival (HR=0.1, 95% CI: 0.01-0.95). The study suggested a poor prognosis for tumors in high-risk locations. In contrast, a retrospective study identified that hydrodissection-assisted ablation of liver tumors near the gastrointestinal tract resulted in a 2-year cumulative local progression

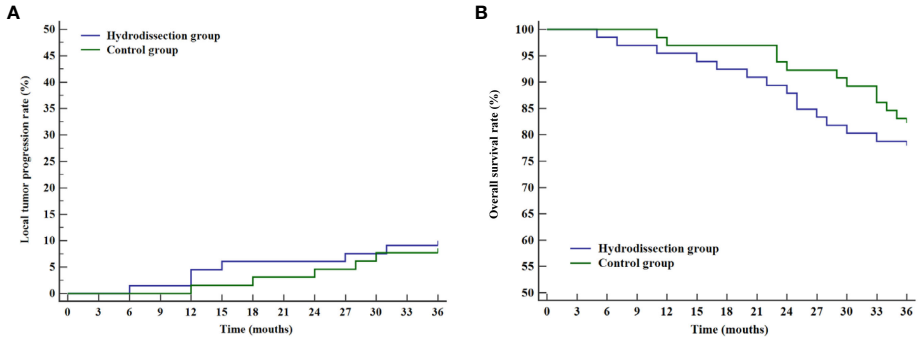

FIGURE 4
Curves of cumulative local tumor progression rates and overall survival rates of the two groups. **(A)** Kaplan-Meier curve of cumulative local tumor progression rates; **(B)** Kaplan-Meier curve of overall survival rates.

rate of 5.7% (36). These findings suggest that the application of hydrodissection decreased local tumor progression in difficult locations, with outcomes similar to those in conventional locations. Stratification analysis of tumors in difficult locations (adjacent to the gastrointestinal tract, diaphragm, and under the liver capsule) revealed no significant variance in cumulative local tumor progression or overall survival rates compared to conventional locations, and no difference between these difficult locations. This highlights the feasibility and consistency of hydrodissection, regardless of tumor location, and broadens its potential therapeutic range. Cox regression analyses further identified prognostic factors affecting patient outcomes. Tumor number and size were independent determinants of overall survival, and minimal ablation margin ≤ 5mm significantly influenced local tumor progression. Notably, the anatomical location of the tumor was not statistically relevant for either outcome metric. Sensitivity analyses validated the robustness of these multivariate models, underscoring the reliability of these prognostic factors.

Nevertheless, this study has several limitations. The first pertains to the intricate relationship between difficult tumor locations and the therapeutic modalities employed, posing

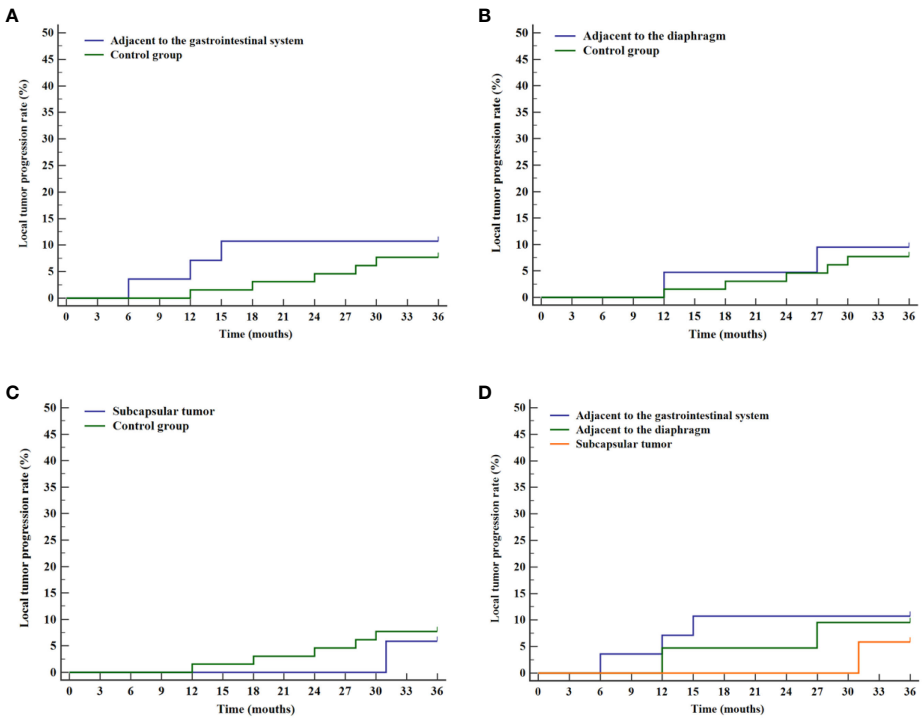

FIGURE 5
Curves of cumulative local tumor progression for various difficult locations and the control group. **(A)** Comparison of cumulative local tumor progression rates between tumor adjacent to the gastrointestinal system and the control group. **(B)** Comparison of cumulative local tumor progression rates between tumor adjacent to the diaphragm and the control group. **(C)** Comparison of cumulative local tumor progression rates between liver subcapsular tumor and the control group. **(D)** Comparison of cumulative local tumor progression rates for tumor in various difficult locations.

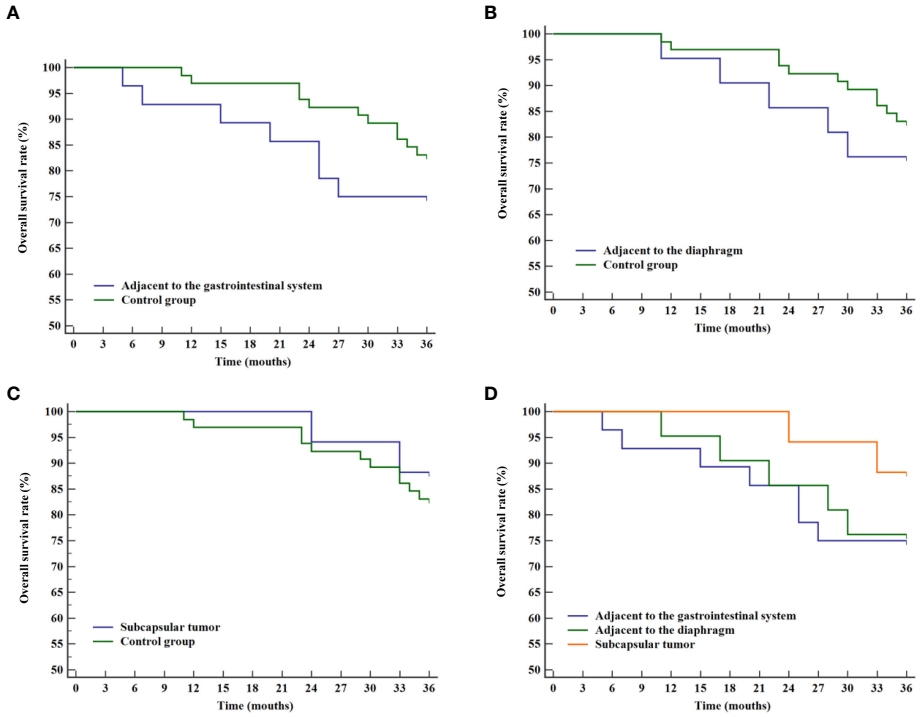

FIGURE 6
Overall survival curves for various difficult locations and the control group. **(A)** Comparison of overall survival rates between tumor adjacent to the gastrointestinal system and the control group. **(B)** Comparison of overall survival rates between tumor adjacent to the diaphragm and the control group. **(C)** Comparison of overall survival rates between liver subcapsular tumor and the control group. **(D)** Comparison of overall survival rates for tumor in various difficult locations.

challenges for isolated analysis. Despite efforts to balance baseline characteristics, the intrinsic interdependence between these variables remains a confounding factor. To account for the variable deemed most clinically significant, difficult tumor locations were specifically incorporated into the Cox regression analyses as an independent variable. This methodological decision, while logical, does not fully resolve the limitations inherent in understanding the relationship between tumor location and

TABLE 4 Univariate analysis of factors associated with local tumor progression and overall survival.

Variables	Overall survival			Local tumor progression		
	HR	95%CI	P	HR	95%CI	P
Age	1.019	0.977-1.064	0.375	1.065	1.005-1.130	0.034
Gender (Male/Female)	0.777	0.306-1.971	0.595	0.648	0.178-2.353	0.509
Tumor location						
Adjacent to the gastrointestinal tract (Yes/No)	0.716	0.282-1.817	0.482	0.888	0.244-3.225	0.856
Adjacent to the diaphragm (Yes/No)	0.889	0.303-2.615	0.831	0.613	0.169-2.228	0.457
Subcapsular tumor (Yes/No)	0.934	0.278-3.144	0.912	0.521	0.143-1.893	0.322
Liver cirrhosis (Yes/No)	0.506	0.200-1.284	0.152	1.829	0.615-5.444	0.278
Tumor number (Single/Multiple)	3.066	1.326-7.092	0.009	2.738	0.895-8.372	0.077
Child-Pugh (A/B)	4.025	1.705-9.052	0.001	3.201	0.985-10.402	0.053
Tumor size (≤3cm/>3cm)	4.845	2.052-11.439	<0.001	2.662	0.895-7.921	0.078
AFP (Positive/Negative)	1.303	0.536-3.166	0.56	1.863	0.609-5.696	0.275
Ablation zone size	1.152	0.689-1.927	0.589	1.293	0.653-2.560	0.461
Minimal ablation margin ≤5mm (Yes/No)	0.296	0.128-0.684	0.004	0.142	0.039-0.515	0.003

TABLE 5 Multivariate analysis of factors associated with local tumor progression and overall survival.

Variables	Overall survival			Local tumor progression		
	HR	95%CI	P	HR	95%CI	P
Age	1.002	0.956-1.050	0.938	1.043	0.982-1.108	0.171
Tumor location						
Adjacent to the gastrointestinal tract (Yes/No)	0.413	0.136-1.256	0.119	0.721	0.158-3.292	0.673
Adjacent to the diaphragm (Yes/No)	0.414	0.111-1.543	0.189	0.42	0.083-2.113	0.293
Subcapsular tumor (Yes/No)	0.833	0.206-3.370	0.789	0.509	0.100-2.581	0.415
Tumor number (Single/Multiple)	3.268	1.277-8.365	0.024	2.433	0.661-8.947	0.181
Child-Pugh (A/B)	2.638	0.903-7.707	0.076	1.582	0.400-6.256	0.513
Tumor size (≤3cm/>3cm)	4.473	1.704-11.743	0.008	1.677	0.475-5.925	0.422
Ablation zone size	1.141	0.639-2.036	0.656	1.201	0.500-2.888	0.682
Minimal ablation margin ≤ 5mm (Yes/No)	0.527	0.207-1.341	0.179	0.207	0.052-0.819	0.025

treatment outcomes. The second limitation stems from the study's retrospective design, which not only constrains the application of standard methods for calculating sample size in non-inferiority tests but also introduces the potential for selection bias and information bias. This may undermine the validity of the results and impact the robustness of the statistical analyses. While the chosen sample size was guided by previous literature and clinical experience, inherent limitations remain unaddressed. Third, the follow-up duration, being relatively brief, might overestimate both the rates of local tumor progression and overall survival. Additionally, the limited follow-up period may not capture late complications or the long-term efficacy of the hydrodissection technique. Therefore, future prospective studies with larger sample sizes and long follow-ups are essential to validate the effects of the hydrodissection technique in assisting microwave ablation in the treatment of hepatocellular carcinoma in difficult locations.

In conclusion, hydrodissection-assisted MWA offers a viable treatment option for HCC in difficult locations, demonstrating safety and mid-term outcomes comparable to those in patients with tumors in conventional locations. Tumor number and size were identified as independent predictors for overall survival, while a higher proportion of patients with a minimal ablation margin of ≤5mm were associated with local tumor progression. No statistically significant impact of tumor location on these outcomes was observed. Although these results are promising, additional research is required for a more comprehensive evaluation.

Data availability statement

The original contributions presented in the study are included in the article/supplementary material. Further inquiries can be directed to the corresponding author.

Ethics statement

The studies involving humans were approved by medical ethics committee of the Affiliated People's Hospital of Ningbo University. The studies were conducted in accordance with the local legislation and institutional requirements. The participants provided their written informed consent to participate in this study.

Author contributions

YS: Conceptualization, Formal Analysis, Methodology, Software, Writing – original draft, Writing – review & editing. MW: Funding acquisition, Investigation, Supervision, Validation, Writing – original draft, Writing – review & editing. RZ: Formal Analysis, Investigation, Methodology, Resources, Visualization, Writing – original draft. PZ: Data curation, Investigation, Methodology, Project administration, Resources, Software, Visualization, Writing – original draft. DM: Data curation, Formal Analysis, Resources, Software, Writing – original draft.

Funding

The author(s) declare financial support was received for the research, authorship, and/or publication of this article. This work was supported by Yinzhou District Science and Technology Plan Project (Yinke [2019] No. 87).

Conflict of interest

The authors declare that the research was conducted in the absence of any commercial or financial relationships that could be construed as a potential conflict of interest.

Publisher's note

References

1. Granata V, Fusco R, De Muzio F, Cutolo C, Setola SV, Simonetti I, et al. Complications risk assessment and imaging findings of thermal ablation treatment in liver cancers: what the radiologist should expect. *J Clin Med* (2022) 11(10):2766. doi: 10.3390/jcm11102766

2. Zheng H, Liu K, Yang Y, Liu B, Zhao X, Chen Y, et al. Microwave ablation versus radiofrequency ablation for subcapsular hepatocellular carcinoma: a propensity score-matched study. *Eur Radiol* (2022) 32(7):4657–66. doi: 10.1007/s00330-022-08537-5

3. Krul MF, Gerritsen SL, Vissers FL, Klompenhouwer EG, Ruers TJ, Kuhlmann KF, et al. Radiofrequency versus microwave ablation for intraoperative treatment of colorectal liver metastases. *Eur J Surg Oncol* (2022) 48(4):834–40. doi: 10.1016/j.ejso.2021.10.012

4. Imajo K, Ogawa Y, Yoneda M, Saito S, Nakajima A. A review of conventional and newer generation microwave ablation systems for hepatocellular carcinoma. *J Med Ultrasonics* (2020) 47(2):265–77. doi: 10.1007/s10396-019-00997-5

5. Izzo F, Granata V, Grassi R, Fusco R, Palaia R, Delrio P, et al. Radiofrequency ablation and microwave ablation in liver tumors: an update. *Oncologist* (2019) 24(10): e990–e1005. doi: 10.1634/theoncologist.2018-0337

6. Ozen M, Raissi D. Current perspectives on microwave ablation of liver lesions in difficult locations. *J Clin Imaging Sci* (2022) 12:61. doi: 10.25259/jcis_126_2022

7. Ishikawa T, Kohno T, Shibayama T, Fukushima Y, Obi S, Teratani T, et al. Thoracoscopic thermal ablation therapy for hepatocellular carcinoma located beneath the diaphragm. *Endoscopy* (2001) 33(8):697–702. doi: 10.1055/s-2001-16216

8. Komorizono Y, Oketani M, Sako K, Yamasaki N, Shibatou T, Maeda M, et al. Risk factors for local recurrence of small hepatocellular carcinoma tumors after a single session, single application of percutaneous radiofrequency ablation. *Cancer* (2003) 97 (5):1253–62. doi: 10.1002/cncr.11168

9. Llovet JM, Vilana R, Brú C, Bianchi L, Salmeron JM, Boix L, et al. Increased risk of tumor seeding after percutaneous radiofrequency ablation for single hepatocellular carcinoma. *Hepatol* (2001) 33(5):1124–9. doi: 10.1053/jhep.2001.24233

10. Smolock AR, Shaw C. Hepatic microwave ablation in challenging locations. *Semin Intervent Radiol* (2019) 36(5):392–7. doi: 10.1055/s-0039-1697003

11. Mukund A, Ramalingam R, Anandpara KM, Patidar Y, Vijayaraghavan R, Sarin SK. Efficacy and safety of percutaneous microwave ablation for hepatocellular carcinomas <4 cm in difficult location. *Br J Radiol* (2020) 93(1116):20191025. doi: 10.1259/bjr.20191025

12. Xiaoyin T, Ping L, Dan C, Min D, Jiachang C, Tao W, et al. Risk assessment and hydrodissection technique for radiofrequency ablation of thyroid benign nodules. *J Cancer* (2018) 9(17):3058–66. doi: 10.7150/jca.26060

13. Garnon J, Cazzato RL, Auloge P, Ramamurthy N, Koch G, Gangi A. Adjunctive hydrodissection of the bare area of liver during percutaneous thermal ablation of sub-cardiac hepatic tumours. *Abdom Radiol (NY)* (2020) 45(10):3352–60. doi: 10.1007/s00261-020-02463-0

14. Delmas L, Koch G, Cazzato RL, Weiss J, Auloge P, Dalili D, et al. Artificial ascites using the guidewire technique during microwave ablation in the liver dome: technique and analysis of fluid repartition. *Abdominal Radiology* (2021) 46(9):4452–9. doi: 10.1007/s00261-021-03077-w

15. Asvadi NH, Anvari A, Uppot RN, Thabet A, Zhu AX, Arellano RS. CT-guided percutaneous microwave ablation of tumors in the hepatic dome: assessment of efficacy and safety. *J Vasc Interv Radiol* (2016) 27(4):496–502. doi: 10.1016/j.jvir.2016.01.010

16. Filippiadis DK, Spiliopoulos S, Konstantos C, Reppas L, Kelekis A, Brountzos E, et al. Computed tomography-guided percutaneous microwave ablation of hepatocellular carcinoma in challenging locations: safety and efficacy of high-power microwave platforms. *Int J Hyperthermia* (2018) 34(6):863–9. doi: 10.1080/02656736.2017.1370728

17. Wang X, Sofocleous CT, Erinjeri JP, Petre EN, Gonen M, Do KG, et al. Margin size is an independent predictor of local tumor progression after ablation of colon cancer liver metastases. *Cardiovasc Intervent Radiol* (2013) 36(1):166–75. doi: 10.1007/s00270-012-0377-1

18. Ahmed M, Solbiati L, Brace CL, Breen DJ, Callstrom MR, Charboneau JW, et al. Image-guided tumor ablation: standardization of terminology and reporting criteria–a 10-year update. *Radiol* (2014) 273(1):241–60. doi: 10.1148/radiol.14132958

19. Goldberg SN, Grassi CJ, Cardella JF, Charboneau JW, Dodd GD, 3rd, Dupuy DE, et al. Image-guided tumor ablation: standardization of terminology and reporting criteria. *Radiol* (2005) 235(3):728–39. doi: 10.1148/radiol.2353042205

20. Ahmed M. Image-guided tumor ablation: standardization of terminology and reporting criteria–a 10-year update: supplement to the consensus document. *J Vasc Interv Radiol* (2014) 25(11):1706–8. doi: 10.1016/j.jvir.2014.09.005

21. Puijk RS, Ruarus AH, Scheffer HJ, Vroomen L, van Tilborg A, de Vries JJJ, et al. Percutaneous liver tumour ablation: image guidance, endpoint assessment, and quality control. *Can Assoc Radiol J* (2018) 69(1):51–62. doi: 10.1016/j.carj.2017.11.001

22. Shiina S, Sato K, Tateishi R, Shimizu M, Ohama H, Hatanaka T, et al. Percutaneous ablation for hepatocellular carcinoma: comparison of various ablation techniques and surgery. *Can J Gastroenterol Hepatol* (2018) 2018:4756147. doi: 10.1155/2018/4756147

23. Nishimura M, Nouso K, Kariyama K, Wakuta A, Kishida M, Wada N, et al. Safety and efficacy of radiofrequency ablation with artificial ascites for hepatocellular carcinoma. *Acta Med Okayama* (2012) 66(3):279–84. doi: 10.18926/amo/48568

24. Kang TW, Lim HK, Lee MW, Kim YS, Choi D, Rhim H. First-line radiofrequency ablation with or without artificial ascites for hepatocellular carcinomas in a subcapsular location: local control rate and risk of peritoneal seeding at long-term follow-up. *Clin Radiol* (2013) 68(12):e641–51. doi: 10.1016/j.crad.2013.07.008

25. Li B, Liu C, Xu XX, Li Y, Du Y, Zhang C, et al. Clinical application of artificial ascites in assisting CT-guided percutaneous cryoablation of hepatic tumors adjacent to the gastrointestinal tract. *Sci Rep* (2017) 7(1):16689. doi: 10.1038/s41598-017-17023-8

26. Makovich Z, Logemann J, Chen L, Mhaskar R, Choi J, Parikh N, et al. Liver tumor ablation in difficult locations: Microwave ablation of perivascular and subdiaphragmatic hepatocellular carcinoma. *Clin Imaging* (2021) 71:170–7. doi: 10.1016/j.clinimag.2020.11.010

27. Garnon J, Koch G, Caudrelier J, Boatta E, Rao P, Nouri-Neuville M, et al. Hydrodissection of the retrohepatic space: A technique to physically separate a liver tumour from the inferior vena cava and the ostia of the hepatic veins. *Cardiovasc Intervent Radiol* (2019) 42(1):137–44. doi: 10.1007/s00270-018-2105-y

28. Kim YS, Rhim H, Paik SS. Radiofrequency ablation of the liver in a rabbit model: creation of artificial ascites to minimize collateral thermal injury to the diaphragm and stomach. *J Vasc Interv Radiol* (2006) 17(3):541–7. doi: 10.1097/01.rvi.0000208305.65202.84

29. Lee EJ, Rhim H, Lim HK, Choi D, Lee WJ, Min KS. Effect of artificial ascites on thermal injury to the diaphragm and stomach in radiofrequency ablation of the liver: experimental study with a porcine model. *AJR Am J Roentgenol* (2008) 190(6):1659–64. doi: 10.2214/ajr.07.2993

30. Park SJ, Lee DH, Han JK. Reducing pain by artificial ascites infusion during radiofrequency ablation for subcapsular hepatocellular carcinoma. *Cardiovasc Intervent Radiol* (2021) 44(4):565–73. doi: 10.1007/s00270-020-02723-y

31. Liu C, He J, Li T, Hong D, Su H, Shao H. Evaluation of the efficacy and postoperative outcomes of hydrodissection-assisted microwave ablation for subcapsular hepatocellular carcinoma and colorectal liver metastases. *Abdominal Radiology* (2021) 46(5):2161–72. doi: 10.1007/s00261-020-02830-x

32. Cheng Z, Yu X, Han Z, Liu F, Yu J, Liang P. Ultrasound-guided hydrodissection for assisting percutaneous microwave ablation of renal cell carcinomas adjacent to intestinal tracts: a preliminary clinical study. *Int J Hyperthermia* (2018) 34(3):315–20. doi: 10.1080/02656736.2017.1338362

33. Kim JH, Lee JY, Yu SJ, Lee DH, Joo I, Yoon JH, et al. Fusion imaging-guided radiofrequency ablation with artificial ascites or pleural effusion in patients with hepatocellular carcinomas: the feasibility rate and mid-term outcome. *Int J Hyperthermia* (2023) 40(1):2213424. doi: 10.1080/02656736.2023.2213424

34. Johnson W, Weekley A, Suz P, Parikh N, El-Haddad G, Mhaskar R, et al. Safety of CT-guided microwave ablation of subcardiac liver tumors. *Cardiovasc Intervent Radiol* (2022) 45(11):1693–700. doi: 10.1007/s00270-022-03235-7

35. Hsieh YC, Limquiaco JL, Lin CC, Chen WT, Lin SM. Radiofrequency ablation following artificial ascites and pleural effusion creation may improve outcomes for hepatocellular carcinoma in high-risk locations. *Abdom Radiol (NY)* (2019) 44 (3):1141–51. doi: 10.1007/s00261-018-1831-6

36. Yang W, Yan K, Wu GX, Wu W, Fu Y, Lee JC, et al. Radiofrequency ablation of hepatocellular carcinoma in difficult locations: Strategies and long-term outcomes. *World J Gastroenterol* (2015) 21(5):1554–66. doi: 10.3748/wjg.v21.i5.1554

frontiers | Frontiers in Oncology

TYPE Original Research
PUBLISHED 22 November 2023
DOI 10.3389/fonc.2023.1235786

OPEN ACCESS

EDITED BY
Francisco Tustumi,
University of São Paulo, Brazil

REVIEWED BY
Robert Damm,
University Hospital Magdeburg, Germany
Bin-Yan Zhong,
The First Affiliated Hospital of Soochow University, China

*CORRESPONDENCE
Wenbo Guo
guowenbo@mail.sysu.edu.cn

†These authors have contributed equally to this work

RECEIVED 06 June 2023
ACCEPTED 06 November 2023
PUBLISHED 22 November 2023

CITATION
Chen S, Cai H, Wu Z, Tang S, Chen L, Wang F, Zhuang W and Guo W (2023) Anlotinib combined with transarterial chemoembolization for unresectable hepatocellular carcinoma associated with hepatitis B virus: a retrospective controlled study. *Front. Oncol.* 13:1235786. doi: 10.3389/fonc.2023.1235786

Anlotinib combined with transarterial chemoembolization for unresectable hepatocellular carcinoma associated with hepatitis B virus: a retrospective controlled study

Song Chen[1†], Hongjie Cai[2†], Zhiqiang Wu[2], Shuangyan Tang[2], Ludan Chen[2], Fan Wang[2], Wenquan Zhuang[2] and Wenbo Guo[2*]

[1]Department of Minimally Invasive Interventional Therapy, State Key Laboratory of Oncology in South China, Guangdong Provincial Clinical Research Center for Cancer, Sun Yat-sen University Cancer Center, Guangzhou, China, [2]Department of Interventional Radiology, The First Affiliated Hospital of Sun Yat-sen University, Guangzhou, China

Purpose: To investigate the efficacy and safety of combined treatment of anlotinib and transarterial chemoembolization (TACE) in patients with unresectable hepatocellular carcinoma (uHCC) associated with hepatitis B virus (HBV) infection.

Methods: We retrospectively collected the data of 96 uHCC patients associated with HBV infection who received either TACE only (TO group; n = 64) or anlotinib combined with TACE (TA group; n = 32) from January 2017 to January 2021. The primary endpoint was overall survival (OS). The secondary outcomes included progression-free survival (PFS), tumor response according to modified Response Evaluation Criteria in Solid Tumors (mRECIST) and RECIST 1.1, and adverse events (AEs).

Results: The median OS and median PFS were significantly longer in the TA group compared to the TO group (17.6 months *vs.* 9.4 months, $p = 0.018$; 6.7 months *vs.* 3.8 months, $p = 0.003$, respectively). In addition, the overall objective response rate (ORR) and disease control rate (DCR) numerically increased in the TA group (mRECIST, ORR 65.6% *vs.* 46.9%, $p = 0.064$, DCR 90.6% *vs.* 85.9%, $p = 0.382$; RECIST 1.1, ORR 46.9% *vs.* 15.6%, $p = 0.001$, DCR 90.6% *vs.* 85.9%, $p = 0.382$, respectively). It was worth noting that no treatment-related mortality occurred during the study. The most common AEs included elevated transaminases (56.3%), decreased appetite (46.9%), and abdominal pain (37.5%) in the TA group. Although the incidence rate of grade 3/4 AEs was higher in the TA group, all of them were controllable.

10.3389/fonc.2023.1235786

Conclusions: The combination of anlotinib and TACE has shown promising results in improving outcomes for patients with HBV-related uHCC, as compared to TACE monotherapy. In addition, this combination therapy has demonstrated a controllable safety profile. However, further validation is urgently needed through randomized controlled trials with large sample sizes.

KEYWORDS

anlotinib, transarterial chemoembolization, unresectable hepatocellular carcinoma, combination therapy, hepatitis B virus

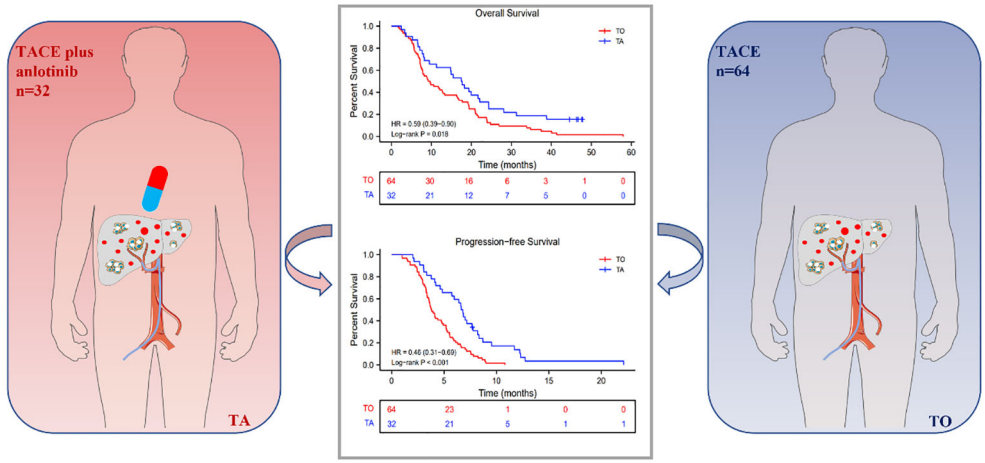

GRAPHICAL ABSTRACT

Introduction

Hepatocellular carcinoma (HCC) is a highly prevalent and deadly form of cancer, ranking sixth and third in terms of incidence and mortality, respectively, among all malignant tumors worldwide. China has the ninth-highest incidence of HCC globally and has over 50% of new HCC cases reported worldwide each year (1). Generally, conventional curative treatment options for HCC included ablation, resection, and transplantation, although the majority of patients are ineligible due to various factors, including tumor size, location, number, liver function, extrahepatic metastases, vascular involvement, and overall patient condition (2, 3).

The Barcelona Clinic Liver Cancer (BCLC) staging system is widely recognized and utilized in clinical practice, and it is also commonly employed in clinical trials for the treatment of HCC (4, 5). According to the BCLC staging system, transarterial chemoembolization (TACE) is recommended as the standard option for intermediate-stage (BCLC-B stage) HCC, while it has been extended for patients with almost all unresectable HCC (uHCC) in many countries, with numerous clinical studies reporting survival advantages in comparison to conservative management or other regimens (6–9). However, based on previously routine TACE, the majority of patients experienced a rapid relapse and poor prognosis within a relatively short period, resulting in a push for the exploration of other feasible options (10, 11).

To our knowledge, TACE exerts therapeutic effect mainly based on constructing intratumoral hypoxia and ischemia environment, which could induce the upregulation of vascular endothelial growth factor (VEGF) and fibroblast growth factor (FGF) at the same time, further promoting tumor growth, invasion, and metastasis. Tyrosine kinase inhibitors (TKIs) can effectively decrease VEGF and FGF, so the combination with TACE has a synergistic antitumor effect theoretically. Although several prospective clinical trials have been reported with negative results regarding the superiority of combination treatment compared to TACE alone, especially for sorafenib, more and more clinical trials presented compelling clinical evidence indicating that patients with uHCC can benefit more from the combination of TACE and TKIs when compared to TACE monotherapy (12–16).

Anlotinib is a novel small-molecule TKI that selectively targets vascular endothelial growth factor receptors (VEGFRs), fibroblast growth factor receptors (FGFRs), platelet-derived growth factor receptors (PDGFRs), and c-kit receptors, demonstrating promising efficacy in treating a variety of malignancies, including advanced non-small cell lung cancer (NSCLC), medullary thyroid carcinoma, soft tissue sarcoma (STS), metastatic cervical cancer, neuroblastoma, and advanced biliary tract cancers (17–19). Recently, anlotinib has shown

its efficacy and safety for patients with uHCC as well, especially in combination with TACE (20, 21).

Although vaccination programs have been implemented and new infections among children have decreased obviously, the percentage of people living with chronic hepatitis B virus (HBV) infection worldwide remained as high as 3.5% of the global population in 2015 (22). Persistent HBV infection is actually responsible for over 50% of all HCC cases worldwide and up to 85% in some areas where the infection is endemic, such as in China (23). Therefore, HCC associated with HBV infection is the major burden for HCC management in China, and the choice of treatment regimens ranks as extremely important.

Anlotinib combined with TACE may have a superior synergistic antitumor effect, but no clinical study has reported the long-term survival of the combination therapy yet. Therefore, our study aims to investigate the efficacy and safety of the combination therapy compared with TACE monotherapy in patients with uHCC associated with HBV infection.

Patients and methods

Patient eligibility

We retrospectively collected uHCC patients who underwent either TACE only or a combination of anlotinib and TACE from January 2017 to January 2021 at the First Affiliated Hospital of Sun Yat-sen University. The unresectable criteria include one or more of the following aspects: i) residual liver volume is insufficient, ii) distant metastasis or macrovascular invasion, iii) liver function or physical condition is poor, and iv) resection is highly risky as assessed by two experienced surgeons.

All patients were preoperatively evaluated by MRI, abdominal dynamic CT, and/or abdominal ultrasonography. The criteria for inclusion were as follows: 1) pathologically or radiologically diagnosed with intermediate to advanced HCC consistent with the European Association for the Study of the Liver (EASL), 2) deemed to be unresectable or incurable according to the above description, 3) liver function scored as Child-Pugh class A or B, 4) performance status score of Eastern Cooperative Oncology Group (ECOG PS) of 0 or 1, and 5) infected with HBV. Exclusion criteria were as follows: 1) <18 years old or ≥75 years old, 2) previous antitumor therapy of any kind, 3) contraindicated to receive TACE or anlotinib, 4) anlotinib administration less than 4 weeks, 5) discontinued anlotinib due to personal reason, 6) incomplete follow-up medical data, and 7) malignant tumors in other organs.

The study was approved by the ethics committee at the First Affiliated Hospital of Sun Yat-sen University, and all recruited patients provided informed consent.

Treatment protocol

TACE therapy

Each patient enrolled underwent at least one TACE session. The catheter tip was selectively or superselectively inserted into the tumor-feeding artery branches based on tumor location, size, and blood supply. The chemoembolization regimen was first performed by emulsion consisting of pharmorubicin and lipiodol and subsequently embolizing the trunk with a microsphere or absorbable gelatin sponge. The embolization endpoint was classified according to the previously established subjective angiographic chemoembolization endpoint (SACE) scale. Generally, the embolization endpoint reached SACE level III or IV, denoting reduced or none antegrade arterial flow without tumor blush (24). All procedures were operated by a physician. Efficacy assessment was performed every 4–6 weeks after TACE, and patients received on-demand TACE according to the investigator's assessment.

Anlotinib therapy

Patients in the TA group were informed about the economic cost, expected outcomes, and possible side effects of anlotinib. With the patients' consent, anlotinib was initially administered (12 mg) once a day for 3 to 5 days after the first TACE session (2 weeks on and 1 week off). If mild to moderate adverse events (AEs) of grade 1/2 occurred, the frequency and dose of anlotinib would be the same as before, but the side effects were promptly addressed. In the event of severe AEs of grade 3/4, the dose of anlotinib would be decreased to 8 mg once a day, or the frequency would be reduced to every 2 days until the AEs were resolved or relieved. If the symptoms persisted, the administration of anlotinib would be temporarily halted until the AEs were alleviated or resolved.

Antiviral therapy

Because all patients enrolled in the study were infected with HBV, they received routine antiviral medication therapy (entecavir or tenofovir alafenamide fumarate) every day.

Assessment and follow-up

The follow-ups were performed every 4–6 weeks after each TACE session, while the interval for the next follow-ups was extended to every 9–12 weeks when patients achieved stable disease. Imaging examination including abdominal MRI with contrast, dynamic CT scans of the chest and abdomen, and/or abdominal ultrasound was used to evaluate the progression-free survival (PFS) and tumor response based on modified Response Evaluation Criteria in Solid Tumors (mRECIST) and RECIST 1.1 criteria. Serum tests were also performed to assess the effectiveness and safety, including liver function, alpha-fetoprotein (AFP) levels, and blood cell count.

Objective response rate (ORR) was defined as the combined percentage of partial response (PR) and complete response (CR). Disease control rate (DCR) was defined as the combined percentage of stable disease (SD) and ORR. Overall survival (OS) refers to the length of time from the start of treatment until death for any reason. PFS refers to the length of time from the start of treatment until either tumor progression or death for any reason. AEs were assessed based on their frequency and severity grade using the Common Terminology Criteria for Adverse Events (CTCAE; version 5.0).

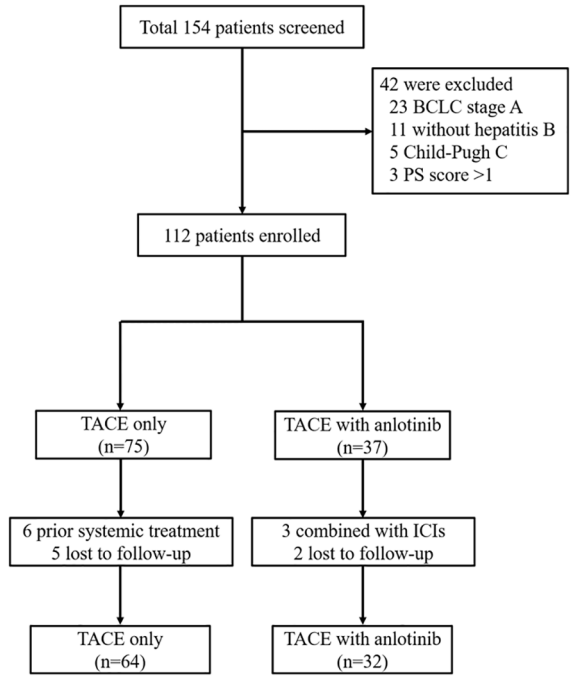

FIGURE 1
Patient enrollment flow diagram. TACE, transarterial chemoembolization; BCLC, Barcelona Clinic Liver Cancer; PS, performance status; ICIs, immune checkpoint inhibitors.

Statistical analysis

R statistical software (version 4.0.3; R Foundation Inc., Vienna, Austria) and SPSS version 25.0 software (SPSS, Chicago, IL, USA) for the statistical analysis were used. The median values and interquartile ranges for the clinical parameters were computed, and then a Student's t-test was performed to compare the continuous variables between the two groups. Survival analyses, including OS and PFS, were performed using the Kaplan–Meier method, and differences were analyzed by the log-rank test. Cox regression analyses were conducted to identify factors associated with survival outcomes. Factors with a p-value < 0.05 in univariate analysis were included in multivariate analysis. The therapeutic efficacy was demonstrated by the ORR and DCR, which were compared using the chi-square test. Statistical significance was defined as two-tailed $p < 0.05$.

Results

Patient characteristics

From January 2017 to January 2021, a total of 154 patients with unresectable treated with TO or TA were screened. Among them, 96 patients were finally eligible and enrolled in the current study, with 64 receiving TACE monotherapy (TO group) and the other 32 patients receiving combination therapy (TA group) (Figure 1).

The baseline characteristics of all patients in the two groups are listed in Table 1. All of the baseline characteristics were well balanced between the two groups including age, gender, BCLC stage, Child-Pugh class, albumin–bilirubin (ALBI) grade, PS score, tumor number, largest size, AFP level, portal vein tumor thrombus (PVTT), and extrahepatic spread. Obviously, the tumor burden was relatively high in the two groups with the median largest size over 11 cm.

TABLE 1 Baseline characteristics of patients in TO and TA groups.

Characteristic	TO (n = 64)	TA (n = 32)	*p*
Age, mean ± SD	53.4 ± 12.4	53.6 ± 13.6	0.960
Gender, n (%)			0.172
Female	5 (7.8%)	6 (18.8%)	
Male	59 (92.2%)	26 (81.2%)	
BCLC stage, n (%)			1.000
B	32 (50.0%)	16 (50.0%)	
C	32 (50.0%)	16 (50.0%)	
CNLC stage, n (%)			0.912
IIb	32 (50.0%)	16 (50.0%)	
IIIa	24 (37.5%)	11 (34.4%)	
IIIb	8 (12.5%)	5 (15.6%)	
Child-Pugh, n (%)			0.636
A	54 (84.4%)	25 (78.1%)	
B	10 (15.6%)	7 (21.9%)	
ALBI grade, n (%)			0.206
1	6 (9.4%)	6 (18.8%)	
2	58 (90.6%)	26 (81.2%)	
Performance status, n (%)			0.527
0	57 (89.1%)	27 (84.4%)	
1	7 (10.9%)	5 (15.6%)	
Tumor number, n (%)			1.000
Multiple	55 (85.9%)	28 (87.5%)	
Solitary	9 (14.1%)	4 (12.5%)	
Largest size (cm), median (Q1, Q3)	11.5 (8.3, 14.3)	11.5 (8.7, 13.1)	0.756
AFP, n (%)			1.000
<400	25 (39.1%)	13 (40.6%)	
≥400	39 (60.9%)	19 (59.4%)	
PVTT, n (%)			0.827
Absence	35 (54.7%)	19 (59.4%)	

(Continued)

10.3389/fonc.2023.1235786

TABLE 1 Continued

Characteristic	TO (n = 64)	TA (n = 32)	*p*
Presence	29 (45.3%)	13 (40.6%)	
Extrahepatic spread, n (%)			0.755
No	56 (87.5%)	27 (84.4%)	
Yes	8 (12.5%)	5 (15.6%)	

TO, TACE only; TA, TACE combined with anlotinib; TACE, transarterial chemoembolization; BCLC, Barcelona Clinic Liver Cancer; CNLC, China Liver Cancer Staging; ALBI, albumin–bilirubin; AFP, alpha-fetoprotein; PVTT, portal vein tumor thrombus.

Efficacy outcomes

The last follow-up date was September 30, 2022. The median follow-up durations in the TO and TA groups were 24.0 months (range, 8.0 to 30.5 months) and 17.5 months (range, 5.0 to 25.4 months), respectively. The median anlotinib treatment duration was 10.7 months (range, 3.8 to 21.9 months).

In the TA and TO groups, the median OS was 9.4 months (95% confidence interval [CI], 7.8 to 16.3 months) and 17.6 months (95% CI, 11.3 to 24.3 months), respectively. Thus, OS was significantly prolonged in the TA group (hazard ratio [HR]: 0.50, 95% CI: 0.27–0.90; p = 0.03; Figure 2A). The median PFS was also longer (HR:

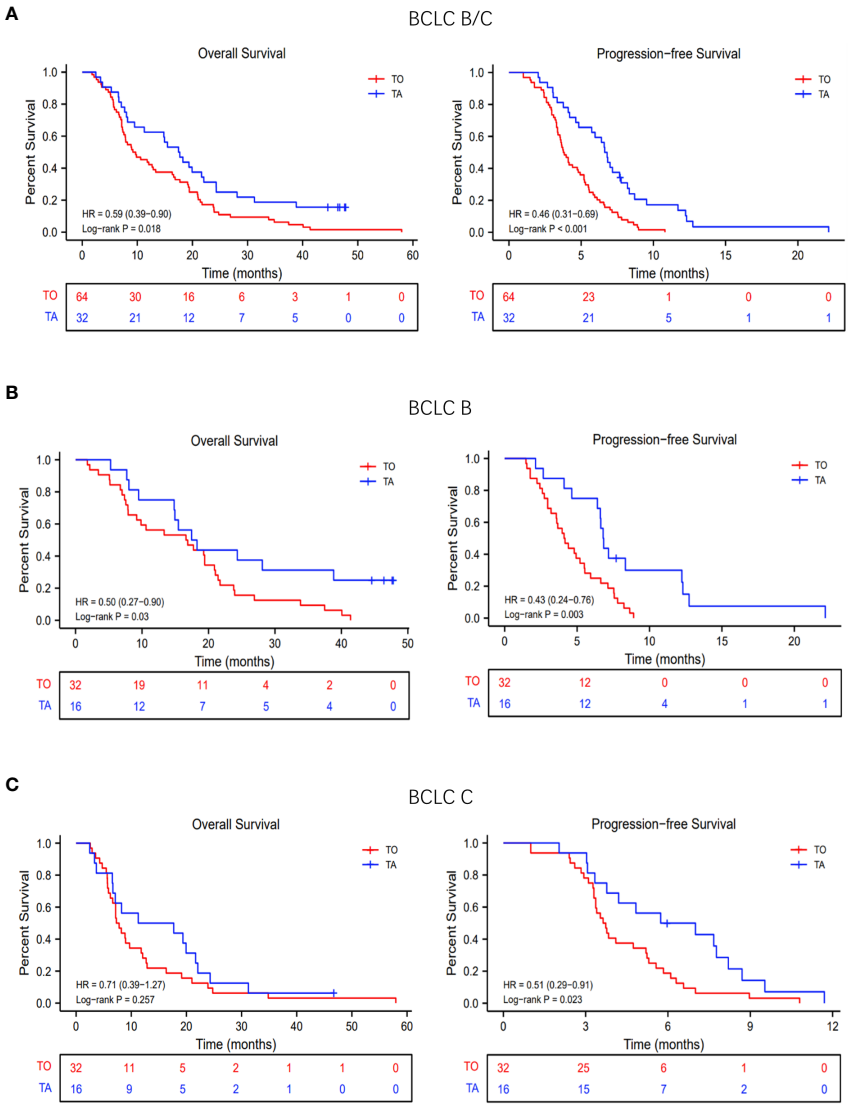

FIGURE 2
Overall survival (OS) and progression-free survival (PFS) with TO or TA regimen. **(A)** The OS and PFS of all patients. **(B)** The OS and PFS of patients with BCLC stage **(B, C)** The OS and PFS of patients with BCLC stage **(C)** TACE, transarterial chemoembolization; TO, TACE only; TA, TACE combined with anlotinib; BCLC, Barcelona Clinic Liver Cancer.

0.43, 95% CI: 0.24–0.76; $p = 0.003$; Figure 2A) in the TA group (3.8 months, 95% CI: 3.5 to 4.9 months) compared with the TO group (6.7 months, 95% CI: 57 to 8.2 months). In the subgroup analysis, based on the BCLC stage (BCLC B/C), the OS and PFS were also longer in the TA group, consistent with the overall population (Figures 2B, C). The forest plot analysis of factors associated with OS and PFS is exhibited in Figure 3. TA provided a clinical benefit in patients with all characteristics except for OS in Child-Pugh class B and ALBI grade 1.

All the patients were evaluated for tumor response in the two groups. According to mRECIST, the ORR and DCR were 65.6% *vs.* 46.9% ($p = 0.064$) and 90.6% *vs.* 85.9% ($p = 0.382$), respectively. According to RECIST 1.1, the ORR and DCR were 46.9% *vs.* 15.6% ($p = 0.001$) and 90.6% *vs.* 85.9% ($p = 0.382$), respectively (Table 2). In the subgroup analysis, the ORR and DCR were higher in the TA group whether for the BCLC-B stage or BCLC-C stage (Table 2).

Univariate and multivariate analyses for survival

Supplementary Table 1 demonstrates the univariate and multivariate analyses for survival. Multivariate analysis demonstrated that the therapeutic regimen was an independent risk factor for both OS (HR 0.58, 95% CI, 0.37–0.91; $p = 0.018$) and PFS (HR 0.39, 95% CI, 0.24–0.62; $p < 0.001$). Multivariate analysis showed that AFP ≥ 400 was a risk factor for PFS (HR 1.80, 95% CI, 1.16–2.78; $p = 0.008$).

Progression reason analysis

As for the progression reason analysis, there were a total of four ways to progress: local lesion progression, intrahepatic metastasis, extrahepatic metastasis, and death. In the two groups, the proportion was 31.3%, 46.9%, 12.5%, and 9.3%, respectively, *vs.* 25.0%, 31.3%, 12.4%, and 31.3%, respectively ($p = 0.054$). Obviously, the proportion of local lesion progression and intrahepatic metastasis in the TA group was less than that in the TO group (Supplementary Figure 1; Table 3).

Subsequent treatment

After tumor progression, 55 patients (85.9%) in the TO group and 30 patients (93.8%) in the TA group received subsequent treatment. With the positive results of the REFLECT study (25), a considerable proportion of the patients converted to lenvatinib with or without programmed death protein 1 (PD-1) after progression. In the TO group, the most common subsequent therapy was anlotinib combined with TACE (Supplementary Table 2).

Safety

All AEs were evaluated as mild to moderate and controllable, with no treatment-associated death occurring. Although more patients experienced AEs in the TA group, especially for grade 3/4 AEs, none of the patients discontinued therapy. The most

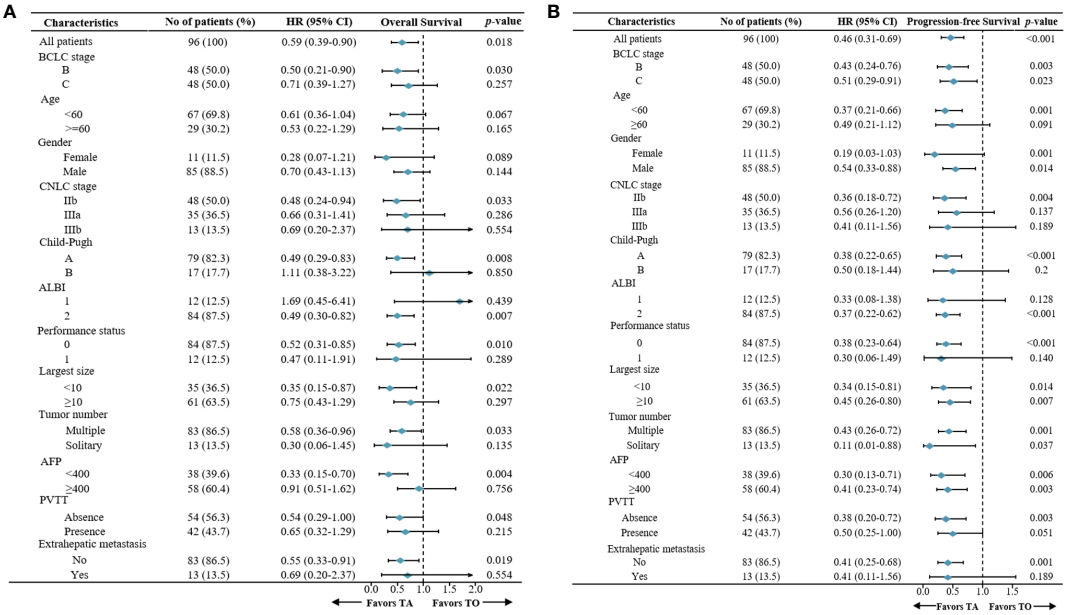

FIGURE 3
Forest plot for **(A)** overall survival and **(B)** progression-free survival of the patients treated with TA or TO. TACE, transarterial chemoembolization; TO, TACE only; TA, TACE combined with anlotinib.

TABLE 2 Tumor response in the total and subgroups according to mRECIST and RECIST 1.1.

	mRECIST							RECIST						
	Total			BCLC B			BCLC C		Total			BCLC B			BCLC C	
	TO (n = 64)	TA (n = 32)	*p*	TO (n = 32)	TA (n = 16)	*p*	TO (n = 32)	TA (n = 16)	TO (n = 64)	TA (n = 32)	*p*	TO (n = 32)	TA (n = 16)	*p*	TO (n = 32)	TA (n = 16)	*p*
CR	0 (0)	3 (9.4%)		0 (0)	1 (6.3%)		0 (0)	2 (12.5%)	0 (0)	0 (0)		0 (0)	0 (0)		0 (0)	0 (0)	
PR	30 (46.9%)	18 (56.2%)		17 (53.1%)	12 (75.0%)		13 (40.6%)	6 (37.5%)	10 (15.6%)	15 (46.9%)		6 (18.8%)	9 (56.3%)		4 (12.5%)	6 (37.5%)	
SD	25 (39.0%)	8 (25.0%)		11 (34.4%)	2 (12.4%)		14 (43.8%)	6 (37.5%)	45 (70.3%)	14 (43.7%)		22 (68.7%)	6 (37.5%)		23 (71.9%)	8 (50.0%)	
PD	9 (14.1%)	3 (9.4%)		4 (12.5%)	1 (6.3%)		5 (15.6%)	2 (12.5%)	9 (14.1%)	3 (9.4%)		4 (12.5%)	1 (6.2%)		5 (15.6%)	2 (125%)	
ORR	30 (46.9%)	21 (65.6%)	0.064	17 (53.1%)	13 (81.3%)	0.055	13 (40.6%)	8 (50.0%)	10 (15.6%)	15 (46.9%)	0.001	6 (18,8%)	9 (56.3%)	0.011	4 (12.5%)	6 (37.5%)	0.054
DCR	55 (85.9%)	29 (90.6%)	0.382	28 (87.5%)	15 (93.8%)	0.454	27 (84.4%)	14 (87.5%)	55 (85.9%)	29 (90.6%)	0.382	28 (87.5%)	15 (93.8%)	0.454	27 (84.4%)	14 (87.5%)	0.571

mRECIST, modified Response Evaluation Criteria in Solid Tumors; BCLC, Barcelona Clinic Liver Cancer; TACE, transarterial chemoembolization; TO, TACE only; TA, TACE combined with anlotinib; CR, complete response; PR, partial response; SD, stable disease; PD, progressive disease; ORR, objective response rate; DCR, disease control rate.

common AEs included elevated transaminases (56.3%), decreased appetite (46.9%), and abdominal pain (37.5%) in the TA group. The details of AEs are summarized in Table 4.

Discussion

We report here the primary results of a retrospective controlled study of anlotinib combined with TACE versus TACE monotherapy in patients with uHCC associated with HBV infection. Anlotinib combined with TACE demonstrated a significant improvement in OS, PFS, and tumor response, further confirming the benefits observed in our previous investigations (20). The study revealed that combination therapy has emerged as a significant independent prognostic factor for improved survival with a manageable safety profile. In summary, we found that anlotinib combined with TACE provided more clinical benefits than TACE monotherapy for patients with uHCC associated with HBV infection with acceptable AEs.

TACE is indeed recommended as the standard treatment for intermediate-stage HCC, while it is the most commonly served as a first-line treatment for uHCC in real-world clinical practice (26). However, TACE monotherapy remains to be further improved with unsatisfactory effectiveness in local recurrence and liver function damage, and TACE combined with TKIs has shown promising prognosis based on the synergistic antitumor effect in previous studies (12–16). The use of drug-eluting beads (DEB-TACE) might contribute to improved outcomes, while it has not been reported with superiority over conventional TACE (cTACE) in terms of survival yet (27, 28), so we opted for cTACE as the standard procedure in our study. There were several reasons for choosing anlotinib combined with TKIs. First, at the time when we decided to investigate the effectiveness of TACE plus TKIs, lenvatinib was not approved by the National Medical Products Administration (NMPA) because the results of the REFLECT study were not reported then. Second, we tried to combine TACE with sorafenib, but the majority of patients refused to continue due to serious side effects and high cost, while anlotinib was approximately one-tenth of the annual economic cost compared to sorafenib with fewer adverse events when first approved in China, which was highly cost-effective and more acceptable. Third, anlotinib is a novel multi-target TKI, which plays a crucial role in inhibiting elements implicated in tumor angiogenesis and signals promoting tumor proliferation, just as lenvatinib and sorafenib.

In both the overall population and the BCLC-B stage subpopulation, the median OS was significantly prolonged in the TA group (overall population, 17.6 *vs.* 9.4 months, $p = 0.0183$; BCLC-B subpopulation, 17.9 *vs.* 16.7 months, $p = 0.03$), while there was no significant difference in median OS between the TA and TO groups (14.5 *vs.* 7.5 months, $p = 0.257$) in the BCLC-C stage subpopulation. On the one hand, the investigated sample was relatively small, influencing the final result. On the other hand, TACE might not be the preferred option for advanced-stage patients, especially for those with vp3/4 portal vein tumor thrombus (PVTT) (29, 30). However, there was an obvious trend for prolonged survival, indicating the advantage of combination

TABLE 3 Different endpoints to progression-free survival.

	TO (n = 64)	TA (n = 32)	*p*
Local lesion progression	20 (31.3%)	8 (25.0%)	
Intrahepatic metastasis	30 (46.9%)	10 (31.3%)	
Extrahepatic metastasis	8 (12.5%)	4 (12.4%)	
death	6 (9.3%)	10 (31.3%)	0.054

Data are presented as n (%),
TO, TACE only; TA, TACE combined with anlotinib; TACE, transarterial chemoembolization.

therapy. Furthermore, the LAUNCH study has demonstrated that TACE combined with TKIs contributed more for advanced patients compared to TKIs monotherapy (31).

In the other subgroup analysis, significant differences were not observed in certain subgroups with small proportional cohorts due to limitations in the number of cases. In general, anlotinib combined with TACE provided survival advantages in patients except for those with Child-Pugh class B or ALBI grade I liver function, indicating that we should take liver function into more consideration when choosing therapy regimens. Additionally, monotherapy might be a preferred option for patients with poor liver function, given that it causes minimal damage to liver function, consistent with a previous study (10, 32). Univariate and multivariate Cox regression analyses indicated that the treatment regimen has emerged as the only significant prognostic factor associated with both PFS and OS, which further confirmed the importance of combination therapy rather than other characteristics in improving efficacy.

In the analysis of different endpoints to PFS, it was obvious that the local lesion progression and intrahepatic metastasis just made up a small proportion in the TA group compared to the TO group. The finding suggested that anlotinib, as an anti-angiogenesis TKI, might have a greater ability to control the recurrence of local or intrahepatic lesions, indicating the synergistic antitumor effect combined with TACE. As reported, local and intrahepatic recurrences principally limited the survival benefit conferred by TACE (33), so the combination of anlotinib might improve prognosis effectively.

Additionally, with the successful prospective trials of anti-programmed death 1 (anti-PD-1) and anti-programmed death ligand 1 (anti-PD-L1) for advanced HCC, the treatment for HCC has stepped into the novel era of immunotherapy (34). Except for the combination of targeted therapy and immunotherapy, locoregional therapy combined with targeted therapy and immunotherapy has also been reported with many positive outcomes (35, 36). The CHANCE001 study demonstrated that TACE combined with PD-(L)1 and molecularly targeted agents (MTAs) significantly improves outcomes versus TACE monotherapy for Chinese patients with uHCC in real-world practice, with an acceptable safety profile (37). Based on the above results, triple combination therapy will be explored next.

The ratio of subsequent therapy was higher in the TA group (93.8% *vs.* 85.9%), and it was also higher than that in the combination group (sorafenib combined with TACE) of the TACTICS trial

TABLE 4 Treatment-related adverse events.

AEs	Any grade			Grade 3/4		
	TO (N = 64)	TA (N = 32)	*p*	TO (N = 64)	TA (N = 32)	*p*
Abdominal pain	25 (39.1)	12 (37.5)	0.882	3 (4.7)	1 (3.1)	<0.001
Nausea	22 (34.4)	10 (31.3)	0.759	0 (0)	0 (0)	1.000
Diarrhea	12 (18.8)	7 (21.9)	0.717	0 (0)	1 (3.1)	0.333
Decreased appetite	20 (31.3)	15 (46.9)	0.165	1 (1.6)	2 (6.3)	0.534
Erythra	0 (0)	5 (15.6)	0.006	0 (0)	2 (6.3)	0.109
Fatigue	6 (9.4)	5 (15.6)	0.571	0 (0)	0 (0)	1.000
Hypoproteinemia	12 (18.8)	5 (15.6)	0.656	2 (3.1)	0 (0)	0.551
Elevated bilirubin	10 (15.6)	6 (18.8)	0.699	1 (1.6)	1 (3.1)	1.000
Elevated transaminases	30 (46.9)	18 (56.3)	0.386	3 (4.7)	2 (6.3)	0.749
Hypothyroidism	0 (0)	6 (18.8)	0.001	0 (0)	1 (3.1)	0.333
Decreased PLT	9 (14.1)	8 (25.0)	0.186	0 (0)	0 (0)	1.000
Hypertension	3 (4.7)	6 (18.8)	0.063	0 (0)	0 (0)	1.000
Hand–foot skin reaction	0 (0)	8 (25.0)	<0.001	0 (0)	2 (6.3)	0.109
Dysphonia	0 (2)	2 (6.3)	0.109	0 (0)	0 (0)	1.000
Proteinuria	2 (3.1)	5 (15.6)	0.071	0 (0)	0 (0)	1.000
Bleeding (gingiva)	1 (1.6)	4 (12.5)	0.081	0 (0)	1 (3.1)	0.333
Joint pain	0 (4)	4 (12.5)	0.012	0 (0)	0 (0)	1.000

TO, TACE only; TA, TACE combined with anlotinib; TACE, transarterial chemoembolization; AEs, adverse events; PLT, platelet count.

(58.8%) (38), demonstrating that subsequent therapy after progression could be performed more frequently in patients treated with anlotinib plus TACE. There were two possible explanations. First, anlotinib combined with TACE provided superior efficacy. Second, anlotinib proved to be less toxic compared to sorafenib, both of which resulted in better patient compliance.

Compared to TACE monotherapy, there was no doubt that more AEs were observed in the combination group. However, compared with TACE combined with sorafenib, these toxicities were mild to moderate and acceptable (39), and no patient discontinued therapy due to the safety profile.

There were several limitations in our study. First, anlotinib has not been approved for HCC yet, but anlotinib combined with penpulimab has been approved in China (40). With more and more clinical studies, anlotinib will be approved for HCC soon or later. Second, respective studies with relatively small samples resulted in various biases affecting survival outcomes. Further validation of these results by multicenter prospective randomized clinical trials is required.

In conclusion, our study first demonstrated that combination therapy with anlotinib and TACE showed significantly better efficacy in terms of long-term survival and tumor response for uHCC patients associated with HBV infection compared to TACE monotherapy, and prospective randomized controlled trials for validation are further needed.

Data availability statement

The raw data supporting the conclusions of this article will be made available by the authors, without undue reservation.

Ethics statement

The studies involving humans were approved by the Ethics Committee of the First Affiliated Hospital of Sun Yat-sen University. The studies were conducted in accordance with the local legislation and institutional requirements. The participants provided their written informed consent to participate in this study.

Author contributions

Conception/design: SC, WZ, and WG. Provision of the study material: SC, HC, WZ, ZW, and WG. Collection of assembly of data: FW, ST, and LC. Data analysis and interpretation: SC and ZW. Manuscript writing or revision: SC and HC. Final manuscript approval: all authors have given their endorsement.

Conflict of interest

The authors declare that the research was conducted in the absence of any commercial or financial relationships that could be construed as a potential conflict of interest.

Publisher's note

Supplementary material

The Supplementary Material for this article can be found online at: https://www.frontiersin.org/articles/10.3389/fonc.2023.1235786/full#supplementary-material

References

1. Sung H, Ferlay J, Siegel RL, Laversanne M, Soerjomataram I, Jemal A, et al. Global cancer statistics 2020: GLOBOCAN estimates of incidence and mortality worldwide for 36 cancers in 185 countries. *CA Cancer J Clin* (2021) 71(3):209–49. doi: 10.3322/caac.21660

2. Forner A, Reig M, Bruix J. Hepatocellular carcinoma. *Lancet* (2018) 391 (10127):1301–14. doi: 10.1016/S0140-6736(18)30010-2

3. Llovet JM, Kelley RK, Villanueva A, Singal AG, Pikarsky E, Roayaie S, et al. Hepatocellular carcinoma. *Nat Rev Dis Primers* (2021) 7(1):6. doi: 10.1038/s41572-020-00240-3

4. Reig M, Forner A, Rimola J, Ferrer-Fabrega J, Burrel M, Garcia-Criado A, et al. BCLC strategy for prognosis prediction and treatment recommendation: The 2022 update. *J Hepatol* (2022) 76(3):681–93. doi: 10.1016/j.jhep.2021.11.018

5. European Association for the Study of the Liver. Electronic address eee, European Association for the Study of the L: EASL Clinical Practice Guidelines: Management of hepatocellular carcinoma. *J Hepatol* (2018) 69(1):182–236. doi: 10.1016/j.jhep.2018.03.019

6. Heimbach JK, Kulik LM, Finn RS, Sirlin CB, Abecassis MM, Roberts LR, et al. AASLD guidelines for the treatment of hepatocellular carcinoma. *Hepatology* (2018) 67 (1):358–80. doi: 10.1002/hep.29086

7. Korean Liver Cancer Study G and National Cancer Center K. 2014 Korean Liver Cancer Study Group-National Cancer Center Korea practice guideline for the management of hepatocellular carcinoma. *Korean J Radiol* (2015) 16(3):465–522. doi: 10.3348/kjr.2015.16.3.465

8. Kudo M, Matsui O, Izumi N, Iijima H, Kadoya M, Imai Y, et al. JSH consensus-based clinical practice guidelines for the management of hepatocellular carcinoma: 2014 update by the liver cancer study group of Japan. *Liver Cancer* (2014) 3(3-4):458–68. doi: 10.1159/000343875

9. Administration NHCotPsRoCM. Consensus statement guidelines for diagnosis and treatment of primary liver cancer in China (2022 edition). *Chin J Clin Hepatol* (2022) 38(02):288–303.

10. Lencioni R, de Baere T, Soulen MC, Rilling WS, Geschwind JF. Lipiodol transarterial chemoembolization for hepatocellular carcinoma: A systematic review of efficacy and safety data. *Hepatology* (2016) 64(1):106–16. doi: 10.1002/hep.28453

11. Lu J, Zhao M, Arai Y, Zhong BY, Zhu HD, Qi XL, et al. Clinical practice of transarterial chemoembolization for hepatocellular carcinoma: consensus statement from an international expert panel of International Society of Multidisciplinary Interventional Oncology (ISMIO). *Hepatobiliary Surg Nutr* (2021) 10(5):661–71. doi: 10.21037/hbsn-21-260

12. Kudo M, Imanaka K, Chida N, Nakachi K, Tak WY, Takayama T, et al. Phase III study of sorafenib after transarterial chemoembolisation in Japanese and Korean patients with unresectable hepatocellular carcinoma. *Eur J Cancer* (2011) 47 (14):2117–27. doi: 10.1016/j.ejca.2011.05.007

13. Lencioni R, Llovet JM, Han G, Tak WY, Yang J, Guglielmi A, et al. Sorafenib or placebo plus TACE with doxorubicin-eluting beads for intermediate stage HCC: The SPACE trial. *J Hepatol* (2016) 64(5):1090–8. doi: 10.1016/j.jhep.2016.01.012

14. Kudo M, Ueshima K, Ikeda M, Torimura T, Tanabe N, Aikata H, et al. Randomised, multicentre prospective trial of transarterial chemoembolisation (TACE) plus sorafenib as compared with TACE alone in patients with hepatocellular carcinoma: TACTICS trial. *Gut* (2020) 69(8):1492–501. doi: 10.1136/gutjnl-2019-318934

15. Fu Z, Li X, Zhong J, Chen X, Cao K, Ding N, et al. Lenvatinib in combination with transarterial chemoembolization for treatment of unresectable hepatocellular carcinoma (uHCC): a retrospective controlled study. *Hepatol Int* (2021) 15(3):663–75. doi: 10.1007/s12072-021-10184-9

16. Cao Y, Ouyang T, Xiong F, Kan X, Chen L, Liang B, et al. Efficacy of apatinib in patients with sorafenib–transarterial chemoembolization refractory hepatocellular carcinoma: a retrospective study. *Hepatol Int* (2021) 15(5):1268–77. doi: 10.1007/s12072-021-10198-3

17. Shen G, Zheng F, Ren D, Du F, Dong Q, Wang Z, et al. Anlotinib: a novel multi-targeting tyrosine kinase inhibitor in clinical development. *J Hematol Oncol* (2018) 11 (1):120. doi: 10.1186/s13045-018-0664-7

18. Su Y, Luo B, Lu Y, Wang D, Yan J, Zheng J, et al. Anlotinib induces a T cell-inflamed tumor microenvironment by facilitating vessel normalization and enhances the efficacy of PD-1 checkpoint blockade in neuroblastoma. *Clin Cancer Res* (2022) 28 (4):793–809. doi: 10.1158/1078-0432.CCR-21-2241

19. Xu Q, Wang J, Sun Y, Lin Y, Liu J, Zhuo Y, et al. Efficacy and safety of sintilimab plus anlotinib for PD-L1-positive recurrent or metastatic cervical cancer: a multicenter, single-arm, prospective phase II trial. *J Clin Oncol* (2022) 40(16):1795–805. doi: 10.1200/JCO.21.02091

20. Guo W, Chen S, Wu Z, Zhuang W, Yang J. Efficacy and safety of transarterial chemoembolization combined with anlotinib for unresectable hepatocellular carcinoma: a retrospective study. *Technol Cancer Res Treat* (2020) 19:1533033820965587. doi: 10.1177/1533033820965587

21. Chen XQ, Zhao YX, Zhang CL, Wang XT, Zhang X, Chen X, et al. Effectiveness and safety of anlotinib with or without PD-1 blockades in the treatment of patients with advanced primary hepatocellular carcinoma: a retrospective, real-world study in China. *Drug Des Devel Ther* (2022) 16:1483–93. doi: 10.2147/DDDT.S358092

22. Fallone CA, Moss SF, Malfertheiner P. Helicobacter pylori infection. *New Engl J Med* (2019) 381(6):587–9. doi: 10.1056/NEJMc1905439

23. Yang JD, Hainaut P, Gores GJ, Amadou A, Plymoth A, Roberts LR. A global view of hepatocellular carcinoma: trends, risk, prevention and management. *Nat Rev Gastroenterol Hepatol* (2019) 16(10):589–604. doi: 10.1038/s41575-019-0186-y

24. Lewandowski RJ, Wang D, Gehl J, Atassi B, Ryu RK, Sato K, et al. A comparison of chemoembolization endpoints using angiographic versus transcatheter intraarterial perfusion/MR imaging monitoring. *J Vasc Interv Radiol* (2007) 18(10):1249–57. doi: 10.1016/j.jvir.2007.06.028

25. Kudo M, Finn RS, Qin S, Han KH, Ikeda K, Piscaglia F, et al. Lenvatinib versus sorafenib in first-line treatment of patients with unresectable hepatocellular carcinoma: a randomised phase 3 non-inferiority trial. *Lancet* (2018) 391(10126):1163–73. doi: 10.1016/S0140-6736(18)30207-1

26. Park JW, Chen M, Colombo M, Roberts LR, Schwartz M, Chen PJ, et al. Global patterns of hepatocellular carcinoma management from diagnosis to death: the BRIDGE Study. *Liver Int* (2015) 35(9):2155–66. doi: 10.1111/liv.12818

27. Golfieri R, Giampalma E, Renzulli M, Cioni R, Bargellini I, Bartolozzi C, et al. Randomised controlled trial of doxorubicin-eluting beads vs conventional chemoembolisation for hepatocellular carcinoma. *Br J Cancer* (2014) 111(2):255–64. doi: 10.1038/bjc.2014.199

28. Salem R, Gordon AC, Mouli S, Hickey R, Kallini J, Gabr A, et al. Y90 radioembolization significantly prolongs time to progression compared with chemoembolization in patients with hepatocellular carcinoma. *Gastroenterology* (2016) 151(6):1155–1163.e1152. doi: 10.1053/j.gastro.2016.08.029

29. Hu J, Bao Q, Cao G, Zhu X, Yang R, Ji X, et al. Hepatic arterial infusion chemotherapy using oxaliplatin plus 5-fluorouracil versus transarterial chemoembolization/embolization for the treatment of advanced hepatocellular carcinoma with major portal vein tumor thrombosis. *Cardiovasc Intervent Radiol* (2020) 43(7):996–1005. doi: 10.1007/s00270-019-02406-3

30. Li S, Lyu N, Han X, Li J, Lai J, He M, et al. Hepatic artery infusion chemotherapy using fluorouracil, leucovorin, and oxaliplatin versus transarterial chemoembolization as initial treatment for locally advanced hepatocellular carcinoma: a propensity score-matching analysis. *J Vasc Interv Radiol* (2021) 32(9):1267–1276 e1261. doi: 10.1016/j.jvir.2021.06.008

31. Peng Z, Fan W, Zhu B, Wang G, Sun J, Xiao C, et al. Lenvatinib combined with transarterial chemoembolization as first-line treatment for advanced hepatocellular carcinoma: a phase III, randomized clinical trial (LAUNCH). *J Clin Oncol* (2023) 41 (1):117–27. doi: 10.1200/JCO.22.00392

32. Zhong B-Y, Yan Z-P, Sun J-H, Zhang L, Hou Z-H, Yang M-J, et al. Prognostic performance of albumin–bilirubin grade with artificial intelligence for hepatocellular carcinoma treated with transarterial chemoembolization combined with sorafenib. *Front Oncol* (2020) 10. doi: 10.3389/fonc.2020.525461

33. Sieghart W, Hucke F, Peck-Radosavljevic M. Transarterial chemoembolization: Modalities, indication, and patient selection. *J Hepatol* (2015) 62(5):1187–95. doi: 10.1016/j.jhep.2015.02.010

34. Zhong B-Y, Jin Z-C, Chen J-J, Zhu H-D, Zhu X-L. Role of transarterial chemoembolization in the treatment of hepatocellular carcinoma. *J Clin Trans Hepatol* (2022) 000(000):000–0. doi: 10.14218/JCTH.2022.00293

35. He M-K, Liang R-B, Zhao Y, Xu Y-J, Chen H-W, Zhou Y-M, et al. Lenvatinib, toripalimab, plus hepatic arterial infusion chemotherapyversuslenvatinib alone for advanced hepatocellular carcinoma. *Ther Adv Med Oncol* (2021) 13:17588359211002720. doi: 10.1177/17588359211002720

36. Fu Y, Peng W, Zhang W, Yang Z, Hu Z, Pang Y, et al. Induction therapy with hepatic arterial infusion chemotherapy enhances the efficacy of lenvatinib and pd1 inhibitors in treating hepatocellular carcinoma patients with portal vein tumor thrombosis. *J Gastroenterol* (2023) 58(4):413–24. doi: 10.1007/s00535-023-01976-x

37. Zhu HD, Li HL, Huang MS, Yang WZ, Yin GW, Zhong BY, et al. Transarterial chemoembolization with PD-(L)1 inhibitors plus molecular targeted therapies for hepatocellular carcinoma (CHANCE001). *Signal Transduct Target Ther* (2023) 8(1):58. doi: 10.1038/s41392-022-01235-0

38. Kudo M, Ueshima K, Ikeda M, Torimura T, Tanabe N, Aikata H, et al. Final results of TACTICS: A randomized, prospective trial comparing transarterial chemoembolization plus sorafenib to transarterial chemoembolization alone in patients with unresectable hepatocellular carcinoma. *Liver Cancer* (2022) 11(4):354–67. doi: 10.1159/000522547

39. Peng Z, Chen S, Xiao H, Wang Y, Li J, Mei J, et al. Microvascular invasion as a predictor of response to treatment with sorafenib and transarterial chemoembolization for recurrent intermediate-stage hepatocellular carcinoma. *Radiology* (2019) 292 (1):237–47. doi: 10.1148/radiol.2019181818

40. Han C, Ye S, Hu C, Shen L, Qin Q, Bai Y, et al. Clinical activity and safety of penpulimab (Anti-PD-1) with anlotinib as first-line therapy for unresectable hepatocellular carcinoma: an open-label, multicenter, phase ib/II trial (AK105-203). *Front Oncol* (2021) 11:684867. doi: 10.3389/fonc.2021.684867

frontiers | Frontiers in Oncology

TYPE Case Report
PUBLISHED 15 December 2023
DOI 10.3389/fonc.2023.1328886

OPEN ACCESS

EDITED BY
Francisco Tustumi,
University of São Paulo, Brazil

REVIEWED BY
Ricardo Yugi Eri,
Faculdade Israelita de Ciências da Saúde Albert Einstein Hospital Israelita Albert Einstein, Brazil
Alfonso Recordare,
Ospedale dell'Angelo, Italy

*CORRESPONDENCE
Xuelin Zhao
zhaoxuelin321@126.com

RECEIVED 27 October 2023
ACCEPTED 04 December 2023
PUBLISHED 15 December 2023

CITATION
Ai H, Gong T, Ma Y, Ma G, Zhao J and Zhao X (2023) Primary hepatic adenosquamous carcinoma: a case report and review of the literature.
Front. Oncol. 13:1328886.
doi: 10.3389/fonc.2023.1328886

Primary hepatic adenosquamous carcinoma: a case report and review of the literature

Haidong Ai[1], Ting Gong[2], Yongbiao Ma[1], Guixu Ma[1], Jingjing Zhao[1] and Xuelin Zhao[1]*

[1]Hepatobiliary and Pancreatic Medical Center, The First Affiliated Hospital of Weifang Medical College (Weifang People's Hospital), Weifang, China, [2]Department of Ophthalmology, The First Affiliated Hospital of Weifang Medical College (Weifang People's Hospital), Weifang, China

Primary hepatic adenosquamous carcinoma is considered a rare subtype of intrahepatic cholangiocarcinoma, with fewer than 100 domestic and international cases reported. This malignancy exhibits a high degree of malignancy, strong invasiveness, and an unfavorable prognosis due to its propensity for early lymph node and intrahepatic metastasis. The etiology of this disease remains uncertain, and preoperative diagnosis is exceedingly challenging owing to the nonspecific clinical features and lack of specificity in imaging studies. Radical surgical resection is the most effective treatment for non-metastatic tumors, while targeted adjuvant therapy administered postoperatively can enhance therapeutic efficacy and delay tumor recurrence. This article documents the diagnostic and therapeutic course of a case of primary hepatic adenosquamous carcinoma treated at our medical institution, along with a comprehensive synthesis of the clinical characteristics and advances in the diagnosis and treatment of this disease, aiming to augment understanding and serve as a reference for future clinical endeavors.

KEYWORDS

primary adenosquamous carcinoma, hepatic tumor, radical surgical resection, adjuvant chemotherapy, immunohistochemistry, case report

Introduction

Primary hepatic adenosquamous carcinoma (ASC) refers to a malignant liver tumor that simultaneously contains components of both adenocarcinoma (AC) and squamous cell carcinoma (SCC). It exhibits high invasiveness and poor prognosis, with an average survival time of less than 1 year. The 5th edition of the WHO classification

of digestive system tumors categorizes ASC as a subtype of intrahepatic cholangiocarcinoma (ICC), which is clinically rare, accounting for only 2%-3% of all ICC cases. To date, there have been fewer than 100 reported cases worldwide (1, 2). Currently, there is no multicenter study with a large sample size or standardized guidelines for the diagnosis and treatment of this disease. This article aims to present a case report on the diagnosis and management process of primary hepatic ASC, along with a summary of the latest research progress both domestically and internationally, in order to enhance our understanding and experience in treating this condition. The following is a detailed account of the case.

Case presentation

A 48-year-old male presented at The First Affiliated Hospital of Weifang Medical College on July 22, 2019, with a complaint of "persistent upper abdominal pain for over one month" He has a history of good physical health, with no known psychological disorders or family history of hereditary diseases. No relevant treatment was administered before admission. Laboratory results revealed the following: alanine aminotransferase (ALT) level (107 U/L, normal range 0-50 U/L), aspartate aminotransferase (AST) level (50 U/L, normal range 0-40 U/L), total bilirubin (TBIL) level (12 umol/L, normal range 0-23 umol/L), alkaline phosphatase (ALP) level (550 U/L, normal range 45-125 U/L), gamma-glutamyltransferase (GGT) level (364 U/L, normal range 4-60 U/L), and carbohydrate antigen 19-9 (CA19-9) level (1839.13 U/L, normal range 0-37 U/L). Other laboratory tests showed no significant abnormalities. Following admission, an abdominal enhanced magnetic resonance imaging (MRI) indicated a mass in the left lobe of the liver, intrahepatic bile duct dilation, and enlarged surrounding lymph nodes (Figures 1A–D). Based on our preoperative assessment, we diagnosed the patient with a primary malignant liver tumor, where intrahepatic cholangiocarcinoma (ICC) appears to be the most likely possibility, although other rare types of malignant liver tumors cannot be ruled out. Preoperative imaging studies indicated the lesion appears in a very close relationship with the right anterior pedicle, and enlarged regional lymph nodes. The tumor exhibits a high degree of invasiveness, making curative surgery challenging and carrying a heightened risk of recurrence. The patient and their family have been adequately informed of the surgical risks, including the potential inability to achieve an R0 resection, as well as the possibility and necessity of postoperative adjuvant chemotherapy, to which the family has expressed understanding and consent to the proposed treatment plan.

The patient underwent left hemihepatectomy, cholecystectomy, and hepatic pedicle lymph node dissection. The operative procedure was as follows: Intraoperative exploration revealed a tumor located in the left half of the liver, compressing the first hepatic hilum. Multiple enlarged lymph nodes were observed in the hepatic pedicle region, with tumor invasion into the cystic duct and adjacent right anterior hepatic duct. Careful dissection of adhesions between the tumor and the right anterior hepatic pedicle was performed while preserving the right anterior hepatic duct. The hepatic hilum was dissected, and a skeletonized lymph node dissection was performed on the hepatic pedicle. The left hepatic artery and left branch of the portal vein were ligated and divided, ensuring complete removal of the tumor and left half of the liver. The surgery lasted for 3.5 hours, with an estimated intraoperative blood loss of approximately 100ml (Figure 2). Postoperative pathological examination revealed the tumor involving the capsule, vascular and neural invasion. The cut surface of the liver was clean, showing no residual tumor tissue. Lymph node metastasis was observed in the hepatic pedicle lymph nodes. Microscopic examination (Figures 3A–F) revealed tumor cells exhibiting both nest-like and glandular structures. Based on the results of immunohistochemistry, the diagnosis was determined to be primary hepatic ASC (with approximately 40% being moderately differentiated AC and 60% being poorly differentiated SCC). Immunohistochemical staining showed that CK7 (+), CK19(+), CK20(+), P40 partial (+), and the Ki-67 proliferation index of 70%.

Preoperatively, we ruled out esophageal cancer, nasopharyngeal cancer, lung cancer, and gastric cancer, which are common sites for SCC. Combining the pathological findings, the definitive diagnosis was primary hepatic ASC. The patient, despite undergoing curative surgical resection, considering the high malignancy of hepatic ASC and its strong invasiveness, postoperative pathology indicated lymph node metastasis at the hepatic hilum. The efficacy of the sole surgical treatment was suboptimal. After the procedure, comprehensive discussions with the patient and their family were held regarding the disease, recommending postoperative systemic chemotherapy or hepatic arterial infusion chemotherapy (HAIC), with the possibility of adjunctive radiotherapy, and duly informing them of potential adverse reactions associated with these treatments. Regrettably, the patient declined any adjunctive therapy postoperatively. On the 5th day post-surgery, an abdominal CT scan revealed no significant peritoneal or perihepatic fluid accumulation (Figure 1E). AST and TBIL gradually returned to normal levels, while serum CA19-9 significantly decreased (Figure 4). After 10 days, the patient was discharged smoothly. Three months later, the patient presented with jaundice accompanied by intermittent abdominal pain, poor appetite, nausea, and vomiting. Subsequent abdominal enhanced MRI indicated a mass in the porta hepatis region, along with multiple enlarged lymph nodes around the liver, in the abdominal cavity, and retroperitoneally, suggesting recurrence (Figures 1F, G). Laboratory tests revealed ALT level 175 U/L, TBIL level 146 umol/L, CA19-9 level 357 U/L (Figure 4). The tumor compressed the biliary duct at the porta hepatis, causing obstructive jaundice, and also exerted pressure on the duodenum, resulting in upper gastrointestinal obstruction. Percutaneous transhepatic cholangial drainage was performed under ultrasound guidance to relieve the biliary obstruction and alleviate jaundice. Nasojejunal catheterization was done via endoscopy to support enteral nutrition (Figure 1H). Upon alleviation of jaundice and improvement in liver function, the patient declined further adjuvant therapies such as chemotherapy and voluntarily requested discharge. Subsequently, through telephone follow-up, we learned that the patient succumbed to severe malnutrition and multi-organ failure six months postoperatively.

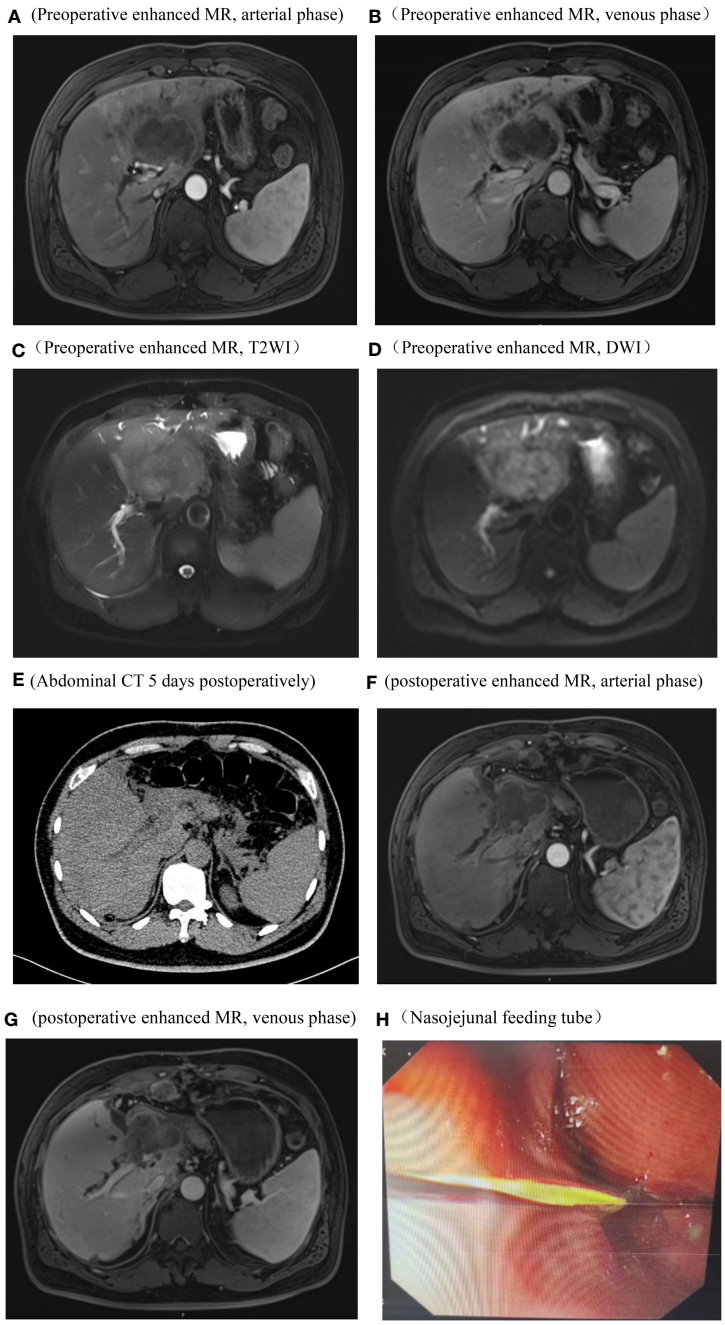

FIGURE 1
Imaging and endoscopic pictures. Preoperative abdominal enhanced MR, arterial phase, The tumor does not exhibit significant enhancement and shows lower signal intensity compared to the surrounding hepatic parenchyma **(A)** Preoperative abdominal enhanced MR, venous phase, the tumor periphery exhibits mild enhancement, while the central region demonstrates significantly lower signal intensity compared to the surrounding hepatic parenchyma **(B)** Preoperative abdominal enhanced MR, T2WI, the tumor demonstrates a long T2 signal, with signal intensity higher than the surrounding hepatic parenchyma **(C)** Preoperative abdominal enhanced MR, DWI, the tumor exhibits restricted diffusion **(D)** Abdominal CT on the 5th day postoperative, no significant fluid accumulation observed in the hepatic periphery or intra-abdominal cavity **(E)** Abdominal enhanced MR in the arterial phase and venous phases, 3 months postoperatively, Imaging reveals an irregular soft tissue mass in the hepatic hilum area following left hepatectomy. Enhanced scanning shows mild, uneven enhancement. Blurring is observed in the hepatic periphery, peritoneum, and abdominal fat interspace, with multiple nodules displaying heterogeneous enhancement within **(F, G)** Endoscopic placement of a nasojejunal nutritional tube **(H)**.

Discussion

ASC is a malignant tumor that comprises both AC and SCC components. It can occur in various organs throughout the body. Primary hepatic ASC, considered a subtype of ICC, is an extremely rare clinical occurrence, accounting for approximately 2%-3% of ICC cases (1, 2). Since its first description as hepatic ASC by Barr et al. (3) in 1975, there have been fewer than 100 reported cases documented internationally. Early diagnosis of primary hepatic ASC presents challenges, with most cases confirmed through

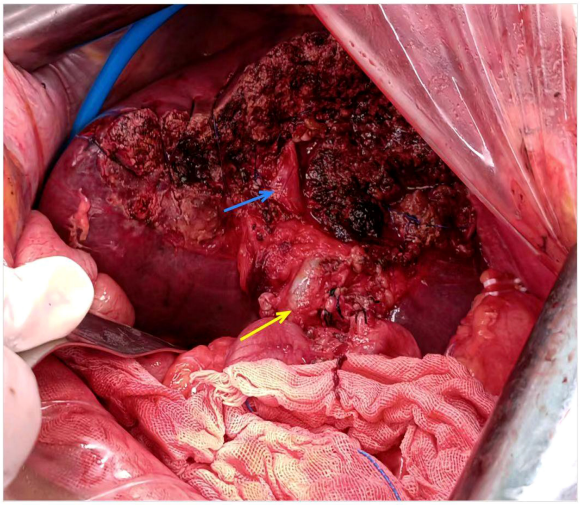

FIGURE 2
Intraoperative pictures. The blue arrow designates right anterior branch of the portal vein, the yellow arrow denotes common bile duct.

postoperative pathological examination. Patients are often diagnosed at an advanced stage, making it a more aggressive and prognostically unfavorable malignancy compared to ICC (4).

The pathogenesis of primary hepatic ASC remains unclear. Most scholars suggest that it arises from the squamous metaplasia of normal bile duct cells under prolonged stimulation from chronic inflammation or viral infection, leading to malignant transformation and concurrent AC components, ultimately culminating in ASC (5, 6). In this case, the patient did not exhibit pathogenic factors such as bile duct cysts or intrahepatic bile duct stones associated with chronic inflammation, nor did they have viral hepatitis. For patients like this, it is conceivable that genetic mutations may trigger the transformation of hepatic multipotent stem cells into SCC. Further research is necessary to elucidate the underlying mechanisms of primary hepatic ASC.

Primary hepatic ASC commonly occurs in elderly patients. Most individuals present with fever, jaundice, abdominal pain, anorexia, and weight loss. Typically, there is no history of hepatitis or liver cirrhosis (7, 8). Laboratory examinations may reveal varying degrees of elevation in serum carcinoembryonic antigen (CEA) and CA19-9, while alpha-fetoprotein (AFP) levels are usually within the normal range. This characteristic is similar to ICC (9). In some cases, there may be an increase in SCC-associated antigens (4, 10–13). Due to the infrequent utilization of tumor marker tests associated with AC in patients with hepatic tumors, coupled with the low incidence rate of primary hepatic ASC, clinicians often lack awareness regarding this particular ailment. Consequently, it becomes arduous to associate this condition with its occurrence during the initial diagnosis.

Primary hepatic ASC lacks highly distinctive radiological features. In CT scans, it may manifest as an indistinct-bordered mass, occasionally accompanied by central necrosis and intrahepatic bile duct stones. Enhanced scans reveal insignificant tumor enhancement. In MRI scans, most tumors exhibit low signal intensity on T1-weighted imaging (T1WI) and high signal intensity on T2-weighted imaging (T2WI). Some cases may demonstrate high signal intensity on T1WI, possibly associated with cystic structures and central necrosis. The tumor's diffusion is restricted, and enhanced scans show minimal tumor enhancement (14–16). In this case, the patient had normal AFP and CEA levels but a significant elevation in CA19-9. MRI showed a single tumor with irregular borders and a low signal-intensity necrotic area in the center. The contrast-enhanced scan indicated no significant enhancement, which aligns with the typical radiological features of primary hepatic ASC. However, careful differentiation from liver abscesses and ICC is necessary since these entities have been reported to be commonly mistaken and misdiagnosed as primary hepatic ASC preoperatively. PET-CT can further delineate the benign or malignant nature of the tumor and exclude systemic metastatic diseases. However, according to the literature we reviewed, ASC does not exhibit specific features on PET-CT scans. For patients highly suspected of hepatic ASC preoperatively, consideration can be given to performing a pathological biopsy to confirm the diagnosis and formulate a more scientifically rational treatment plan for the patient. Given the extreme rarity and lack of specific clinical manifestations of ASC, conventional preoperative pathological biopsy for such patients may pose certain difficulties. Therefore, preoperative diagnosis of primary hepatic ASC is extremely challenging, and in the vast majority of cases, confirmation relies on postoperative pathology and immunohistochemistry results.

Histologically, ASC comprises two cellular components: AC and SCC. AC is characterized by the formation of glands of various sizes containing intracellular and extracellular mucins. SCC, on the other hand, exhibits regular tumor cell morphology with clear boundaries, nest-like distribution, eosinophilic cytoplasm, and varying degrees of keratin pearls and intercellular bridges (17, 18). According to the prevailing diagnostic criteria established by the WHO, ASC can be definitively diagnosed when both AC and SCC components exceed 10%. In this case, well-differentiated AC

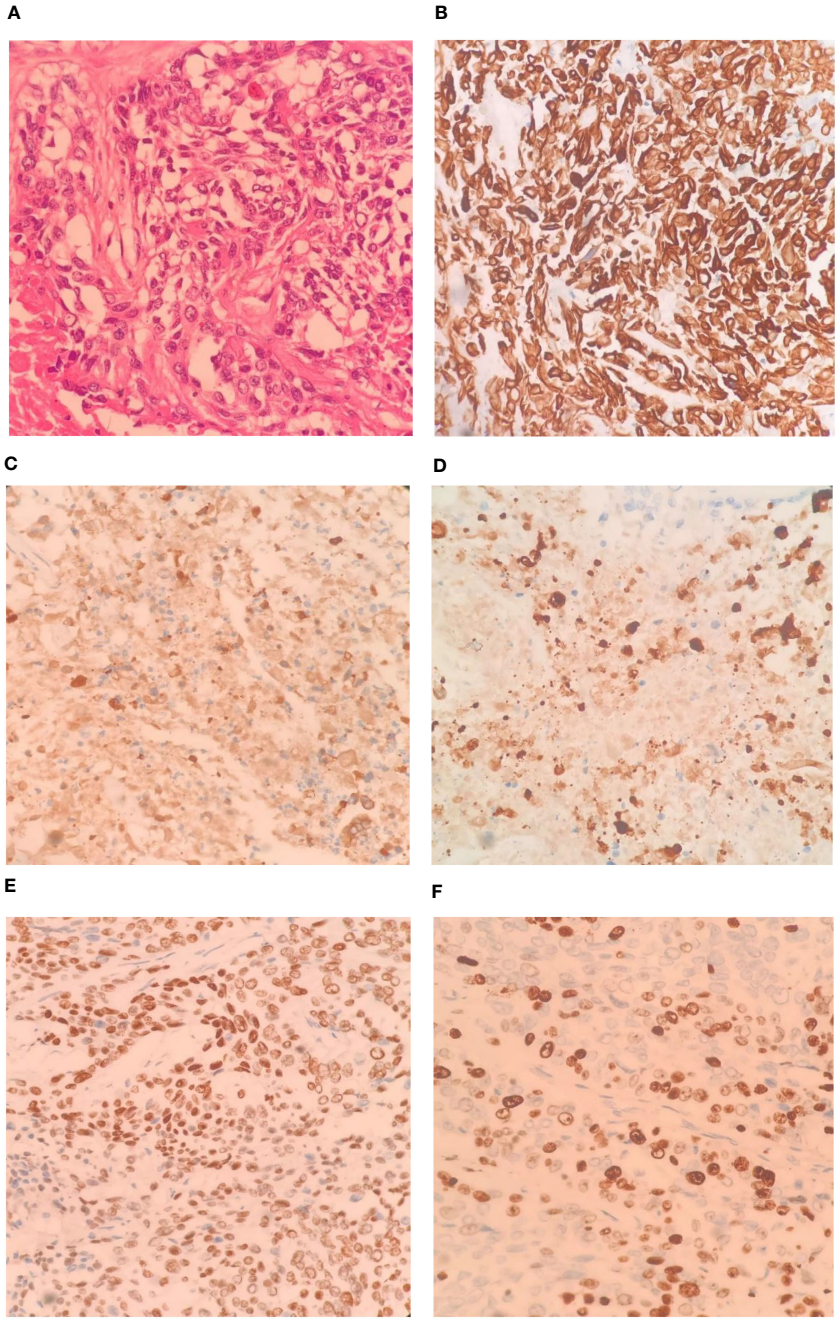

FIGURE 3
Pathological images and immunohistochemistry staining were conducted as follows: Tumor tissue sections stained (HE ×400), The tumor cells exhibit a pattern of solid nests, glandular formations, and reticular arrangements. Some of the nest formations show central keratinization. The cells possess abundant cytoplasm, large and deeply stained nuclei, and notable cellular atypia (**A**, ×400); CK-7 immunohistochemical staining exhibited diffuse positivity (**B**, ×400); CK-19 immunohistochemical staining exhibited diffuse positivity (**C**, ×400); CK-20 immunohistochemical staining displayed diffuse positivity (**D**, ×400); P40 immunohistochemical staining showed partial positivity (**E**, ×400); Ki-67 positive index is approximately 70%. (**F**, ×400).

accounts for approximately 40% while poorly differentiated SCC accounts for approximately 60%, meeting the diagnostic criteria for primary hepatic ASC. Immunohistochemically, different types of cytokeratins (CKs) are expressed in hepatocytes and biliary epithelial cells. In immunohistochemical staining of hepatocellular carcinoma (HCC), CK20 typically shows positive reactivity, while CK7 and CK19 show negative reactivity. However, in ICC, CK20 is mostly negative, while CK7 and CK19 are positive. As primary hepatic ASC represents a subtype of ICC, its immunohistochemical profile generally aligns with the characteristics of ICC: CK20(-), CK7(+), CK19(+), and the presence of SCC-associated tumor markers p63/p40(+) can further aid in the accurate diagnosis (9). The postoperative pathological and immunohistochemical results in this case largely conform to the aforementioned characteristics.

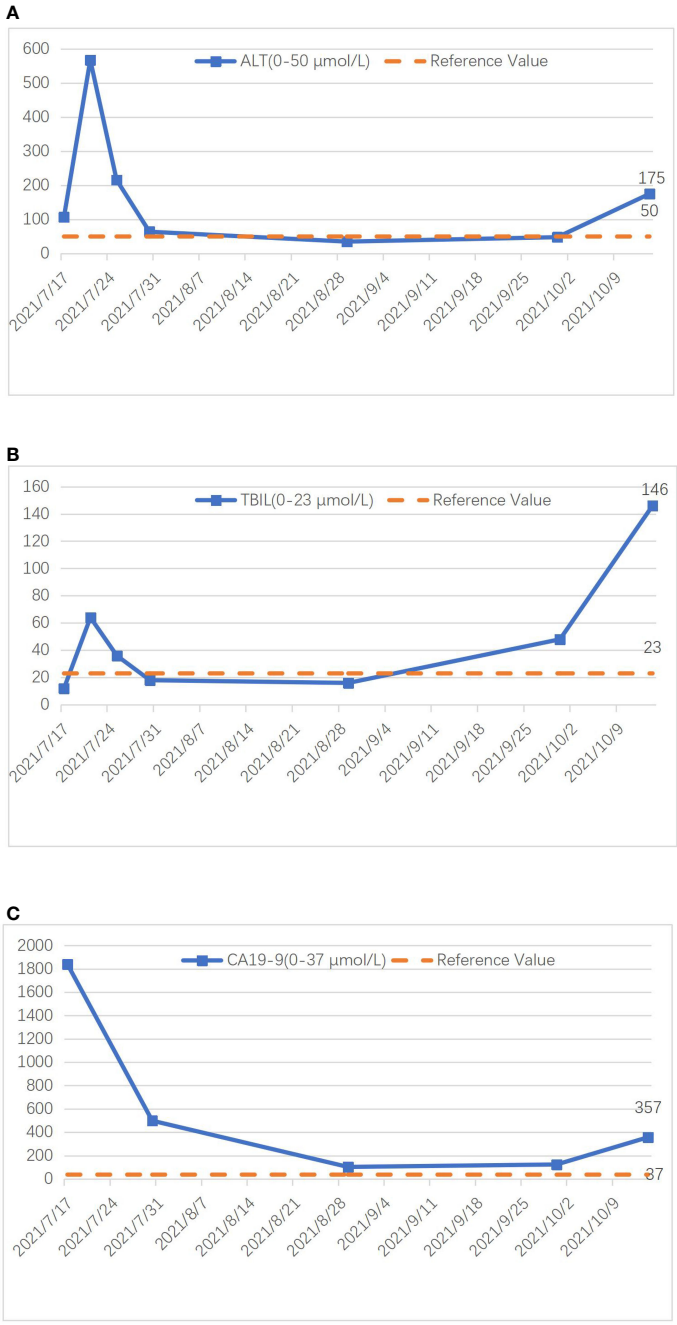

FIGURE 4
Graph illustrating the changing trends of ALT **(A)**, TBIL **(B)**, and CA19-9 **(C)** during treatment.

Curative surgical resection stands as the primary therapeutic modality for non-metastatic primary hepatic ASC. The surgical approach follows the treatment principles of ICC, encompassing the excision of the affected liver lobe coupled with clearance of the hepatic hilum lymph nodes. The specific surgical technique and extent of lymph node clearance are determined based on lesion location, local vascular, biliary, lymphatic infiltration, and dissemination. Performing curative resection according to tumor location, along with thorough clearance of the hepatic hilum lymph nodes, can maximize patient prognosis. We believe that an anatomical liver lobectomy, with a margin width exceeding 1cm, and comprehensive clearance of the hepatic hilum lymph nodes can confer substantial benefits to patients by prolonging tumor recurrence and improving overall prognosis.

Primary hepatic ASC exhibits a poor prognosis. Takahashi et al. (19) employed DNA ploidy quantitative analysis techniques, indicating that the SCC component demonstrates a more malignant biological behavior closely associated with rapid tumor growth and invasive clinical characteristics. Hence, there is reason to believe that a higher proportion of SCC component corresponds to increased malignancy. Based on previous case reports, the average survival time for such cases falls short of 1 year. While curative

surgical resection stands as the foremost therapeutic approach for non-metastatic primary hepatic ASC, even in most cases where curative resection is performed, there is still a propensity for early tumor recurrence, lymph node metastasis, and even distant metastasis. Solely relying on surgical intervention yields a less optimistic prognosis (16, 20). Research has shown that patients with primary hepatic ASC who undergo adjuvant chemotherapy experience longer survival (median survival: 15 months vs. 6 months) (9). Studies conducted by Kang (11) and Demir (21) also indicate a significant extension in survival for patients with primary hepatic ASC who receive adjuvant chemotherapy, with the highest reported survival reaching 8 years. Watanabe et al. (22) summarized treatment and prognosis data for 71 patients with primary hepatic ASC from PubMed. Among the 48 patients who solely underwent surgical treatment, 39 (92.9%) died within 12 months postoperatively. In contrast, Among the 7 patients who received adjuvant chemotherapy after surgery, 5 patients did not experience tumor recurrence during the 8-15 months follow-up period. It is worth mentioning that one patient missed the opportunity for curative surgery at initial diagnosis but underwent surgical resection following systemic chemotherapy with tegafur/gimeracil/oteracil (S-1) and transcatheter hepatic arterial injection (TAI) of cisplatin. The patient then received adjuvant cisplatin chemotherapy for 6 months, resulting in a favorable prognosis with no tumor recurrence during the 6-month follow-up period. These studies collectively affirm the effectiveness of adjuvant chemotherapy. Watanabe's research (22) suggests that combination therapy with systemic chemotherapy and hepatic arterial infusion cisplatin demonstrates favorable efficacy for unresectable primary hepatic ASC patients, and may even create opportunities for curative resection. This indirectly confirms the efficacy of HAIC treatment. The aim of using HAIC is to locally deliver higher concentrations of chemotherapeutic agents and alleviate systemic toxicity. We believe that HAIC treatment can be considered for patients with significant local tumor invasion, high-risk recurrence postoperatively, and those unable to tolerate systemic chemotherapy. Referring to the chemotherapy regimen of ICC, the combination of gemcitabine and cisplatin is considered the most effective first-line treatment (23), which may also yield good results for hepatic ASC patients. Consequently, comprehensive treatment based on surgery has gradually emerged as a novel direction in recent research. In the future, the combined treatment approach of surgery with adjuvant chemotherapy holds the potential to become the optimal choice for treating primary hepatic ASC. Moreover, the conversion therapy model, chemotherapy-surgery-postoperative chemotherapy, may also offer a glimmer of hope for survival among advanced-stage patients who have missed the opportunity for surgical intervention.

In this case, the patient declined any adjuvant therapy postoperatively, including chemotherapy and radiotherapy. The prognosis was poor, with tumor recurrence occurring only 3 months after surgery, accompanied by intrahepatic and intra-abdominal lymph node metastasis. The patient passed away 6 months after the surgery, greatly deviating from our expectations and serving as a profound reminder of the postoperative significance of adjuvant chemotherapy. Perhaps mere surgical treatment cannot achieve satisfactory efficacy for hepatic ASC with lymph node metastasis. Active cooperation with adjuvant chemotherapy postoperatively is essential to further improve the prognosis of such patients. The patient's refusal of further adjuvant chemotherapy postoperatively delayed the optimal treatment window, resulting in an unsatisfactory prognosis, which we deeply regret. This is a limitation in our case and calls for the reflection of experiences and lessons learned from this treatment process. We cannot predict whether neoadjuvant chemotherapy would yield better therapeutic effects preoperatively, as it is a relatively unfamiliar field in the treatment of hepatic ASC. Additionally, not every patient is highly sensitive to chemotherapy, and disease progression could lead to the loss of the opportunity for curative surgery. For patients with the opportunity for R0 resection, we recommend early surgical intervention combined with adjuvant chemotherapy as the optimal treatment choice for such cases.

For advanced primary hepatic ASC patients who have lost the opportunity for surgery and those who experience postoperative recurrence, ongoing attempts are being made to explore the efficacy of molecular targeted therapy and immunotherapy. In recent years, targeted drugs and immunotherapy have shown good efficacy in patients with advanced ICC (24). As a clinical subtype of ICC, hepatic ASC shares many similarities with ICC. We have reason to believe that with in-depth research on the molecular mechanisms, gene sequencing technology, and therapeutic targets of ASC, molecular targeted therapy and immunotherapy may become breakthroughs in the future treatment of ASC. In the case of poor prognosis in advanced-stage hepatic ASC patients, further exploration is warranted regarding the utilization of local treatment, targeted therapy, immunotherapy, and their combination. Additionally, considering the higher sensitivity of the SCC component compared to AC towards radiation therapy, which has shown good efficacy in treating SCC in other sites, some scholars advocate for implementing radiotherapy in hepatic ASC cases with a higher proportion of SCC. However, due to limited sample size and experience, the effectiveness of these treatment modalities requires further confirmation through additional accumulation of cases. ASC exhibits severe malignant biological behavior, characterized by highly invasive and rapid growth mechanisms that remain unclear. Despite aggressive treatments, overall therapeutic outcomes for most patients remain unsatisfactory, possibly due to tumor heterogeneity and the malignant features of SCC, among other influencing factors. Improving early diagnosis rates would contribute to enhancing patient prognosis.

Conclusion

In light of the aforementioned exposition, primary hepatic ASC is an extremely rare and highly malignant liver tumor. It exhibits rapid disease progression and presents significant challenges in preoperative diagnosis. Most patients are diagnosed at advanced stages, leading to poor prognosis and high mortality rates. We believe that an integrated treatment approach combining surgery with adjuvant chemotherapy can effectively prolong patient survival.

Data availability statement

The original contributions presented in the study are included in the article/supplementary material, further inquiries can be directed to the corresponding author.

Ethics statement

Written informed consent was obtained from the individual(s) for the publication of any potentially identifiable images or data included in this article.

Author contributions

HA: Writing – original draft. TG: Writing – review & editing. YM: Writing – review & editing. GM: Writing – review & editing. JZ: Writing – review & editing. XZ: Writing – review & editing.

Funding

The author(s) declare that no financial support was received for the research, authorship, and/or publication of this article.

Conflict of interest

The authors declare that the research was conducted in the absence of any commercial or financial relationships that could be construed as a potential conflict of interest.

Publisher's note

All claims expressed in this article are solely those of the authors and do not necessarily represent those of their affiliated organizations, or those of the publisher, the editors and the reviewers. Any product that may be evaluated in this article, or claim that may be made by its manufacturer, is not guaranteed or endorsed by the publisher.

References

1. Harino T, Tomimaru Y, Noguchi K, Nagase H, Ogino T, Hirota M, et al. [A rare case of adenosquamous carcinoma in the liver with hepatolithiasis]. *Gan To Kagaku Ryoho* (2019) 46(4):772–4.

2. Nakajima T, Kondo Y. A clinicopathologic study of intrahepatic cholangiocarcinoma containing a component of squamous cell carcinoma. *Cancer* (1990) 65(6):1401–4. doi: 10.1002/1097-0142(19900315)65:6<1401::AID-CNCR2820650626>3.0.CO;2-K

3. Barr RJ, Hancock DE. Adenosquamous carcinoma of the liver. *Gastroenterology* (1975) 69(6):1326–30. doi: 10.1016/S0016-5085(19)32328-5

4. Nam KH, Kim JY. Primary adenosquamous carcinoma of the liver: a case report. *Clin Mol Hepatol* (2016) 22(4):503–8. doi: 10.3350/cmh.2016.0077

5. Gresham GA, Rue LW 3rd. Squamous cell carcinoma of the liver. *Hum Pathol* (1985) 16(4):413–6. doi: 10.1016/S0046-8177(85)80234-3

6. Greenwood N, Orr WM. Primary squamous-cell carcinoma arising in a solitary non-parasitic cyst of the liver. *J Pathol* (1972) 107(2):145–8. doi: 10.1002/path.1711070211

7. Takeda T, Murata K, Ikeda M, Chatani N, Kobayashi M, Aoki Y, et al. [Primary adenosquamous carcinoma of the liver presenting with hematochezia due to tumor invasion of the colon]. *Nihon Shokakibyo Gakkai Zasshi* (2013) 110(11):1959–67.

8. Zhou SY, Qiao ZG, Li CL, Chen TB. Primary adenosquamous carcinoma of the liver. *Kaohsiung J Med Sci* (2020) 36(10):857–8. doi: 10.1002/kjm2.12252

9. Gou Q, Fu S, Xie Y, Zhang M, Shen Y. Treatment and survival patterns of primary adenosquamous carcinoma of the liver: A retrospective analysis. *Front Oncol* (2021) 11:621594. doi: 10.3389/fonc.2021.621594

10. Zhang Z, Nonaka H, Nagayama T, Hatori T, Ihara F, Zhang L, et al. Double cancer consisting of adenosquamous and hepatocellular carcinomas of the liver. *Pathol Int* (2001) 51(12):961–4. doi: 10.1046/j.1440-1827.2001.01302.x

11. Kang GH, Lee BS, Kang DY. A case of primary adenosquamous carcinoma of the liver. Korean. *JHepatobiliary Pancreat Surg* (2013) 17(1):38–41. doi: 10.14701/kjhbps.2013.17.1.38

12. Hamaya K, Nose S, Mimura T, Sasaki K. Solid adenosquamous carcinoma of the liver. A case report and review of the literature. *Acta Pathol Jpn* (1991) 41(11):834–40. doi: 10.1111/j.1440-1827.1991.tb01627.x

13. Yamamoto K, Takenaka K, Kajiyama K, Maeda T, Shirabe K, Shimada M, et al. A primary adenosquamous carcinoma of the liver with an elevated level of serum squamous cell carcinoma related antigen. *Hepatogastroenterology* (1996) 43(9):658–62.

14. Tan Y, Xiao EH. Rare hepatic Malignant tumors: dynamic CT, MRI, and clinicopathologic features: with analysis of 54 cases and review of the literature. *Abdom Imaging* (2013) 38(3):511–26. doi: 10.1007/s00261-012-9918-y

15. Asayama Y, Tajima T, Okamoto D, Nishie A, Ishigami K, Ushijima Y, et al. Imaging of cholangiolocellular carcinoma of the liver. *Eur J Radiol* (2010) 75(1):e120–5. doi: 10.1016/j.ejrad.2009.09.010

16. Yan L, Xie F, Yang C, Yu L, Zheng T, Fu J, et al. The comparison of surgical patients with primary hepatic squamous cell carcinoma or adenosquamous carcinoma and surgical patients with hepatocellular carcinoma. *World J Surg Oncol* (2015) 13:90. doi: 10.1186/s12957-015-0464-2

17. Kobayashi M, Okabayashi T, Okamoto K, Namikawa T, Araki K. A clinicopathologic study of primary adenosquamous carcinoma of the liver. *J Clin Gastroenterol* (2005) 39(6):544–8. doi: 10.1097/01.mcg.0000165705.74079.fc

18. Park SY, Cha EJ, Moon WS. Adenosquamous carcinoma of the liver. *Clin Mol Hepatol* (2012) 18(3):326–9. doi: 10.3350/cmh.2012.18.3.326

19. Takahashi H, Hayakawa H, Tanaka M, Okamura K, Kosaka A, Mizumoto R, et al. Primary adenosquamous carcinoma of liver resected by right trisegmentectomy: report of a case and review of the literature. *J Gastroenterol* (1997) 32(6):843–7. doi: 10.1007/BF02936966

20. Yeh CN, Jan YY, Chen MF. Adenosquamous carcinoma of the liver: clinicopathologic study of 10 surgically treated cases. *World J Surg* (2003) 27(2):168–72. doi: 10.1007/s00268-002-6585-0

21. Moon D, Kim H, Han Y, Byun Y, Choi Y, Kang J, et al. Preoperative carbohydrate antigen 19-9 and standard uptake value of positron emission tomography-computed tomography as prognostic markers in patients with pancreatic ductal adenocarcinoma. *JHepatobiliary Pancreat Sci* (2022) 29(10):1133–41. doi: 10.1002/jhbp.845

22. Watanabe Y, Osaki A, Kimura K, Yakubo S, Takaku K, Sato M, et al. Unresectable primary hepatic adenosquamous carcinoma successfully treated with systemic and transcatheter hepatic arterial injection chemotherapies followed by conversion surgery: a case report and literature review. *BMC Gastroenterol* (2021) 21(1):491. doi: 10.1186/s12876-021-02070-3

23. Benson AB 3rd, D'Angelica M, Abrams T, Are C, Bloomston P, Chang DT, et al. Hepatobiliary cancers, version 2.2014. *J Natl Compr Canc Netw* (2014) 12(8):1152–82. doi: 10.6004/jnccn.2014.0112

24. Moris D, Palta M, Kim C, Allen PJ, Morse MA, Lidsky ME, et al. Advances in the treatment of intrahepatic cholangiocarcinoma: An overview of the current and future therapeutic landscape for clinicians. *CA Cancer J Clin* (2023) 73(2):198–222. doi: 10.3322/caac.21759

frontiers | Frontiers in Oncology

TYPE Original Research
PUBLISHED 17 January 2024
DOI 10.3389/fonc.2023.1348679

OPEN ACCESS

EDITED BY
Francisco Tustumi,
University of São Paulo, Brazil

REVIEWED BY
Xiaolong Li,
Fudan University, China
Eric Nakamura,
University of São Paulo, Brazil

*CORRESPONDENCE
Xiuming Zhang
zhangxiuming360@163.com
Zheng Kang
1366101002@qq.com

†These authors have contributed equally to this work

RECEIVED 03 December 2023
ACCEPTED 27 December 2023
PUBLISHED 17 January 2024

CITATION
Pan C, Dai F, Sheng L, Li K, Qiao W, Kang Z and Zhang X (2024) Clinical application of spectral CT perfusion scanning in evaluating the blood supply source of portal vein tumor thrombus in hepatocellular carcinoma. *Front. Oncol.* 13:1348679. doi: 10.3389/fonc.2023.1348679

Clinical application of spectral CT perfusion scanning in evaluating the blood supply source of portal vein tumor thrombus in hepatocellular carcinoma

Chunhan Pan[1†], Feng Dai[2†], Liuli Sheng[3], Kang Li[3], Wei Qiao[3], Zheng Kang[3*] and Xiuming Zhang[3*]

[1]Department of Radiology, The Affiliated Cancer Hospital of Nanjing Medical University, Jiangsu Cancer Hospital and Jiangsu Institute of Cancer Research, Nanjing, China, [2]Department of Intervention, The Second Hospital of Nanjing, Nanjing, China, [3]Department of Radiology, Jiangsu Cancer Hospital, Jiangsu Institute of Cancer Research and The Affiliated Cancer Hospital of Nanjing Medical University, Nanjing, China

Purpose: To evaluate the characteristic of blood supply of liver portal vein tumor thrombus (PVTT) using perfusion indexes and spectral parameters.

Methods: Between July 2020 and December 2022, the study enrolled 25 liver cancer patients completed with PVTT (male=20, female=5; age 41-74 years (59.48 ± 9.12)) from the Interventional Department of Jiangsu Cancer Hospital. There were 11 cases of type III PVTT, 12 of type II PVTT, and 2 of type I PVTT (Cheng's classification). All patients underwent spectral perfusion scans through dual-layer spectral detector computed tomography. The PVTTs were divided into proximal and distal groups based on the distance between the tumor thrombus and the main portal vein. The perfusion analysis was performed on the 120-kVp conventional images to generate hepatic perfusion index (HPI). The spectral based images (SBIs) during the artery and venous peak phases were extracted from the perfusion data. The iodine map and 40&100-keV virtual monoenergetic image (VMI) were generated from SBI data. HPI, iodine concentration (IC), CT value at 40 and 100-keV, and spectral slope (40-100keV) of the primary lesion, proximal and distal PVTT, and liver parenchyma were measured and compared. The correlation between the primary lesion and proximal and distal PVTT was analyzed.

Results: The IC and spectral slope during the arterial and venous peak phases and HPI of the primary lesion, proximal PVTT, and distal PVTT were highly correlated ($P<0.001$). The differences between the IC and spectral slope during the arterial and venous peak phases and HPI of the primary lesion, proximal PVTT were statistically significant ($P<0.001$). The differences between the IC during venous peak phase and HPI of primary lesion, distal PVTT were statistically significant ($P<0.001$), and there was no statistically significant difference in arterial phase IC, arterial and venous phase spectral slopes.

Conclusion: The IC, slope, and HPI of the distal and proximal PVTT were highly correlated with the primary lesion, indicating that PVTT was similar to the primary lesion in the liver that they were both mainly supplied by the hepatic artery. However, there was still significant heterogeneity between the proximal PVTT and the primary lesion, while the difference in the distal PVTT was relatively small.

KEYWORDS

PVTT, hepatocellular carcinoma (HCC), spectral computed tomography, spectral based image, virtual monoenergetic images

1 Introduction

Portal vein tumor thrombus (PVTT) is the most common form of vascular invasion, and its incidence ranges from 44% to 62.2% at the time of HCC diagnosis in China (1). The median survival time of HCC patients complicated with PVTT is about 2.7 months if they only receive supportive treatment (2). The local treatment of PVTT includes various methods such as transarterial chemoembolization (TACE) and iodine particle implantation surgery, and the choice of treatment plan is closely related to the blood supply of the primary lesion and PVTT. Dual-layer spectral detector CT (SDCT) has high application value in liver cancer, which can evaluate the properties and hemodynamics of primary lesions, PVTT, and liver parenchyma with multiple parameters (3). Perfusion combined with spectral detector CT can comprehensively or semi-quantitatively evaluate the blood supply of PVTT. Through energy spectrum images and quantitative analysis methods such as virtual monoenergetic image (VMI), iodine map and spectral slope, various related information of PVTT and primary lesions can be analyzed. This study used SDCT to evaluate the blood supply of PVTT, aiming to provide a basis for selecting the best treatment method for PVTT patients.

2 Materials and methods

2.1 Characteristics of patient and tumors

Between July 2020 and December 2022, the study enrolled 25 liver cancer patients completed with PVTT [male=20, female=5; age 41-74 (59.48 ± 9.12)] from the Interventional Department of Jiangsu Cancer Hospital (Table 1). This retrospective study was approved by the institutional review board. All patients provided written informed consent before study participation according to the institutional. The inclusion criteria were as follows: 1: patients were histopathologically diagnosed with locally advanced HCC complicated with PVTT, or the patients had three diagnostic criteria: cirrhosis, typical imaging manifestations of HCC and elevated AFP; 2: patients showed adequate renal function with a serum creatinine level of no more than 2.0 mg/dL (177 umol/L); 3: patients had no history of iodine allergy. 4: patients had not received any treatment related to HCC.

2.2 CT scanning parameter

A clinical SDCT scanner (IQon, Philips Healthcare, Best, The Netherlands) was applied in this research, and 25 patients were scanned in a head-first, supine position. A body weight-adapted volume of a non-ionic, iodinated contrast agent (iohexol 350 mg/mL) was administered intravenously via the peripheral vein at a mean flow of 3.5 mL/s, followed by a 30 mL of saline flush. The perfusion scanning range was centered around the lesion, covering a total of 8cm and included five cycles of cyclic scanning. Phantom scans were performed five times through the 100 mAs of fixed tube current. The additional scan parameters used in patients and phantom scans were collimation at 64 × 0.625 mm, rotation time at 0.5s, pitch 0.671, and tube voltage at 120 keV.

TABLE 1 Clinical factors of patients.

Clinical factors	No. (%)
Sex	
Male	20 (80)
Female	5 (20)
Age (years)	
40-50	2 (8)
50-60	10 (40)
>60	13 (52)
PVTT classification	
Type I	2 (8)
Type II	12 (48)
Type III	11 (44)
Type IV	0

2.3 Region of interest (ROI) design and image reconstruction

During the arterial and venous peak phases of the CT scanning (Figure 1), the circular ROIs of at least 500 mm^2 were placed on the primary lesion, proximal and distal PVTT, and liver parenchyma. To minimize any measurement error from different ROIs, we took the average value of three measurements. The ROIs of liver parenchyma and primary lesion were measured at the same level. ROIs did not include nonrepresentative structures like blood vessels, bile ducts, and lymph nodes. The perfusion analysis was performed on the 120-kVp conventional images to generate perfusion results (like hepatic perfusion index (HPI) (Figure 1).The spectral based images (SBIs) at the artery and venous phases were extracted from perfusion data. The iodine map and 40-100 keV VMI were generated from SBI, at a reconstructed slice thickness of 1 mm and an increment of 1 mm. The iodine concentration (IC), CT value at 40 and 100-keV, and spectral slope (40-100keV) of the primary lesion, proximal and distal PVTT, and liver parenchyma were measured (Figure 2).

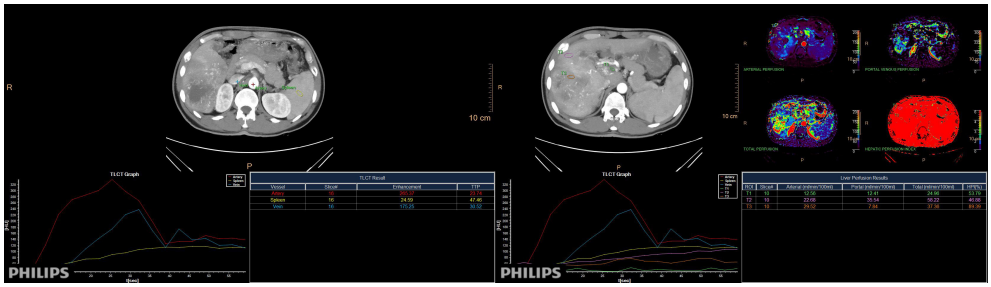

FIGURE 1
The peak time curve and perfusion analysis diagram of arteries, veins, and spleen. Directly obtain the HPI value of the region of interest through measurement.

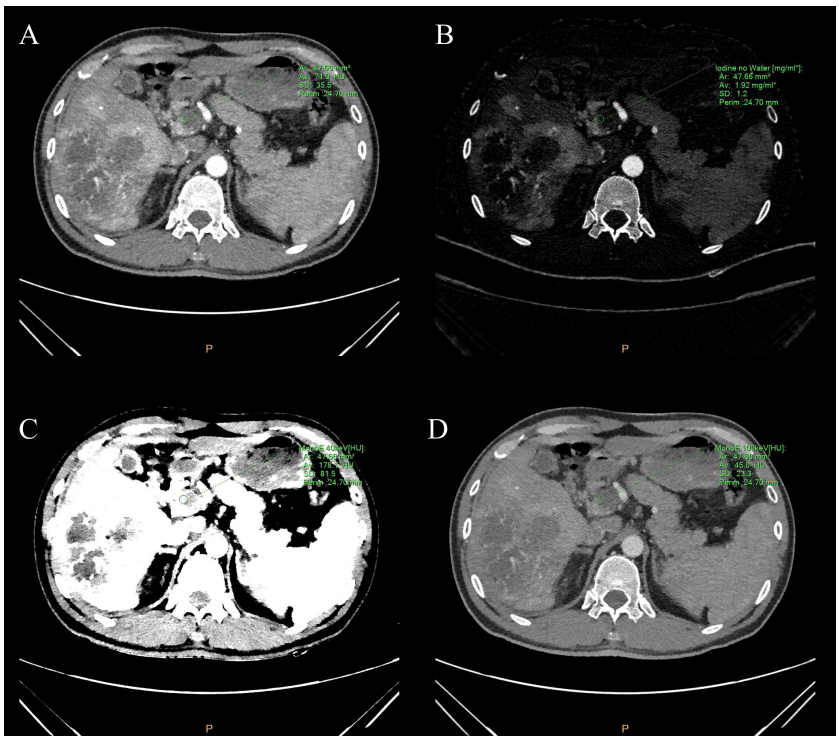

FIGURE 2
(A) Conventional image, **(B)** iodine map image, and **(C, D)** 40&100-keV virtual monoenergetic images of the portal vein tumor thrombus during the peak arterial phase. The green circle represents the measured ROI in the portal vein tumor thrombus. ROI is plotted by using spectral CT post-processing software. The green letters around are some spectral parameters.

2.4 Statistical analysis

The SPSS version 26.0 (SPSS, Inc., Chicago, IL, USA) was used for data analysis. The measurement data was described as mean ± standard deviation, and the K-S test was used to evaluate whether the measurable variables exhibit a normal distribution. A scatter plot was created to observe whether its distribution was linear. Pearson correlation analysis was used to evaluate the correlation between each group of data for normal distribution variables. Paired samples were subjected to paired sample T-test, and the mean difference between groups was analyzed. The statistical significance was defined as *P* value of no more than 0.05.

3 Results

The IC and spectral slope during the arterial and venous peak phases and HPI of the primary lesion, proximal PVTT, and distal PVTT were highly correlated (P<0.001) (Table 2; Figures 3, 4). The differences between the IC and spectral slope during the arterial and venous peak phases and HPI of the primary lesion, proximal PVTT were statistically significant (P<0.001) (Table 3). The differences between the IC during venous peak phase and HPI of primary lesion, distal PVTT were statistically significant (P<0.001), and there was no statistically significant difference in arterial phase IC, arterial and venous phase spectral slopes (Table 4).

4 Discussion

4.1 The treatment methods of PVTT

The primary causes of PVTT development include gene mutation, active replication of HBV, and direct invasion of the portal vein by tumor (4–6). The Barcelona Clinic Liver Cancer guidelines classify HCC accompanied by PVTT as advanced stage (BCLC C stage), and such patients are only eligible for palliative systemic treatment (7) Despite the varying burden of HCC faced by various countries, more proactive management methods are proposed for advanced HCC cases (8–10), including local, locoregional and systemic therapies. Local therapies include surgery (liver resection and transplantation) and radiotherapy the 3-dimensional conformal radiotherapy (3D-CRT), external beam radiotherapy (EBRT)) (10).Locoregional therapies include transarterial chemoembolization (TACE), transarterial radioembolization (TARE), and hepatic artery infusion chemotherapy (HAIC) (11). Systemic therapies include immunotherapy with nivolumab, pembrolizumab and others, and targeted therapy with sorafenib, regorafenib, Lenvatinib etc (12). The use of drugs combined with other methods like radiation therapy (RT), TACE, TARE, and HAIC can effectively control HCC development. However, the main treatment method has always been a focus of clinical discussion, and various treatment methods through hepatic artery perfusion need to clarify whether the target lesion has hepatic artery blood supply and the degree of hepatic artery

TABLE 2 Correlation analysis of primary lesion, proximal and distal PVTT.

	Primary lesion	Proximal PVTT	Distal PVTT	Correlation P
IC (arterial)	1.74 ± 0.35	3.16 ± 1.24	1.84 ± 0.50	<0.001
IC (venous)	1.88 ± 0.42	2.07 ± 0.30	1.73 ± 0.32	<0.001
Slope (arterial)	1.83 ± 0.64	3.24 ± 1.38	2.00 ± 0.62	<0.001
Slope (venous)	2.16 ± 0.59	2.42 ± 0.41	2.13 ± 0.51	<0.001
HPI (%)	66.61 ± 7.92	54.46 ± 5.62	55.97 ± 6.64	<0.001

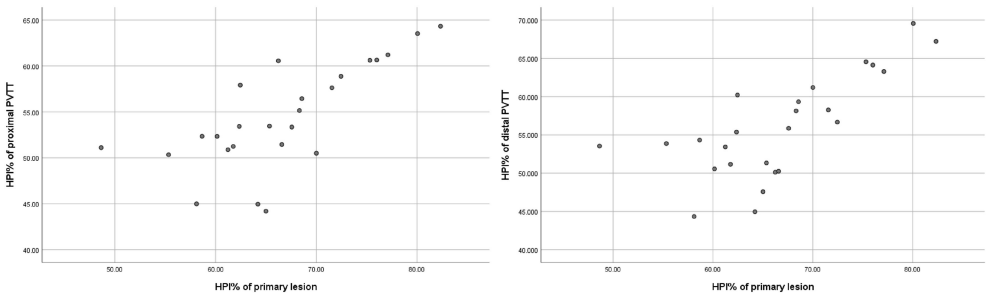

FIGURE 3
The scatter plot of HPI% from the primary lesion and proximal and distal PVTT.

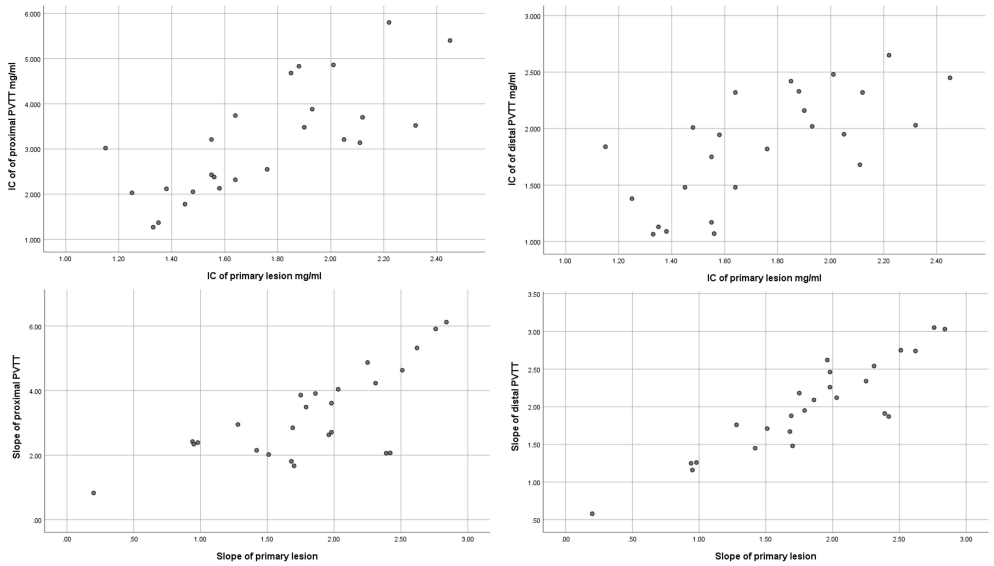

FIGURE 4
The scatter plot of IC from the primary lesion and proximal and distal PVTT during the peak arterial phase. The scatter plot of slope from the primary lesion and proximal and distal PVTT during the peak arterial phase.

TABLE 3 Paired t-test between primary lesion and proximal PVTT.

	Primary lesion	Proximal PVTT	95%CI	t	P
IC (arterial)	1.74 ± 0.35	3.16 ± 1.24	-1.42(-1.83, -1.00)	-7.08	<0.001
IC (venous)	1.88 ± 0.42	2.07 ± 0.30	-0.18(-0.25, -0.11)	-5.42	<0.001
Slope (arterial)	1.83 ± 0.64	3.24 ± 1.38	-1.40(-1.82, -0.99)	-6.92	<0.001
Slope (venous)	2.16 ± 0.59	2.42 ± 0.41	-0.26(-0.38, -0.14)	-4.57	<0.001
HPI(%)	66.61 ± 7.92	54.46 ± 5.62	12.15(9.89, 14.41)	11.11	<0.001

TABLE 4 Paired t-test between primary lesion and distal PVTT.

	Primary lesion	Distal PVTT	95%CI	t	P
IC (arterial)	1.74 ± 0.35	1.84 ± 0.50	-0.10(-0.25, 0.05)	-1.41	0.172
IC (venous)	1.88 ± 0.42	1.73 ± 0.32	0.16(0.08, 0.24)	4.19	<0.001
Slope (arterial)	1.83 ± 0.64	2.00 ± 0.62	-0.17(-0.28, -0.06)	-3.17	0.004
Slope (venous)	2.16 ± 0.59	2.13 ± 0.51	0.03(-0.08, 0.14)	-0.59	0.559
HPI (%)	66.61 ± 7.92	55.97 ± 6.64	10.65(8.36, 12.93)	9.63	<0.001

blood supply, which will directly affect the efficacy of TACE for lesion treatment and whether other methods need to be combined.

4.2 The application of CT in PVTT evaluation

Perfusion CT can objectively and quantitatively evaluate the blood perfusion of the tumor and its adjacent tissues (13). SDCT can offer energy spectrum images and quantitative analysis methods in liver diseases, such as virtual mono energy images (VMIs), virtual plain scans, iodine density maps, atomic number maps, and energy spectrum curves; it can further provide valuable information for disease localization and qualitative diagnosis (14). Moreover, it can provide more tissue characteristics beyond a conventional CT scanner (15). The function of spectral slop (40-100 keV) is similar to spectral attenuation curves, it can plot the CT numbers of tissues at different energy levels of VMIs. Although hepatic arteries are not the main blood supply to the liver, they are the dominant blood supply to liver tumors due to neoplastic

angiogenesis (16), which is the basis for the TACE. Our research showed that the blood supply of PVTT was similar to that of liver cancer lesions, and both were primarily supplied by arteries, which was of great significance for selecting the optimal treatment method for advanced HCC patients complicated with PVTT. Moreover, this study found that the mean HPI value was significantly higher in the primary lesion than in the liver parenchyma, and the high HPI values could explain the reduction of the portal perfusion inflow and a simultaneous increase in arterial inflow in the primary lesion, which further validated the reliability of the selection of control criteria in this study. The difference in mean values between the primary lesion and proximal PVTT was statistically significant, while there was a statistically significant difference in IC values and HPI between the primary lesion and distal PVTT during the venous peak period. There was no statistically significant difference in mean values between the remaining items. PVTT might obstruct the portal vein blood flow of the tumor (17) and the corresponding segment of liver parenchyma to influence perfusion parameters. Nevertheless, the blood supply of the distal PVTT was less affected by the main portal vein, so the values of IC and spectral slope from the distal PVTT were similar.

4.3 Selection of Treatment plans guided by PVTT blood supply evaluation

According to the guidelines for HCC in China, patients with liver cancer combined with PVTT can apply TACE, systemic therapy, radiotherapy, chemotherapy, or surgical resection according to the situation. Surgical resection is widely recognized as a curative treatment measure, but it can only be targeted at patients with PVTT I-II who have good liver function. Various guidelines agreed that TACE was the preferred and effective palliative treatment for advanced liver cancer (18, 19). Chung et al (20) enrolled 83(66.4%) of the 125 advanced HCC patients complicated with PVTT who were treated with TACE and 42 (33.6%) who received supportive care. They found that repeated TACE had more significant survival benefits than supportive care in treating patients with Child-Pugh class A HCC. With the diversification of treatment methods, Li et al. (21) conducted a meta-analysis that included seven studies with 1,018 patients, in which 602 patients received TACE and I^{125} irradiation stent placement and 416 underwent TACE and stent placement without endovascular brachytherapy (EVBT).The study found that I^{125} irradiation stent could improve the cumulative stent patency rate in 6 and 12months and the survival rate in 12 and 24months, indicating that the I^{125} radiation stent was more effective in treating HCC with PVTT and TACE combined with EVBT may become an alternative treatment method for HCC with PVTT. Kim et al. found that HCC patients complicated with PVTT who received TACE with RT had a longer median time to progression and OS than those who got TACE or sorafenib ($P < 0.001$) (22).

Based on the above studies, it was found that HCC combined with PVTT still needed to be combined with other different treatment methods on the basis of TACE, which was basically consistent with the results of this study. This study showed that PVTT was similar to the primary lesion which was mainly supplied by the hepatic artery, and TACE was effective. However, the efficacy of TACE in treating PVTT was not as good as that of primary lesions. As a result, the author believed that although PVTT was mainly supplied by the hepatic artery, there was still significant heterogeneity between proximal PVTT and primary lesions. Most parameters of distal PVTT were not statistically different from primary lesions, but the difference in HPI was still significant. Therefore, TACE alone was not effective in treating PVTT. Therefore, considering the blood supply characteristics of PVTT, a comprehensive treatment plan combined with TACE should become the mainstream treatment method for patients with advanced hepatocellular carcinoma accompanied by portal vein tumor thrombus. Before selecting the treatment plan, performing spectral perfusion analysis on PVTT to evaluate its hepatic artery blood supply and the degree of difference with liver cancer and choosing an appropriate combination plan may have high reference value for improving the treatment efficacy.

In summary, both PVTT and primary lesions were supplied by the hepatic artery, but the degree of blood supply and tumor tissue still had certain heterogeneity compared to the liver cancer. A comprehensive treatment plan based on TACE combined with various methods should become the mainstream treatment method for patients with advanced hepatocellular carcinoma and portal vein cancer thrombus.

4.4 Limitation

This study used a clear proportion of blood supply to primary liver cancer lesions as a reference standard, and the evaluation method mainly relied on imaging, which was relatively single. In the later stage, DSA angiography results will be considered to further clarify the conclusions of this study. If part of patients have pathological results as support, the conclusion will be more clear. Due to the fact that the patients collected in this study are mainly with advanced liver cancer and the inclusion criteria are relatively strict, the sample size is relatively small, and the results have certain limitations. In the later stage, the sample size will be further expanded to make the conclusions more accurate.

Data availability statement

The original contributions presented in the study are included in the article/supplementary material. Further inquiries can be directed to the corresponding author.

Ethics statement

The studies involving humans were approved by Ethics Committee of Jiangsu Cancer Hospital. The studies were conducted in accordance with the local legislation and institutional requirements. Written informed consent for participation was not required from the participants or the participants' legal guardians/ next of kin in accordance with the national legislation and

institutional requirements. Written informed consent was obtained from the individual(s) for the publication of any potentially identifiable images or data included in this article.

Author contributions

XZ: Methodology, Project administration, Writing – original draft, Writing – review & editing. CP: Data curation, Methodology, Writing – original draft. FD: Formal Analysis, Investigation, Writing – review & editing. LS: Investigation, Writing – review & editing. KL: Investigation, Software, Writing – review & editing. WQ: Conceptualization, Methodology, Writing – review & editing. ZK: Data curation, Methodology, Project administration, Writing – review & editing.

Funding

The author(s) declare financial support was received for the research, authorship, and/or publication of this article. This work was supported by grants from the Roentgen special fund for image research of Jiangsu Medical Association (SYH-32011500008 2021003) and The Jiangsu Cancer Hospital Young Talents Plan (Jiangsu China).

Conflict of interest

The authors declare that the research was conducted in the absence of any commercial or financial relationships that could be construed as a potential conflict of interest.

Publisher's note

All claims expressed in this article are solely those of the authors and do not necessarily represent those of their affiliated organizations, or those of the publisher, the editors and the reviewers. Any product that may be evaluated in this article, or claim that may be made by its manufacturer, is not guaranteed or endorsed by the publisher.

References

1. Sun JX, Guo RP, Bi XY, Wu MC, Tang ZY, Lau WY, et al. Guidelines for diagnosis and treatment of hepatocellular carcinoma with portal vein tumor thrombus in China (2021 edition). *Liver Cancer* (2022) 11(4):315–28. doi: 10.1159/000523997

2. Tao ZW, Cheng BQ, Zhou T, Gao YJ. Management of hepatocellular carcinoma patients with portal vein tumor thrombosis: A narrative review. *Hepatobiliary Pancreat Dis Int* (2022) 21(2):134–44. doi: 10.1016/j.hbpd.2021.12.004

3. Hennedige T, Venkatesh SK. Imaging of hepatocellular carcinoma: diagnosis, staging and treatment monitoring. *Cancer Imaging* (2013) 12(3):530–47. doi: 10.1102/1470-7330.2012.0044

4. Fan XX, Li YR, Yi X, Chen GQ, Jin SX, Dai YL, et al. Epigenome-wide DNA methylation profiling of portal vein tumor thrombosis (PVTT) tissues in hepatocellular carcinoma patients. *Neoplasia* (2020) 22(11):630–43. doi: 10.1016/j.neo.2020.09.007

5. Chen C, Chen DP, Gu YY, Hu LH, Wang D, Lin JH, et al. Vascular invasion in hepatitis B virus-related hepatocellular carcinoma with underlying cirrhosis: possible associations with ascites and hepatitis B viral factors? *Tumour Biol* (2015) 36(8):6255–63. doi: 10.1007/s13277-015-3311-8

6. Intagliata NM, Caldwell SH, Tripodi A. Diagnosis, development, and treatment of portal vein thrombosis in patients with and without cirrhosis. *Gastroenterology* (2019) 156(6):1582–1599.e1581. doi: 10.1053/j.gastro.2019.01.265

7. European Association for the Study of the Liver. EASL Clinical Practice Guidelines: Management of hepatocellular carcinoma. *J Hepatol* (2018) 69(1):182–236. doi: 10.1016/j.jhep.2018.03.019

8. Benson AB, D'Angelica MI, Abbott DE, Abrams TA, Alberts SR, Anaya DA, et al. Guidelines insights: hepatobiliary cancers, version 2.2019. *J Natl Compr Canc Netw* (2019) 17(4):302–10. doi: 10.6004/jnccn.2019.0019

9. Yau T, Tang VYF, Yao TJ, Fan ST, Lo CM, Poon RTP. Development of Hong Kong Liver Cancer staging system with treatment stratification for patients with hepatocellular carcinoma. *Gastroenterology* (2014) 146(7):1691–1700.e1693. doi: 10.1053/j.gastro.2014.02.032

10. Leung TWT, Tang AMY, Zee B, Lau WY, Lai PBS, Leung KL, et al. Construction of the Chinese University Prognostic Index for hepatocellular carcinoma and comparison with the TNM staging system, the Okuda staging system, and the Cancer of the Liver Italian Program staging system: a study based on 926 patients. *Cancer* (2002) 94(6):1760–9. doi: 10.1002/cncr.10384

11. Chen CP. Role of external beam radiotherapy in hepatocellular carcinoma. *Clinics liver Dis* (2020) 24(4):701–17. doi: 10.1016/j.cld.2020.07.006

12. Galle PR, Finn RS, Qin SK, Ikeda M, Zhu AX, Kim TY, et al. Patient-reported outcomes with atezolizumab plus bevacizumab versus sorafenib in patients with unresectable hepatocellular carcinoma (IMbrave150): an open-label, randomised, phase 3 trial. *Lancet Oncol* (2021) 22(7):991–1001. doi: 10.1016/s1470-2045(21)00151-0

13. Ippolito D, Sironi S, Pozzi M, Antolini L, Invernizzi F, Ratti L, et al. Perfusion CT in cirrhotic patients with early stage hepatocellular carcinoma: assessment of tumor-related vascularization. *Eur J Radiol* (2010) 73(1):148–52. doi: 10.1016/j.ejrad.2008.10.014

14. Chellini D, Kinman K. Dual-energy CT principles and applications. *Radiol Technol* (2020) 91(6):561ct–76ct.

15. Rajiah P, Parakh A, Kay F, Baruah D, Kambadakone AR, Leng S. Update on multienergy CT: physics, principles, and applications. *Radiographics* (2020) 40(5):1284–308. doi: 10.1148/rg.2020200038

16. Morse MA, Sun WJ, Kim R, He AR, Abada PB, Mynderse M, et al. The role of angiogenesis in hepatocellular carcinoma. *Clin Cancer Res* (2019) 25(3):912–20. doi: 10.1158/1078-0432.Ccr-18-1254

17. Li H, Liu J, Chen M, Li Hang, Long LL. Therapeutic evaluation of radiotherapy with contrast-enhanced ultrasound in non-resectable hepatocellular carcinoma patients with portal vein tumor thrombosis. *Med Sci Monit* (2018) 24:8183–9. doi: 10.12659/msm.911073

18. Kudo M, Kawamura Y, Hasegawa K, Tateishi R, Kariyama K, Shiina S, et al. Management of hepatocellular carcinoma in Japan: JSH consensus statements and recommendations 2021 update. *Liver Cancer* (2021) 10(3):181–223. doi: 10.1159/000514174

19. Zhou J, Sun HC, Wang Z, Cong WM, Wang JH, Zeng MS, et al. Guidelines for the diagnosis and treatment of hepatocellular carcinoma (2019 edition). *Liver Cancer* (2020) 9(6):682–720. doi: 10.1159/000509424

20. Zhou J, Sun HC, Wang Z, Cong WM, Wang JH, Zeng MS, et al. Transarterial chemoembolization can be safely performed in patients with hepatocellular carcinoma invading the main portal vein and may improve the overall survival. *Radiology* (2011) 258(2):627–34. doi: 10.1148/radiol.10101058

21. Zhou J, Sun HC, Wang Z, Cong WM, Wang JH, Zeng MS, et al. I^{125} irradiation stent for treatment of hepatocellular carcinoma with portal vein thrombosis: A meta-analysis. *Cancer Radiother* (2021) 25(4):340–9. doi: 10.1016/j.canrad.2020.12.003

22. Zhou J, Sun HC, Wang Z, Cong WM, Wang JH, Zeng MS, et al. Comparison of chemoembolization with and without radiation therapy and sorafenib for advanced hepatocellular carcinoma with portal vein tumor thrombosis: a propensity score analysis. *J Vasc Interv Radiol* (2015) 26(3):320–329.e326. doi: 10.1016/j.jvir.2014.10.019

frontiers | Frontiers in Oncology

TYPE Original Research
PUBLISHED 25 January 2024
DOI 10.3389/fonc.2024.1332188

OPEN ACCESS

EDITED BY
Francisco Tustumi,
University of São Paulo, Brazil

REVIEWED BY
Jianguo Xu,
Sichuan University, China
Xiaopeng Yao,
Southwest Medical University, China
Daniel Szor,
University of São Paulo, Brazil

*CORRESPONDENCE
Xisheng Dai
mathdxs@163.com
Enming Cui
cem2008@163.com

†These authors share first authorship

RECEIVED 03 November 2023
ACCEPTED 09 January 2024
PUBLISHED 25 January 2024

CITATION
Yu Z, Liu Y, Dai X, Cui E, Cui J and Ma C (2024) Enhancing preoperative diagnosis of microvascular invasion in hepatocellular carcinoma: domain-adaptation fusion of multi-phase CT images.
Front. Oncol. 14:1332188.
doi: 10.3389/fonc.2024.1332188

Enhancing preoperative diagnosis of microvascular invasion in hepatocellular carcinoma: domain-adaptation fusion of multi-phase CT images

Zhaole Yu[1†], Yu Liu[2†], Xisheng Dai[1*], Enming Cui[3*], Jin Cui[3] and Changyi Ma[3]

[1]School of Automation, Guangxi University of Science and Technology, Liuzhou, Guangxi, China, [2]Laboratory of Artificial Intelligence of Biomedicine, Guilin University of Aerospace Technology, Guilin, Guangxi, China, [3]Department of Radiology, Jiangmen Central Hospital, Jiangmen, Guangdong, China

Objectives: In patients with hepatocellular carcinoma (HCC), accurately predicting the preoperative microvascular invasion (MVI) status is crucial for improving survival rates. This study proposes a multi-modal domain-adaptive fusion model based on deep learning methods to predict the preoperative MVI status in HCC.

Materials and methods: From January 2008 to May 2022, we collected 163 cases of HCC from our institution and 42 cases from another medical facility, with each case including Computed Tomography (CT) images from the pre-contrast phase (PCP), arterial phase (AP), and portal venous phase (PVP). We divided our institution's dataset (n=163) into training (n=119) and test sets (n=44) in an approximate 7:3 ratio. Additionally, we included cases from another institution (n=42) as an external validation set (test1 set). We constructed three single-modality models, a simple concatenated multi-modal model, two current state-of-the-art image fusion model and a multi-modal domain-adaptive fusion model (M-DAFM) based on deep learning methods. We evaluated and analyzed the performance of these constructed models in predicting preoperative MVI using the area under the receiver operating characteristic curve (AUC), decision curve analysis (DCA), and net reclassification improvement (NRI) methods.

Results: In comparison with all models, M-DAFM achieved the highest AUC values across the three datasets (0.8013 for the training set, 0.7839 for the test set, and 0.7454 for the test1 set). Notably, in the test set, M-DAFM's Decision Curve Analysis (DCA) curves consistently demonstrated favorable or optimal net benefits within the 0-0.65 threshold probability range. Additionally, the Net Reclassification Improvement (NRI) values between M-DAFM and the three single-modal models, as well as the simple concatenation model, were all greater than 0 (all $p < 0.05$). Similarly, the NRI values between M-DAFM and the two current state-of-the-art image fusion models were also greater than 0. These findings collectively indicate that M-DAFM effectively integrates valuable information from multi-phase CT images, thereby enhancing the model's preoperative predictive performance for MVI.

Conclusion: The M-DAFM proposed in this study presents an innovative approach to improve the preoperative predictive performance of MVI.

KEYWORDS

hepatocellular carcinoma, microvascular invasion, multi-modal, domain adaptation, feature fusion

1 Introduction

Microvascular invasion (MVI) is one of the significant factors contributing to postoperative recurrence of hepatocellular carcinoma (HCC) (1–4), exerting a pronounced impact on disease recurrence and shortened survival in HCC patients (5–7). When MVI is positive in cases of HCC, the short-term recurrence rate of small liver cancers (8) (liver cell tumors <2cm) is higher, and patients with liver cell tumors ≥2cm exhibit lower long-term survival rates (9). Therefore, MVI is commonly regarded as a marker to assess the malignancy degree of HCC (10). However, in clinical practice, the presence of MVI can only be confirmed through histopathological examination of resected tumor tissue postoperatively (11, 12). Accurately predicting the preoperative MVI status in a noninvasive manner remains a challenge.

Prior research has demonstrated the feasibility of preoperative MVI prediction in HCC using Computed Tomography (CT) images (13), and many studies have extracted radiological features from CT images to construct radiological models for predicting the preoperative MVI status (2, 14, 15). Since the extraction of radiological features relies on the subjective expertise of radiologists, less experienced radiologists may overlook valuable features (16). Additionally, radiological features are often considered low to mid-level features, which may not fully capture the heterogeneity of HCC (17).

Deep learning based on Convolutional Neural Networks (CNN) has the capacity to automatically extract high-level features relevant to the target problem in CT images, surpassing explicitly designed low and mid-level features (18–21). Research has indicated that deep learning methods exhibit excellent performance in differentiating liver lesions and classifying fibrosis, offering diagnostic accuracy comparable to pathological gold standards (22, 23). In previous studies, deep learning methods have been applied to predict the preoperative status of MVI. For example, Liu et al. (24) used AP-phase CT images to construct a deep learning model and combined it with clinical factors for preoperative MVI prediction. Jiang et al. (25), on the other hand, built deep models using arterial phase (AP), portal venous phase (PVP), and delayed phase (DP) CT images separately and concatenated the deep features from these three phases to predict the preoperative MVI status. While these studies have achieved certain effectiveness in preoperative MVI prediction, they also exhibit certain limitations. For instance, Liu et al. used only a single-phase CT image, limiting their ability to comprehensively evaluate tumor characteristics. Jiang et al., although combining information from different phases of CT images, did not address the issue of feature distribution differences during the fusion process.

To address these issues, our study proposes a multimodal domain-adaptive fusion model based on deep learning. This model employs deep learning methods to extract information from CT images acquired at different phases, enabling a more comprehensive evaluation of HCC characteristics. Furthermore, it employs domain adaptation to align the feature distributions of various CT images, thereby enhancing the quality of the fused features. To the best of our knowledge, there is limited research considering the differences in data distribution between different modalities when utilizing multimodal image information. Our study aims to investigate the effectiveness of the domain-adaptive fusion method for preoperative MVI prediction in HCC, in comparison to single-modal and multimodal simple concatenation methods. Our research provides a novel approach to effectively integrate multimodal image information for predicting the preoperative MVI status.

2 Materials and methods

The ethics committee of our hospital has granted approval for this retrospective study. Since the data is sourced from an existing institution and imposes no additional burden on the patients, the requirement for informed consent has been waived. Figure 1 provides a schematic representation of the study's design.

2.1 Patients

We conducted a retrospective study by querying our medical institution's pathology database from January 2008 to May 2022 to identify patients who underwent hepatic resection surgery for HCC. The patient data collected by our institution predominantly employs major resection as the types of resection. The inclusion criteria for our study were as follows: (a) patients who did not receive any other anti-tumor treatments before surgery (including liver resection, liver transplantation, chemotherapy, radiation therapy, radiofrequency ablation, immunosuppressive therapy); (b) liver nodules with comprehensive histopathological

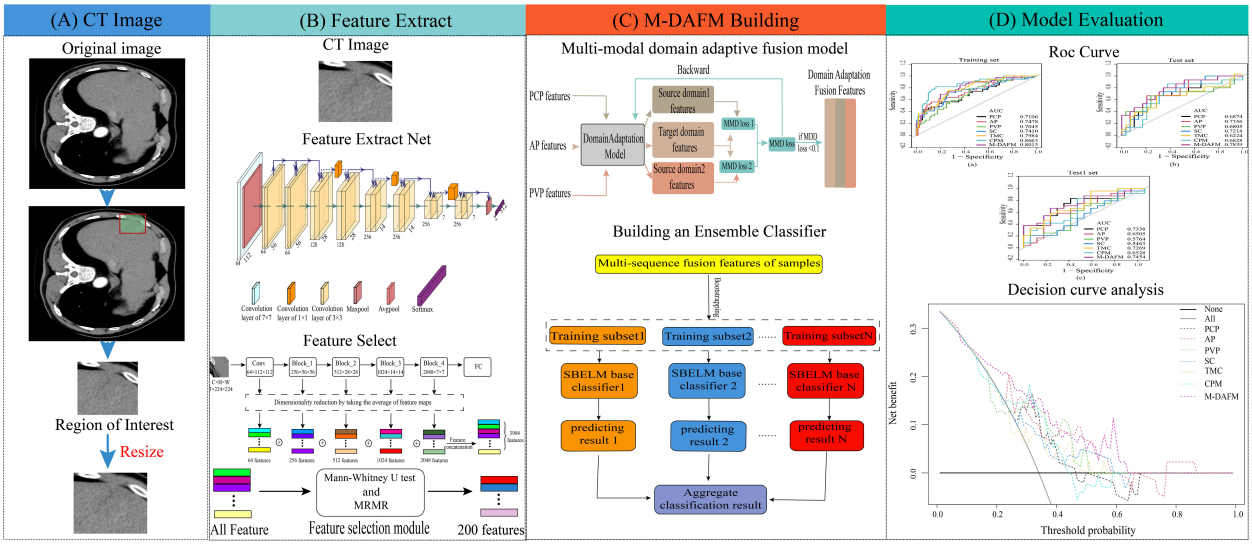

FIGURE 1
The overall design flowchart. **(A)** ROI extraction process; **(B)** DL feature extraction process; **(C)** M-DAFM building process; **(D)** Model evaluation.

descriptions in the pathology reports; (c) a time interval of no more than 4 weeks between preoperative CT examination [including pre-contrast phase (PCP), arterial phase (AP), portal venous phase (PVP)] and surgery. We excluded HCC patients with pathological results obtained through puncture and patients with artifacts in imaging and incomplete clinical information. A total of 163 patients with CT images from our institution met the inclusion and exclusion criteria. Subsequently, we randomly divided this dataset into a training set (n=119) and a test set (n=44) in an approximate ratio of 7:3. Statistical analysis revealed that in the training set, the rate of MVI was found to be 32.8% (39/119). Furthermore, we gathered 42 cases from external medical institutions to constitute an external validation set (test1 set). These cases adhere to the inclusion and exclusion criteria of our institution, and undergo the same preprocessing procedures as our institution's pathology. This was done to further assess the predictive performance of the model on previously unseen data. The inclusion and exclusion criteria of our medical institution are presented in Electronic Supplementary Material S1.

2.2 Medical history and laboratory parameters

Age, gender, hepatocirrhosis status, and the presence of hepatitis B surface antigen (HBsAg) were documented for every patient. A range of serum biochemical parameters related to liver function were assessed for each patient within two weeks before or after the CT examination. These parameters encompassed α-fetoprotein (AFP), Carbohydrate antigen 199 (CA199), total bilirubin (TBIL), direct bilirubin (DBIL), indirect bilirubin (IBIL), alanine aminotransferase (ALT), aspartate aminotransaminase (AST), albumin, total protein, alkaline phosphatase (ALP), and platelet count (PLT). The baseline characteristics of the included cohorts are summarized in the Table 1.

TABLE 1 Baseline characteristics of the CT training set and test set.

Characteristics	CT Dataset					
	Training (n=119)			Test (n=44)		
	MVI negative (n=80)	MVI positive (n=39)	p Value	MVI negative (n=29)	MVI positive (n=15)	p Value
Age (years)	56.26 ± 10.86	55.90 ± 12.08	0.869	58.00 ± 8.30	52.60 ± 9.21	0.055
Gender (n)			0.364			0.319
Male	62 (77.5%)	33 (84.6%)		27 (93.1%)	12 (80%)	
Female	18 (22.5%)	6 (15.4%)		2 (6.9%)	3 (20%)	
HBsAg status			0.605			0.171

(Continued)

TABLE 1 Continued

Characteristics	CT Dataset					
	Training (n=119)			Test (n=44)		
	MVI negative (n=80)	MVI positive (n=39)	p Value	MVI negative (n=29)	MVI positive (n=15)	p Value
Negative	21 (26.2%)	12 (30.8%)		10 (34.4%)	2 (13.3%)	
Positive	59 (73.8%)	27 (69.2%)		19 (65.6%)	13 (86.7%)	
Hepatocirrhosis status			0.647			1.000
Absent	28 (35%)	12 (30.7%)		7 (24.1%)	4 (26.6%)	
Present	52 (65%)	27 (69.3%)		22 (75.8%)	11 (73.4%)	
Log10AFP	3.21 ± 3.85	3.80 ± 4.25	0.044*	2.78 ± 3.43	3.55 ± 3.97	0.117
CA199	36.58 ± 62.24	80.60 ± 94.72	0.003*	22.52 ± 18.95	25.45 ± 22.26	0.650
TBIL	20.05 ± 12.57	14.28 ± 12.66	0.021*	19.94 ± 10.71	17.96 ± 8.10	0.534
DBIL	8.95 ± 8.32	6.67 ± 9.29	0.178	9.00 ± 4.78	8.20 ± 4.86	0.605
IBIL	11.10 ± 5.58	7.72 ± 4.58	0.001*	10.95 ± 6.60	9.76 ± 3.85	0.525
ALT	182.10 ± 367.57	101.70 ± 87.90	0.181	213.65 ± 248.3	328.54 ± 384.18	0.236
AST	134.23 ± 161.64	106.26 ± 85.78	0.314	171.33 ± 172.80	33.97 ± 373.67	0.046
Albumin	35.72 ± 5.73	33.22 ± 5.49	0.026*	33.63 ± 4.76	32.53 ± 3.77	0.439
Total protein	62.19 ± 8.68	59.02 ± 8.64	0.063	59.55 ± 8.07	55.12 ± 7.01	0.079
ALP	100.21 ± 42.96	119.01 ± 59.68	0.052	101.10 ± 69.79	197.20 ± 422.91	0.235
PLT	169.19 ± 56.65	178.05 ± 72.87	0.468	155.23 ± 91.47	199.40 ± 87.27	0.131

AFP, α-fetoprotein; CA199, Carbohydrate antigen 199; TBIL, total bilirubin; DBIL, direct bilirubin; IBIL, indirect bilirubin; ALT, alanine aminotransferase; AST, aspartate aminotransaminase; ALP, alkaline phosphatase; PLT, platelet count. * $P < 0.05$ indicates statistical significance; The numbers following ± represent the standard deviation.

2.3 Imaging scans

The CT scanning devices used in this study were the 16-detector CT (SOMATOM Sensation 16, Siemens Healthineers), the 64-detector CT (Aquilion 64, Canon Medical Systems), and the dual-source CT (SOMATOM Force, Siemens Healthineers). Patients maintained a supine position and held their breath during the procedure. The scanning sequences consisted of the pre-contrast phase (PCP), the arterial phase (AP, 30 seconds after contrast injection), and the portal venous phase (PVP, 60-70 seconds after contrast injection). The CT parameters included: tube voltage set at 120 kV, effective tube current-exposure time product ranging from 200 to 350 mAs, matrix size of 512×512, and a slice thickness of either 1.0 or 3.0 mm.

2.4 Radiologist assessment

The study utilized three different-phase CT images: PCP, AP, and PVP. Two radiologists, each possessing more than 5 and 11 years of expertise in abdominal imaging, independently conducted image assessments. These assessments were carried out in isolation from each other, with no knowledge of their respective ratings and no access to pathological findings. The degree of their confidence in detecting MVI was documented using a 5-point scale: 5, indicating a definite positive diagnosis; 4, signifying a probable positive finding; 3, expressing uncertainty; 2, suggesting a potential negative result; and 1, denoting a definite negative assessment (12). In cases of discordance, these two radiologists held discussions to reach a consensus score.

The summary of radiological features encompassed the following criteria: (1) tumor diameter (<5cm = 0; ≥5cm = 1); (2) the number of tumors (<2 = 0; ≥2 = 1); (3) the presence of a pseudocapsule (absent = 0; present = 1); (4) intratumoral necrosis (absent = 0; present = 1); (5) intratumoral hemorrhage (absent = 0; present = 1); (6) peritumoral enhancement during the arterial phase (AP) (absent = 0; present = 1); (7) AP hyperenhancement (absent = 0; present = 1); (8) wash-in and wash-out patterns (absent = 0; present = 1). Scores equal to or greater than 4 signified a heightened likelihood of MVI presence. Each image was individually examined and rated. In cases of multiple lesions, the option of surgical resection was considered.

2.5 Pathological diagnosis

The reference criteria for identifying MVI relied on the pathological examination of surgical specimens. MVI was specifically characterized as the presence of a tumor within a vascular space lined with endothelial cells, as visualized under

microscopy (26). Moreover, to ensure precision, all our pathological findings underwent thorough review by a pathologist with twelve years of experience.

2.6 Tumor segmentation

After extracting patient images from our institutional picture archiving and communication system (PACS), we perform image de-identification and store them in the NIfTI format. Subsequently, these images are imported into 3D-Slicer (version 5.0.2). Next, we proceed with delineating the region of interest (ROI) on the CT images for each phase separately. The entire tumor is outlined at three distinct layers: the initial layer, the section with the maximum cross-sectional area, and the final layer. To ensure comprehensive coverage of the tumor, an additional 1-centimeter extension is applied at the margins. This delineation process is semi-automated to save the effort of radiologists and reduce the interference of subjective factors. The flowchart for image segmentation and preprocessing is presented in Electronic Supplementary Material S2.

2.7 Building the multi-modal domain adaptive fusion model

Multi-modal domain adaptive fusion model (M-DAFM) utilizesa convolutional neural network to extract feature information from the target task. It can predict the occurrence of MVI in HCC within a given ROI without the need for precise lesion segmentation. The training process of M-DAFM in this study consists of three stages: first, deep learning models are employed to extract features from single-phase CT images; then, domain adaptation techniques (27) are applied to align the distributions of features among the single-phase CT images and fuse these features; finally, an ensemble sparse Bayesian extreme learning machine (ESBELM) is used for preoperative prediction of MVI status in HCC. Detailed parameters for training the deep learning model can be found in Electronic Supplementary Material S3.

In the feature extraction stage, we employ a pre-trained ResNet18 model on ImageNet to extract features from multiple single-phase CT images, including PCP, AP, and PVP. Each single-phase image yields 3904 features. For a comprehensive understanding of the deep feature extraction process, please refer to Electronic Supplementary Material S4.

In the domain adaptation feature fusion stage, we perform feature selection using Mann-Whitney U test (28) and Maximum Relevance Minimum Redundancy (MRMR) algorithm (29) on the features extracted from individual single-phase images, selecting the top 200 features most relevant to the target task. Domain adaptation is a learning paradigm within transfer learning that primarily addresses distributional differences between the target domain and the source domain, enabling the adaptation of the source domain distribution to the target domain. In clinical practice, CT images from the PCP, AP, and PVP phases typically reflect relevant information about tumors from different perspectives. Consequently, there are often distributional differences among them. To alleviate these differences, we employ domain adaptation methods, treating the AP phase features as the target domain and the PCP and PVP phase features as the source domain, the Maximum Mean Discrepancy (MMD) (30) is utilized as the loss function to quantify the distributional differences between the source and target domains. This alignment aims to ensure that PCP, AP and PVP features exhibit similar distributions. The domain adaptation fusion algorithm proposed in this article can be divided into three steps: 1) We select the AP phase CT image features as the target domain and the PCP and PVP phase CT image features as two source domains. The purpose is to use the target domain as a standard to make the data distribution of the source domains closer to the target domain. 2) We use maximum mean discrepancy (MMD) as the model's loss function to measure the distribution difference between the source domain (PCP and PVP features) and the target domain (AP features). By training the model to reduce these distribution differences, we make the distribution of the source domain tend to be consistent with the target domain. 3) We use a feature concatenation strategy to fuse the distribution-consistent PCP, AP, and PVP features, aiming to improve the model's performance on unknown datasets. For a detailed description of the feature fusion process, please refer to Electronic Supplementary Material S5.

In the classification stage, we construct an ESBELM classifier. This classifier incorporates Bayesian linear regression algorithms into the framework of extreme learning machines (31) to reduce feature dimensions and mitigate model overfitting. Additionally, the classifier enhances model classification performance through the ensemble of multiple base classifiers. Detailed information about classifier construction can be found in Electronic Supplementary Material S6.

2.8 Statistical analysis

In this study, model performance was evaluated using metrics including accuracy, sensitivity, specificity, positive predictive value (PPV), negative predictive value (NPV), and area under the receiver operating characteristic curve (AUC). Comparing these metrics aids in assessing the model's classification capability, accuracy, and reliability. The formulas for calculating classification performance metrics are provided in Electronic Supplementary Material S7.

Net reclassification improvement (NRI) is a metric used to evaluate the improvement of a predictive model, particularly for comparing the performance differences between two models in a classification task. The formula for calculating the metrics is provided in Electronic Supplementary Material S8.

Decision curve analysis (DCA) is a method for evaluating the performance of medical diagnostic or predictive models. The primary objective of DCA is to assess the impact of model classification results at different thresholds, assisting medical decision-makers in making more informed choices in various scenarios, thus enhancing overall patient benefit.

All statistical analyses were performed using Python 3.7 (https://www.python.org/), MATLAB R2020b (https://www.mathworks.com/products/matlab.html), and R 4.3.0 (http://

www.rproject.org). The deep learning model was constructed using Python. Mann-Whitney U test and Maximum MRMR algorithm were computed and analyzed using Python. The ESBELM classifier was built using MATLAB for classification. The "pROC" package in RStudio was utilized to plot ROC curves, the NRI value was calculated used the "glm" package in RStudio.

3 Results

3.1 Performance analysis of different classifiers

In this experiment, we conducted a comparative analysis among ESBELM, Ensemble Random Forest (ERF), and Extreme Learning Machine (ELM) to validate the superiority of ESBELM. The experimental results can be found in Tables 2, 3. On the test set, ESBELM achieved AUC values of 0.7011, 0.7011, and 0.6805 when using single-phase features PCP, AP, and PVP as inputs, respectively. Additionally, M-DAFM achieved an AUC value of 0.7839, all of which outperformed the predictive performance of ERF and ELM.

3.2 Analyzing the predictive performance of different models

We will compare the proposed M-DAFM model with the following models: (1) Single-modal model: Construct a deep learning model using only one phase of CT images (PCP, AP, or PVP) from patients for preoperative prediction of MVI; (2) Simple concatenation model (SC): Employ deep learning methods to extract deep features from PCP, AP, and PVP phase CT images of patients separately, followed by straightforward concatenation for preoperative prediction of MVI.; (3) State-of-the-Art models, where we selected two state-of-the-art image fusion models: TMC (Trusted Multi-View Classification model) (32), which dynamically acquires the credibility of different modalities and integrates information from each modality based on its credibility, thereby effectively improving the predictive performance of the model; CPM (Cross Partial Multi-View Networks) (33), which integrates information from different modalities by constructing a non-parametric classification loss function, allowing the model to learn the consistency and complementary information of different modalities for the target task, thereby enhancing model performance.

TABLE 2 AUC values of different classifiers on the training set.

Classifier / Input features	ERF	ELM	ESBELM
PCP	*0.6476*	*0.6865*	***0.7167***
AP	*0.5641*	*0.7170*	***0.7420***
PVP	*0.6229*	*0.6788*	***0.7045***
DAFF	*0.6877*	*0.7423*	***0.8013***

PCP, AP and PVP correspond to the features extracted from these three models, and DAFF represents domain-adaptive fused features.
The bold values are highlighted to emphasize the superiority of the classifier used in this study compared to other classifiers. The bolding of DAFF is intended to highlight the fused features obtained by the algorithm proposed in this paper.

TABLE 3 AUC values of different classifiers on the test set.

Classifier / Input feature	ERF	ELM	SBELM
PCP	*0.6000*	*0.6621*	***0,7011***
AP	*0.5333*	*0.6920*	***0.7011***
PVP	*0.5828*	*0.6575*	***0.6805***
DAFF	*0.6460*	*0.7011*	***0.7839***

PCP, AP and PVP correspond to the features extracted from these three models, and DAFF represents domain-adapted fused features.
The bold values are highlighted to emphasize the superiority of the classifier used in this study compared to other classifiers. The bolding of DAFF is intended to highlight the fused features obtained by the algorithm proposed in this paper.

Table 4 presents the diagnostic performance of each model for preoperative prediction of MVI; Figure 2 shows the ROC (receiver operating characteristic) curves of each model on the training set, test set, and test1 set; Table 5 demonstrates the improvement performance of M-DAFM compared to other models; Figure 3 displays the DCA curves of each model on the test set.

As evident from Table 4 and Figure 2, M-DAFM achieved AUC values in the test set close to those in the training set (<5%). This indicates that M-DAFM successfully learned relevant and effective information highly correlated with the target task in the training set. Moreover, M-DAFM exhibited good predictive performance on the test1 set with an AUC of 0.7454, indicating strong generalization capabilities. In other words, the model performed well on datasets with substantial differences from the training set. In comparison, the AUC values of single-modal models (PCP, AP, PVP) and the SC were consistently lower than M-DAFM across all three datasets. The AUC values of TMC and CPM in the test set are significantly lower than those in the training set, indicating a certain degree of overfitting. This implies that both TMC and CPM models have overly adapted to the noise or specific characteristics of the training set during the training process, leading to suboptimal performance on unseen data. Therefore M-DAFM exhibits superior predictive and generalization performance compared to other models, while TMC and CPM require further optimization to enhance their generalization performance on unknown data.

According to Table 5, the NRI values of M-DAFM compared to the single-modal models (PCP, AP, PVP) and the SC are 0.4805 ($p < 0.05$), 0.3471 ($p < 0.05$), 0.5379 ($p < 0.05$), and 0.3816 ($p < 0.05$), respectively. This indicates that M-DAFM exhibits a significantly improved predictive performance compared to these models. Furthermore, the NRI values of M-DAFM compared to the current state-of-the-art models, TMC and CPM, are 0.1556 ($p = 0.39$) and 0.4092 ($p < 0.05$), respectively, suggesting that M-DAFM still demonstrates some improvement in predictive performance compared to the current state-of-the-art models.

According to Figure 3, we visually represented the DCA curves for all models in the test set. It can be observed that, within the 0-0.65 threshold range, M-DAFM consistently achieves better or the best net benefit compared to other models.

TABLE 4 Comparison of classification performance between M-DAFM and PCP, AP, PVP, TMC, CPM and SC models.

Sets	Model	AUC	Sensitivity	Specificity	Accuracy	PPV	NPV
Training Set	*PCP*	*0.7106*	*0.4359 (17/39)*	*0.9375 (75/80)*	*0.7731 (92/119)*	*0.7727 (17/22)*	*0.7732 (75/97)*
	AP	*0.7478*	*0.5641 (22/39)*	*0.8750 (70/80)*	*0.7731 (92/119)*	*0.6875 (22/32)*	*0.8046 (70/87)*
	PVP	*0.7045*	*0.7949 (31/39)*	*0.5625 (45/80)*	*0.6387 (76/119)*	*0.4697 (31/66)*	*0.8491 (45/53)*
	SC	*0.7410*	*0.7179 (28/39)*	*0.7375 (59/80)*	*0.7311 (87/119)*	*0.5714 (28/49)*	*0.8429 (59/70)*
	TMC	*0.7984*	*0.7576 (25/33)*	*0.7361 (53/72)*	*0.7429 (78/105)*	*0.5682 (25/44)*	*0.8689 (53/61)*
	CPM	*0.8663*	*0.8205 (32/39)*	*0.8375 (67/80)*	*0.8319 (99/119)*	*0.7111 (32/45)*	*0.9054 (67/74)*
	M-DAFM	*0.8013*	*0.6923 (27/39)*	*0.8000 (64/80)*	*0.7647 (91/119)*	*0.6279 (27/43)*	*0.8421 (64/76)*
Test set	*PCP*	*0.6874*	*0.6667 (10/15)*	*0.7931 (23/29)*	*0.7500 (33/44)*	*0.6250 (10/16)*	*0.8214 (23/28)*
	AP	*0.7356*	*0.6667 (10/15)*	*0.7931 (23/29)*	*0.7500 (33/44)*	*0.6250 (10/16)*	*0.8214 (23/28)*
	PVP	*0.6805*	*0.6667 (10/15)*	*0.7586 (22/29)*	*0.7273 (32/44)*	*0.5882 (10/17)*	*0.8148 (22/27)*
	SC	*0.7218*	*0.7333 (11/15)*	*0.6552 (19/29)*	*0.6818 (30/44)*	*0.5238 (11/21)*	*0.8261 (19/23)*
	TMC	*0.6224*	*0.6429 (9/14)*	*0.7143 (20/28)*	*0.6905 (29/42)*	*0.5294 (9/17)*	*0.8000 (20/25)*
	CPM	*0.6828*	*0.8667 (13/15)*	*0.6207 (18/29)*	*0.7045 (31/44)*	*0.5417 (13/24)*	*0.9000 (18/20)*
	M-DAFM	*0.7839*	*0.8000 (12/15)*	*0.6552 (19/29)*	*0.7045 (31/44)*	*0.5455 (12/22)*	*0.8636 (19/22)*
Test1 set	*PCP*	*0.7338*	*0.8333 (20/24)*	*0.6111 (11/18)*	*0.7381 (31/42)*	*0.7407 (20/27)*	*0.7333 (11/15)*
	AP	*0.6505*	*0.5833 (14/24)*	*0.7778 (14/18)*	*0.6667 (28/42)*	*0.7778 (14/18)*	*0.5833 (14/24)*
	PVP	*0.5764*	*0.7083 (17/24)*	*0.5000 (9/18)*	*0.6190 (26/42)*	*0.6538 (17/26)*	*0.5625 (9/16)*
	SC	*0.5463*	*0.9583 (23/24)*	*0.2222 (4/18)*	*0.6429 (27/42)*	*0.6216 (23/37)*	*0.8000 (4/5)*
	TMC	*0.7269*	*0.9583 (23/24)*	*0.4444 (8/18)*	*0.7381 (31/42)*	*0.6970 (23/33)*	*0.8889 (8/9)*
	CPM	*0.6528*	*0.8333 (20/24)*	*0.5556 (10/18)*	*0.7143 (30/42)*	*0.7143 (20/28)*	*0.7143 (10/14)*
	M-DAFM	*0.7454*	*0.6667 (16/24)*	*0.7778 (14/18)*	*0.7143 (30/42)*	*0.8000 (16/20)*	*0.6364 (14/22)*

SC, simple concatenation; TMC, trusted multi-view classification model; CPM, cross partial multi-view model; M-DAFM, multi-modal domain adaptive fusion model.

In summary, through quantitative visual comparisons and analyses from various perspectives, including AUC, NRI, and DCA, we found that M-DAFM demonstrates excellent performance in preoperative prediction of MVI. Based on these analytical results, it can be concluded that M-DAFM not only excels in predictive performance but also holds significant potential for clinical applications.

4 Discussion

The diagnosis of MVI can only be confirmed through postoperative pathological examination, while the preoperative diagnosis of MVI relies on liver biopsy (34). However, due to factors such as tumor heterogeneity and challenges in sample acquisition, preoperative liver biopsy faces several limitations (35). If it were possible to predict the status of MVI preoperatively, doctors could tailor personalized treatment plans for patients at an earlier stage, thereby improving patient survival rates.

With the application of deep learning in the medical field, there have been studies that use deep learning methods to construct deep models for the preoperative prediction of MVI (22–24). In clinical practice, CT images at different phases can reveal the tumor's vascular characteristics and its surrounding relationships at different time points. PCP images primarily display the basic anatomical features of the liver; AP images significantly enhance the detection of hepatic arterial blood flow, and PVP images can detect the blood flow and vascular distribution in the portal vein of the liver. Therefore, finding an objective and efficient way to integrate multi-phase image information, complementing the characteristics of each phase, may prove effective for diagnosis. This study innovatively predicts MVI by constructing the M-DAFM, which combines effective information from PCP, AP, and PVP modalities. Experimental validation demonstrates the superiority of multi-modal image fusion.

Comparative experiments with different classifiers reveal, as shown in Tables 2, 3, that ESBELM performs the best in classifying MVI. This is possibly because CT image data often contain complex features and non-linear relationships, such as tumor morphology, texture, and vascular distribution. In contrast, ERF is insensitive to complex non-linear relationships, ELM is prone to overfitting when dealing with complex data, while ESBELM, by introducing ensemble strategies and Bayesian optimization algorithms,

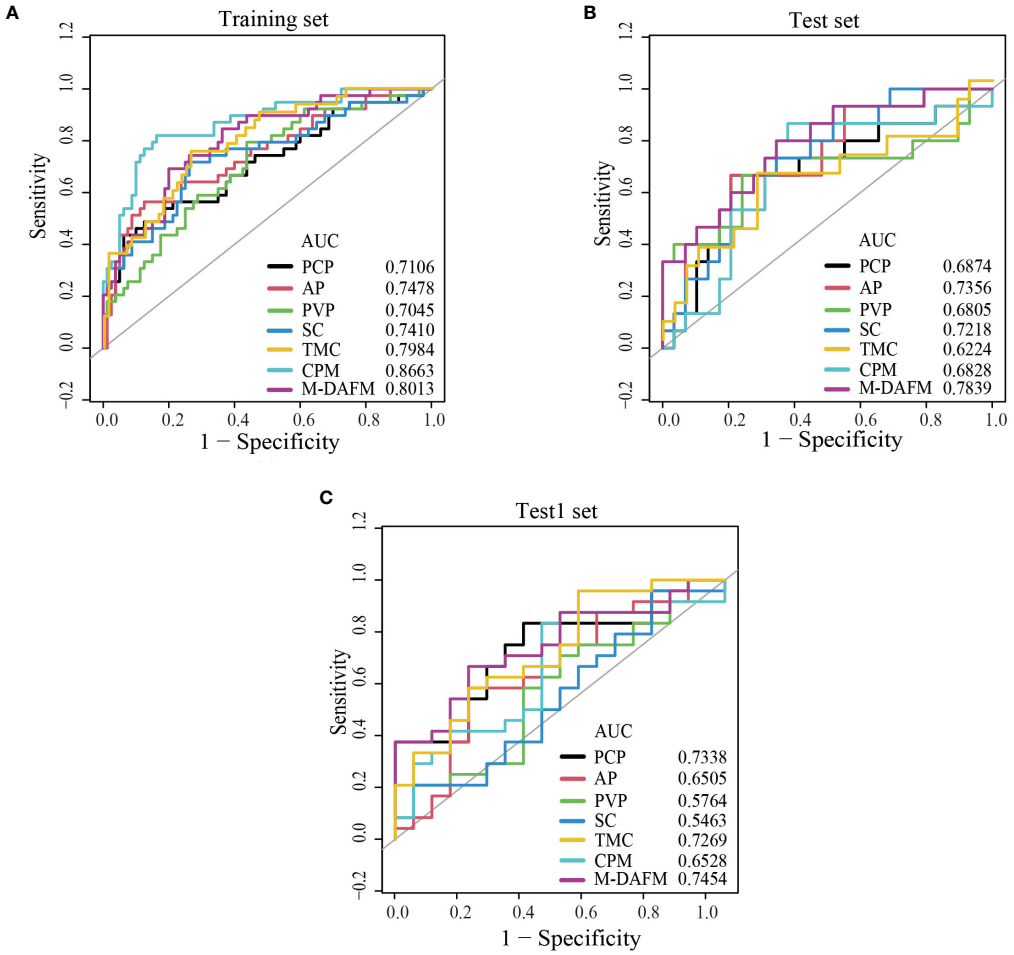

FIGURE 2
ROC curves of PCP, AP, PVP, SC, TMC, CPM models, and M-DAFM on the training **(A)**, test **(B)** and test1 **(C)** sets. SC, simple concatenation; TMC, trusted multi-view classification model; CPM, cross partial multi-view model. M-DAFM, multi-modal domain adaptive fusion model.

enhances its ability to handle high-dimensional and non-linear relationships while mitigating model overfitting.

Comparative experiments between single-modal models and multi-modal fusion models: As shown in Figure 2 and Table 4, M-DAFM demonstrates superior performance in preoperative MVI prediction (The AUC values for the training set, test set, and Test1 set are 0.8013, 0.7839, and 0.7454, respectively). This could be attributed to the successful reduction of inter-modal differences by M-DAFM, allowing the model to better leverage complementary information from each modality for preoperative MVI prediction. In contrast, the performance of single-modal models (PCP, AP, PVP) in this aspect is significantly lower than that of M-DAFM, possibly due to the limited effective information provided by a single CT modality image, restricting the performance of single-modal models in preoperative MVI prediction tasks.On the other hand, the performance of SC in preoperative MVI prediction is relatively average, and even its predictive performance in the test set and Test1 set is inferior to some single-modal models. This may be because each modality typically predicts MVI from different perspectives, and SC does not consider the correlation between modalities, leading to negative interactions between modalities and affecting the predictive performance of SC.Regarding TMC and CPM, although they also integrate information from multiple modalities, the strategies adopted by these models may struggle to effectively distinguish between valuable information and noise within CT images, which often contain rich and complex microscopic information, encompassing multi-level structures of

TABLE 5 NRI comparison of M-DAFM with AP, PCP, PVP, TMC, CPM and SC models in the test set.

Model 1 / Model 2		All-phase
M-DAFM	*PCP*	*NRI [95% CI]: 0.4805 [0.1393 - 0.8216] –P<0.05*
	AP	*NRI [95% CI]: 0.3471 [0.006 - 0.6882] – P<0.05*
	PVP	*NRI [95% CI]: 0.5379 [0.1416 - 0.9342] –P<0.05*
	SC	*NRI [95% CI]: 0.3816 [0.0396 - 0.7237] –P<0.05*
	TMC	*NRI [95% CI]: 0.1556 [-0.2049 - 0.516] –P=0.39*
	CPM	*NRI [95% CI]: 0.4092 [0.0798 - 0.7386] –P<0.05*

SC, simple concatenation; TMC, trusted multi-view classification model; CPM, cross partial multi-view model; M-DAFM, multi-modal domain adaptive fusion model.

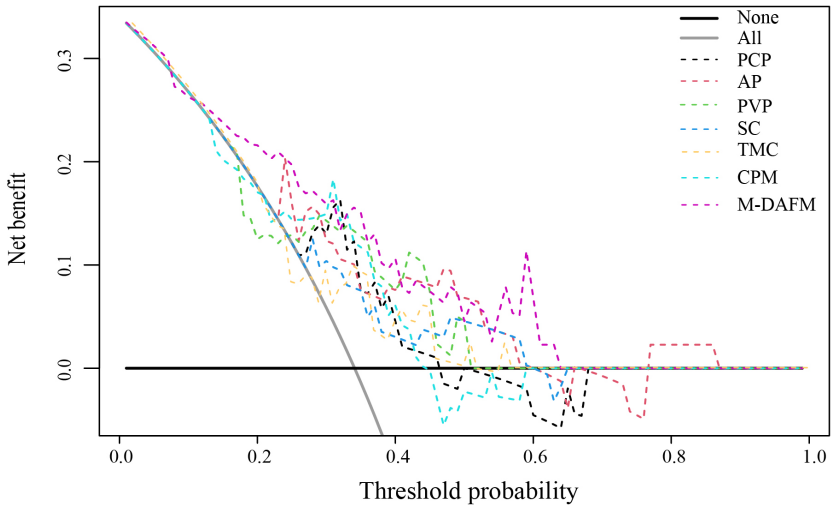

FIGURE 3
Decision curve analysis (DCA) of PCP, AP, PVP, SC, TMC, CPM models, and M-DAFM on the test set. SC, simple concatenation; TMC, trusted multi-view classification model; CPM, cross partial multi-view model. M-DAFM, multi-modal domain adaptive fusion model.

tumor lesions. This difficulty in effective discrimination may result in suboptimal predictive performance for these models.

The method proposed in this paper for preoperative prediction of MVI has three advantages in clinical practice:1) In terms of tumor segmentation, we employ a semi-automatic segmentation algorithm that only requires radiologists to perform rough segmentation of the tumor area. This significantly reduces the workload for radiologists in tumor segmentation, while reducing subjective interventions during the segmentation process. Consequently, it enhances the consistency and repeatability of the final results.2) Regarding feature extraction, we utilize a convolutional neural network for automatic, accurate, and objective extraction of specific features from the tumor region.3) In clinical practice, doctors often employ various methods for disease diagnosis. Inspired by this, our study considers the PCP, AP, and PVP of CT images as three distinct modalities. Using a domain adaptation approach, we design a multimodal fusion network to build a more robust and accurate preoperative prediction model, which holds practical significance.

This retrospective study has certain limitations. Firstly, the extensive time span of data collection may introduce variations in data quality. However, our experimental results demonstrate the effectiveness of the proposed method, highlighting the robustness of M-DAFM. Further improvements in data quality may enhance the model's performance. Secondly, this study lacks multi-center CT image data for further validation of the model's universality. Lastly, this study only explores the diagnostic performance of deep learning models, which enhances practical portability but may compromise accuracy. As for analyzing clinical models as a single modality within the multi-modal fusion model, we will continue to investigate in our future research.

5 Conclusions

This study introduces a novel approach for preoperative MVI prediction by effectively integrating information from multi-phase CT images through mitigating the distribution differences between different modalities.

Data availability statement

The original contributions presented in the study are included in the article/Supplementary Material. Further inquiries can be directed to ZY, 1023494842@qq.com.

Ethics statement

The studies involving humans were approved by the institutional review board of Jiangmen Central Hospital, which waived the requirement for written informed consent for participation. The studies were conducted in accordance with the local legislation and institutional requirements.

Author contributions

ZY: Conceptualization, Methodology, Writing – original draft. YL: Conceptualization, Methodology, Writing – review & editing. XD: Conceptualization, Supervision, Writing – review & editing. EC: Conceptualization, Data curation, Writing – review & editing. JC: Data curation, Investigation, Writing – review & editing. CM: Conceptualization, Data curation, Writing – review & editing.

Funding

The author(s) declare financial support was received for the research, authorship, and/or publication of this article. This work was supported by the National Natural Science Foundation of China (81960324, 12261027) and Guangdong Basic and Applied Basic Research Foundation [2021A1515220080].

Conflict of interest

The authors declare that the research was conducted in the absence of any commercial or financial relationships that could be construed as a potential conflict of interest.

Publisher's note

Supplementary material

The Supplementary Material for this article can be found online at: https://www.frontiersin.org/articles/10.3389/fonc.2024.1332188/full#supplementary-material

References

1. Lee S, Kim SH, Lee JE, Sinn DH, Park CK. Preoperative gadoxetic acid–enhanced MRI for predicting microvascular invasion in patients with single hepatocellular carcinoma. *J Hepatol* (2017) 67(3):526–34. doi: 10.1016/j.jhep.2017.04.024

2. Xu X, Zhang HL, Liu QP, Sun SW, Zhang J, Zhu FP, et al. Radiomic analysis of contrast-enhanced CT predicts microvascular invasion and outcome in hepatocellular carcinoma. *J Hepatol* (2019) 70(6):1133–44. doi: 10.1016/j.jhep.2019.02.023

3. Gao F, Qiao K, Yan B, Wu M, Wang L, Chen J, et al. Hybrid network with difference degree and attention mechanism combined with radiomics (H-DARnet) for MVI prediction in HCC. *Magnetic Resonance Imaging* (2021) 83:27–40. doi: 10.1016/j.mri.2021.06.018

4. Hong SB, Choi SH, Kim SY, Shim JH, Lee SS, Byun JH, et al. MRI features for predicting microvascular invasion of hepatocellular carcinoma: a systematic review and meta-analysis. *Liver Cancer* (2021) 10(2):94–106. doi: 10.1159/000513704

5. Benson AB, D'Angelica MI, Abbott DE, Anaya DA, Anders R, Are C, et al. Hepatobiliary cancers, version 2.2021, NCCN clinical practice guidelines in oncology. *J Natl Compr Cancer Network* (2021) 19(5):541–65. doi: 10.6004/jnccn.2021.0022

6. Sumie S, Nakashima O, Okuda K, Kuromatsu R, Kawaguchi A, Nakano M, et al. The significance of classifying microvascular invasion in patients with hepatocellular carcinoma. *Ann Surg Oncol* (2014) 21:1002–9. doi: 10.1245/s10434-013-3376-9

7. Yang L, Gu D, Wei J, Yang C, Rao S, Wang W, et al. A radiomics nomogram for preoperative prediction of microvascular invasion in hepatocellular carcinoma. *Liver Cancer* (2018) 8(5):373–86. doi: 10.1159/000494099

8. Yamashita YI, Tsuijita E, Takeishi K, Fujiwara M, Kira S, Mori M, et al. Predictors for microinvasion of small hepatocellular carcinoma≤ 2 cm. *Ann Surg Oncol* (2012) 19:2027–34. doi: 10.1245/s10434-011-2195-0

9. Shindoh J, Andreou A, Aloia TA, Zimmitti G, Lauwers GY, Laurent A, et al. Microvascular invasion does not predict long-term survival in hepatocellular carcinoma up to 2 cm: reappraisal of the staging system for solitary tumors. *Ann Surg Oncol* (2013) 20:1223–9. doi: 10.1245/s10434-012-2739-y

10. Erstad DJ, Tanabe KK. Prognostic and therapeutic implications of microvascular invasion in hepatocellular carcinoma. *Ann Surg Oncol* (2019) 26:1474–93. doi: 10.1245/s10434-019-07227-9

11. Zhang X, Li J, Shen F, Lau WY. Significance of presence of microvascular invasion in specimens obtained after surgical treatment of hepatocellular carcinoma. *J Gastroenterol Hepatol* (2018) 33(2):347–54. doi: 10.1111/jgh.13843

12. Min JH, Lee MW, Park HS, Lee DH, Park HJ, Lim S. Interobserver variability and diagnostic performance of gadoxetic acid–enhanced MRI for predicting microvascular invasion in hepatocellular carcinoma. *Radiology* (2020) 297(3):573–81. doi: 10.1148/radiol.2020201940

13. Lewin M, Laurent-Bellue A, Desterke C, Radu A, Feghali JA, Farah J, et al. Evaluation of perfusion CT and dual-energy CT for predicting microvascular invasion of hepatocellular carcinoma. *Abdominal Radiol* (2022) 47(6):2115–27. doi: 10.1007/s00261-022-03511-7

14. He M, Zhang P, Ma X, He B, Fang C, Jia F. Radiomic feature-based predictive model for microvascular invasion in patients with hepatocellular carcinoma. *Front Oncol* (2020) 10:574228. doi: 10.3389/fonc.2020.574228

15. Gao L, Xiong M, Chen X, Han Z, Yan C, Ye R, et al. Multi-region radiomic analysis based on multi-sequence MRI can preoperatively predict microvascular invasion in hepatocellular carcinoma. *Front Oncol* (2022) 12:818681. doi: 10.3389/fonc.2022.818681

16. Ni M, Zhou X, Lv Q, Li Z, Gao Y, Tan Y, et al. Radiomics models for diagnosing microvascular invasion in hepatocellular carcinoma: which model is the best model? *Cancer Imaging* (2019) 19:1–10. doi: 10.1186/s40644-019-0249-x

17. Wang W, Chen Q, Iwamoto Y, Aonpong P, Lin L, Hu H, et al. Deep fusion models of multi-phase CT and selected clinical data for preoperative prediction of early recurrence in hepatocellular carcinoma. *IEEE Access* (2020) 8:139212–20. doi: 10.1109/access.2020.3011145

18. Krizhevsky A, Sutskever I, Hinton GE. Imagenet classification with deep convolutional neural networks. *Communications of the ACM* (2017) 60(6):84–90. doi: 10.1145/3065386

19. Liu Z, Mao H, Wu CY, Feichtenhofer C, Darrell T, Xie S. (2022). A convnet for the 2020s, in: *Proceedings of the IEEE/CVF conference on computer vision and pattern recognition*. New Orleans, LA, USA: Institute of Electrical and Electronics Engineers (IEEE), pp. 11976–86. doi: 10.1109/CVPR52688.2022.01167

20. He K, Zhang X, Ren S, Sun J. (2016). Deep residual learning for image recognition, in: *Proceedings of the IEEE conference on computer vision and pattern recognition*. Las Vegas, NV, USA: Institute of Electrical and Electronics Engineers (IEEE), pp. 770–8. doi: 10.1109/cvpr.2016.90

21. He K, Chen X, Xie S, Li Y, Dollár P, Girshick R. (2022). Masked autoencoders are scalable vision learners, in: *Proceedings of the IEEE/CVF conference on computer vision and pattern recognition*. New Orleans, LA, USA: Institute of Electrical and Electronics Engineers (IEEE), pp. 15979–88. doi: 10.1109/CVPR52688.2022.01553

22. Yasaka K, Akai H, Abe O, Kiryu S. Deep learning with convolutional neural network for differentiation of liver masses at dynamic contrast-enhanced CT: a preliminary study. *Radiology* (2018) 286(3):887–96. doi: 10.1148/radiol.2017170706

23. Wang K, Lu X, Zhou H, Gao Y, Zheng J, Tong M, et al. Deep learning Radiomics of shear wave elastography significantly improved diagnostic performance for assessing liver fibrosis in chronic hepatitis B: a prospective multicentre study. *Gut* (2019) 68(4):729–41. doi: 10.1136/gutjnl-2018-316204

24. Liu SC, Lai J, Huang JY, Cho CF, Lee PH, Lu MH, et al. Predicting microvascular invasion in hepatocellular carcinoma: a deep learning model validated across hospitals. *Cancer Imaging* (2021) 21:1–16. doi: 10.1186/s40644-021-00425-3

25. Jiang YQ, Cao SE, Cao S, Chen JN, Wang GY, Shi WQ, et al. Preoperative identification of microvascular invasion in hepatocellular carcinoma by XGBoost and deep learning. *J Cancer Res Clin Oncol* (2021) 147:821–33. doi: 10.1007/s00432-020-03366-9

26. Rodriguez-Peralvarez M, Luong TV, Andreana L, Meyer T, Dhillon AP, Burroughs AK. A systematic review of microvascular invasion in hepatocellular carcinoma: diagnostic and prognostic variability. *Ann Surg Oncol* (2013) 20:325–39. doi: 10.1245/s10434-012-2513-1

27. Herath S, Harandi M, Porikli F. (2017). Learning an invariant hilbert space for domain adaptation, in: *Proceedings of the IEEE conference on computer vision and pattern recognition*. Honolulu, HI, USA: Institute of Electrical and Electronics Engineers (IEEE), pp. 3845–54. doi: 10.1109/cvpr.2017.421

28. Dührkop K, Nothias LF, Fleischauer M, Reher R, Ludwig M, Hoffmann MA, et al. Systematic classification of unknown metabolites using high-resolution fragmentation mass spectra. *Nat Biotechnol* (2021) 39(4):462–71. doi: 10.1101/2020.04.17.046672

29. Peng H, Long F, Ding C. Feature selection based on mutual information criteria of max-dependency, max-relevance, and min-redundancy. *IEEE Trans Pattern Anal Mach Intell* (2005) 27(8):1226–38. doi: 10.1109/tpami.2005.159

30. Gretton A, Borgwardt KM, Rasch MJ, Schölkopf B, Smola A. A kernel two-sample test. *J Mach Learn Res* (2012) 13(1):723–73. doi: 10.5555/2503308.2188410

31. Huang GB, Zhu QY, Siew CK. Extreme learning machine: theory and applications. *Neurocomputing* (2006) 70(1-3):489–501. doi: 10.1016/j.neucom.2005.12.126

32. Han Z, Zhang C, Fu H, Zhou JT. Trusted multi-view classification with dynamic evidential fusion. *IEEE Trans Pattern Anal Mach Intell* (2022) 45(2):2551–66. doi: 10.1109/TPAMI.2022.3171983

33. Zhang C, Han Z, Fu H, Zhou JT, Hu Q. CPM-Nets: Cross partial multi-view networks. *Adv Neural Inf Process Syst* (2019) 32:559–69. doi: 10.5555/3454287.3454338

34. Sheng H, Mao M, Huang K, Zheng H, Liu W, Liang Y. A clinical tool to predict the microvascular invasion risk in patients with hepatocellular carcinoma. *Technol Cancer Res Treat* (2023) 22:15330338231182526. doi: 10.1177/15330338231182526

35. Hu HT, Wang Z, Huang XW, Chen SL, Zheng X, Ruan SM. Ultrasound-based radiomics score: a potential biomarker for the prediction of microvascularinvasion in hepatocellular carcinoma. *Eur Radiol* (2019) 29:2890–901. doi: 10.1007/s00330-018-5797-0

10.3389/fonc.2024.1332188

Glossary

CT	Computed tomography
PCP	Pre-contrast phase
AP	Arterial phase
PVP	Portal venous phase
CNN	Convolutional neural networks
ROI	Region of interest
MVI	Microvascular invasion
HCC	Hepatocellular carcinoma
M-DAFM	Multi-modal domain adaptive fusion model
SC	Simple connection
TMC	Trusted multi-view classification model
CPM	Cross partial multi-view model
MRMR	Maximum relevance minimum redundancy
MMD	Maximum mean discrepancy
NRI	Net reclassification improvement
PPV	Positive predictive value
NPV	Negative predictive value
ELM	Extreme learning machine
ERF	Ensemble random forest
ESBELM	Ensemble sparse Bayesian extreme learning machine
AUC	Area under the receiver operating characteristic curve
ROC	Receiver operating characteristic
DCA	Decision curve analysis

frontiers | Frontiers in Oncology

TYPE Systematic Review
PUBLISHED 16 February 2024
DOI 10.3389/fonc.2024.1344798

OPEN ACCESS

EDITED BY
Francisco Tustumi,
University of São Paulo, Brazil

REVIEWED BY
Jiqiao Zhu,
Capital Medical University, China
Abdullah Esmail,
Houston Methodist Hospital, United States
Phillipe Abreu,
Jackson Health System, United States

*CORRESPONDENCE
Henry W. C. Leung
070506@tool.caaumed.org.tw
Agnes L. F. Chan
agnes.lf@gmail.com

†These authors share first authorship

RECEIVED 26 November 2023
ACCEPTED 16 January 2024
PUBLISHED 16 February 2024

CITATION
Leung JH, Wang S-Y, Leung HWC and Chan ALF (2024) Comparative efficacy and safety of multimodality treatment for advanced hepatocellular carcinoma with portal vein tumor thrombus: patient-level network meta-analysis.
Front. Oncol. 14:1344798.
doi: 10.3389/fonc.2024.1344798

Comparative efficacy and safety of multimodality treatment for advanced hepatocellular carcinoma with portal vein tumor thrombus: patient-level network meta-analysis

John Hang Leung[1†], Shyh-Yau Wang[2†], Henry W. C. Leung[3*] and Agnes L. F. Chan[4*]

[1]Department of Obstetrics and Gynecology, Ditmanson Medical Foundation Chia-Yi Christian Hospital, Chiayi, Taiwan, [2]Department of Radiology, An-Nan Hospital, China Medical University, Tainan, Taiwan, [3]Department of Radiation Oncology, An-Nan Hospital, China Medical University, Tainan, Taiwan, [4]Department of Pharmacy, An-Nan Hospital, China Medical University, Tainan, Taiwan

Background: Portal vein tumor thrombus (PVTT) is a common complication and an obstacle to treatment, with a high recurrence rate and poor prognosis. There is still no global consensus or standard guidelines on the management of hepatocellular carcinoma (HCC) with PVTT. Increasing evidence suggests that more aggressive treatment modalities, including transarterial chemoembolization, radiotherapy, targeted therapy, and various combination therapies, may improve the prognosis and prolong the survival of advanced hepatocellular carcinoma (aHCC) patients with PVTT. We aim to comprehensively review and compare the efficacy and safety of these advanced options for aHCC with PVTT.

Methods: A comprehensive literature search was conducted on PubMed and EMBASE for phase II or III randomized controlled trials (RCTs) investigating multimodality treatments for aHCC with PVTT. Kaplan–Meier curves for overall survival (OS) and progression-free survival were constructed to retrieve individual patient-level data to strengthen the comparison of the benefits of all multimodality treatments of interest. Each study was pooled in a fixed-effects network meta-analysis (NMA). We also conducted subgroup analyses using risk ratios extracted from each study, including viral etiology, Barcelona Clinic Liver Cancer (BCLC) staging, alpha-fetoprotein (AFP) levels, macrovascular invasion or portal vein tumor thrombosis, and extrahepatic spread. Multimodality treatments were ranked using SUCRA scores.

Results: We identified 15 randomized controlled trials with 16 multimodality regimens that met the inclusion criteria. Among them, 5,236 patients with OS results and 5,160 patients with PFS results were included in the analysis. The hepatic arterial infusion chemotherapy of fluorouracil, leucovorin, and oxaliplatin (HAIC-FO) showed OS and PFS benefits over all the other therapies. In terms of OS, HAIC-FO, nivolumab, and TACE+Len were superior to sorafenib, lenvatinib, and donatinib monotherapies, as well as HAIC-FO+Sor. In terms of PFS, TACE +Len showed better benefits than lenvatinib, donatinib, and tremelimumab +durvalumab. A low heterogeneity (I^2 < 50%) and consistency were observed.

The SUCRA score for OS ranked HAIC-FO+sorafenib as the best treatment option among all multimodality treatments in hepatitis B, MVI, or PVTT with EHS and AFP 400 μg/L subgroups.

Conclusion: HAIC-FO and HAIC-FO+sorafenib are statistically better options for unresectable hepatocellular carcinoma with PVTT among the multimodality treatments, and their effective and safe implementation may provide the best outcomes for HCC-PVTT patients.

KEYWORDS

patient-level NMA, multimodality treatments, hepatic arterial infusion chemotherapy, advanced or metastatic hepatocellular carcinoma, portal vein tumor thrombosis

Introduction

Hepatocellular carcinoma (HCC) is one of the most common types of primary liver cancer and the third leading cause of cancer mortality, with an estimated 830,180 deaths worldwide in 2020. In Taiwan, liver and intrahepatic cholangiocarcinoma and hepatocellular carcinoma (HCC) were ranked as the second leading causes of cancer death in 2020 (1). The symptoms of early HCC are often imperceptible, and approximately 70%–80% of patients are diagnosed at an advanced stage (2). In HCC involving the invasion of intrahepatic blood vessels (portal or hepatic vein branches), patients are less tolerant to treatment and only survive for approximately 2–4 months without treatment (3, 4). Studies have found that HCC prognosis is related to the presence and extent of portal vein tumor thrombus (PVTT) (5). In addition, PVTT extension in hepatitis B virus-related HCC may involve genetic abnormalities of KDM6A, CUL9, FDG6, AKAP3, RNF139, etc. (6) Therefore, PVTT is an independent risk factor associated with a disappointing prognosis in HCC patients.

According to the Barcelona liver cancer staging system (BCLC staging), HCC with PVTT is classified as BCLC C stage. The only treatment that patients can benefit from is oral sorafenib; however, in China, Europe, and the United States, the median survival time is only 3 to 6 months and approximately 6 to 9 months (7–9). However, the BCLC staging system does not clarify the extent of PVTT, which is significantly associated with prognosis after treatment. Currently, there are only two detailed classification systems recognized globally, namely, the Chinese Cheng's classification and the Japanese Liver Cancer Study Group's VP staging classification system, which divide PVTT into several subgroups (10). Depending on the degree of PVTT, patients may select surgical resection, which may provide a better survival benefit. However, numerous studies have demonstrated that postoperative 5-year survival ranges from 10% to 59% (11–13). Approximately 44%–62% of patients with HCC will develop PVTT, and only a few of them will undergo a curative operation after being carefully selected. Thus, in many cases, non-operative treatment is the only available treatment option in actual clinical practice; non-operative treatment includes transarterial chemoembolization (TACE), transarterial radioembolization (TARE), hepatic arterial infusion chemotherapy (HAIC), sorafenib therapy, and radiotherapy (RT). Combinations of these treatments have also been used to improve outcomes.

Recently, HAIC combined with systemic therapies, such as sorafenib, lenvatinib, and programmed cell death protein-1 (PD-1), has been used in advanced hepatocellular carcinoma (aHCC) in phase II and III randomized controlled trials and clinical trials, and the results have shown its superiority to sorafenib monotherapy (14–19). HAIC is now accepted as a treatment option for unresectable HCC and is promoted in the clinical setting (20–22). In addition, HAIC and lenvatinib may also induce significant local immune modulation in the intrahepatic tumor microenvironment and increase the infiltration of T lymphocytes in the immunosuppressive microenvironment of HCC (23). Therefore, HAIC has been combined with several therapeutic agents and modalities, including multikinase inhibitors, immunotherapy to augment its treatment efficacy. Therefore, we performed a network meta-analysis (NMA) to comprehensively review and compare the efficacy and toxicity of these newer multimodal treatments for advanced hepatocellular carcinoma and PVTT subgroups.

Materials and methods

Search strategy

We performed a systematic literature search of PubMed and EMBASE databases for phase II or phase III randomized controlled trials (RCTs) investigating any targeted therapy, immunotherapy, and HAIC used alone or in combination with systemic or local therapy for the treatment of aHCC patients who had no prior history of systemic therapy. The detailed search strategies are described in the Supplementary Materials (online only). From the selected articles, we manually searched for additional references to

identify potentially overlooked studies. This study was conducted in accordance with the Preferred Reporting Items for Systematic Reviews and Meta-Analyses (PRISMA) guidelines (24).

Selection criteria

All trials had to meet the following criteria for inclusion: trials had to 1) be phase II or III RCTs comparing monotherapies or combination therapies of atezolizumab–bevacizumab, nivolumab, sorafenib, lenvatinib, tremelimumab+durvalumab, durvalumab, cabozantinib+atezolizumzb, donatinib, sintilimab+bevacizumab biosimilar (BevBiol), HAIC-FOLFOX (FO), HAIC plus sorafenib (HAICSor), HAIC-FO+sorafenib, TACE+lenvatinib (Len), or TACE+radiotherapy (RT), published in English from 1 January 2018 to 31 June 2022; 2) include patients with pathologically proven advanced inoperable HCC with PVTT, Barcelona Clinic Liver Cancer (BCLC) stage B or C; 3) have detailed data on methods, the characteristics of the patient population, overall survival, progression-free survival, and the disease control rate; 4) compare at least two arms that consisted of the abovementioned regimens of interest; 5) define and evaluate the disease control rate based on a comparison of abdominal computed tomography or magnetic resonance imaging before and after treatment according to the modified Response Evaluation Criteria in Solid Tumors (mRECIST) guidelines for HCC (25); and 6) present the results of severe adverse events (SAEs), defined as ≥grade 3 adverse events. Among the several publications from the same trial, only the latest or complete publication data were selected. Case reports, case series, and reviews were excluded.

Data extraction

All eligible studies were reviewed and screened by two independent reviewers based on the study selection criteria described above. Any discrepancy was adjudicated by a third reviewer. Data from all eligible studies were extracted and summarized in a standardized table, including the study's first author; characteristics of the population; intervention; vascular invasion; and outcomes in terms of PFS, overall survival (OS), and SAEs. In addition, we extracted primary outcome data from a subgroup of aHCC patients after we manually screened and appraised studies that did not only include PVTT aHCC patients.

Quality assessment of the literature

The quality of the included studies was assessed by two independent investigators using the GRADE method of the Cochrane Collaboration's tools for assessing the risk of bias, which comprises six domains: selection bias, performance bias, detection bias, attrition bias, reporting bias, and other biases. Each domain was explicitly assessed as having a low risk of bias, a high risk of bias, or an unclear risk of bias (defined as a lack of information or bias uncertainty). The risk of publication bias presented in the form of a funnel plot assesses bias in terms of the overall clinical efficacy rate using Review Manager (RevMan) software version 5.4.1 (26).

Extraction of individual patient data

Due to the rapid advancement and novel modalities recently used in the field of aHCC treatment and the complexity of HCC etiology, more precise statistical methods are needed to make comparisons between different modalities. Therefore, a graphical reconstructive algorithm outlined by Guyot et al. (27, 28) was employed to obtain the PFS and OS data of individual patients (IPD) in each trial arm by using WebPlotDigitizer to digitize the Kaplan–Meier curves from the included studies. An IPD network meta-analysis is recognized as the gold standard approach for evidence synthesis (29, 30).

Data analysis

This NMA included a comparison of direct and indirect treatments, and it comprehensively compared the efficacy and safety of 15 novel molecularly targeted drugs (MTDs), immunotherapy, HAIC, and their combination in the treatment of aHCC with PVTT (10–17, 31–37). All analyses were performed using the Bayesian Markov Chain Monte Carlo method in WinBUGS 1.4.3 (MRC Biostatistics Unit, Cambridge, and Imperial College School of Medicine, London, UK) and NetMetaXL (version 1.6.1) (38).

Network meta-analysis

A network map of 16 multimodality regimens is shown in Supplementary Figure 1. Each node represents a regimen, and the node size is proportional to the sample size. The connecting lines represent comparisons between regimens, and the thickness of the lines is proportional to the number of studies compared. The main primary outcomes were OS, PFS, and SAEs. Bayesian Markov Chain Monte Carlo methods were used to make indirect comparisons of OS, PFS, and SAEs between the modalities of interest, and the results are presented in league tables. The relative risk of SAEs between the different regimens is presented as the odds ratio (OR) and corresponding 95% CI, with an OR >1 indicating a higher risk of SAEs than the other regimens. Cochran's Q statistic from the fixed-effect NMA model can be decomposed into within-design heterogeneity (Q^{het}) and between-design heterogeneity, which is termed design inconsistency (Qinc). DIC statistics comparison in fitted consistency and inconsistency models can be used to assess between-design heterogeneity (39). The I^2 test was used to assess within-study heterogeneity, with values of <50%, 50%–75%, and >75% being considered low, moderate, and considerable, respectively (40, 41).

We also conducted subgroup analyses to assess differences in OS according to HCC etiology (HBV) and the presence of PVTT or macrovascular invasion (MVI) and/or extrahepatic spread (EHS). RCTs without subgroup data were excluded, such as the Scoop-2 trial performed by Kondo et al.

Multimodality treatments were ranked according to their probability of being the best treatment based on the SUCRA score, which was calculated using the formula described in Salanti, Ades, and Ioannidis (2011) (42). The SUCRA values were obtained from the distribution of ranking probabilities. The higher the SUCRA value and close to 100%, the higher the treatment ranking in the network.

Sensitivity analysis

We re-ran the model to compare the results by including and excluding one study with a potential high risk of bias, with forest plots describing the effect estimates for the paired multimodality regimens in the sensitivity analysis.

Results

Characteristics of the included RCTs

Fifteen RCTs containing 16 modality regimens with a total of 5,638 patients and 5,562 patients with OS and PFS results were identified through searches of the PubMed and EMBASE electronic databases (online Supplementary Figure 2). The study and patient characteristics are presented in Table 1 (14–17, 31–37, 43–47).

Among all the studies, 12 studies were phase III randomized clinical trials, 2 were phase II RCTs, and 2 were RCTs. The publication years of the included studies ranged from 2018 to 2023, with updated outcome data. The median age of the patients was 49 to 72 years old. The age of the patients in the Scoop-2 phase II trial was slightly higher (72.0 ± 7.0) than in the other studies. All studies were conducted in the Asia-Pacific region, comprising 20 countries; therefore, they included patients from the Asia-Pacific, European, and North American regions. The patients from the Asia-Pacific region represented 67% in REFLECT, 50.4% in IMbrave150, and 40% in CheckMate 459. The proportion of patients with HBV ranged from 8.6% to 94%, while 1.5%–32% had HCV. In total, 5 of the 15 RCTs included patients with 100% PVTT. The percentage of patients with PVTT in the remaining RCTs ranged from 19% to 80% (Table 1). The probabilities of SAEs are presented in a heatmap in Figure 1.

Overall survival

HAIC-FO showed a statistically significant OS benefit over all modalities of interest, except for nivolumab, TACE+Len, TACE +Sor, tremelimumab+Dur, and Ate+Bev. Three modalities were superior to sorafenib: HAIC-FO (OR = 0.28, 95% CI = 0.11–0.64), nivolumab (OR = 0.54, 95% CI = 0.36–0.79), and TACE+Len (OR = 0.78, 95% CI = 0.66–0.92) (Table 2). A low heterogeneity (I^2 = 38%) and no evidence of inconsistency (each study data point must have a posterior mean deviance contribution of approximately 1) were observed, indicating consistency (Supplementary Figures 3B).

Figures 2, 3 are pooled reconstructed Kaplan–Meier curves of the OS of monotherapies and combined transarterial therapies. A visual examination of Figure 2 shows that durvalumab and nivolumab provide long-term benefits over sorafenib, donatinib, and lenvatinib, and tremelimumab+Dur also shows long-term benefits relative to the other combination regimens shown in Figure 3.

Progression-free survival

HAIC-FO was significantly superior to all modalities of interest, except for TACE+Len (OR = 0.42, 95% CI = 0.13–1.32), HAIC+Sor (OR = 0.41, 95% CI = 0.13–1.21), and TACE+Sor (OR = 0.49, 95% CI = 0.10–2.37) (Table 2). TACE+Len and HAIC+Sor were significantly better than lenvatinib, durvalumab, and tremelimumab+durvalumab. In addition, donatinib was also favored over durvalumab (OR = 0.54, 95% CI = 0.32–0.90) and tremelimumab+Dur (OR = 0.45, 95% CI = 0.27–0.77). A low heterogeneity (I^2 = 9%) and no evidence of inconsistency (each study data point must have a posterior mean deviance contribution of approximately 1) were observed, indicating consistency (Supplementary Figures 4A). Kaplan–Meier curves of the PFS of the monotherapy regimens and combination regimens and pooled plots of the PFS and OS of all multimodality regimes are shown in Supplementary Figures 5–8.

Online Supplementary Figure 9 shows the SUCRA score plot for OS versus PFS. HAIC-FO ranked higher in OS and PFS, while HAIC+sorafenib had a higher ranking in PFS (SUCRA score: 0.7893) than OS (SUCRA score: 0.3313).

Quality assessment of the studies

Figure 4 shows the risk of bias in the 15 RCTs included in this network meta-analysis. All included studies were determined to have high-quality evidence according to the criteria for risk of bias using the GRADE method, with all reporting random sequence generation and concealed allocation. No studies reported the blinding of participants and personnel. Four studies clearly mentioned specific methods used for the blinding of the outcome assessor. Overall, study quality was assessed as high because of the low heterogeneity determined based on I^2 <50% (9% for PFS; 38% for OS) (Supplementary Figure 7), and no inconsistency was observed because all studies were along the line of equality (Supplementary Figure 4).

Regarding the funnel plot for the assessment of publication bias in the network meta-analysis (Figure 5), the central line suggests the null hypothesis that study-specific effect sizes do not differ from the respective comparison-specific pooled effect estimates. The dots in different colors represent the comparisons of different regimens. All

TABLE 1 Baseline characteristics of the population included in the clinical trials of interests.

	Study	Treatment (*n*)	Study design	Median age	Etiology HBV/ HCV	BCLC stage B/C, *N*	PVTT, *N* (%)	Extrahepatic metastasis, *N* (%)	Serum AFP ≧400 g/mL (*N*)	Primary outcomes	Tx cycles median	Treatment duration (weeks)
	PD-1 inhibitor+anti-VEGF vs. sorafenib											
1	**Cheng 2022** (43) ※	Ate+Bev = 336 Sorafenib = 165	Phase III	64 (56–71) 66 (59–71)	129/48; 62/26	B/C: 52/ 276 B/C: 26/133	129 (38) 71 (43)	212 (63) 93 (56)	126 61	PFS, OS, SAE	Ate: 5 Bev 4	6
	HAIC vs. sorafenib											
2	**Lyu, 2022** (32) **FOHAIC-1※**	HAIC = 130 Sorafenib = 132	Phase III	54 (45–61) 53 (45–62)	120/2 114/4	B/C: 5/ 125 B/C: 9/123	82 (55.8) 80 (54.4)	75 (51) 80 (54.4)	69 64	PFS, OS, SAE	HAIC: 8	10.4 (HAIC) 14 (sorafenib)
3	**Choi, 2018** (31) ※	HAIC = 29 Sorafenib = 29	Randomized prospective	60.3 ± 9.5 60.2 ± 7.3	21/0 8/5	NA	29 (100) 29 (100)	NA	29 29	PFS, OS, SAE	HAIC 4.4	17.6
	Sorafenib+HAIC (SoraHAIC) vs. sorafenib											
4	**Kudo, 2018** (14) **(SILIUS)※**	SoraHAIC = 102 Sorafenib = 103	Phase III	69 (62–75) 68 (62–75)	26/47 22/76	B/C: 32/27 B/C: 70/76	64 (62) 58 (57)	26 (25) 27 (27)	42 35	PFS, OS, SAE	2	19.2
5	**He MK, 2019** (15) ※	SoraHAIC = 125 Sorafenib = 122	Randomized clinical trial	49 (41–55) 49 (40–56)	62/101 89/99	NA	125 (100) 122(100)	38/125 (30.4) 42/122 (34.4)	+	PFS, OS, SAE	4	19.6 (SoraHAIC) 8.14 (sorafenib)
6	**Kondo, 2019** (16) **Scoop-2**	SoraHAIC = 35 Sorafenib = 33	Phase II	72.0 ± 7.0 70.9 ± 9.1	4/20 3/21	B/C: 14/19 B/C: 13/18	21 (60) 22 (67)	10 (29) 8 (24)	+	PFS, OS, SAE	2.2	11.2
7	**Zheng, 2022** (17) ※	SoraHAIC = 32 Sorafenib = 32	Phase II	56 ± 11 55 ± 10	28/2 29/3	NA	32 (100) 32 (100)	4 (12) 5 (16)	+	PFS, OS, SAE	5.5	28
	Lenvatinib vs. sorafenib											
8	**Kudo, 2018** (44) **※(REFLECT)**	Lenvatinib = 478 Sorafenib = 476	Phase III	63 (20–88) 62 (22–88)	251/91: 53/ 19 228/126: 21/45	B/C: 104/ 374 B/C: 92/384	109 (23%) 90 (19%)	291 (61) 295 (62)	AFP ≧200 183/154	PFS, OS, SAE	2	8
	Nivolumab vs. sorafenib											
9	**Yau, 2022** (45) ※ **(CheckMate 459)**	Nivolumab = 371 Sorafenib = 372	Phase III	65(57–71) 65 (58–72)	116/87 117/86	B/C: 53/ 303 B/C: 63/291	124 (33) 118 (32)	222 (60) 207 (56)	124 142	PFS, OS, SAE	3.5	7

(Continued)

10.3389/fonc.2024.1344798

TABLE 1 Continued

	Study	Treatment (*n*)	Study design	Median age	Etiology HBV/ HCV	BCLC stage B/C, *N*	PVTT, *N* (%)	Extrahepatic metastasis, *N* (%)	Serum AFP ≧400 g/mL (*N*)	Primary outcomes	Tx cycles median	Treatment duration (weeks)
	Donatinib vs. sorafenib											
10	**Qin, 2021 (33)**	Donatinib = 328 Sorafenib = 331	Phase III	53 (46–62) 53 (46–63)	293/7 301/5	B/C: 42/ 286 B/C: 41/290	241 (73) 243 (73)	241 (73) 243 (73)	173 177	PFS, OS, SAE	7.4	14.8
	Cabozantinib+Ate vs. sorafenib											
11	**Kelley, 2022 (35) (COSMIC-32)**	Cabozantinib+Ate = 432 Sorafenib = 217 Cabozantinib = 188	Phase III	64 (58–70) 64 (57–71) 64 (58–71)	127/136 64/67 59/60	B/C: 140/ 292 B/C: 72/ 145 B/C: 66/122	84 (19) 35 (16) 40 (21)	232 (54) 122 (56) 102 (54)	163 65 65	PFS, OS, SAE	8	24
	Tremelimumab+durvalumab vs. durvalumab or sorafenib											
12	**Abou-Alfa, 2022 (37)**	Tremelimumab+durvalumab = 393 vs. durvalumab = 389 or sorafenib = 389	Phase III	65 (22–86) 64 (20–86) 64 (18–88)	122/110 119/107 119/104	B/C: 77/ 316 B/C: 80/ 309 B/C: 66/323	103 (26.2) 94 (24.2) 100 (25.7)	209 (53.2) 212 (54.5) 203 (52.2)	145 (16.9) 137 (35.2) 124 (31.9)	PFS, OS, SAE	5	19.6
	Sintilimab plus Bev biosimilar vs. sorafenib											
13	**Ren, 2021 (34)**	Sintilimab plus BevBiol vs. sorafenib	Phase III	53 (21–82) 54 (28–77)	359/6 179/8	B/C: 56/ 324 B/C: 27/164	105 (80) 50 (26)	279 (73) 144 (75)	165 (43) 81 (42)	PFS, OS, SAE	7 4	22 vs. 12.4
	TACE+radiotherapy (RT) vs. sorafenib											
14	**Yoon, 2018 (36)**	TACE+RT Sorafenib	Phase III	55 (42–77) 55(33–82)	36/1 40/0	B/C: NA	45 (100) 45 (100)	8 (17.8) 0 (0)	+	PFS, OS, SAE	5 2	31 (TACE) 11.7 (RT)
15	**TACE+lenvatinib vs. Lenvatinib**											
	Peng, 2023 (46)	TACE+lenvatinib	Phase III	56 (48–63)	148/4	NA	122 (72)	94 (55)	83 (49)	PFS, OS	4	32.8
		Lenvatinib		54 (46.0–64.)	144/6		117 (70)	95 (57)	87 (52)	SAE	5.1	20.4
16	**Ding, 2021 (47)**	TACE+lenvatinib TACE+sorafenib	Phase III	57 ± 11 56 ± 11	30/1 29/3	NA	32 (100) 32 (100)	13 (91) 9 (28)	16 (50) 18 (56)	PFS, OS, SAE	6.9 3.0	18.8 12.4

N, number; BCLC, Barcelona Clinic Liver Cancer; HBV/HCV, Hepatitis B virus (B)/ Hepatitis C virus (C); AFP, alpha fetoprotein; PVTT, portal vein tumor thrombosis; OS, overall survival; PFS, progression free survival; SAE, severe adverse event; PVTT, Portal vein tumor thrombosis; FOLFOX, Oxaliplatin+Leucovorin+5-FU); ※, The study focused on patients with AHCC with PVTT or showed subgroup analysis data. HAIC, Hepatic arterial infusion chemotherapy; Tx, treatment.

10.3389/fonc.2024.1344798

A

	HEMATOLOGY SAE probablity				
	Neutropenia	Thrombpcytopenia	Anemia	Leukopenia	Decreasde WBC count
Ate+Bev	0	0	0	0	0.00
Lenvantinib	0	0	0	0	0.00
Sorafenib	0.107	0.103	0.124	0.06	0.08
HAIC-FO	0	0	0	0	0.00
Nivolumab	0	0	0	0	0.00
HAIC-Cis+Sor	0.017	0.34	0	0	0.13
HAIC-Fo+Sora	0.097	0.349	0.048	0.03	0.00
Donatinib	0	0	0	0	0.00
Cabozantinib+Ate	0	0	0	0	0.03
Tremelimumab+Dur	0	0	0.028	0	0.00
Sintilinab+Bevbiol	0	0	0.03	0	0.02
TACE+RT	0.02	0	0	0	0.00
Cabozantinib	0	0	0	0	0.00
Durvatinib	0	0	0.023	0	0.00

B

	Non-Hematology SAE probability								
	Hypertension	Elevated AST	Elevated ALT	Diarrhea	Nausea/Vomiting	Fatique	Hand-Foot Syndrome	GGT	Proteinurea
Ate+Bev	0.12	0.05	0.02	0.01	0	0.02	0	0	0.04
Lenvantinib	0.637	0.05	0	0.04	0.02	0.048	0.03	0	0.060
Sorafenib	1.092	0.658	0.184	0.77	0.153	0.302	1.293	0.140	0.081
HAIC-FO	0	0.144	0.047	0.00	0	0	0	0	0
Nivolumab	0	0.07	0	0.00	0	0.01	0	0	0
HAIC-Cis+Sor	0.29	0.182	0.147	0.14	0.162	0.14	0.35	0	0
HAIC-Fo+Sora	0.054	0.06	0.143	0.31	0.137	0.095	0.295	0	0
Donatinib	0.09	0.02	0.02	0.02	0	0	0.06	0	0.01
Cabozantinib+Ate	0.09	0.09	0.09	0.04	0.02	0.03	0.08	0	0
Tremelimumab+Dur	0.018	0.052	0.052	0.04	0	0.021	0	0.021	0
Sintilinab+Bevbiol	0.014	0.03	0.03	0.02	0.02	0.029	0	0.05	0.05
TACE+RT	0	0.133	0.133	0.02	0	0	0	0	0
Cabozantinib	0.08	0.1	0.05	0.06	0.04	0.04	0.09	0	0
Durvatinib	0.018	0.01	0.067	0.02	0	0	0	0.018	0

FIGURE 1
Heatmap of grade 3–5 toxicity spectra based on each of the specific adverse events for multidisciplinary treatment in advanced hepatocellular carcinoma with PVTT. **(A)** Hematology SAE. **(B)** Non-hematology SAE. Abbreviations: Ate+Bev, atezolizumab–bevacizumab; HAIC-FO, hepatic arterial infusion chemotherapy plus FOLFOX; HAIC-Cis+Sor, HAIC (cisplatin+5Fu or cisplatin) plus sorafenib; Dur, durvalumab; RT, radiotherapy. The deep color presented a higher risk.

the dots are evenly distributed on both sides of the funnel plot and symmetrical, indicating no potential publication bias in this network meta-analysis, except for one study (32) which was outside the funnel plot.

The sensitivity analysis results showed that the estimates for treatment comparisons are very similar to those in our main analysis, despite the inclusion of the biased study. This indicates that the results of our study are robust (Supplementary Figure 10).

Subgroup analysis

When analyzing HCC etiology and HBV subgroups according to the SUCRA score, NMA observed an OS benefit of HAIC-FO +sorafenib, followed by HAIC-FO and tremelimumab+Dur. The combination of cabozantinib+Ate was ranked first for PFS. In the HCV subgroup, Ate+Bev had an OS benefit over all the other treatments, followed by nivolumab, and it was ranked first based on the SUCRA score. Lenvatinib was ranked first for PFS. After stratifying by BCLC category, nivolumab and tremelimumab+Dur were ranked first in OS for BCLC B and C patients, respectively. Lenvatinib was ranked first for PFS. In MVI/PVTT/EHS and the AFP ≧400 mg/L subgroup, SUCRA scores ranked HAIC-FO+Sor as the best treatment in terms of OS and HAIC-FO as the best treatment in terms of PFS (Table 3).

Drug safety

The included RCTs reported 15 different treatment modalities, and we compared their adverse events ≧grade 3. The network analysis result is presented in Table 2. Nivolumab showed a significantly lower risk of SAEs than all other treatment modalities, except for durvalumab (OR = 0.55, 95% CI = 0.36–0.84) and TACE+RT (OR = 0.62, 95% CI = 0.20–1.95), followed by durvatinib (OR = 1.11, 95% CI = 0.37–3.50), donatinib (OR = 0.83, 95% CI = 0.54–1.27), and HAIC+Sor (OR = 0.55, 95% CI = 0.29–1.06).

Heatmaps of the subgroup analyses of hematologic and non-hematologic SAEs are shown in Figure 1. Sorafenib caused a high percentage of neutropenia (10.7%). HAIC-Fo+sorafenib and HAIC-Cis+Sor caused a high percentage of thrombocytopenia. The top 3 non-hematological SAEs with the highest incidence were sorafenib-

TABLE 2 Network comparisons of outcomes among different treatments.

PFS														
HAIC-FO														
0.42 (0.13 – 1.32)	**TACE+Len**													
0.41 (0.13 – 1.21)	0.97 (0.47 – 2.00)	**HAIC +Sor**												
0.49 (0.10 – 2.37)	1.16 (0.39 – 3.49)	1.21 (0.32 – 4.47)	**TACE + Sor**											
0.39 (0.13 – 1.08)	0.91 (0.48 – 1.75)	0.94 (0.55 – 1.60)	0.78 (0.22 – 2.78)	**Donatinib**										
0.39 (0.12 – 1.21)	0.93 (0.43 – 2.04)	0.96 (0.48 – 1.95)	0.80 (0.21 – 3.08)	1.02 (0.55 – 1.91)	**Ate+Bev**									
0.31 (0.11 – 0.83)	0.73 (0.41 – 1.30)	0.76 (0.49 – 1.17)	0.63 (0.18 – 2.16)	0.81 (0.60 – 1.10)	0.79 (0.45 – 1.35)	**Sorafenib**								
0.30 (0.09 – 0.92)	0.70 (0.32 – 1.57)	0.73 (0.36 – 1.48)	0.61 (0.16 – 2.33)	0.78 (0.41 – 1.46)	0.76 (0.35 – 1.65)	0.96 (0.56 – 1.68)	**Cabozantinib +Ate**							
0.29 (0.09 – 0.83)	0.69 (0.36 – 1.36)	0.72 (0.41 – 1.24)	0.59 (0.16 – 2.13)	0.76 (0.48 – 1.19)	0.75 (0.39 – 1.41)	0.94 (0.67 – 1.32)	0.98 (0.51 – 1.87)	**Nivolumab**						
0.29 (0.09 – 0.84)	0.69 (0.33 – 1.40)	0.71 (0.38 – 1.30)	0.59 (0.16 – 2.18)	0.75 (0.44 – 1.27)	0.74 (0.37 – 1.46)	0.93 (0.61 – 1.43)	0.97 (0.48 – 1.96)	0.99 (0.57 – 1.71)	**Sintiliman +Bevbiol**					
0.29 (0.09 – 0.84)	0.67 (0.33 – 1.39)	0.70 (0.37 – 1.31)	0.58 (0.16 – 2.17)	0.74 (0.43 – 1.27)	0.73 (0.36 – 1.46)	0.92 (0.59 – 1.43)	0.96 (0.46 – 1.94)	0.97 (0.56 – 1.70)	0.99 (0.53 – 1.85)	**HAIC-FO+Sor**				
0.26 (0.07 – 0.95)	0.62 (0.22 – 1.71)	0.64 (0.25 – 1.65)	0.53 (0.12 – 2.36)	0.68 (0.27 – 1.66)	0.66 (0.24 – 1.82)	0.84 (0.36 – 1.95)	0.88 (0.31 – 2.36)	0.89 (0.36 – 2.21)	0.90 (0.35 – 2.29)	0.92 (0.35 – 2.36)	**TACE+RT**			
0.25 (0.08 – 0.70)	0.58 (0.38 – 0.90)	0.60 (0.34 – 1.07)	0.50 (0.15 – 1.62)	0.64 (0.40 – 1.03)	0.63 (0.32 – 1.20)	0.79 (0.55 – 1.14)	0.83 (0.43 – 1.58)	0.84 (0.51 – 1.38)	0.85 (0.48 – 1.49)	0.86 (0.49 – 1.53)	0.94 (0.37 – 2.38)	**Lenvatinib**		
0.21 (0.07 – 0.61)	0.49 (0.24 – 0.99)	0.51 (0.28 – 0.93)	0.42 (0.11 – 1.56)	0.54 (0.32 – 0.90)	0.53 (0.27 – 1.04)	0.67 (0.44 – 1.02)	0.70 (0.35 – 1.39)	0.71 (0.42 – 1.21)	0.72 (0.39 – 1.31)	0.73 (0.40 – 1.36)	0.80 (0.31 – 2.06)	0.85 (0.49 – 1.46)	**Durvalumab**	
0.18 (0.05 – 0.52)	0.41 (0.20 – 0.84)	0.43 (0.23 – 0.78)	0.36 (0.09 – 1.32)	0.45 (0.27 – 0.77)	0.45 (0.22 – 0.88)	0.56 (0.36 – 0.86)	0.59 (0.29 – 1.17)	0.60 (0.35 – 1.03)	0.60 (0.33 – 1.11)	0.61 (0.33 – 1.14)	0.67 (0.26 – 1.74)	0.71 (0.40 – 1.25)	0.84 (0.53 – 1.32)	**Tremelimumab + Dur**

(Continued)

10.3389/fonc.2024.1344798

TABLE 2 Continued

OS														
HAIC-FO														
0.51 (0.19 – 1.31)	**Nivolumab**													
0.52 (0.18 – 1.47)	1.02 (0.51 – 2.02)	**TACE +Len**												
0.60 (0.13 – 2.51)	1.16 (0.34 – 3.90)	1.14 (0.42 – 3.15)	**TACE +Sor**											
0.42 (0.16 – 1.04)	0.82 (0.50 – 1.35)	0.81 (0.41 – 1.57)	0.70 (0.21 – 2.39)	**Tremelimumab +Dur**										
0.38 (0.14 – 1.00)	0.74 (0.41 – 1.35)	0.73 (0.35 – 1.52)	0.64 (0.18 – 2.22)	0.91 (0.52 – 1.58)	**Ate+Bev**									
0.33 (0.13 – 0.81)	0.64 (0.38 – 1.05)	0.63 (0.32 – 1.23)	0.55 (0.16 – 1.87)	0.78 (0.57 – 1.06)	0.86 (0.49 – 1.48)	**Durvalumab**								
0.32 (0.12 – 0.80)	0.62 (0.35 – 1.07)	0.61 (0.30 – 1.22)	0.53 (0.15 – 1.83)	0.75 (0.46 – 1.25)	0.83 (0.45 – 1.51)	0.97 (0.58 – 1.61)	**Cabozantinib +Ate**							
0.28 (0.11 – 0.64)	0.54 (0.36 – 0.79)	0.53 (0.30 – 0.95)	0.46 (0.14 – 1.51)	0.66 (0.48 – 0.90)	0.72 (0.46 – 1.13)	0.84 (0.61 – 1.16)	0.87 (0.59 – 1.29)	**Sorafenib**						
0.25 (0.07 – 0.82)	0.49 (0.20 – 1.22)	0.49 (0.17 – 1.35)	0.42 (0.10 – 1.79)	0.60 (0.25 – 1.46)	0.66 (0.26 – 1.69)	0.77 (0.32 – 1.87)	0.80 (0.31 – 2.02)	0.91 (0.40 – 2.09)	**TACE+RT**					
0.26 (0.10 – 0.65)	0.51 (0.31 – 0.84)	0.50 (0.26 – 0.98)	0.44 (0.13 – 1.49)	0.62 (0.40 – 0.98)	0.69 (0.39 – 1.19)	0.80 (0.51 – 1.25)	0.82 (0.49 – 1.39)	0.95 (0.69 – 1.31)	1.04 (0.43 – 2.55)	**Donatinib**				
0.26 (0.09 – 0.68)	0.50 (0.28 – 0.89)	0.49 (0.24 – 1.02)	0.43 (0.13 – 1.52)	0.61 (0.36 – 1.05)	0.68 (0.36 – 1.26)	0.79 (0.46 – 1.35)	0.81 (0.45 – 1.47)	0.93 (0.61 – 1.44)	1.02 (0.40 – 2.62)	0.98 (0.58 – 1.69)	**Sintilimab +BevBiol**			
0.26 (0.10 – 0.65)	0.51 (0.30 – 0.85)	0.50 (0.32 – 0.77)	0.43 (0.14 – 1.33)	0.61 (0.38 – 1.00)	0.68 (0.38 – 1.21)	0.79 (0.48 – 1.30)	0.82 (0.48 – 1.41)	0.94 (0.65 – 1.35)	1.03 (0.42 – 2.56)	0.99 (0.61 – 1.62)	1.01 (0.58 – 1.76)	**Lenvatinib**		
0.24 (0.08 – 0.65)	0.47 (0.24 – 0.90)	0.46 (0.21 – 1.01)	0.40 (0.11 – 1.45)	0.57 (0.31 – 1.06)	0.63 (0.31 – 1.27)	0.74 (0.40 – 1.37)	0.76 (0.39 – 1.47)	0.87 (0.51 – 1.48)	0.96 (0.36 – 2.57)	0.92 (0.50 – 1.71)	0.94 (0.47 – 1.86)	0.93 (0.48 – 1.77)	**HAIC+ Sor**	
0.19 (0.07 – 0.48)	0.36 (0.20 – 0.64)	0.35 (0.17 – 0.74)	0.31 (0.09 – 1.10)	0.44 (0.25 – 0.76)	0.48 (0.25 – 0.90)	0.56 (0.33 – 0.98)	0.58 (0.32 – 1.06)	0.67 (0.42 – 1.04)	0.73 (0.28 – 1.86)	0.70 (0.40 – 1.22)	0.71 (0.38 – 1.33)	0.71 (0.40 – 1.26)	0.76 (0.38 – 1.54)	**HAIC-FO + Sor**

(Continued)

10.3389/fonc.2024.1344798

TABLE 2 Continued

SAE															
Nivolumab															
0.55 (0.36 – 0.85)	**Durvalumab**														
0.61 (0.21 – 1.95)	1.11 (0.37 – 3.50)	**TACE +RT**													
0.46 (0.29 – 0.72)	0.83 (0.54 – 1.27)	0.74 (0.24 – 2.22)	**Donatinib**												
0.35 (0.11 – 1.18)	0.64 (0.20 – 2.11)	0.57 (0.12 – 2.74)	0.77 (0.24 – 2.60)	**TACE+Sor**											
0.32 (0.21 – 0.49)	0.58 (0.43 – 0.77)	0.52 (0.17 – 1.54)	0.70 (0.46 – 1.07)	0.90 (0.28 – 2.87)	**Tremelimumab +Dur**										
0.30 (0.21 – 0.41)	0.54 (0.40 – 0.71)	0.48 (0.16 – 1.37)	0.65 (0.47 – 0.89)	0.84 (0.26 – 2.62)	0.93 (0.70 – 1.23)	**Sorafenib**									
0.22 (0.14 – 0.36)	0.41 (0.26 – 0.64)	0.36 (0.11 – 1.10)	0.49 (0.30 – 0.79)	0.63 (0.19 – 2.08)	0.70 (0.45 – 1.10)	0.76 (0.53 – 1.07)	**Sintilimab +BevBiol**								
0.22 (0.13 – 0.36)	0.39 (0.24 – 0.64)	0.35 (0.11 – 1.07)	0.47 (0.28 – 0.79)	0.61 (0.18 – 2.04)	0.67 (0.41 – 1.10)	0.73 (0.49 – 1.09)	0.96 (0.56 – 1.64)	**Ate+Bev**							
0.20 (0.13 – 0.30)	0.36 (0.24 – 0.53)	0.32 (0.10 – 0.95)	0.43 (0.28 – 0.65)	0.55 (0.18 – 1.67)	0.61 (0.41 – 0.91)	0.66 (0.50 – 0.88)	0.88 (0.56 – 1.37)	0.91 (0.56 – 1.49)	**Lenvatinib**						
0.16 (0.09 – 0.30)	0.29 (0.16 – 0.53)	0.26 (0.08 – 0.85)	0.35 (0.19 – 0.65)	0.46 (0.16 – 1.24)	0.51 (0.28 – 0.91)	0.54 (0.32 – 0.92)	0.72 (0.39 – 1.34)	0.75 (0.38 – 1.44)	0.82 (0.53 – 1.27)	**TACE +Len**					
0.14 (0.08 – 0.25)	0.26 (0.15 – 0.45)	0.23 (0.07 – 0.74)	0.31 (0.18 – 0.54)	0.40 (0.11 – 1.36)	0.45 (0.26 – 0.77)	0.48 (0.30 – 0.76)	0.63 (0.36 – 1.14)	0.66 (0.36 – 1.22)	0.73 (0.42 – 1.25)	0.88 (0.44 – 1.77)	**HAIC-FO + Sor**				
0.13 (0.08 – 0.20)	0.23 (0.15 – 0.36)	0.21 (0.06 – 0.62)	0.28 (0.17 – 0.45)	0.36 (0.11 – 1.18)	0.40 (0.25 – 0.62)	0.43 (0.30 – 0.61)	0.57 (0.34 – 0.93)	0.59 (0.34 – 1.01)	0.65 (0.41 – 1.01)	0.78 (0.42 – 1.48)	0.89 (0.50 – 1.58)	**Cabozantinib +Ate**			
0.08 (0.04 – 0.15)	0.15 (0.08 – 0.27)	0.13 (0.04 – 0.43)	0.18 (0.09 – 0.33)	0.23 (0.06 – 0.81)	0.25 (0.14 – 0.47)	0.27 (0.16 – 0.47)	0.36 (0.19 – 0.69)	0.38 (0.19 – 0.74)	0.41 (0.22 – 0.76)	0.50 (0.23 – 1.07)	0.57 (0.28 – 1.17)	0.64 (0.33 – 1.23)	**HAIC-FO**	
0.04 (0.02 – 0.08)	0.08 (0.04 – 0.15)	0.07 (0.02 – 0.23)	0.10 (0.05 – 0.18)	0.12 (0.03 – 0.44)	0.14 (0.07 – 0.25)	0.15 (0.09 – 0.25)	0.20 (0.10 – 0.38)	0.21 (0.10 – 0.40)	0.23 (0.12 – 0.41)	0.27 (0.13 – 0.58)	0.31 (0.15 – 0.64)	0.35 (0.18 – 0.67)	0.55 (0.25 – 1.18)	**HAIC+ Sor**

Comparisons should be read from left to right. Cells narked in red color are significant (OR<1). For OS, PFS, and SAE an OR < 1.

HAIC, hepatic arterial infusion chemotherapy; TACE, transarterial chemoembolization; RT, external beam radiotherapy; Sor, Sorafenib; Sor, Sorafenic; Der, dervalumab; Ate, atezolizumab; FO, FOLFOX.

10.3389/fonc.2024.1344798

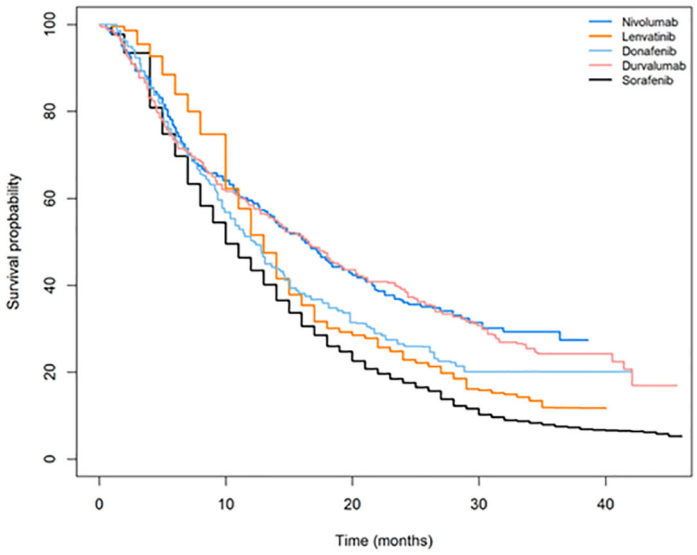

Number at risk

Nivolumab	371	216	147	63	0
Lenvatinib	646	443	138	41	0
Donafenib	328	188	95	25	2
Durvalumab	389	256	161	87	8
Sorafenib	2637	1339	446	66	0

FIGURE 2
Reconstructed Kaplan–Meier curves of OS for individual patient data extracted from single-agent systemic therapies for aHCC.

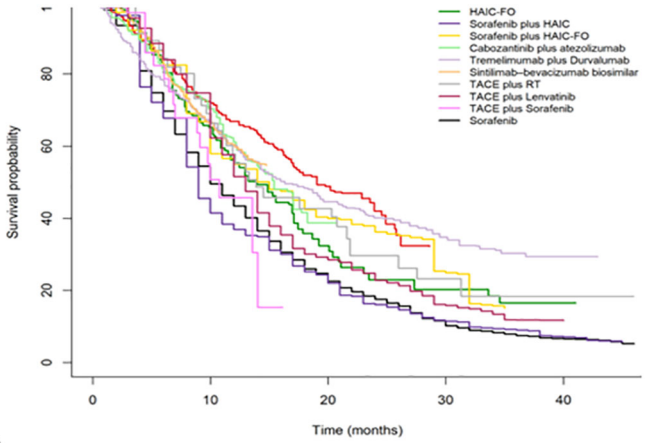

Number at risk

Atezolizumab plus bevacizumab	336	233	134	0	0
HAIC-FO	130	76	31	10	0
Sorafenib plus HAIC	166	87	48	22	3
Sorafenib plus HAIC-FO	157	77	28	3	0
Cabozantinib plus atezolizumab	432	208	0	0	0
Tremelimumab plus Durvalumab	389	71	35	20	1
Sintilimab–bevacizumab biosimilar	380	126	0	0	0
TACE plus RT	45	30	18	6	2
TACE plus Lenvatinib	202	121	23	0	0
TACE plus Sorafenib	32	12	0	0	0
Sorafenib	2637	1339	446	66	0

FIGURE 3
Kaplan–Meier curves of OS for individual patient data extracted from combination systemic therapies for aHCC.

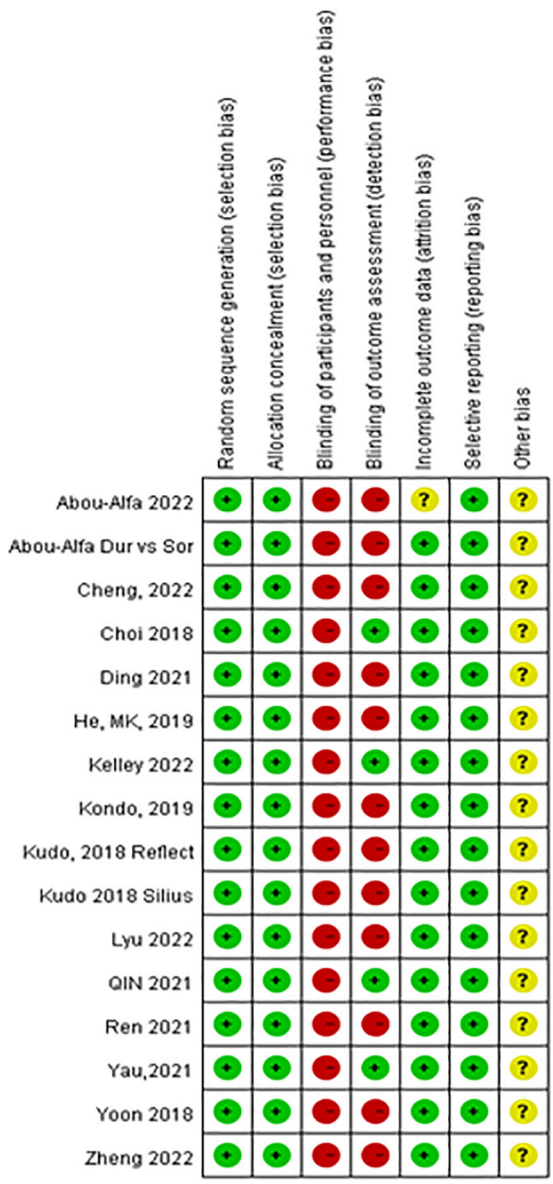

FIGURE 4
Risk of bias of the included 15 randomized control trials [review authors' judgments about each risk of bias item for each included study: low risk (+), high risk (–), and unclear risk ()?].

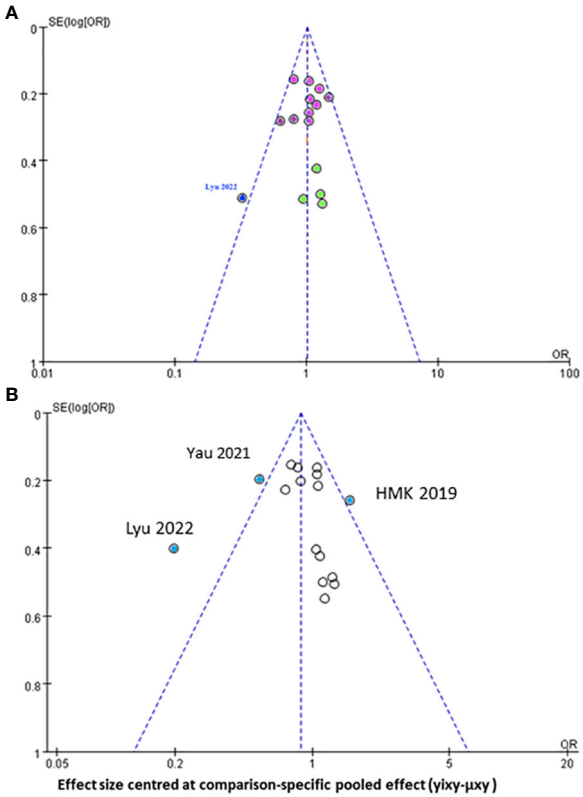

FIGURE 5
Funnel plot for the assessment of publication bias for **(A)** progression free survival **(B)** overall survival of all mutimodal regimens in network meta-analysis.

induced hand–foot syndrome (1.293), hypertension (1.092), and diarrhea (0.77).

Discussion

Systemic therapies have played an important role in the treatment of aHCC for decades. The emergence of TKI therapy in 2007 and immunotherapy in 2017 paved the way for multidisciplinary therapy to gradually expand treatment options. As a result, the median OS for patients with poor prognosis in aHCC is expected to improve from 7 months to 2 years. However, for patients with aHCC complicated by PVTT, the prognosis after surgical resection is still poor. Between 44% and 62% of HCC patients will develop PVTT, and only a few who are strictly selected will undergo curative surgery. Therefore, it is necessary to identify patients who cannot undergo surgical treatment and provide more active treatment strategies to prolong their survival time (13). In recent years, with the continuous advancement of surgical technology, local therapy, radiotherapy, molecular target therapy, and immunotherapy have been combined to formulate precise treatment options to improve the prognosis of patients with aHCC complicated by PVTT.

To the best of our knowledge, this current study is the first to conduct a patient-level network analysis to comprehensively compare the benefits and safety profiles of the most updated modalities of interest for patients with aHCC-PVTT. The results of this study demonstrate that, for patients with unresectable HCC, locoregional monotherapy (HAIC-FOLFOX) or combined targeted agents (TACE+Len, HAIC+Sor, and TACE+Sor) are superior to all studied treatment modalities in terms of OS (Table 2). The results of this latest network analysis support the results of Deng J et al. (48) TACE+lenvatinib showed better results, but no significant advantage was found between TACE+lenvatinib and TACE+sorafenib. The results of this current network study may also be explained by the concept of the tumor microenvironment, which is mainly composed of tumor cells, infiltrating immune cells around the tumor, new vessels and endothelial cells, tumor-associated fibroblasts, and an extracellular matrix (49). The tumor microenvironment undergoes a process of dynamic change. As tumor cells proliferate indefinitely,

TABLE 3 SUCRA score for OS and PFS in the entire cohort and in relative subgroups, derived from individual patient data meta-analysis.

	Entire cohort		HBV		HCV		MVI/ PVTT/EHS		AFP ≥400 μg/L		BCLC B		BCLC C	
	OS	PFS	OS	PFS	OS	PFS	OS	PFS	OS	PFS	OS	PFS	OS	PFS
HAIC-FO+sorafenib	0.08213	0.4336	0.9882				0.9816	0.3234	0.9914					
HAIC-FO	0.9846	0.9816	0.8502				0.9059	0.9612	0.01276					
Nivolumab	0.8764	0.4715	0.4887		0.8434		0.6948	0.3396	0.8145		0.2455		0.843	
Tremelimumab+Dur	0.7892	0.0642	0.7383		0.3641		0.5587		0.8045		0.8085		0.7752	
Ate+Bev	0.6897	0.7251	0.4347	0.5385	0.9525	0.5847	0.4914	0.6054	0.4129	0.4704	0.5397	0.5759	0.752	0.6607
Durvalumab	0.5687	0.1666	0.443		0.2921		0.3075		0.6023		0.6624		0.3935	
Cabozantinib+Ate	0.5315	0.4829	0.5399	0.7975	0.02749	0.3873	0.3335	0.6198		0.04939				
Sorafenib	0.3825	0.5325	0.1624	0.2894	0.5395	0.2661	0.1933	0.395	0.4114	0.6416	0.4625	0.4503	0.214	0.2301
Donatinib	0.3273	0.7473												
Sintilimab+BevBiol	0.3235	0.4545	0.1494	0.2482			0.1593	0.3184	0.3765	0.5917	0.2048	0.375	0.3316	0.3934
Lenvatinib	0.3233	0.2897	0.2053	0.6264	0.481	0.7619	0.1561	0.1526	0.4063	0.9872	0.5767	0.5988	0.1907	0.7157
HAIC+Sor	0.2756	0.7718						0.7847	0.1674	0.2597				
TACE+RT	0.3456	0.3788												

Blank space: no data available.
HAIC-FO, hepatic arterial infusion chemotherapy-FOLFOX; HBV/HCV, hepatitis B virus (B)/hepatitis C virus (C); BCLC, Barcelona Clinic Liver Cancer; OS, overall survival; PFS, progression-free survival; TACE+RT, transarterial chemoembolization+radiotherapy; BevBiol, bevacizumab biosimilar.

they stimulate the production of proangiogenic factors and immunosuppressive cells, resulting in an immunosuppressive microenvironment (50–52). Lenvatinib is a novel anti-angiogenesis multikinase inhibitor, and it inhibits the combination of vascular endothelial growth factor (VEGF) and vascular endothelial growth factor receptor (VEGFR) (53). VEGF is highly expressed in HCC and is the most representative pro-angiogenic factor in the tumor microenvironment, so it is a key mediator in inhibiting the tumor microenvironment (52). Therefore, lenvatinib can alleviate immunosuppression in the tumor microenvironment by inhibiting the binding mechanism of VEGF and VEGFR, and immune checkpoint inhibitors (ICIs) work under the condition of T lymphocyte infiltration. Therefore, lenvatinib can inhibit the formation of tumor blood vessels, increase the infiltration of T lymphocytes in the immunosuppressive microenvironment, and provide an effective immunotherapy microenvironment for anti-PD-1 treatment. Therefore, lenvatinib combined with anti-PD-1 therapy has a synergistic effect (49).

Overall survival is considered the most reliable and clinically meaningful endpoint for evaluating drug efficacy in oncology trials, and it provides objective, accurate, and easy-to-interpret data in NMA studies. In our subgroup analysis, we found that age, etiology, APF, PVTT, and EHS were the main prognostic factors affecting the clinical outcome of overall survival, and this is generally consistent with the main results of the examined studies. The results of the subgroup analyses showed that, compared with all other modalities of interest, the HAIC-FO+sorafenib and HAIC-FO regimens showed significant improvements in OS in HBV and MVI/PVTT/EHS subgroups (Table 3). These results provide reassurance that HAIC-based target therapy may effectively control tumor burden, provide a higher response rate than MTDs or ICIs alone in patients with portal vein thrombosis or a high intrahepatic tumor burden, and reduce the risk of postoperative recurrence (13).

In the SUCRA ranking plot, HAIC-FOLFOX ranked the highest in terms of OS and PFS, while HAIC-Sor ranked higher in PFS and lower in OS. The remaining MTD or ICI monotherapy rankings were comparable. The advances in molecular therapy and immune therapy are likely to have challenged the locoregional modalities with chemotherapy. However, due to the different mechanisms of both therapies, chemotherapeutic agents inhibit the DNA synthesis of the tumor, and molecular agents inhibit the multikinases involved in cell proliferation. Therefore, multikinases are limited to patients with Child–Pugh class A liver disease, and HAIC with chemotherapeutic agents benefits patients with Child–Pugh class B or C liver disease. The emergence of immune agents seems to have brought new hope to patients and oncologists regarding the systemic treatment of aHCC. Unfortunately, the development of immunotherapeutic agents appears to be limited by mechanisms involving the hyperactivation of the Wnt/β-catenin signaling pathway, which occurs in 50% of HCCs with a 5-year relapse rate of up to 70%, despite its marginal survival benefit for hepatovirus-infected HCC (54). Therefore, the replacement of conventional chemotherapy with MTA and immunotherapy is particularly controversial. Our result may accelerate studies in which MTD or ICI is added to locoregional modalities such as TACE or SBRT, as it is believed that these combinations may be sufficient to kill tumor cells and subsequently improve tumor-killing efficacy for treating aHCC (55, 56).

Another issue in this study may be heterogeneity due to the slightly different chemotherapy regimens, doses, and HAIC concomitant drug selection. We found that the dose and duration

of HAIC-FOLFOX (fluorouracil, leucovorin, and oxaliplatin) used in 60% (3/5) of the locoregional studies were almost the standard starting dose and duration and that they needed to be adjusted during treatment according to the clinical condition of the patients. The doses and durations of the HAIC–cisplatin plus 5-fluorouracil and HAIC–cisplatin regimens were also similar in the remaining studies. Based on this finding, it was determined that the dose, duration, and alternative agents used in HAIC may not affect the efficacy, but special attention may need to be paid to SAEs when selecting molecular therapies or immunotherapies combined with HAIC (54).

A comparison of safety (SAE ≥ grade 3) in this NMA may be challenging, as several covariates may influence the occurrence of SAEs, such as different follow-up times and treatment durations, as well as the response of individual patients to the drugs, e.g., patient idiosyncrasy to drugs and late onset of the effects of SAEs. Therefore, simply comparing the reported rates of adverse events of any grade is not feasible to obtain a detailed comparison of the toxicity profile of the included regimens. For this reason, our analysis focused on SAE ≥grade 3 and used Bayesian NMA to optimize data extrapolation and minimize reporting bias in SAE comparisons. Regarding serious adverse events, nivolumab, durvalumab, and TACE+RT ranked in the upper left corner of the legend table due to their relatively low incidence of grade 3–5 SAEs. After integrating the SAE chromatography of the regimens of interest, we observed that nivolumab provided a lower severe toxicity than the other regimens. This result is also supported by a published study conducted by Pan et al. (55) Overall, we suggest that nivolumab might be a good alternative to sorafenib or in combination with MTD, ICI, SBRT, or TACE as a sequential line for aHCC with PVTT (13, 56, 57).

The strength of this study is that we included updated published data from phase II and III randomized clinical trials and focused on the incidence of grade III SAEs, minimizing reporting bias. The first limitation is that the reported data (PFS and OS) require a longer follow-up time; some study results may be underestimated. Second, approximately 30% of the study population consisted of 100% patients with aHCC and PVTT, and in most of the remaining studies, only more than 50% of the study population had aHCC with PVTT, so selection bias may exist. Third, given the increasing understanding of post-marketing SAE reporting analyses, the results of toxicity analyses should be interpreted with caution. Finally, the potential risks of bias may be caused by performance bias because all included randomized clinical trials employed an open-labeled study design. However, the overall assessment showed that the quality of the evidence was high. Despite these limitations, the sensitivity analysis was robust. We believe that this study can provide clinicians with new treatment options for aHCC with PVTT and improve patient survival rates and quality of life.

Conclusion

In conclusion, PVTT remains an obstacle to the treatment of HCC, resulting in a high recurrence rate and poor prognosis. Except for sorafenib and lenvatinib, there is currently no standard treatment regimen for HCC associated with PVTT, but more active treatment modalities have been proposed and practiced clinically, which may improve the prognosis and survival time of patients with HCC associated with PVTT.

By conducting a robust NMA on individual patient-level data from RCTs, our current study provides further evidence that supports multimodality treatment as a better option for aHCC with MVI or PVTT. In view of the different efficacies observed in different subgroups (for example, HAIC-FO+sorafenib is slightly better for aHCC patients with MVI/PVTT/EHS and AFP ≧400 mg/L), multimodality treatment should be individualized by taking these subgroup factors into consideration. In the future, phase III randomized controlled trials are needed to develop better multimodality treatment strategies to manage HCC patients with PVTT.

Data availability statement

The original contributions presented in the study are included in the article/Supplementary Material. Further inquiries can be directed to the corresponding authors.

Author contributions

AC: Conceptualization, Data curation, Writing – original draft. S-YW: Writing – review & editing. JL: Software, Writing – original draft. HL: Writing – review & editing.

Funding

The author(s) declare financial support was received for the research, authorship, and/or publication of this article. This study was supported by TAINAN MUNICIPAL AN-NAN HOSPITAL-CHINA MEDICAL UNIVERSITY ANHRF 111-33.

Conflict of interest

The authors declare that the research was conducted in the absence of any commercial or financial relationships that could be construed as a potential conflict of interest.

Publisher's note

Supplementary material

The Supplementary Material for this article can be found online at: https://www.frontiersin.org/articles/10.3389/fonc.2024.1344798/full#supplementary-material

References

1. Cancer. net. *Liver cancer: statistics* . Available at: https://www.cancer.net/cancer-types/liver-cancer/statistics.

2. Cheng S, Chen M, Cai J. Chinese expert consensus on multidisciplinary diagnosis and treatment of hepatocellular carcinoma with portal vein tumor thrombus: 2016 edition. *Oncotarget* (2017) 8(5):8867–76. doi: 10.18632/oncotarget.12817

3. Woo HY, Heo J. New perspectives on the management of hepatocellular carcinoma with portal vein thrombosis. *Clin Mol Hepatol* (2015) 21(2):115–21. doi: 10.3350/cmh.2015.21.2.115

4. Yin J, Bo WT, Sun J, Xiang X, Lang JY, Zhong JH, et al. New evidence and perspectives on the management of hepatocellular carcinoma with portal vein tumor thrombus. *J Clin Transl Hepatol* (2017) 5(2):169–76. doi: 10.14218/JCTH.2016.00071

5. Sun JX, Shi J, Li N, Guo WX, Wu MC, Lau WY, et al. Portal vein tumor thrombus is a bottleneck in the treatment of hepatocellular carcinoma. *Cancer Biol Med* (2016) 13(4):452–8.

6. Huang J, Deng Q, Wang Q, Li KY, Dai JH, Li N, et al. Exome sequencing of hepatitis B virus-associated hepatocellular carcinoma. *Nat Genet* (2012) 44(10):1117–21. doi: 10.1038/ng.2391

7. Llovet JM, Ricci S, Mazzaferro V, Hilgard P, Gane E, Blanc JF, et al. Sorafenib in advanced hepatocellular carcinoma. *N Engl J Med* (2008) 359:378–90. doi: 10.1056/NEJMoa0708857

8. Cheng AL, Kang YK, Chen Z, Tsao CJ, Qin S, Kim JS, et al. Efficacy and safety of sorafenib in patients in the Asia-Pacific region with advanced hepatocellular carcinoma: a phase III randomised, double-blind, placebo-controlled trial. *Lancet Oncol* (2009) 10:25–34. doi: 10.1016/S1470-2045(08)70285-7

9. Tan WF, Qiu ZQ, Yu Y, Ran RZ, Yi B, Lau WY, et al. Sorafenib extends the survival time of patients with multiple recurrences of hepatocellular carcinoma after liver transplantation. *Acta Pharmacol Sin* (2010) 31(12):1643–8. doi: 10.1038/aps.2010.124

10. Mähringer-Kunz A, Steinle V, Düber C, Weinmann A, Koch S, Schmidtmann I, et al. Extent of portal vein tumour thrombosis in patients with hepatocellular carcinoma: The more, the worse? *Liver Int* (2019) 39:324–31. doi: 10.1111/liv.13988

11. Chen ZH, Zhang XP, Lu YG, Li LQ, Chen MS, Wen TF, et al. Actual long-term survival in HCC patients with portal vein tumor thrombus after liver resection: a nationwide study. *Hepatol Int* (2020) 14:754–64. doi: 10.1007/s12072-020-10032-2

12. Zhang XP, Gao YZ, Chen ZH, Chen MS, Li LQ, Wen TF, et al. An eastern hepatobiliary surgery hospital/portal vein tumor thrombus scoring system as an aid to decision making on hepatectomy for hepatocellular carcinoma patients with portal vein tumor thrombus: A multicenter study. *Hepatology* (2019) 69:2076–90. doi: 10.1002/hep.30490

13. Qiu G, Xie K, Jin Z, Jiang C, Liu H, Wan H, et al. The multidisciplinary management of hepatocellular carcinoma with portal vein tumor thrombus. *Biosci Trends.* (2021) 15(3):148–54. doi: 10.5582/bst.2021.01173

14. Kudo M, Ueshima K, Yokosuka O, Ogasawara S, Obi S, Izumi N, et al. Sorafenib plus low-dose cisplatin and fluorouracil hepatic arterial infusion chemotherapy versus sorafenib alone in patients with advanced hepatocellular carcinoma (SILIUS): a randomised, open label, phase 3 trial. *Lancet Gastroenterol Hepatol* (2018) 3(6):424–32. doi: 10.1016/S2468-1253(18)30078-5

15. He M, Li Q, Zou R, Shen J, Fang W, Tan G, et al. Sorafenib plus hepatic arterial infusion of oxaliplatin, fluorouracil, and leucovorin vs sorafenib alone for hepatocellular carcinoma with portal vein invasion: A randomized clinical trial. *JAMA Oncol* (2019) 5(7):953–60. doi: 10.1001/jamaoncol.2019.0250

16. Kondo M, Morimoto M, Kobayashi S, Ohkawa S, Hidaka H, Nakazawa T, et al. Randomized, phase III trial of sequential hepatic arterial infusion chemotherapy and sorafenib versus sorafenib alone as initial therapy for advanced hepatocellular carcinoma: SCOOP-2 trial. *BMC Cancer.* (2019) 19(1):954. doi: 10.1186/s12885-019-6198-8

17. Zheng K, Zhu X, Fu S, Cao G, Li WQ, Xu L, et al. Sorafenib plus hepatic arterial infusion chemotherapy versus sorafenib for hepatocellular carcinoma with major portal vein tumor thrombosis: A randomized trial. *Radiology* (2022) 303(2):455–64. doi: 10.1148/radiol.211545

18. Zhao Y, Lai J, Liang R, et al. Sorafenib plus hepatic arterial infusion chemotherapy with oxaliplatin versus sorafenib alone for advanced hepatocellular carcinoma. *J Interv Med* (2019) 2(2):78–83. doi: 10.1016/j.jimed.2019.07.005

19. He MK, Liang RB, Zhao Y, Xu YJ, Chen HW, Zhou YM, et al. Lenvatinib, toripalimab, plus hepatic arterial infusion chemotherapy versus lenvatinib alone for advanced hepatocellular carcinoma. *Ther Adv Med Oncol* (2021) 13:17588359211002720. doi: 10.1177/17588359211002720

20. Zhang J, Zhang X, Mu H, Yu G, Xing W, Wang L, et al. Surgical conversion for initially unresectable locally advanced hepatocellular carcinoma using a triple combination of angiogenesis inhibitors, anti-PD-1 antibodies, and hepatic arterial infusion chemotherapy: a retrospective study. *Front Oncol* (2021) 11:729764. doi: 10.3389/fonc.2021.729764

21. Liu BJ, Gao S, Zhu X, Guo JH, Kou FX, Liu SX, et al. Real-world study of hepatic artery infusion chemotherapy combined with anti-PD-1 immunotherapy and tyrosine kinase inhibitors for advanced hepatocellular carcinoma. *Immunotherapy* (2021) 13:1395–405. doi: 10.2217/imt-2021-0192

22. Chen LT, Martinelli E, Cheng AL, Pentheroudakis G, Qin S, Bhattacharyya GS, et al. Pan-Asian adapted ESMO clinical practice guidelines for the management of patients with intermediate and advanced/relapsed hepatocellular carcinoma: a TOS-ESMO initiative endorsed by CSCO, ISMPO, JSMO, KSMO, MOS and SSO. *Ann Oncol* (2020) 31:334–51. doi: 10.1016/j.annonc.2019.12.001

23. Llovet J, Montal R, Sia D, Finn RS. Molecular therapies and precision medicine for hepatocellular carcinoma, Nat. *Rev Clin Oncol* (2018) 15(10):599–616. doi: 10.1038/s41571-018-0073-4

24. Parums DV. Editorial: review articles, systematic reviews, meta-analysis, and the updated preferred reporting items for systematic reviews and meta-analyses (PRISMA) 2020 guidelines. *Med Sci Monit* (2021) 27:e934475. doi: 10.12659/MSM.934475

25. Lencioni R, Llovet JM. Modified RECIST (mRECIST) assessment for hepatocellular carcinoma. *Semin Liver Dis* (2010) 30(1):52–60. doi: 10.1055/s-0030-1247132

26. *Review Manager (RevMan) computer program, version 5.4.1 Copenhagen: The Cochrane Collaboration* (London, England: The Cochrane Collaboration) (2020). Available at: https://training.cochrane.org/system/files/uploads/protected_file/RevMan5.4_user_guide.pdf

27. Liu N, Zhou Y, Lee JJ. IPD from KM: reconstruct individual patient data from published Kaplan-Meier survival curves. *BMC Med Res Methodol* (2021) 21:111. doi: 10.1186/s12874-021-01308-8

28. Guyot P, Ades AE, Ouwens MJ, Welton NJ. Enhanced secondary analysis of survival data: reconstructing the data from published Kaplan-Meier survival curves. *BMC Med Res Methodol* (2012) 12:9. doi: 10.1186/1471-2288-12-9

29. Riley RD, Lambert PC, Abo-Zaid G. Meta-analysis of individual participant data: rationale, conduct, and reporting. *BMJ* (2010) 340:c221. doi: 10.1136/bmj.c221

30. Higgins JPT, Li T, Deeks JJ, Higgins JPT, Thomas J, Chandler J, et al. Choosing effect measures and computing estimates of effect, in: *Cochrane Handbook for Systematic Reviews of Interventions version 6.3 (updated February 2022)* (2022). Cochrane. Available at: www.training.cochrane.org/handbook (Accessed on 1 March, 2023).

31. Choi JH, Chung WJ, Bae SH, Song DS, Song MJ, Kim YS, et al. Randomized, prospective, comparative study on the effects and safety of sorafenib vs. hepatic arterial infusion chemotherapy in patients with advanced hepatocellular carcinoma with portal vein tumor thrombosis. *Cancer Chemother Pharmacol* (2018) 82(3):469–78.

32. Lyu N, Wang X, JB L, JF L, QF C, SL L, et al. Arterial chemotherapy of oxaliplatin plus fluorouracil versus sorafenib in advanced hepatocellular carcinoma: A biomolecular exploratory, randomized, phase III trial (FOHAIC-1). *J Clin Oncol* (2022) 40(5):468–80. doi: 10.1200/JCO.21.01963

33. Qin S, Bi F, Gu S, Bai Y, Chen Z, Wang Z, et al. Donafenib versus sorafenib in first-line treatment of unresectable or metastatic hepatocellular carcinoma: A randomized, open-label, parallel-controlled phase II-III trial. *J Clin Oncol* (2021) 39(27):3002–11. doi: 10.1200/JCO.21.00163

34. Ren Z, Xu J, Bai Y, Xu A, Cang S, Du C, et al. Sintilimab plus a bevacizumab biosimilar (IBI305) versus sorafenib in unresectable hepatocellular carcinoma (ORIENT-32): a randomised, open-label, phase 2-3 study. *Lancet Oncol* (2021) 22(7):977–90. doi: 10.1016/S1470-2045(21)00252-7

35. Kelley RK, Rimassa L, Cheng AL, Kaseb A, Qin S, Zhu AX, et al. Cabozantinib plus atezolizumab versus sorafenib for advanced hepatocellular carcinoma (COSMIC-312): a multicentre, open-label, randomised, phase 3 trial. *Lancet Oncol* (2022) 23(8):995–1008. doi: 10.1016/S1470-2045(22)00326-6

36. Yoon SM, Ryoo BY, Lee SJ, Kim JH, Shin JH, An JH, et al. Efficacy and safety of transarterial chemoembolization plus external beam radiotherapy vs sorafenib in hepatocellular carcinoma with macroscopic vascular invasion: A randomized clinical trial. *JAMA Oncol* (2018) 4(5):661–9. doi: 10.1001/jamaoncol.2017.5847

37. Abou-Alfa GK, Lau G, Kudo M, Chan SL, Kelley, Furuse K, et al. Tremelimumab plus durvalumab in unresectable hepatocellular carcinoma. *NEJM Evidence* (2022) 1(8). doi: 10.1056/EVIDoa2100070

38. Brown S, Hutton B, Clifford T. A Microsoft-excel-based tool for running and critically appraising network meta-analyses–an over view and application of NetMetaXL. *Syst Rev* (2014) 3:110. doi: 10.1186/2046-4053-3-110

39. Freeman SC, Fisher D, White IR, Auperin A, Carpenter JR. Identifying inconsistency in network meta-analysis: Is the net heat plot a reliable method? *Stat Med* (2019) 38(29):5547–64. doi: 10.1002/sim.8383

40. Higgins JPT, Thompson SG, Deeks JJ, Altman DG. Measuring inconsistency in meta-analyses. *BMJ* (2003) 327(7414):557–60. doi: 10.1136/bmj.327.7414.557

41. Dias S, Welton NJ, Sutton AJ, Caldwell DM, Lu G, Ades AE. Evidence synthesis for decision making 4: inconsistency in networks of evidence based on randomized controlled trials. *Med Decis Making* (2013) 33:641–56. doi: 10.1177/0272989X12455847

42. Salanti G, Ades AE, Ioannidis JP. Graphical methods and numerical summaries for presenting results from multiple-treatment meta-analysis: an overview and tutorial. *J Clin Epidemiol.* (2011) 64(2):163–71. doi: 10.1016/j.jclinepi.2010.03.016

43. Cheng AL, Qin S, Ikeda M, Galle PR, Ducreux M. Updated efficacy and safety data from IMbrave150: Atezolizumab plus bevacizumab vs. sorafenib for unresectable hepatocellular carcinoma. *J Hepatol* (2022) 76(4):862–73. doi: 10.1016/j.jhep.2021.11.030

44. Ding X, Sun W, Li W, Shen Y, Guo X. Transarterial chemoembolization plus lenvatinib versus transarterial chemoembolization plus sorafenib as first-line treatment for hepatocellular carcinoma with portal vein tumor thrombus: A prospective randomized study. *Cancer* (2021) 127(20):3782–3793. doi: 10.1002/cncr.33677

45. Yau T, Park JW, Finn RS, Cheng AL, Mathurin P. Nivolumab versus sorafenib in advanced hepatocellular carcinoma (CheckMate 459): a randomised, multicentre, open-label, phase 3 trial. *Lancet Oncol* (2022) 23(1):77–90. doi: 10.1016/S1470-2045(21)00604-5

46. Kudo M, Finn RS, Qin S, Han KH, Ikeda K. Lenvatinib versus sorafenib in first-line treatment of patients with unresectable hepatocellular carcinoma: a randomised phase 3 non-inferiority trial. *Lancet* (2018) 391(10126):1163–1173. doi: 10.1016/S0140-6736(18)30207-1

47. Peng Z, Fan W, Zhu B, Wang G, Sun J. Lenvatinib Combined With Transarterial Chemoembolization as First-Line Treatment for Advanced Hepatocellular Carcinoma: A Phase III, Randomized Clinical Trial (LAUNCH). *J Clin Oncol* (2023) 41(1):117–127. doi: 10.1200/JCO.22.00392

48. Deng J, Liao Z, Gao J. Efficacy of transarterial chemoembolization combined with tyrosine kinase inhibitors for hepatocellular carcinoma patients with portal vein tumor thrombus: A systematic review and meta-analysis. *Curr Oncol* (2023) 30(1):1243–54. doi: 10.3390/curroncol30010096

49. Wang Y, Jiang M, Zhu J, Qu J, Qin K, Zhao D, et al. The safety and efficacy of lenvatinib combined with immune checkpoint inhibitors therapy for advanced hepatocellular carcinoma. *BioMed Pharmacother.* (2020) 132:110797. doi: 10.1016/j.biopha.2020.110797

50. Ovais M, Mukherjee S, Pramanik A, Das D, Mukherjee A, Raza A, et al. Designing stimuli-responsive upconversion nanoparticles that exploit the tumor microenvironment. *Adv Mater* (2020) 32(22):e2000055. doi: 10.1002/adma.202000055

51. Martin JD, Cabral H, Stylianopoulos T, Jain RK. Improving cancer immunotherapy using nanomedicines: progress, opportunities and challenges. *Nat Rev Clin Oncol* (2020) 17(4):251–66. doi: 10.1038/s41571-019-0308-z

52. Sharonov G, Serebrovskaya EO, Yuzhakova DV, Britanova OV, Chudakov DM. B cells, plasma cells and antibody repertoires in the tumour Microenvironment. *Nat Rev Clin Oncol* (2020) 17(4):251–66. doi: 10.1038/s41577-019-0257-x

53. Thomas H. Liver cancer: Lenvatinib non-inferior to sorafenib for hepatocellular carcinoma. *Nat Rev Gastroenterol Hepatol* (2018) 15(4):190.

54. Hou Z, Liu J, Jin Z, Qiu G, Xie Q, Mi S, et al. Use of chemotherapy to treat hepatocellular carcinoma. *Biosci Trends* (2022) 16(1):31–45. doi: 10.5582/bst.2022.01044

55. Pan Y, Wang R, Hu D, Xie W, Fu Y, Hou J, et al. Comparative safety and efficacy of molecular-targeted drugs, immune checkpoint inhibitors, hepatic arterial infusion chemotherapy and their combinations in advanced hepatocellular carcinoma: findings from advances in landmark trials. *Front Biosci (Landmark Ed).* (2021) 26(10):873–81.

56. Marinelli B, Kim E, D'Alessio A, Cedillo M, Sinha I, Debnath N, et al. Integrated use of PD-1 inhibition and transarterial chemoembolization for hepatocellular carcinoma: evaluation of safety and efficacy in a retrospective, propensity score-matched study. *J Immunother Cancer.* (2022) 10(6):e004205. doi: 10.1136/jitc-2021-004205

57. Choi HS, Kang KM, Jeong BK, Jeong H, Lee YH, Ha IB, et al. Effectiveness of stereotactic body radiotherapy for portal vein tumor thrombosis in patients with hepatocellular carcinoma and underlying chronic liver disease. *Asia Pac J Clin Oncol* (2021) 17(3):209–15. doi: 10.1111/ajco.13361

frontiers | Frontiers in Oncology

TYPE Original Research
PUBLISHED 27 February 2024
DOI 10.3389/fonc.2024.1355927

OPEN ACCESS

EDITED BY
Francisco Tustumi,
University of São Paulo, Brazil

REVIEWED BY
Prakash Kumar Sasmal,
All India Institute of Medical Sciences Bhubaneswar, India
Farzad Kakaee,
Tabriz University of Medical Sciences, Iran
Tushar Mishra,
All India Institute of Medical Sciences Bhubaneswar, India

*CORRESPONDENCE
Zunqiang Xiao
Zqxiao@zcmu.edu.cn
Huang Jing
Huangjingonline@163.com

RECEIVED 14 December 2023
ACCEPTED 05 February 2024
PUBLISHED 27 February 2024

CITATION
Fu T, Bao Y, Zhong Z, Gao Z, Ye T, Zhang C, Jing H and Xiao Z (2024) Machine learning-based diagnostic model for preoperative differentiation between xanthogranulomatous cholecystitis and gallbladder carcinoma: a multicenter retrospective cohort study. *Front. Oncol.* 14:1355927. doi: 10.3389/fonc.2024.1355927

Machine learning-based diagnostic model for preoperative differentiation between xanthogranulomatous cholecystitis and gallbladder carcinoma: a multicenter retrospective cohort study

Tianwei Fu[1], Yating Bao[2], Zhihan Zhong[1], Zhenyu Gao[1], Taiwei Ye[1], Chengwu Zhang[1], Huang Jing[2*] and Zunqiang Xiao[1*]

[1]General Surgery, Cancer Center, Department of Hepatobiliary & Pancreatic Surgery and Minimally Invasive Surgery, Zhejiang Provincial People's Hospital (Affiliated People's Hospital), Hangzhou Medical College, Hangzhou, Zhejiang, China, [2]Department of Hepatopancreatobiliary Surgery, The Affiliated Lihuili Hospital of Ningbo University, Ningbo University, Ningbo, Zhejiang, China

Background: Xanthogranulomatous cholecystitis (XGC) and gallbladder carcinoma (GBC) share similar imaging and serological profiles, posing significant challenges in accurate preoperative diagnosis. This study aimed to identify reliable indicators and develop a predictive model to differentiate between XGC and GBC.

Methods: This retrospective study involved 436 patients from Zhejiang Provincial People's Hospital and The Affiliated Lihuili Hospital of Ningbo University. Comprehensive preoperative imaging, including ultrasound, Computed Tomography (CT), Magnetic Resonance Imaging (MRI), and blood tests, were analyzed. Machine learning (Random Forest method) was employed for variable selection, and a multivariate logistic regression analysis was used to construct a nomogram for predicting GBC. Statistical analyses were performed using SPSS and RStudio software.

Results: The study identified gender, Murphy's sign, absolute neutrophil count, glutamyl transpeptidase level, carcinoembryonic antigen level, and comprehensive imaging diagnosis as potential risk factors for GBC. A nomogram incorporating these factors demonstrated high predictive accuracy for GBC, outperforming individual or combined traditional diagnostic methods. External validation of the nomogram showed consistent results.

Conclusion: The study successfully developed a predictive nomogram for distinguishing GBC from XGC with high accuracy. This model, integrating

multiple clinical and imaging indicators, offers a valuable tool for clinicians in making informed diagnostic decisions. The findings advocate for the use of comprehensive preoperative evaluations combined with advanced analytical tools to improve diagnostic accuracy in complex medical conditions.

KEYWORDS

xanthogranulomatous cholecystitis, gallbladder carcinoma, diagnostic nomogram, machine learning, preoperative imaging

Introduction

Gallbladder diseases are frequently encountered in the clinical setting and comprise gallbladder malignant carcinoma and xanthogranulomatous cholecystitis (XGC). It is vital to correctly diagnose these two diseases, given their contrasting treatment options. Xanthogranulomatous cholecystitis is a special pathological type of chronic cholecystitis (1–3). In clinical practice, it is challenging to distinguish xanthogranulomatous cholecystitis from gallbladder carcinoma (GBC) via preoperative examinations (4). The imaging features of XGC and GBC include gallbladder wall thickening, gallbladder wall enhancement, and invasion of surrounding tissues (5, 6). They also have similar clinical manifestations, such as abdominal pain, jaundice, weight loss, and loss of appetite. Xanthogranulomatous cholecystitis is usually treated by cholecystectomy. However, owing to the similarities in imaging results and a lack of specific serological biomarkers, xanthogranulomatous cholecystitis is often misdiagnosed. Indeed, the diagnosis can only be confirmed via pathological examination or fine-needle aspiration following cholecystectomy (7, 8). The latter is not a recommended diagnostic option according to current guidelines because of the potential risks of bile leakage, tumor dissemination, and sampling error. Therefore, there is an urgent need to develop a non-invasive method to pre-operatively distinguish between XGC and GBC.

Abdominal ultrasound, computed tomography, magnetic resonance imaging, and other imaging examinations are routine preoperative examinations performed for XGC and GBC patients. The thickening pattern of the gallbladder wall can be divided into two types, namely focal and diffuse (9). Although the pattern of wall thickening in gallbladder cancer differs from that in benign disease, it is less specific. Therefore, there are many cases of misdiagnosis in clinical work (10). In addition, XGC can coexist with GBC (11). Due to the comparable clinical manifestations and imaging features, it is difficult to differentiate between XGC and GBC in the clinical setting. Therefore, XGC is frequently misdiagnosed as GBC, leading to unnecessary radical cholecystectomy and significantly increasing the complexity of the surgical intervention and the incidence of intraoperative and postoperative complications, such as biliary fistula, surgical site infection, bleeding, and organ damage. Conversely, GBC may also be misdiagnosed as XGC, and incomplete preoperative evaluation leads to missing the optimal treatment window or unnecessary surgical treatment for GBC patients. At present, with the exception of postoperative pathological diagnosis, there is no satisfactory preoperative model to distinguish GBC from xanthogranulomatous cholecystitis. Therefore, accurate clinical diagnosis is essential for the ensuing treatments of XGC and GBC patients.

Materials

The subjects were patients who underwent cholecystectomy and a histologically-confirmed diagnosis of XGC and GBC in Zhejiang Provincial People's Hospital and The Affiliated Lihuili Hospital of Ningbo University from January 2011 to January 2022. The clinical data of 109 patients with XGC were retrospectively analyzed, and 16 patients with incomplete imaging data were excluded. Similarly, the clinical data of 229 patients with GBC were analyzed, among which 14 patients with missing data, 16 patients with incomplete imaging data, and 2 patients with secondary gallbladder malignancy were excluded. Finally, 93 patients with XGC and 197 patients with GBC were eligible to participate in the training cohort, and the patients were divided into the XGC and GBC groups. Similarly, 40 patients with XGC and 106 patients with GBC were enrolled in The Affiliated Lihuili Hospital of Ningbo University as the validation cohort. Details of the inclusion and exclusion criteria for patients in this study are illustrated in Figure 1.

The comprehensive preoperative imaging diagnosis was conducted through abdominal ultrasound, abdominal-enhanced computed tomography (CT), magnetic resonance cholangiopancreatography

Abbreviations: XGC, Xanthogranulomatous cholecystitis; GBC, GBC; L, Bsolute lymphocyte count; N, Bsolute neutrophil count; M, Bsolute monocyte count; CEA, Carcinoembryonic antigen; PT, prothrombin time; ALB, Albumin; ALP, Alkaline phosphatase; ALT, Alanine transaminase; AST, Aspartate aminotransferase; auROC, Area under the receiver operating characteristic curve; BMI, Body mass index; GGT, Gammaglutamyl transpeptidase; IQR, Interquartile range; NPV, Negative predictive value; PPV, Positive predictive value; SD, Standard deviation; TBIL, Total bilirubin; DBIL, direct bilirubin; TBA, total bile acid; AFP, alpha fetoprotein; CA19-9, Carbohydrate antigen19-9; CA15-3, Carbohydrate antigen15-3; CA125, Carbohydrate antigen125.

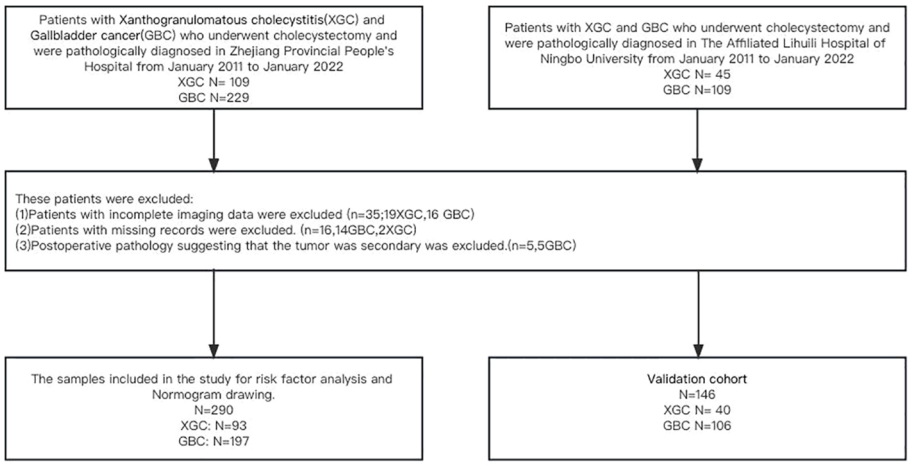

FIGURE 1
Flow diagram of the study design. A total of 290 patients with postoperative pathological diagnosis of XGC and GBC were included in the study of Zhejiang Provincial People's Hospital, including 93 patients with XGC and 193 patients with GBC. The Affiliated Lihuili Hospital of Ningbo University was included in this study as a validation cohort.

(MRCP), and abdominal-enhanced magnetic resonance (MRI). Due to the absence of retrospective imaging records, the abdominal ultrasound diagnosis relied solely on its report. The imaging data of both training and validation cohorts were reviewed by the same two experienced radiologists, who were blinded to the patient's clinical, laboratory, or pathological details during re-evaluation. If their interpretations differed, a consensus was reached through discussion and mutual consensus. The Kappa-Cohen index was used to assess inter-observer agreement. Comprehensive preoperative imaging diagnosis represents the comprehensive evaluation of the patient by imaging, and the evaluation criteria are as follows: (1) When all imaging examinations (ultrasound, CT, and MRI) indicate benign gallbladder disease, the preoperative diagnosis was defined as "benign gallbladder disease". (2) When the results of imaging examination in the diagnosis of benign and malignant gallbladder were inconsistent, the preoperative comprehensive diagnosis was "suspected GBC". (3) The preoperative diagnosis was labeled as "GBC" if all imaging tests uniformly suggested malignancy.

All experiments were conducted in accordance with the Declaration of Helsinki. All procedures performed involving human participants in the study adhered to the ethical standards of the Institutional Review Board (IRB). Due to the study's retrospective design, involving the use and analysis of past data, the IRB approved a waiver for the requirement of written informed consent.

Methods

Continuous variables following a normal distribution were represented by mean ± standard deviation (SD), while those following a skewed distribution were expressed as quartile range (IQR) and median. For comparison, the Mann-Whitney U test was used. Frequency data were expressed as numbers and percentages and compared using the Chi-square test or Fisher's exact test. The receiver-operating characteristic (ROC) curve analysis was used to assess the ability of each tumor marker and imaging method to differentiate xanthogranulomatous cholecystitis (XGC) from GBC (GBC).

The "Random Forest" method in machine learning was used for model variable selection. After the transformation of continuous variables into binary variables according to the best cutoff value, all variables were included in the multivariate logistic regression analysis according to their importance. Collinearity diagnosis was conducted for each variable included in the model. The OR and 95% CI of each independent risk factor in the model were calculated. A nomogram was subsequently constructed to predict the probability of GBC. The Hosmer-Lemesow test was used to evaluate the suitability of the nomogram ($P > 0.05$ indicating good fit), and correction curves were plotted to compare the relationship between the predicted probability and the actual probability. Sensitivity, specificity, positive predictive value (PPV), negative predictive value (NPV), and 95% CI were calculated for different risk cutoff points. The data set of The Affiliated Lihuili Hospital of Ningbo University was used for external validation of the nomogram. DeLong's test was used to estimate the difference between the ROC curves of the training and validation cohorts.

All statistical analyses were performed using SPSS software (version 26.0.0.0) and RStudio software (RStudio 2022.07.2 + 576,© 2009-2022 RStudio, PBC). All reported levels of statistical significance were bilateral, and statistical significance was set to 0.05.

Results

In this study, clinical data of 290 patients in Zhejiang Provincial People's Hospital and 146 patients in The Affiliated Lihuili Hospital of Ningbo University was collected and analyzed. Table 1 summarizes the demographic characteristics, clinical symptoms, and data on laboratory and imaging data for both the training and

10.3389/fonc.2024.1355927

TABLE 1 Demographic and clinical characteristics of the study population.

Baselines variables	Training cohort				Validation cohort			
	Total (n = 290)	Xanthogranulomatous cholecystitis (n = 93)	Gallbladder carcinoma (n = 197)	P value	Total (n = 146)	Xanthogranulomatous cholecystitis (n =40)	Gallbladder carcinoma (n =106)	P value
Gendar, female (%)	166 (57.2%)	34 (36.6%)	132 (67.0%)	< 0.001	77(52.7%)	14(35.0%)	63(59.4%)	0.010
Age(years),median (IQR)	64.90 ±7.0	63.75 ±14.3	65.44 ±10.6	0.314	66.85 ±10.91	63.80 ±13.73	68.00 ±9.45	0.080
BMI(kg/m2),mean (SD)	22.79 ± 3.19	23.26 ± 2.78	22.57 ± 3.36	0.066	23.54 ±3.12	24.40 ±3.94	23.21±2.70	0.039
Epigastric pain, n (%)	213 (73.4%)	88 (94.6%)	125 (63.5%)	< 0.001	83(56.8%)	28(70.0%)	55(51.9%)	0.061
Ventosity, n (%)	92 (31.7%)	42 (45.2%)	50 (25.4%)	0.001	46(31.5%)	15(37.5%)	31(29.2%)	0.452
Fever, n (%)	81 (27.9%)	31 (33.3%)	50 (25.4%)	0.205	35(24.0%)	11(27.5%)	24(22.6%)	0.542
Emesis, n (%)	75 (25.9%)	32 (34.4%)	43 (22.8%)	0.032	29(19.9%)	11(27.5%)	18(17.0%)	0.168
Jaudice, n (%)	58 (20.0%)	22 (24.7%)	36 (18.3%)	0.362	23(15.8%)	4(10.0%)	19(17.9%)	0.313
Murphy, n (%)	79 (27.2%)	57 (61.3%)	22 (11.2%)	< 0.001	23(15.8%)	16(42.5%)	6(5.7%)	< 0.001
Radiating pain, n (%)	82 (27.2%)	41 (44.1%)	41 (20.8%)	< 0.001	32(21.9%)	10(25.0%)	22(20.8%)	0.365
Weight loss, n (%)	23 (7.9%)	7 (7.5%)	16 (8.1%)	1	11(7.5%)	1(2.5%)	10(9.4%)	0.290
Abdominal surgery, n (%)	14 (4.8%)	3 (3.2%)	11 (5.6%)	0.561	9(6.2%)	4(10.0%)	5(4.7%)	0.258
Malignant individual, n (%)	30 (10.3%)	14 (15.1%)	16 (8.1%)	0.109	12(8.2%)	3(7.5%)	9(8.5%)	1
Personal gallstones history, n (%)	195 (67.6%)	82 (88.2%)	114 (57.9%)	< 0.001	91(62.3%)	33(82.5%)	58(54.7%)	0.002
Personal polyp history, n (%)	18 (6.2%)	2 (2.2%)	16 (8.1%)	0.082	4(2.7%)	1(2.5%)	3(2.8%)	1
L(*10^9/L), median (IQR)	1.48 (1.10, 1.88)	1.50 (1.10, 1.89)	1.44 (1.10, 1.88)	0.989	1.5 (1.1, 1.9)	1.41 (1.04, 1.85)	1.50 (1.10, 1.90)	0.656
N(*10^9/L), median (IQR)	4.23 (3.07, 6.79)	5.95 (3.38, 9.03)	4.00 (3.00, 5.52)	< 0.001	4.43 (3.30, 6.25)	5.92(3.39, 7.48)	4.40 (3.23, 5.70)	0.024
M(*10^9/L), median (IQR)	0.37 (0.30, 0.51)	0.40 (0.30, 0.60)	0.34 (0.29, 0.50)	0.008	0.50 (0.40, 0.63)	0.44(0.30, 0.60)	0.50 (0.40, 0.70)	0.028
ALB(g/L), mean (SD)	38.13 ± 5.39	36.38 ± 5.18	38.97 ± 5.29	< 0.001	39.10 ±6.21	36.63±6.15	40.03± 5.99	0.003
ALT (U/L), median (IQR)	28 (14, 90)	39 (17, 95)	26(14,88)	0.068	26(17,74)	36(20, 116)	24(17,74)	0.439
AST(U/L), median (IQR)	28 (21, 69)	31 (20, 75)	27 (21, 68)	0.918	27(21,48)	31(21, 80)	26(20,46)	0.335
GGT(U/L), median (IQR)	60 (25, 261)	125 (41, 266)	40 (21, 253)	< 0.001	60 (30,196)	126(35, 237)	51(24,167)	0.032
ALP(U/L),median (IQR)	114 (82, 223)	130 (96, 236)	105 (80, 212)	0.021	104 (78,186)	114(83, 177)	98(75,208)	0.796

(Continued)

TABLE 1 Continued

Baselines variables	Training cohort				Validation cohort			
	Total (n = 290)	Xanthogranulomatous cholecystitis (n = 93)	Gallbladder carcinoma (n = 197)	P value	Total (n = 146)	Xanthogranulomatous cholecystitis (n =40)	Gallbladder carcinoma (n =106)	P value
DBIL(umol/L), median (IQR)	3.6 (2.2, 12.3)	5.1 (2.5, 13.9)	3.2 (2.2, 9.7)	0.042	4.3 (2.7, 9.5)	4.1 (2.4, 9.7)	4.6(3.1,9.3)	0.114
IBIL(umol/L), median (IQR)	12.2 (8.8, 20.6)	12.4 (9.0, 23.4)	12.1 (8.8, 19.5)	0.612	8.9 (6.9, 13.7)	10.8 (8.0, 19.7)	8.5(6.4,11.9)	0.017
TBA(umol/L), median (IQR)	6.9 (3.7, 17.6)	7 .0(4.0, 15.6)	6.8 (3.5, 21.1)	0.970	6.0 (3.3, 18.8)	5.8 (3.3, 13.9)	20.7(6.0,196.7)	0.729
PT(s), median (IQR)	11.8 (11.1, 12.5)	12.1 (11.4, 12.8)	11.7 (11.0, 12.3)	< 0.001	11.6 (11.0, 12.2)	11.7 (11.3, 12.3)	11.5(10.9,12.1)	0.178
AFP(ug/L), median (IQR)	2.4 (1.8, 3.4)	2.1 (1.7, 3.3)	2.5 (1.9, 3.6)	0.079	2.5 (1.7, 4.0)	2.3 (1.7, 3.1)	2.6(1.7,4.5)	0.219
CEA(ug/L), median (IQR)	2.6 (1.6, 5.1)	2.0 (1.2, 2.9)	2.9 (1.8, 5.7)	< 0.001	1.8 (1.2, 5.2)	1.6 (1.1, 2.9)	1.9(1.2,6.8)	0.047
CA125(U/L), median (IQR)	16.8 (10.6, 33.0)	21.9 (11.5, 38.0)	16.6 (10.6, 30.3)	0.183	17.8 (9.7, 42.1)	13.0(10.3, 30.5)	18.8(9.2,50.7)	0.146
CA19-9(U/L), median (IQR)	37.4 (13.0, 180.5)	54.2 (15.0, 194.0)	33.1 (12.5, 154.1)	0.150	49.4 (12.8, 316.7)	52.9 (12.5, 94.9)	49.1 (13.4,461.9)	0.203
CA15-3(U/L), median (IQR)	11.0 (8.5, 16.7)	10.7 (8.1, 15.7)	11.5 (8.7, 17.1)	0.197	11.5 (7.3,15.6)	12.2 (7.0, 16.5)	11.1(7.5,15.4)	0.640
Comprehensive preoperative imaging diagnosis				< 0.001				< 0.001
Benign diseases of gallbladder	117 (40.3%)	77 (82.8%)	40 (20.3%)		55(37.7%)	33(82.5%)	17(19.8%)	
Suspected gallbladder carcinoma	68 (23.4%)	8 (8.6%)	60(30.5%)		48(32.9%)	3(7.5%)	42(42.5%)	
Gallbladder carcinoma	105 (36.2%)	8 (8.6%)	97 (49.2%)		43(29.5%)	4(10.0%)	47(37.3%)	

XGC, Xanthogranulomatous; GBC, Gallbladder carcinoma; L, lymphocyte; N, neutrophile granulocyte; M, monocyte; ALB, serum albumin; ALT, alanine aminotransferase; AST, aspartate aminotransferase; GGT, gamma-glutamyl transpeptidase; ALP, alkaline phosphatase; DBIL, direct bilirubin; IBIL, indirect bilirubin; TBA, total bile acid; PT, prothrombin time; AFP, alpha-fetal protein; CA 19-9, cancer antigen 19-9; CEA, carcinoembryonic antigen; CA 153, cancer antigen 153.

validation cohorts. Univariate analysis revealed that gender, right upper quadrant abdominal pain, vomiting, abdominal distention, Murphy's sign, radiating pain, history of gallstones, absolute neutrophil count (N), prothrombin time (PT), comprehensive preoperative imaging diagnosis, as well as levels of albumin (ALB), GGT, alkaline phosphatase (ALK), direct bilirubin (DBIL), and CEA were potential risk factors for the differential diagnosis of XGC and GBC (all $P < 0.05$).

The results of preoperative ultrasonography, enhanced CT, MRI, and enhanced MR of patients are summarized in Table 2. As displayed in Figure 2, contrast-enhanced CT and contrast-enhanced MRI had the highest discriminatory power, with AUCs (95% CI) of 0.819 (0.769–0.868) and 0.885 (0.764–1), respectively. Comprehensive preoperative imaging had an AUC (95% CI) of 0.821 (0.772–0.869). However, the AUC (95% CI) of unenhanced MRI was 0.729 (0.665–0.793), while that of the US was 0.692 (0.638–0.746). The inter-observer agreement between the two radiologists was good. The Kappa-Cohen index was 0.810 in the training cohort and 0.782 in the validation cohort.

The thirty-three characteristic variables in the study were included and ranked by importance using the random forest method (Figure 3). Finally, the top six variables with Mean decrease Gini (A larger value indicates a greater importance of the variable) were selected for inclusion in the model, and the continuous variables included N, GGT, and CEA. For the convenience of model construction and scoring, continuous variables were divided into binary variables according to the best cutoff value of ROC curve analysis (Table 3).

Serum CEA

The preoperative serum CEA levels of 93 patients in the XGC group and 197 patients in the GBC group were statistically

10.3389/fonc.2024.1355927

TABLE 2 The simple frequency distribution of preoperative US, enhanced CT, MR, enhanced MR and comprehensive imaging diagnosis results in XGC and GBC groups was shown.

		XGC	GBC	Total
US	Benign gallbladder disease	73	79	152
	GBC	20	118	138
enhanced CT	Benign gallbladder disease	62	40	102
	GBC	5	99	104
MR	Benign gallbladder disease	45	47	92
	GBC	6	64	70
enhanced MR	Benign gallbladder disease	9	3	12
	GBC	1	20	21
comprehensive imaging diagnosis	Benign gallbladder disease	77	40	117
	GBC	16	157	173
	Total	93	197	290

analyzed. The median level of serum carcinoembryonic antigen in the GBC group was 2.9 μg/L (range: 0.2–244.9 μg/L), which was significantly higher than 2.0 μg/L in the XGC group (range: 0.4–6.9 μg/L) ($P < 0.001$). The ROC curve of serum carcinoembryonic antigen value for diagnosis was then drawn. The AUC value was found to be 0.693. According to the ROC curve analysis of CEA level, the optimal cutoff value of CEA was 3.2 ug/L when the Youden index was the highest. The sensitivity and specificity were 51.3% and 79.6%, respectively (Figure 2B). Subsequently, unifactor analysis was performed (Table 3). The difference between the two groups was statistically significant ($P < 0.001$).

Multiple Logistic regression analysis was conducted to identify independent predictors for differentiating XGC from GBC. Then, stepwise inclusion and exclusion methods were used to analyze the model, which finally yielded six independent predictors for the differentiation of XGC and GBC (Table 4). In the comprehensive preoperative imaging diagnosis, compared with "benign gallbladder disease," the OR value of "GBC" was (OR = 17.45; 95% CI: 6.61–46.06), and the OR value of "suspected GBC" was (OR = 13.51; 95% CI: 4.87–37.44). Similarly, female gender (OR = 4.21; 95% CI: 1.91–9.32) and CEA ≥ 3.2μg/L (OR = 4.05; 95% CI: 1.31–12.46) were independent risk factors for the diagnosis of GBC. Contrastingly, a positive Murphy's sign, GGT ≥ 29 U/L, and $N \geq 5.60 \times 10^9$/L were associated with a lower risk of GBC, with OR values of 0.15 (95% CI: 0.07–0.34), 0.27 (95% CI: 0.09–0.82), and 0.41 (95% CI: 0.18–0.91), respectively.

Based on the multifactor model, the nomogram was constructed with the six independent risk factors (Figure 4). In the nomogram, each predictor was assigned a score according to its classification. A patient's total score corresponded to the likelihood of GBC. The p-value of the Hosmer-Lemesshow test for this model was 0.700 ($P > 0.05$, good model fitting) (Figure 5). Subsequently, a nomogram calibration chart was developed to evaluate the predictive value of the model by curves of prediction probability and actual probability. The AUC of the nomogram was 0.936 (95% CI, 0.909–0.963), with accuracy, sensitivity, specificity, NPV, and PPV of 87.2%, 76.3%, 92.4%, 82.6%, and 89.2%, respectively. Moreover, the optimal cutoff value of the nomogram was 0.65, corresponding to 155 points, and the corresponding sensitivity and specificity were 88.8% and 86.0%, respectively. Furthermore, comparing the AUCs revealed that among the two commonly used combinations, the nomogram had the highest discriminant ability and outperformed that of the combination of radiographic diagnosis and CEA levels, which had an AUC of 0.861 ($P < 0.01$) (Figure 6). According to the American Joint Committee on Cancer (AJCC) GBC staging, the model characteristics of GBC patients in the training cohort are demonstrated in Table 5. As shown in Table 6, comparing the

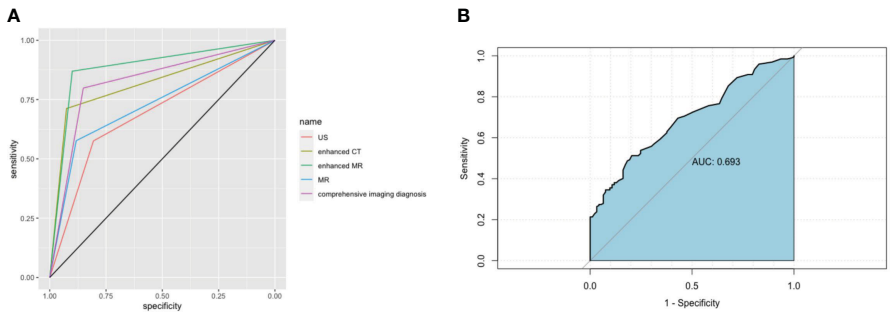

FIGURE 2
Imaging and receiver operating characteristic (ROC) curve analysis of serum markers in XGC and GBC patients prior to cholecystectomy. **(A)** The areas under the AUC curve were 0.691, 0.819, 0.885, 0.729, and 0.821, respectively, for ultrasonography, enhanced CT, enhanced MRI, plain MRI, and comprehensive imaging diagnosis. **(B)** Serum CEA. The critical value of serum CEA (μg/L) in differentiating XGC and GBC showed that the area under the AUC curve was 0.693.

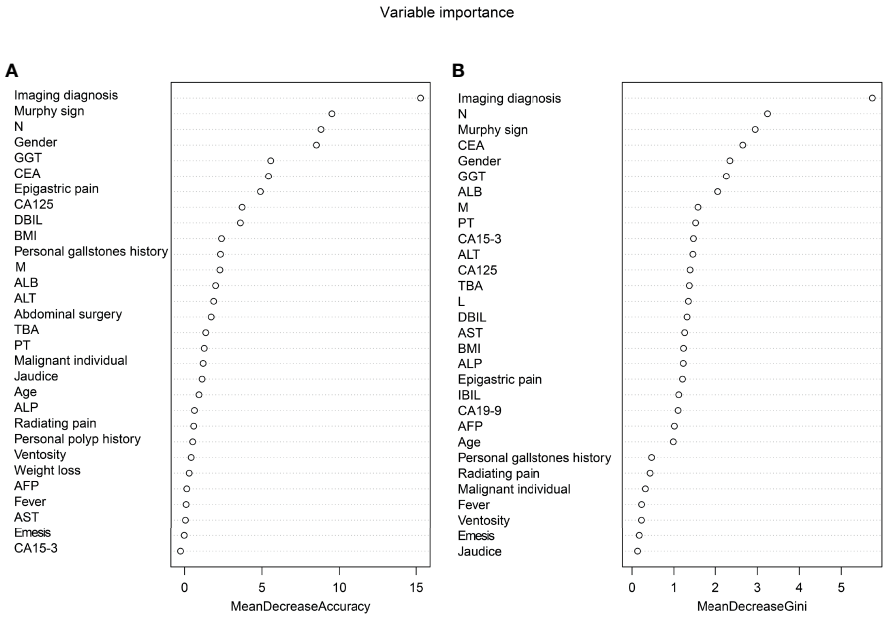

FIGURE 3
Ranking of input variables in the random forest model to predict GBC. **(A)** The mean decrease in accuracy. **(B)** Mean decrease Gini. Variables are listed from most important to least important based on the mean decrease in accuracy and mean reduction in the Gini coefficient.

preoperative imaging examination and intraoperative frozen results of GBC patients with AJCC stage I and II, there was no statistically significant difference between them.

The nomogram was validated externally in one validation cohort. The AUC value of the nomogram in The Affiliated Lihuili Hospital of Ningbo University was 0.924 (Figure 7). The ROC curve of the nomogram based on the validation cohort was not significantly different from the training cohort (P = 0.657).

The nomogram was then incorporated into a web page (https://nomomodel.shinyapps.io/dynnomapp/). When distinguishing between XGC and GBC, the probability of XGC could be determined after inputting the relevant data (Figure 8).

Discussion

XGC, also referred to as fibroxanthogranulomatous cholecystitis or waxy histiocytic granuloma, is a rare type of benign cholecystitis caused by chronic inflammation in the gallbladder (1). XGCs's etiology is elusive and is hypothesized to be caused by the rupture or ulceration of the Ro-Arsal sinus. This causes bile to penetrate the gallbladder wall and infiltrate the interstitial space, leading to an inflammatory response to phagocytize the bile. Microscopically, foam cells, multinucleated giant cells, fibrous tissue hyperplasia, and phagocytes with lipids in the cytoplasm can be visualized in sections (2, 3). The imaging and

TABLE 3 Univariate analysis of the GGT, N and CEA as a categorical variable.

Laboratory test index	Total (n = 290)	Xanthogranulomatous cholecystitis (n = 93)	Gallbladder carcinoma (n = 197)	P value
GGT(U/L)				< 0.001
<29	83 (29%)	7 (8%)	76 (39%)	
≥29	207 (71%)	86 (92%)	121 (61%)	
N(*10^9/L)				< 0.001
<5.60	188 (67%)	38(41%)	150(76%)	
≥5.60	102 (33%)	55(59%)	47(24%)	
CEA(ug/L)				< 0.001
<3.2	170 (5%)	74(80%)	96(49%)	
≥3.2	120 (%)	19(20%)	101(51%)	

XGC, Xanthogranulomatous; GBC, Gallbladder carcinoma; N, neutrophile granulocyte; GGT, gamma-glutamyl transpeptidase; CEA, carcinoembryonic antigen.

TABLE 4 Multivariate Logistic regression analysis of risk factors for XGC and GBC.

Characteristic	Comparisons	UV OR (95% CI)	UV P	MV OR (95% CI)	MV P
Gendar, female (%)	Female vs. male	3.52(2.10-5.90)	<0.01	4.21(1.91-9.32)	<0.01
Murphy,yes	Yes vs. no	0.08(0.04-0.15)	<0.01	0.15(0.07-0.34)	<0.01
N≥5.60*10^9/L	Yes vs. no	0.22(0.13-0.37)	<0.01	0.41(0.18-0.91)	0.041
GGT≥29U/L	Yes vs. no	0.13(0.06-0.30)	<0.01	0.27(0.09-0.82)	0.004
CEA≥3.2 ug/L	Yes vs. no	4.10(2.30-7.29)	<0.01	4.05(1.31-12.46)	0.004
Comprehensive preoperative imaging diagnosis	Suspected gallbladder carcinoma vs. benign gallbladder diseases	14.43(6.29-33.13)	<0.01	13.51(4.87-37.44)	<0.01
	Gallbladder carcinoma vs. benign gallbladder diseases	23.34(10.32-52.78)	<0.01	17.45(6.61-46.06)	<0.01

XGC, Xanthogranulomatous ; GBC, Gallbladder carcinoma; N, neutrophile granulocyte; GGT, gamma-glutamyl transpeptidase; CEA, carcinoembryonic antigen.

serological data, as well as the clinical symptoms of XGC and GBC, are similar. However, significant differences exist in their treatment modalities. The preferred treatment modality for XGC is cholecystectomy. When hilar invasion, intrahepatic bile duct dilatation, vascular invasion, or other potentially invasive conditions are present, surgical intervention should extend beyond the gallbladder to include the resection of adjacent affected organs (12). Due to severe fibrosis and inflammation, undissected Callot's triangle, unclear anatomy, life-threatening hemorrhage, and major bile duct injury, the frequency of conversion to open surgery in patients with XGC is higher than that in patients with other forms of cholecystitis. The conversion rate is between 10% and 80% (13–15). However, XGC is ultimately a benign disease with aggressive characteristics, and the use of intraoperative frozen sections aids in distinguishing XGC from GBC. However, in a retrospective study, 42 of 142 XGC patients had a preoperative diagnosis of GBC. In this subset of patients, the accuracy of frozen sections was 93%, and the accuracy of macroscopic diagnosis by the surgeon was 50% (16).

This study's primary novel findings include the identification of several potential indicators for distinguishing XGC from GBC. These indicators are gender, the presence of Murphy's sign, absolute neutrophil count, levels of glutamyl transpeptidase, carcinoembryonic antigen levels, and comprehensive preoperative imaging diagnosis. The difference in the serum tumor marker levels between XGC and GBC remains controversial (17–19). Xiao et al. (20) found significant differences in absolute neutrophil count and CEA level in the results of preoperative laboratory tests between XGC and GBC, while there were no significant differences in the levels of AFP, CA12-5, and CA242. Moreover, Yu et al. (21) noted that the levels of tumor biomarkers are typically elevated in XGC and that CA19-9 and CA12-5 levels can increase the incidence of

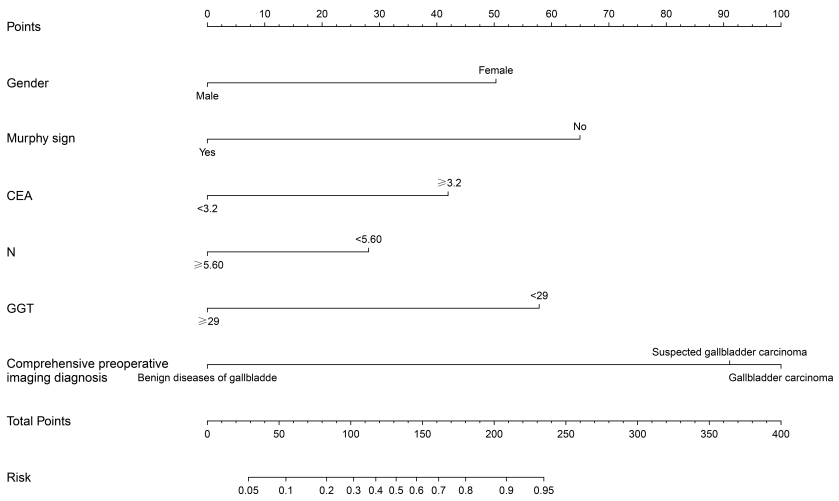

FIGURE 4
Construction of nomogram of xanthogranulomatous cholecystitis (XGC) and GBC (GBC) patients. The nomogram was established according to six possible independent predictors of cancer: gender, Murphy's sign, CEA, neutrophils absolute value (N), glutamyl transpeptienzyme (GGT), and comprehensive preoperative imaging diagnosis. For each patient, the values of the six risk factors are represented as dots by projecting them onto the topmost line (point scale). Summing the six variables and projecting the total points' value downward onto the bottom-most line can determine the probability of GBC.

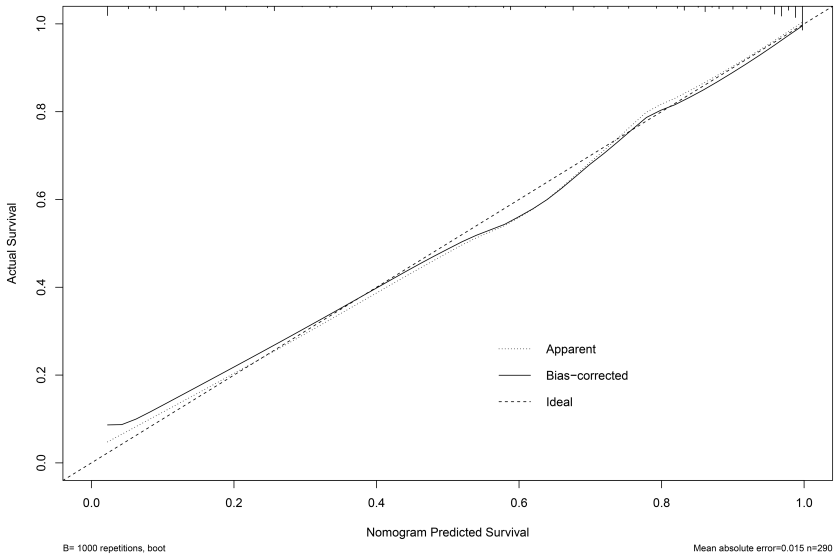

FIGURE 5
Calibration plot of Normogram for the probability of diagnosis of gallbladder malignancy.

XGC and XGC misdiagnosis. XGC is frequently accompanied by Mirizzi syndrome and internal fistula, and CA19-9 levels were elevated in 26.09% of patients. In this study, CEA was the only serum tumor marker with a statistical difference and included in the model, and its optimal cutoff value was 3.2 μg/L. Furthermore, there was no significant difference in the level of AFP, CA19-9, CA12-5, and CA15-3 between the two groups.

Similarly, the female gender and negative Murphy's sign were risk factors for GBC. Notably, the occurrence of GBC in women is two to six times higher than in men and progressively rises with advancing age (22). In patients with cholelithiasis, epigastric pain and a positive Murphy's sign are most commonly associated with acute gallbladder inflammation. Conversely, most patients with GBC do not exhibit severe symptoms. However, there is no universally accepted consensus in this regard. Regarding laboratory tests, the count of neutrophils and the level of GGT act as protective factors in diagnosing GBC. These findings are consistent with the study conducted by Xiao et al. (20). Statistically significant differences in neutrophil counts were also found in this study. The authors contend that most patients with XGC present symptoms of acute cholecystitis, whereas patients with GBC may only exhibit radiographic abnormalities and present without significant gallbladder inflammation. Serum GGT level is extensively used for the diagnosis of liver and biliary tract diseases and predominantly reflects biliary tract involvement in clinical practice. Bile duct obstruction and other diseases lead to cholestasis. The increase in cell membrane permeability induces the synthesis of bile salts, resulting in elevated GGT levels, which enter the blood circulation through the injured biliary duct epithelial cells (23). In this study, the serum GGT level of XGC patients was generally greater than 29 U/L, indicating biliary tract injury. In XGC, the granuloma of the gallbladder wall compresses the bile

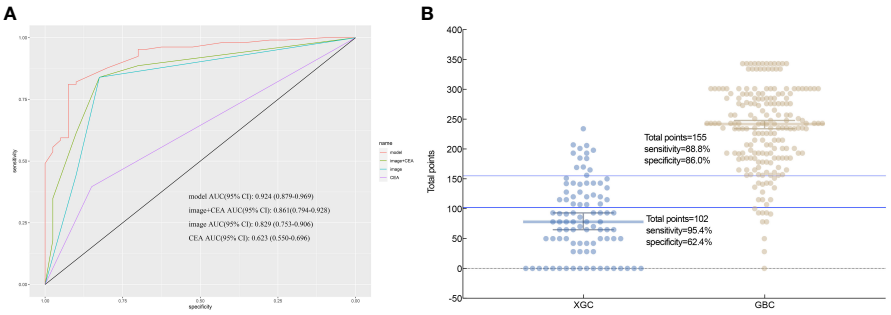

FIGURE 6
According to nomogram scores, the performance of the novel model (nomogram), image+CEA, image, and CEA in differentiating patients with xanthogranulomatous cholecystitis (XGC) and GBC (GBC) were compared. **(A)** Receiver operating characteristic (ROC) curve. The area under the ROC curve of the model, image+CEA, image, and CEA, was 0.936, 0.861, 0.821, and 0.654, respectively. It reflects the good discriminant ability of the nomogram to predict GBC. **(B)** Interactive dot diagram for the performance of the nomogram in differentiating XGC and GBC. X-axis: patients in XGC and GBC groups; Y-axis: the scale for total points of each XGC and GBC patient; each dot; each dot is a data point for the result of each patient. The horizontal blue line represents the optimal critical value that maximizes the sum of sensitivity and specificity.

TABLE 5 Distribution of model characteristics in each AJCC stage of GBC patients.

Characteristic	AJCC stage I (n=37)	AJCC stage II (n=36)	AJCC stage III (n=78)	AJCC stage IV (n=46)	Total (n=197)
Gendar, female (%)	22(59.5%)	23(63.9%)	55(70.5%)	32(69.6%)	132(67.0%)
Murphy, no	34(91.9%)	33(91.7%)	71(91.0%)	38(82.6%)	175(88.8%)
N <5.60*10^9/L	29(78.4%)	29(80.6%)	67(85.9%)	25(54.3%)	150(76.1%)
GGT <29U/L	14(37.8%)	19(52.8%)	28(35.9%)	15(32.6%)	76(38.6%)
CEA ≥3.2 ug/L	12(32.4%)	17(47.2%)	45(57.7%)	27(58.7%)	101(51.3%)
Comprehensive preoperative imaging diagnosis					
Benign gallbladder diseases	9(24.4%)	13(36.2%)	13(16.7%)	5(10.9%)	40(20.3%)
Suspected gallbladder carcinoma	14(37.8%)	8(22.2%)	25(32.1%)	13(28.3%)	60(30.5%)
Gallbladder carcinoma	14(37.8%)	15(41.6%)	40(51.2%)	28(60.8%)	97(49.3%)
Total points	226(160,279)	234(184,291)	250(193,293)	243(181,279)	242(185,285)

AJCC, American Joint Committee on Cancer; GBC, Gallbladder carcinoma; N,neutrophile granulocyte; GGT, gamma-glutamyl transpeptidase; CEA, carcinoembryonic antigen.

duct, invades the surrounding liver, and even forms a fistula with the intrahepatic bile duct. The bile duct is uninjured in the early stages of GBC. Consequently, a GGT level lower than 29 U/L is considered an independent risk factor of GBC.

Similar to other biliary tract diseases, the differentiation between XGC and GBC relies on imaging modalities, including US, CT, and MRI. In XGC patients, the rupture or ulceration of the Rokitansky-Aschoff sinus facilitates bile entry into the gallbladder and infiltration into the interstitial space. However, features of the unclear hepatic silhouette or mucosal interruption are usually challenging to distinguish from GBC, with tumors invading the serous layer of the gallbladder. Interestingly, the OR for comprehensive imaging diagnosis was highest for GBC diagnosis in this study. Additionally, the complexity in differentiating XGC from GBC through imaging techniques is compounded by the thickening of the gallbladder wall, which can be a result of either acute or chronic inflammation of the gallbladder. Therefore, accurate identification of XGC and GBC by imaging technology remains challenging. Given that most patients in the study did not receive contrast-enhanced MRI, there is a lack of data regarding contrast-enhanced MRI for these patients. However, comprehensive preoperative imaging diagnosis was higher than that of enhanced CT alone in 80.7% (234/290) of cases. In XGC and GBC patients included in this study, the accuracy of preoperative diagnosis with CT enhancement and MRI enhancement was 78.2% (161/206) and 87.9% (29/33), respectively. In the comprehensive imaging diagnosis, the accuracy of XGC and GBC was 78.2% (77/93) and 78.2% (157/197). Regardless of whether a single imaging examination or comprehensive imaging modality is used, we can observe that there is a considerable proportion of GBC patients misdiagnosed as benign gallbladder diseases. Employing comprehensive imaging diagnosis can decrease the rate of such misdiagnoses in patients with GBC. Furthermore, Figure 9 illustrates one case of XGC and one case of GBC misdiagnosed by comprehensive imaging. In these two cases, the surgeon successfully selected the appropriate surgical approach for the patient by combining intraoperative frozen pathological results and model risk assessment.

TABLE 6 Characteristics of GBC patients with AJCC stage I and stage II.

Characteristic	AJCC stage I (n=37)	AJCC stage II (n=36)	P value
Imaging showed gallbladder wall thickening, n (%)	30(81.1%)	31(86.1%)	0.754
Imaging gallbladder wall thickness (*mm), median (IQR)	15(8,20)	12(10,15)	0.384
Abdominal ultrasound misdiagnosis, n (%)	17(45.9%)	16(44.4%)	1
Comprehensive preoperative imaging misdiagnosis, n (%)	9(24.3%)	13(36.1%)	0.315
Intraoperative frozen section pathology, n (%)	30(81.1%)	34(94.4%)	0.152
Intraoperative frozen section pathology misdiagnosis, n (%)	2(6.7%)	3(8.8%)	1
Unexpected gallbladder cancer, n (%)	7(18.9%)	1(2.8%)	0.152
Combined adenoma, n (%)	7(18.9%)	3(8.8%)	0.308
Combined with intraepithelial neoplasia, n (%)	10(27.0%)	6(16.7%)	0.398

AJCC, American Joint Committee on Cancer; GBC, Gallbladder carcinoma.

Although the AUC of enhanced CT and enhanced MR was relatively high, the differentiation between XGC and GBC remains problematic in clinical practice. First, XGC is a relatively rare disease, and most patients are diagnosed with gallbladder inflammation due to the limitations of imaging features. Only a minority of patients further undergo MR examination. Therefore, we speculate that tests with high sensitivity and specificity are difficult to popularize in this population. This could have contributed to the perplexity in differentiating the two diseases. Second, radiologists re-evaluated the diagnosis in established patients with XGC and GBC in this study. However, in clinical practice, XGC and GBC should be distinguished from other

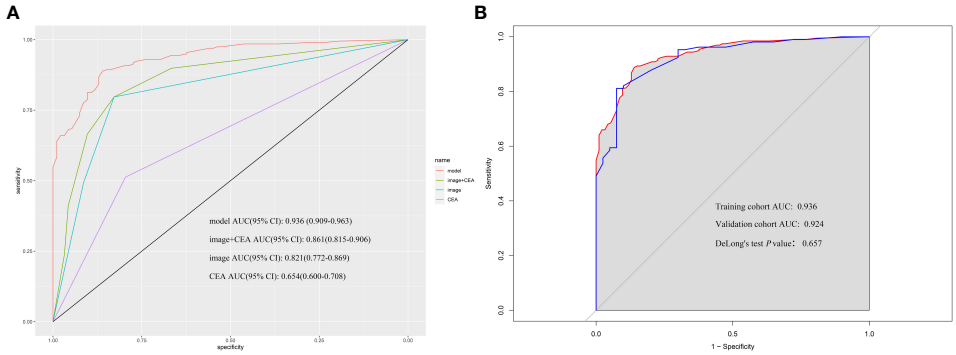

FIGURE 7
(A) According to nomogram scores, the performance of the novel model (nomogram), image+CEA, image, and CEA in the validation cohort. The area under the receiver operating characteristic (ROC) curve of the model, image+CEA, image, and CEA were 0.924, 0.861, 0.829, and 0.623, respectively. **(B)** The area under the ROC curve of the model in the training cohort and validation cohort was 0.936 and 0.924. The *P*-value of DeLong's test was 0.657.

gallbladder diseases such as gallbladder polyps, gallbladder adenomyosis, and secondary GBC, while GBC in the neck of gallbladder even needs to be differentiated from diseases such as hilar cholangiocarcinoma. Therefore, the scope of diagnosis of enrolled patients was significantly limited, whereas radiologists conduct comprehensive differential diagnoses in real-life situations, which also adds to the difficulty in identifying XGC and GBC. Moreover, there was an unmet need for a preoperative diagnostic model combined with other independent risk factors to facilitate clinicians' decision-making.

Most studies on the preoperative diagnosis of XGC and GBC focus on their differential diagnosis using various preoperative imaging examinations (10, 24, 25). However, reports on the demographics, clinical symptoms, and laboratory tests of XGC and GBC patients are scarce. This study is the first to design a diagnostic criteria chart to assist clinicians in diagnosing and treating XGC and GBC. To the best of our knowledge, this is the most extensive single-center study to construct a diagnostic nomogram for differentiating XGC from GBC. Compared with traditional methods, machine learning methods (random forest) have greatly improved the rigor of screening risk factors. By analyzing the demographics, clinical, laboratory, and imaging data of 93 patients with XGC and 197 patients with GBC, a nomogram with desirable predictive value for XGC and GBC was developed. The nomogram was subsequently well-calibrated. The valuable nomogram comprised variables such as gender, Murphy's sign, absolute neutrophil count, glutamyl transpeptidase level, carcinoembryonic antigen level, and comprehensive imaging diagnosis. Moreover, the AUC value of the nomogram in predicting XGC and GBC was 0.936 (95% CI: 0.894–0.954). As anticipated, the nomogram outperformed any single risk factor or combination of risk factors in the predictive model (Figures 2, 6). Furthermore, the data from the Affiliated Lihuili Hospital of Ningbo University were used for external validation. The results demonstrated that the model had optimal diagnostic performance (Figure 7).

FIGURE 8
As shown in the figure above, the appropriate option was selected according to the patient's gender, Murphy's sign, CEA value, absolute neutrophil count, GGT value, and comprehensive imaging diagnosis. The right image shows the probability that the patient is diagnosed with gallbladder carcinoma.

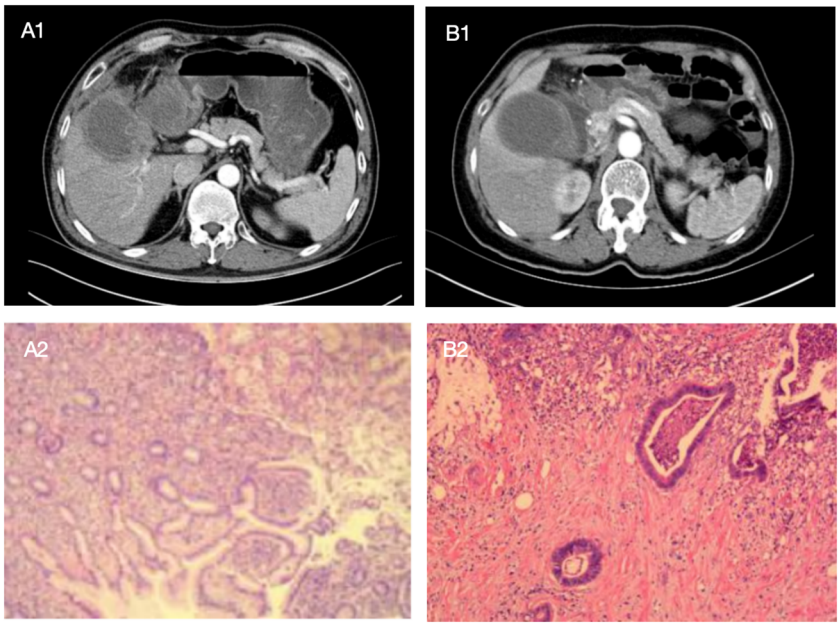

FIGURE 9
The following are two cases in which the model was applied to intraoperative decision making, with preoperative enhanced CT images of patients and postoperative pathological sections as above. Patient A showed a high-density mass with blurred margins in the arterial phase of enhanced CT. The mass was located in the neck of the gallbladder. The patient was a 52-year-old man with Murphy's sign, N 7.4*10^9/L, GGT 149U/L, and CEA 0.8ug/L. Comprehensive preoperative imaging diagnosis **(A1)** was considered suspicious of gallbladder cancer, but its probability of predicting gallbladder cancer was 0.239. In this case, the boundary and anatomical structure of the liver of the gallbladder were blurred during the operation, and the frozen section pathology showed no abnormality after complete resection of the gallbladder. The surgeon chose simple cholecystectomy based on the conjecture of the model, and no "gallbladder cancer" was found in postoperative routine pathology **(A2)**. Patient B showed a high-density mass with blurred margins in the arterial phase of enhanced CT. The mass was located in the neck of the gallbladder. The patient was a 68-year-old female with negative Murphy's sign, N 4.35*10^9/L, GGT 15U/L, and CEA 2.3ug/L. Comprehensive preoperative imaging diagnosis **(B1)** considered benign gallbladder disease, but its probability of predicting gallbladder cancer was 0.880. In this case, no gallbladder cancer was found by repeated frozen pathology during operation, but radical resection of gallbladder cancer was still performed after the surgeon conjecturing according to the model, and postoperative routine pathology **(B2)** showed "gallbladder cancer".

Given that it is difficult to identify patients with XGC and GBC in clinical practice accurately, the nomogram sites were stratified into three groups based on optimal truncation points: low-, medium-, and high-risk groups. The total points, probability of GBC, sensitivity, and specificity are listed as follows: < 93, < 0.25, > 0.970, and < 0.559 in the low-risk group; 93–170, 0.25–0.75, 0.970–0.812 and 0.559–0.892 in the medium-risk group; > 170, > 0.75, < 0.812 and > 0.892 in the high-risk group. In the nomogram, the probability of the optimal cutoff value was determined to be 0.65 according to the Youden index, corresponding to 155 points. The sum of sensitivity (88.8%) and specificity (86.0%) for GBC diagnosis was the highest. Compiling comprehensive preoperative patient information and using the nomogram for scoring allows for risk stratification of GBC, offering a practical tool for clinicians. For patients in the intermediate-high risk group and those suspected of GBC based on imaging, an intraoperative frozen section is essential. When all imaging tests suggest benign gallbladder disease, but the surgeon remains unable to exclude GBC, this model aids the surgeon in deciding whether to opt for an intraoperative frozen section.

As shown in Table 5, patients in the training cohort were subjected to subgroup analysis according to AJCC stage of GBC, and the distribution of model characteristics of patients in each stage was compared. The proportion of women was higher than that of men in each stage. Compared with AJCC stage I, II and III patients, the proportion of Murphy's sign positive and N ≥5.60*10^9/L increased in stage IV patients. The authors consider that this may be related to the tumor invasion of surrounding organs in patients with stage IV, which is more similar to cholecystitis in symptoms and inflammatory indicators. In addition, no significant differences were observed between stages of GGT grouping. It is worth to note that the proportion of patients with CEA ≥3.2 ug/L in stage III and IV was higher than that in stage I and II, which the authors hold that may be related to lymph node metastasis. In the preoperative comprehensive imaging diagnosis, the proportion of GBC patients with stage III and IV diagnosed as benign gallbladder diseases was only 16.7% and 10.9%.

Due to the low degree of invasion and insignificant imaging features of AJCC stage I and II, Table 6 summarizes the imaging and pathological features of a total of 73 GBC patients in these two stages. Among the 37 patients in AJCC I stage, there were 1 case of carcinoma *in situ*, 7 cases of tumor invasion into the lamina propria, and 29 cases of tumor invasion into the muscular layer. Contrary to our expectations, the gallbladder wall thickness of stage I patients was generally higher than that of stage II patients. Although the two were not statistically significant, the authors suggest that this phenomenon may be related to a greater probability of adenoma or intraepithelial neoplasia in the former group. The missed diagnosis rate of AJCC stage I and II GBC patients by abdominal

ultrasound alone was 45.9% and 44.4%, respectively, while the missed diagnosis rate of comprehensive imaging diagnosis was 24.3% and 36.1%, respectively. This suggests that abdominal ultrasound combined with cross-sectional scan is helpful to reduce the rate of missed diagnosis, and intraoperative frozen section should be performed to determine the nature of GBC when an imaging examination is considered. In these two stage GBC patients, "unsuspected gallbladder carcinoma" was found in 7 and 1 cases, respectively. Among the 64 cases of intraoperative frozen section, 2 cases were misdiagnosed, and 3 cases were only reported as intraepithelial neoplasia. Therefore, the accuracy of intraoperative frozen section in patients with AJCC stage 1 and 2 GBC in this study was 92.2%.

This study has some limitations that need to be considered. First, the nomogram was developed and validated in China, whereas XGC and GBC are uncommon conditions in Western populations. Consequently, the results of the nomogram may not be generalizable to the global population. Second, this study was retrospective, and the sample size of this study was small. Hence, the accuracy of the model must be verified by a larger sample size. Moreover, the diagnostic model constructed in this study may be unsuitable for the differentiation of benign gallbladder diseases except XGC from GBC.

Approximately 60%–70% of GBC patients are incidentally detected by pathologists after cholecystectomy for benign diseases (26, 27). In a study of 187 cases of GBC combined with 20 articles, 15 cases (8%) had normal gross appearance during the surgical operation (28). For these patients, it was difficult for surgeons to select the intraoperative frozen sections for pathological examination. Consequently, the decision to perform an intraoperative frozen section in most instances relies on the imaging examination and the judgment of the treating surgeon, indicating a lack of objective criteria for evaluation.

In conclusion, factors such as gender, Murphy's sign, absolute neutrophil count, glutamyl transpeptidase level, serum carcinoembryonic antigen level, and comprehensive imaging diagnosis emerge as potential independent risk factors for GBC. This nomogram is anticipated to serve as a novel and precise instrument for distinguishing GBC from XGC.

Data availability statement

The original contributions presented in the study are included in the article/supplementary material. Further inquiries can be directed to the corresponding authors.

Ethics statement

The studies involving humans were approved by Ethics Review Committee of Zhejiang Provincial People's Hospital. The studies were conducted in accordance with the local legislation and institutional requirements. Written informed consent for participation was not required from the participants or the participants' legal guardians/next of kin in accordance with the national legislation and institutional requirements.

Author contributions

TF: Conceptualization, Data curation, Formal analysis, Funding acquisition, Investigation, Methodology, Software, Writing – original draft, Writing – review & editing. YB: Data curation, Formal analysis, Funding acquisition, Validation, Writing – original draft. ZZ: Data curation, Formal analysis, Writing – original draft. ZG: Data curation, Formal analysis, Writing – original draft. TY: Data curation, Formal analysis, Writing – original draft. CZ: Supervision, Writing – original draft. HJ: Supervision, Writing – review & editing, Validation. ZX: Supervision, Writing – review & editing.

Funding

The author(s) declare that no financial support was received for the research, authorship, and/or publication of this article.

Conflict of interest

The authors declare that the research was conducted in the absence of any commercial or financial relationships that could be construed as a potential conflict of interest.

Publisher's note

References

1. Zhao F, Lu PX, Yan SX, Wang GF, Yuan J, Zhang SZ, et al. CT and MR features of xanthogranulomatous cholecystitis: an analysis of consecutive 49 cases. *Eur J Radiol.* (2013) 82:1391–7. doi: 10.1016/j.ejrad.2013.04.026.

2. Benbow EW. Xanthogranulomatous cholecystitis associated with carcinoma of the gallbladder. *Postgrad Med J.* (1989) 65:528–31. doi: 10.1136/pgmj.65.766.528.

3. Roberts KM, Parsons MA. Xanthogranulomatous cholecystitis: clinicopathological study of 13 cases. *J Clin Pathol.* (1987) 40:412–7. doi: 10.1136/jcp.40.4.412.

4. Suzuki H, Wada S, Araki K, Kubo N, Watanabe A, Tsukagoshi M, et al. Xanthogranulomatous cholecystitis: Difficulty in differentiating from GBC. *World J Gastroenterol.* (2015) 21:10166–73. doi: 10.3748/wjg.v21.i35.10166.

5. Truant S, Chater C, Pruvot FR. Greatly enlarged thickened gallbladder. Diagnosis: Xanthogranulomatous cholecystitis (XGC). *JAMA Surg*. (2015) 150:267–8. doi: 10.1001/jamasurg.2014.492.

6. Goshima S, Chang S, Wang JH, Kanematsu M, Bae KT, Federle MP. Xanthogranulomatous cholecystitis: diagnostic performance of CT to differentiate from GBC. *Eur J Radiol*. (2010) 74:e79–83. doi: 10.1016/j.ejrad.2009.04.017.

7. Hijioka S, Mekky MA, Bhatia V, Sawaki A, Mizuno N, Hara K, et al. Can EUS-guided FNA distinguish between GBC and xanthogranulomatous cholecystitis? *Gastrointest Endosc*. (2010) 72:622–7. doi: 10.1016/j.gie.2010.05.022.

8. Park SW, Cho WT, Shin E. An unusual cause of abnormal weight loss. *Gastroenterology*. (2020) 158:e13–e4. doi: 10.1053/j.gastro.2019.09.043.

9. Runner GJ, Corwin MT, Siewert B, Eisenberg RL. Gallbladder wall thickening. *AJR Am J Roentgenol*. (2014) 202:W1–w12. doi: 10.2214/AJR.12.10386.

10. Gupta P, Marodia Y, Bansal A, Kalra N, Kumar MP, Sharma V, et al. Imaging-based algorithmic approach to gallbladder wall thickening. *World J Gastroenterol*. (2020) 26:6163–81. doi: 10.3748/wjg.v26.i40.6163.

11. Kwon AH, Sakaida N. Simultaneous presence of xanthogranulomatous cholecystitis and GBC. *J Gastroenterol*. (2007) 42:703–4. doi: 10.1007/s00535-007-2072-6.

12. Nacif LS, Hessheimer AJ, Rodríguez Gómez S, Montironi C, Fondevila C. Infiltrative xanthogranulomatous cholecystitis mimicking aggressive GBC: A diagnostic and therapeutic dilemma. *World J Gastroenterol*. (2017) 23:8671–8. doi: 10.3748/wjg.v23.i48.8671.

13. Şimşek G, Şahin A, Metin ŞH, Ulutaş ME, Arslan K. The management of xanthogranulomatous cholecystitis. *Turk J Surg*. (2021) 37:242–6. doi: 10.47717/turkjsurg.

14. Makimoto S, Takami T, Hatano K, Kataoka N, Yamaguchi T, Tomita M, et al. Xanthogranulomatous cholecystitis: a review of 31 patients. *Surg Endosc*. (2021) 35:3874–80. doi: 10.1007/s00464-020-07828-6.

15. Yucel O, Uzun MA, Tilki M, Alkan S, Kilicoglu ZG, Goret CC. Xanthogranulomatous cholecystitis: analysis of 108 patients. *Indian J Surg*. (2017) 79:510–4. doi: 10.1007/s12262-016-1511-0.

16. Deng YL, Cheng NS, Zhang SJ, Ma WJ, Shrestha A, Li FY, et al. Xanthogranulomatous cholecystitis mimicking GBC: An analysis of 42 cases. *World J Gastroenterol*. (2015) 21:12653–9. doi: 10.3748/wjg.v21.i44.12653.

17. Misra S, Chaturvedi A, Misra NC, Sharma ID. Carcinoma of the gallbladder. *Lancet Oncol*. (2003) 4:167–76. doi: 10.1016/S1470-2045(03)01021-0.

18. Hundal R, Shaffer EA. GBC: epidemiology and outcome. *Clin Epidemiol*. (2014) 6:99–109. doi: 10.2147/CLEP.S37357

19. Wang YF, Feng FL, Zhao XH, Ye ZX, Zeng HP, Li Z, et al. Combined detection tumor markers for diagnosis and prognosis of GBC. *World J Gastroenterol*. (2014) 20:4085–92. doi: 10.3748/wjg.v20.i14.4085.

20. Xiao J, Zhou R, Zhang B, Li B. Noninvasive preoperative differential diagnosis of GBC and xanthogranulomatous cholecystitis: A retrospective cohort study of 240 patients. *carcinoma Med*. (2022) 11:176–82. doi: 10.1002/cam4.4442.

21. Yu H, Yu TN, Cai XJ. Tumor biomarkers: help or mislead in the diagnosis of xanthogranulomatous cholecystitis?-analysis of serum CA 19-9, carcinoembryonic antigen, and CA 12-5. *Chin Med J (Engl)*. (2013) 126:3044–7. doi: 10.3760/cma.j.issn.0366-6999.20120341.

22. Randi G, Franceschi S, La Vecchia C. GBC worldwide: geographical distribution and risk factors. *Int J carcinoma*. (2006) 118:1591–602. doi: 10.1002/ijc.21683.

23. Sotil EU, Jensen DM. Serum enzymes associated with cholestasis. *Clin Liver Dis*. (2004) 8:41–54, vi. doi: 10.1016/S1089-3261(03)00136-3.

24. Zhang F, Chen W, Zhang L, Hou C, Zhang M. Usefulness of ultrasound in differentiating xanthogranulomatous cholecystitis from GBC. *Ultrasound Med Biol*. (2019) 45:2925–31. doi: 10.1016/j.ultrasmedbio.2019.07.682.

25. Zhou QM, Liu CX, Zhou JP, Yu JN, Wang Y, Wang XJ, et al. Machine learning-based radiological features and diagnostic predictive model of xanthogranulomatous cholecystitis. *Front Oncol*. (2022) 12:792077. doi: 10.3389/fonc.2022.792077.

26. Fuks D, Regimbeau JM, Le Treut YP, Bachellier P, Raventos A, Pruvot FR, et al. Incidental GBC by the AFC-GBC-2009 study group. *World J Surg*. (2011) 35:1887–97. doi: 10.1007/s00268-011-1134-3.

27. Duffy A, Capanu M, Abou-Alfa GK, Huitzil D, Jarnagin W, Fong Y, et al. GBC (GBC): 10-year experience at Memorial Sloan-Kettering carcinoma Centre (MSKCC). *J Surg Oncol*. (2008) 98:485–9. doi: 10.1002/jso.21141.

28. Jamal K, Ratansingham K, Siddique M, Nehra D. Routine histological analysis of a macroscopically normal gallbladder–a review of the literature. *Int J Surg*. (2014) 12:958–62. doi: 10.1016/j.ijsu.2014.07.010.

frontiers | Frontiers in Oncology

TYPE Original Research
PUBLISHED 28 February 2024
DOI 10.3389/fonc.2024.1372007

OPEN ACCESS

EDITED BY
Francisco Tustumi,
University of São Paulo, Brazil

REVIEWED BY
Hasan Cagri Yildirim,
Hacettepe University, Türkiye
Kazuto Tajiri,
University of Toyama University Hospital, Japan

*CORRESPONDENCE
Pil Soo Sung
pssung@catholic.ac.kr

RECEIVED 17 January 2024
ACCEPTED 09 February 2024
PUBLISHED 28 February 2024

CITATION
Han JW, Sung PS, Yoo J-S, Cho HS, Lee SK, Yang H, Kim JH, Nam H, Lee HL, Kim HY, Lee SW, Song DS, Song MJ, Kwon JH, Kim CW, Bae SH, Jang JW, Choi JY and Yoon SK (2024) Differential liver function at cessation of atezolizumab-bevacizumab versus lenvatinib in HCC: a multicenter, propensity-score matched comparative study. *Front. Oncol.* 14:1372007. doi: 10.3389/fonc.2024.1372007

Differential liver function at cessation of atezolizumab-bevacizumab versus lenvatinib in HCC: a multicenter, propensity-score matched comparative study

Ji Won Han[1,2], Pil Soo Sung[1,2]*, Jae-Sung Yoo[1,2], Hee Sun Cho[1,2], Soon Kyu Lee[1,3], Hyun Yang[1,4], Ji Hoon Kim[1,5], Heechul Nam[1,5], Hae Lim Lee[1,6], Hee Yeon Kim[1,6], Sung Won Lee[1,6], Do Seon Song[1,7], Myeong Jun Song[1,8], Jung Hyun Kwon[1,3], Chang Wook Kim[1,5], Si Hyun Bae[1,4], Jeong Won Jang[1,2], Jong Young Choi[1,2] and Seung Kew Yoon[1,2]

[1]The Catholic University Liver Research Center, College of Medicine, The Catholic University of Korea, Seoul, Republic of Korea, [2]Division of Gastroenterology and Hepatology, Department of Internal Medicine, College of Medicine, Seoul St. Mary's Hospital, The Catholic University of Korea, Seoul, Republic of Korea, [3]Division of Gastroenterology and Hepatology, Department of Internal Medicine, College of Medicine, Incheon St. Mary's Hospital, The Catholic University of Korea, Incheon, Republic of Korea, [4]Division of Gastroenterology and Hepatology, Department of Internal Medicine, College of Medicine, Eunpyeong St. Mary's Hospital, The Catholic University of Korea, Seoul, Republic of Korea, [5]Division of Gastroenterology and Hepatology, Department of Internal Medicine, College of Medicine, Uijeongbu St. Mary's Hospital, The Catholic University of Korea, Uijeongbu, Republic of Korea, [6]Division of Gastroenterology and Hepatology, Department of Internal Medicine, College of Medicine, Bucheon St. Mary's Hospital, The Catholic University of Korea, Bucheon, Republic of Korea, [7]Division of Gastroenterology and Hepatology, Department of Internal Medicine, St. Vincent's Hospital, College of Medicine, The Catholic University of Korea, Suwon, Republic of Korea, [8]Division of Gastroenterology and Hepatology, Department of Internal Medicine, Daejeon St. Mary's Hospital, College of Medicine, The Catholic University of Korea, Daejeon, Republic of Korea

Background: Atezolizumab+bevacizumab (AB) and lenvatinib have been proposed as first-line treatment options for patients with advanced hepatocellular carcinoma (HCC), but comparative efficacy and associated factors are controversial.

Materials and methods: This real-world multicenter study analysed patients with HCC who received AB (n=169) or lenvatinib (n=177).

Results: First, 1:1 propensity score matching (PSM) was performed, resulting in 141 patients in both the AB and lenvatinib groups. After PSM, overall survival (OS) was better in the AB group than in the lenvatinib group [hazard ratio (HR)=0.642, P=0.009], but progression-free survival (PFS) did not vary between the two groups (HR=0.817, P=0.132). Objective response rate (ORR) was also similar between AB and lenvatinib (34.8% vs. 30.8%, P=0.581). In a subgroup of patients with objective responses (OR, n=78), OS (HR=0.364, P=0.012) and PFS (HR=0.536, P=0.019) were better in the AB group (n=41) than in the lenvatinib group (n=37). Time-to-progression from time of OR was also better in the AB

group (HR=0.465, P=0.012). Importantly, residual liver function was a significant factor related to OS in both treatments. Child-Pugh score following cessation of the respective treatments was better in the AB group (n=105) than in the lenvatinib group (n=126) (median 6 versus 7, P=0.008), and proportion of salvage treatment was also higher in the AB group (52.4% versus 38.9%, P=0.047). When we adjusted for residual liver function or salvage treatment, there was no difference in OS between the two treatments.

Conclusion: Our study suggests that residual liver function and subsequent salvage treatments are major determinants of clinical outcomes in patients treated with AB and lenvatinib; these factors should be considered in future comparative studies.

KEYWORDS

HCC, atezolizumab plus bevacizumab, lenvatinib, residual liver function, survival

1 Introduction

The REFLECT and IMbrave150 trials have shown that lenvatinib and atezolizumab plus bevacizumab (AB) have better clinical outcomes than sorafenib in advanced, unresectable hepatocellular carcinoma (HCC) (1, 2). In the REFLECT trial, lenvatinib showed comparable overall survival (OS) compared to sorafenib (median 13.6 versus 12.3 months), whereas it had better progression-free survival (PFS) (median 7.4 versus 3.7 months, P<0.001) and objective response rate (ORR) (24.1% versus 9.2%, P<0.001) (1). In the IMbrave150 trial, AB had superior OS (19.2 versus 13.4 months, P<0.001), PFS (6.9 versus 4.3 months, P<0.001), and ORR (30.0% versus 11.9%, P<0.001) to lenvatinib (2).

Consequently, these therapeutic regimens have been endorsed as first-line treatment options for patients with advanced HCC. Notwithstanding these recommendations, a prevailing debate exists concerning which of the two is the most optimal for first-line treatment. Some investigations posit that AB is superior to lenvatinib in terms of OS (3–5), whereas alternative studies assert the contrary (6, 7). Moreover, some reports indicated no significant difference in efficacy between the two regimens (8–10).

Liver function, tumor size, tumor extension into adjacent structures, patient performance status, and extrahepatic metastases serve as pivotal prognostic indicators in individuals diagnosed with HCC (11). Additionally, hepatitis B or C infections, as well as serum concentrations of tumor markers—namely alpha-fetoprotein (AFP) and protein induced by vitamin K absence or antagonist-II (PIVKA-II)—should be taken into account when assessing prognostic factors. Furthermore, subsequent treatment can extend survival in patients who discontinue first-line therapy due to tumor progression or adverse events (AEs) whose performance status and liver function are adequate to tolerate further treatment (12), suggesting that the capability of patients to undergo second-line therapy following the termination of initial treatment stands as a significant factor closely associated with clinical outcomes.

However, previous studies comparing these two treatments did not take into account various prognostic factors including residual liver function and salvage treatment, nor did they conduct subgroup analyses based on these factors. In this real-world, multi-center study utilizing propensity-score matching (PSM), we conducted comparative analyses between lenvatinib and AB in terms of OS, PFS, and ORR. Of note, we conducted subgroup analyses that considered baseline factors, as well as residual function and salvage treatments, to determine which factors influence the differences in clinical outcomes between the two treatments.

2 Materials and methods

2.1 Study cohort

Ethical approval for this research was granted by the Institutional Review Board of the Catholic University of Korea (approved number: XC23RADI0081), and the investigation was conducted in adherence to the principles delineated in the Declaration of Helsinki. A retrospective analysis was undertaken on 346 consecutive patients with unresectable HCC who were treated with AB or lenvatinib at seven affiliated hospitals in Korea. For the AB arm, patients were enrolled between September 2020 and December 2022; for the lenvatinib arm, the enrollment period was from January 2019 to December 2022. Diagnoses of HCC were confirmed either histologically or through radiological examinations, specifically contrast-enhanced

computed tomography (CT) and/or magnetic resonance imaging (MRI). Inclusion criteria comprised: (1) histologically or radiologically confirmed intermediate to advanced HCC not amenable to surgical resection; (2) minimum age of 18 years; and (3) an Eastern Cooperative Oncology Group (ECOG) performance status score not exceeding 2. Exclusion criteria included: (1) absence of follow-up post-initiation of therapy; (2) less than a two-week treatment course with lenvatinib; (3) fewer than two cycles of AB; and (4) prior malignancies other than HCC within the past five years.

2.2 Therapeutic protocol

Lenvatinib dosing was stratified by patient body weight: 8 mg daily for those weighing less than 60 kg and 12 mg daily for those above 60 kg. The AB therapeutic regimen consisted of intravenous administration of 1200 mg atezolizumab in conjunction with 15 mg/kg bevacizumab, repeated tri-weekly until either disease progression or onset of unacceptable toxicity.

2.3 Efficacy and adverse event assessment

Patients were stratified by the Barcelona Clinic Liver Cancer (BCLC) stage, utilizing radiological and laboratory data at the time of enrollment. Periodic imaging, via CT or MRI, was scheduled at 4-12 weeks intervals for lenvatinib and every 3-4 cycles for AB to evaluate treatment responses based on the modified Response Evaluation Criteria in Solid Tumors (mRECIST), as previously delineated (13). OS and PFS were measured from treatment initiation to the date of death, last follow-up, or disease progression. ORR was calculated as the sum of the "complete" and "partial" responses at the response evaluation. The disease control rate (DCR) was calculated as the sum of the complete response (CR), partial response (PR), and stable disease (SD). Additionally, the modified albumin-bilirubin (mALBI) score was quantified to gauge hepatic function using a predetermined formula (14). AEs were characterized according to the Common Terminology Criteria for Adverse Events version 4.0 (15).

2.4 Statistical methods

Statistical computations were conducted employing R statistical software (version 4.0.3; R Foundation Inc., Vienna, Austria; http://cran.r-project.org, accessed on 6 September 2021) and SPSS version 23.0 software (IBM Corp., Armonk, NY, USA). Continuous variables were compared via Student's t-test, and categorical variables were compared via chi-square test. To counterbalance baseline differences between the AB (n=169) and lenvatinib (n=177) cohorts, PSM was applied using one-to-one nearest-neighbor matching within a 0.20 caliper width, resulting in 141 patients in each matched group. Kaplan-Meier estimations were employed for survival analyses, and Cox regression modeling was utilized for survival outcome determinants. Statistical significance was established at p-values < 0.05.

3 Results

3.1 Baseline characteristics

Table 1 shows the comparison of baseline characteristics between AB (n=169) and lenvatinib (n=177) groups before and after PSM. Before PSM, demographic characteristics including gender, age, and etiology were comparable between the two groups. Additive combined treatment on each regimen was comparably performed in the two groups. However, the proportion of treatment-naïve patients was significantly higher in the AB group (60/169, 35.5% versus 36/177, 20.3%, P=0.002). Regarding laboratory tests, the serum levels of aspartate aminotransferase (AST), alanine aminotransferase (ALT), albumin, platelets, international normalized ratio (INR), and creatinine as well as tumor markers such as AFP and PIVKA-II showed no significant differences between the two groups. However, the total bilirubin level was higher in the lenvatinib group (mean 1.2 versus 1.0 mg/dL, P=0.009). Furthermore, ascites, Child-Pugh class, and ECOG were not different between the two groups. Tumor factors including largest intrahepatic tumor size, multiple intrahepatic tumors, portal vein invasion (PVI), and extrahepatic spread were comparable, and mUICC and BCLC stages were also not different between the two groups. PSM was performed, and there was no difference in the baseline characteristics between the two groups. All subsequent analyses were performed using the matched cohort unless stated that an unmatched cohort was used.

3.2 Comparison of clinical outcomes

We investigated whether there are differences in clinical outcomes such as OS, PFS, ORR, and DCR between the two treatments. In the unmatched cohort, AB showed better OS and PFS compared to lenvatinib (Figure 1A). In the matched cohort, AB also showed significantly better OS than lenvatinib (median 599 versus 277 days, HR=0.642, P=0.009) (Figure 1B). However, PFS was not different between the two groups (median 168 days for AB, versus 126 days for lenvatinib, HR=0.817, P=0.132) (Figure 1B). Before and after PSM, ORR and DCR were not significantly different between the two groups (Table 2). In the matched cohort, ORR was 30.8% (37/120) in the lenvatinib group and 34.8% (41/118) in the AB group (P=0.581). Furthermore, DCR was 70.0% (84/120) in the lenvatinib group and 75.4% (89/118) in the AB group (P=0.384).

Next, we investigated which treatment would be beneficial in each subgroup in terms of OS and PFS. As a result, in the respective patient subgroups of age >65 years, viral etiology, ALBI grade 1, AFP>1000 ng/mL, PIVKA-II>1000 mAU/mL, ECOG 0, Child-Pugh 5A, largest intrahepatic tumor >5 cm, multiple intrahepatic tumors, or PVI, AB had significant benefits in OS (Supplementary Table 1). In addition, patient subgroups of ALBI grade 1, PIVKA-II>1000, largest intrahepatic tumor >5 cm, multiple intrahepatic tumors, or PVI also showed benefits in PFS from AB compared to lenvatinib (Supplementary Table 2).

TABLE 1 Comparison of baseline characteristics between lenvatinib and atezolizumab+bevacizumab groups before and after propensity-score matching.

	Before matching		P	After matching		P
	Lenvatinib n=177	AB n=169		Lenvatinib n=141	AB n=141	
Male gender	152 (85.9)	144 (85.2)	0.981	118 (83.7)	118 (83.7)	1.000
Age, years	63.6 ± 11.8	63.8 ± 11.5	0.906	63.8 ± 11.8	63.6 ± 11.2	0.852
Treatment naïve	36 (20.3)	60 (35.5)	0.002	36 (25.5)	34 (24.1)	0.890
Viral etiology	127 (71.8)	113 (66.9)	0.385	100 (70.9)	97 (68.8)	0.795
HBV	109 (61.6)	102 (60.4)	0.902	86 (61.0)	87 (61.7)	1.000
HCV	18 (10.2)	12 (7.1)	0.411	14 (9.9)	11 (7.8)	0.675
Alcohol	47 (26.6)	45 (26.6)	1.000	41 (29.1)	34 (24.1)	0.419
Others	20 (11.3)	25 (14.8)	0.420	16 (11.3)	22 (15.6)	0.383
Combined treatment	28 (15.8)	24 (14.2)	0.787	21 (14.9)	20 (14.2)	1.000
Radiotherapy	24 (13.6)	20 (11.8)	0.749	17 (12.1)	16 (11.3)	1.000
TACE	4 (2.3)	0 (0.0)	0.144	4 (2.8)	0 (0.0)	0.131
Surgery	0 (0.0)	3 (1.8)	0.230	0 (0.0)	3 (2.1)	0.246
Laboratory tests						
AST, U/L	86.4 ± 99.1	79.7 ± 81.9	0.492	78.9 ± 82.0	76.4 ± 85.5	0.801
ALT, U/L	44.4 ± 62.3	37.5 ± 34.3	0.201	39.8 ± 57.8	35.5 ± 35.5	0.448
Total bilirubin, mg/dL	1.2 ± 0.8	1.0 ± 0.7	0.009	1.1 ± 0.7	1.0 ± 0.7	0.298
Albumin, g/dL	3.7 ± 0.5	3.8 ± 0.5	0.818	3.7 ± 0.5	3.8 ± 0.4	0.594
Platelet, 10^9/L	167.0 ± 98.0	179.9 ± 93.7	0.213	173.2 ± 98.9	173.1 ± 90.7	0.990
INR	2.2 ± 13.7	1.1 ± 0.1	0.299	1.1 ± 0.1	1.1 ± 0.1	0.305
Creatinine, mg/dL	0.9 ± 0.7	0.9 ± 0.6	0.802	0.8 ± 0.3	0.9 ± 0.6	0.577
AFP, ng/mL	29673.3 ± 251757.9	12036.0 ± 33419.1	0.357	34560.4 ± 281596.2	12854.0 ± 35836.0	0.365
PIVKA-II, mAU/mL	22275.3 ± 59208.0	21379.1 ± 58625.5	0.888	21021.3 ± 59381.1	20959.3 ± 62518.5	0.993
Ascites	35 (19.8)	33 (19.5)	1.000	30 (21.3)	27 (19.1)	0.767
Child-Pugh class B	29 (16.4)	18 (10.7)	0.209	24 (17.0)	15 (10.6)	0.168
ECOG			0.212			0.229
1	63 (35.6)	55 (32.5)		48 (34.0)	43 (30.5)	
2	1 (0.6)	5 (3.0)		1 (0.7)	5 (3.5)	
Largest intrahepatic tumor size	7.1 ± 7.4	7.7 ± 5.5	0.376	7.3 ± 7.8	7.1 ± 5.5	0.809
Multiple intrahepatic tumor	131 (74.0)	121 (71.6)	0.701	102 (72.3)	98 (69.5)	0.694
Portal vein invasion	96 (54.2)	85 (50.3)	0.531	69 (48.9)	68 (48.2)	1.000
mUICC stage			0.644			0.405
2	9 (5.1)	5 (3.0)		7 (5.0)	5 (3.5)	
3	20 (11.3)	15 (8.9)		18 (12.8)	10 (7.1)	
4A	57 (32.2)	53 (31.4)		42 (29.8)	42 (29.8)	
4B	91 (51.4)	96 (56.8)		74 (52.5)	84 (59.6)	
BCLC stage			0.480			0.394
B	23 (13.0)	17 (10.1)		20 (14.9)	15 (10.6)	

(Continued)

TABLE 1 Continued

	Before matching		P	After matching		P
	Lenvatinib n=177	AB n=169		Lenvatinib n=141	AB n=141	
Laboratory tests						
C	154 (87.0)	152 (89.9)		120 (85.1)	126 (89.4)	
Extrahepatic spread	106 (59.9)	103 (60.9)	0.927	87 (61.7)	90 (63.8)	0.805
Lung	64 (36.2)	62 (36.7)	1.000	51 (36.2)	53 (37.6)	0.902
Lymph node	36 (20.3)	28 (16.6)	0.445	32 (22.7)	26 (18.4)	0.461
Adrenal	5 (2.8)	6 (3.6)	0.938	3 (2.1)	6 (4.3)	0.498
Bone	16 (9.0)	23 (13.6)	0.241	14 (9.9)	19 (13.5)	0.459
Peritoneal seeding	7 (4.0)	8 (4.7)	0.927	5 (3.5)	8 (5.7)	0.570

Data are given as n (%) or mean ± standard deviation. AB, Atezolizumab plus Bevacizumab; HBV, Hepatitis B Virus; HCV, Hepatitis C Virus; TACE, Transarterial Chemoembolization; AST, Aspartate Aminotransferase; ALT, Alanine Aminotransferase; INR, International Normalized Ratio; AFP, Alpha-fetoprotein; PIVKA-II, Protein Induced by Vitamin K Absence or Antagonist-II; ECOG, Eastern Cooperative Oncology Group; mUICC, Modified Union for International Cancer Control; BCLC, Barcelona Clinic Liver Cancer.

3.3 Factors associated with the clinical outcomes

We subsequently analysed factors associated with the OS (Table 3), PFS (Supplementary Table 3), and objective response (OR) (Supplementary Table 4) in the total, lenvatinib, and AB groups using multivariate analyses. Among the lenvatinib subgroup, high AST level, low albumin level, multiple intrahepatic tumors, high mUICC stage, and poor residual liver function after cessation of treatment were factors associated with poor OS. In the AB subgroup, high AST level, low albumin level, poor ECOG, and poor residual liver function were associated with poor OS, whereas multiple intrahepatic tumors or high mUICC stage were not significant. In terms of PFS, high AST level, poor baseline Child-Pugh score (CPS), multiple intrahepatic tumors, and high mUICC stage were related to poor PFS in the lenvatinib group, whereas low albumin level, ascites, poor ECOG, and high mUICC stage were significant in the AB group. Regarding OR, AST and ECOG were associated factors only in the total cohort, but not in the two treatment subgroups.

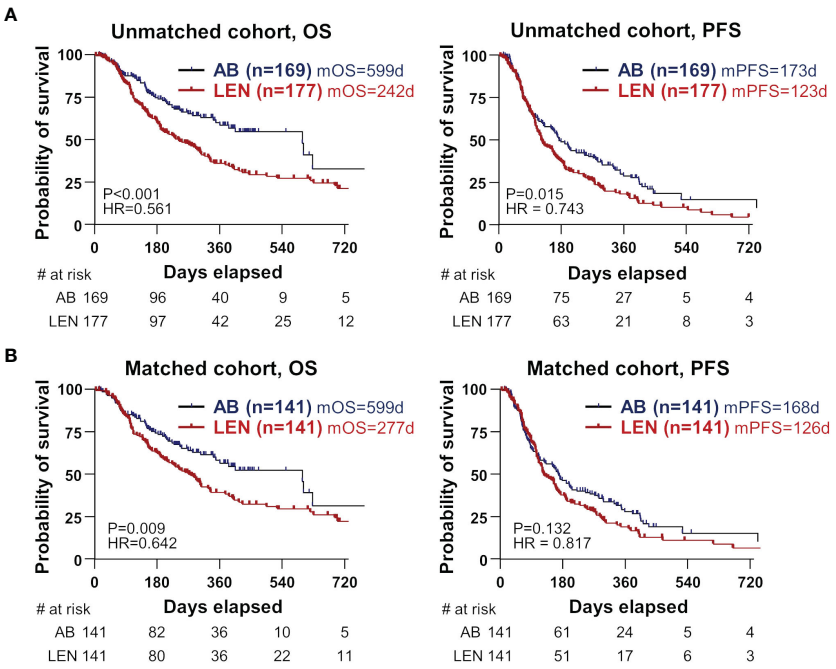

FIGURE 1
Survival differences between the two treatments in unmatched and matched cohorts. **(A, B)** OS and PFS were compared between AB- and LEN-treated patients, before **(B)** and after propensity-score matching. OS, overall survival; PFS, progression-free survival; AB, atezolizumab+bevacizumab; LEN, lenvatinib; m, median; d, days; HR, hazard ratio.

TABLE 2 Best responses of each treatment before and after matching.

	Before matching		P	After matching		P
	Lenvatinib n=177	AB n=169		Lenvatinib n=141	AB n=141	
CR	7 (4.0)	7 (4.1)		6 (4.3)	7 (5.0)	
PR	37 (20.9)	42 (24.9)		31 (22.0)	34 (24.1)	
SD	56 (31.6)	57 (33.7)		47 (33.3)	48 (34.0)	
PD	49 (27.7)	36 (21.3)		36 (25.5)	29 (20.6)	
undetermined	28 (15.8)	27 (16.0)		21 (14.9)	23 (16.3)	
ORR	44 (29.5)	49 (34.5)	0.381	37 (30.8)	41 (34.8)	0.581
DCR	100 (67.1)	106 (74.7)	0.197	84 (70.0)	89 (75.4)	0.384

Data are given as n (%). AB, Atezolizumab plus Bevacizumab; CR, Complete Response; PR, Partial Response; SD, Stable Disease; PD, Progressive Disease; ORR, Objective Response Rate; DCR, Disease Control Rate.

3.4 Differences in survival between the two treatments according to treatment response

We hypothesized that there might be a difference in the OS in patients who achieved OR, because of the better OS in the AB group without superior ORR. We compared OS in patients who achieved OR, and observed significantly better OS in the AB group (n=41) compared to the lenvatinib group (n=37) (median not reached versus 527 days, HR=0.364, P=0.012) (Figure 2A, left). Furthermore, PFS was also superior in the AB group compared to the lenvatinib group (median 405 versus 250 days, HR=0.536, P=0.019) (Figure 2A, right). Of note, time-to-progression (TTP) from the time point of OR was significantly better in the AB group (median 301 versus 165 days, HR=0.465, P=0.012) (Figure 2B). However, there was no difference in OS and PFS among disease-controlled patients (Supplementary Figure 1A), as well as in OS among patients with PD (Supplementary Figure 1B).

3.5 AEs and their association with the survivals

Table 4 shows the safety profiles of respective treatments. AEs of any grade or serious AEs of grade 3 or more did not differently occur in the two groups. Hand-foot syndrome was only observed in the lenvatinib group (19/141, 13.5%), and thyroiditis was observed more in the AB group (18/141, 12.8% versus 2/141, 1.4%, P=0.001). Variceal bleeding also significantly occurred in the AB group (9/141, 6.4% versus 1/141, 0.6%, P=0.007). However, the chemotherapy was stopped due to AEs more frequently in the lenvatinib group (22/141, 15.6% versus 9/141, 6.4%, P=0.022). Additionally, we have clarified that the median timing of the best responses between the two treatments—70.5 days for lenvatinib and 64 days for AB (P=0.149)—is not significantly different. This indicates that the most common timing for the best responses in both treatments corresponds to the first response evaluation.

TABLE 3 Multivariate Cox-regression analyses* of factors associated with overall survival in the matched cohort.

	Total (n=282)		Lenvatinib (n=141)		AB (n=141)	
	HR	P	HR	P	HR	P
AST	1.002 (1.00-1.00)	0.087	1.005 (1.00-1.01)	0.002	1.005 (1.00-1.01)	0.022
Albumin	0.546 (0.37-0.81)	0.003	0.524 (0.33-0.83)	0.006	0.174 (0.06-0.48)	<0.001
ECOG	1.799 (1.28-2.52)	0.001	1.104 (0.65-1.88)	0.716	2.946 (1.64-5.30)	<0.001
Multiple intrahepatic tumor	1.975 (1.24-3.15)	0.004	3.065 (1.63-5.74)	0.001	1.213 (0.49-2.96)	0.672
Portal vein invasion	1.467 (1.00-2.15)	0.049	1.212 (0.67-2.20)	0.529	1.594 (0.66-3.83)	0.297
mUICC stage	not included		1.728 (1.30-2.30)	0.001	not included	
Residual liver function**	1.241 (1.14-1.36)	<0.001	1.304 (1.16-1.47)	<0.001	1.252 (1.08-1.46)	0.004

AB, Atezolizumab plus Bevacizumab; HR, hazard ratio; AST, Aspartate Aminotransferase; ECOG, Eastern Cooperative Oncology Group; mUICC, Modified Union for International Cancer Control.
*Only factors with P<0.02 in univariate analyses were included for multivariate analyses.
**Child-Pugh score at the time of cessation of lenvatinib or Atezo+Bev.

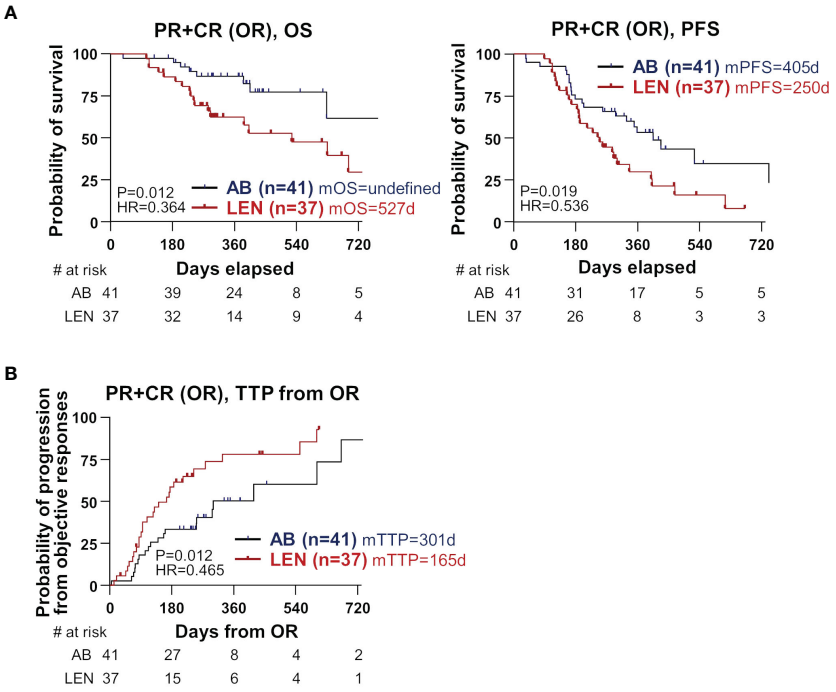

FIGURE 2
Differences in clinical outcome between the two treatments among the subgroup that achieved objective responses. **(A)** OS and PFS were compared between AB- and LEN-treated patients. **(B)** TTP from the time of OR was compared between the two treatments. PR, partial response; CR, complete response; OR, objective responses; OS, overall survival; PFS, progression-free survival; AB, atezolizumab+bevacizumab; LEN, lenvatinib; m, median; d, days; HR, hazard ratio, TTP, time-to-progression.

TABLE 4 Safety and the duration of chemotherapy of the matched cohort.

	Lenvatinib n=141	AB n=141	P
Adverse events of any grade	64 (45.4)	66 (46.8)	0.905
Hand-foot syndrome	19 (13.5)	0 (0)	<0.001
Diarrhea	7 (5.0)	3 (2.1)	0.334
General weakness, poor oral intake	10 (7.1)	8 (5.7)	0.808
Hypertension	7 (5.0)	3 (2.1)	0.334
Proteinuria	3 (2.1)	5 (3.5)	0.720
Thyroiditis	2 (1.4)	18 (12.8)	0.001
Varix bleeding	1 (0.6)	9 (6.4)	0.007
Hepatic encephalopathy	2 (1.4)	0 (0)	0.478
Decreased liver function	7 (5.0)	16 (11.3)	0.082
Pneumonitis	0 (0)	1 (0.7)	1.000
Serious adverse events	33 (23.4)	27 (19.1)	0.467
Cessation of chemotherapy due to adverse events	22 (15.6)	9 (6.4)	0.022
Median chemotherapy duration, days	102	91	0.907
Median timing of the best responses, days	70.5	64	0.149

AB, Atezolizumab plus Bevacizumab.

Specifically, in the lenvatinib group, older patients (who discontinued treatment) had a significantly higher age than those who continued, indicating a higher susceptibility or lower tolerance to AEs among the elderly. Conversely, age did not play a significant role in treatment discontinuation within the AB group. Additionally, the incidence of general weakness/poor oral intake was markedly higher among patients who stopped lenvatinib due to AEs (22.7%) compared to those who did not (4.2%), highlighting that certain AEs, particularly general weakness and poor oral intake, were critical factors in the decision to discontinue lenvatinib. Other notable AEs such as variceal bleeding, liver function abnormalities, autoimmune side effects, and renal function abnormalities did not significantly impact the decision to discontinue treatment in either group. Thus, older age and a decline in general condition may be more closely associated with treatment discontinuation in lenvatinib compared to AB, though further large-scale studies are needed for confirmation (Supplementary Table 5).

We investigated whether the occurrence of AEs causes a difference in survival between the two groups. Among patients with any grade of AE, there was no difference in OS or PFS between the two groups (Supplementary Figures 2A, B). Among patients without AEs, there was a tendency for better PFS (P=0.057) observed in the AB group (Supplementary Figure 2B). Furthermore, significantly better OS was observed in the AB group (P<0.001) (Supplementary Figure 2A). A similar tendency was observed when we divided patients according to serious AEs (Supplementary Figures 2C, D).

3.6 Impact of residual liver function on survival following the cessation of treatment

We finally hypothesized that residual liver function at the cessation of treatment and subsequent salvage treatment might be associated with the better OS of AB in our cohort. The inclusion criteria for the salvage treatment were as follows; (1) sufficient liver reserve function, classified as Child-Pugh A and B7; (2) ECOG performance status ranging from 0 to 2; and (3) patient consent to undergo salvage treatment. Residual liver function represented by CPS and the frequency and types of salvage treatment are presented in Supplementary Table 6. At the time of treatment cessation, the AB group demonstrated superior residual liver function and ECOG performance status. Specifically, median CPS was significantly better in the AB group compared to the lenvatinib group (6 versus 7, P=0.008) (Figure 3A). The frequency of salvage treatment was also higher in the AB group (55/105, 52.4% versus 49/126, 38.9%, P=0.048), but there was no difference in the frequency of salvage treatment between the two treatments in each Child-Pugh class group (Figure 3B). Furthermore, in patients with the residual function of Child-Pugh A, there was no difference in OS between the two groups, and this result was also observed in the Child-Pugh B-C subgroup (Figure 3C). Also, there was no survival difference between the two groups when we performed subgroup analyses according to the salvage treatment or none (Figure 3D). There was no significant difference in tumor characteristics, including tumor markers, size, number, portal vein invasion, and extrahepatic spread, between the two treatment groups at the point of salvage treatment initiation

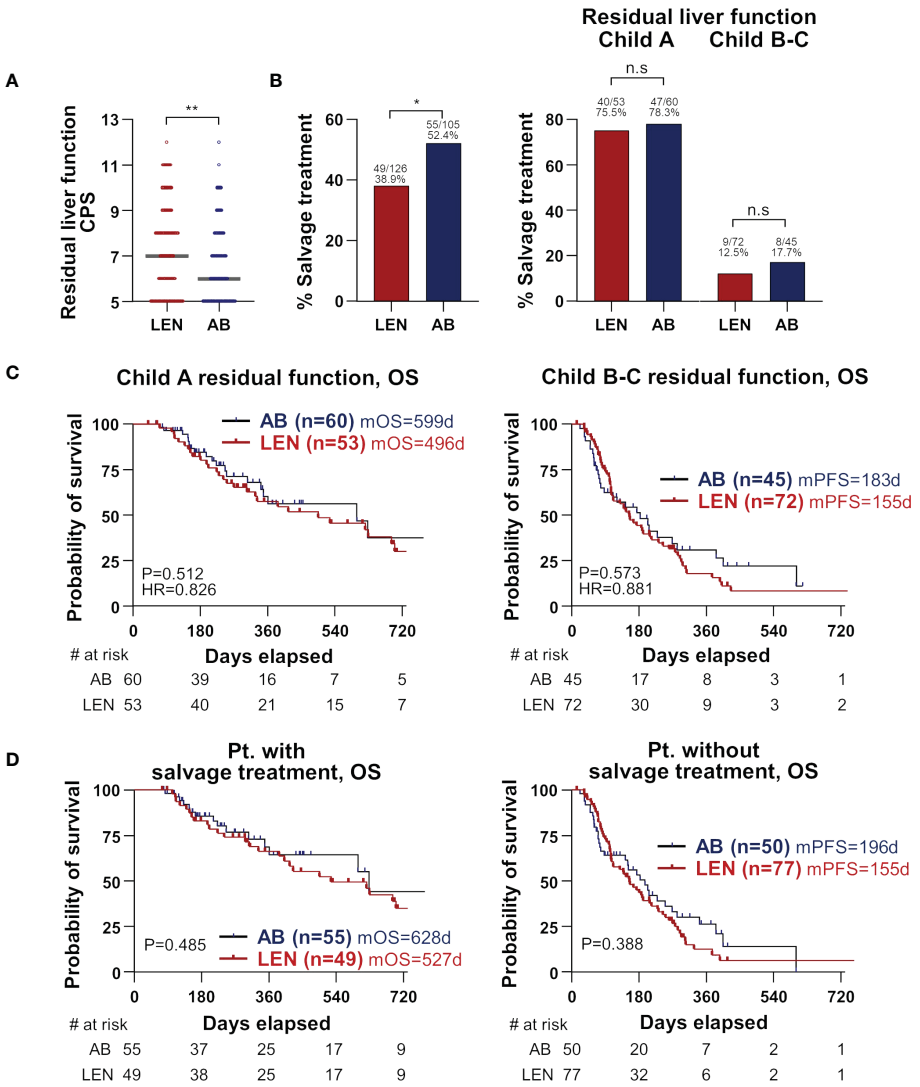

FIGURE 3
Importance of residual liver function at treatment cessation. **(A)** Residual liver function at treatment cessation is represented by CPS and compared between the two treatments. Median values are presented by grey lines. **(B)** The percentages who received salvage treatments following treatment cessation were compared between the two treatments (left). Patients were divided by Child-Pugh classes, and again the two treatments were compared for the percentages of salvage treatment (right). **(C, D)** Subgroup analyses according to residual liver function **(C)** and salvage treatment **(D)** were performed. OS and PFS were compared between the two treatments. CPS, Child-Pugh score; OS, overall survival; PFS, progression-free survival; AB, atezolizumab+bevacizumab; LEN, lenvatinib; m, median; d, days; HR, hazard ratio; Pt., patients.

(Supplementary Table 6). These results suggest that residual liver function and subsequent salvage treatment have an important role in the survival difference between AB and lenvatinib treatments.

4 Discussion

In the present study, we conducted a real-world, multi-center study using PSM, which provides a robust comparison between AB and lenvatinib in treating unresectable HCC. AB demonstrated superior OS compared to lenvatinib, without a significant difference in PFS or ORR. This underscores that PFS alone may not reflect the true benefit of a treatment, particularly in the context of immunotherapy for HCC, which is in line with the previous report (16). Our research highlights other factors influencing OS benefits with AB treatment, such as the importance of residual liver function post-treatment and the role of salvage treatments. Interestingly, in patients who achieved OR by respective treatments, OS, PFS, and TTP were better in the AB group, suggesting durable response can be achieved by this regimen compared to lenvatinib. Of note, our study highlights that residual liver function following the cessation of respective treatments, as measured by the CPS, is a critical determinant of OS, and the difference in residual liver function might be associated with the different frequency of subsequent salvage treatment and OS between two groups. Treatment discontinuation due to AEs was more frequent in the lenvatinib group, but the incidence of serious AEs was not different between the two treatments. The superiority of AB in OS was diminished in patients who underwent serious AEs, suggesting the prediction, monitoring, and management of AEs are also important in both treatments. Subgroup analysis showed that the subgroups of patients with high tumor burden or preserved liver function had significant survival benefits from AB.

Studies comparing these two regimens have conflicting results, although most studies used matched cohorts using PSM or inverse probability of treatment weighting (3–6, 8, 9). Some studies showed that AB has superior OS (4, 5) or PFS (3–5) compared to lenvatinib. Other reports showed that these two treatments have comparable OS and PFS (8, 9). However, another study demonstrated that lenvatinib was associated with longer OS and PFS (6). Two recent meta-analyses also reported different results (17, 18). A study analysing 6,628 patients from 8 studies showed that there was no difference in OS and PFS between two treatments (17), but another study analysing 3,690 patients from 8 studies showed longer PFS of AB treatment (17). These results might be related to the characteristics of the cohort, which can be baseline or post-treatment events such as AEs, residual liver function, and salvage treatments. Our study particularly focused on the analysis of factors associated with the difference in clinical outcomes between the two treatments.

One of the important findings is that we first identified that residual liver function after treatment cessation is significantly associated with the patient survival in both treatments, which can be associated with the difference of clinical outcomes between two treatments. We showed that this residual liver function affected the difference in OS between the two regimens. Patients who have better residual liver function after cessation of the primary treatments might have better survival because of eligibility for further treatment. Moreover, there were no survival differences between the two treatments if residual liver function was adjusted for. This underscores the need to maintain liver function during systemic therapies. Previous studies reported that AB caused worsening of ALBI score 3 weeks after treatment, but tended to be maintained thereafter (19–21). Other reports showed that lenvatinib treatment was associated with worsening of ALBI score at 2 and 4 weeks of treatment (22). A recent comparative study confirmed that this difference of dynamic changes within 6 weeks after respective treatments (3). However, these studies were focused on the short-term changes in liver function following each treatment, which would not be directly related to preserved liver function at the time of treatment cessation that is necessary for subsequent treatment. Rather, our study directly compared residual liver function at the cessation of each treatment regardless of the time point and found that CPS was significantly better in the AB group, which might be related to better OS.

Our second critical finding is that subsequent opportunity to receive salvage treatment is related to the survival difference between the two treatments. The AB group more frequently received salvage treatment, which resulted in better OS than the lenvatinib group. In addition, there was no survival difference between the two treatments if the salvage treatment was adjusted. Subsequent treatment was significantly associated with better survival in lenvatinib-treated HCC patients (23). In the AB treatment, salvage treatment was also analysed and its importance was also discussed in a recent report, but a direct comparison of salvage treatment between lenvatinib and AB treatments, or its prognostic impact were not examined (5). The frequency of salvage treatment can be heterogeneous among different cohorts; for example, post-progression treatment was performed in 77.6% following AB treatment in the Japanese cohort (5), but it was 52.4% in our cohort. Therefore, subsequent treatments following cessation might be associated with the heterogeneous survival results from previous studies. These findings imply that future comparative studies should consider residual liver function and subsequent treatment after the treatment cessation.

The third notable finding is that even in the subgroup that achieved OR, AB showed better OS and PFS. Furthermore, TTP from the time of OR was longer in AB than lenvatinib, suggesting that AB treatment could have long-term anti-tumor effects. Immunotherapies in HCC can induce durable responses which can result in prolonged survival (24, 25). The CheckMate459 trial also showed that nivolumab was more durable than sorafenib in terms of disease control (26). This relatively long-term effect of immunotherapies can be explained by the augmentation of tumor-specific memory responses which mainly recognize cancer cells (27). Moreover, our study also showed that treatment discontinuation due to AEs was significantly higher in the lenvatinib treatment, which can influence the durability of the treatment responses. Thus, the long-term beneficial effect of AB treatment, compared to lenvatinib treatment, should be investigated in future translational and clinical research.

We also performed detailed subgroup analyses using a matched cohort to identify which treatment would be beneficial in terms of OS and PFS in the respective subgroups. A recent experimental report suggested that the limited role of anti-PD-1 treatment in NASH-related HCC might be due to the pathologic CD8+PD-1+ T cells (28). In the latest results from the IMbrave150 study, treatment with AB showed better OS and PFS in patients with viral causes like HBV and HCV compared to sorafenib (29). Moreover, a recent network meta-analysis revealed that AB treatment could be beneficial in terms of survival in the subgroup of viral etiology (30). Our study also confirmed that AB treatment might have a comparative benefit in OS in viral etiology, but not in non-viral etiology. In addition to the etiology, we first observed that patients with high tumor burden reflected by tumor markers, size, number of intrahepatic tumors, and PVI had a benefit in OS and PFS from AB treatment than lenvatinib treatment. In addition, tumor size, tumor markers, or PVI were not factors associated with poor clinical outcomes in the AB subgroup, unlike the lenvatinib subgroup. These findings could support the treatment decision between the two treatments, although more data need to be accumulated in future studies.

Despite the retrospective design, our multi-center real-world study is the first to suggest that residual liver function and subsequent salvage treatments are the major determinants of clinical outcomes in HCC patients treated with AB and lenvatinib. These factors might be associated with the conflicting results of previous comparative studies, and this point should be considered in future studies. Importantly, cautious monitoring and management to maintain liver function during those treatments would consequently improve patient outcomes in advanced HCC.

Data availability statement

The original contributions presented in the study are included in the article/Supplementary Material. Further inquiries can be directed to the corresponding author.

Ethics statement

The studies involving humans were approved by Ethical approval for this research was granted by the Institutional Review Board of the Catholic University of Korea (approved number: XC23RADI0081). The studies were conducted in accordance with the local legislation and institutional requirements. The ethics committee/institutional review board waived the requirement of written informed consent for participation from the participants or the participants' legal guardians/next of kin because this study was a retrospective study.

Author contributions

JH: Writing – original draft, Writing – review & editing, Conceptualization, Data curation, Formal analysis, Investigation, Methodology, Resources, Visualization. PS: Writing – original draft, Writing – review & editing, Funding acquisition, Resources, Supervision, Validation. JY: Resources, Writing – review & editing. HC: Resources, Writing – review & editing. SL: Resources, Writing – review & editing. HY: Resources, Writing – review & editing. JKim: Resources, Writing – review & editing. HN: Resources, Writing – review & editing. HL: Resources, Writing – review & editing. HK: Resources, Writing – review & editing. SL: Resources, Writing – review & editing. DS: Resources, Writing – review & editing. MS: Resources, Writing – review & editing. JKwon: Resources, Writing – review & editing. CK: Resources, Writing – review & editing. SB: Resources, Writing – review & editing. JJ: Resources, Writing – review & editing. JC: Resources, Writing – review & editing. SY: Resources, Writing – review & editing.

Funding

The author(s) declare financial support was received for the research, authorship, and/or publication of this article. This research was supported by Basic Science Research Program through the National Research Foundation of Korea (NRF) funded by the Ministry of Education (2022R1I1A1A01063636) (to JH). This work was also supported by the Basic Science Research Program through an NRF grant funded by the Ministry of Science and ICT (grant number: NRF-2019R1A2C3005212) (to PS). This study was supported by Research Fund of Seoul St. Mary's Hospital, The Catholic University of Korea (to JH).

Conflict of interest

The authors declare that the research was conducted in the absence of any commercial or financial relationships that could be construed as a potential conflict of interest.

The author(s) declared that they were an editorial board member of Frontiers, at the time of submission. This had no impact on the peer review process and the final decision.

Publisher's note

Supplementary material

The Supplementary Material for this article can be found online at: https://www.frontiersin.org/articles/10.3389/fonc.2024.1372007/full#supplementary-material

References

1. Kudo M, Finn RS, Qin S, Han KH, Ikeda K, Piscaglia F, et al. Lenvatinib versus sorafenib in first-line treatment of patients with unresectable hepatocellular carcinoma: a randomised phase 3 non-inferiority trial. *Lancet*. (2018) 391:1163–73. doi: 10.1016/S0140-6736(18)30207-1

2. Finn RS, Qin S, Ikeda M, Galle PR, Ducreux M, Kim TY, et al. Atezolizumab plus bevacizumab in unresectable hepatocellular carcinoma. *N Engl J Med*. (2020) 382:1894–905. doi: 10.1056/NEJMoa1915745

3. Maesaka K, Sakamori R, Yamada R, Doi A, Tahata Y, Miyazaki M, et al. Comparison of atezolizumab plus bevacizumab and lenvatinib in terms of efficacy and safety as primary systemic chemotherapy for hepatocellular carcinoma. *Hepatol Res*. (2022) 52:630–40. doi: 10.1111/hepr.13771

4. Niizeki T, Tokunaga T, Takami Y, Wada Y, Harada M, Shibata M, et al. Comparison of efficacy and safety of atezolizumab plus bevacizumab and lenvatinib as first-line therapy for unresectable hepatocellular carcinoma: A propensity score matching analysis. *Target Oncol*. (2022) 17:643–53. doi: 10.1007/s11523-022-00921-x

5. Hiraoka A, Kumada T, Tada T, Hirooka M, Kariyama K, Tani J, et al. Does first-line treatment have prognostic impact for unresectable HCC?-Atezolizumab plus bevacizumab versus lenvatinib. *Cancer Med*. (2023) 12:325–34. doi: 10.1002/cam4.4854

6. Rimini M, Rimassa L, Ueshima K, Burgio V, Shigeo S, Tada T, et al. Atezolizumab plus bevacizumab versus lenvatinib or sorafenib in non-viral unresectable hepatocellular carcinoma: an international propensity score matching analysis. *ESMO Open*. (2022) 7:100591. doi: 10.1016/j.esmoop.2022.100591

7. Persano M, Rimini M, Tada T, Suda G, Shimose S, Kudo M, et al. Clinical outcomes with atezolizumab plus bevacizumab or lenvatinib in patients with hepatocellular carcinoma: a multicenter real-world study. *J Cancer Res Clin Oncol*. (2023) 149:5591–602. doi: 10.1007/s00432-022-04512-1

8. Kim BK, Cheon J, Kim H, Kang B, Ha Y, Kim DY, et al. Atezolizumab/bevacizumab vs. Lenvatinib as first-line therapy for unresectable hepatocellular carcinoma: a real-world, multi-center study. *Cancers (Basel)*. (2022) 14. doi: 10.3390/cancers14071747

9. Casadei-Gardini A, Rimini M, Tada T, Suda G, Shimose S, Kudo M, et al. Atezolizumab plus bevacizumab versus lenvatinib for unresectable hepatocellular carcinoma: a large real-life worldwide population. *Eur J Cancer*. (2023) 180:9–20. doi: 10.1016/j.ejca.2022.11.017

10. Su CW, Teng W, Lin PT, Jeng WJ, Chen KA, Hsieh YC, et al. Similar efficacy and safety between lenvatinib versus atezolizumab plus bevacizumab as the first-line treatment for unresectable hepatocellular carcinoma. *Cancer Med*. (2023) 12:7077–89. doi: 10.1002/cam4.5506

11. Han JW, Jang JW. Predicting outcomes of atezolizumab and bevacizumab treatment in patients with hepatocellular carcinoma. *Int J Mol Sci*. (2023) 24. doi: 10.3390/ijms241411799

12. An L, Liao H, Yuan K. Efficacy and safety of second-line treatments in patients with advanced hepatocellular carcinoma after sorafenib failure: A meta-analysis. *J Clin Transl Hepatol*. (2021) 9:868–77. doi: 10.14218/JCTH.2021.00054

13. Llovet JM, Lencioni R. mRECIST for HCC: Performance and novel refinements. *J Hepatol*. (2020) 72:288–306. doi: 10.1016/j.jhep.2019.09.026

14. Toyoda H, Johnson PJ. The ALBI score: From liver function in patients with HCC to a general measure of liver function. *JHEP Rep*. (2022) 4:100557. doi: 10.1016/j.jhepr.2022.100557

15. Chen AP, Setser A, Anadkat MJ, Cotliar J, Olsen EA, Garden BC, et al. Grading dermatologic adverse events of cancer treatments: the Common Terminology Criteria for Adverse Events Version 4.0. *J Am Acad Dermatol*. (2012) 67:1025–39. doi: 10.1016/j.jaad.2012.02.010

16. Gyawali B, Hey SP, Kesselheim AS. A comparison of response patterns for progression-free survival and overall survival following treatment for cancer with PD-1 inhibitors: A meta-analysis of correlation and differences in effect sizes. *JAMA Netw Open*. (2018) 1:e180416. doi: 10.1001/jamanetworkopen.2018.0416

17. Du S, Cao K, Wang Z, Lin D. Clinical efficacy and safety of atezolizumab plus bevacizumab versus lenvatinib in the treatment of advanced hepatocellular carcinoma: A systematic review and meta-analysis. *Med (Baltimore)*. (2023) 102:e33852. doi: 10.1097/MD.0000000000033852

18. Liu J, Yang L, Wei S, Li J, Yi P. Efficacy and safety of atezolizumab plus bevacizumab versus lenvatinib for unresectable hepatocellular carcinoma: a systematic review and meta-analysis. *J Cancer Res Clin Oncol*. (2023) 149:16191-201. doi: 10.1007/s00432-023-05342-5

19. Ando Y, Kawaoka T, Kosaka M, Shirane Y, Johira Y, Miura R, et al. Early tumor response and safety of atezolizumab plus bevacizumab for patients with unresectable hepatocellular carcinoma in real-world practice. *Cancers (Basel)*. (2021) 13. doi: 10.3390/cancers13163958

20. Hayakawa Y, Tsuchiya K, Kurosaki M, Yasui Y, Kaneko S, Tanaka Y, et al. Early experience of atezolizumab plus bevacizumab therapy in Japanese patients with unresectable hepatocellular carcinoma in real-world practice. *Invest New Drugs*. (2022) 40:392–402. doi: 10.1007/s10637-021-01185-4

21. Hiraoka A, Kumada T, Tada T, Hirooka M, Kariyama K, Tani J, et al. Atezolizumab plus bevacizumab treatment for unresectable hepatocellular carcinoma: Early clinical experience. *Cancer Rep (Hoboken)*. (2022) 5:e1464. doi: 10.1002/cnr2.1464

22. Hiraoka A, Kumada T, Atsukawa M, Hirooka M, Tsuji K, Ishikawa T, et al. Early relative change in hepatic function with lenvatinib for unresectable hepatocellular carcinoma. *Oncology*. (2019) 97:334–40. doi: 10.1159/000502095

23. Lee J, Han JW, Sung PS, Lee SK, Yang H, Nam HC, et al. Comparative analysis of lenvatinib and hepatic arterial infusion chemotherapy in unresectable hepatocellular carcinoma: A multi-center, propensity score study. *J Clin Med*. (2021) 10. doi: 10.3390/jcm10184045

24. El-Khoueiry AB, Sangro B, Yau T, Crocenzi TS, Kudo M, Hsu C, et al. Nivolumab in patients with advanced hepatocellular carcinoma (CheckMate 040): an open-label, non-comparative, phase 1/2 dose escalation and expansion trial. *Lancet*. (2017) 389:2492–502. doi: 10.1016/S0140-6736(17)31046-2

25. Zhu AX, Finn RS, Edeline J, Cattan S, Ogasawara S, Palmer D, et al. Pembrolizumab in patients with advanced hepatocellular carcinoma previously treated with sorafenib (KEYNOTE-224): a non-randomised, open-label phase 2 trial. *Lancet Oncol*. (2018) 19:940–52. doi: 10.1016/S1470-2045(18)30351-6

26. Sangro B, Sarobe P, Hervas-Stubbs S, Melero I. Advances in immunotherapy for hepatocellular carcinoma. *Nat Rev Gastroenterol Hepatol*. (2021) 18:525–43. doi: 10.1038/s41575-021-00438-0

27. Postow MA, Callahan MK, Wolchok JD. Immune checkpoint blockade in cancer therapy. *J Clin Oncol*. (2015) 33:1974–82. doi: 10.1200/JCO.2014.59.4358

28. Pfister D, Nunez NG, Pinyol R, Govaere O, Pinter M, Szydlowska M, et al. NASH limits anti-tumour surveillance in immunotherapy-treated HCC. *Nature*. (2021) 592:450–6. doi: 10.1038/s41586-021-03362-0

29. Cheng A-L, Qin S, Ikeda M, Galle PR, Ducreux M, Kim T-Y, et al. Updated efficacy and safety data from IMbrave150: Atezolizumab plus bevacizumab vs. sorafenib for unresectable hepatocellular carcinoma. *J Hepatol*. (2022) 76:862–73. doi: 10.1016/j.jhep.2021.11.030

30. Vogel A, Rimassa L, Sun HC, Abou-Alfa GK, El-Khoueiry A, Pinato DJ, et al. Comparative efficacy of atezolizumab plus bevacizumab and other treatment options for patients with unresectable hepatocellular carcinoma: A network meta-analysis. *Liver Cancer*. (2021) 10:240–8. doi: 10.1159/000515302

frontiers | Frontiers in Oncology

TYPE Original Research
PUBLISHED 29 February 2024
DOI 10.3389/fonc.2023.1327147

OPEN ACCESS

EDITED BY
Francisco Tustumi,
University of São Paulo, Brazil

REVIEWED BY
Marina Alessandra Pereira,
Universidade de São Paulo, Brazil
Eric Nakamura,
University of São Paulo, Brazil
Fan Feng,
The 302th Hospital of PLA, China

*CORRESPONDENCE
Weidong Pei
peiwd@aliyun.com

RECEIVED 24 October 2023
ACCEPTED 08 December 2023
PUBLISHED 29 February 2024

CITATION
Zhang Z-H, Du Y, Wei S and Pei W (2024) Multilayered insights: a machine learning approach for personalized prognostic assessment in hepatocellular carcinoma. *Front. Oncol.* 13:1327147. doi: 10.3389/fonc.2023.1327147

Multilayered insights: a machine learning approach for personalized prognostic assessment in hepatocellular carcinoma

Zhao-Han Zhang[1], Yunxiang Du[2], Shuzhen Wei[2] and Weidong Pei[3]*

[1]Shenyang No.20 High School, Shenyang, China, [2]Department of Oncology, Huai'an 82 Hospital, China RongTong Medical Healthcare Group Co., Ltd., Chengdu, China, [3]Department of Discipline Development, China RongTong Medical Healthcare Group Co., Ltd., Chengdu, China

Background: Hepatocellular carcinoma (HCC) is a complex malignancy, and precise prognosis assessment is vital for personalized treatment decisions.

Objective: This study aimed to develop a multi-level prognostic risk model for HCC, offering individualized prognosis assessment and treatment guidance.

Methods: By utilizing data from The Cancer Genome Atlas (TCGA) and the Surveillance, Epidemiology, and End Results (SEER) database, we performed differential gene expression analysis to identify genes associated with survival in HCC patients. The HCC Differential Gene Prognostic Model (HCC-DGPM) was developed through multivariate Cox regression. Clinical indicators were incorporated into the HCC-DGPM using Cox regression, leading to the creation of the HCC Multilevel Prognostic Model (HCC-MLPM). Immune function was evaluated using single-sample Gene Set Enrichment Analysis (ssGSEA), and immune cell infiltration was assessed. Patient responsiveness to immunotherapy was evaluated using the Immunophenoscore (IPS). Clinical drug responsiveness was investigated using drug-related information from the TCGA database. Cox regression, Kaplan-Meier analysis, and trend association tests were conducted.

Results: Seven differentially expressed genes from the TCGA database were used to construct the HCC-DGPM. Additionally, four clinical indicators associated with survival were identified from the SEER database for model adjustment. The adjusted HCC-MLPM showed significantly improved discriminative capacity (*AUC*=0.819 *vs.* 0.724). External validation involving 153 HCC patients from the International Cancer Genome Consortium (ICGC) database verified the performance of the HCC-MLPM (*AUC*=0.776). Significantly, the HCC-MLPM exhibited predictive capacity for patient response to immunotherapy and clinical drug efficacy ($P < 0.05$).

Conclusion: This study offers comprehensive insights into HCC prognosis and develops predictive models to enhance patient outcomes. The

evaluation of immune function, immune cell infiltration, and clinical drug responsiveness enhances our comprehension and management of HCC.

KEYWORDS

hepatocellular carcinoma, prognosis risk model, machine learning, immune function, drug responsiveness

1 Introduction

Primary liver cancer, a prevalent malignancy of the digestive system, ranks as the sixth most frequently occurring tumor globally and is the second leading cause of mortality (1, 2). Hepatocellular carcinoma (HCC) is the prevailing pathological subtype of primary liver cancer, accounting for 75%-85% of all cases (3). The poor prognosis of HCC arises from its early propensity for metastasis, often involving dissemination to the portal vein or distant organs (4). Patients with early-stage HCC have access to a potentially curative treatment option with a long-term survival rate exceeding 5% at 60 years, while patients with advanced-stage tumors experience a median survival period ranging from 1 to 2 years (5–7). Therefore, timely identification, early intervention, and the implementation of rational and effective treatment strategies are crucial for patients diagnosed with HCC (8).

Surgical resection is considered represents the primary therapeutic approach for patients with early-stage HCC and often leads to favorable outcomes (9, 10). However, for individuals diagnosed with intermediate or advanced-stage HCC, surgical resection is no longer a feasible option due to tumor progression and metastasis. Local regional therapies, such as ablation, arterial-directed therapies, or external beam radiation therapy, are the preferred treatment modalities for patients with localized liver disease that cannot be surgically removed or are not suitable for surgery. Systemic therapies are recommended for patients who undergo disease progression after local regional therapies or those with metastases outside the liver (11). This focus on systemic therapies highlights the importance of considering the tumor microenvironment, drug responsiveness, and immunotherapy as crucial factors (12–14). Targeted therapies are particularly relevant for patients diagnosed with intermediate or advanced-stage HCC (15, 16). Sorafenib, initially approved for advanced HCC treatment, is hindered by the development of resistance (17, 18). Subsequently, other multi-kinase inhibitors, such as Lenvatinib, Regorafenib, Cabozantinib, and the VEGFR2 inhibitor ramucirumab, have been approved as second-line targeted treatment options (19). With a deeper understanding of the interplay between the immune system and cancer, immune checkpoint inhibitors (ICI) have been integrated into the therapeutic arsenal for patients with advanced HCC. Nivolumab, an ICI agent, has been FDA approval for the management of advanced HCC (20, 21). Given the expanding range of treatment methods, the selection of the most suitable treatment plan for patients has become critical.

Therefore, to provide optimal treatment approaches for different stages of HCC progression, conventional methods often assign patients to specific stages based on the Barcelona Clinic Liver Cancer (BCLC) classification (6, 22). BCLC staging, widely utilized in HCC, categorizes patients into different stages based on factors such as tumor size, number, liver function, and symptoms (23). Treatment strategies, such as surgical resection, liver transplantation, radiofrequency ablation, radiation therapy, and targeted therapy, are determined for patients according to their corresponding stages (6). However, significant heterogeneity exists among patients, including genetic variations, immune environments, and tumor heterogeneity. Relying solely on conventional staging methods may insufficiently consider individual patient characteristics and the complexities of the disease, potentially leading to inaccurate prognosis assessments and suboptimal personalized treatments.

Recent advancements in tumor genomics research have facilitated the utilization of extensive tumor genomic data to gain insights into the complexity and individual variations of tumors. The Cancer Genome Atlas (TCGA) database, as a comprehensive repository of diverse cancer-related data, offers new opportunities for exploring prognostic risk assessment in HCC (24, 25). Therefore, in contrast to conventional approaches, we consider incorporating factors such as molecular biology information and the tumor microenvironment based on clinical indicators. By leveraging the potential of powerful machine learning and big data analysis techniques, we can extract valuable insights from extensive tumor genomic data to construct prognostic risk assessment models.

Through a comprehensive analysis of clinical indicators, molecular biology information, tumor microenvironment, and other multi-level factors, o our objective is to establish a

Abbreviations: AUC, Area under the curve; BCLC, Barcelona Clinic Liver Cancer; DEG, Differentially expressed gene; GSEA, Gene Set Enrichment Analysis; HCC, Hepatocellular carcinoma; HCC-DGPM, Hepatocellular Carcinoma Differential Gene Prognostic Model; HCC-MLPM, Hepatocellular Carcinoma Multilevel Prognostic Model; HR, Hazard ratios; ICGC, International Cancer Genome Consortium; IPS, Immunophenoscore; KM, Kaplan-Meier; NCCN, National Comprehensive Cancer Network; OS, Overall survival; ROC, Receiver operating characteristic; SEER, Surveillance, Epidemiology, and End Results; ssGSEA, Single-sample Gene Set Enrichment Analysis; TCGA, The Cancer Genome Atlas.

comprehensive and accurate HCC prognostic risk model and explore its association with drug responsiveness and immunotherapy (26, 27). By improving the accurate assessment of prognostic risk in HCC patients, we can provide essential evidence to inform the development of personalized treatment plans, thus improving prognosis assessment and treatment outcomes for patients. Moreover, by leveraging the extensive resources of databases such as TCGA and SEER, this study has the potential to make significant breakthroughs and advancements in the field of HCC prognostic assessment and personalized treatment.

2 Research design and methods

2.1 Research workflow

The research workflow (depicted in Figure 1) comprised the subsequent steps: 1) Identification of differentially expressed genes (DEGs) associated with survival through gene expression analysis; 2) Development of the HCC Differential Gene Prognostic Model (HCC-DGPM) by integrating significant DEGs; 3) Selection of clinical indices linked to survival; 4) Model adjustment and validation, culminating in the HCC Multilevel Prognostic Model (HCC-MLPM); 5) Evaluation of immune function and analysis of clinical drug responsiveness.

2.2 Data collection and preparation

The dataset for liver cancer was obtained from the TCGA database through the website, and the gene expression matrices of adjacent non-cancerous and cancerous tissues were used for the analysis. The dataset consisted of 50 samples of normal liver tissue and 370 samples of liver cancer. Additionally, data from 30,684 patients diagnosed with primary liver cancer between 1988 and 2015 were extracted from the SEER database using SEER*stat software 8.4.0 (https://seer.cancer.gov/). After data cleansing, a total of 3,017 patient records were available for further analysis.

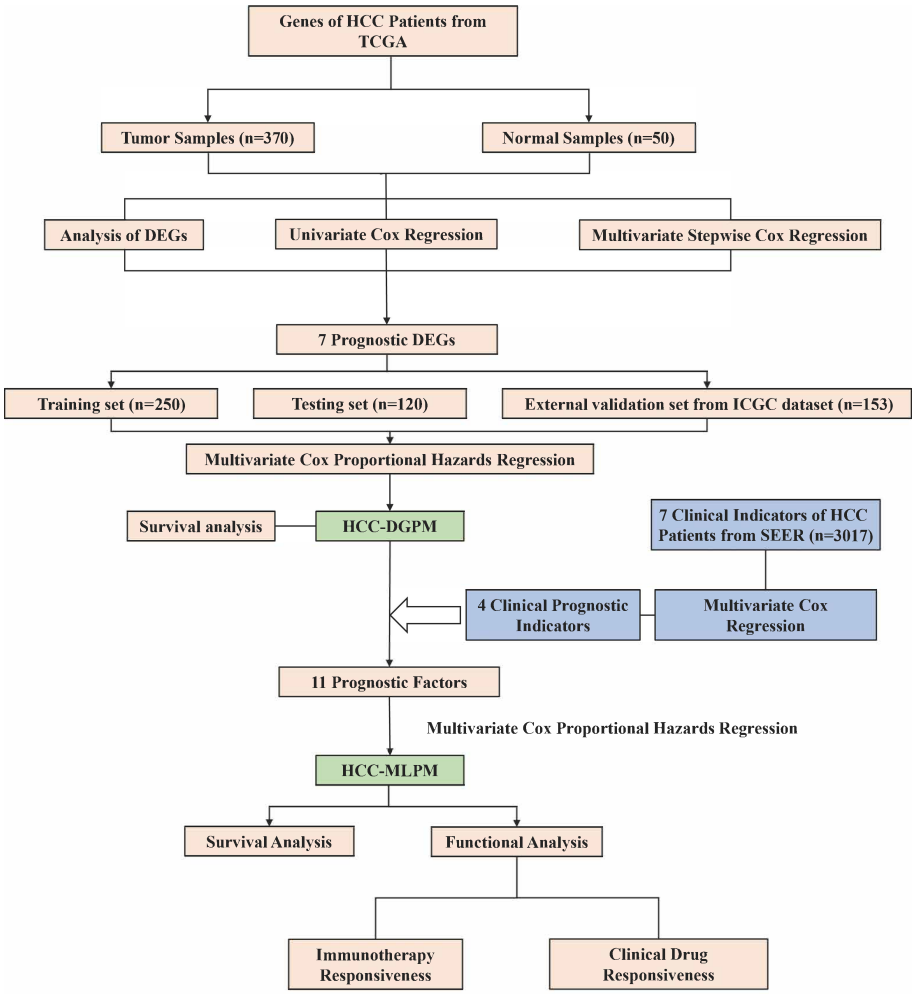

FIGURE 1
Research workflow for the construction of hepatocellular carcinoma prognostic model. HCC, Hepatocellular carcinoma; TCGA, The Cancer Genome Atlas; SEER, Surveillance, Epidemiology, and End Results; DEGs, Differentially expressed genes; HCC-DGPM, HCC Differential Gene Prognostic Model; HCC-MLPM, Hepatocellular Carcinoma Multilevel Prognostic Model.

The International Cancer Genome Consortium (ICGC) database provided data from 369 HCC patients for the study. After further data cleaning, cases with incomplete clinical information were excluded, resulting in a final sample size of 153 cases.

It is important to note that all the included patients were diagnosed with primary liver cancer. The year of the initial diagnosis was categorized into 5-year intervals and considered as an ordinal variable. Age 45 was chosen as the threshold to classify cases with early-onset HCC, and age was divided into 10-year intervals.

2.3 Selection of HCC prognostic DEGs

The "limma" package in R was used to identify the DEGs between cancerous and adjacent non-cancerous tissues (28). The DEG threshold was set as an absolute log2-fold change (FC) ≥ 1 and an adjusted $P < 0.05$. Volcano plots illustrating the DEGs were generated using the "ggplot2" package (https://ggplot2.tidyverse.org/). Subsequent screening involved conducting both univariate and stepwise multivariate Cox regression analyses. In the univariate Cox regression analysis, each DEG was evaluated individually to assess its association with the survival outcome. In this context, the survival outcomes were solely considered as "death". This analysis facilitated the identification of genes that exhibited a significant correlation with patient survival. Subsequently, a stepwise multivariate Cox regression analysis was performed.

2.4 Construction and validation of HCC-DGPM

The patients from the TCGA dataset were randomly assigned to training (n = 250) and testing (n = 120) sets in a 7:3 ratio, facilitated by the "caret" R package for random assignment (29). The training set was used to train the model, while the testing set was used to assess the predictive performance of the model. HCC-DGPM was constructed using the multivariate Cox regression method. External validation set was performed using the ICGC dataset (n = 153). The performance of HCC-DGPM was evaluated using receiver operating characteristic (ROC) curves, with a higher area under the curve (AUC) indicating improved predictive accuracy. To enhance the precision of our prognostic model, calibration curves were utilized, employing the "rms", "survival", and "ResourceSelection" R packages (https://CRAN.R-project.org/package). These curves are a measure of how closely the model's predictions align with actual outcomes. The closer these curves lie to the 45-degree line, the more accurate the model is, indicating a high degree of concordance between predicted and observed results. The HCC-DGPM was validated with Kaplan-Meier (KM) curves, and the methodology for establishing the cutoff value for risk groups was not initially specified. The cutoff value used for delineating high and low risk groups was determined by the method that maximizes (sensitivity + specificity - 1). The established cutoff value for the risk score was 1.65.

2.5 Model adjustment and validation

To improve the model's performance, we performed multivariate Cox regression analysis to identify clinical indicators associated with HCC patient survival using the SEER database. SSubsequently, these indicators were used to refine the HCC-DGPM, resulting in the HCC-MLPM. ROC curves and KM curves were generated to assess the performance of the HCC-MLPM and provide additional validation of its effectiveness.

2.6 Immune evaluation of the model

Gene Set Enrichment Analysis (GSEA) was performed to investigate the impact of the risk score on the biological function of HCC patients. The annotated gene setlist was selected using a significance threshold of $P < 0.05$. Moreover, the "ssGSEA" R package was used to estimate the infiltration levels of 28 distinct immune cell types in HCC patients (30), taking into account their risk scores. The IPS was used to assess patient responsiveness to immunotherapy (31).

2.7 Clinical drug responsiveness evaluation

To explore the variations in clinical drug responsiveness among patients, we analyzed the clinical drug information and patients' drug responsiveness data retrieved from the TCGA database. We evaluated the effects of chemotherapy drugs such as Gemcitabine, Cisplatin, Doxorubicin, 5-fluorouracil (5-FU), Oxaliplatin, Adriamycin, and Cytoxan, alongside targeted therapy agents including Sorafenib, Everolimus, Sunitinib, and Temsirolimus. This comprehensive assessment was crucial as it is well-recognized that therapeutic efficacy varies significantly between treatments, independent of other evaluated variables.

Based on the risk scores generated by our model, patients were categorized into high-risk and low-risk groups. Subsequently, a proportional stacked bar chart was used to visually represent and analyze the disease progression in these two patient groups.

2.8 Statistical analysis

Cox regression models were employed to calculate hazard ratios (HR) and assess the relationship between gene expression and survival outcomes. The KM method was utilized to generate survival curves, and the log-rank test was applied to compare these curves. The Jonckheere-Terpstra test and Cochran-Mantel-Haenszel test were performed to evaluate the trend association between the diagnosis year and patient characteristics for numerical and categorical data, respectively. Cox proportional hazards regression models were used to HRs and their corresponding 95% confidence intervals for prognostic factors related to overall survival (OS). In the multivariate Cox regression analyses, a stepwise procedure was conducted with an entry criterion of $P < 0.05$ to identify the most statistically significant

prognostic factors. The significance level for all statistical tests was set at $P < 0.05$. Statistical analyses were conducted using SAS 13.2 (SAS Institute, Cary, NC, USA), and the KM curves were plotted using R Software.

2.9 Availability of data

The data utilized in this study can be obtained by contacting the authors due to restrictions imposed by the data providers, namely TCGA, SEER, and GSEA databases. Access to these databases is available via their dedicated websites: TCGA (https://portal.gdc.cancer.gov/), SEER (https://seer.cancer.gov/), GSEA (http://software.broadinstitute.org/gsea/index.jsp), and ICGC (https://icgcportal.genomics.cn/). Researchers interested in accessing the data may reach out to the authors for additional information and support in acquiring the required permissions and data access.

3 Results

3.1 Analysis of differential gene expression

To establish a prognostic model, 370 HCC samples and 50 samples of normal liver tissue from TCGA were involved. Compared to normal group, a total of 1761 DEGs were identified, comprising 1,091 upregulated genes and 670 downregulated genes in HCC group. The expression patterns of these DEGs are illustrated in Figure 2A through volcano plots.

3.2 Identification of genes associated with patient prognosis

To further identify the prognostic genes, a univariate Cox regression was performed on the 1,761 genes to identify genes significantly associated with patient prognosis. This analysis yielded a subset of 89 genes that showed a significant association at a significance level of $P < 0.001$. Further analysis using multivariate Cox stepwise regression identified seven genes significantly associated with the survival of HCC patients: MYBL2, SF3B4, CDCA8, NUF2, HMMR, PON1, and PAGE1 (Table 1).

KM analysis was performed to assess the impact of the seven identified genes on patient survival. The results revealed a significant correlation between these genes and patient prognosis, as evidenced by distinct survival patterns observed in patient groups with high and low expression levels of these genes. Moreover, the survival analysis demonstrated that patients with higher gene expression levels had a significantly poorer prognosis compared to those with lower expression levels (Figures 2B–H).

3.3 Construction and validation of the HCC-DGPM

Therefore, HCC-DGPM was constructed through univariate Cox proportional hazards regression analysis using the expression levels of the seven identified genes (MYBL2, SF3B4, CDCA8, NUF2, HMMR, PON1, and PAGE1) as covariates. The regression coefficients were used to assign weights to each gene, allowing for the development of a risk score formula to calculate the individual risk score for each patient The risk score formula is defined as follows: Risk score = (Expression level of MYBL2 × 0.4820) + (Expression level of SF3B4 × 3.0446) + (Expression level of CDCA8 × 3.1851) + (Expression level of NUF2 × 0.1932) + (Expression level of HMMR × 3.1205) + (Expression level of P0N1 × 0.7698) + (Expression level of PAGE1 × 1.2691).

ROC curve was performed to assess the predictive ability of the HCC-DGPM in determining patient outcomes. The training dataset exhibited an AUC of 0.723 (Figure 3A) for the HCC-DGPM, while the testing and external validation sets showed AUC values of 0.724 & 0.719 (Figures 3B, C). These results suggest that the HCC-DGPM has a moderate predictive ability to distinguish between high-risk and low-risk patients. To enhance the credibility of our model's accuracy, we performed calibration curve analyses following the ROC assessments (Figures 3D–F). The results from these calibration curves lend further credence to the model's predictive acumen, highlighting its prospective value in a clinical setting.

In addition, survival analysis was conducted based on the newly calculated risk score, allowing for the classification of patients into high-risk and low-risk groups for model validation purposes. The KM curves demonstrated significant differences in survival between the high-risk and low-risk groups (Figures 3G–H).

3.4 Model adjustment

Clinical indicators, including Age, Race, Sex, tumor size (T), node involvement (N), metastasis (M), and stage, were screened from the SEER database due to their potential correlation with patient survival in HCC. Four indicators were identified as significantly associated with survival outcomes (Table 2). Multivariate Cox regression analysis was conducted to determine the clinical factors significantly associated with patient survival. Four indicators were found to be significantly correlated with survival outcomes (Table 2). Next, the identified clinical indicators from the SEER database were integrated with the risk scores obtained from the 7 DEGs, resulting in the development of a novel predictive model (HCC-MLPM). The adjusted predictive HCC-MLPM is represented by the following formula: Risk Score = (Expression level of MYBL2 × 0.4820) + (Expression level of SF3B4 × 3.0446) + (Expression level of CDCA8 × 3.1851) + (Expression level of NUF2 × 0.1932) + (Expression level of HMMR × 3.1205) + (Expression level of PON1 × 0.7698) + (Expression level of PAGE1 × 1.2691) + (Age × 1.5079) + (T × 2.9376) + (N × 0.8721) + (M × 3.0453).

3.5 Evaluation of HCC-MLPM

The performance of the HCC-MLPM was evaluated using both the training and testing datasets. In the training dataset, the HCC-MLPM demonstrated improved predictive ability with an AUC of 0.826 (Figure 4A). In the testing dataset, the HCC-MLPM achieved

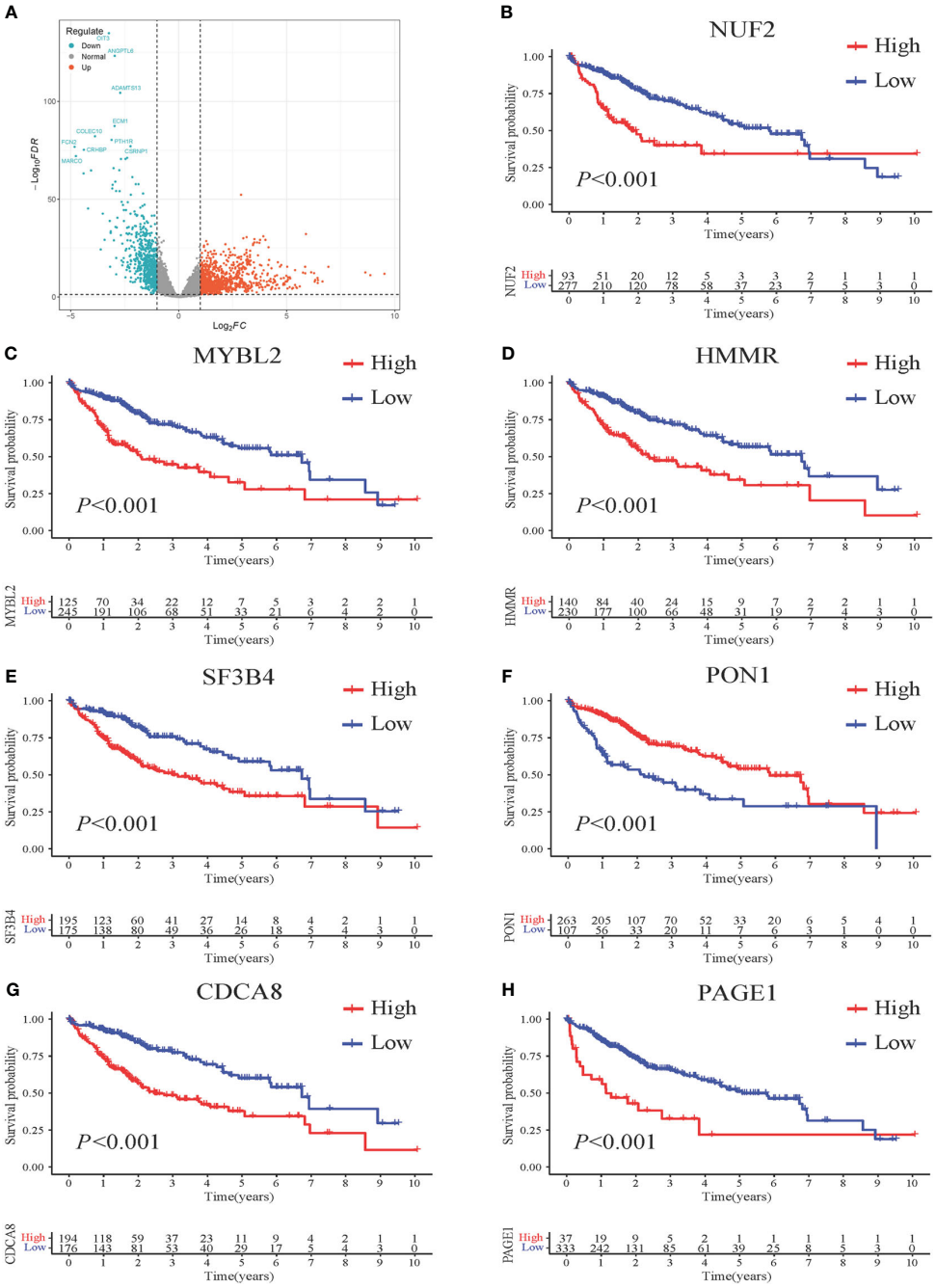

FIGURE 2
Survival impact of 7 DEGs screened from HCC patients. **(A)** Volcano plots illustrating the DEGs from HCC *vs*. normal. Genes upregulated in HCC are represented in red, while genes downregulated in HCC are shown in blue. The x-axis represents the log2-fold change in gene expression, indicating the magnitude of change, and the y-axis represents the statistical significance (-log10 p-value) of the differential expression. **(B–H)** Kaplan-Meier (KM) curves demonstrating the association between gene expression levels and patient survival. High-risk patients are depicted in red, while low-risk patients are represented in blue. The x-axis represents the survival time, and the y-axis represents the survival probability.

an AUC of 0.819 (Figure 4B), further validating its enhanced predictive capacity. Similarly, the HCC-MLPM exhibited satisfactory predictive capability in the external validation dataset, achieving an AUC of 0.776 (Figure 4C). These results indicate that the HCC-MLPM effectively discriminates between high-risk and low-risk patients in this external validation set. Calibration curves were subsequently integrated, serving as an additional verification stratum for the model's validity (Figures 4D–F).

Furthermore, by utilizing the scoring system derived from the adjusted model, patients were categorized into high-risk and low-risk groups. KM curves showed that patients in the low-risk group had superior overall survival outcomes compared to those in the high-risk group (Figures 4G–H). These findings indicate that the integration of risk scores based on differential gene expression, along with the selected clinical indicators, significantly improved the predictive performance of the HCC-MLPM.

TABLE 1 Differential genes associated with OS in HCC patients.

Name	HR	HR.95L	HR.95H	*P value*
MYBL2	0.4820	0.31979	0.7264	0.000488
SF3B4	3.0446	1.90062	4.8770	3.63e-06
CDCA8	3.1851	1.65058	6.1463	0.000552
NUF2	0.1932	0.08874	0.4205	3.43e-05
HMMR	3.1205	1.73930	5.5985	0.000136
PON1	0.7698	0.67562	0.8771	8.47e-05
PAGE1	1.2691	1.11467	1.4448	0.000318

3.6 Stratified survival analysis based on clinical indicators

This section delves into a detailed survival analysis of HCC patients within the HCC-MLPM framework, stratified according to key clinical indicators. The KM curves display distinct survival probabilities over time for groups stratified by key clinical indicators: Age (Figure 5A), T (Figure 5B), N (Figure 5C), and M (Figure 5D). These curves reveal considerable variation in survival outcomes across these different clinical stratifications (P<0.001), underscoring the significant impact of each indicator on survival. They highlight the potential utility of these clinical indicators in refining the HCC-MLPM.

3.7 Gene set enrichment analysis

To assess the immune function associated with the HCC-MLPM, Gene Set Enrichment Analysis (GSEA) was performed. The analysis revealed that high-risk patients showed a stronger association with

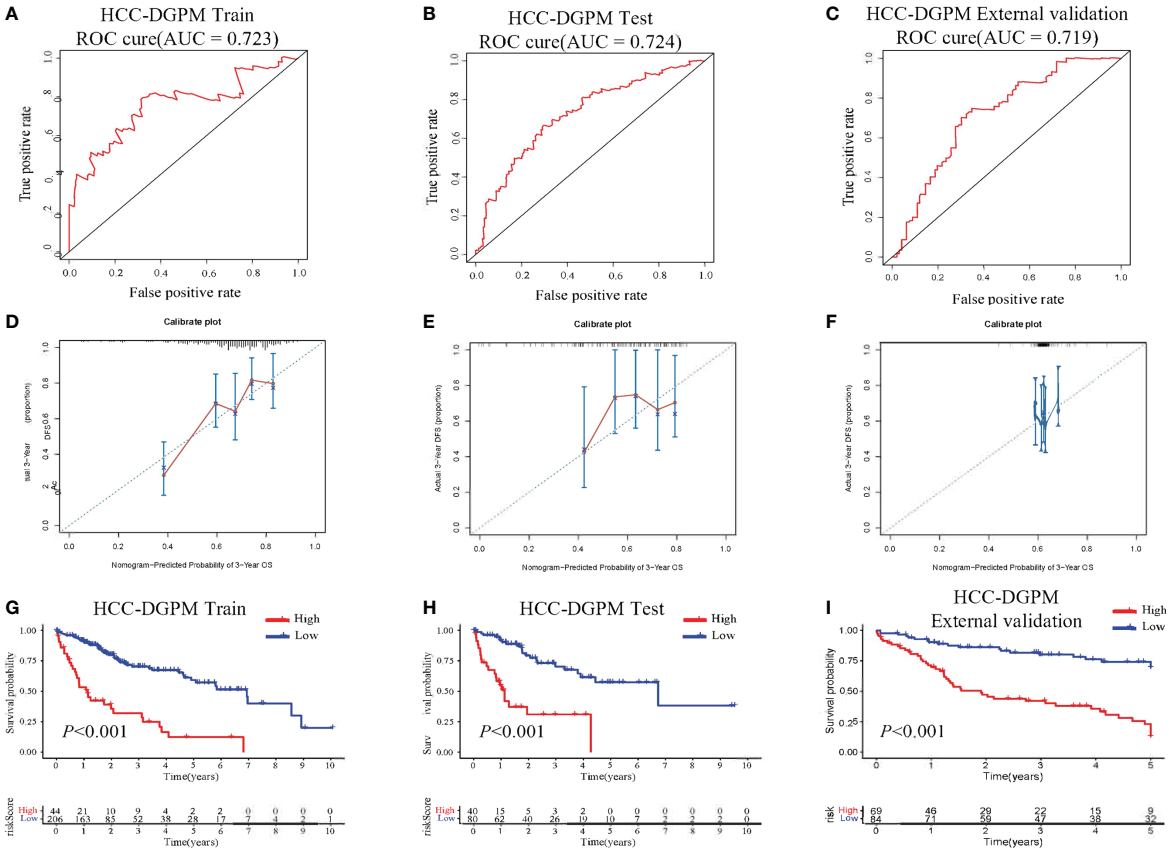

FIGURE 3
Performance Evaluation of the HCC-DGPM. **(A)** ROC curve of the training dataset. **(B)** ROC curve of the testing set. **(C)** ROC curve of the external validation set. The x-axis represents the false-positive rate, while the y-axis represents the true-positive rate. **(D–F)** Calibration curves for the training, testing, and external validation sets, respectively. **(G–I)** KM curves for overall survival (OS) in the training, testing and external validation set sets respectively (red: High risk; blue: Low risk).

TABLE 2 Risk factors in the SEER database.

risk factors	HR	HR.95L	HR.95H	*P value*
Age	1.5079	1.2375	1.8374	4.63e-05
T	2.9376	2.5259	3.4165	2e-16
N	0.8721	0.7641	0.9954	0.0425
M	3.0453	2.4834	3.7343	2e-16

cellular processes related to the cell cycle and DNA replication, indicating a more aggressive tumor phenotype compared to low-risk patients (Figures 6A–C). Moreover, the high-risk group exhibited a closer association with immune response compared to the low-risk group. This was evident from the enrichment of gene sets related to the toll-like receptor signaling pathway, cytokine-cytokine receptor interaction, and chemokine signaling pathway. These findings highlight a significant correlation between the risk score and the immune status of HCC (Figures 6D–F).

3.8 Immune assessment of the HCC-MLPM

Using the single-sample Gene Set Enrichment Analysis (ssGSEA) method, we conducted an analysis of immune cell infiltration in HCC patients, comparing the high-risk and low-risk groups. Violin plots further illustrated significantly lower infiltration levels of activated B cells, activated CD8+ T cells, natural killer cells, immature B cells, mast cells, and memory CD4+ T cells in the high-risk group. Conversely, the infiltration level of activated CD4+ T cells was significantly higher in the high-risk group (Figure 7A). Additionally, we examined the expression changes of immune checkpoint markers between the high-risk and low-risk groups. Remarkably, the high-risk group exhibited a significant upregulation in the expression levels of most immune checkpoint markers (Figure 7B). These findings indicate that the high-risk group of HCC patients displays lower levels of immune cell infiltration, particularly in specific immune cell subsets, along with higher expression of immune checkpoint markers. These observations suggest the presence of a potentially

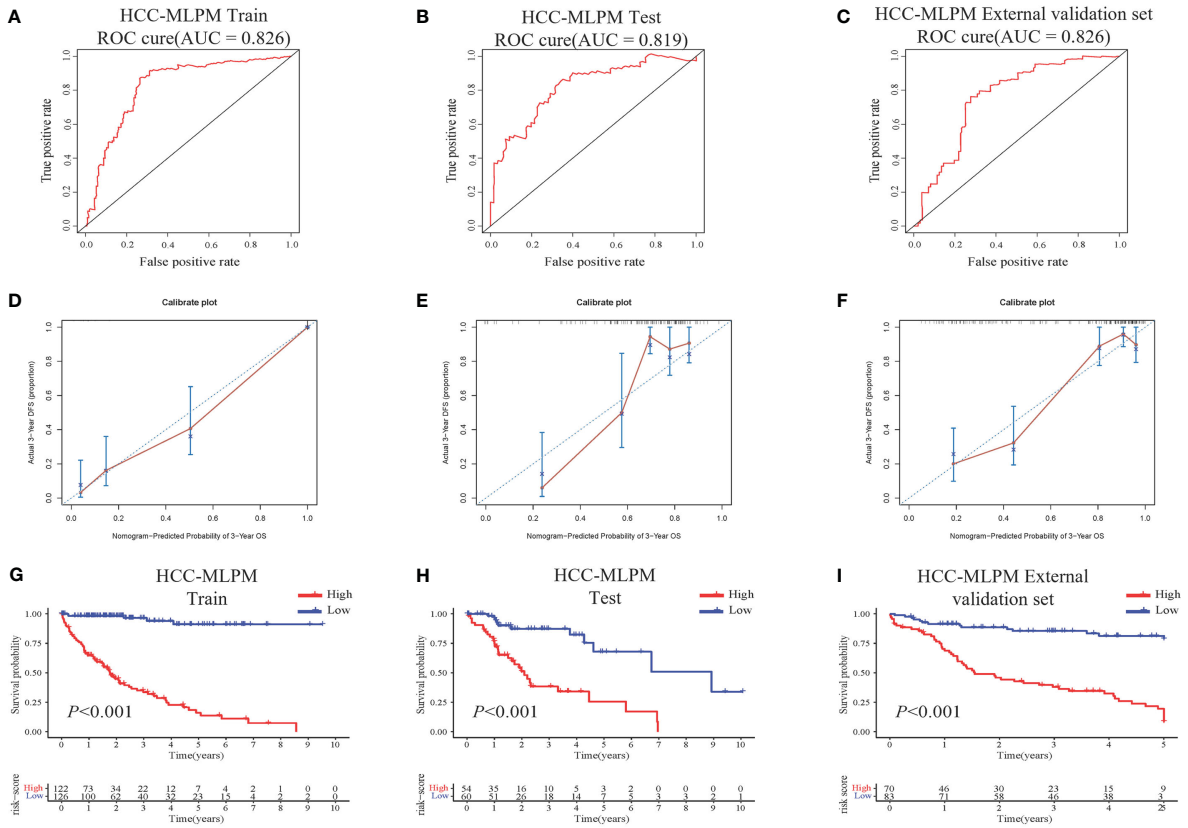

FIGURE 4
Performance Evaluation of the HCC-MLPM. **(A)** ROC curve of the training dataset. **(B)** ROC curve of the testing set. **(C)** ROC curve of the external validation set. **(D–F)** Calibration curves for the training, testing, and external validation sets, respectively. **(G–I)** KM survival curves for OS of the training, testing and external dataset respectively (red: High risk; bule: Low risk).

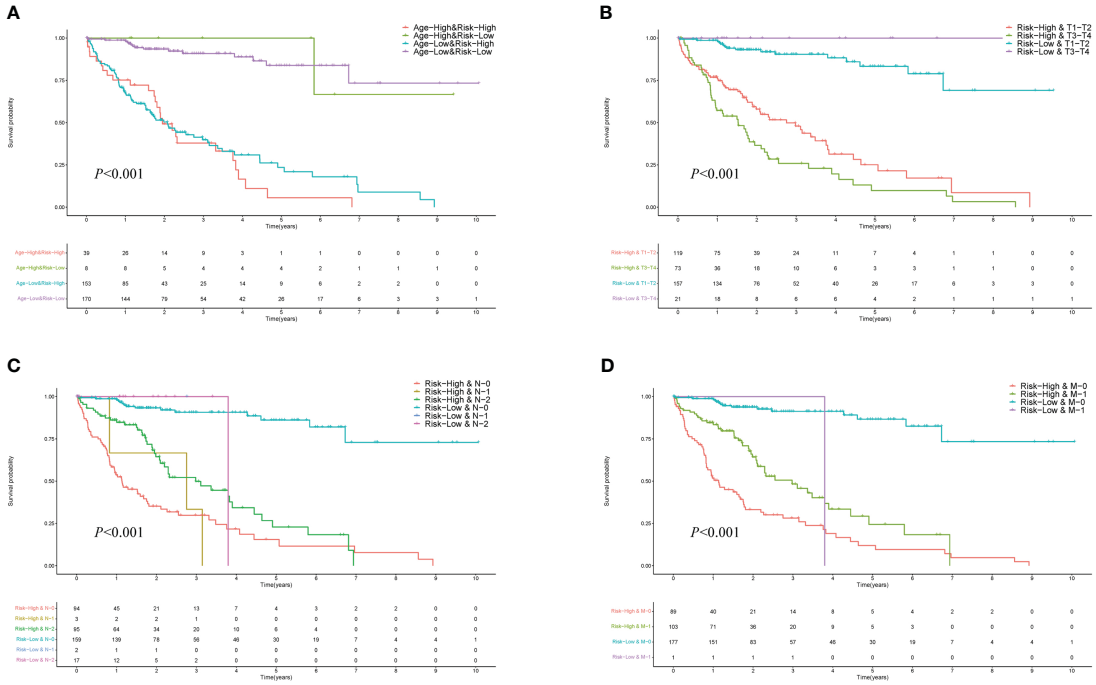

FIGURE 5
Performance for Different Clinical Indicators in HCC-MLPM. **(A)** KM curves for Age. **(B)** KM curves for tumor size (T). **(C)** KM curves for node involvement (N). **(D)** KM curves for metastasis (M).

immunosuppressive microenvironment in the high-risk group, which may contribute to disease progression and poorer prognosis.

To assess the responsiveness of patients in both groups to immunotherapy, we utilized an unsupervised clustering approach based on the characteristics of the tumor microenvironment, specifically the IPS. The patients were categorized into four groups: immune-enriched/fibrotic (IE/F), immune-enriched (IE), fibrotic (F), and immune-depleted (D). Among these groups, IE/F and IE demonstrated a more favorable response to immunotherapy, while F and D were associated with relatively poorer responses. In our analysis, we observed a higher proportion of patients in the low-risk group with an IE/F microenvironment. However, the proportions of IE and F were comparable between the two patient groups (IPS) (Figure 7C).

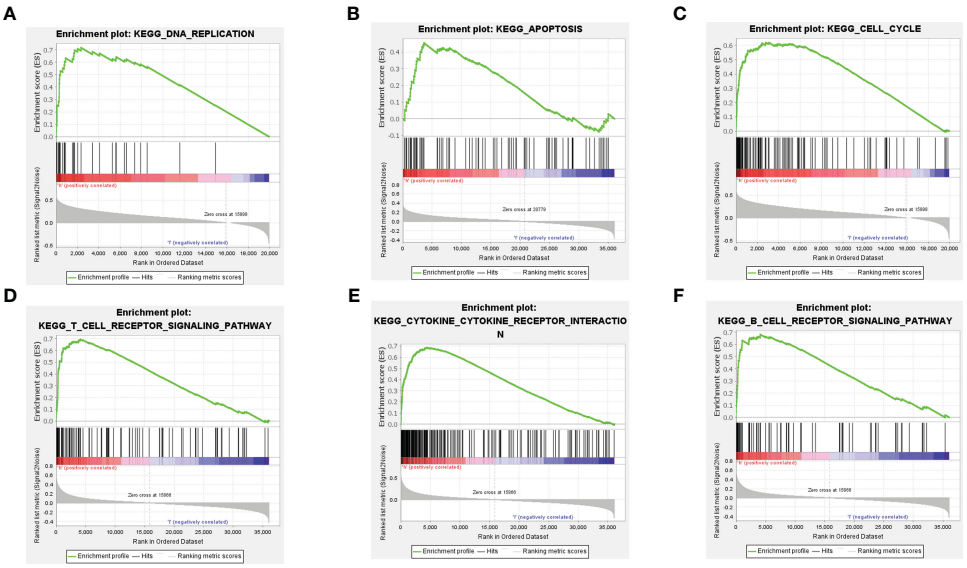

FIGURE 6
Gene Set Enrichment Analysis (GSEA) of the HCC-MLPM. **(A–C)** DNA replication, apoptosis and cell cycle enrichment analysis by GSEA. **(D-F)** T and B cell receptor pathway, cytokine receptor interaction pathway enrichment analysis by GSEA.

10.3389/fonc.2023.1327147

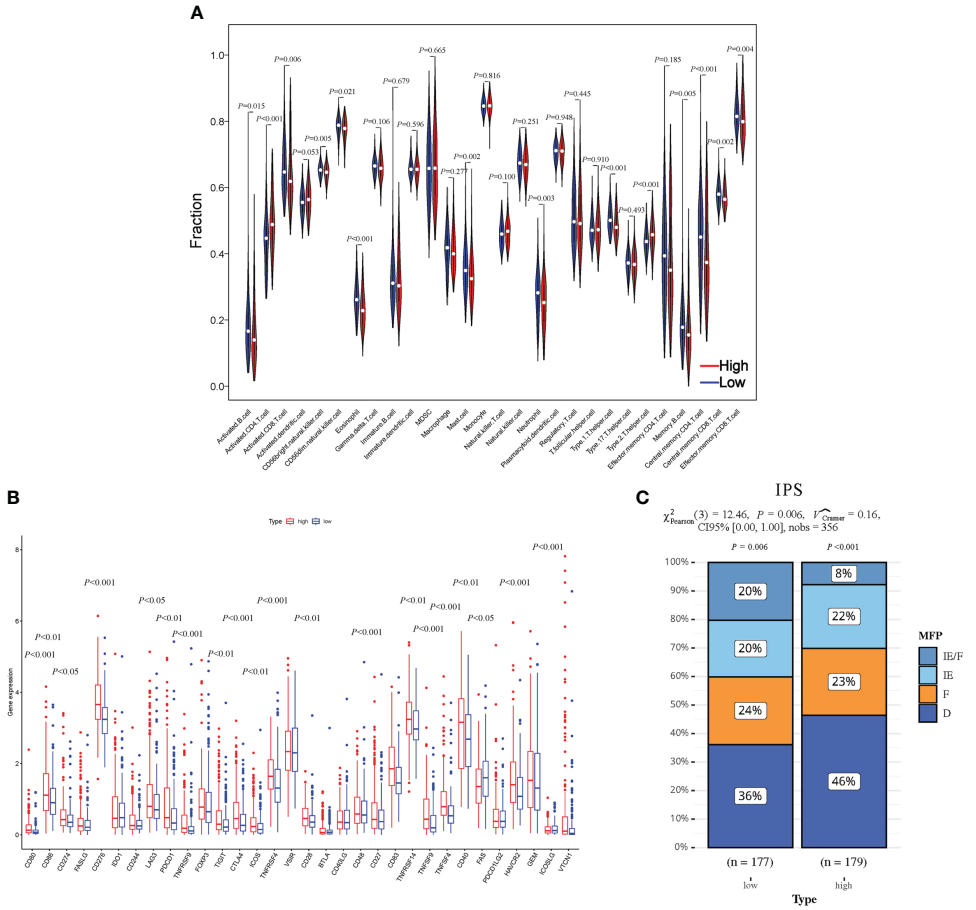

FIGURE 7
Evaluation of the HCC-MLPM on tumor immunity. **(A)** The Violin plots for infiltration levels of specific immune cell types. **(B)** Boxplot for infiltration levels of immune checkpoint markers. **(C)** The performance for immunotherapy. IE/F, Immune-enriched/Fibrotic; IE, Immune-enriched; F, Fibrotic; D, Depleted; High, high risk; Low, low risk. (red: High risk; bule: Low risk).

3.9 Assessment of clinical drug responsiveness

To investigate the clinical drug responsiveness predicted by HCC-MLPM, we utilized drug information obtained from the TCGA database. We examined the correlation between drug targets (Sorafenib) and cytotoxic drugs with the risk scores derived from our model. The results revealed significant differences in drug responsiveness between the high-risk and low-risk groups. Notably, a higher proportion of patients in the low-risk group demonstrated disease stability when treated with both targeted therapy and chemotherapy regimens (Figures 8A, B). This finding suggests that these treatment approaches were more likely to be effective in the low-risk group, providing potential therapeutic options for this particular subgroup of patients.

4 Discussion

We have successfully developed a machine learning-based prognostic risk model specifically designed for patients with HCC. This study integrates diverse indicators from a multicenter dataset, providing a comprehensive tool to aid in personalized treatment decisions for HCC patients. Remarkably, this model accurately predicts patient survival outcomes and offers insights into the effectiveness of immunotherapy and other clinical drug treatments in HCC patients.

The molecular pathogenesis of HCC is highly complex and heterogeneous. Currently, clinical treatment decisions for HCC patients are primarily based on limited clinical and pathological indicators (32). However, the development and progression of HCC are influenced by various factors, such as genetic variations, aberrant cell signaling pathways, and alterations in the immune environment (33, 34). Therefore, there is an urgent need to develop a dependable prognostic risk assessment model to enable personalized treatment for HCC. Previous studies have predominantly focused on individual tumor indicators, including age, stage, pathological type, tumor size, and other clinical factors, which have been extensively utilized in clinical assessments (35, 36). With advancements in genomics and immunology, there is a growing emphasis on the molecular characteristics of HCC and the impact of the immune environment on patient prognosis. Researchers have made efforts to predict patient prognosis from a biological perspective by integrating diverse information sources, such as gene expression data, protein expression

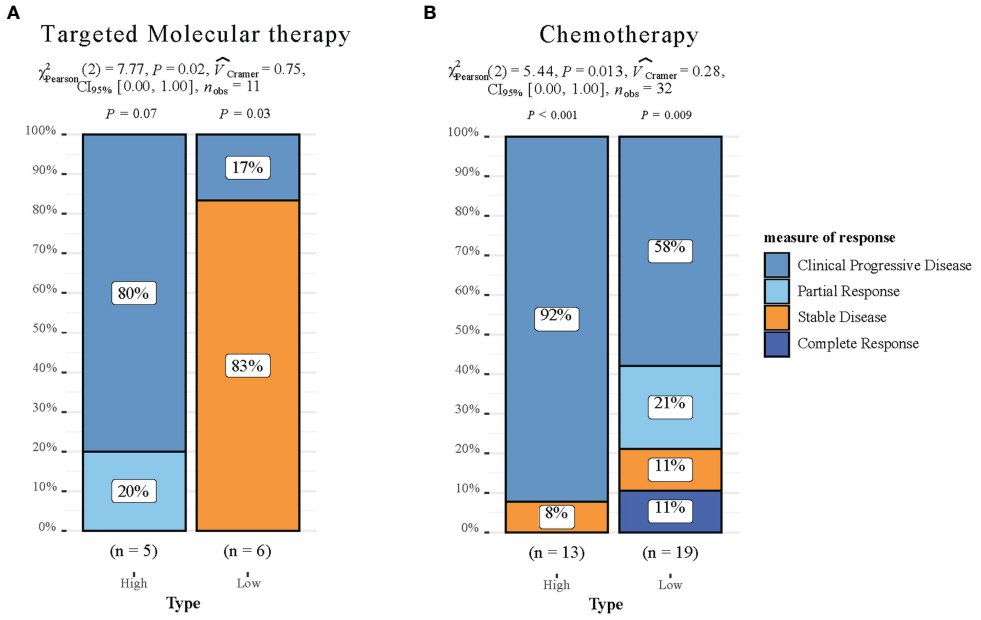

FIGURE 8
Drug responsiveness Evaluation of the HCC-MLPM. **(A)** Performance for predicting targeted molecular therapy of HCC-MLPM. **(B)** Performance for chemotherapy of HCC-MLPM. (High: high risk; Low: low risk).

data, and immune cell infiltration (37, 38). However, these evaluation methods provide a limited perspective on patient prognosis, resulting in inherent limitations. In contrast, our study not only takes into account clinical and pathological indicators that reflect the overall patient condition and disease severity but also places significant emphasis on the biological characteristics of liver cell tumors. This approach involves the identification of differentially expressed genes in HCC and the unveiling of potential biological mechanisms. By utilizing a modeling approach that incorporates comprehensive multi-level indicators, our model can offer a more comprehensive and dependable prognostic risk assessment for HCC patients (39, 40). Similar methodologies have demonstrated favorable outcomes in studies focusing on diverse cancer types, underscoring their potential utility in personalized medicine. Specifically, researchers investigating breast cancer, bladder cancer, and colorectal cancer have achieved robust predictive results by integrating comprehensive models with diverse datasets encompassing clinical, gene expression, and proteomic information (41–43). These investigations additionally validate the feasibility of our modeling approach.

In terms of methodology, our research has made significant advancements. Cox regression, an advanced machine learning technique, has provided strong technical support. Machine learning, in comparison to traditional statistical methods, excels in managing complex data structures and relationships, facilitating the extraction of potential features and patterns from extensive clinical and gene expression data (41). By employing the feature selection and optimization process of Cox regression, we have identified the most relevant indicators for prognosticating HCC patients. This approach effectively reduces the dimensionality of the feature space and enhances the predictive performance of the model (AUC = 0.724 *vs.* 0.819). Importantly, our research leverages the generalizability of machine learning, enabling the evaluation of the model's predictive performance and reliability across diverse datasets from multiple centers, including TCGA, SEER, and ICGC. The comprehensive integration of biological factors, clinical and pathological features, and multi-level indicators in our model substantially enhances its capacity to capture the intricacies of patient survival in HCC.

Our research findings include 11 risk factors, including 7 identified from the TCGA dataset (MYBL2, SF3B4, CDCA8, NUF2, HMMR, P0N1, and PAGE1), and an additional 4 acquired from the SEER database (Age, T, N, M). Several studies have recognized the substantial impact of certain factors on patient outcomes in HCC (44, 45). Our stratified survival analysis revealed that age plays a critical role in determining survival rates, aligning with previous findings. Furthermore, the correlation observed between smaller tumor size and better prognoses in our study underscores the importance of early detection and diagnosis in HCC, as reflected in the Kaplan-Meier curves for T. N and M, which indicate the aggressive progression of HCC, were also found to significantly affect survival rates in our analysis. These findings advocate for a nuanced understanding of HCC, indicating the inadequacy of generic treatment strategies. Moreover, our study validated these risk factors against the National Comprehensive Cancer Network (NCCN) guidelines (11), confirming the model's emphasis on tumor staging and its reliability.

Apart from established clinical factors, our research innovatively identified 7 genes that influence prognosis. These genes play critical roles in regulating cell-cell interactions, extracellular matrix remodeling, angiogenesis, and inflammatory responses within the tumor microenvironment. For example,

MYBL2 plays an important role in regulating the cell cycle, as its high expression is correlated with the staging and grading of various cancers (46). SF3B4 is involved in regulating the cell cycle, cell differentiation, and immune deficiency. Mutations in SF3B4 can lead to abnormal cell growth and contribute to disease development (47). CDCA8 controls the process of cell mitosis and has been identified as an unfavorable prognostic predictor in liver cancer (48). NUF2 participates in chromosome segregation and has been positively correlated with differential immune cell infiltration and various immune biomarkers (49). HMMR is associated with the infiltration levels of neutrophils, CD8+ T cells, and CD4+ T cells in the immune system, as well as the prognosis of patients with cancer (50). PON1 plays a role in cell adhesion and migration, contributing to the regulation of tumor development, oxidative stress, and inflammatory responses (51). PAGE1 is involved in cell apoptosis and immune regulation (52). These gene abnormalities play a role in altering the tumor microenvironment, which impacts the growth, infiltration, and metastasis of HCC. By integrating these differential gene factors into the prognostic risk assessment model, we capture the intricacies of patient survival in HCC.

In addition to assessing the model's performance in predicting patient survival, our research closely integrates with clinical treatment through the evaluation of patients' immune infiltration status and their responses to clinical drugs. This enhances our comprehensive understanding of HCC. In recent years, immunotherapy has emerged as a significant breakthrough in HCC treatment, utilizing the patient's immune system to target tumor cells (53, 54). We examined the association between the model's predictive results and the immune status by employing GSEA analysis and assessing immune cell infiltration. The results indicated a significant correlation ($P < 0.05$) between high-risk patients and malignant tumor phenotypes, particularly in terms of cell cycle, DNA replication, and immune responses. We have discerned a significant elevation in the infiltration levels of Type2 T helper (Th2) cells within the cohort of high-risk HCC patients ($P < 0.001$), indicating a Th2-dominated immune microenvironment. The cytokines secreted by Th2 cells, such as IL-4 and IL-10, may facilitate tumor growth and assist in the tumor's evasion of immune surveillance. Therapeutic interventions targeting the Th2 cell pathway, such as PD-1/PD-L1 and CTLA-4 inhibitors, have demonstrated potential in the treatment of other cancers (55, 56). This observation underscores the importance of considering the immune microenvironment when devising therapeutic strategies for HCC.

Additionally, we introduced the novel IPS to assess both the immune system's activity level and the extent of immune cell infiltration in the tumor microenvironment. This was done with the aim of identifying potential variations in patient response to immunotherapy. The IPS quantifies patients' potential responsiveness to immunotherapy based on the analysis of expression patterns in immune-related genes. Higher IPS scores generally reflect a more active immune system and an increased likelihood of positive response to immunotherapy (31). We computed IPS scores for patients in both the high-risk and low-risk groups, facilitating a comparison of their immunotherapy responsiveness. The findings showed that the low-risk group exhibited significantly higher responsiveness to immunotherapy ($P < 0.05$), providing theoretical support for the application of immunotherapy in low-risk patients.

Although our research has shown promising results, it is important to acknowledge its limitations. First, the development and prognosis of HCC are influenced by various biological and environmental factors. While we thoroughly considered clinical data and genetic information, it is conceivable that other factors, not accounted for in the model, may also contribute. This underscores the necessity for continual improvement and refinement. Secondly, as our model lacks support from Supplementary Databases, it is advisable to conduct further prospective studies to validate and refine it in relation to immunotherapy and clinical drug responsiveness.

In conclusion, we have successfully developed a machine learning-based prognostic risk model for HCC, providing robust support for personalized treatment strategies in HCC patients. Furthermore, this study highlights the potential importance of utilizing multi-level modeling approaches in the realm of personalized medicine.

Data availability statement

The data utilized in this study can be obtained by contacting the authors due to restrictions imposed by the data providers, namely the TCGA, SEER, and GSEA databases. Access to these databases is available via their dedicated websites: TCGA (https://portal.gdc.cancer.gov/), SEER (https://seer.cancer.gov/), GSEA (http://software.broadinstitute.org/gsea/index.jsp), and ICGC (https://icgcportal.genomics.cn/). Researchers interested in accessing the data may reach out to the authors for additional information and support in acquiring the required permissions and data access.

Author contributions

Z-HZ: Data curation, Methodology, Software, Writing – original draft. YD: Supervision, Validation, Writing – review & editing. SW: Investigation, Writing – original draft. WP: Methodology, Supervision, Validation, Writing – original draft, Writing – review & editing.

Funding

The author(s) declare that no financial support was received for the research, authorship, and/or publication of this article.

Conflict of interest

Authors YD, SW and WP were employed by the company China RongTong Medical Healthcare Group Co., Ltd.

The remaining author declares that the research was conducted in the absence of any commercial or financial relationships that could be construed as a potential conflict of interest.

Publisher's note

References

1. McGlynn KA, Petrick JL, El-Serag HB. Epidemiology of hepatocellular carcinoma. *Hepatology* (2021) 73 (Suppl 1):4–13. doi: 10.1002/hep.31288

2. Samant H, Amiri HS, Zibari GB. Addressing the worldwide hepatocellular carcinoma: epidemiology, prevention and management. *J Gastrointest Oncol* (2021) 12 Suppl 2:S361–73. doi: 10.21037/jgo.2020.02.08

3. Yao J, Liang X, Liu Y, Li S, Zheng M. Trends in incidence and prognostic factors of two subtypes of primary liver cancers: A surveillance, epidemiology, and end results-based population study. *Cancer Control.* (2022) 29:10732748211051548. doi: 10.1177/10732748211051548

4. Moon AM, Singal AG, Tapper EB. Contemporary epidemiology of chronic liver disease and cirrhosis. *Clin Gastroenterol Hepatol* (2020) 18:2650–66. doi: 10.1016/j.cgh.2019.07.060

5. European Association for the Study of the Liver. Electronic address: easloffice@easloffice.eu and European Association for the Study of the Liver. EASL Clinical Practice Guidelines: Management of hepatocellular carcinoma. *J Hepatol* (2018) 69:182–236. doi: 10.1016/j.jhep.2018.03.019

6. Llovet JM, Kelley RK, Villanueva A, Singal AG, Pikarsky E, Roayaie S, et al. Hepatocellular carcinoma. *Nat Rev Dis Primers.* (2021) 7:6. doi: 10.1038/s41572-020-00240-3

7. Marrero JA, Kulik LM, Sirlin CB, Zhu AX, Finn RS, Abecassis MM, et al. Diagnosis, staging, and management of hepatocellular carcinoma: 2018 practice guidance by the american association for the study of liver diseases. *Hepatology* (2018) 68:723–50. doi: 10.1002/hep.29913

8. Ayuso C, Rimola J, Vilana R, Burrel M, Darnell A, García-Criado Á, et al. Diagnosis and staging of hepatocellular carcinoma (HCC): current guidelines. *Eur J Radiol* (2018) 101:72–81. doi: 10.1016/j.ejrad.2018.01.025

9. Allaire M, Goumard C, Lim C, Le Cleach A, Wagner M, Scatton O. New frontiers in liver resection for hepatocellular carcinoma. *JHEP Rep* (2020) 2:100134. doi: 10.1016/j.jhepr.2020.100134

10. Kabir T, Tan ZZ, Syn NL, Wu E, Lin JD, Zhao JJ, et al. Laparoscopic versus open resection of hepatocellular carcinoma in patients with cirrhosis: meta-analysis. *Br J Surg* (2021) 109:21–9. doi: 10.1093/bjs/znab376

11. Benson AB, D'Angelica MI, Abbott DE, Anaya DA, Anders R, Are C, et al. Hepatobiliary cancers, version 2.2021, NCCN clinical practice guidelines in oncology. *J Natl Compr Cancer Network* (2021) 19:541–65. doi: 10.6004/jnccn.2021.0022

12. Shimose S, Iwamoto H, Tanaka M, Niizeki T, Shirono T, Kajiwara A, et al. Multimolecular-targeted agents for intermediate-stage hepatocellular carcinoma influence time to stage progression and overall survival. *Oncology* (2021) 99:756–65. doi: 10.1159/000518612

13. D'Angelo S, Secondulfo M, De Cristofano R, Sorrentino P. Sorafenib and entecavir: the dioscuri of treatment for advanced hepatocellular carcinoma? *World J Gastroenterol* (2013) 19:2141–3. doi: 10.3748/wjg.v19.i14.2141

14. Shen X, Li N, Li H, Zhang T, Wang F, Li Q. Increased prevalence of regulatory T cells in the tumor microenvironment and its correlation with TNM stage of hepatocellular carcinoma. *J Cancer Res Clin Oncol* (2010) 136:1745–54. doi: 10.1007/s00432-010-0833-8

15. Lim H, Ramjeesingh R, Liu D, Tam VC, Knox JJ, Card PB, et al. Optimizing survival and the changing landscape of targeted therapy for intermediate and advanced hepatocellular carcinoma: A systematic review. *J Natl Cancer Inst* (2021) 113:123–36. doi: 10.1093/jnci/djaa119

16. Foerster F, Gairing SJ, Müller L, Galle PR. NAFLD-driven HCC: Safety and efficacy of current and emerging treatment options. *J Hepatol* (2022) 76:446–57. doi: 10.1016/j.jhep.2021.09.007

17. Couri T, Pillai A. Goals and targets for personalized therapy for HCC. *Hepatol Int* (2019) 13:125–37. doi: 10.1007/s12072-018-9919-1

18. Lee S-W, Lee T-Y, Peng Y-C, Yang S-S, Yeh H-Z, Chang C-S. Sorafenib treatment on Chinese patients with advanced hepatocellular carcinoma: A study on prognostic factors of the viral and tumor status. *Med (Baltimore).* (2019) 98:e17692. doi: 10.1097/MD.0000000000017692

19. Faivre S, Rimassa L, Finn RS. Molecular therapies for HCC: Looking outside the box. *J Hepatol* (2020) 72:342–52. doi: 10.1016/j.jhep.2019.09.010

20. Finkelmeier F, Waidmann O, Trojan J. Nivolumab for the treatment of hepatocellular carcinoma. *Expert Rev Anticancer Ther* (2018) 18:1169–75. doi: 10.1080/14737140.2018.1535315

21. Paik J. Nivolumab plus relatlimab: first approval. *Drugs* (2022) 82:925–31. doi: 10.1007/s40265-022-01723-1

22. Sidali S, Trépo E, Sutter O, Nault J-C. New concepts in the treatment of hepatocellular carcinoma. *United Eur Gastroenterol J* (2022) 10:765–74. doi: 10.1002/ueg2.12286

23. Guiu B, Garin E, Allimant C, Edeline J, Salem R. TARE in hepatocellular carcinoma: from the right to the left of BCLC. *Cardiovasc Intervent Radiol* (2022) 45:1599–607. doi: 10.1007/s00270-022-03072-8

24. Liñares-Blanco J, Pazos A, Fernandez-Lozano C. Machine learning analysis of TCGA cancer data. *PeerJ Comput Sci* (2021) 7:e584. doi: 10.7717/peerj-cs.584

25. Liu J, Sun G, Pan S, Qin M, Ouyang R, Li Z, et al. The Cancer Genome Atlas (TCGA) based m6A methylation-related genes predict prognosis in hepatocellular carcinoma. *Bioengineered* (2020) 11:759–68. doi: 10.1080/21655979.2020.1787764

26. Donisi C, Puzzoni M, Ziranu P, Lai E, Mariani S, Saba G, et al. Immune checkpoint inhibitors in the treatment of HCC. *Front Oncol* (2020) 10:601240. doi: 10.3389/fonc.2020.601240

27. Llovet JM, Montal R, Sia D, Finn RS. Molecular therapies and precision medicine for hepatocellular carcinoma. *Nat Rev Clin Oncol* (2018) 15:599–616. doi: 10.1038/s41571-018-0073-4

28. Ritchie ME, Phipson B, Wu D, Hu Y, Law CW, Shi W, et al. limma powers differential expression analyses for RNA-sequencing and microarray studies. *Nucleic Acids Res* (2015) 43:e47. doi: 10.1093/nar/gkv007

29. Kuhn M. Building predictive models in R using the caret package. *J Stat Software* (2008) 28:1–26. doi: 10.18637/jss.v028.i05

30. Hänzelmann S, Castelo R, Guinney J. GSVA: gene set variation analysis for microarray and RNA-seq data. *BMC Bioinf* (2013) 14:7. doi: 10.1186/1471-2105-14-7

31. Bagaev A, Kotlov N, Nomie K, Svekolkin V, Gafurov A, Isaeva O, et al. Conserved pan-cancer microenvironment subtypes predict response to immunotherapy. *Cancer Cell* (2021) 39:845–865.e7. doi: 10.1016/j.ccell.2021.04.014

32. Reig M, Forner A, Rimola J, Ferrer-Fàbrega J, Burrel M, Garcia-Criado Á, et al. BCLC strategy for prognosis prediction and treatment recommendation: The 2022 update. *J Hepatol* (2022) 76:681–93. doi: 10.1016/j.jhep.2021.11.018

33. Dhanasekaran R, Bandoh S, Roberts LR. Molecular pathogenesis of hepatocellular carcinoma and impact of therapeutic advances. *F1000Res* (2016) 5:F1000 Faculty Rev–879. doi: 10.12688/f1000research.6946.1

34. Macdonald GA. Pathogenesis of hepatocellular carcinoma. *Clin Liver Dis* (2001) 5:69–85. doi: 10.1016/S1089-3261(05)70154-9

35. Ma L, Deng K, Zhang C, Li H, Luo Y, Yang Y, et al. Nomograms for predicting hepatocellular carcinoma recurrence and overall postoperative patient survival. *Front Oncol* (2022) 12:843589. doi: 10.3389/fonc.2022.843589

36. Zhang H, Du X, Dong H, Xu W, Zhou P, Liu S, et al. Risk factors and predictive nomograms for early death of patients with advanced hepatocellular carcinoma: a large retrospective study based on the SEER database. *BMC Gastroenterol* (2022) 22:348. doi: 10.1186/s12876-022-02424-5

37. Hu B, Yang X-B, Sang X-T. Molecular subtypes based on immune-related genes predict the prognosis for hepatocellular carcinoma patients. *Int Immunopharmacol.* (2021) 90:107164. doi: 10.1016/j.intimp.2020.107164

38. Song X, Du R, Gui H, Zhou M, Zhong W, Mao C, et al. Identification of potential hub genes related to the progression and prognosis of hepatocellular carcinoma through integrated bioinformatics analysis. *Oncol Rep* (2020) 43:133–46. doi: 10.3892/or.2019.7400

39. Yang B, Zhang Y, Pang S, Shang X, Zhao X, Han M. Integrating multi-omic data with deep subspace fusion clustering for cancer subtype prediction. *IEEE/ACM Trans Comput Biol Bioinform* (2021) 18:216–26. doi: 10.1109/TCBB.2019.2951413

40. Vangimalla RR, Sreevalsan-Nair J. HCNM: heterogeneous correlation network model for multi-level integrative study of multi-omics data for cancer subtype prediction. *Annu Int Conf IEEE Eng Med Biol Soc* (2021) 2021:1880–6. doi: 10.1109/EMBC46164.2021.9630781

41. Pou SA, Díaz M del P, Osella AR. Applying multilevel model to the relationship of dietary patterns and colorectal cancer: an ongoing case-control study in Córdoba, Argentina. *Eur J Nutr* (2012) 51:755–64. doi: 10.1007/s00394-011-0255-7

42. Hiatt RA, Porco TC, Liu F, Balke K, Balmain A, Barlow J, et al. A multilevel model of postmenopausal breast cancer incidence. *Cancer Epidemiol Biomarkers Prev* (2014) 23:2078–92. doi: 10.1158/1055-9965.EPI-14-0403

43. Peng C, Li A, Wang M. Discovery of bladder cancer-related genes using integrative heterogeneous network modeling of multi-omics data. *Sci Rep* (2017) 7:15639. doi: 10.1038/s41598-017-15890-9

44. Liu M, Xu M, Tang T. Association between chemotherapy and prognostic factors of survival in hepatocellular carcinoma: a SEER population-based cohort study. *Sci Rep* (2021) 11:23754. doi: 10.1038/s41598-021-02698-x

45. Ding J, Wen Z. Survival improvement and prognosis for hepatocellular carcinoma: analysis of the SEER database. *BMC Cancer*. (2021) 21:1157. doi: 10.1186/s12885-021-08904-3

46. Chen X, Lu Y, Yu H, Du K, Zhang Y, Nan Y, et al. Pan-cancer analysis indicates that MYBL2 is associated with the prognosis and immunotherapy of multiple cancers as an oncogene. *Cell Cycle* (2021) 20:2291–308. doi: 10.1080/15384101.2021.1982494

47. Yan L, Yang X, Yang X, Yuan X, Wei L, Si Y, et al. The role of splicing factor SF3B4 in congenital diseases and tumors. *Discovery Med* (2021) 32:123–32.

48. Shuai Y, Fan E, Zhong Q, Chen Q, Feng G, Gou X, et al. CDCA8 as an independent predictor for a poor prognosis in liver cancer. *Cancer Cell Int* (2021) 21:159. doi: 10.1186/s12935-021-01850-x

49. Xie X, Jiang S, Li X. Nuf2 is a prognostic-related biomarker and correlated with immune infiltrates in hepatocellular carcinoma. *Front Oncol* (2021) 11:621373. doi: 10.3389/fonc.2021.621373

50. Ma X, Xie M, Xue Z, Yao J, Wang Y, Xue X, et al. HMMR associates with immune infiltrates and acts as a prognostic biomaker in lung adenocarcinoma. *Comput Biol Med* (2022) 151 Pt A:106213. doi: 10.1016/j.compbiomed.2022.106213

51. Cai D, Zhao Z, Hu J, Dai X, Zhong G, Gong J, et al. Identification of the tumor immune microenvironment and therapeutic biomarkers by a novel molecular subtype based on aging-related genes in hepatocellular carcinoma. *Front Surg* (2022) 9:836080. doi: 10.3389/fsurg.2022.836080

52. Cui Y, Jiang N. Identification of a seven-gene signature predicting clinical outcome of liver cancer based on tumor mutational burden. *Hum Cell* (2022) 35:1192–206. doi: 10.1007/s13577-022-00708-2

53. Rodríguez Pérez Á, Campillo-Davo D, Van Tendeloo VFI, Benítez-Ribas D. Cellular immunotherapy: a clinical state-of-the-art of a new paradigm for cancer treatment. *Clin Transl Oncol* (2020) 22:1923–37. doi: 10.1007/s12094-020-02344-4

54. Abbott M, Ustoyev Y. Cancer and the immune system: the history and background of immunotherapy. *Semin Oncol Nurs*. (2019) 35:150923. doi: 10.1016/j.soncn.2019.08.002

55. Zhang H, Dai Z, Wu W, Wang Z, Zhang N, Zhang L, et al. Regulatory mechanisms of immune checkpoints PD-L1 and CTLA-4 in cancer. *J Exp Clin Cancer Res* (2021) 40:184. doi: 10.1186/s13046-021-01987-7

56. Pandey P, Khan F, Qari HA, Upadhyay TK, Alkhateeb AF, Oves M. Revolutionization in cancer therapeutics *via* targeting major immune checkpoints PD-1, PD-L1 and CTLA-4. *Pharmaceuticals* (2022) 15:335. doi: 10.3390/ph15030335

frontiers | Frontiers in Oncology

TYPE Systematic Review
PUBLISHED 18 March 2024
DOI 10.3389/fonc.2024.1366607

OPEN ACCESS

EDITED BY
Giorgio Treglia,
Ente Ospedaliero Cantonale (EOC), Switzerland

REVIEWED BY
Pierluigi Romano,
University Hospital of Padua, Italy
Sjaak Pouwels,
Elisabeth Tweesteden Hospital (ETZ), Netherlands
Gianluca Rompianesi,
University of Naples Federico II, Italy

*CORRESPONDENCE
Francesco Giovinazzo
giovinazzo_francesco@live.com

RECEIVED 06 January 2024
ACCEPTED 13 February 2024
PUBLISHED 18 March 2024

CITATION
Martinino A, Bucaro A, Cardella F, Wazir I, Frongillo F, Ardito F and Giovinazzo F (2024) Liver transplantation vs liver resection in HCC: promoting extensive collaborative research through a survival meta-analysis of meta-analyses. *Front. Oncol.* 14:1366607. doi: 10.3389/fonc.2024.1366607

Liver transplantation vs liver resection in HCC: promoting extensive collaborative research through a survival meta-analysis of meta-analyses

Alessandro Martinino[1], Angela Bucaro[2], Francesca Cardella[3], Ishaan Wazir[4], Francesco Frongillo[2], Francesco Ardito[5] and Francesco Giovinazzo[2]*

[1]Department of Surgery, Duke University, Durham, NC, United States, [2]General Surgery and Liver Transplant Unit, Fondazione Policlinico Universitario Agostino Gemelli IRCCS, Rome, Italy, [3]Surgical Oncology of Gastrointestinal Tract Unit, Vanvitelli University, Naples, Italy, [4]Vardhaman Mahavir Medical College & Safdarjung Hospital, New Delhi, India, [5]Hepatobilairy and General Surgery Unit, Fondazione Policlinico Universitario Agostino Gemelli IRCCS, Rome, Italy

Background: HCC is a major global health concern, necessitating effective treatment strategies. This study conducts a meta-analysis of meta-analyses comparing liver resection (LR) and liver transplantation (LT) for HCC.

Methods: The systematic review included meta-analyses comparing liver resection vs. liver transplantation in HCC, following PRISMA guidelines. Primary outcomes included 5-year overall survival (OS) and disease-free survival (DFS). AMSTAR-2 assessed study quality. Citation matrix and hierarchical clustering validated the consistency of the included studies.

Results: A search identified 10 meta-analyses for inclusion. The median Pearson correlation coefficient for citations was 0.59 (IQR 0.41-0.65). LT showed better 5-year survival and disease-free survival in all HCC (OR): 0.79; 95% CI: 0.67-0.93, I^2:57% and OR: 0.44; 95% CI: 0.25-0.75, I^2:96%). Five-year survival in early HCC and ITT was 0.63 (95% CI: 0.50-0.78, I^2:0%) and 0.60 (95% CI: 0.39-0.92, I^2:0%). Salvage LT vs. Primary LT did not differ between 5-year survival and disease-free survival (OR: 0.62; 95% CI: 0.33-1.15, I^2:0% and 0.93; 95% CI: 0.82-1.04, I^2:0%).

Conclusion: Overall, the study underscores the superior survival outcomes associated with LT over LR in HCC treatment, supported by comprehensive meta-analysis and clustering analysis. There was no difference in survival or recurrence rate between salvage LT and primary LT. Therefore, considering the organ shortage, HCC can be resected and transplanted in case of recurrence.

KEYWORDS

liver transplantation, liver resection, hepatocellular carcinoma, survival, meta-analysis

Introduction

Hepatocellular carcinoma (HCC), with 782000 cases diagnosed and 746 000 deaths in 2012 and an age-adjusted worldwide incidence of 10·1 cases per 100 000 person-years (1), is the sixth most common cancer and the third-leading cause of cancer-related mortality in the world (1, 2).

HCC usually develops in the setting of chronic liver diseases, such as cirrhosis, infections like hepatitis B or C, non-alcoholic fatty liver disease, or alcohol-related liver disease (1–3). Most HCCs (80%) occur in sub-Saharan Africa and eastern Asia, where the main risk factors are chronic hepatitis B and aflatoxin B1 exposure. Instead, in the USA, Europe, and Japan, hepatitis C is the leading risk factor, together with excessive alcohol intake (1, 4, 5).

The management of HCC depends on several factors, including the size and number of tumours, the underlying liver function, and the patient's overall health status (6, 7). Liver resection (LR) and transplantation (LT) are the most effective curative treatments for HCC, with promising outcomes in survival and disease-free survival (DFS) (1, 8–10). In patients without clinically significant portal hypertension (CSPH), compensated liver function, and early HCC stages, LR achieves 70% 5-year survival in HCC. However, the survival rate decreases by 50% when those adverse factors are present (1). On the other hand, 5-year survival in HCC after LT is more than 70% with a recurrence rate of less than 10–15% (1) (11). However, the choice of the two treatments is also limited by the availability of donor organs. Therefore, choosing between LT and LR for HCC in several cases is still controversial (7, 10).

As robust evidence is missing with contrasting results, the objective of the present study was to perform a survival meta-analysis of meta-analyses to compare LT and LR in HCC. The primary outcomes were 5-year overall and disease-free survival after the two different types of treatment.

Methods

The systematic review and meta-analysis were conducted according to the Preferred Reporting Items for Systematic Reviews and Meta-Analyses (PRISMA) guidelines.

A computerised search of PubMed, Scopus and Cochrane Library was carried out. Reference lists of all obtained and relevant articles were screened manually and cross-referenced to identify any additional studies. Articles published from the time of inception to June 2023 were included. An advanced search was performed using the following terms: [(transplant) OR (transplantation)] AND (hepatocellular) OR (HCC) OR (liver cancer).

Outcomes of interest

The primary outcomes were 5-year graft overall (OS) and disease-free survival (DFS) in liver resection vs. liver transplantation in all HCCs. The secondary outcomes were OS and DSF in early HCC, Intention to treat, and salvage liver transplantation for HCC.

Inclusion criteria

The systematic review included meta-analyses comparing liver resection vs. liver transplantation in HCC and reporting the primary and secondary outcomes. Abstracts, letters, comments, editorials and expert opinions, unpublished articles and abstracts, reviews without original data, and case reports were excluded from the analysis. Studies were included only when reporting the number or the rate of events (deaths or recurrences). Two reviewers (AM and IW) independently screened the titles and abstracts of all retrieved articles. The full texts of articles that could fulfil the inclusion criteria were obtained and checked for eligibility.

Internal validity (methodological quality)

The internal validity of the meta-analyses was assessed by the Assessment of Multiple Systematic Reviews 2 (AMSTAR-2) method. AMSTAR is a standardised and reliable method for assessing the quality of systematic reviews that include randomised or non-randomised studies of healthcare interventions, or both. FG and FC completed the AMSTAR proforma for all included reviews, and discrepancies were discussed to reach a consensus. Studies were, finally, classified on the level of quality through the online tool calculator (12).

Cytation matrix and dendrogram analysis

A sample citation matrix was created by measuring the primary overlap of every included study (Supplementary Table 1), and the Pearson correlation coefficient (r) was calculated. r was visualised through a heatmap. A hierarchical cluster analysis of the r was visualised through a dendrogram clusterisation and a silhouette analysis used to identify the number of clusters (13).

Data analysis

The results of the meta-analyses were combined using a summary meta-analysis model for odds ratios (OR) and hazard ratio (HR) with 95% confidence intervals.

The fixed-effect method was used to combine the results without statistically significant heterogeneity. The random-effect method was used when heterogeneity was confirmed ($p \leq 0{\cdot}10$). Potential publication bias was investigated by funnel plot. Egger's and Begger's tests were used to assess funnel plot asymmetry and biases [12], and Makaskill's test was used to quantify the bias (14). $P < 0{\cdot}05$ (two-tailed) was considered to indicate statistical significance [13]. Trim-and-fill method was used to adjust for the publication biases.

The meta-analysis of meta-analyses and hierarchical analysis was performed using the R software suite (v3.4.0, https://www.R-project.org). Statistical heterogeneity between metanalysis was evaluated by $\chi 2$ and I2, with significance set at $p \leq 0{,}10$ (14–16).

Results

Literature search

The PRISMA flow diagram reports the number of studies screened, assessed, and excluded (Figure 1). 19 full-text articles were assessed for eligibility, and 10 meta-analyses comparing an overall 105 studies were included in the umbrella review (11, 17–25). The characteristics of the included meta-analyses are shown in Table 1.

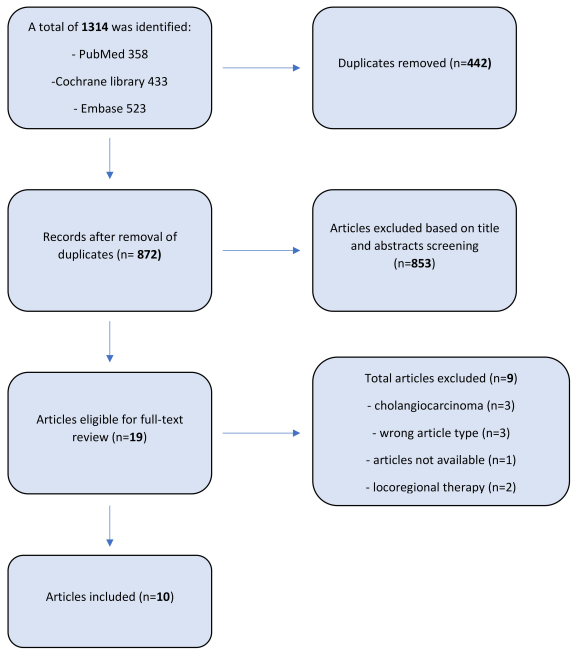

FIGURE 1
PRISMA flow diagram.

Quality assessment

Authors of five of the eight meta-analyses cited the previously published meta-analyses, and only one study had no prior studies available to cite (Table 2). Every included study used Medline/PubMed as part of the literature search, and nine studies also used Embase (Table 3). There was variation in the utilisation of other databases, but every study (excluding two) used at least two electronic databases. According to the AMSTAR quality assessment, four studies rated low quality and six critically low quality (Table 4). The median Pearson correlation coefficient was 0.59 (IQR 0.41-0.65) for all the included studies (Figure 2A). Hierarchical clustering of the r identified 3 clusters after silhouette analysis (Cluster Sizes and Average Silhouette Widths: Cluster 1 (26 data points): Average Silhouette Width of 0.443; Cluster 2 (62 data points): Average Silhouette Width of 0.724; Cluster 3 (12 data points): Average Silhouette Width of 0.909); (Median: 0.7341 IQR: 0.5543- 0.8369; Mean: 0.6731 Range 0.1244-0.9534. (Figure 2B).

Primary outcome

5 years overall survival

LT showed better 5-year survival in all HCC (Odd Ratio (OR): 0.79; 95% CI: 0.67-0.93, I^2:57%), (Figure 3A), Egger's test showed a significant funnel plot asymmetry (t = -2.62, df = 5, p = 0.0468). Begg's test did not find funnel plot asymmetry (z = -1.05, p = 0.2931) (Figure 3B). After the 5-year survival Trim-and-fill method, both Egger's and Begg's tests did not show evidence of publication bias (t = -0.07, df = 9, p-value = 0.9437 and z = -0.08, p-value = 0.9372, respectively) (Figure 3C).

5 years disease survival

DFS favoured LT for all HCC (OR: 0.44; 95% CI: 0.25-0.75, I^2:96%) (Figure 4A). The Egger's test (t = 0.02, df = 3, p-value = 0.9879) and Begg's test (z = -0.68, p-value = 0.4969) did not indicate significant publication bias in the original analysis (Figure 4B). After applying the Trim-and-fill method, the Egger's test (t = 0.02,

TABLE 1 Included studies.

Authors	Journal	Publication Year	Range of Years of Included Studies	No. of Primary Studies	No. of Retrospective Study	Finding Direction
Dhir et al. (17)	HPB	2012	1990-2011	10	10	LT
Rahman et al. (11)	J Gastrointest Surg	2012	2000-2012	9	9	LT
Li et al. (19)	World J Gastroenterol	2012	1996-2011	11	11	LT
Zheng et al. (25)	Transplantation	2014	Inception to 8 March 2013	62	not specified	LT
Proneth et al. (22)	Ann Surg Oncol	2014	1990-2013	7	7	LT

(Continued)

TABLE 1 Continued

Authors	Journal	Publication Year	Range of Years of Included Studies	No. of Primary Studies	No. of Retrospective Study	Finding Direction
Xu et al. (24)	Hepatobiliary Pancreat Dis Int	2014	1990-2012	17	17	LT
Menahem et al. (21)	Liver Transplantation	2017	Inception to 8 March 2015	9	9	No differences
Schoenberg et al. (23)	Medicine	2017	1990-2016	54	54	LT
Li et al. (20)	Clinical Transplantation	2017	Inception to 8 March 2017	6	6	LT
Koh et al. (18)	Hepatobiliary Surg Nutr	2022	Inception to 8 March 2021	35	34	LT

TABLE 2 Number of meta-analyses.

Authors	Publication Year	Date of Last Literature Search (mo/yr)	No. of Meta-Analyses Possible to Cite	No. of Meta-Analyses Cited
Hong-Yu Li (19)	2012	01/04/2010	1	0
Mashaal Dhir (17)	2012	31/03/2011	0	0
Atiq Rahman (11)	2012	01/03/2012	2	0
Zheng Zheng (25)	2014	01/04/2012	4	0
Xin-Sen Xu (24)	2014	01/07/2012	5	1
Andrea Proneth (22)	2014	01/09/2013	6	1
Benjamin Menahem (21)	2017	01/12/2016	7	0
Markus B. Schoenberg (23)	2017	01/03/2017	8	3
Wei Li (20)	2018	01/06/2017	9	1
Jin Hean Koh (18)	2022	01/03/2021	11	1

TABLE 3 Search methodology.

Authors	Year of Publication	Medline/ PubMed	Embase	Cochrane Library	Other	Language Limitations
Mashaal Dhir (17)	2012	yes	no	no	no	Only English
Atiq Rahman (11)	2012	yes	yes	yes	no	no
Hong-Yu Li (19)	2012	yes	yes	yes	no	Only English
Zheng Zheng (25)	2014	yes	yes	yes	no	nr
Andrea Proneth (22)	2014	yes	yes	yes	no	Only English
Xin-Sen Xu (24)	2014	yes	yes	yes	no	Only English
Benjamin Menahem (21)	2017	yes	yes	yes	no	Only English
Markus B. Schoenberg (23)	2017	yes	yes	no	no	Only English
Wei Li (20)	2017	yes	yes	yes	no	nr
Jin Hean Koh (18)	2022	yes	yes	no	no	Only English

TABLE 4 Amstar 2 evaluation.

Domains	Items-Authors	Hong-yu (19)	Kostakis (26)	Koh (18)	Zheng Zheng (25)	Xin-sen Xu (24)	Schoenberg (23)	Proneth (22)	Rahaman (11)	Dhir (17)	Menahem (21)
	1. Did the research questions and inclusion criteria for the review include the components of PICO?	yes	yes	yes	yes	yes	yes	yes	yes	yes	yes
Critical	2. Did the report of the review contain an explicit statement that the review methods were established prior to the conduct of the review and did the report justify any significant deviations from the protocol?	yes	no	yes	yes	yes	yes	Partial yes	yes	yes	yes
	3. Did the review authors explain their selection of the study designs for inclusion in the review?	yes	no	no	yes	no	no	yes	no	no	no
Critical	4. Did the review authors use a comprehensive literature search strategy?	yes	no	Partial yes	yes	yes	yes	yes	yes	no	Partial yes
	5. Did the review authors perform study selection in duplicate?	yes	no	yes	yes	yes	yes	yes	yes	no	yes
	6. Did the review authors perform data extraction induplicate?	yes	no	yes	yes	yes	yes	yes	yes	no	yes
Critical	7. Did the review authors provide a list of excluded studies and justify the exclusions?	no	no	no	no	Partial yes	Partial yes	yes	Partial Yes	no	no
	8. Did the review authors describe the included studies in adequate detail?	Partial yes	Partial yes	yes	Partial yes	Partial yes	yes	Partial yes	yes	yes	yes
Critical	9. Did the review authors use a satisfactory technique for assessing the risk of bias (RoB) in individual studies that were included in the review?	yes	no	no	yes	no	Partial yes	yes	yes	no	no
	10. Did the review authors report on the sources of funding for the studies included in the review?	no	no	no	no	no	no	no	no	no	no
Critical	11. If meta-analysis was performed did the review authors use appropriate methods for statistical combination of results?	yes	yes	yes	yes	yes	yes	yes	yes	yes	yes
	12. If meta-analysis was performed, did the review authors assess the potential impact of RoB in individual studies on the results of the meta-analysis or other evidence synthesis?	yes	no	no	yes	no	yes	yes	yes	yes	no
Critical	13. Did the review authors account for RoB in individual studies when interpreting/discussing the results of the review?	yes	no	no	no	no	yes	yes	no	yes	no
	14. Did the review authors provide a satisfactory explanation for, and discussion of, any heterogeneity observed in the results of the review?	yes	yes	yes	no	yes	yes	no	yes	yes	no

(Continued)

10.3389/fonc.2024.1366607

10.3389/fonc.2024.1366607

TABLE 4 Continued

Domains	Items-Authors	Hong-yu (19)	Kostakis (26)	Koh (18)	Zheng Zheng (25)	Xin-sen Xu (24)	Schoenberg (23)	Proneth (22)	Rahaman (11)	Dhir (17)	Menahem (21)
Critical	15. If they performed quantitative synthesis did the review authors carry out an adequate investigation of publication bias (small study bias) and discuss its likely impact on the results of the review?	yes	no	no	yes	no	no	no	yes	yes	no
	16. Did the review authors report any potential sources of conflict of interest, including any funding they received for conducting the review?	no	no	yes	yes	yes	yes	no	no	yes	yes
	Overall AMSTAR 2 Rating	Low quality	Critially Low quality	Critially Low quality	Critially Low quality	Critially Low quality	Low quality	Low quality	Low quality	Critially Low quality	Critially Low quality

df = 3, p-value = 0.9879) and Begg's test (z = -0.76, p-value = 0.4485) still did not show significant evidence of publication bias (Figure 4C).

HR Overall and disease-free survival

Two studies reported the HR for overall and disease-free survival favouring LT over liver resection (1.30, 95% CI: 1.10-1.55, I^2: 24% and 2.46, 95% CI: 2.03-2.99, I^2: 47%) (Figures 5A, B).

Secondary outcomes

Five-year survival in early HCC and ITT was 0.63 (95% CI: 0.50-0.78, I^2:0%), (Figure 6A) and 0.60 (95% CI: 0.39-0.92, I^2:0%), respectively (Figure 6B). Salvage LT vs. Primary LT did not differ between 5-year survival and DFS (OR: 0.62; 95% CI: 0.33-1.15, I^2:0% and 0.93; 95% CI: 0.82-1.04, I^2:0%) (Figures 7A, B).

Discussion

Comparing the outcomes of LT and LR in HCC is crucial because it can inform the decision-making process for selecting the most appropriate treatment option for individual patients (1, 11, 21). By identifying the best treatment between LT and LR, healthcare providers improve the patient's overall survival and quality of life. Furthermore, there is a shortage of donor organs worldwide, so optimising organ allocation is central to HCC. In some cases, LR may be a viable alternative to LT as a definitive treatment, especially for patients with early-stage HCC and those with limited underlying liver disease or bridge therapy in case of cancer recurrences (10, 27–29). The study included a large cohort of patients, which is a relatively large sample size and may increase the reliability of the findings.

Furthermore, the study conducted a systematic review and meta-analysis of multiple meta-analyses, which may provide a more comprehensive picture of the topic. Also, the study conducted subgroup analyses for different types of HCC and liver transplantation, which may help identify specific factors that influence outcomes.

LT showed better OS and DFS than LR for HCC. However, survival after retransplantation for cancer recurrences was equal to primary LT for HCC. The finding agreed with the included meta-analyses, independently from the correlation matrix and the cluster analysis.

The results of the meta-analysis provide valuable insights into the comparative effectiveness of liver transplantation (LT) and liver resection for hepatocellular carcinoma (HCC) in terms of 5-year overall survival, disease-free survival, and hazard ratio (HR) for overall survival. These findings align with the evolving body of research in the field, which examines the optimal treatment approaches for HCC patients.

While the meta-analysis indicates funnel plot asymmetry through Egger's test, this could suggest the presence of

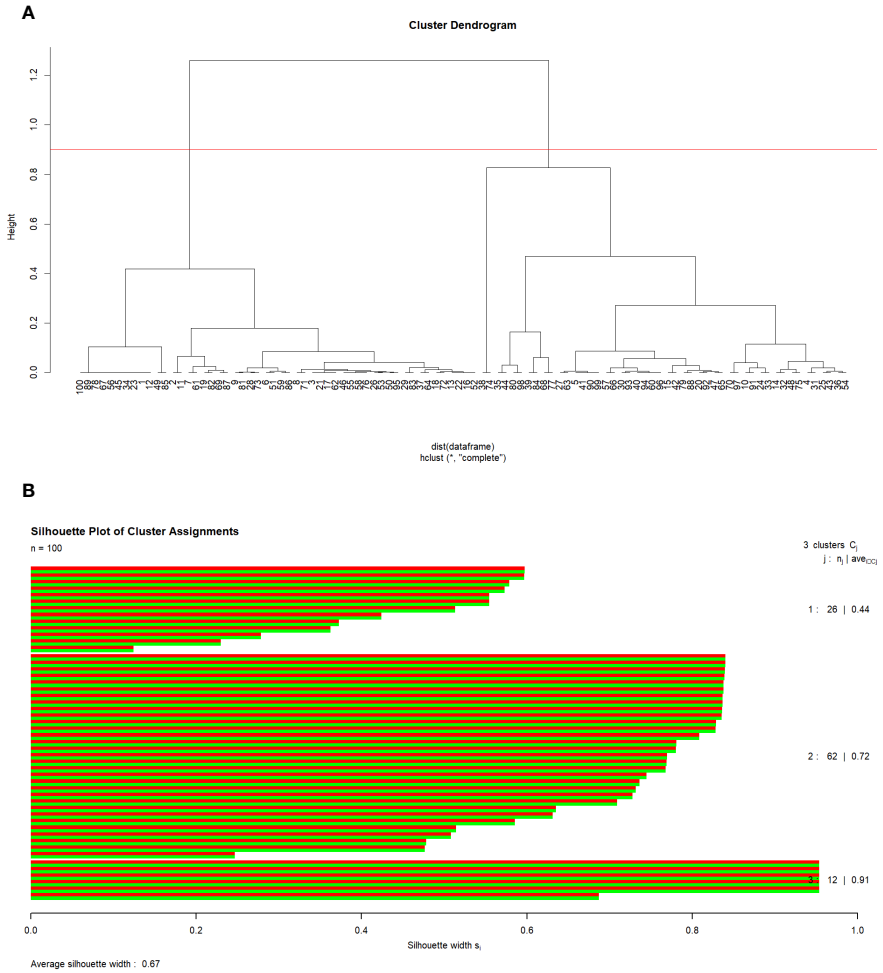

FIGURE 2
(A) Cluster Dendrogram. **(B)** Silhouette Plot of Cluster Assignments.

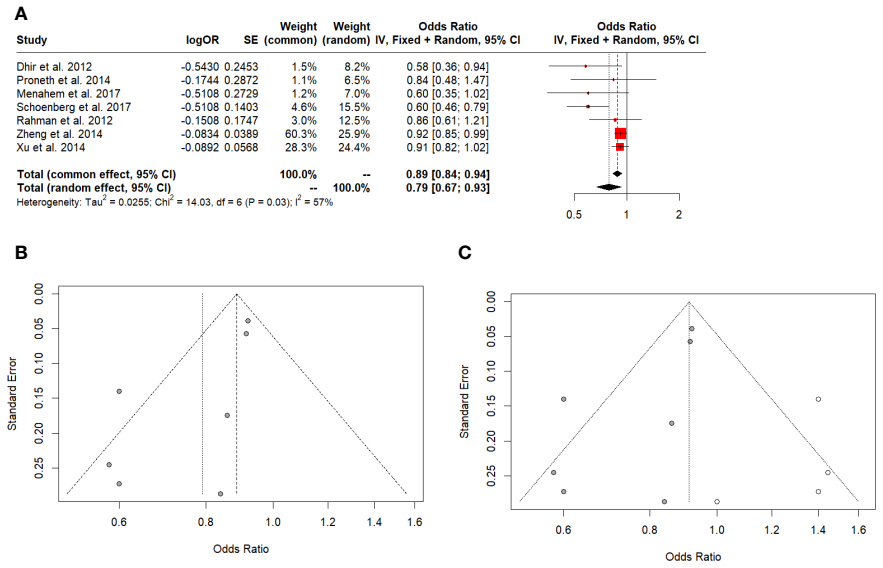

FIGURE 3
(A) 5-year overall survival in all HCC. **(B)** Funnel plot. **(C)** Funnel plot after Trim-and-fill.

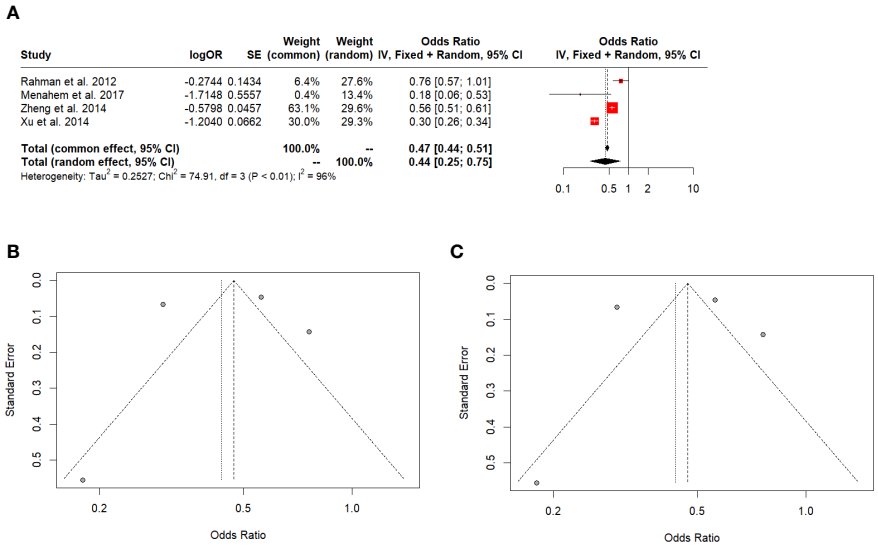

FIGURE 4
(A) 5-year disease-free survival in all HCC. **(B)** Funnel plot. **(C)** Funnel plot after Trim-and-fill.

publication bias that may skew the results. Using the Trim-and-fill method to address publication bias enhances the reliability of the findings. The favourable disease-free survival outcomes favouring LT over liver resection for all HCC cases align with previous research suggesting that LT can lead to more extended periods without recurrence (30, 31). The absence of significant publication bias in the initial analysis and after using the Trim-and-fill method adds confidence to these findings.

Furthermore, the HR analysis suggests that LT may be associated with better overall survival than liver resection, as the HR favours LT. The I^2 value of 24% suggests moderate heterogeneity, indicating relatively consistent results among the studies included.

The quality assessment of the included studies reveals that there was at least a critical flaw in the meta-analysis methodology. Many of the studies under consideration did not adequately address the potential risks of bias in their analyses, nor did they thoroughly discuss how these biases might influence the outcomes reported in the review. This oversight raises concerns about the robustness and reliability of the findings presented in these studies (32). Biases, whether related to study design, data collection, or reporting, can introduce systematic errors that may distort the overall conclusions of a meta-analysis. Failing to acknowledge and address these biases can undermine the validity and credibility of the study's results. It is essential for future research to comprehensively evaluate and report on the potential biases and their potential impact to ensure the accuracy and reliability of the meta-analytic findings.

There was some heterogeneity in the data, particularly in the DFS analysis, possibly due to differences in study design and patient populations. Therefore, despite the present findings, individual patient factors and clinical considerations should still be considered when determining the most appropriate treatment approach for HCC (31).

The correlation analysis of the present study indicates a moderate association level between the variables, while

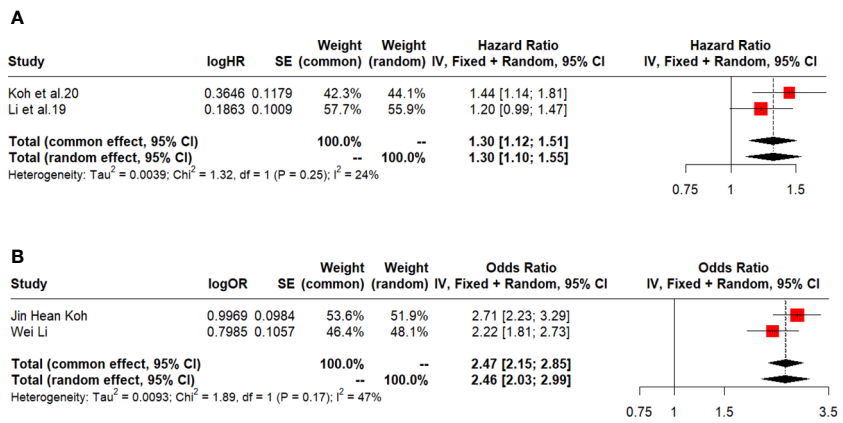

FIGURE 5
(A) HR overall survival. **(B)** HR disease free survival.

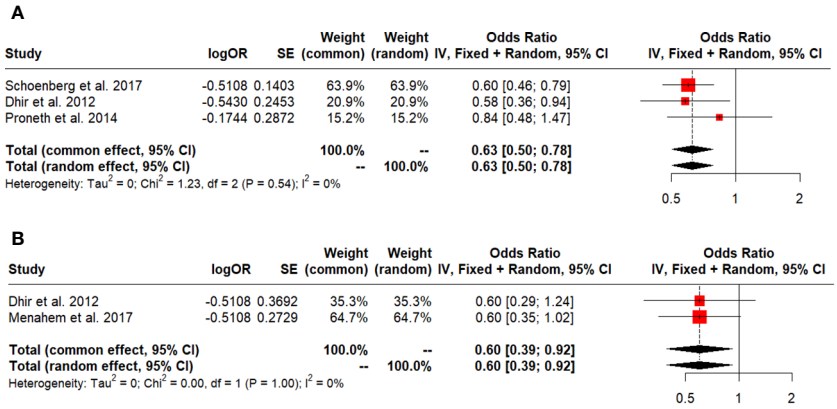

FIGURE 6
(A) Five-year survival in early HCC. **(B)** Five-year survival in ITT.

hierarchical clustering identified three distinct clusters based on the correlation coefficients. The integration of hierarchical clustering analysis to validate the consistency of findings adds further strength to the results. The silhouette analysis suggests these clusters are well-defined, with different data points forming cohesive groups. The three clusters showed good separation and assignment of data points to clusters, confirming a consistent agreement among the meta-analyses about the advantage of LT over LR, independently from the included studies.

Several potential sources of bias in this study should be considered. While the results and conclusions of the study may provide valuable insights into the overall management of HCC, it is essential to consider the heterogeneity of the patient population and the specific clinical contexts when interpreting the findings for different subgroups of patients. A limitation of the present study was the difficulties in drawing the same conclusions for patients with HCC within or outside Milan criteria, undergoing a first or a salvage transplantation. Similarly, whether the manuscript included three meta-analyses, reporting outcomes in ITT patients, the lack of robust data may result in a positive outcome for the LT group and in a disadvantage in the LR group. Another potential source of bias is measurement bias, as the determination of survival and disease-free survival may be affected by factors such as follow-up time, surveillance protocols, and the definition of recurrence. Finally, there may be publication bias, as studies with negative or null findings may be less likely to be published or included in systematic reviews and meta-analyses (33, 34).

By systematically analysing the citation matrix, the authors identified clusters of meta-analysis indicating potential overlap or duplication. However, the association was moderate, and the primary outcomes results consistent. The integration of hierarchical clustering analysis to validate the consistency of findings added further strength to the results. The silhouette analysis suggested these clusters were well-defined, with different data points forming cohesive groups. The three clusters showed good separation and assignment of data points to clusters, confirming a consistent agreement among the meta-analyses about the advantage of LT over LR, independently from the included studies.

Future research could explore the impact of patient-specific characteristics on treatment effectiveness, investigate new biomarkers for patient selection, develop individualised treatment

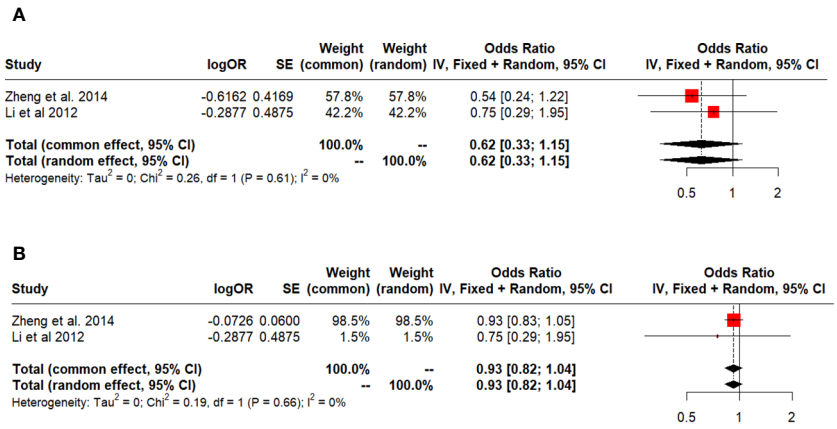

FIGURE 7
(A) Salvage vs primary (overall). **(B)** Salvage vs primary (disease free).

algorithms, and assess novel therapies in combination with surgical interventions to improve outcomes.

In conclusion, the study's findings consistently suggest that LT offers better 5-year and disease-free survival rates than LR for HCC. These results hold significance for clinical practice, as they provide insights into the most effective treatment approach for HCC patients. The study underscores the importance of addressing biases and limitations in meta-analyses and highlights potential areas for future research to enhance HCC treatment strategies.

Data availability statement

The original contributions presented in the study are included in the article/Supplementary Material. Further inquiries can be directed to the corresponding author.

Author contributions

AM: Conceptualization, Formal analysis, Methodology, Writing – original draft, Writing – review & editing. AB: Writing – original draft, Writing – review & editing. FC: Writing – original draft, Writing – review & editing. IW: Writing – original draft, Writing – review & editing. FF: Writing – original draft, Writing – review & editing. FA: Writing – original draft, Writing – review & editing. FG: Writing – original draft, Writing – review & editing.

Funding

The author(s) declare that no financial support was received for the research, authorship, and/or publication of this article.

Conflict of interest

The authors declare that the research was conducted in the absence of any commercial or financial relationships that could be construed as a potential conflict of interest.

Publisher's note

Supplementary material

The Supplementary Material for this article can be found online at: https://www.frontiersin.org/articles/10.3389/fonc.2024.1366607/full#supplementary-material

References

1. Forner A, Reig M, Bruix J. Hepatocellular carcinoma. *Lancet (London England)*. (2018) 391:1301–14. doi: 10.1016/S0140-6736(18)30010-2

2. Konyn P, Ahmed A, Kim D. Current epidemiology in hepatocellular carcinoma. *Expert Rev Gastroenterol hepatol*. (2021) 15:1295–307. doi: 10.1080/17474124.2021.1991792

3. Massarweh NN, El-Serag HB. Epidemiology of hepatocellular carcinoma and intrahepatic cholangiocarcinoma. *Cancer Control*. (2017) 24:1073274817729245. doi: 10.1177/1073274817729245

4. Kulik L, El-Serag HB. Epidemiology and management of hepatocellular carcinoma. *Gastroenterology*. (2019) 156:477–491.e471.

5. Morgan TR, Mandayam S, Jamal MM. Alcohol and hepatocellular carcinoma. *Gastroenterology*. (2004) 127:S87–96. doi: 10.1053/j.gastro.2004.09.020

6. Yang JD, Heimbach JK. New advances in the diagnosis and management of hepatocellular carcinoma. *BMJ*. (2020) 371:m3544. doi: 10.1136/bmj.m3544

7. Yang JD, Hainaut P, Gores GJ, Amadou A, Plymoth A, Roberts LR. A global view of hepatocellular carcinoma: trends, risk, prevention and management. *Nat Rev Gastroenterol hepatol*. (2019) 16:589–604. doi: 10.1038/s41575-019-0186-y

8. Gilles H, Garbutt T, Landrum J. Hepatocellular carcinoma. *Crit Care Nurs Clin North Am*. (2022) 34:289–301. doi: 10.1016/j.cnc.2022.04.004

9. Zhang W, Zhang B, Chen XP. Adjuvant treatment strategy after curative resection for hepatocellular carcinoma. *Front Med*. (2021) 15:155–69. doi: 10.1007/s11684-021-0848-3

10. Vibert E, Schwartz M, Olthoff KM. Advances in resection and transplantation for hepatocellular carcinoma. *J Hepatol*. (2020) 72:262–76. doi: 10.1016/j.jhep.2019.11.017

11. Rahman A, Assifi MM, Pedroso FE, Maley WR, Sola JE, Lavu H, et al. Is resection equivalent to transplantation for early cirrhotic patients with hepatocellular carcinoma? A meta-analysis. *J gastrointestinal Surg*. (2012) 16:1897–909. doi: 10.1007/s11605-012-1973-8

12. Shea BJ, Reeves BC, Wells G, Thuku M, Hamel C, Moran J, et al. AMSTAR 2: a critical appraisal tool for systematic reviews that include randomised or non-randomised studies of healthcare interventions, or both. *BMJ*. (2017) 358:j4008. doi: 10.1136/bmj.j4008

13. Zhang Z, Murtagh F, Van Poucke S, Lin S, Lan P. Hierarchical cluster analysis in clinical research with heterogeneous study population: highlighting its visualization with R. *Ann Trans Med*. (2017) 5:75. doi: 10.21037/atm

14. Trikalinos TA, Salanti G, Zintzaras E, Ioannidis JP. Meta-analysis methods. *Adv Genet*. (2008) 60:311–34. doi: 10.1016/S0065-2660(07)00413-0

15. Lin L. Comparison of four heterogeneity measures for meta-analysis. *J Eval Clin Pract*. (2020) 26:376–84. doi: 10.1111/jep.13159

16. Higgins JP, Thompson SG, Deeks JJ, Altman DG. Measuring inconsistency in meta-analyses. *BMJ*. (2003) 327:557–60. doi: 10.1136/bmj.327.7414.557

17. Dhir M, Lyden ER, Smith LM, Are C. Comparison of outcomes of transplantation and resection in patients with early hepatocellular carcinoma: a meta-analysis. *HPB (Oxford)*. (2012) 14:635–45. doi: 10.1111/j.1477-2574.2012.00500.x

18. Koh JH, Tan DJH, Ong Y, Lim WH, Ng CH, Tay PWL, et al. Liver resection versus liver transplantation for hepatocellular carcinoma within Milan criteria: a meta-analysis of 18,421 patients. *Hepatobiliary Surg Nutr*. (2022) 11:78–93. doi: 10.21037/hbsn

19. Li HY, Wei YG, Yan LN, Li B. Salvage liver transplantation in the treatment of hepatocellular carcinoma: a meta-analysis. *World J Gastroenterol*. (2012) 18:2415–22. doi: 10.3748/wjg.v18.i19.2415

20. Li W, Li L, Han J, Wu H. Liver transplantation vs liver resection in patients with HBV-related hepatocellular carcinoma beyond Milan criterion: A meta-analysis. *Clin transpl*. (2018) 32:e13193. doi: 10.1111/ctr.13193

21. Menahem B, Lubrano J, Duvoux C, Mulliri A, Alves A, Costentin C, et al. Liver transplantation versus liver resection for hepatocellular carcinoma in intention to treat: An attempt to perform an ideal meta-analysis. *Liver Transplant*. (2017) 23:836–44. doi: 10.1002/lt.24758

22. Proneth A, Zeman F, Schlitt HJ, Schnitzbauer AA. Is resection or transplantation the ideal treatment in patients with hepatocellular carcinoma in cirrhosis if both are

possible? A systematic review and metaanalysis. *Ann Surg Oncol*. (2014) 21:3096–107. doi: 10.1245/s10434-014-3808-1

23. Schoenberg MB, Bucher JN, Vater A, Bazhin AV, Hao J, Guba MO, et al. Resection or transplant in early hepatocellular carcinoma. *Deutsches Arzteblatt Int*. (2017) 114:519–26. doi: 10.3238/arztebl.2017.0519

24. Xu XS, Liu C, Qu K, Song YZ, Zhang P, Zhang YL. Liver transplantation versus liver resection for hepatocellular carcinoma: a meta-analysis. *Hepatobiliary pancreatic Dis Int*. (2014) 13:234–41. doi: 10.1016/S1499-3872(14)60037-0

25. Zheng Z, Liang W, Milgrom DP, Zheng Z, Schroder PM, Kong NS, et al. Liver transplantation versus liver resection in the treatment of hepatocellular carcinoma: a meta-analysis of observational studies. *Transplantation*. (2014) 97:227–34. doi: 10.1097/TP.0b013e3182a89383

26. Kostakis ID, Machairas N, Prodromidou A, Stamopoulos P, Garoufalia Z, Fouzas I, et al. Comparison between salvage liver transplantation and repeat liver resection for recurrent hepatocellular carcinoma: A systematic review and meta-analysis. *Transplant Proc*. (2019) 51:433–6. doi: 10.1016/j.transproceed.2019.01.072

27. Vogel A, Martinelli Eclinicalguidelines@esmo.org EGCEa and Committee EG. Updated treatment recommendations for hepatocellular carcinoma (HCC) from the ESMO Clinical Practice Guidelines. *Ann Oncol*. (2021) 32:801–5. doi: 10.1016/j.annonc.2021.02.014

28. Lee KK, Kim DG, Moon IS, Lee MD, Park JH. Liver transplantation versus liver resection for the treatment of hepatocellular carcinoma. *J Surg Oncol*. (2010) 101:47–53. doi: 10.1002/jso.21415

29. Krenzien F, Schmelzle M, Struecker B, Raschzok N, Benzing C, Jara M, et al. Liver transplantation and liver resection for cirrhotic patients with hepatocellular carcinoma: comparison of long-term survivals. *J gastrointestinal Surg*. (2018) 22:840–8. doi: 10.1007/s11605-018-3690-4

30. Kanneganti M, Mahmud N, Kaplan DE, Taddei TH, Goldberg DS. Survival benefit of liver transplantation for hepatocellular carcinoma. *Transplantation*. (2020) 104:104–12. doi: 10.1097/TP.0000000000002816

31. Di Sandro S, Sposito C, Ravaioli M, Lauterio A, Magistri P, Bongini M, et al. Surgical treatment of hepatocellular carcinoma: multicenter competing-risk analysis of tumor-related death following liver resection and transplantation under an intention-to-treat perspective. *Transplantation*. (2023) 107:1965–75. doi: 10.1097/TP.0000000000004593

32. Viswanathan M, Ansari MT, Berkman ND, Chang S, Hartling L, McPheeters M, et al. Risk of bias of individual studies in systematic reviews of health care interventions. In: *Methods Guide for Effectiveness and Comparative Effectiveness Reviews*. Agency for Healthcare Research and Quality (US, Rockville (MD (2012). p. 2008–.

33. Joober R, Schmitz N, Annable L, Boksa P. Publication bias: what are the challenges and can they be overcome? *J Psychiatry Neurosci*. (2012) 37:149–52. doi: 10.1503/jpn.110175

34. Nair AS. Publication bias - Importance of studies with negative results! *Indian J anaesthesia*. (2019) 63:505–7. doi: 10.4103/ija.IJA_142_19

35. Adam R, Azoulay D, Castaing D, et al. Liver resection as a bridge to transplantation for hepatocellular carcinoma on cirrhosis: a reasonable strategy? *Ann Surg*. (2003) 238:508–518; discussion 518-509. doi: 10.1097/01.sla.0000090449.87109.44

36. Adam R, Bhangui P, Vibert E, et al. Resection or transplantation for early hepatocellular carcinoma in a cirrhotic liver: does size define the best oncological strategy? *Ann Surg*. (2012) 256:883–91. doi: 10.1097/SLA.0b013e318273bad0

37. Aksoy SO, Unek T, Sevinc AI, et al. Comparison of resection and liver transplant in treatment of hepatocellular carcinoma. *Exp Clin Transplant*. (2020) 18:712–8. doi: 10.6002/ect

38. Baccarani U, Isola M, Adani GL, et al. Superiority of transplantation versus resection for the treatment of small hepatocellular carcinoma. *Transplant Int*. (2008) 21:247–54. doi: 10.1111/j.1432-2277.2007.00597.x

39. Belghiti J, Cortes A, Abdalla EK, et al. Resection prior to liver transplantation for hepatocellular carcinoma. *Ann Surg*. (2003) 238:885–892; discussion 892-883. doi: 10.1097/01.sla.0000098621.74851.65

40. Bellavance EC, Lumpkins KM, Mentha G, et al. Surgical management of early-stage hepatocellular carcinoma: resection or transplantation? *J gastrointestinal Surg*. (2008) 12:1699–708. doi: 10.1007/s11605-008-0652-2

41. Bigourdan JM, Jaeck D, Meyer N, et al. Small hepatocellular carcinoma in Child A cirrhotic patients: hepatic resection versus transplantation. *Liver Transplant*. (2003) 9:513–20. doi: 10.1053/jlts.2003.50070

42. Bismuth H, Chiche L, Adam R, Castaing D, Diamond T, Dennison A. Liver resection versus transplantation for hepatocellular carcinoma in cirrhotic patients. *Ann Surg*. (1993) 218:145–51. doi: 10.1097/00000658-199308000-00005

43. Borie F, Bouvier AM, Herrero A, et al. Treatment and prognosis of hepatocellular carcinoma: a population based study in France. *J Surg Oncol*. (2008) 98:505–9. doi: 10.1002/jso.21159

44. Bronowicki JP, Boudjema K, Chone L, et al. Comparison of resection, liver transplantation and transcatheter oily chemoembolization in the treatment of hepatocellular carcinoma. *J Hepatol*. (1996) 24:293–300. doi: 10.1016/S0168-8278(96)80007-9

45. Canter RJ, Patel SA, Kennedy T, et al. Comparative analysis of outcome in patients with hepatocellular carcinoma exceeding the milan criteria treated with liver transplantation versus partial hepatectomy. *Am J Clin Oncol*. (2011) 34:466–71. doi: 10.1097/COC.0b013e3181ec63dd

46. Cha CH, Ruo L, Fong Y, et al. Resection of hepatocellular carcinoma in patients otherwise eligible for transplantation. *Ann Surg*. (2003) 238:315–321; discussion 321-313. doi: 10.1097/01.sla.0000086548.84705.ef

47. Chan SC, Fan ST, Chok KS, et al. Survival advantage of primary liver transplantation for hepatocellular carcinoma within the up-to-7 criteria with microvascular invasion. *Hepatol Int*. (2012) 6:646–56. doi: 10.1007/s12072-011-9318-3

48. Chan AC, Chan SC, Chok KS, et al. Treatment strategy for recurrent hepatocellular carcinoma: salvage transplantation, repeated resection, or radiofrequency ablation? *Liver Transplant*. (2013) 19:411–9. doi: 10.1002/lt.v19.4

49. Chapman WC, Klintmalm G, Hemming A, et al. Surgical treatment of hepatocellular carcinoma in North America: can hepatic resection still be justified? *J Am Coll Surg*. (2015) 220:628–37. doi: 10.1016/j.jamcollsurg.2014.12.030

50. Choi GH, Kim DH, Kang CM, et al. Prognostic factors and optimal treatment strategy for intrahepatic nodular recurrence after curative resection of hepatocellular carcinoma. *Ann Surg Oncol*. (2008) 15:618–29. doi: 10.1245/s10434-007-9671-6

51. Chuan W, Li C, Wen TF, et al. Short-term and long-term outcomes of surgical treatment for HCC within Milan criteria with cirrhotic portal hypertension. *Hepatogastroenterology*. (2014) 61:2185–90.

52. Cillo U, Vitale A, Brolese A, et al. Partial hepatectomy as first-line treatment for patients with hepatocellular carcinoma. *J Surg Oncol*. (2007) 95:213–20. doi: 10.1002/jso.20641

53. Closset J, Van de Stadt J, Delhaye M, El Nakadi I, Lambilliotte JP, Gelin M. Hepatocellular carcinoma: surgical treatment and prognostic variables in 56 patients. *Hepatogastroenterology*. (1999) 46:2914–8.

54. Colella G, Bottelli R, De Carlis L, et al. Hepatocellular carcinoma: comparison between liver transplantation, resective surgery, ethanol injection, and chemoembolization. *Transplant Int*. (1998) 11 Suppl 1:S193–196. doi: 10.1111/j.1432-2277.1998.tb01113.x

55. Concejero A, Chen CL, Wang CC, et al. Living donor liver transplantation for hepatocellular carcinoma: a single-center experience in Taiwan. *Transplantation*. (2008) 85:398–406. doi: 10.1097/TP.0b013e3181622ff8

56. Dai Y, Li C, Wen TF, Yan LN. Comparison of liver resection and transplantation for Child-pugh A cirrhotic patient with very early hepatocellular carcinoma and portal hypertension. *Pak J Med Sci*. (2014) 30:996–1000. doi: 10.12669/pjms.305.5038

57. De Carlis L, Sammartino C, Giacomoni A, et al. [Surgical treatment of hepatocellular carcinoma: resection or transplantation? Results of a multivariate analysis]. *Chirurgia italiana*. (2001) 53:579–86.

58. De Carlis L, Giacomoni A, Pirotta V, et al. Surgical treatment of hepatocellular cancer in the era of hepatic transplantation. *J Am Coll Surg*. (2003) 196:887–97. doi: 10.1016/S1072-7515(03)00140-6

59. Del Gaudio M, Ercolani G, Ravaioli M, et al. Liver transplantation for recurrent hepatocellular carcinoma on cirrhosis after liver resection: University of Bologna experience. *Am J Transplant*. (2008) 8:1177–85. doi: 10.1111/j.1600-6143.2008.02229.x

60. Dima SO, Iacob S, Botea F, et al. Multimodal treatment of hepatocellular carcinoma: an eastern European experience. *Hepatogastroenterology*. (2009) 56:1696–703.

61. El-Gazzaz G, Wong W, El-Hadary MK, et al. Outcome of liver resection and transplantation for fibrolamellar hepatocellular carcinoma. *Transplant Int*. (2000) 13 Suppl 1:S406–409. doi: 10.1111/tri.2000.13.issue-S1

62. Facciuto ME, Koneru B, Rocca JP, et al. Surgical treatment of hepatocellular carcinoma beyond Milan criteria. Results of liver resection, salvage transplantation, and primary liver transplantation. *Ann Surg Oncol*. (2008) 15:1383–91. doi: 10.1245/s10434-008-9851-z

63. Fan HL, Chen TW, Hsieh CB, et al. Liver transplantation is an alternative treatment of hepatocellular carcinoma beyond the Milan criteria. *Am J Surg*. (2010) 200:252–7. doi: 10.1016/j.amjsurg.2009.07.049

64. Fan ST, Poon RT, Yeung C, et al. Outcome after partial hepatectomy for hepatocellular cancer within the Milan criteria. *Br J Surg*. (2011) 98:1292–300. doi: 10.1002/bjs.7583

65. Farinati F, Gianni S, Marin G, Fagiuoli S, Rinaldi M, Naccarato R. Does the choice of treatment influence survival of patients with small hepatocellular carcinoma in compensated cirrhosis? *Eur J Gastroenterol Hepatol*. (2001) 13:1217–24. doi: 10.1097/00042737-200110000-00015

66. Figueras J, Jaurrieta E, Valls C, et al. Resection or transplantation for hepatocellular carcinoma in cirrhotic patients: outcomes based on indicated treatment strategy. *J Am Coll Surg*. (2000) 190:580–7. doi: 10.1016/S1072-7515(00)00251-9

67. Foltys D, Zimmermann T, Kaths M, et al. Hepatocellular carcinoma in Child's A cirrhosis: a retrospective analysis of matched pairs following liver transplantation vs. liver resection according to the intention-to-treat principle. *Clin transpl*. (2014) 28:37–46. doi: 10.1111/ctr.12273

68. Franssen B, Alshebeeb K, Tabrizian P, et al. Differences in surgical outcomes between hepatitis B- and hepatitis C-related hepatocellular carcinoma: a retrospective analysis of a single North American center. *Ann Surg*. (2014) 260:650–656; discussion 656-658. doi: 10.1097/SLA.0000000000000917

69. Fuks D, Dokmak S, Paradis V, Diouf M, Durand F, Belghiti J. Benefit of initial resection of hepatocellular carcinoma followed by transplantation in case of recurrence: an intention-to-treat analysis. *Hepatology*. (2012) 55:132–40. doi: 10.1002/hep.24680

70. Graham JA, Newman DA, Smirniotopolous J, Shetty K, Slidell MB, Johnson LB. Transplantation for hepatocellular carcinoma in younger patients has an equivocal survival advantage as compared with resection. *Transplant Proc*. (2013) 45:265–71. doi: 10.1016/j.transproceed.2012.07.151

71. Harada N, Shirabe K, Ikeda Y, Korenaga D, Takenaka K, Maehara Y. Surgical management of hepatocellular carcinoma in Child-Pugh class B cirrhotic patients: hepatic resection and/or microwave coagulation therapy versus living donor liver transplantation. *Ann transpl*. (2012) 17:11–20. doi: 10.12659/AOT.883689

72. Ho CM, Lee PH, Chen CL, Ho MC, Wu YM, Hu RH. Long-term outcomes after resection versus transplantation for hepatocellular carcinoma within UCSF criteria. *Ann Surg Oncol*. (2012) 19:826–33. doi: 10.1245/s10434-011-1975-x

73. Hsueh KC, Lee TY, Kor CT, et al. The role of liver transplantation or resection for patients with early hepatocellular carcinoma. *Tumour Biol*. (2016) 37:4193–201. doi: 10.1007/s13277-015-4243-z

74. Huang ZY, Liang BY, Xiong M, et al. Severity of cirrhosis should determine the operative modality for patients with early hepatocellular carcinoma and compensated liver function. *Surgery*. (2016) 159:621–31. doi: 10.1016/j.surg.2015.09.002

75. Hwang S, Lee SG, Moon DB, et al. Salvage living donor liver transplantation after prior liver resection for hepatocellular carcinoma. *Liver Transpl*. (2007) 13:741–6. doi: 10.1002/(ISSN)1527-6473

76. Iwatsuki S, Starzl TE, Sheahan DG, et al. Hepatic resection versus transplantation for hepatocellular carcinoma. *Ann Surg*. (1991) 214:221–228; discussion 228-229. doi: 10.1097/00000658-199109000-00005

77. Jiang L, Liao A, Wen T, Yan L, Li B, Yang J. Living donor liver transplantation or resection for Child-Pugh A hepatocellular carcinoma patients with multiple nodules meeting the Milan criteria. *Transplant Int*. (2014) 27:562–9. doi: 10.1111/tri.2014.27.issue-6

78. Kaido T, Morita S, Tanaka S, et al. Long-term outcomes of hepatic resection versus living donor liver transplantation for hepatocellular carcinoma: a propensity score-matching study. *Dis Markers*. (2015) 2015:425926. doi: 10.1155/2015/425926

79. Kim BW, Park YK, Kim YB, Wang HJ, Kim MW. Salvage liver transplantation for recurrent hepatocellular carcinoma after liver resection: feasibility of the Milan criteria and operative risk. *Transplant Proc*. (2008) 40:3558–61. doi: 10.1016/j.transproceed.2008.03.175

80. Koniaris LG, Levi DM, Pedroso FE, et al. Is surgical resection superior to transplantation in the treatment of hepatocellular carcinoma? *Ann Surg*. (2011) 254:527–537; discussion 537-528. doi: 10.1097/SLA.0b013e31822ca66f

81. Kooby DA, Egnatashvili V, Graiser M, et al. Changing management and outcome of hepatocellular carcinoma: evaluation of 501 patients treated at a single comprehensive center. *J Surg Oncol*. (2008) 98:81–8. doi: 10.1002/jso.21049

82. Kuroda S, Tashiro H, Kobayashi T, Oshita A, Amano H, Ohdan H. Selection criteria for hepatectomy in patients with hepatocellular carcinoma classified as Child-Pugh class B. *World J surg*. (2011) 35:834–41. doi: 10.1007/s00268-010-0929-y

83. Langer B, Greig PD, Taylor BR. Surgical resection and transplantation for hepatocellular carcinoma. *Cancer Treat Res*. (1994) 69:231–40.

84. Launois B, Chauvin J, MaChado ML, Bourdonnec P, Campion JP, Bardaxoglou E. [Surgical treatment of hepatocarcinoma in cirrhosis]. *Annales gastroenterologie d'hepatologie*. (1996) 32:35–39; discussion 39-40.

85. Lei JY, Yan LN, Wang WT. Transplantation vs resection for hepatocellular carcinoma with compensated liver function after downstaging therapy. *World J Gastroenterol*. (2013) 19:4400–8. doi: 10.3748/wjg.v19.i27.4400

86. Li C, Zhu WJ, Wen TF, et al. Child-Pugh A hepatitis B-related cirrhotic patients with a single hepatocellular carcinoma up to 5 cm: liver transplantation vs. resection. *J gastrointestinal Surg*. (2014) 18:1469–76. doi: 10.1007/s11605-014-2550-0

87. Li C, Liu JY, Peng W, et al. Liver resection versus transplantation for multiple hepatocellular carcinoma: a propensity score analysis. *Oncotarget*. (2017) 8:81492–500. doi: 10.18632/oncotarget.v8i46

88. Lim C, Shinkawa H, Hasegawa K, et al. Salvage liver transplantation or repeat hepatectomy for recurrent hepatocellular carcinoma: An intent-to-treat analysis. *Liver Transplant*. (2017) 23:1553–63. doi: 10.1002/lt.24952

89. Llovet JM, Fuster J, Bruix J. Intention-to-treat analysis of surgical treatment for early hepatocellular carcinoma: resection versus transplantation. *Hepatology*. (1999) 30:1434–40. doi: 10.1002/(ISSN)1527-3350

90. Margarit C, Escartin A, Castells L, Vargas V, Allende E, Bilbao I. Resection for hepatocellular carcinoma is a good option in Child-Turcotte-Pugh class A patients with cirrhosis who are eligible for liver transplantation. *Liver Transplant*. (2005) 11:1242–51. doi: 10.1002/(ISSN)1527-6473

91. Mazziotti A, Grazi GL, Cavallari A. Surgical treatment of hepatocellular carcinoma on cirrhosis: a Western experience. *Hepatogastroenterology*. (1998) 45 Suppl 3:1281–7.

92. Meyerovich G, Goykhman Y, Nakache R, et al. Resection vs transplant listing for hepatocellular carcinoma: an intention-to-treat analysis. *Transplant Proc*. (2019) 51:1867–73. doi: 10.1016/j.transproceed.2019.02.030

93. Michel J, Suc B, Montpeyroux F, et al. Liver resection or transplantation for hepatocellular carcinoma? Retrospective analysis of 215 patients with cirrhosis. *J Hepatol*. (1997) 26:1274–80.

94. Michelakos T, Xourafas D, Qadan M, et al. Hepatocellular carcinoma in transplantable child-Pugh A cirrhotics: should cost affect resection vs transplantation? *J gastrointestinal Surg*. (2019) 23:1135–42. doi: 10.1007/s11605-018-3946-z

95. Moon DB, Lee SG, Hwang S. Liver transplantation for hepatocellular carcinoma: single nodule with Child-Pugh class A sized less than 3 cm. *Dig Dis*. (2007) 25:320–8. doi: 10.1159/000106912

96. Ng KK, Lo CM, Liu CL, Poon RT, Chan SC, Fan ST. Survival analysis of patients with transplantable recurrent hepatocellular carcinoma: implications for salvage liver transplant. *Arch Surg*. (2008) 143:68–74; discussion 74. doi: 10.1001/archsurg.2007.15

97. Obed A, Tsui TY, Schnitzbauer AA, et al. Liver transplantation as curative approach for advanced hepatocellular carcinoma: is it justified? *Langenbeck's Arch Surg / Deutsche Gesellschaft fur Chirurgie*. (2008) 393:141–7. doi: 10.1007/s00423-007-0250-x

98. Otto G, Heuschen U, Hofmann WJ, Krumm G, Hinz U, Herfarth C. Survival and recurrence after liver transplantation versus liver resection for hepatocellular carcinoma: a retrospective analysis. *Ann Surg*. (1998) 227:424–32. doi: 10.1097/00000658-199803000-00015

99. Park MS, Lee KW, Kim H, et al. Primary living-donor liver transplantation is not the optimal treatment choice in patients with early hepatocellular carcinoma with poor tumor biology. *Transplant Proc*. (2017) 49:1103–8. doi: 10.1016/j.transproceed.2017.03.016

100. Perry JF, Charlton B, Koorey DJ, et al. Outcome of patients with hepatocellular carcinoma referred to a tertiary centre with availability of multiple treatment options including cadaveric liver transplantation. *Liver Int*. (2007) 27:1240–8. doi: 10.1111/j.1478-3231.2007.01569.x

101. Peters NA, Javed AA, He J, Wolfgang CL, Weiss MJ. Association of socioeconomics, surgical therapy, and survival of early stage hepatocellular carcinoma. *J Surg Res*. (2017) 210:253–60. doi: 10.1016/j.jss.2016.11.042

102. Philosophe B, Greig PD, Hemming AW, et al. Surgical management of hepatocellular carcinoma: resection or transplantation? *J gastrointestinal Surg*. (1998) 2:21–7. doi: 10.1016/S1091-255X(98)80099-1

103. Poon RT, Fan ST, Lo CM, Liu CL, Wong J. Difference in tumor invasiveness in cirrhotic patients with hepatocellular carcinoma fulfilling the Milan criteria treated by resection and transplantation: impact on long-term survival. *Ann Surg*. (2007) 245:51–8. doi: 10.1097/01.sla.0000225255.01668.65

104. Rayya F, Harms J, Bartels M, Uhlmann D, Hauss J, Fangmann J. Results of resection and transplantation for hepatocellular carcinoma in cirrhosis and noncirrhosis. *Transplant Proc*. (2008) 40:933–5. doi: 10.1016/j.transproceed.2008.03.045

105. Ringe B, Pichlmayr R, Wittekind C, Tusch G. Surgical treatment of hepatocellular carcinoma: experience with liver resection and transplantation in 198 patients. *World J surg*. (1991) 15:270–85. doi: 10.1007/BF01659064

106. Ruzzenente A, Capra F, Pachera S, et al. Is liver resection justified in advanced hepatocellular carcinoma? Results of an observational study in 464 patients. *J gastrointestinal Surg*. (2009) 13:1313–20. doi: 10.1007/s11605-009-0903-x

107. Sangro B, Herraiz M, Martinez-Gonzalez MA, et al. Prognosis of hepatocellular carcinoma in relation to treatment: a multivariate analysis of 178 patients from a single European institution. *Surgery*. (1998) 124:575–83. doi: 10.1016/S0039-6060(98)70105-9

108. Sapisochin G, Castells L, Dopazo C, et al. Single HCC in cirrhotic patients: liver resection or liver transplantation? Long-term outcome according to an intention-to-treat basis. *Ann Surg Oncol*. (2013) 20:1194–202. doi: 10.1245/s10434-012-2655-1

109. Sapisochin G, Bilbao I, Balsells J, et al. Optimization of liver transplantation as a treatment of intrahepatic hepatocellular carcinoma recurrence after partial liver resection: experience of a single European series. *World J surg*. (2010) 34:2146–54. doi: 10.1007/s00268-010-0583-4

110. Scatton O, Zalinski S, Terris B, et al. Hepatocellular carcinoma developed on compensated cirrhosis: resection as a selection tool for liver transplantation. *Liver Transplant*. (2008) 14:779–88. doi: 10.1002/(ISSN)1527-6473

111. Seshadri RM, Besur S, Niemeyer DJ, et al. Survival analysis of patients with stage I and II hepatocellular carcinoma after a liver transplantation or liver resection. *HPB (Oxford)*. (2014) 16:1102–9. doi: 10.1111/hpb.12300

112. Shabahang M, Franceschi D, Yamashiki N, et al. Comparison of hepatic resection and hepatic transplantation in the treatment of hepatocellular carcinoma among cirrhotic patients. *Ann Surg Oncol*. (2002) 9:881–6. doi: 10.1007/BF02557525

113. Shah SA, Cleary SP, Tan JC, et al. An analysis of resection vs transplantation for early hepatocellular carcinoma: defining the optimal therapy at a single institution. *Ann Surg Oncol*. (2007) 14:2608–14. doi: 10.1245/s10434-007-9443-3

114. Shao Z, Lopez R, Shen B, Yang GS. Orthotopic liver transplantation as a rescue operation for recurrent hepatocellular carcinoma after partial hepatectomy. *World J Gastroenterol*. (2008) 14:4370–6. doi: 10.3748/wjg.14.4370

115. Shen BY, Li HW, Regimbeau JM, Belghiti J. Recurrence after resection of hepatocellular carcinoma. *Hepatobiliary pancreatic Dis Int*. (2002) 1:401–5.

116. Shen JY, Li C, Wen TF, et al. Transplantation versus hepatectomy for HCC beyond the Milan criteria: A propensity score analysis. *Int J Surg (London England)*. (2017) 44:33–42. doi: 10.1016/j.ijsu.2017.05.034

117. Sogawa H, Shrager B, Jibara G, Tabrizian P, Roayaie S, Schwartz M. Resection or transplant-listing for solitary hepatitis C-associated hepatocellular carcinoma: an intention-to-treat analysis. *HPB (Oxford)*. (2013) 15:134–41. doi: 10.1111/j.1477-2574.2012.00548.x

118. Sotiropoulos GC, Druhe N, Sgourakis G, et al. Liver transplantation, liver resection, and transarterial chemoembolization for hepatocellular carcinoma in cirrhosis: which is the best oncological approach? *Digestive Dis Sci*. (2009) 54:2264–73. doi: 10.1007/s10620-008-0604-4

119. Squires MH 3rd, Hanish SI, Fisher SB, et al. Transplant versus resection for the management of hepatocellular carcinoma meeting Milan Criteria in the MELD exception era at a single institution in a UNOS region with short wait times. *J Surg Oncol*. (2014) 109:533–41. doi: 10.1002/jso.23531

120. Sung PS, Yang H, Na GH, et al. Long-term outcome of liver resection versus transplantation for hepatocellular carcinoma in a region where living donation is a main source. *Ann transpl*. (2017) 22:276–84. doi: 10.12659/AOT.904287

121. Tan KC, Rela M, Ryder SD, et al. Experience of orthotopic liver transplantation and hepatic resection for hepatocellular carcinoma of less than 8 cm in patients with cirrhosis. *Br J Surg*. (1995) 82:253–6. doi: 10.1002/bjs.1800820239

122. Tiao GM, Bobey N, Allen S, et al. The current management of hepatoblastoma: a combination of chemotherapy, conventional resection, and liver transplantation. *J Pediatr*. (2005) 146:204–11. doi: 10.1016/j.jpeds.2004.09.011

123. Vargas V, Castells L, Balsells J, et al. Hepatic resection or orthotopic liver transplant in cirrhotic patients with small hepatocellular carcinoma. *Transplant Proc*. (1995) 27:1243–4.

124. Vennarecci G, Ettorre GM, Antonini M, et al. First-line liver resection and salvage liver transplantation are increasing therapeutic strategies for patients with hepatocellular carcinoma and child a cirrhosis. *Transplant Proc*. (2007) 39:1857–60. doi: 10.1016/j.transproceed.2007.05.073

125. Weimann A, Schlitt HJ, Oldhafer KJ, Hoberg S, Tusch G, Raab R. Is liver transplantation superior to resection in early stage hepatocellular carcinoma? *Transplant Proc*. (1999) 31:500–1. doi: 10.1016/S0041-1345(98)01727-8

126. Wu Z, Chen W, Ouyang T, Liu H, Cao L. Management and survival for patients with stage-I hepatocellular carcinoma: An observational study based on SEER database. *Med (Baltimore)*. (2020) 99:e22118. doi: 10.1097/MD.0000000000022118

127. Yamamoto J, Iwatsuki S, Kosuge T, et al. Should hepatomas be treated with hepatic resection or transplantation? *Cancer*. (1999) 86:1151–8. doi: 10.1002/(ISSN)1097-0142

128. Yamashita Y, Yoshida Y, Kurihara T, et al. Surgical results for recurrent hepatocellular carcinoma after curative hepatectomy: Repeat hepatectomy versus salvage living donor liver transplantation. *Liver Transplant*. (2015) 21:961–8. doi: 10.1002/lt.24111

129. Yang A, Ju W, Yuan X, et al. Comparison between liver resection and liver transplantation on outcomes in patients with solitary hepatocellular carcinoma meeting UNOS criteria: a population-based study of the SEER database. *Oncotarget*. (2017) 8:97428–38. doi: 10.18632/oncotarget.v8i57

130. Yokoi H, Isaji S, Yamagiwa K, et al. The role of living-donor liver transplantation in surgical treatment for hepatocellular carcinoma. *J Hepatobiliary Pancreat Surg*. (2006) 13:123–30. doi: 10.1007/s00534-005-1018-8

131. Zaydfudim VM, Vachharajani N, Klintmalm GB, et al. Liver resection and transplantation for patients with hepatocellular carcinoma beyond Milan criteria. *Ann Surg*. (2016) 264:650–8. doi: 10.1097/SLA.0000000000001866

132. Zhou J, Wang Z, Qiu SJ, et al. Surgical treatment for early hepatocellular carcinoma: comparison of resection and liver transplantation. *J Cancer Res Clin Oncol*. (2010) 136:1453–60. doi: 10.1007/s00432-010-0802-2

frontiers | Frontiers in Oncology

TYPE Review
PUBLISHED 28 March 2024
DOI 10.3389/fonc.2024.1370390

OPEN ACCESS

EDITED BY
Francisco Tustumi,
University of São Paulo, Brazil

REVIEWED BY
Eric Toshiyuki Nakamura,
University of São Paulo, Brazil
Daniel Szor,
University of São Paulo, Brazil

*CORRESPONDENCE
Hao Zhang
zhbest@outlook.com

†These authors have contributed equally to this work

RECEIVED 14 January 2024
ACCEPTED 15 March 2024
PUBLISHED 28 March 2024

CITATION
Dong R, Zhang T, Wan W and Zhang H (2024) Repeat hepatectomy versus thermal ablation therapy for recurrent hepatocellular carcinoma: a systematic review and meta-analysis.
Front. Oncol. 14:1370390.
doi: 10.3389/fonc.2024.1370390

Repeat hepatectomy versus thermal ablation therapy for recurrent hepatocellular carcinoma: a systematic review and meta-analysis

Renhua Dong[1†], Ting Zhang[2†], Wenwu Wan[1] and Hao Zhang[1*]

[1]Department of Hepatobiliary and Pancreatic Surgery, Meishan People's Hospital, Meishan, Sichuan, China, [2]Department of Gastroenterology, Meishan People's Hospital, Meishan, Sichuan, China

Background: This meta-analysis was conducted to assess the survival benefits of repeat hepatectomy (RH) and thermal ablation therapy (TAT) in managing recurrent hepatocellular carcinoma (HCC).

Methods: A comprehensive search was conducted in the PubMed, SinoMed, Embase, Cochrane Library, Medline, and Web of Science databases using relevant keywords to identify all studies published on this specific topic. Pooled odds ratios (ORs) with corresponding 95% confidence intervals (CIs) were estimated using a fixed-effects model.

Results: This meta-analysis included a total of 21 studies, comprising 2580 patients with recurrent HCC, among whom 1189 underwent RH and 1394 underwent TAT. Meta-analysis results demonstrated that the RH group exhibited superior overall survival (OS) (HR=0.85, 95%CI 0.76~0.95, P=0.004) and recurrence-free survival (RFS) (HR=0.79, 95%CI 0.7~0.9, P<0.01) compared to the TAT group. Regarding postoperative complications, the TAT group experienced fewer complications than the RH group (OR=3.23, 95%CI 1.48~7.07, P=0.003), while no significant difference in perioperative mortality was observed between the two groups (OR=2.11, 95%CI 0.54~8.19, P=0.28).

Conclusion: The present study demonstrates that, in comparison to TAT, RH may confer superior survival benefits for patients with recurrent HCC.

KEYWORDS

repeat hepatectomy, thermal ablation therapy, meta-analysis, recurrent hepatocellular carcinoma, systematic review

Introduction

The postoperative recurrence rate of hepatocellular carcinoma (HCC) is significantly high, with an incidence exceeding 50% at 3 years and surpassing 70% at 5 years (1). Therefore, it is crucial to develop an effective strategy for managing recurrent HCC in order to improve patient survival. Salvage liver transplantation is considered the primary therapeutic approach for patients with recurrent HCC due to its comprehensive consideration of excising cancerous tissue and addressing the entire cirrhotic liver, thereby offering patients the most promising prospects for survival (2). However, it should be noted that this treatment option's feasibility is severely limited by donor scarcity, restricting its applicability and benefits to a select group of patients (3, 4). Consequently, repeat hepatectomy (RH) and thermal ablation therapy (TAT) have emerged as viable alternative treatment modalities for individuals experiencing recurrent HCC (5, 6).

Although hepatectomy is regarded as the gold standard for the treatment of HCC (7), RH is controversial in the treatment of recurrent HCC due to the excessive damage to liver function caused by surgical resection and the extremely difficult to reoperation (8). As a minimally invasive and repeatable treatment, TAT is currently considered a good choice for treating recurrent HCC (9). Several published studies have compared the effectiveness of these two surgical methods in the treatment of recurrent liver cancer, but there is still controversy in terms of survival. Numerous studies have conducted comparative analyses of the efficacy between repeat hepatectomy and thermal ablation therapy in the treatment of recurrent liver cancer (10–12). However, controversy remains surrounds the question of which surgical approach is more effective in significantly prolonging patient survival. Several meta-analyses on this topic have been published, but these studies exhibit certain methodological concerns (13, 14). For instance, in the meta-analysis conducted by Liu et al (15) and Yang et al (14), the comparison of prognoses between the two patient groups was based on 1-year or three-year survival rates, overlooking the situations of patients lost to follow-up or censored. Additionally, Yuan et al. (13) meta-analysis included data that were not appropriately matched or corrected for multiple factors. These factors may contribute to bias in the results of the meta-analysis. Simultaneously, new research on the treatment of recurrent liver cancer using these two surgical modalities has been published (16–18). Given these circumstances, there is a necessity to update the meta-analysis on this topic. Therefore, this study conducts a meta-analysis to explore the clinical efficacy of repeat hepatectomy and thermal ablation therapy in treating recurrent liver cancer.

Methods

Search strategies

This study adhered to the Preferred Reporting Items for Systematic Reviews and Meta-Analyses (PRISMA) guidelines (19). Two investigators (H.Z. and T.Z.) independently conducted a comprehensive literature search on the treatment of recurrent HCC using TAT and RH. The search was performed in PubMed, Embase, Cochrane Library, Medline, and Web of Science databases utilizing relevant MESH terms and free-text variations such as ("repeat hepatectomy" OR "repeat liver resection" OR "repeat hepatic resection") and ("thermal ablation" OR "radiofrequency ablation" OR "microwave ablation" OR "ablation") and ("recurrent hepatocellular carcinoma" OR "recurrent HCC" OR "HCC recurrence"). No restrictions were imposed on publication date or journal category. The literature search included articles published in English and Chinese before December 31, 2023. Additionally, we thoroughly examined the reference lists of identified studies to identify any relevant publications that might have been overlooked. While meta-analyses are commonly employed to evaluate controversies in randomized controlled trials (RCTs), they can also be applied to retrospective studies. To ensure more robust conclusions, our analysis included both randomized controlled trials and comparable retrospective studies.

Inclusion and exclusion criteria

The inclusion criteria were as follows: (1) patients diagnosed with recurrent HCC who underwent RH (open or laparoscopy), with a comparison group undergoing TAT. (2) ensured comparability in baseline patient characteristics across the included studies. (3) outcome measures should encompass survival data, including but not limited to overall survival (OS), recurrence-free survival (RFS), and other relevant metrics. Conversely, the exclusion criteria include: (1) studies lacking a control group for comparison. (2) materials presented solely in the form of case reports, abstracts, conference presentations, or those involving animal experiments. (3) incomplete full-text articles where the abstract fails to provide comprehensive information about the study.

Data extraction and quality assessment

The article selection and data extraction were conducted by two authors (R.H. and T.Z.). In case of any disagreement regarding the inclusion or exclusion of an article, consultation with the author (H.Z.) was sought for resolution. Following completion of data extraction, a thorough review was performed by the author (H.Z.), and in case of any discrepancies, the data were re-extracted for subsequent analysis and discussion. The extracted information from included studies encompassed details such as first author, publication date, study design, number of cases, age distribution, gender composition, overall survival rate, recurrence-free survival rate, major morbidity rates and mortality rates. In addition, all included studies were evaluated for quality using the ROBINS-I tool.

Data synthesis and analysis

The meta-analysis was conducted using RevMan 5.3 software, a Cochrane-endorsed tool for systematic reviews. Dichotomous variables were assessed utilizing the odds ratio (OR) and a 95%

confidence interval (CI) as statistical measures for effect analysis. Hazard Ratio (HR) was used to analyze overall survival (OS) and recurrence-free survival (RFS). In cases where explicit HR values were not provided in the literature, we applied the method of Parmar et al. (20) to extract HR values. Heterogeneity within included studies was examined using the Mantel-Haenszel test with I^2 values categorized as follows: low heterogeneity when $I^2 \leq 25\%$, moderate heterogeneity when $25\% < I^2 \leq 50\%$, and high heterogeneity when I2 > 50%. A fixed-effects model was used under conditions of low or moderate heterogeneity; otherwise, a random-effects model was adopted. Sensitivity analysis employing the one-out method was conducted to assess our findings' robustness, while a funnel plot based on primary outcomes served as an evaluation tool for publication bias in this study. Throughout all analyses, statistical significance is considered at P value <0.05 for overall effect.

Results

Search results

The flow diagram illustrating the search results is presented in Figure 1. Following the devised retrieval strategy, a total of 324 relevant references were identified after eliminating duplicates. After reviewing the titles and abstracts, 49 articles with potential relevance were retained. Among these, 28 studies were excluded during full-text analysis due to reasons such as overlapping centers or patient cohorts (2 studies), lack of significant outcomes (10 studies), meeting one or more exclusion criteria (13 studies) and baseline data inconsistent (21–23). Ultimately, a meta-analysis was conducted on a selected set of 21 studies (10–12, 16–18, 24–38), comprising one randomized controlled trial (12) and twenty retrospective studies.

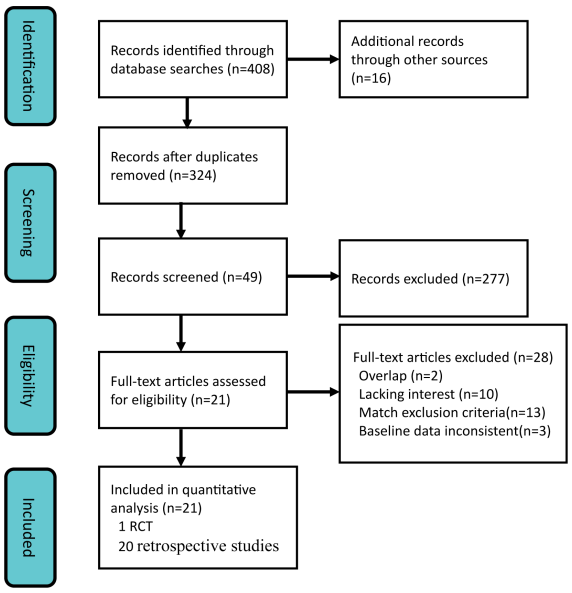

FIGURE 1
PRISMA flow chart of the literature selection.

Characteristics and quality of included studies

The basic characteristics of the included studies are presented in Table 1. All publications spanned from 2007 to 2023 and encompassed a total cohort of 2580 patients, including 1186 patients in the RH group and 1394 patients in the TAT group. Of these 21 studies, 16 were conducted in China (including Hong Kong and Taiwan), 3 in Japan and 2 in Korea. In the included studies, there was no statistically significant difference in baseline data (such as tumor size and number of tumors, etc.) between the two groups. Both RH and TAT groups in each study were from the same single or multiple centers during the same period. The ROBINS-I tool was used to assess the quality of the 21 included studies, and the specific results are shown in Supplementary Table S1.

Overall survival and recurrence free survival

The HR values of OS in all included studies (10–12, 16–18, 24–38) were extracted as the effect size for meta-analysis. The heterogeneity among studies was low (I^2 = 21%). Therefore, a fixed-effect model was employed for combined analysis. The results of the meta-analysis demonstrated that patients with recurrent liver cancer who received RH had significantly higher OS compared to those in the TAT group (HR=0.85, 95%CI 0.76~0.95, P=0.004) (Figure 2). Results showed that patients with recurrent liver cancer who underwent RH had significantly higher OS than those in the TAT group.

The HR data from 14 studies (10–12, 16–18, 27, 28, 31–33, 35, 37, 38) on RFS were included for meta-analysis. Given the low heterogeneity among the study groups (I^2 = 0%), a fixed effect model was employed for data integration. The meta-analysis results showed that patients with recurrent liver cancer who underwent RH had significantly higher RFS than those in the TAT group (HR=0.79, 95%CI 0.7~0.9, P<0.01) (Figure 3).

Postoperative complications and mortality

Ten studies (12, 16, 18, 25, 31, 32, 35–38) provided data on severe postoperative complications (Clavien-Dindo grade III or higher).The incidence of severe postoperative complications was 11.4% (88/769) in the RH group and 3.6% (31/860) in the TAT group. The heterogeneity of these trials was moderate (I^2 = 53%); therefore, a random effects model was employed to pool data. The meta-analysis results revealed a significantly lower incidence of severe postoperative complications in the TAT group compared to the RH group (OR=3.23, 95%CI 1.48~7.07, P=0.003) (Figure 4).

Eleven studies (12, 16, 18, 28, 31–33, 35–38) provided perioperative mortality. The perioperative mortality of the RH

TABLE 1 Characteristics of the included studies.

Author	Year	Country	Study design	Patients (n)	Age (mean ± SD)		Sex (M/F)		Child–Pugh (A/B)		Tumor size (mean ± SD,cm)		Tumor number (single/multiple)	
					RH	TAT	RH	TAT	RH	TAT	RH	TAT	RH	TAT
Choi	2007	Korea	N-RCT	23	NA	NA	NA	NA	NA	NA	NA	NA	NA	NA
Liang	2008	China	N-RCT	110	48.8 ± 12.0	54.6 ± 10.8	39/5	54/12	44/0	64/2	≤3(26)	≤3(44)	34/10	48/18
Ueno	2009	Japan	N-RCT	19	68.0 ± 6.8	68.0 ± 4.3	4/5	10/0	8/1	7/3	1.8 ± 0.38	1.8 ± 0.35	NA	NA
Umeda	2010	Japan	N-RCT	87	64.8 ± 0.79		63/24		29/0	51/7	3.2 ± 0.57	3.1 ± 0.30	18/11	34/24
Chan	2012	China	N-RCT	74	52.0 ± 10.3	59.0 ± 11.0	NA	NA	29/0	40/5	2.1 ± 1.2	2.2 ± 1.3	21/7	29/16
Hirokawa	2011	Japan	N-RCT	31	69.0 ± 7.3	67.0 ± 7.3	8/2	17/4	10/1	21/3	1.9 ± 0.7	1.7 ± 0.6	7/3	16/5
Cheng	2012	China	N-RCT	104	56.3 ± 12.3	61.0 ± 11.1	40/14	39/11	51/3	50/0	2.9 ± 1.8	2.3 ± 1.9	NA	NA
Zhang	2014	China	N-RCT	66	47 ± 13	52 ± 13	25/2	37/2	27/0	37/2	3.2 ± 1.0	2.7 ± 1.1	25/2	32/7
Wang	2015	China	N-RCT	290	50.2 ± 10.1	52.7 ± 10.9	113/15	148/14	NA	NA	2.4 ± 0.9	2.3 ± 0.7	89/39	107/55
Song	2015	Korea	N-RCT	117*	52.5 ± 9.8	53.6 ± 10.9	31/8	58/20	39/0	78/0	NA	NA	32/7	65/13
Chen	2018	China	N-RCT	105	73.5 ± 3.5	73.7 ± 2.9	41/7	51/6	NA	NA	2.6 ± 1.14	2.5 ± 1.2	28/20	30/27
Peng	2018	China	N-RCT	102*	55.3 ± 14.3	56.0 ± 14.3	46/5	45/6	48/3	49/2	2.4 ± 1.0	2.4 ± 0.9	43/8	43/8
Xia	2019	China	RCT	240	53.0 ± 8.8		216/24		NA	NA	NA	NA	NA	NA
Xiao	2019	China	N-RCT	35	NA	NA	10/1	18/6	11/0	24/0	NA	NA	5/6	11/13
Feng	2020	China	N-RCT	96*	56.6 ± 9.	58.2 ± 7.5	42/6	42/6	47/1	46/2	2.5 ± 0.5	2.5 ± 0.5	37/11	34/14
Lu	2020	China	N-RCT	240*	50.3 ± 10.5	50.9 ± 11.6	108/12	104/16	120/0	120/0	2.4 ± 1.1	2.2 ± 1.0	106/14	106/14
Wang	2020	China	N-RCT	71*	NA	NA	23/2	40/6	NA	NA	≤3(20)	≤3(39)	19/6	38/8
Zhong	2021	China	N-RCT	454*	NA	NA	194/33	191/36	222/5	224/3	<3 (128)	<3 (135)	171/56	172/55
Shi	2022	China	N-RCT	44*	53.2 ± 11.3	55.2 ± 10.0	17/5	17/5	NA	NA	2.9 ± 1.4	3.4 ± 1.3	14/8	15/7
Wang	2023	China	N-RCT	120*	52.0 ± 8.9	53.0 ± 14.0	54/6	54/6	NA	NA	2.5 ± 0.4	2.4 ± 0.4	NA	NA
Wan	2023	China	N-RCT	152*	56.1 ± 8.7	57.6 ± 8.4	66/10	69/7	63/13	61/15	4.6 ± 2.1	4.9 ± 2.1	62/14	57/19

RH, repeat hepatectomy; TAT, thermal ablation therapy; NA, not available; RCT, randomized controlled trial; NOS, Newcastle-Ottawa scale; SD, standard deviation.
*Data after propensity matching scores.

group was 0.5% (4/805), while that of the TAT group was 0.2% (2/890). The heterogeneity of these trials was low (I^2 = 48%); therefore, the fixed effect model was used to pool data. Meta-analysis results indicated no statistically significant difference in perioperative mortality between the two groups (OR=2.11, 95%CI 0.54~8.19, P=0.28) (Figure 5).

Sensitivity analysis and publication bias

Sensitivity analysis was conducted by sequentially excluding individual studies and subsequently performing a pool analysis again. The findings demonstrated that the results of overall survival and recurrence-free survival were basically consistent with the

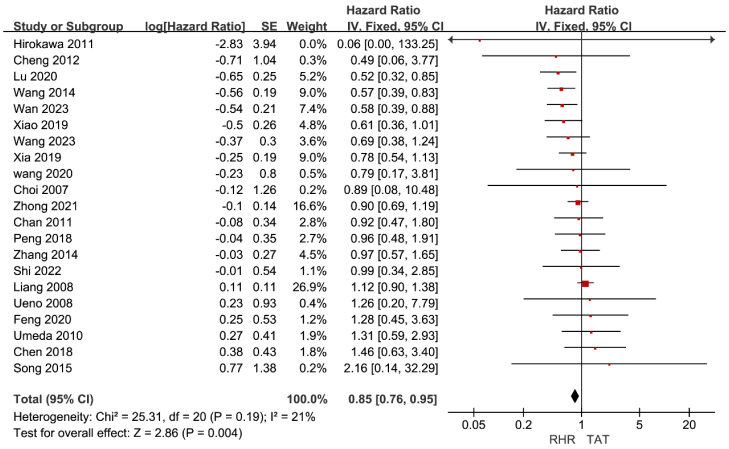

FIGURE 2
Forest plots of pooled data on overall survival.

original results, indicating that the meta-analysis results were robust. Figure 6 illustrates the funnel plot of the included studies. Notably, all plots within the funnel plot display a symmetrical distribution, indicating an absence of discernible publication bias in this meta-analysis.

Discussion

Recurrence following hepatectomy poses a formidable challenge in the management of HCC (6). When addressing recurrent HCC, it is imperative to concurrently pursue the comprehensive elimination of the tumor and the optimal preservation of residual liver function (5). RHR and TAT stand out as commonly employed modalities for treating recurrent HCC (6). During the initial operation, only a portion of the liver tissue is retained post-hepatectomy, resulting in a significantly diminished liver function reserve compared to the first intervention (12). Additionally, postoperative adhesions pose substantial challenges to reoperation. RHR, with its associated heightened risks of bleeding, infection, and liver failure, exacerbates the complexity of treating recurrent HCC (38). Consequently, some scholars advocate for the utilization of TAT in the management of recurrent HCC, asserting its comparable efficacy to RHR [27]. Literature has reported that only approximately 30% of patients experiencing recurrence after HCC resection have the opportunity for subsequent re-resection, with thermal ablation offering a relatively broad range of applicability (39). Nonetheless, an ongoing debate persists regarding the survival benefits of both RHR and TAT in patients with recurrent HCC (12, 30).

Previous meta-analysis have reported that there was no significant difference between RH and TAT in terms of OS and RFS for patients with recurrent HCC (13). Additionally, RH was associated with higher postoperative complications and mortality (15). However, we conducted a meta-analysis by incorporating newly published studies (16–18) that met the inclusion criteria and re-including data after propensity score matched (16–18, 31, 33, 35–38), which yielded different results from the previous studies. Our findings demonstrate that RH is superior to TAT in terms of OS and RFS in patients with recurrent HCC. This superiority may be attributed to the ability of RH to more thoroughly remove tumor tissue, thereby reducing the risk of residual cancer cells and their spread (18). Moreover, RH proves more effective in controlling local disease, which is crucial for prolonging patient survival time (16). Our sensitivity analysis

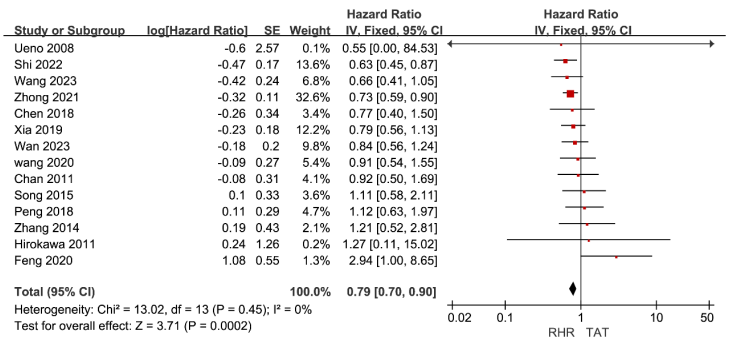

FIGURE 3
Forest plots of pooled data on recurrence free survival.

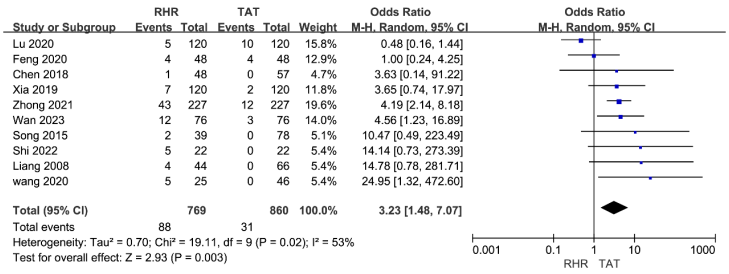

FIGURE 4
Forest plots of pooled data on severe postoperative complications.

confirms the robustness of our meta-analysis results, further enhancing the reliability of these findings.

Similarly, it is imperative to acknowledge that TAT represents a technical modality for tumor ablation utilizing high-temperature physical methods, encompassing radiofrequency and microwave ablation techniques (40). TAT possesses distinctive advantages and can be performed via percutaneous, laparoscopic, or open surgery approaches (41). Percutaneous TAT is widely employed in clinical practice as it obviates the need for traditional open surgery (42), thereby reducing patient's pain and recovery time while enhancing surgical safety. Currently, TAT exhibits extensive applicability across various types and sizes of liver cancer including primary and secondary liver cancer (43). Due to its minimal invasiveness and low postoperative complications, TAT is also regarded as an appropriate treatment option for HCC (12). The findings of this meta-analysis further validate that the perioperative complication rate associated with TAT for recurrent liver cancer is significantly lower compared to that observed with RH. The lower complication rate means patients recover faster and have a shorter hospital stay, making it a potentially safer option for those who can't handle major surgery.

However, it is important to note that our study did not find any statistically significant difference in perioperative mortality rates between the two treatment modalities. This shows that although surgery and ablation are technically and operationally different, they are both acceptable in terms of safety. Additionally, it should be acknowledged that while targeting the tumor with TAT, there is a possibility of overlooking certain adjacent satellite lesions (44).

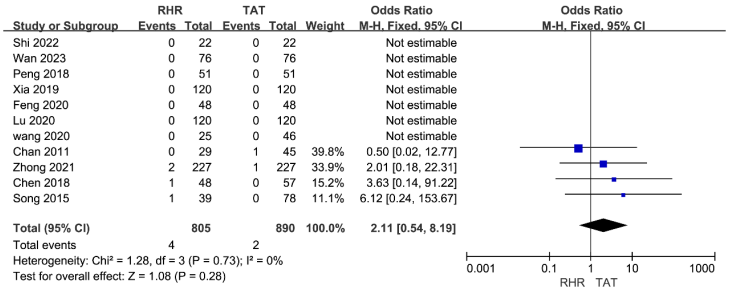

FIGURE 5
Forest plots of pooled data on mortality.

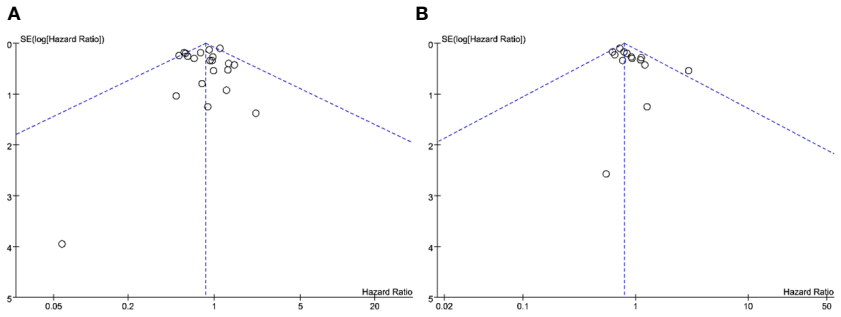

FIGURE 6
Funnel plot analysis: **(A)** funnel plot of overall survival; **(B)** funnel plot of recurrence-free survival.

Hepatectomy can remove both primary tumor lesions and satellite lesions metastasized through portal vein branches (30). Additionally, factors such as tumor morphology, distribution, and ablation range have a much stronger effect on TAT than RH (45). These factors may be the reason why RH is superior to TAT in OS and RFS with recurrent HCC.

The meta-analysis had several limitations. First, almost all the studies included were retrospective studies and only one RCTs was included for evaluation. Therefore, potential confounding factors will reduce the reliability of the meta-analysis results, even if the included study adopts propensity score matching analysis [33]. Second, most of the studies included in the meta-analysis were completed in the Asian region, and the results may be affected by institutional and regional differences. Third, included studies have different surgical indication for recurrent HCC, and the background of the two groups of patients in the same study is inevitably different. Owing to the limitation of data acquisition, this study did not conduct subgroup analysis on tumor size or number, cirrhosis, and recurrence time of recurrent HCC. It is not further clear which patients with recurrent HCC will benefit more from RH. Above reasons may result in a limitation of the conclusion. Therefore, a large sample size, multicenter randomized controlled trial needs to be completed to determine which treatment is most effective for recurrent HCC.

Conclusion

In conclusion, RH demonstrates a significantly superior survival benefit compared to TAT in the treatment of recurrent HCC. Therefore, in clinical decision-making, RH should be considered as the preferred choice for eligible patients with recurrent HCC. While, it is also necessary to recognize that TAT is an important alternative for the management of recurrent HCC.

Author contributions

HZ: Writing – review & editing, Writing – original draft, Visualization, Validation, Supervision, Software, Resources, Project administration, Methodology, Investigation, Formal analysis, Data curation, Conceptualization. RD: Writing – original draft, Visualization, Validation, Supervision, Software, Resources, Project administration, Methodology, Investigation, Formal analysis, Data curation, Conceptualization. TZ: Writing – review & editing, Visualization, Validation, Supervision, Software, Resources, Project administration, Methodology, Investigation, Formal analysis, Data curation, Conceptualization. WW: Writing – original draft, Visualization, Validation, Supervision, Software, Resources, Project administration, Methodology, Investigation, Formal analysis, Data curation, Conceptualization.

Funding

The author(s) declare that no financial support was received for the research, authorship, and/or publication of this article.

Conflict of interest

The authors declare that the research was conducted in the absence of any commercial or financial relationships that could be construed as a potential conflict of interest.

Publisher's note

Supplementary material

The Supplementary Material for this article can be found online at: https://www.frontiersin.org/articles/10.3389/fonc.2024.1370390/full#supplementary-material

References

1. Forner A, Reig M, Bruix J. Hepatocellular carcinoma. *Lancet*. (2018) 391:1301–14. doi: 10.1016/S0140-6736(18)30010-2

2. Belghiti J, Cortes A, Abdalla EK, Régimbeau J-M, Prakash K, Durand F, et al. Resection prior to liver transplantation for hepatocellular carcinoma. *Ann Surg*. (2003) 238:885–892; discussion 892-893. doi: 10.1097/01.sla.0000098621.74851.65

3. Guerrini GP, Gerunda GE, Montalti R, Ballarin R, Cautero N, De Ruvo N, et al. Results of salvage liver transplantation. *Liver Int*. (2014) 34:e96–e104. doi: 10.1111/liv.12497

4. Menahem B, Lubrano J, Duvoux C, Mulliri A, Alves A, Costentin C, et al. Liver transplantation versus liver resection for hepatocellular carcinoma in intention to treat: An attempt to perform an ideal meta-analysis. *Liver Transpl*. (2017) 23:836–44. doi: 10.1002/lt.24758

5. Lee MW, Lim HK. Management of sub-centimeter recurrent hepatocellular carcinoma after curative treatment: Current status and future. *World J Gastroenterol*. (2018) 24:5215–22. doi: 10.3748/wjg.v24.i46.5215

6. Wen T, Jin C, Facciorusso A, Donadon M, Han H-S, Mao Y, et al. Multidisciplinary management of recurrent and metastatic hepatocellular carcinoma after resection: an international expert consensus. *Hepatobiliary Surg Nutr*. (2018) 7:353–71. doi: 10.21037/hbsn.2018.08.01

7. Akoad ME, Pomfret EA. Surgical resection and liver transplantation for hepatocellular carcinoma. *Clin Liver Dis*. (2015) 19:381–99. doi: 10.1016/j.cld.2015.01.007

8. Kobayashi Y, Shindoh J, Igata Y, Okubo S, Hashimoto M. A novel scoring system for evaluating the difficulty of lysis of adhesion and surgical risk at repeat hepatectomy. *J Hepatobiliary Pancreat Sci*. (2020) 27:191–9. doi: 10.1002/jhbp.708

9. Ryu T, Takami Y, Wada Y, Hara T, Sasaki S, Saitsu H. Efficacy of surgical microwave ablation for recurrent hepatocellular carcinoma after curative hepatectomy. *HPB (Oxford)*. (2020) 22:461–9. doi: 10.1016/j.hpb.2019.08.001

10. Ueno M, Uchiyama K, Ozawa S, Nakase T, Togo N, Hayami S, et al. Prognostic impact of treatment modalities on patients with single nodular recurrence of hepatocellular carcinoma. *Surg Today*. (2009) 39:675–81. doi: 10.1007/s00595-008-3942-0

11. Zhang T, Li K, Luo H, Zhang W, Zhang L, Gao M. Long-term outcomes of percutaneous microwave ablation versus repeat hepatectomy for treatment of late recurrent small hepatocellular carcinoma: a retrospective study. *Natl Med J China*. (2014) 94:2570–1. doi: 10.3760/cma.j.issn.0376-2491.2014.33.004

12. Xia Y, Li J, Liu G, Wang K, Qian G, Lu Z, et al. Long-term effects of repeat hepatectomy vs percutaneous radiofrequency ablation among patients with recurrent hepatocellular carcinoma: A randomized clinical trial. *JAMA Oncol*. (2020) 6:255. doi: 10.1001/jamaoncol.2019.4477

13. Yuan B-H, Zhu Y-K, Zou X-M, Zhou H-D, Li R-H, Zhong J-H. Repeat hepatic resection versus percutaneous ablation for the treatment of recurrent hepatocellular carcinoma: meta-analysis. *BJS Open*. (2022) 6:zrac036. doi: 10.1093/bjsopen/zrac036

14. Yang Y, Yu H, Tan X, You Y, Liu F, Zhao T, et al. Liver resection versus radiofrequency ablation for recurrent hepatocellular carcinoma: a systematic review and meta-analysis. *Int J Hyperthermia*. (2021) 38:875–86. doi: 10.1080/02656736.2021.1933218

15. Liu J, Zhao J, Gu H a. O, Zhu Z. Repeat hepatic resection VS radiofrequency ablation for the treatment of recurrent hepatocellular carcinoma: an updated meta-analysis. *Minim Invasive Ther Allied Technol*. (2022) 31:332–41. doi: 10.1080/13645706.2020.1839775

16. Shi T, Xu C, Feng Y, Wei Y, Lv H, Zhu Q. Surgical resection versus radiofrequency ablation for early recurrent hepatocellular carcinoma. *Eur J Gastroenterol Hepatol*. (2022) 34:844–51. doi: 10.1097/MEG.0000000000002393

17. Wang W-Q, Lv X, Li J, Li J, Wang J-L, Yuan T, et al. Repeat hepatectomy versus microwave ablation for solitary and small (≤3 cm) recurrent hepatocellular carcinoma with early or late recurrence: A propensity score matched study. *Eur J Surg Oncol*. (2023) 49:1001–8. doi: 10.1016/j.ejso.2022.12.016

18. Wan W, Zhang H, Ji T, Zhang L, Luo K, Xiong D. Optimal treatment strategy for recurrent hepatocellular carcinoma based on recurrence time and tumor size: A propensity score matching study. *Clinics Res Hepatol Gastroenterol*. (2023) 47:102157. doi: 10.1016/j.clinre.2023.102157

19. Moher D, Shamseer L, Clarke M, Ghersi D, Liberati A, Petticrew M, et al. Preferred reporting items for systematic review and meta-analysis protocols (PRISMA-P) 2015 statement. *Syst Rev*. (2015) 4:1. doi: 10.1186/2046-4053-4-1

20. Parmar MK, Torri V, Stewart L. Extracting summary statistics to perform meta-analyses of the published literature for survival endpoints. *Stat Med*. (1998) 17:2815–34. doi: 10.1002/(sici)1097-0258(19981230)17:24<2815::aid-sim110>3.0.co;2-8

21. Eisele RM, Chopra SS, Lock JF, Glanemann M. Treatment of recurrent hepatocellular carcinoma confined to the liver with repeated resection and radiofrequency ablation: a single center experience. *Technol Health Care*. (2013) 21:9–18. doi: 10.3233/THC-120705

22. Wang C, Li K, Huang Z, Yuan Y, He W, Zheng Y, et al. Repeat hepatectomy versus percutaneous ablation for recurrent hepatocellular carcinoma: emphasis on the impact of early or late recurrence. *J Cancer Res Clin Oncol*. (2023) 149:15113–25. doi: 10.1007/s00432-023-05286-w

23. Luo J, Wu F, Tang M. Comparison of reoperation and adiofrequency ablation for recurrent small hepatocellular carcinoma. *Chin J Gen Surg*. (2011) 20:676–9.

24. Choi G-H, Kim D-H, Kang C-M, Kim K-S, Choi J-S, Lee W-J, et al. Prognostic factors and optimal treatment strategy for intrahepatic nodular recurrence after curative resection of hepatocellular carcinoma. *Ann Surg Oncol*. (2008) 15:618–29. doi: 10.1245/s10434-007-9671-6

25. Liang H-H, Chen M-S, Peng Z-W, Zhang Y-J, Zhang Y-Q, Li J-Q, et al. Percutaneous radiofrequency ablation versus repeat hepatectomy for recurrent hepatocellular carcinoma: A retrospective study. *Ann Surg Oncol*. (2008) 15:3484–93. doi: 10.1245/s10434-008-0076-y

26. Umeda Y, Matsuda H, Sadamori H, Matsukawa H, Yagi T, Fujiwara T. A prognostic model and treatment strategy for intrahepatic recurrence of hepatocellular carcinoma after curative resection. *World J Surg*. (2011) 35:170–7. doi: 10.1007/s00268-010-0794-8

27. Hirokawa F, Hayashi M, Miyamoto Y, Asakuma M, Shimizu T, Komeda K, et al. Appropriate treatment strategy for intrahepatic recurrence after curative hepatectomy for hepatocellular carcinoma. *J Gastrointest Surg*. (2011) 15:1182–7. doi: 10.1007/s11605-011-1484-z

28. Chan ACY, Poon RTP, Cheung TT, Chok KSH, Chan SC, Fan ST, et al. Survival analysis of re-resection versus radiofrequency ablation for intrahepatic recurrence after hepatectomy for hepatocellular carcinoma. *World J Surg*. (2012) 36:151–6. doi: 10.1007/s00268-011-1323-0

29. Ho C-M, Lee P-H, Shau W-Y, Ho M-C, Wu Y-M, Hu R-H. Survival in patients with recurrent hepatocellular carcinoma after primary hepatectomy: Comparative effectiveness of treatment modalities. *Surgery*. (2012) 151:700–9. doi: 10.1016/j.surg.2011.12.015

30. Wang K, Liu G, Li J, Yan Z, Xia Y, Wan X, et al. Early intrahepatic recurrence of hepatocellular carcinoma after hepatectomy treated with re-hepatectomy, ablation or chemoembolization: A prospective cohort study. *Eur J Surg Oncol (EJSO)*. (2015) 41:236–42. doi: 10.1016/j.ejso.2014.11.002

31. Song KD, Lim HK, Rhim H, Lee MW, Kim Y, Lee WJ, et al. Repeated Hepatic Resection versus Radiofrequency Ablation for Recurrent Hepatocellular Carcinoma after Hepatic Resection: A Propensity Score Matching Study. *Radiology*. (2015) 275:599–608. doi: 10.1148/radiol.14141568

32. Chen S, Peng Z, Xiao H, Lin M, Chen Z, Jiang C, et al. Combined radiofrequency ablation and ethanol injection versus repeat hepatectomy for elderly patients with recurrent hepatocellular carcinoma after initial hepatic surgery. *Int J Hyperthermia*. (2018) 34:1029–37. doi: 10.1080/02656736.2017.1387941

33. Peng Z, Wei M, Chen S, Lin M, Jiang C, Mei J, et al. Combined transcatheter arterial chemoembolization and radiofrequency ablation versus hepatectomy for recurrent hepatocellular carcinoma after initial surgery: a propensity score matching study. *Eur Radiol*. (2018) 28:3522–31. doi: 10.1007/s00330-017-5166-4

34. Xiao H, Chen Z-B, Jin H-L, Li B, Xu L-X, Guo Y, et al. Treatment selection of recurrent hepatocellular carcinoma with microvascular invasion at the initial hepatectomy. *Am J Transl Res*. (2019 11(3):1864–75.

35. Feng Y, Wu H, Huang DQ, Xu C, Zheng H, Maeda M, et al. Radiofrequency ablation versus repeat resection for recurrent hepatocellular carcinoma (≤ 5 cm) after initial curative resection. *Eur Radiol*. (2020) 30:6357–68. doi: 10.1007/s00330-020-06990-8

36. Lu L, Mei J, Kan A, Ling Y, Li S, Wei W, et al. Treatment optimization for recurrent hepatocellular carcinoma: Repeat hepatic resection versus radiofrequency ablation. *Cancer Med*. (2020) 9:2997–3005. doi: 10.1002/cam4.2951

37. Wang Y, Liao Y, Liu W, Zhang Y, Yuan Y, Qiu Y, et al. Surgical Resection versus Re-Ablation for Intrahepatic Recurrent Hepatocellular Carcinoma after Initial Ablation Therapy. *Dig Surg*. (2021) 38:46–57. doi: 10.1159/000511157

38. Zhong J-H, Xing B-C, Zhang W-G, Chan AW-H, Chong CCN, Serenari M, et al. Repeat hepatic resection versus radiofrequency ablation for recurrent hepatocellular carcinoma: retrospective multicentre study. *Br J Surg*. (2021) 109:71–8. doi: 10.1093/bjs/znab340

39. Xu X-F, Xing H, Han J, Li Z-L, Lau W-Y, Zhou Y-H, et al. Risk factors, patterns, and outcomes of late recurrence after liver resection for hepatocellular carcinoma: A multicenter study from China. *JAMA Surg*. (2019) 154:209–17. doi: 10.1001/jamasurg.2018.4334

40. Koza A, Bhogal RH, Fotiadis N, Mavroeidis VK. The role of ablative techniques in the management of hepatocellular carcinoma: indications and outcomes. *Biomedicines*. (2023) 11:1062. doi: 10.3390/biomedicines11041062

41. Zhu F, Rhim H. Thermal ablation for hepatocellular carcinoma: what's new in 2019. *Chin Clin Oncol*. (2019) 8:58. doi: 10.21037/cco.2019.11.03

42. Viganò L, Laurenzi A, Solbiati L, Procopio F, Cherqui D, Torzilli G. Open liver resection, laparoscopic liver resection, and percutaneous thermal ablation for patients with solitary small hepatocellular carcinoma (≤30 mm): review of the literature and proposal for a therapeutic strategy. *Dig Surg*. (2018) 35:359–71. doi: 10.1159/000489836

43. Liu M, Huang G-L, Xu M, Pan F-S, Lu M, Zheng K-G, et al. Percutaneous thermal ablation for the treatment of colorectal liver metastases and hepatocellular carcinoma: a comparison of local therapeutic efficacy. *Int J Hyperthermia*. (2017) 33:446–53. doi: 10.1080/02656736.2017.1278622

44. Ding J, Jing X, Wang Y, Wang F, Wang Y, Du Z. Thermal ablation for hepatocellular carcinoma: a large-scale analysis of long-term outcome and prognostic factors. *Clin Radiol*. (2016) 71:1270–6. doi: 10.1016/j.crad.2016.07.002

45. Weinstein JL, Ahmed M. Percutaneous ablation for hepatocellular carcinoma. *AJR Am J Roentgenol*. (2018) 210:1368–75. doi: 10.2214/AJR.17.18695

frontiers | Frontiers in Oncology

TYPE Original Research
PUBLISHED 23 April 2024
DOI 10.3389/fonc.2024.1405178

OPEN ACCESS

EDITED BY
Fabricio Ferreira Coelho,
University of São Paulo, Brazil

REVIEWED BY
Bin-Yan Zhong,
The First Affiliated Hospital of Soochow University, China
Francisco Tustumi,
University of São Paulo, Brazil

*CORRESPONDENCE
Guohong Han
hangh@fmmu.edu.cn

RECEIVED 22 March 2024
ACCEPTED 05 April 2024
PUBLISHED 23 April 2024

CITATION
Sun J, Xia D, Bai W, Li X, Wang E, Yin Z and Han G (2024) Tumor burden affects the progression pattern on the prognosis in patients treated with sorafenib.
Front. Oncol. 14:1405178.
doi: 10.3389/fonc.2024.1405178

Tumor burden affects the progression pattern on the prognosis in patients treated with sorafenib

Jun Sun[1], Dongdong Xia[1,2], Wei Bai[1,2], Xiaomei Li[1,2], Enxing Wang[1], ZhanXin Yin[1,2] and Guohong Han[1,2*]

[1]Department of Liver Disease and Digestive Interventional Radiology, National Clinical Research Center for Digestive Diseases and Xijing Hospital of Digestive Diseases, Air Force Medical University, Xi'an, Shaanxi, China, [2]Department of Liver Diseases and Interventional Radiology, Digestive Diseases Hospital, Xi'an International Medical Center Hospital, Northwestern University, Xi'an, Shaanxi, China

The progression pattern of tumors has an impact on the survival of patients with advanced hepatocellular carcinoma (HCC) and has been applied in the design of clinical trials for multiple second-line drugs. Previous research results have been contradictory, and the clinical impact of different progression patterns and their role in survival are still in question.

Purpose: The study aims to analyze the impact of different progression patterns and tumor burden size on survival of HCC patients, as well as their interactions, through a retrospective cohort study.

Patients and methods: The study involved 538 patients who had undergone treatment with sorafenib and had shown radiographic progression. The progression pattern was analyzed using Cox regression by including an interaction term between progression pattern and tumor burden, which was then visualized through a graphical analysis. Tumor burden was categorized into low, medium, and high subgroups based on the six-and-twelve criteria, allowing for an exploration of the effect of progression pattern on survival in different tumor burden situations.

Results: Compared to patients with only intrahepatic progression (NIH/IHG) with an overall survival (OS) of 14.1/19.9 months and post-progression survival (PPS) of 8.1/13.1 months respectively, patients with extrahepatic lesions (NEH/EHG) had worse overall and postprogressive survival (OS: 9.3/9.2 months, PPS: 4.9/5.1 months). The hazard ratio for extrahepatic progression (NEH/EHG) compared to intrahepatic progression (NIH/IHG) at low, medium, and high tumor burden were [HR 2.729, 95%CI 1.189-6.263], [HR 1.755, 95%CI 1.269-2.427], and [HR 1.117, 95%CI 0.832-1.499], respectively.

Conclusion: The study concluded that the interaction between the tumor progression patterns and tumor burden significantly affects the prognosis of HCC patients. As the tumor burden increases, the sensitivity of the patient's risk of death to the progression pattern decreases. These findings are valuable in personalized treatment and trial design.

KEYWORDS

HCC, sorafenib, progression pattern, tumor burden, interaction

1 Introduction

Tumor progression is generally considered a discouraging event and is seen as a reflection of treatment failure that requires shifting to another treatment approach (1–3). However, in fact, progression may have different patterns, and the progression pattern is an important factor that affects the subsequent survival of liver cancer patients, distinguishing them according to the location of lesion progression (4–9). The 2020 trial design and endpoints in hepatocellular carcinoma: AASLD (American Association for the Study of Liver Diseases) consensus conference mentioned that the trial design of second-line treatment for advanced hepatocellular carcinoma should take into account the different progression patterns after first-line treatment and this has been applied to the clinical trial design of multiple second-line drugs (4, 7–10). Stratifying patients based on their progression patterns provides a validated predictor of treatment outcomes and has become a relevant parameter for informing patients, designing and analyzing clinical trials. In clinical trials, reasonable survival assumptions are key to determining the potential impact of new drugs on expected lifespan.

However, past related research has yielded conflicting results (Table 1) (11–17). In 2013, Maria Reig et al. for the first time explored the relationship between survival and progression patterns in patients who progressed after receiving sorafenib treatment and had good liver function and performance scores, and found that new extrahepatic lesions (NEH) were a poor prognostic factor, providing evidence that different types of progression should be considered when stratifying patients and emphasized the need for further analysis and clarification of the prognostic significance of different progression types (11). In 2015, Massimo Colombo et al. found that although NEH was an independent prognostic factor, the post-progression survival of patients with extrahepatic growth (EHG) was similar to that of NEH patients, with respective time periods of 3.2 and 3.1 months (12). In the sub-analysis of the SORAMIC trial in 2020, NEH was not a poor prognostic factor (with respective median survival times of 14.8 and 14.9 months compared to overall survival), and only lung metastasis was a poor prognostic factor (7.6 months) (15). In SIRT treatment, Bruno Sangro et al. found that the NEH or NIH progression patterns represented a poor prognosis (16). Of course, more research points to NEH as an independent prognostic factor.

Advanced hepatocellular carcinoma is characterized by significant heterogeneity, with tumor burden, metastases, liver function reserve, and overall health status all significantly impacting patient survival time and quality of life (18). Moreover, studies have shown that even in patients with liver cancer accompanied by extrahepatic metastases, more than 80% of deaths are attributed to intrahepatic tumor progression, with liver failure resulting from late-stage progression being the main cause of death (19). Previous studies have also found that as tumor burden increases, the correlation between imaging response and survival rate after Transarterial chemoembolization (TACE) treatment weakens, possibly due to a balance between the positive impact of imaging response and the negative impact on liver function in patients with high tumor burden (20). Therefore, in the progression patterns of advanced liver cancer, can intrahepatic tumor burden affect the prognosis of progression patterns, with the negative impact on liver function resulting from the rapid deterioration in patients with high tumor burden being consistent with the negative impact of extrahepatic lesion progression?

Therefore, we propose the following hypothesis: In cases of low tumor burden, the appearance of extrahepatic lesion progression (NEH/EHG) signifies poor prognosis, but with increasing tumor burden, the sensitivity of extrahepatic lesion progression prognosis gradually decreases.

2 Patients and methods

2.1 Study population

This study retrospectively included 1048 patients with HCC who received sorafenib at our Center from January 2010 to October 2019, including patients with advanced HCC or those who were resistant to TACE therapy. Diagnosis was made by imaging or histological assessment according to American Association for the Study of Liver Diseases (AASLD) or European Association for the Study of Liver Diseases (EASL) guidelines. Exclusion criteria included: (1) accompanied by other malignant tumors; (2) Received any local treatment (ablation or TACE, etc.) within 4 weeks prior to the initiation of sorafenib; (3) Child-Pugh grade C patients; (4) Patients with ECOG physical status score over 2 points; (5) Patients who lacked progressive imaging until the last follow-up.

Patients received an initial dose of sorafenib of 400mg BID and the dose was adjusted in the event of intolerable adverse reactions. In the event of intolerable toxicity, the dose of sorafenib is reduced accordingly, or even temporary or permanent discontinuation of sorafenib therapy, but patients are usually encouraged to continue sorafenib therapy when adverse reactions can be tolerated.

2.2 Data collection

Commonly variables collected for the analysis were baseline demographic patient characteristics, radiological images and serum parameters.

Multiphase computed tomography (CT) or dynamic enhanced magnetic resonance imaging (MRI) imaging was performed before treatment initiation and every 8 weeks after treatment, and tumor response (complete response, partial response, disease stabilization, tumor progression) was evaluated according to modified response evaluation criteria in solid tumors (mRECIST) (21).

The progress time of imaging evaluation of patients was recorded, and the type of progress was registered: IHG: ≥20% increase in the size of intrahepatic lesions compared with baseline (intrahepatic growth); NIH: new intrahepatic lesion; EHG: ≥20% increase in the size of extrahepatic lesions compared with baseline (extrahepatic growth); NEH: new extrahepatic lesion and/or vascular invasion (11).

Tumor burden was categorized into low, medium, and high subgroups based on the six-and-twelve criteria (The sum of tumor numbers and maximum diameters was delimited by truncation values of six and twelve) (22).

TABLE 1 Previous studies on the prognostic significance of progression patterns in patients with advanced hepatocellular carcinoma.

Author	Year	Treatment	Independent prognostic factor
Maria Reig	2013	sorafenib	NEH
Massimo Iavarone	2015	sorafenib	NEH
Yi-Hsiang Huang	2015	sorafenib	NEH
Sadahisa Ogasawara	2016	sorafenib	NEH
Kerstin Schütte	2020	sorafenib/sorafenib plus SIRT	New pulmonary metastases
Bruno Sangro	2020	SIRT	NEH/NIH
Maria Reig	2020	ramucirumab	NEH

SIRT, selective internal radiation treatment; NEH, new extrahepatic lesion and/or vascular invasion; NIH: new intrahepatic lesion.

The primary outcome points were overall survival and post-progression survival. Follow-up was conducted by a professional clinical follow-up team every 8 weeks until death or the last follow-up date or contact was lost. On October 9, 2021, a final follow-up was conducted and a final survival assessment was made for all patients. The procedures followed in this study conformed to the ethical guidelines of the Helsinki Declaration of 1975 and were approved by the Ethics Committee of Xijing Hospital (Xi'an, China). According to institutional guidelines, all patients signed a written informed consent for treatment and to provide their clinical data in subsequent research before receiving sorafenib therapy.

2.3 Statistical analysis

Quantitative variables are presented as means with standard deviation (SD) or medians with interquartile range median with interquartile range, and were compared by Student's t test or Mann-Whitney U test. Categorical variables were presented as absolute and relative frequencies and compared by Chi-square test or Fisher's exact test. The interaction multiplicative terms of progression pattern and tumor load were included in COX regression, and the interaction was analyzed by drawing viewable views. Survival curves were plotted using the Kaplan-Meier (KM) method. For all analyses, a corresponding p value less than 0.05 was considered statistically significant. All calculations were performed with SPSS v22 (SPSS Inc., Chicago, IL) and R version 4.1.0 (R Foundation for Statistical Computing, Vienna, Austria).

3 Results

3.1 Baseline characteristics

A total of 538 patients with hepatocellular carcinoma that progressed after receiving sorafenib were included in this study (Figure 1). Chronic hepatitis B virus infection was the main cause in 463 patients (86.1%). The patients were mainly with medium-high tumor burden: 52 patients (9.7%) in low-load group, 251 patients (46.7%) in medium-load group, and 235 patients (43.7%) in high-load group. In the mode of progression, there were 246 cases (45.7%) of intrahepatic lesions, 148 cases (27.5%) of new extrahepatic lesions, 103 cases (19.1%) of new intrahepatic lesions, and 41 cases (7.6%) of extrahepatic lesions. The baseline data of all patients are shown in Table 2.

3.2 Survival analysis

The median follow-up was 11.8 months (IQR 6.2–24.7 months). In the general population, the median survival of patients with different progression modes (NEH, EHG, NIH, IHG) was 9.3 (95% CI 8.1-11.6) months, 9.2 (95%CI 6.2-11.8) months, 14.1 (95%CI 11.3-16.6) months, and 19.6 (95%CI 15.8-24.8) months, respectively (p<0.001); The post-progression survival was 4.9 (95%CI 3.8-6.4) months, 5.1 (95%CI 4.2-7.5) months, 8.1 (95%CI

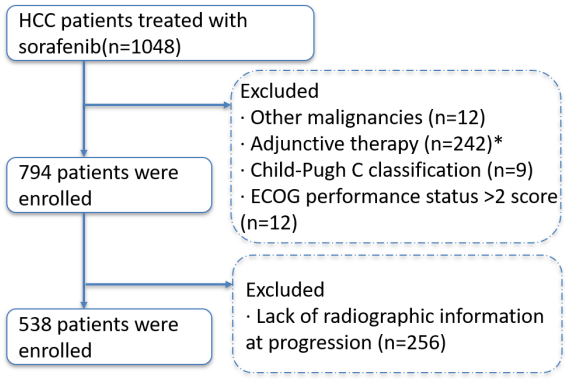

FIGURE 1
Selection flow diagram. **Comment:** * Received any local treatment (ablation or TACE, etc.) within 4 weeks prior to the initiation of sorafenib.

7.0-10.1) months, 13.1 (95%CI 9.5-16.5) months, respectively (p<0.001) (Figure 2).

But in people with a high tumor burden, the median survival of patients with different progression modes (NEH, EHG, NIH, IHG) was 9.2 (95%CI 7.0-10.4) months, 9.3 (95%CI 6.2-16.3) months, 8.3 (95%CI 7.5-10.8) months, and 12.1 (95%CI 9.3-17.9) months, respectively (p=0.068); The post-progression survival was 4.9 (95%CI 3.2-7.0) months, 4.8 (95%CI 4.2-11.3) months, 5.0 (95% CI 4.1-6.9) months, 6.6 (95%CI 5.9-12.0) months (p=0.07). and it was difficult to distinguish survival based on the mode of progression. The effect of progression patterns on patient survival was no longer statistically significant.

TABLE 2 Demographic and baseline characteristics of the patients.

Variables	Total cohorts(n=538)
Age, y (SD)	52.96(11.12)
Males (%)	457(84.9%)
Etiology (%)	
HBV	463(86.1%)
HCV	18(3.3%)
others	57(10.6%)
BCLC-C (%)	422(78.4%)
Largest tumour size, mm (IQR)	8.4(6.0-11.7)
Tumour number (IQR)	2(1-3)
Six-and-twelve (%)	
Low	52(9.7%)
Intermediate	251(46.7%)
High	235(43.7%)
Progression pattern (%)	
NIH	103(19.1%)
IHG	246(45.7%)
EHG	41(7.6%)
NEH	148(27.5%)
ECOG PS (%)	
0	258(48.0%)
1	261(48.5%)
2	19(3.5%)
ALBI 1 (%)	250(46.5%)
Child-Pugh A (%)	415(77.1%)
AFP, ng/ml (IQR)	449.3(20.44-11693)
NLR (IQR)	2.82(1.89-4.20)
ALB, g/L (SD)	39.37(5.04)
Bilirubin (μmol/L) (%)	16.80(12.50-22.50)
AST, U/L (IQR)	49(33-79)
INR (IQR)	1.09(1.02-1.17)
Creatinine, μmol/l (IQR)	86(76-96)
Macrovascular invasion (%)	230(42.8%)
Extrahepatic spread (%)	231(42.9%)
Ascites (%)	101(18.8%)

AFP, alpha-fetoprotein; ALB, albumin; ABLI, albumin-bilirubin; AST, aspartate aminotransferase; BCLC, Barcelona Clinic Liver Cancer; HBV, hepatitis B virus; INR, international normalized ratio; IQR, interquartile range; PS, performance status.

3.3 Interaction analysis

The multivariate Cox regression analysis included factors related to the guidelines recommended grouping criteria for clinical trials, in addition to tumor load and the multiplicative interaction terms of tumor load and pattern of progression (progression limited to intrahepatic/extrahepatic progression). The results showed that MVI, AFP, tumor burden, progression pattern and the multiplicative interaction terms of tumor load and mode of progression were statistically significant for the prognosis of patients (p< 0.001) (Table 3). A restricted cube plot (Figure 3) shows that the risk of death in patients with liver-limited progression (NIH/IHG) increases with the enlarging in tumor load until the risk is close to that in patients with extrahepatic progression at high tumor load.

3.4 Relationship between progression patterns and mortality risk under different tumor burden

Multivariate COX regression analysis was performed according to the clinical trial grouping criteria recommended by the guidelines. The pattern of progression was found to be independent prognostic factor p<0.001 for both overall median survival and post-progression survival (Table 4). Patients with extrahepatic progression or new extrahepatic progression had a 1.549 times higher risk of death (95% CI 1.256-1.909).

However, when subgroups were differentiated according to tumor load, it was found that the sensitivity of patients' risk of death to the pattern of progression decreased with increasing tumor load. The hazard ratio for extrahepatic progression (NEH/EHG) compared to intrahepatic progression (NIH/IHG) at low, medium, and high tumor burden were [HR 2.729, 95%CI 1.189-6.263], [HR 1.755, 95%CI 1.269-2.427], and [HR 1.117, 95%CI 0.832-1.499], respectively.

4 Discussion

Based on a retrospective analysis of 538 patients with hepatocellular carcinoma who progressed after treatment with sorafenib, we found that there was a significant interaction between tumor burden and progression pattern on the outcome of hepatocellular carcinoma. At the same time, the changes of the relationship between death risk and progression pattern of patients

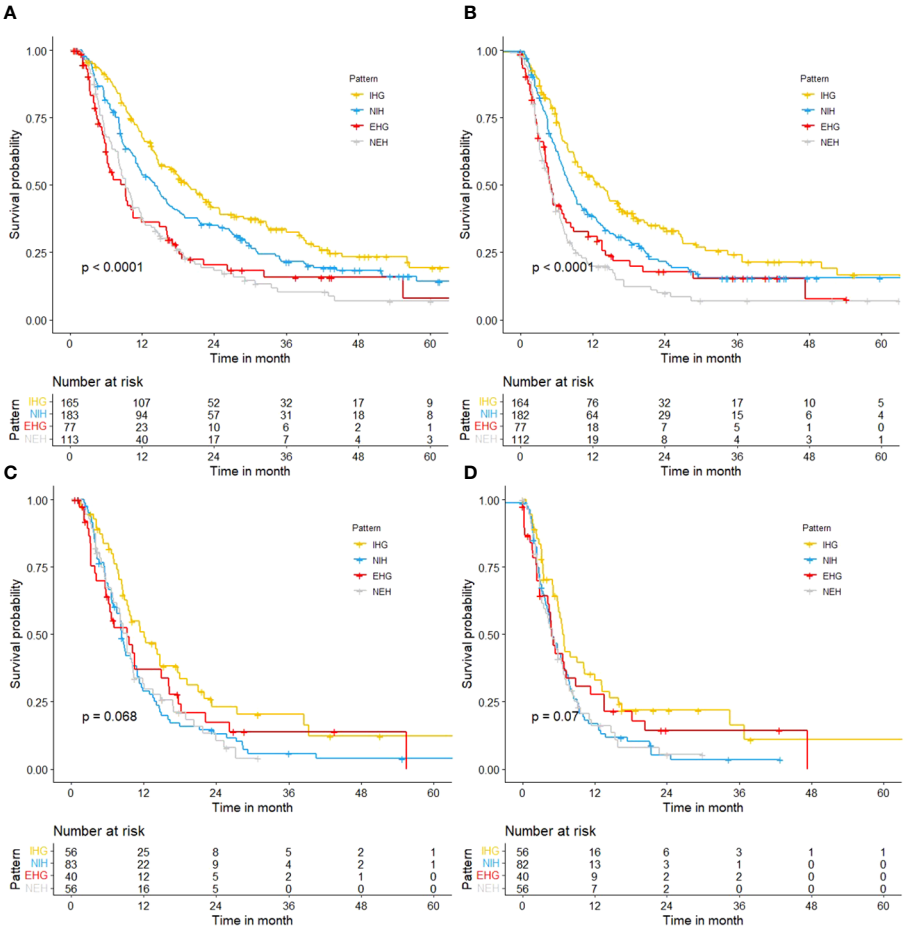

FIGURE 2
Kaplan-Meier curves. **(A)** OS of different progression patterns in total cohort; **(B)** PPS of different progression patterns in total cohort; **(C)** OS of different progression patterns in patients with a high tumor burden; **(D)** PPS of different progression patterns in patients with a high tumor burden.

under different tumor burden were further analyzed using tumor burden as stratification condition. Our study partly explains why previous studies have reached different conclusions about the progression pattern of advanced liver cancer tumors, in which tumor burden was not included in the analysis (11–17).

According to the tumor burden model established previously by our research group (six-and-twelve) (22), we divided the tumor burden into three subgroups of low, medium and high, and found that as the tumor burden increases, the sensitivity of the patient's risk of death to the progression pattern decreases: In patients with low and moderate tumor loads, patients with extrahepatic progression (NEH/EHG) had a significantly worse prognosis than those with intrahepatic progression (NIH/IHG). In patients with high tumor burden, the progression pattern no longer significantly stratified patient survival. Meanwhile, in patients whose progression was limited to the liver (NIH/IHG), median survival of different subgroups of at-risk individuals was significantly differentiated based on tumor burden; However, it is difficult to distinguish different risk groups based on tumor burden when there is extrahepatic lesion progression. This may be because the negative effects of rapid deterioration of liver function in patients with high tumor burden after progression are similar to the negative effects of extra-hepatic lesion progression.

With the development of first-line therapy such as molecular targeted therapy and immunotherapy, the therapeutic strategy of second-line therapy is also about to change dramatically (23, 24). Appropriate stratification factors should be considered in the trial design of second-line therapy for advanced liver cancer, otherwise patient characteristics may influence clinical trial results in patients with treatment failure (4). Our study suggests that the interaction between progression patterns and tumor burden in trial design should be fully considered in trial design and personalized treatment.

In our study, high tumor burden and medium tumor burden together accounted for more than 90% of the total population, which is consistent with the popular situation of our country, and the influence of tumor burden on our patients is more important (25). In the general population, overall survival and post-progression of new and extra-hepatic lesions were poor (OS: 9.3, 9.2; PPS: 4.9 months, 5.1 months). For patients with high tumor burden, regardless of intrahepatic progression or extrahepatic progression, the survival time after progression was only about

TABLE 3 Analysis of interaction between tumor burden and progression pattern.

Variables	HR (95%CI)	*p* value
	OS	
ECOG PS (≥1 vs 0)	1.134 (0.922-1.393)	0.233
MVI (yes vs no)	1.472 (1.184-1.830)	<0.001
AFP (>400ng/ml vs ≤400ng/ml)	1.574 (1.285-1.928)	<0.001
Tumor burden	1.103 (1.072-1.928)	<0.001
Progression pattern (Intrahepatic vs extrahepatic)	3.918 (2.177-7.050)	<0.001
Interaction between tumor burden and progression pattern	0.920 (0.878-0.965)	<0.001
	PPS	
ECOG PS (≥1 vs 0)	1.060 (0.863-1.302)	0.579
MVI (yes vs no)	1.299 (1.044-1.617)	0.019
AFP (>400ng/ml vs ≤400ng/ml)	1.648 (1.343-2.022)	<0.001
Tumor burden	1.087 (1.058-1.117)	<0.001
Progression pattern (Intrahepatic vs extrahepatic)	4.311 (2.408-7.720)	<0.001
Interaction between tumor burden and progression pattern	0.915 (0.873-0.958)	<0.001

AFP, alpha-fetoprotein; MVI, Macrovascular invasion.

half a year (4.9 months, 4.8 months, 5.0 months, 6.6 months). Therefore, for patients with higher tumor burden and better liver function reserve, active treatment with higher objective remission rate and disease control rate is recommended, because the objective remission rate of sorafenib is low, once the tumor progression is not controlled, it is difficult to bring better survival benefits to patients. At the same time, our study found that AFP had significant prognostic significance in different subgroups, and its prognostic value and significance should be further explored.

Advanced liver cancer has considerable heterogeneity, and tumor burden, metastasis, liver function reserve, and systemic condition all have considerable influence on the survival time and quality of life of patients (18, 26). However, the degree of influence of these factors varies. In 2018, Giannini et al. used clinical characteristics to classify heterogeneous BCLC stage C patients. In a retrospective analysis of 835 patients with stage C BCLC, median overall survival was significantly different based on criteria leading to advanced tumor stage (ECOG score 1-2, macrovascular infiltration, or extrahepatic spread) (18). At the same time, these factors will also influence each other and interact with each other, instead of simply adding or subtracting. However, the current research mainly divides patients into different groups according to a certain factor. In the follow-up studies of prognostic factors, faced with complex individuals, we should study more the interaction between multiple factors, rather than just explore the independent prognostic effect of a single factor.

Intrahepatic tumor burden, macrovascular invasion and extrahepatic metastasis, as well as severe liver function impairment, are key factors for poor prognosis, and these factors are often reflected in multiple clinical prediction models (27–32). However, tumor burden is rarely considered in the trial design of second-line therapy, possibly because its role is often overwritten by adverse prognostic factors such as liver function and extrahepatic metastasis (7–10, 33, 34). Patients with high tumor burden are more likely to suffer from rapid deterioration of liver function or even liver failure, resulting in death, after the progression of intrahepatic tumor, and this risk should not be ignored (19). The liver function and tumor burden can be in a certain interaction between need further exploration in the future. On the one hand, normal liver tissue is affected in patients with large tumor burden, and people with poor liver function should be more than patients with small tumor burden. On the other hand, as the patient's liver function declines, the sensitivity of tumor burden to survival prognosis may also gradually decrease.

The study also has some limitations. First, the risk of selection bias is inevitable in observational studies. Secondly, the cause of

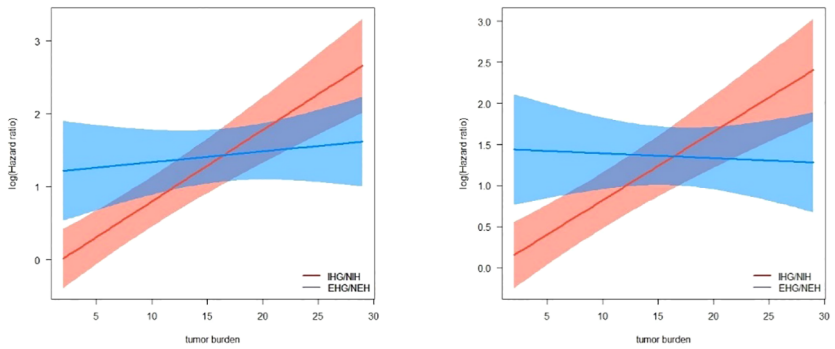

FIGURE 3
Interactive visualization of the interaction between tumor burden and progression patterns with OS/PPS as the endpoint.

TABLE 4 Multivariate cox regression analysis under different tumor loads.

Variables	OS		PPS	
	HR (95%CI)	*p* value	HR (95%CI)	*p* value
Total				
ECOG (≥1 vs 0)	1.283(1.047-1.571)	0.160	1.177(0.960-1.443)	0.117
MVI (yes vs no)	1.629(1.313-2.020)	0.001	1.435(1.155-1.782)	0.001
AFP (>400ng/ml vs ≤400ng/ml)	1.702(0.391-2.084)	<0.001	1.728(1.410-2.117)	<0.001
Progression pattern (Intrahepatic vs extrahepatic)	1.549(1.256-1.909)	<0.001	1.558(1.261-1.925)	<0.001
Low				
ECOG (≥1 vs 0)	3.243(1.466-7.174)	0.004	4.008(1.676-9.586)	0.002
MVI (yes vs no)	0.667(0.191-2.330)	0.526	0.495(0.141-1.739)	0.273
AFP (>400ng/ml vs ≤400ng/ml)	3.706(1.707-8.046)	0.001	3.853(1.693-8.768)	0.001
Progression pattern (Intrahepatic vs extrahepatic)	2.729(1.189-6.263)	0.018	1.776(0.736-4.282)	0.201
Intermediate				
ECOG (≥1 vs 0)	1.151(0.844-1.571)	0.375	1.069(0.782-1.460)	0.676
MVI (yes vs no)	1.621(1.148-2.289)	0.006	1.439(1.014-2.043)	0.042
AFP (>400ng/ml vs ≤400ng/ml)	1.680(1.234-2.287)	0.001	1.744(0.281-2.374)	<0.001
Progression pattern (Intrahepatic vs extrahepatic)	1.755(1.269-2.427)	0.001	1.913(1.378-2.654)	<0.001
High				
ECOG (≥1 vs 0)	1.059(0.787-1.424)	0.706	0.992(0.737-1.336)	0.959
MVI (yes vs no)	1.351(1.000-1.824)	0.050	1.185(0.878-1.598)	0.268
AFP (>400ng/ml vs ≤400ng/ml)	1.455(1.088-1.947)	0.012	1.469(1.096-1.968)	0.010
Progression pattern (Intrahepatic vs extrahepatic)	1.117(0.832-1.499)	0.462	1.117(0.832-1.498)	0.462

AFP, alpha-fetoprotein; MVI, Macrovascular invasion.

Chinese patients is mainly hepatitis B, and the tumor burden is also relatively high, which has some differences with other areas of tumors, and needs to be further verified in multi-center and other areas. At the same time, we only considered the interaction between tumor burden and progressive mode, and did not consider the interaction between tumor burden and progressive mode and liver function. This part of work needs to be further explored in the future.

5 Conclusion

In conclusion, interaction between the tumor progression patterns and tumor burden significantly affects the prognosis of HCC patients. As the tumor burden increases, the sensitivity of the patient's risk of death to the progression pattern decreases. Therefore, the interaction between progression mode and tumor burden should be fully considered in trial design and personalized treatment.

Data availability statement

The data that support the findings of this study are available on request from the corresponding author, Guohong Han, upon reasonable request. Requests to access these datasets should be directed to Jun Sun, 438831443@qq.com.

Ethics statement

The studies involving humans were approved by Ethics Committee of Xijing Hospital. The studies were conducted in accordance with the local legislation and institutional requirements. Written informed consent for participation was not required from the participants or the participants' legal guardians/next of kin in accordance with the national legislation and institutional requirements.

Author contributions

JS: Writing – review & editing, Writing – original draft, Visualization, Software, Methodology, Investigation, Data curation, Conceptualization. DX: Writing – review & editing, Validation, Supervision, Software, Project administration, Methodology, Investigation, Conceptualization. WB: Writing – review & editing, Supervision, Resources, Project administration,

Methodology, Investigation, Formal Analysis, Data curation, Conceptualization. XL: Writing – review & editing, Resources, Investigation, Data curation. EW: Writing – review & editing, Methodology, Investigation, Data curation, Conceptualization. ZY: Writing – review & editing, Resources, Project administration, Methodology, Investigation, Data curation, Conceptualization. GH: Writing – review & editing, Validation, Supervision, Software, Resources, Project administration, Methodology, Investigation, Funding acquisition, Formal Analysis, Data curation, Conceptualization.

Funding

The author(s) declare that no financial support was received for the research, authorship, and/or publication of this article.

Conflict of interest

The authors declare that the research was conducted in the absence of any commercial or financial relationships that could be construed as a potential conflict of interest.

Publisher's note

References

1. Easl clinical practice guidelines: management of hepatocellular carcinoma. *J Hepatol*. (2018) 69:182–236. doi: 10.1016/j.jhep.2018.03.019

2. Vogel A, Meyer T, Sapisochin G, Salem R, Saborowski A. Hepatocellular carcinoma. *Lancet*. (2022) 400:1345–62. doi: 10.1016/S0140-6736(22)01200-4

3. Marrero JA, Kulik LM, Sirlin CB, Zhu AX, Finn RS, Abecassis MM, et al. Diagnosis, staging, and management of hepatocellular carcinoma: 2018 practice guidance by the american association for the study of liver diseases. *Hepatology*. (2018) 68:723–50. doi: 10.1002/hep.29913

4. Llovet JM, Villanueva A, Marrero JA, Schwartz M, Meyer T, Galle PR, et al. Trial design and endpoints in hepatocellular carcinoma: aasld consensus conference. *Hepatology*. (2021) 73 Suppl 1:158–91. doi: 10.1002/hep.31327

5. Llovet JM, Kelley RK, Villanueva A, Singal AG, Pikarsky E, Roayaie S, et al. Hepatocellular carcinoma. *Nat Rev Dis Primers*. (2021) 7:6. doi: 10.1038/s41572-020-00240-3

6. Villanueva A. Hepatocellular carcinoma. *N Engl J Med*. (2019) 380:1450–62. doi: 10.1056/NEJMra1713263

7. Zhu AX, Kang YK, Yen CJ, Finn RS, Galle PR, Llovet JM, et al. Ramucirumab after sorafenib in patients with advanced hepatocellular carcinoma and increased alpha-fetoprotein concentrations (reach-2): a randomised, double-blind, placebo-controlled, phase 3 trial. *Lancet Oncol*. (2019) 20:282–96. doi: 10.1016/S1470-2045(18)30937-9

8. Chau I, Peck-Radosavljevic M, Borg C, Malfertheiner P, Seitz JF, Park JO, et al. Ramucirumab as second-line treatment in patients with advanced hepatocellular carcinoma following first-line therapy with sorafenib: patient-focused outcome results from the randomised phase iii reach study. *Eur J Cancer*. (2017) 81:17–25. doi: 10.1016/j.ejca.2017.05.001

9. Bruix J, Qin S, Merle P, Granito A, Huang YH, Bodoky G, et al. Regorafenib for patients with hepatocellular carcinoma who progressed on sorafenib treatment (resorce): a randomised, double-blind, placebo-controlled, phase 3 trial. *Lancet*. (2017) 389:56–66. doi: 10.1016/S0140-6736(16)32453-9

10. Abou-Alfa GK, Meyer T, Cheng AL, El-Khoueiry AB, Rimassa L, Ryoo BY, et al. Cabozantinib in patients with advanced and progressing hepatocellular carcinoma. *N Engl J Med*. (2018) 379:54–63. doi: 10.1056/NEJMoa1717002

11. Reig M, Rimola J, Torres F, Darnell A, Rodriguez-Lope C, Forner A, et al. Postprogression survival of patients with advanced hepatocellular carcinoma: rationale for second-line trial design. *Hepatology*. (2013) 58:2023–31. doi: 10.1002/hep.26586

12. Iavarone M, Cabibbo G, Biolato M, Della Corte C, Maida M, Barbara M, et al. Predictors of survival in patients with advanced hepatocellular carcinoma who permanently discontinued sorafenib. *Hepatology*. (2015) 62:784–91. doi: 10.1002/hep.27729

13. Lee I, Chen Y, Chao Y, Huo TI, Li CP, Su CW, et al. Determinants of survival after sorafenib failure in patients with bclc-c hepatocellular carcinoma in real-world practice. *Med (Baltimore)*. (2015) 94:e688. doi: 10.1097/MD.0000000000000688

14. Ogasawara S, Chiba T, Ooka Y, Suzuki E, Kanogawa N, Saito T, et al. Post-progression survival in patients with advanced hepatocellular carcinoma resistant to sorafenib. *Invest New Drugs*. (2016) 34:255–60. doi: 10.1007/s10637-016-0323-1

15. Schütte K, Schinner R, Fabritius MP, Möller M, Kuhl C, Iezzi R, et al. Impact of extrahepatic metastases on overall survival in patients with advanced liver dominant hepatocellular carcinoma: a subanalysis of the soramic trial. *Liver Cancer*. (2020) 9:771–86. doi: 10.1159/000510798

16. de la Torre-Aláez M, Jordán-Iborra C, Casadei-Gardini A, Bilbao JI, Rodriguez-Fraile M, Sancho L, et al. The pattern of progression defines post-progression survival in patients with hepatocellular carcinoma treated with sirt. *Cardiovasc Intervent Radiol*. (2020) 43:1165–72. doi: 10.1007/s00270-020-02444-2

17. Reig M, Galle PR, Kudo M, Finn R, Llovet JM, Metti AL, et al. Pattern of progression in advanced hepatocellular carcinoma treated with ramucirumab. *Liver Int*. (2021) 41:598–607. doi: 10.1111/liv.14731

18. Giannini EG, Bucci L, Garuti F, Brunacci M, Lenzi B, Valente M, et al. Patients with advanced hepatocellular carcinoma need a personalized management: a lesson from clinical practice. *Hepatology*. (2018) 67:1784–96. doi: 10.1002/hep.29668

19. Uchino K, Tateishi R, Shiina S, Kanda M, Masuzaki R, Kondo Y, et al. Hepatocellular carcinoma with extrahepatic metastasis. *Cancer*. (2011) 117:4475–83. doi: 10.1002/cncr.25960

20. Wang Z, Wang E, Bai W, Xia D, Ding R, Li J, et al. Exploratory analysis to identify candidates benefitting from combination therapy of transarterial chemoembolization and sorafenib for first-line treatment of unresectable hepatocellular carcinoma: a multicenter retrospective observational study. *Liver Cancer*. (2020) 9:308–25. doi: 10.1159/000505692

21. Lencioni R, Llovet J. Modified recist (mrecist) assessment for hepatocellular carcinoma. *Semin Liver Dis*. (2010) 30:52–60. doi: 10.1055/s-0030-1247132

22. Wang Q, Xia D, Bai W, Wang E, Sun J, Huang M, et al. Development of a prognostic score for recommended tace candidates with hepatocellular carcinoma: a multicentre observational study. *J Hepatol*. (2019) 70:893–903. doi: 10.1016/j.jhep.2019.01.013

23. Gordan JD, Kennedy EB, Abou-Alfa GK, Beg MS, Brower ST, Gade TP, et al. Systemic therapy for advanced hepatocellular carcinoma: asco guideline. *J Clin Oncol*. (2020) 38:4317–45. doi: 10.1200/JCO.20.02672

24. Cabibbo G, Reig M, Celsa C, Torres F, Battaglia S, Enea M, et al. First-line immune checkpoint inhibitor-based sequential therapies for advanced hepatocellular carcinoma: rationale for future trials. *Liver Cancer*. (2022) 11:75–84. doi: 10.1159/000520278

25. Wang ZX, Li J, Wang EX, Xia DD, Bai W, Wang QH, et al. Validation of the six-and-twelve criteria among patients with hepatocellular carcinoma and performance score 1 receiving transarterial chemoembolization. *World J Gastroenterol*. (2020) 26:1805–19. doi: 10.3748/wjg.v26.i15.1805

26. Yoo JJ, Chung GE, Lee JH, Nam JY, Chang Y, Lee JM, et al. Sub-classification of advanced-stage hepatocellular carcinoma: a cohort study including 612 patients treated with sorafenib. *Cancer Res Treat*. (2018) 50:366–73. doi: 10.4143/crt.2017.126

27. Labeur TA, Berhane S, Edeline J, Blanc JF, Bettinger D, Meyer T, et al. Improved survival prediction and comparison of prognostic models for patients with hepatocellular carcinoma treated with sorafenib. *Liver Int*. (2019) 40:215–28. doi: 10.1111/liv.14270

28. Berhane S, Fox R, Garcia-Finana M, Cucchetti A, Johnson P. Using prognostic and predictive clinical features to make personalised survival prediction in advanced hepatocellular carcinoma patients undergoing sorafenib treatment. *Br J Cancer*. (2019) 121:117–24. doi: 10.1038/s41416-019-0488-4

29. Edeline J, Blanc JF, Campillo-Gimenez B, Ma YT, King J, Faluyi O, et al. Prognostic scores for sorafenib-treated hepatocellular carcinoma patients: a new application for the hepatoma arterial embolisation prognostic score. *Eur J Cancer*. (2017) 86:135–42. doi: 10.1016/j.ejca.2017.08.036

30. Choi GH, Han S, Shim JH, Ryu MH, Ryoo BY, Kang YK, et al. Prognostic scoring models for patients undergoing sorafenib treatment for advanced stage hepatocellular carcinoma in real-life practice. *Am J Clin Oncol*. (2017) 40:167–74. doi: 10.1097/COC.0000000000000132

31. Adhoute X, Penaranda G, Raoul JL, Blanc JF, Edeline J, Conroy G, et al. Prognosis of advanced hepatocellular carcinoma: a new stratification of barcelona clinic liver cancer stage c: results from a french multicenter study. *Eur J Gastroenterol Hepatol*. (2016) 28:433–40. doi: 10.1097/MEG.0000000000000558

32. Takeda H, Nishikawa H, Osaki Y, Tsuchiya K, Joko K, Ogawa C, et al. Clinical features associated with radiological response to sorafenib in unresectable hepatocellular carcinoma: a large multicenter study in Japan. *Liver Int*. (2015) 35:1581–9. doi: 10.1111/liv.12591

33. Qin S, Li Q, Gu S, Chen X, Lin L, Wang Z, et al. Apatinib as second-line or later therapy in patients with advanced hepatocellular carcinoma (ahelp): a multicentre, double-blind, randomised, placebo-controlled, phase 3 trial. *Lancet Gastroenterol Hepatol*. (2021) 6:559–68. doi: 10.1016/S2468-1253(21)00109-6

34. Finn RS, Ryoo BY, Merle P, Kudo M, Bouattour M, Lim HY, et al. Pembrolizumab as second-line therapy in patients with advanced hepatocellular carcinoma in keynote-240: a randomized, double-blind, phase iii trial. *J Clin Oncol*. (2020) 38:193–202. doi: 10.1200/JCO.19.01307

frontiers | Frontiers in Oncology

TYPE Original Research
PUBLISHED 02 May 2024
DOI 10.3389/fonc.2024.1387587

OPEN ACCESS

EDITED BY
Vahid Rashedi,
University of Social Welfare and Rehabilitation Sciences, Iran

REVIEWED BY
Umar Saeed,
Ajou University, Republic of Korea
Ruimei Feng,
Shanxi Medical University, China
Raziye Özdemir,
Karabük University, Türkiye

*CORRESPONDENCE
Di Wu
wudi0729@126.com
Boheng Liang
14927462@qq.com

†These authors have contributed equally to this work

RECEIVED 19 February 2024
ACCEPTED 08 April 2024
PUBLISHED 02 May 2024

CITATION
Wang D, Hu X, Xu H, Chen Y, Wang S, Lin G, Yang L, Chen J, Zhang L, Qin P, Wu D and Liang B (2024) Trend analysis and age-period-cohort effects on morbidity and mortality of liver cancer from 2010 to 2020 in Guangzhou, China.
Front. Oncol. 14:1387587.
doi: 10.3389/fonc.2024.1387587

Trend analysis and age-period-cohort effects on morbidity and mortality of liver cancer from 2010 to 2020 in Guangzhou, China

Dedong Wang[1,2,3†], Xiangzhi Hu[1†], Huan Xu[2], Yuanyuan Chen[2], Suixiang Wang[2], Guozhen Lin[2], Lei Yang[3], Jinbin Chen[4], Lin Zhang[2], Pengzhe Qin[2], Di Wu[1,2,3*] and Boheng Liang[2*]

[1]Department of Public Health and Preventive Medicine, School of Medicine, Jinan University, Guangzhou, China, [2]Department of Biostatistics and Cancer Registration, Guangzhou Center for Disease Control and Prevention, Guangzhou, China, [3]The State Key Lab of Respiratory Disease, School of Public Health, Guangzhou Medical University, Guangzhou, China, [4]Guangzhou Key Laboratory for Clinical Rapid Diagnosis and Early Warning of Infectious Diseases, KingMed School of Laboratory Medicine, Guangzhou Medical University, Guangzhou, Guangdong, China

Introduction: Liver cancer is one of the most common malignant gastrointestinal tumors worldwide. This study intends to provide insight into the epidemiological characteristics and development trends of liver cancer incidence and mortality from 2010 to 2020 in Guangzhou, China.

Methods: Data were collected from the Cancer Registry and Reporting Office of Guangzhou Center for Disease Control and Prevention. Cross-sectional study, Joinpoint regression (JPR) model, and Age-Period-Cohort (APC) model were conducted to analyze the age-standardized incidence rate (ASIR) and age-standardized mortality rate (ASMR) trend of liver cancer among the entire study period.

Results: The age-standardized incidence and mortality of liver cancer in Guangzhou showed an overall decreasing trend. The disparity in risk of morbidity and mortality between the two sexes for liver cancer is increasing. The cohort effect was the most significant among those born in 1965~1969, and the risk of liver cancer incidence and mortality in the total population increased and then decreased with the birth cohort. Compared with the birth cohort born in 1950~1954 (the reference cohort), the risk of liver cancer incidence and mortality in the males born in 1995~1999 decreased by 32% and 41%, respectively, while the risk in the females decreased by 31% and 32%, respectively.

Conclusions: The early detection, prevention, clinical diagnosis, and treatment of liver cancer in Guangzhou have made remarkable achievements in recent years. However, the risk of liver cancer in the elderly and the middle-aged males is still

at a high level. Therefore, the publicity of knowledge related to the prevention and treatment of liver cancer among the relevant population groups should be actively carried out to enhance the rate of early diagnosis and treatment of liver cancer and to advocate a healthier lifestyle.

KEYWORDS

liver cancer, trend analysis, joinpoint, age-period-cohort model, cross-sectional study

1 Introduction

Liver cancer is a malignant tumor of the gastrointestinal tract with strong insidiousness, heterogeneity, rapid progression, high recurrence rate, and poor overall prognosis (1). Additionally, there is a clear regional disparity in the occurrence of liver cancer, with East Asia and sub-Saharan Africa experiencing a higher incidence risk, accounting for 85% of cases worldwide. Liver cancer is the fifth most common cancer worldwide and the second leading cause of cancer death, with 854,000 new cases and 810,000 deaths annually (2, 3). According to the data of the latest report released by the National Cancer Center, liver cancer in China is located in fourth place in the incidence of malignant tumors and second place in the mortality rate. A study by the research team of Professor Chen of the National Cancer Center also reported that although the incidence of liver cancer in our country has been steadily declining, the trend has remained stable, and the prediction through the APC model shows that the number of liver cancer cases in the Chinese population will stabilize at around 160,000 and the number of deaths will stabilize at around 140,000 annually during 2020~2024 (4). Therefore, liver cancer is still an important public health problem in China. The occurrence of liver cancer is related to various risk factors, such as the infection of Hepatitis B virus (HBV), intake of toxic and harmful substances, metabolic abnormalities, cirrhosis, and smoking. Furthermore, it is especially crucial to note that with the development of the social and economic environment, lifestyles and eating habits have also changed dramatically among individuals, resulting in a significant increase in exposure to various risk factors. Guangzhou, as the economic center city of the Pearl River Delta region, has its own unique food culture and regional characteristics (5). According to relevant statistics, Guangzhou is one of the regions with a high incidence of liver cancer in China, and there is an obvious tendency for the high-risk group to become younger. In addition, coastal regions such as Guangxi, Fujian, and Hainan are also areas with high incidences of liver cancer. Taken together, these regions share several common factors associated with the development of liver cancer, including frequent hepatitis, a preference for fish and raw foods, and humid environments (6).

A large number of studies have been conducted both domestically and internationally using the JPR model and the APC model to determine the prevalence of chronic non-communicable diseases, which can also be used to predict the future burden of cancers (7–11). Research reported that the death rate of liver cancer in both sexes in Korea has decreased gradually since 1993, with the cohort effect primarily responsible for this trend, which was consistent with the trend of liver cancer mortality in Serbia during 1991~2015 and Mexico during 1998~2018 (12–14). Zhang's study demonstrated a gradual decline in the male-to-female incidence ratio (IRR) in the U.S. population under 50 years of age from 2001~2015, with a diminishing incidence advantage of liver cancer for males and a gradual increase in incidence risk for females with the birth cohort (15). In domestic, the incidence and mortality rates of liver cancer in Hubei Province during 1990~2019 suggested an unfavorable upward trend in contrast to the steady decline trend in China, and the risk of death due to HBV was found to be the highest in all age groups according to the classification of specific etiologies (16, 17). Research in 2024 displayed significant regional disparities in liver cancer incidence in five regions: Shanghai, Jiashan, Hong Kong, Harbin and Zhongshan, with a higher incidence in southwest China. And the cohort effect of males born in 1916~1962 and females born in 1916~1949 among Zhongshan City was gradually considerable, as opposed to the downward trend in other regions (18). In Guangzhou, only one research used the APC model to investigate the incidence and mortality risk of liver cancer from 2004 to 2015 (19). Thus, it is significant to assess the changes in age, period, and cohort effects of liver cancer in Guangzhou in recent years.

With a special focus on the separate effects of age and the birth cohort utilizing the APC model, this study sought to clarify and assess the trends of liver cancer morbidity and mortality in Guangzhou over the past eleven years among the total population, males, and females. Based on this, the total changes in unique exposures among different birth cohorts over time were taken into account, aiming to grasp the epidemiologic characteristics of liver cancer in the local area and to identify the key points of control for liver cancer prevention and treatment in different high-risk groups. In addition, focusing on specific areas and populations for accurate prevention and control not only contributes to exploring the pathogenesis but also provides scientific evidence for the development of population-based strategies and interventions for the prevention and control of liver cancer.

2 Materials and methods

2.1 Data sources

Guangzhou is located in the south of mainland China and at the northern edge of the Pearl River Delta. It consists of 11 districts:

Yuexiu District, Haizhu District, Liwan District, Tianhe District, Baiyun District, Huangpu District, Huadu District, Panyu District, Nansha District, Conghua District, and Zengcheng District. The permanent population in 2020 is approximately 9.85 million. The incidence data of liver cancer was obtained from the Information System of Tumor Registry and Report of Guangzhou City, the case data of primary liver cancer patients from 2010 to 2020 were collected according to the International Classification of Diseases (ICD-10) coded by C22, including sex, name, gender, age, address, occupation, date of birth, date of death, and diagnosis. The death data were primarily based on deaths reported in the Cause of Death Registration Information System of the Guangzhou Center for Disease Control and Prevention (GZCDC), which screened for underlying causes of death from liver cancer between 2010~2020. Population data are provided by the Statistics Bureau of Guangzhou Municipality, including population numbers divided into five years.

2.2 Joinpoint regression model analysis

In comparison to the traditional single regression model, the JPR model can identify statistically significant segments of change in the trend of morbidity and mortality of liver cancer, avoiding subjective judgment in the descriptive analysis to some extent. The average annual percentage change (AAPC), estimated annual percentage change (EAPC), and corresponding 95% confidence intervals (CIs) were calculated for each trend segment and tested for significance using Monte Carlo permutations. The Bayesian Information Criterion (BIC) was used to determine the optimal connectivity points. In this study, we analyzed the trend change in incidence and mortality of liver cancer on a population-based basis, with the dependent variable obeying a Poisson distribution, and ultimately a log-linear model was selected. The grid search method (GSM) (20) is used to determine the number of optimal connection points. In addition, "constant variance" was selected for the "heteroscedasticity errors option". Statistically significant trends in the ASIR and ASMR among different age groups were identified, representing a monotonically increasing or decreasing trend when APC > or < 0, respectively.

2.3 Construction and analysis of the APC model

The APC model is a multiple regression model that quantifies the event risk based on Poisson distribution while the interaction effects were controlled (21). The model has the unique advantage of being able to decompose temporal variation into three dimensions (age, period, and cohort) (22, 23). Age effects are defined as variations in physiologic factors associated with age differences of individuals. Conversely, period effects reflect the influence of anthropogenic factors on disease rates in populations. Factors such as the development of technologies for early screening and diagnosis of diseases, changes in registration and reporting systems, and advanced treatment may affect the rate of disease at different periods. The cohort effect derives from changes in potentially life-threatening factors early in the generations, so it illustrates factual changes in disease rates (24). Due to the low incidence and mortality of liver cancer in people under 20 years old, the age group among 20~85 years old was divided into groups of 5 years, and the age group above 85 years old was divided into a separate group. It was eventually divided into 14 groups. The common form of the model is expressed as follows:

$$\text{Log}\left[\text{r}\left(a,p\right)\right] = f(a) + g(p) + h(\text{c})$$

where $f(a)$ refers to the age effect, $g(p)$ refers to the period effect, and $h(c)$ refers to the birth cohort effect. The age-cohort (AC), age-period (AP), and age-trend (AT) models were developed to compare the Akaike Information Criterion (AIC) of the different APC sub-models. Finally, the APC model was identified as the most appropriate. The limitation of the model lies in the liner independent of the above three factors. In order to obtain the unique solution of the parameter, we used the period zero linear trend method (ZLT-P) contained in the method of "Equality Restrictions" in the APC model to orthogonally decompose the time effect into an unidentifiable linear trend and a linear deviation independent of specific constraints (25). That is to say, the linear trend of the period effect is shrunk to zero in this study, and the linear degree of freedom is assigned to the other two factors, so as to achieve the division of the linear trend for the three factors.

2.4 Stability evaluation of parameter estimation methods of the APC model

The method of "Equality Restrictions", proposed by HolfFord and Clayton (26, 27), is based on the hypothesis that the effects of age, cohort, and period can be orthogonally decomposed into linear and non-linear components. The linear deviations of the time effects and specific combinations of slopes are identifiable, and the defined effects building on these identifiable functions are therefore also reliable (25). Depending on the constraints, this method contains two different sets of parameter estimates. The cohort zero linear trend method (ZLT-C) and the ZLT-P method are the terms applied to describe the two scenarios in which the dominant effect in the constraints is the period effect or the cohort effect, respectively. In this study, the sensitivity of the constraint methods and the credibility of the results were assessed in terms of the stability of the parameter estimates, the consistency of parameter estimates with biological evidence, and the evaluation of the model fitting performance (28).

2.5 Quality control of the data

The data of the Information System of Tumor Registry and Report of Guangzhou City were obtained from 120 networked hospitals with oncology capacity, and the quality and accuracy of the data were widely recognized. The Guangzhou Center for Disease Control and Prevention is responsible for coding, re-checking, merging cases across districts, and excluding patients with non-Guangzhou household registration and duplicate information (especially checking whether the coding is correct).

The data were audited by IARC crgtools software to review the data after the above operations, and the data were validated based on the electronic medical record information collected back when the doubtful cases were identified. Finally, the complete database was established. The completion rate of follow-up visits for the malignant tumor surveillance population in Guangzhou exceeds 90% annually. The death surveillance data from the Cause of Death Registration Information System of GZCDC also integrated data from the Statistics Center of the Guangzhou Municipal Health and Wellness Commission, data on deaths from canceled accounted from the Public Security Bureau, and data on the deaths of infants, children and young people from the Department of Maternity and Infantry. In addition, the de-identification process was used to enhance the privacy of monitoring data and ensure the sensitization of data.

During 2010~2020, the proportion of submissions with morphological verification (MV%) of liver cancer in Guangzhou was 31.2%~48.2%. The mortality-to-incidence ration (M/I) of liver cancer spanned 80.5%~90.9%. Additionally, the proportion of submissions with a sole death certificate was 0.28%~0.76%. The morphological verification should not be too high because the pathological tissue of liver cancer is not easy to obtain, it is often confirmed by other laboratory-assisted diagnostic techniques. All of the above indicators pointed to good data quality. The incidence and mortality rates of liver cancer were stabilized compared with those of Guangzhou during 2004~2015, indicating that the data were highly credible. The requirement for ethics committee approval was waived due to the retrospective nature and anonymity of this study.

2.6 Statistical analysis

EXCEL 2019 was used to build a database of surveillance data, with statistical indicators including the number of morbidities, deaths, crude rates, and standardized rates, stratified by gender and age groups. Age-standardized rates were calculated using the age composition of the population from the sixth national census in 2010. Trend analysis was performed using the Joinpoint regression program (4.8.0.1) (29). The APC model was constructed and analyzed using the "Epi" package in the R language (30). All $p<0.05$ were considered statistically significant.

3 Results

3.1 Overall report on morbidity and mortality of liver cancer in Guangzhou, 2010~2020

In this study, a total of 26895 cases of liver cancer were identified during 2010~2020, with an average crude incidence rate of 28.03 per 100,000, of which 21502 were males and 5393 were females, and the crude incidence rate was significantly higher in males (44.61 per 100,000) than in females (11.28 per 100,000); In the past 11 years, a total of 23086 liver cancer deaths were confirmed, with an average crude death rate of 24.10 per 100,000, and the death rate reached 85.85%, including 18284 males and 4802 females. Among all liver cancer cases, the elderly over 64 years old accounted for 97.91%, but no more than half of liver cancer patients have undergone pathological examination (Supplementary Table S1).

3.2 Trends in AISR and ASMR among Guangzhou residents during 2010~2020

During 2010~2020, the ASIR of liver cancer patients declined from 23.23 per 100,000 to 22.28 per 100,000. Specifically, we discovered that the ASIR of the total population, males and females exhibited a growing trend from 2010 to 2015 (Figures 1A–C; Table 1). After 2015, all the populations showed a consistent downward trend. Both crude incidence and ASIR were considerably higher in males than in females. ASMR displayed a fluctuating decreasing trend from 2010 to 2020, it declined from 22.63 per 100,000 in 2010 to 18.26 per 100,000 in 2020 (Figures 1D–F; Table 2). As was shown in Figure 1G, the male-to-female incidence-mortality ratio is rapidly increasing following a consistent drop until 2016, with a growing gender disparity in morbidity-mortality risk.

3.3 Occupational composition and regional distribution of patients with liver cancer

Figures 1H, I depicted the age distribution of liver cancer cases across various occupations among males and females. It was evident that retired individuals had a relatively higher proportion of cases among the elderly of liver cancer, which progressively increased with age. The vast majority of cases affected those over the age of 50 years old. Compared with other occupations, the proportion of retirees (35.3% vs.24.1%) and farmers (5.7% vs. 5.3%) in females with liver cancer was higher than that of males. There was a greater percentage of males with liver cancer who were technicians (9.2% vs. 7.4%), enterprise managers (5.5% vs. 3.3%), and individual household (2.5% vs. 1.1%). In addition, no gender disparity was observed in the proportion of students with liver cancer in all occupational types.

Furthermore, Yuexiu District had the highest incidence, with an average of 933 cases per year over 11 years. Especially during 2016~2018, the number of cases from Yuexiu District exceeded 1,000 cases. Tianhe District had the second-highest number of cases, with an average of around 300 cases per year. On the contrary, Nansha District had the lowest number of cases, with an annual average of 51 cases (Figures 2A, B).

3.4 Age distribution of cases and deaths of liver cancer patients in Guangzhou, 2010~2020

Figures 2C, D exhibited the comprehensive age-density distribution of liver cancer incidence and mortality among males and females in Guangzhou during 2010~2020. Up to the age of 34 years old, the incidence densities of liver cancer in males and females remained

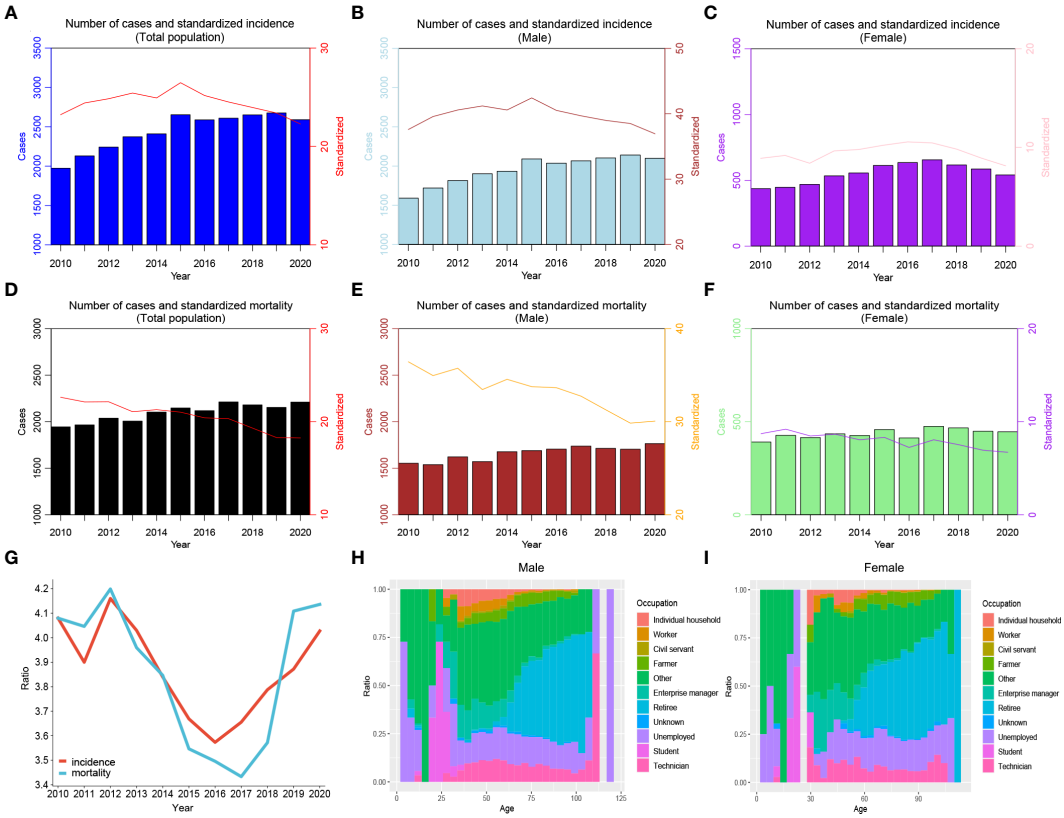

FIGURE 1
Trends of cases and age-standardized rates of liver cancer in Guangzhou, 2010~2020. **(A–C)** Number of cases and standardized incidence rates for the whole population, males and females; **(D–F)** Number of deaths and standardized mortality rates for the whole population, males and females; **(G)** Male-to-female ratios of liver cancer incidence and mortality; **(H)** The occupational composition of male liver cancer patients; **(I)** The occupational composition of female liver cancer patients.

relatively similar. However, among the population aged 34~74 years old, the incidence densities of liver cancer in males increased rapidly and are notably higher than those in females. Subsequently, over 74 years old, the incidence densities of liver cancer in males decreased significantly, while the densities in females exhibited a slight fluctuating pattern. Notably, over 87 years old, the incidence density among females started to decline. The age range with higher incidence densities among females occurred later compared to males, with two small peaks observed around the ages of 74 and 87 years old, respectively. The age distribution of incidence and mortality in different years appeared with the mountain range diagram, indicating it gradually moving towards the younger generation (Figures 3A–F).

3.5 Joinpoint regression fitting results of ASRs of liver cancer in Guangzhou, 2010~2020

3.5.1 Trends in regression fits for ASRs

The results indicated that the ASIR of liver cancer in the Guangzhou population generally declined during the 11 years, with females exhibiting a more rapid average rate of decline than males (AAPC=−0.9% vs. AAPC=−0.4%) (Figures 4A, D; Tables 3, 4). The risk of liver cancer steadily grows with age, and it rapidly increases over 85 years old (Figures 4B, E). Only one node is displayed in the optimal models for different populations. During 2010~2015, the ASIR of the total population, males showed a monotonous increasing trend (APC = 2.1%, 1.8%, respectively). During 2015~2020, the ASIR decreased steadily, and APC was −6.13%, −5.33%, respectively. For females, the ASIR exhibited a monotonically growing trend (APC=2.5%), and during 2016~2020, it suggested a falling trend (APC=−5.7%). As for ASMR, only the whole population showed a connection point, with consistently decreasing rates for both males and females.

3.5.2 Trend analysis of ASIR and ASMR for different age groups

As illustrated in Figures 4C–F, the risk of liver cancer incidence in the elderly aged 40~44 years and 70 years old and above is still on the rise, especially in the people aged 70~74 years (AAPC=6.9%). Furthermore, Tables 5, 6 suggested that although the rates of all age groups have decreased, the incidence and mortality of elderly people aged 65 years old and above are still at a high level. Thus, the elderly people still deserved a lot of attention. The risk of disease is still rising for middle-aged males (AAPC = 1.4%; AAPC = 0.5%). The mortality risk declined significantly among all age groups, with the 30~39 years old group experiencing a substantial decrease (AAPC > 5%). The incidence of females aged 35~39 showed a slight increase trend (AAPC=1%). Also, the incidence of elderly

TABLE 1 Crude incidence and ASIR of liver cancer in Guangzhou, 2010~2020.

Year	Crude incidence/100,000			Standardized incidence/100,000		
	Male	Female	Total	Male	Female	Total
2010	39.99	9.64	24.53	37.60	8.78	23.23
2012	41.78	10.22	26.20	39.58	9.15	24.42
2012	43.81	10.51	27.34	40.58	9.00	24.85
2013	45.41	11.46	28.60	41.20	9.62	25.43
2014	45.71	11.42	28.69	40.58	9.26	24.93
2015	48.67	13.23	31.05	42.43	10.55	26.48
2016	46.65	12.70	29.73	40.52	9.95	25.18
2017	46.00	12.09	29.06	39.69	9.50	24.52
2018	45.45	11.77	28.58	38.99	9.13	23.96
2019	45.08	11.17	28.06	38.51	8.59	23.4
2020	42.90	9.90	26.29	36.94	7.97	22.28

people aged over 70 years old increased but there was no significant statistical significance. For the risk of death, we observed a downward trend in women of all age groups.

3.6 Results of APC model of liver cancer morbidity and mortality in Guangzhou, 2010~2020

The age-trend (AT), age-cohort (AC), and age-period (AP) models were fitted and evaluated for liver cancer in Guangzhou City based on the number of incidences and fatalities in each age group, respectively. Ultimately, the APC model was selected for analyzing the data as the findings indicated that it had the best fitting effect and the smallest AIC value (Tables 7, 8).

As depicted in Figures 5A, C, the age, cohort, and period effects of the liver cancer patients compared to the reference cohort were displayed by the curves that flowed from left to right. Age-induced rates were presented on the left vertical axis, while the relative risk (RR) of the other two effects was displayed on the right vertical axis. The results showed that under the influence of age effect, the ASIR and ASMR of liver cancer in the total population of Guangzhou increased steadily, and rose exponentially after the age of 70 years old. The birth cohort effect of population-wide incidence exhibited the highest RR (1.42, 95%CI: 1.15~1.76) in the 1970~1974 cohort compared to that in the 1945~1949 cohort, which gradually declined after 1975 to 0.58 in 1995. For the cohort effect on mortality, those born in 1925~1950 had a relatively low risk of death (RR<1), and the effect in the birth cohort gradually increased after 1950 and peaked in 1965 (RR=1.32, 95% CI:1~1.74). During 1965 and 1995, there was a downward trend in the

TABLE 2 Crude mortality and ASMR of liver cancer in Guangzhou, 2010~2020.

Year	Crude mortality/100,000			Standardized mortality/100,000		
	Male	Female	Total	Male	Female	Total
2010	38.09	9.87	24.23	36.44	8.72	22.63
2011	37.38	10.64	24.18	34.96	9.2	22.13
2012	39.15	10.24	24.85	35.75	8.47	22.15
2013	37.53	10.58	24.19	33.46	8.66	21.08
2014	39.66	10.22	25.05	34.56	8.06	21.3
2015	39.34	10.78	25.14	33.77	8.32	21.03
2016	39.07	9.52	24.34	33.66	7.24	20.42
2017	38.67	10.59	24.65	32.75	8.06	20.33
2018	37.03	10.05	23.51	31.29	7.54	19.32
2019	35.90	9.38	22.59	29.85	6.94	18.3
2020	36.08	8.99	22.44	30.07	6.72	18.26

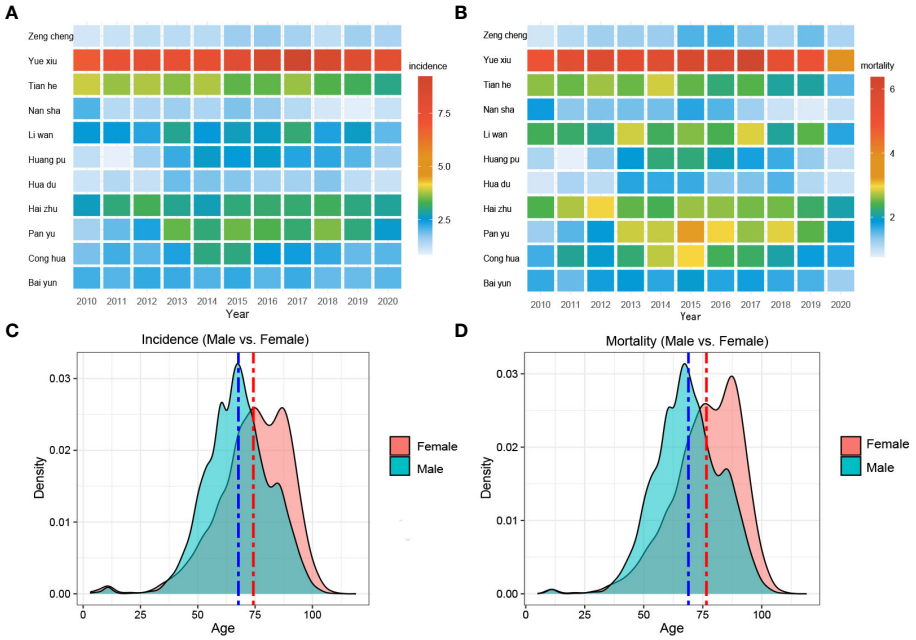

FIGURE 2
Morbidity, mortality, and age composition of liver cancer in various districts of Guangzhou. **(A)** Morbidity and **(B)** mortality in different districts of Guangzhou, 2010~2020; **(C)** Morbidity density and **(D)** mortality density in different age groups among males and females, 2010~2020.

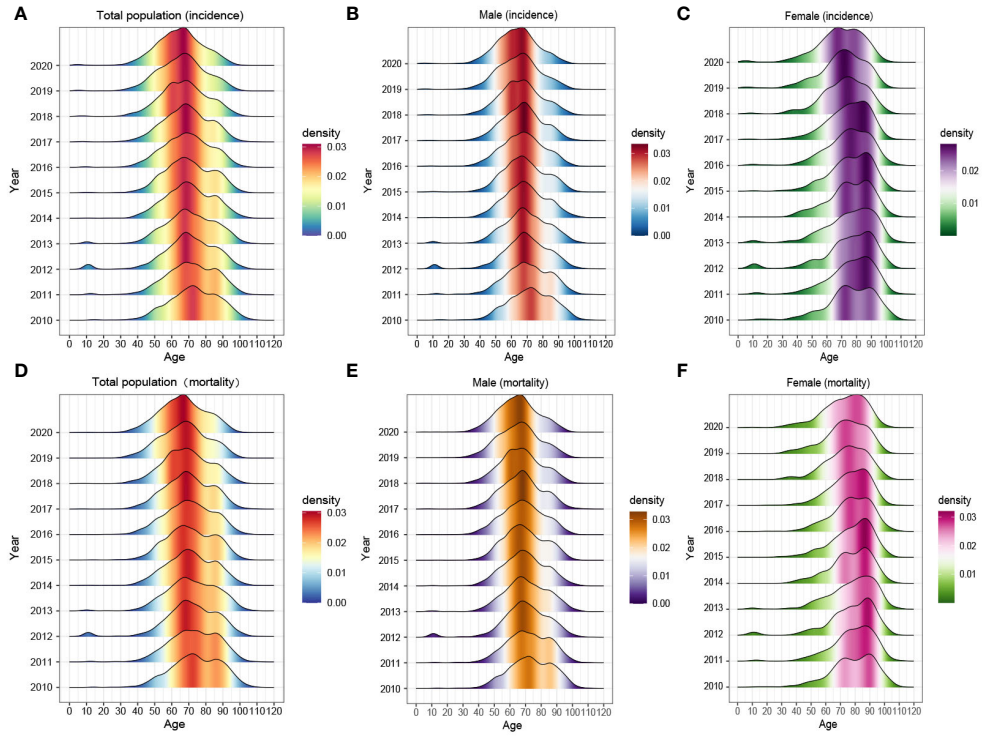

FIGURE 3
The age composition of **(A–C)** morbidity and **(D–F)** mortality of the whole population, males and females in Guangzhou, 2010~2020.

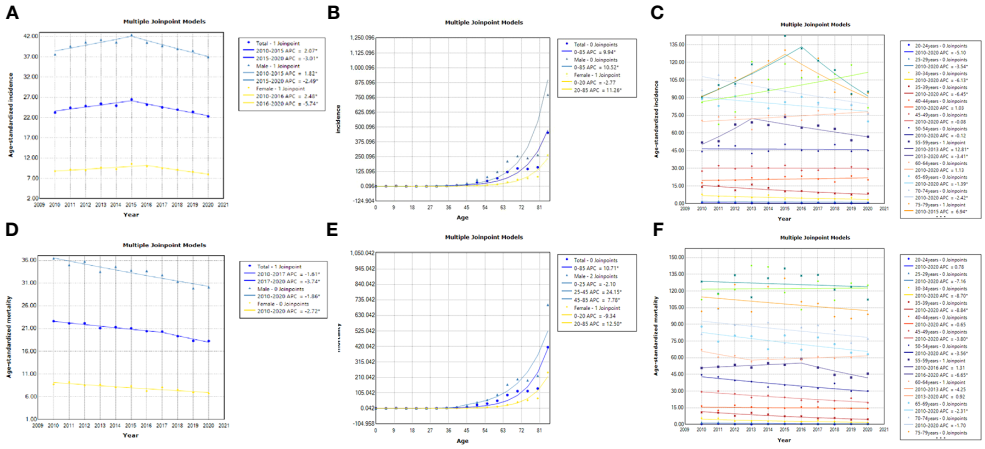

FIGURE 4
Results of the JPR model for ASIR and ASMR for the whole population, males and females, Guangzhou, 2010~2020. **(A, D)** Trends in ASIR and ASMR among different populations; **(B, E)** Age-related trends in liver cancer incidence and mortality among different populations; **(C, F)** Trends in ASIR and ASMR among different age groups.

cohort effect, with the youngest generation presenting the lowest risk (RR=0.68, 95%CI: 0.49 to 0.96).

Since the incidence density of males and females varies with age, APC models are constructed separately (Figures 5B, D). In terms of the age effect, the incidence rate for males increased significantly faster than that for females. The birth cohort effect can be categorized into two phases of incidence for both sexes, with an upward trend followed by a steady decline until 1970 and 1960, respectively. The RR values of morbidity and mortality decreased from 0.79 (95%CI: 0.54~1.15) and 0.68 (95%CI: 0.46~1.02) in males born in 1925~1929 to 0.68 (95%CI: 1~1.74) and 0.59 (95%CI: 0.39~0.90) in males born in 1995~1999. For females, the RR values of morbidity and mortality were 0.55 (95%CI: 0.27~1.11) and 0.51 (95%CI: 1~1.74), respectively, and it is unfavorable that RR rose to 0.69 (95% CI: 0.35-1.38) and 0.68 (95% CI: 0.33-1.41) in the latest birth cohort. Furthermore, compared to the reference cohort, among males, the risk of morbidity and mortality for liver cancer decreased by 32% and 41%, respectively. For women, the risk of morbidity and mortality decreased by 32% and 41%, respectively (Tables 9, 10).

3.7 Verification of robustness of results in estimable function method

The age, period, and cohort effects under the estimable function method in this study essentially followed the same pattern in terms

TABLE 3 Trend of ASIR for liver cancer in Guangzhou, 2010~2020.

Group	Year	EAPC (95%CI)	*Z*	*P*	AAPC (95%CI)	*Z*	*P*
Total	2010-2015	2.1* (-0.8, 3.4)	3.9	0.008	-0.5 (-1.2, 0.2)	-1.4	0.175
	2015-2020	-3.0* (-4.2, -1.8)	-5.8	0.001			
Male	2010-2015	1.8* (0.5, 3.2)	3.4	0.015	-0.4 (-1.1, -0.4)	-1.0	0.340
	2015-2020	-2.5* (-3.8, -1.2)	-4.7	0.003			
Female	2010-2016	2.5* (0.5, 4.5)	3.1	0.022	-0.9 (-2.4, 0.6)	-1.2	0.246
	2016-2020	-5.7* (-9.1, -2.2)	-3.9	0.008			

ASIR, age-standardized incidence; ASMR, age-standardized mortality; EAPC, estimated annual percentage change; AAPC, average annual percentage change.

TABLE 4 Trend of ASMR for liver cancer in Guangzhou, 2010-2020.

Group	Year	EAPC (95%CI)	*Z*	*P*	AAPC (95%CI)	*Z*	*P*
Total	2010-2017	-1.6* (-2.3, -1.0)	-6.1	0.001	-2.3* (-2.9, -1.6)	-6.5	0.001
	2017-2020	-3.7* (-6.1, -1,4)	-1.4	0.009			
Male	2010-2020	–	–	–	-1.9* (-2.4, -1.4)	-8.3	0.001
Female	2010-2020	–	–	–	-2.7* (-3.7, -1.8)	-6.4	0.001

TABLE 5 Changes in the incidence of different age groups, 2010~2020.

Age group	Period	AAPC (95%CI)		
		Total	Male	Female
20-24	2010-2020	-5.1 (-12.1, 2.5)	-3.4 (-17.8, 13.4)	-4.1 (-15.5, 8.8)
25-29	2010-2020	-3.5* (-6.6, -0.4)	-3.3 (-10.9, 5.1)	-3 (-12.9, 7.9)
30-34	2010-2020	-6.1* (-9.7, -2.4)	-6.2* (-10.1, -2.2)	-6.6* (-12.4, -0.4)
35-39	2010-2020	-6.4* (-9, -3.9)	-6.0* (-8.8, -3.1)	1* (0.4, 6.3)
40-44	2010-2020	1* (0.9, 3)	1.4* (0.6, 3.4)	-0.8 (-6.1, 4.8)
45-49	2010-2020	-0.1 (-1.3, 1.2)	0.5* (0.2, 1.8)	-0.8 (-6.4, 5.2)
50-54	2010-2020	-0.1 (-1.5, 1.2)	0.2 (-1.2, 1.6)	-1.6 (-4.3, 1.1)
55-59	2010-2020	1.2 (-2.2, 4.7)	1.5 (-1.4, 4.6)	0 (-2.4, 2.4)
60-64	2010-2020	1.1 (-0.1, 2.4)	1.5* (0, 2.9)	-2.5 (-6.3, 1.6)
65-69	2010-2020	-1.4* (-2.7, 0)	-0.9 (-2.2, 0.4)	-3.2 (-12.3, 6.7)
70-74	2010-2020	6.9* (1.1, 13.1)	-2.6* (-4, -1.3)	0.5 (-5.4, 6.8)
75-79	2010-2020	-0.1 (-3.3, 3.1)	-0.5 (-3.3, 2.5)	3.4 (-4.3, 11.7)
80-84	2010-2020	0.0 (-4.7, 4.9)	-0.4 (-6.1, 5.6)	3.9 (-1.9, 10)
85+	2010-2020	-5.1 (-12.1, 2.5)	1 (-2.2, 4.4)	-4.1 (-15.5, 8.8)

of the stability of the parameter estimates under the above two constraints, with minor variations in the slope and magnitude of the increase in morbidity or mortality (Figures 5A–D). In terms of the consistency between the parameter estimates and the biological evidence, the age effects of both ZLT-C and ZLT-P methods increase with age, indicating that the risk of liver cancer increased exponentially with age, which was in accordance with the expected pattern of the age effect. For the cohort effect, both exhibited an upward tendency followed by a downward trend during 1925~2000, which was in line with the typical cohort effect pattern. All of the above suggested that the results are robust.

4 Discussion

In this study, the ASIR and ASMR of liver cancer among males and females in Guangzhou exhibited a declining trend during 2010~2020, which was in line with the pattern of declining

TABLE 6 Changes in the mortality of different age groups, 2010~2020.

Age group	Period	AAPC (95%CI)		
		Total	Male	Female
20-24	2010-2020	0.8* (0.1, 2.1)	-12.4 (-27, 5.1)	-8.1 (-23.7, 10.6)
25-29	2010-2020	-7.2 (-16.5, 3.2)	-8.8 (-17.8, 1.2)	-1.3 (-19.2, 20.6)
30-34	2010-2020	-8.7* (-13.1, -4.1)	-9.3* (-13.5, -5)	-0.3 (-13.9, 15.5)
35-39	2010-2020	-8.8* (-11.3, -6.3)	-7.8* (-10.3, -5.2)	-15.2 (-31.2, 4.6)
40-44	2010-2020	-0.7 (-2.5, 1.2)	0.4 (-1.9, 2.8)	-5.5* (-10.6, -0.2)
45-49	2010-2020	-3.8* (-5.2, -2.4)	-3.2* (-5, -1.4)	-5.3 (-10.7, 0.5)
50-54	2010-2020	-3.6* (-4.9, -2.2)	-3.1* (-4.5, -1.8)	-5.1 (-10.4, 0.5)
55-59	2010-2020	-2.0 (-4.1, -1)	-2 (-4.2, 0.3)	-3.3 (-7, 0.6)
60-64	2010-2020	-0.7 (-2.1, 0.8)	0.5 (-0.7, 1.8)	-4.2* (-6.4, -1.9)
65-69	2010-2020	-2.3* (-3.9, -0.7)	-2.0* (-3.5, -0.4)	-2.8 (-6.2, 0.8)
70-74	2010-2020	-1.7 (-3.6, 0.3)	-1.8 (-4, 0.4)	-0.7 (-4.6, 3.3)
80-84	2010-2020	-1.1 (-3.5, 1.3)	-1.4 (-3.8, 1)	-0.7 (-4.3, 3)
85+	2010-2020	-0.4 (-2.0, 1.3)	-0.4 (-2.8, 2.1)	0.9 (-2.8, 4.6)

TABLE 7 Comparison of fitting results for the incidence of different sub-models of APC.

Term	Model	Residual degree of freedom	Residual	AIC	*P*-value
Total liver cancer incidence	Age	21	49.9	246.6	<0.01
	Age-trend	20	49.7	248.5	<0.01
	Age-period	20	49.4	248.7	<0.01
	Age-cohort	15	32.5	241.2	<0.01
	Age-period-cohort	15	32.1	239.4	<0.01
Male liver cancer incidence	Age	22	46.7	234.1	<0.01
	Age-trend	21	46.6	236.1	<0.01
	Age-period	21	46.4	236.4	<0.01
	Age-cohort	16	37.7	236.8	<0.01
	Age-period-cohort	16	37.4	236.0	<0.01
Female liver cancer incidence	Age	21	8.3	160.9	<0.01
	Age-trend	20	7.6	162.2	<0.01
	Age-period	20	7.2	162.4	<0.01
	Age-cohort	15	4.7	169.4	<0.01
	Age-period-cohort	15	4.5	156.0	<0.01

mortality of liver cancer among urban and rural population in China reported by Sun et al. (31). APC analysis suggested that the effect of birth cohort increased initially and subsequently reduced over time. Individuals born in 1965~1969 had the relatively highest risk of liver cancer incidence and mortality, validating the previous trend of increasing risk in middle-aged populations. Fortunately, those born during 1995~1999 experienced a lower risk of liver cancer as compared to the reference cohort (1950~1954). In addition, the incidence and mortality of liver cancer varied greatly among different districts in Guangzhou, especially in Yuexiu District, which might be caused by the higher proportion of the elderly, living habits, and urbanization rate.

Although the ASIR and ASMR of liver cancer in Guangzhou appeared to be a downward trend, the risk remained higher relative to other regions in southern China. A study reported that the prevalence of HBsAg in the population under 50 years old in Guangzhou in 2018 (9.5%) was substantially lower than that ten years ago (12.45%), but it was still higher than the national average (6.1%) and southern cities (7.4%) (32). A series of driving stimuli caused by HBV promotes the transformation of liver cells, leading to DNA damage, aging, chronic inflammation, hepatitis, cirrhosis, impairing the immune system, and eventually leading to liver cancer (33–35). China began to promote the use of hepatitis B vaccine in 1992, and the inclusion of hepatitis B vaccine in the child immunization program in 2002 was an important measure for the prevention and control of the hepatitis B epidemic (36, 37). Despite the fact that the vaccination proved to be effective primary prevention measure, comprehensive neonatal hepatitis B vaccination policy has only been implemented in East Asian countries such as China and South Korea for about 30 years, and the average duration of hepatitis B vaccination is only 5~10 years, indicating that risk inhibition has not yet been fully reflected. The current decline in the incidence of liver cancer is mainly related to measures to control aflatoxin intake (38). The current downward trend may be mainly related to a decrease in aflatoxin intake.

The male-to-female incidence and mortality ratio of liver cancer declined and then continued to rise, and the gender disparity is still growing. According to previous epidemiological researches, males were nearly threefold more probable than females to suffer from liver cancer. It was discovered more than 60 years ago that sex

TABLE 8 Comparison of fitting results for the mortality of different sub-models of APC.

Term	Model	Residual degree of freedom	Residual	AIC	*P*-value
Total liver cancer mortality	Age	21	39.6	230.9	<0.01
	Age-trend	20	31.9	225.2	<0.01
	Age-period	20	31.8	225.1	<0.01
	Age-cohort	15	24.9	228.3	<0.01
	Age-period-cohort	15	24.5	226.4	<0.01
Male liver cancer mortality	Age	21	42.9	225.8	<0.01
	Age-trend	20	38.2	223.1	<0.01
	Age-period	20	38.1	223.0	<0.01
	Age-cohort	15	28.9	223.8	<0.01
	Age-period-cohort	15	28.6	221.5	<0.01
Female liver cancer mortality	Age	21	7.6	153.1	<0.01
	Age-trend	20	6.4	153.8	<0.01
	Age-period	20	6.3	153.7	<0.01
	Age-cohort	16	4.1	159.5	<0.01
	Age-period-cohort	16	4.0	151.4	<0.01

hormones exerted a major impact on the shape and function of the liver in humans, and that estrogen in women had a more effective protective effect on the liver (39).

The average age of the occurrence and death in males is 7~8 years earlier than in females. The estrogen/androgen signaling pathway is not only associated with HBV gene transcription and viral replication but also influences the occurrence of liver cancer by inducing epigenetic modifications (40). There is also growing evidence that there are significant gender disparities in HBV-related liver cancer, with women experiencing a better prognosis (41). Various behavioral risk factors such as smoking, alcohol consumption, host stress, immune response, and psychological, metabolic, and sex differences in tumor biology have been attributed to this (42). In addition, Guangzhou is also profoundly affected by traditional alcohol culture, and the study showed that the drinking rate of local adults was much higher than that of the national adults in 2018 (39.8%) (43). The per capita alcohol consumption of males in Guangzhou (15.74g) was significantly higher than that in females (3.13g) (44, 45). Long-term alcohol users frequently develop cirrhosis, and drinking 100 grams of alcohol daily increases the risk of cirrhosis by 27 times. Studies have shown that East Alcohol consumption of Asians are prone to cancer, among which liver cancer, esophageal cancer, and breast cancer are most common types (46). Therefore, health education for males with bad drinking behavior should be strengthened. Retirees, unemployed people, professionals and technicians are the occupational categories with a higher incidence of liver cancer. Above population might be exposed to more carcinogens in their long-term life and work, such as environmental pollution and toxins. Additionally, rising age can result in a chronic immune system deterioration, allowing the hepatitis virus to continue living in the body and develop into liver cancer.

JPR model analysis showed that the ASIR and ASMR of liver cancer in Guangzhou residents decreased steadily during 2010 ~2020, which was not only related to the improved awareness and healthier living habits of residents, but also inseparable from the medical investment and policy support of Guangzhou government in the prevention and control of chronic diseases. According to the optimal JPR model, the trend of ASIR exhibited only one link point in 2015. Guangdong province issued the

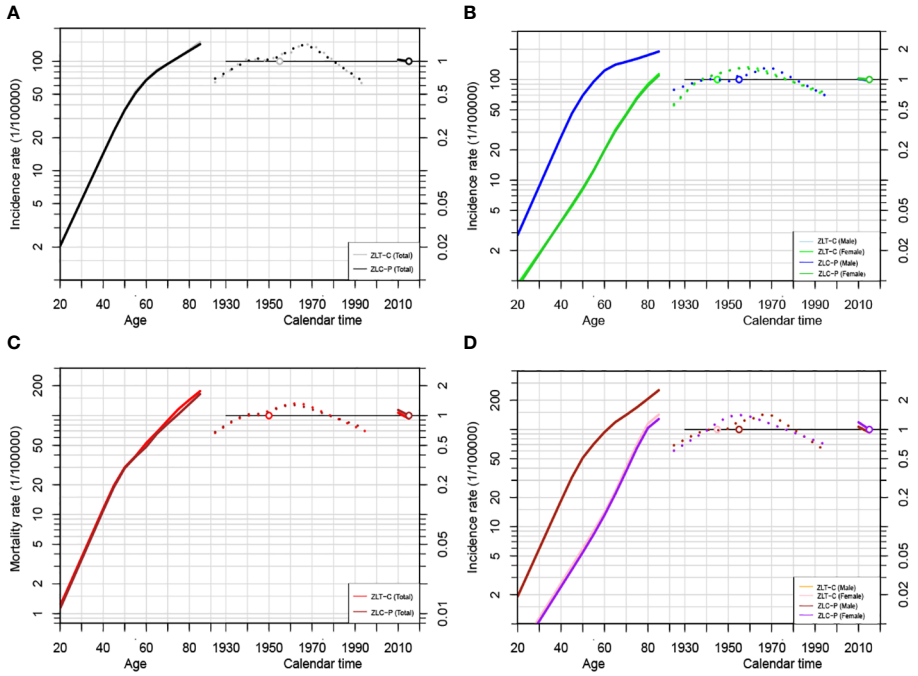

FIGURE 5
Age-Period-Cohort modeling results of liver cancer incidence and mortality in Guangzhou, 2010~2020. **(A)** APC analysis for incidence of the total population by ZLT-P and ZLT-C method; **(B)** APC analysis for incidence of males and females by ZLT-P and ZLT-C method; **(C)** APC analysis for mortality of the total population by ZLT-P and ZLT-C method; **(D)** APC analysis for mortality of males and females by ZLT-P and ZLT-C method.

"Guangdong Three-Year Action Plan for Cancer Prevention and Treatment (2015~2017)" in 2016, environmental protection and tobacco control had been vigorously strengthened, and tumor surveillance and follow-up have been enhanced, resulting in the improved screening rate of liver cancer and reducing the burden of cancer. Unfortunately, the risk of morbidity in the 40~49 age group is still rising, which can be attributed to the psychological state of anxiety associated with the high-pressure life, unhealthy dietary habits, and increased frequency of smoking and alcohol consumption among the middle-aged population. In the elderly aged over 65 years old, the incidence has declined but still remains at a high level. Therefore, the early screening and management of liver cancer in the elderly population is still the focus of prevention and treatment.

APC model analysis quantitatively explored the three effects and investigated the impacts of factors such as natural environment, social economy, lifestyle, diet, and medical technology on the trend of incidence and mortality from a macro perspective. In our study, by comparing the residuals of the APC sub-models, it is evident that the cohort effect is more significant relative to that of the birth cohort. The results of the age effect proved that the risk of liver cancer incidence and mortality among Guangzhou residents increased with age and rose exponentially once they reached 70 years old, which was related to the increase of basic diseases and the reduction of physiological functions in the elderly. Although Guangzhou is economically prosperous, the city is densely populated and still in the stage of mild aging. Data released by the Guangzhou Municipal Health Commission in 2023 indicated that there would be 483,100 floating population aged over 60 years old in Guangzhou in 2022, an increase of 12.28% compared with last year. As for the cohort effect, the RR values for the risk of liver cancer in the total population decreased with the birth cohort, which is consistent with the results of national and another research in Guangzhou on liver cancer during 2004~2015 (17, 19). The prevalence of HBsAg in Guangzhou decreased significantly from 1992 to 1995. Additionally, The Xijiang Drinking Water Project, initiated by Guangzhou in 2009, improved sanitation management, made it possible for locals to have access to the cleaner water, and successfully prevented the hepatitis virus infection. With certain slight deviations from other regions, the RR values of incidence risk for males and females increased linearly during 1925~1970 and 1925~1965 before steadily dropping. This pattern was essentially similar to the trend in Tianjin, China. Men born after 1920 experienced a monotonically declining risk of liver cancer as the birth cohort became younger in Australia, Serbia, and South Korea (14, 16, 47, 48). The period during 1925 ~1945 was characterized by civil war, deteriorating living circumstances, underdeveloped medical technology, lack of an effective medical security system, and an immature tumor surveillance and reporting system. After 1949, the living conditions of Guangzhou inhabitants gradually improved. During 1958~1965, the "Great Leap Forward", the "People's Commune Movement" led to low social productivity and economic downturn. The development of AFP and ultrasonography screening techniques in 1970 further improved

TABLE 9 Results of APC model on the incidence of liver cancer .

Group	Age-period-cohort(Incidence/RR)		
	Total	Male	Female
Age			
20-24	0.28 (0.20, 0.38)	0.22 (0.14, 0.34)	0.21 (0.11, 0.40)
25-29	0.63 (0.48, 0.80)	0.62 (0.44, 0.86)	0.37 (0.22, 0.63)
30-34	2.04 (1.50, 2.77)	2.85 (1.97, 4.12)	0.91 (0.44, 1.88)
35-39	3.31 (2.67, 4.10)	5.00 (3.89, 6.42)	1.31 (0.79, 2.18)
40-44	5.38 (4.71, 6.14)	8.77 (7.55, 10.10)	1.88 (1.37, 2.58)
45-49	8.74 (7.89, 9.68)	15.30 (13.70, 17.20)	2.69 (2.18, 3.32)
50-54	14.10 (12.10, 16.50)	26.90 (22.20, 32.60)	3.85 (2.86, 5.19)
55-59	22.90 (18.20, 28.80)	46.00 (35.10, 60.40)	5.54 (3.47, 8.83)
60-64	36.10 (28.60, 45.60)	69.50 (54.20, 89.00)	8.12 (4.60, 14.30)
65-69	53.00 (43.20, 65.10)	95.30 (76.30, 119)	12.40 (7.34, 20.90)
70-74	94.90 (82.50, 109)	150 (127, 176)	45.30 (33.50, 61.10)
75-79	108 (94.70, 124)	161 (139, 186)	66.40 (49.20, 89.60)
80-84	127 (108, 150)	174 (144, 211)	89.60 (60.10, 133)
85-89	149 (113, 197)	189 (136, 263)	113 (62.80, 203)
Period			
2010-2014	1.01 (0.98, 1.04)	1.01 (0.98, 1.04)	1.01 (0.93, 1.09)
2015-2019	0.97 (0.94, 1.01)	0.98 (0.94, 1.02)	0.98 (0.90, 1.07)
Cohort			
1925-1929	0.64 (0.46, 0.88)	0.79 (0.54, 1.15)	0.55 (0.27, 1.11)
1930-1934	0.76 (0.62, 0.94)	0.86 (0.68, 1.09)	0.72 (0.46, 1.15)
1935-1939	0.92 (0.81, 1.04)	0.94 (0.82, 1.07)	0.92 (0.65, 1.30)
1940-1944	1.05 (0.91, 1.21)	1.01 (0.87, 1.17)	1.03 (0.77, 1.38)
1945-1949	1.02 (0.89, 1.17)	1.00 (0.84, 1.18)	1.13 (0.83, 1.55)
1950-1954	1.01 (0.85,1.20)	0.95 (0.78, 1.15)	1.21 (0.82, 1.79)
1955-1959	1.15 (0.95, 1.40)	1.10 (0.89, 1.37)	1.29 (0.81, 2.07)
1960-1964	1.18 (0.95, 1.48)	1.10 (0.87, 1.40)	1.33 (0.74, 2.36)
1965-1969	1.42 (1.12, 1.80)	1.28 (0.98, 1.67)	1.26 (0.73, 2.17)
1970-1974	1.42 (1.15, 1.76)	1.30 (1.02, 1.66)	1.15 (0.80, 1.65)
1975-1979	1.22 (1.08, 1.37)	1.16 (1.01, 1.34)	1.04 (0.88, 1.22)
1980-1984	1.01 (0.97, 1.06)	1.02 (0.97, 1.07)	0.94 (0.86, 1.02)
1985-1989	0.84 (0.75, 0.95)	0.89 (0.78, 1.02)	0.85 (0.65, 1.12)
1990-1994	0.70 (0.56, 0.88)	0.78 (0.6, 1.01)	0.77 (0.48, 1.24)
1995-1999	0.58 (0.42, 0.81)	0.68 (0.47, 1.00)	0.69 (0.35, 1.38)

TABLE 10 Results of APC model on the mortality of liver cancer.

Group	Age-period-cohort (Mortality/RR)		
	Total	Male	Female
Age			
20-24	1.20 (0.83, 1.72)	1.91 (1.29, 2.83)	0.51 (0.24, 1.07)
25-29	2.10 (1.63, 2.71)	3.37 (2.57, 4.44)	0.76 (0.44, 1.32)
30-34	3.70 (3.16, 4.33)	5.96 (5.00, 7.09)	1.15 (0.80, 1.67)
35-39	6.51 (5.82, 7.28)	10.50 (9.17, 12.00)	1.74 (1.34, 2.26)
40-44	11.40 (9.69, 13.50)	18.50 (15.20, 22.50)	2.63 (1.95, 3.54)
45-49	19.60 (15.30, 25.20)	32.20 (24.10, 42.80)	3.96 (2.53, 6.20)
50-54	29.90 (23.00, 39.00)	51.00 (38.10, 68.50)	5.98 (3.26, 10.90)
55-59	38.80 (30.80, 48.90)	70.70 (54.90, 90.90)	9.08 (4.86, 16.90)
60-64	52.70 (43.10, 64.40)	93.90 (74.90, 117)	14.00 (8.63, 22.90)
65-69	68.10 (57.40, 80.80)	119 (97.50, 145)	23.20 (15.90, 33.80)
70-74	89.30 (78.20, 102)	141 (119, 167)	41.10 (30.00, 56.30)
75-79	116 (99.00, 136)	169 (142, 200)	71.30 (51.30, 99.10)
80-84	143 (120, 172)	206 (168, 253)	114 (72.50, 181)
85-89	176 (132, 234)	253 (180, 356)	142 (74.30, 271)
Period			
2010-2014	1.06 (1.02, 1.10)	1.06 (1.02, 1.10)	1.08 (0.98, 1.19)
2015-2019	0.93 (0.89, 0.96)	0.93 (0.89, 0.97)	0.91 (0.82, 1.01)
Cohort			
1925-1929	0.66 (0.47, 0.94)	0.68 (0.46, 1.02)	0.60 (0.28, 1.27)
1930-1934	0.78 (0.63, 0.97)	0.78 (0.61, 1.01)	0.70 (0.42, 1.17)
1935-1939	0.91 (0.78, 1.07)	0.90 (0.77, 1.05)	0.82 (0.56, 1.19)
1940-1944	0.99 (0.87, 1.14)	0.99 (0.83, 1.18)	0.97 (0.75, 1.26)
1945-1949	1.01 (0.86, 1.18)	0.98 (0.83, 1.15)	1.17 (0.84, 1.61)
1950-1954	1.11 (0.92, 1.34)	1.02 (0.82, 1.25)	1.38 (0.88, 2.15)
1955-1959	1.22 (0.99, 1.50)	1.22 (0.96, 1.55)	1.42 (0.81, 2.49)
1960-1964	1.31 (1.03, 1.67)	1.24 (0.95, 1.63)	1.36 (0.72, 2.57)
1965-1969	1.32 (1.00, 1.74)	1.41 (1.05, 1.91)	1.25 (0.72, 2.16)
1970-1974	1.21 (0.98, 1.48)	1.39 (1.06, 1.81)	1.14 (0.80, 1.61)
1975-1979	1.08 (0.98, 1.19)	1.19 (1.03, 1.38)	1.03 (0.89, 1.18)
1980-1984	0.96 (0.92, 1.00)	1.00 (0.95, 1.06)	0.93 (0.84, 1.02)
1985-1989	0.86 (0.76, 0.98)	0.84 (0.73, 0.98)	0.84 (0.62, 1.13)
1990-1994	0.77 (0.61, 0.97)	0.71 (0.53, 0.94)	0.76 (0.45, 1.26)
1995-1999	0.68 (0.49, 0.96)	0.59 (0.39, 0.90)	0.68 (0.33, 1.41)

the detection level of liver cancer. However, the cohort effect gradually diminished as the birth cohort progressed. From 1967 to 1976, the patriotic health movement and rural cooperative medical care were widely popularized (49). Since 1978, there has been a steady decrease in the incidence and mortality risk of liver cancer due to the promotion of reform and open policy, improved social and medical environments, and a higher quality of living conditions. Overall, the cohort effect of morbidity was most

significant for males born in 1970~1974 and females born in 1960~1964, confirming the previously increasing risk of morbidity in males aged 40~49 years old, with the cohort born in 1965~1969 having the highest risk of death. Overall, the above-mentioned findings effectively demonstrated the significant impact of early life exposure on individual's vulnerability to diseases and eventual death in late adulthood.

Furthermore, we used the ZLT-P formula in the method of "Equality Restrictions" to solve the unidentifiable problem of the model, and further verified the robustness of the results with the ZLT-C method in our current study, discovering that the trends of the two models are basically the similar. Mason, Rogers, and Holford (26) proposed that the stability of parameter estimates is critical when employing the same method for parameter estimation. Second, verifiable experience and theory supported the conclusion that the RR values of the age effect conformed to the exponential growth of the biological curves (50). The cohort effect also reasonably reflected the fluctuation of natural disasters in the three years after the Anti-Japanese War, and the protective effect followed the founding of the People's Republic of China, especially after the reform and open policy. Finally, the test statistics of the model, such as AIC and deviation statistics, demonstrated the statistical superiority of our model results.

In conclusion, during 2010~2020, the ASIR and ASMR of liver cancer in Guangzhou showed a downward trend, indicating that the early screening, prevention, clinical diagnosis, and treatment of liver cancer in Guangzhou have achieved remarkable outcomes in recent years. However, it doesn't mean we can ease up on our efforts to prevent liver cancer. The results of the APC model suggested that the latest birth cohort in Guangzhou had a lower risk of liver cancer. Compared with the reference cohort, the risk of liver cancer in males decreased by 32% and 41% and decreased by 31% and 32% in females, respectively. Furthermore, more attention should be paid to high-risk groups such as middle-aged males aged 40~44 and the elderly over 65 years old. Efforts should be focused on tertiary prevention to better tackle the disease burden caused by liver cancer. In the future, it is absolutely essential to identify the causes of disease through large-scale epidemiological cohorts and make targeted interventions for high-risk populations. Secondly, early detection, diagnosis, and treatment should be strengthened to control the rapid progression of liver cancer. Finally, it is imperative to conduct a thorough assessment of the impact of clinical treatment interventions, enhance the quality of life and the input-output ratio. Specifically, it is important for adults to be properly vaccinated. Hepatitis B patients should maintain healthy diets and antiviral therapies to reduce inflammatory stimuli triggered via alcohol and tobacco use in the middle-aged population, and receive regular medical screenings.

Of course, our study has certain limitations. As it focuses on descriptive analysis of trends, the contribution of various specific exposure factors cannot be quantified. Also, rapidly advancing medical technologies and governmental measures affect the level of cancer screening, and continuous monitoring of cancer trends can help to adjust prevention and control measures. In the future, it is necessary to further expand the period range and collect information on specific subtypes or specific etiological types of liver cancer. Furthermore, the survival analysis of the included subjects helps to obtain more complete results and provides more rigorous data support for the policy of liver cancer.

Data availability statement

The original contributions presented in the study are included in the article/Supplementary Material. Further inquiries can be directed to the corresponding authors.

Ethics statement

Ethical approval was not required for the study involving humans in accordance with the local legislation and institutional requirements. Written informed consent to participate in this study was not required from the participants or the participants' legal guardians/next of kin in accordance with the national legislation and the institutional requirements.

Author contributions

DWa: Conceptualization, Funding acquisition, Writing – original draft, Writing – review & editing. XH: Formal analysis, Methodology, Software, Writing – original draft, Writing – review & editing. HX: Data curation, Writing – review & editing. YC: Methodology, Supervision, Writing – review & editing. SW: Data curation, Writing – review & editing. GL: Data curation, Supervision, Writing – review & editing. LY: Writing – review & editing. JC: Data curation, Writing – review & editing. LZ: Project administration, Supervision, Writing – review & editing. PQ: Data curation, Methodology, Supervision, Writing – review & editing. DWu: Supervision, Writing – review & editing. BL: Project administration, Supervision, Writing – review & editing.

Funding

The author(s) declare financial support was received for the research, authorship, and/or publication of this article. This work was funded by the National Natural Science Foundation of China (81803325), Natural Science Foundation of Guangdong Province (2021A1515011175, 2024A1515011646), Guangzhou Science and Technology Project (202102080126), Basic Research Project of Key Laboratory of Guangzhou (202102100001, 202206080008), Medical

Science and Technology Foundation of Guangdong (A2024733), The Key Project of Medicine Discipline of Guangzhou (2021-2023-12).

Acknowledgments

We thanks to all hospitals and health workers which involved in the Cancer Surveillance System of Guangzhou in this research.

Conflict of interest

The authors declare that the research was conducted in the absence of any commercial or financial relationships that could be construed as a potential conflict of interest.

Publisher's note

Supplementary material

The Supplementary Material for this article can be found online at: https://www.frontiersin.org/articles/10.3389/fonc.2024.1387587/full#supplementary-material

References

1. Gravitz L. Liver cancer. *Nature*. (2014) 516:S1. doi: 10.1038/516S1a

2. Forner A, Reig M, Bruix J. Hepatocellular carcinoma. *Lancet (London England)*. (2018) 391:1301–14. doi: 10.1016/S0140-6736(18)30010-2

3. Llovet JM, Kelley RK, Villanueva A, Singal AG, Pikarsky E, Roayaie S, et al. Hepatocellular carcinoma. *Nat Rev Dis Primers*. (2021) 7:6. doi: 10.1038/s41572-020-00240-3

4. Younossi ZM, Wong G, Anstee QM, Henry L. The global burden of liver disease. *Clin Gastroenterol Hepatol*. (2023) 21:1978–91. doi: 10.1016/j.cgh.2023.04.015

5. Zhou Y, Li Y, Zhou T, Zheng J, Li S, Li HB. Dietary natural products for prevention and treatment of liver cancer. *Nutrients*. (2016) 8:156. doi: 10.3390/nu8030156

6. Dong H, Chen Y, Li K, Liang B, Lin G, Qin P. Mortality and trends of liver cancer in Guangzhou City, 2010–2019. *Pract Prev Med*. (2021) 28:1315–8. doi: 10.3969/j.issn.1006-3110.2021.11.009

7. Abolhosseini M, Khorrami Z, Safi S, Akbari ME, Moshtaghion SM, Mohammadi SF, et al. A joinpoint and age-period-cohort analysis of ocular cancer secular trends in Iran from 2004 to 2016. *Sci Rep*. (2023) 13:1074. doi: 10.1038/s41598-022-26349-x

8. Wu W, Feng A, Ma W, Li D, Zheng S, Xu F, et al. Worldwide long-term trends in the incidence of nonalcoholic fatty liver disease during 1990-2019: A joinpoint and age-period-cohort analysis. *Front Cardiovasc Med*. (2022) 9:891963. doi: 10.3389/fcvm.2022.891963

9. Gao Y, Liu X. Secular trends in the incidence of and mortality due to Alzheimer's disease and other forms of dementia in China from 1990 to 2019: an age-period-cohort study and joinpoint analysis. *Front Aging Neurosci*. (2021) 13:709156. doi: 10.3389/fnagi.2021.709156

10. Sedeta E, Sung H, Laversanne M, Bray F, Jemal A. Recent mortality patterns and time trends for the major cancers in 47 countries worldwide. *Cancer epidemiol Biomarkers Prev*. (2023) 32:894–905. doi: 10.1158/1055-9965.EPI-22-1133

11. Tapper EB, Parikh ND. Mortality due to cirrhosis and liver cancer in the United States, 1999-2016: observational study. *BMJ (Clinical Res ed)*. (2018) 362:k2817. doi: 10.1136/bmj.k2817

12. Álvarez CS, Espinosa-Tamez P, López-Ridaura R, Lamadrid-Figueroa H, Melchor-Ruan J, McGlynn KA, et al. Liver cancer mortality in Mexico: trend analysis from 1998 to 2018. *Salud Publica Mexico*. (2022) 64:14–25. doi: 10.21149/12518

13. Ilic I, Sipetic Grujicic S, Grujicic J, Radovanovic D, Zivanovic Macuzic I, Kocic S, et al. Long-term trend of liver cancer mortality in Serbia, 1991-2015: an age-period-cohort and joinpoint regression analysis. *Healthc (Basel Switzerland)*. (2020) 8:283. doi: 10.3390/healthcare8030283

14. Park J, Jee YH. Age-period-cohort analysis of liver cancer mortality in Korea. *Asian Pacific J Cancer Prev APJCP*. (2015) 16:8589–94. doi: 10.7314/APJCP.2015.16.18.8589

15. Zhang X, El-Serag HB, Thrift AP. Sex and race disparities in the incidence of hepatocellular carcinoma in the United States examined through age-period-cohort analysis. *Cancer Epidemiol Biomarkers Prev*. (2020) 29:88–94. doi: 10.1158/1055-9965.EPI-19-1052

16. Liu H, Li J, Zhu S, Zhang X, Zhang F, Zhang X, et al. Long-term trends in incidence, mortality and burden of liver cancer due to specific etiologies in Hubei Province. *Sci Rep*. (2024) 14:4924. doi: 10.1038/s41598-024-53812-8

17. Wang F, Mubarik S, Zhang Y, Wang L, Wang Y, Yu C, et al. Long-term trends of liver cancer incidence and mortality in China 1990-2017: A joinpoint and age-period-cohort analysis. *Int J Environ Res Public Health*. (2019) 16:2878. doi: 10.3390/ijerph16162878

18. Jiang L, Zhao N, Xu M, Pei J, Lin Y, Yao Q, et al. Incidence trends of primary liver cancer in different geographical regions of China from 1978 to 2012 and projections to 2032: An age-period-cohort analysis. *Int J Cancer*. (2024) 154:465–76. doi: 10.1002/ijc.34724

19. Luo A, Dong H, Lin X, Liao Y, Liang B, Chen L, et al. Time trends of major cancers incidence and mortality in Guangzhou, China 2004-2015: A Joinpoint and Age-Period-Cohort Analysis. *Cancer Med*. (2021) 10:2865–76. doi: 10.1002/cam4.3744

20. Fong Y. Fast bootstrap confidence intervals for continuous threshold linear regression. *J Comput Graph Stat*. (2019) 28:466–70. doi: 10.1080/10618600.2018.1537927

21. Wang S, Dong Z, Wan X. Global, regional, and national burden of inflammatory bowel disease and its associated anemia, 1990 to 2019 and predictions to 2050: An analysis of the global burden of disease study 2019. *Autoimmun Rev*. (2023) 23:103498. doi: 10.1016/j.autrev.2023.103498

22. Chien CR, Chen TH. A Bayesian model for age, period, and cohort effects on mortality trends for lung cancer, in association with gender-specific incidence and case-fatality rates. *J Thorac Oncol*. (2009) 4:167–71. doi: 10.1097/JTO.0b013e318194fabc

23. Riaz SP, Coupland VH, Lüchtenborg M, Peake MD, Møller H. Mesothelioma incidence projections in South East England. *Eur Respir J*. (2012) 40:965–8. doi: 10.1183/09031936.00168111

24. Liu J, Han W, Wang H, Wang Z, Li B, Hong L. Spatiotemporal trends and age-period-cohort analysis for the burden of endometriosis-related infertility: an analysis of the global burden of disease study 2019. *J Personal Med*. (2023) 13:1284. doi: 10.3390/jpm13091284

25. O'Brien RM. A simplified approach for establishing estimable functions in fixed effect age-period-cohort multiple classification models. *Stat Med*. (2021) 40:1160–71. doi: 10.1002/sim.8831

26. Holford TR. The estimation of age, period and cohort effects for vital rates. *Biometrics*. (1983) 39:311–24. doi: 10.2307/2531004

27. Clayton D, Schifflers E. Models for temporal variation in cancer rates. I: Age-period and age-cohort models. *Stat Med*. (1987) 6:449–67. doi: 10.1002/sim.4780060405

28. Hobcraft J, Menken J, Preston S. Age, period, and cohort effects in demography: a review. *Popul Index*. (1982) 48:4–43. doi: 10.2307/2736356

29. Irimata KE, Bastian BA, Clarke TC, Curtin SC, Badwe R, Rui P. Guidance for selecting model options in the national cancer institute joinpoint regression software. *Vital Health Stat Ser 1 Progr collect proced*. (2022) 194:1–22. doi: 10.15620/cdc:118050

30. Rodrigues W, Simões TC, Magnago C, Dantas ESO, Guimarães RM, Jesus JC, et al. The influence of the age-period-cohort effects on male suicide in Brazil from 1980 to 2019. *PloS One*. (2023) 18:e0284224. doi: 10.1371/journal.pone.0284224

31. Sun Y, Wang Y, Li M, Cheng K, Zhao X, Zheng Y, et al. Long-term trends of liver cancer mortality by gender in urban and rural areas in China: an age-period-cohort analysis. *BMJ Open*. (2018) 8:e020490. doi: 10.1136/bmjopen-2017-020490

32. Yang QY, Huang Y, Wang W, Zhang CH, Xu JX, Zhang ZB. Comparative analysis on seroprevalence of hepatitis B in Guangzhou in 2008 and 2018. *Zhonghua liu xing bing xue za zhi = Zhonghua liuxingbingxue zazhi*. (2021) 42:1061–6.

33. Yeh SH, Li CL, Lin YY, Ho MC, Wang YC, Tseng ST, et al. Hepatitis B virus DNA integration drives carcinogenesis and provides a new biomarker for HBV-related HCC. *Cell Mol Gastroenterol Hepatol*. (2023) 15:921–9. doi: 10.1016/j.jcmgh.2023.01.001

34. Liu Z, Jiang Y, Yuan H, Fang Q, Cai N, Suo C, et al. The trends in incidence of primary liver cancer caused by specific etiologies: Results from the Global Burden of Disease Study 2016 and implications for liver cancer prevention. *J Hepatol*. (2019) 70:674–83. doi: 10.1016/j.jhep.2018.12.001

35. Liu Y, Guo LW, Xu HF, Kang RH, Zheng LY, Zhang LY, et al. Risk of liver cirrhosis in HBV/HCV-infected individuals with first-degree relatives who have liver cancer: development and validation of a simple model. *Cancer Prev Res (Philadelphia Pa)*. (2022) 15:111–20. doi: 10.1158/1940-6207.CAPR-21-0220

36. Liu J, Liang W, Jing W, Liu M. Countdown to 2030: eliminating hepatitis B disease, China. *Bull World Health Organ*. (2019) 97:230–8. doi: 10.2471/BLT.18.219469

37. Wu Z, Bao H, Yao J, Chen Y, Lu S, Li J, et al. Suitable hepatitis B vaccine for adult immunization in China: a systematic review and meta-analysis. *Hum Vaccines Immunother*. (2019) 15:220–7. doi: 10.1080/21645515.2018.1509172

38. Liu Y, Liu L. Changes in the epidemiology of hepatocellular carcinoma in Asia. *Cancers*. (2022) 14:4473. doi: 10.3390/cancers14184473

39. Perea LME, Antunes JLF, Peres MA. Approaches to the problem of nonidentifiability in the age-period-cohort models in the analysis of cancer mortality: a scoping review. *Eur J Cancer Prev*. (2022) 31:93–103. doi: 10.1097/CEJ.0000000000000713

40. Zheng B, Zhu YJ, Wang HY, Chen L. Gender disparity in hepatocellular carcinoma (HCC): multiple underlying mechanisms. *Sci China Life Sci*. (2017) 60:575–84. doi: 10.1007/s11427-016-9043-9

41. Birrer DL, Linecker M, López-López V, Brusadin R, Navarro-Barrios Á, Reese T, et al. Sex disparities in outcomes following major liver surgery: new powers of estrogen? *Ann Surg*. (2022) 276:875–81. doi: 10.1097/SLA.0000000000005635

42. Bashir Hamidu R, Chalikonda DM, Hann HW. Gender disparity in host responses to hepatitis B-related hepatocellular carcinoma: a case series. *Vaccines*. (2021) 9:838. doi: 10.3390/vaccines9080838

43. Li Y, Wang L, Jiang Y, Zhang M, Wang L. Risk factors for noncommunicable chronic diseases in women in China: surveillance efforts. *Bull World Health Organ*. (2013) 91:650–60. doi: 10.2471/BLT.13.117549

44. Kelly JT, Su G, Zhang L, Qin X, Marshall S, González-Ortiz A, et al. Modifiable lifestyle factors for primary prevention of CKD: A systematic review and meta-analysis. *J Am Soc Nephrol JASN*. (2021) 32:239–53. doi: 10.1681/ASN.2020030384

45. Polyzos SA, Chrysavgis L, Vachliotis ID, Chartampilas E, Cholongitas E. Nonalcoholic fatty liver disease and hepatocellular carcinoma:Insights in epidemiology, pathogenesis, imaging, prevention and therapy. *Semin Cancer Biol*. (2023) 93:20–35. doi: 10.1016/j.semcancer.2023.04.010

46. Rumgay H, Shield K, Charvat H, Ferrari P, Sornpaisarn B, Obot I, et al. Global burden of cancer in 2020 attributable to alcohol consumption: a population-based study. *Lancet Oncol*. (2021) 22:1071–80. doi: 10.1016/S1470-2045(21)00279-5

47. Liu C, Wu J, Chang Z. Trends and age-period-cohort effects on the prevalence, incidence and mortality of hepatocellular carcinoma from 2008 to 2017 in Tianjin, China. *Int J Environ Res Public Health*. (2021) 18:6034. doi: 10.3390/ijerph18116034

48. Livingston M, Room R, Chikritzhs T, Taylor N, Yuen WS, Dietze P. Trends in alcohol-related liver disease mortality in Australia: An age-period-cohort perspective. *Addict (Abingdon England)*. (2023) 118:2156–63. doi: 10.1111/add.16275

49. Liu W, Liu Q, Huang Q, Lu Y, Xie S, Lin A, et al. Time trend analysis of primary liver cancer incidence in Sihui county of Guangdong Province, China (1987-2011). *BMC Cancer*. (2016) 16:796. doi: 10.1186/s12885-016-2817-9

50. Luo L, Hodges JS. Constraints in random effects age-period-cohort models. *Sociol Method*. (2020) 50:276–317. doi: 10.1177/0081175020903348

frontiers | Frontiers in Oncology

TYPE Original Research
PUBLISHED 15 May 2024
DOI 10.3389/fonc.2024.1401496

OPEN ACCESS

EDITED BY
Francisco Tustumi,
University of São Paulo, Brazil

REVIEWED BY
Jonathan Soldera,
University of Caxias do Sul, Brazil
Zeynep Kucukakcali,
İnönü University, Türkiye
William Matsui,
The University of Texas at Austin,
United States

*CORRESPONDENCE
Jianmin Wang
wangjm8605@163.com

†These authors have contributed equally to this work

RECEIVED 15 March 2024
ACCEPTED 29 April 2024
PUBLISHED 15 May 2024

CITATION
Jiang X, Zhou R, Jiang F, Yan Y, Zhang Z and Wang J (2024) Construction of diagnostic models for the progression of hepatocellular carcinoma using machine learning.
Front. Oncol. 14:1401496.
doi: 10.3389/fonc.2024.1401496

Construction of diagnostic models for the progression of hepatocellular carcinoma using machine learning

Xin Jiang[1,2†], Ruilong Zhou[3†], Fengle Jiang[1,2], Yanan Yan[1,2], Zheting Zhang[1,2] and Jianmin Wang[1,2*]

[1]Innovation Center for Cancer Research, Clinical Oncology School of Fujian Medical University, Fujian Cancer Hospital, Fuzhou, China, [2]Fujian Key Laboratory of Advanced Technology for Cancer Screening and Early Diagnosis, Fuzhou, China, [3]Faculty of Medicine, The Chinese University of Hong Kong, Hong Kong, Hong Kong SAR, China

Liver cancer is one of the most prevalent forms of cancer worldwide. A significant proportion of patients with hepatocellular carcinoma (HCC) are diagnosed at advanced stages, leading to unfavorable treatment outcomes. Generally, the development of HCC occurs in distinct stages. However, the diagnostic and intervention markers for each stage remain unclear. Therefore, there is an urgent need to explore precise grading methods for HCC. Machine learning has emerged as an effective technique for studying precise tumor diagnosis. In this research, we employed random forest and LightGBM machine learning algorithms for the first time to construct diagnostic models for HCC at various stages of progression. We categorized 118 samples from GSE114564 into three groups: normal liver, precancerous lesion (including chronic hepatitis, liver cirrhosis, dysplastic nodule), and HCC (including early stage HCC and advanced HCC). The LightGBM model exhibited outstanding performance (accuracy = 0.96, precision = 0.96, recall = 0.96, F1-score = 0.95). Similarly, the random forest model also demonstrated good performance (accuracy = 0.83, precision = 0.83, recall = 0.83, F1-score = 0.83). When the progression of HCC was categorized into the most refined six stages: normal liver, chronic hepatitis, liver cirrhosis, dysplastic nodule, early stage HCC, and advanced HCC, the diagnostic model still exhibited high efficacy. Among them, the LightGBM model exhibited good performance (accuracy = 0.71, precision = 0.71, recall = 0.71, F1-score = 0.72). Also, performance of the LightGBM model was superior to that of the random forest model. Overall, we have constructed a diagnostic model for the progression of HCC and identified potential diagnostic characteristic gene for the progression of HCC.

KEYWORDS

liver cancer, machine learning, random forest model, LightGBM model, the progression of HCC

Introduction

According to the recent data on global cancer burden in 2020, liver cancer ranked as the sixth most common cancer in terms of incidence rate and the third highest in terms of mortality (1). A considerable percentage of patients diagnosed with hepatocellular carcinoma (HCC) are at an advanced stage. Therefore, the identification of diagnostic markers is of immense importance (2–4). The development of HCC is a gradual process. Patients with chronic liver disease experience persistent liver inflammation, fibrosis, and abnormal regeneration of liver cells. These abnormalities can lead to cirrhosis and gradually give rise to dysplastic nodules of precancerous lesions. Finally, the patients will develop HCC (5). However, the marker gene for HCC progression remain unclear.

Thus, there is an urgent need to identify markers and develop precise diagnostic model for progression of HCC. With the development of artificial intelligence, machine learning has shown promise in cancer diagnosis and treatment (6, 7). For example, Zhang (8) developed a machine learning-based model for the early detection of liver cancer by utilizing low-depth whole genome sequencing of cell-free DNA. The model achieved an AUC of 0.995, a sensitivity of 0.968, and a specificity of 0.988 in differentiating between liver cancer and non-liver cancer. According to feature selection, Tang (9) used Least Absolute Shrinkage and Selector Operation (Lasso), Support Vector Machine (SVM), and Random Forest (RF) to construct HCC classification models for HCC saliva samples. The diagnostic accuracy of the LASSO-HCC model was 0.706, the diagnostic accuracy of the SVM-HCC model was 0.812, and the diagnostic accuracy of the RF-HCC model was 0.859.

However, these studies exclusively focused on particular stages in the progression of HCC. In this research, we aim to develop an accurate diagnostic model for the progression of HCC by utilizing machine learning algorithms, such as RF and LightGBM. The RF and LightGBM models are two commonly used machine learning algorithms known for their strong performance and effectiveness in dealing with classification and regression problems.

RF is an ensemble learning algorithm that enhances prediction accuracy by constructing multiple decision trees and taking the average of the predictions from these trees. RF can reduce overfitting, is tolerant to missing values, and can assess the importance of each feature, aiding in data comprehension (10, 11). LightGBM is a distributed and high-performance algorithm designed for gradient-boosting decision trees, specifically based on the Histogram algorithm, characterized by efficiency, speed, and high accuracy. Principle of LightGBM is to iteratively train multiple decision trees and train the next tree based on the results of the previous tree to minimize the loss function (12, 13). Combining the RF and LightGBM models can yield more comprehensive and accurate results in research. These two algorithms have outstanding performance in cancer diagnostics (14).

In this research, we classified 118 samples from GSE114564 into three groups: normal liver, precancerous lesion, and HCC. The RF model and LightGBM model showed strong performance and identified 12 characteristic genes. Additionally, the diagnostic model still exhibited high efficacy when categorizing the progression of HCC into six finely stratified stages. To the best of our knowledge, this research represented the first application of machine learning to comprehensively cover all stages of HCC progression.

Materials and methods

Patients

This research employed the RNA-sequencing dataset GSE114564 (15), retrieved from the GEO database, which included transcriptome data from 118 tissue samples representing different stages of HCC. The dataset included 15 normal liver samples, 20 chronic hepatitis samples, 10 liver cirrhosis samples, 10 dysplastic nodule samples, 18 early stage HCC samples, and 45 advanced HCC samples. This comprehensive dataset covers almost all stages for progression of HCC.

Data processing

We obtained the file "GSE114564_Liver_Cancer_FPKM.txt.gz" from the GEO database (https://www.ncbi.nlm.nih.gov/geo/query/acc.cgi?acc=GSE114564). FPKM (fragments per kilobase of exon model per million mapped fragments) of 118 samples were used as the input file, which can effectively eliminate the impact of sequencing depth and gene length on the results. Following that, we conducted an 8:2 random split (16–18) to partition the 118 available samples into training and validation sets. The 8:2 ratio is commonly regarded as a reasonable choice, because it ensures an adequate sample size for the training set, while also providing a certain number of samples for the validation set to evaluate model performance. Next, we kept genes that are expressed (FPKM>0) in at least three samples and these genes are in scanpy (19) (scanpy.pp.filter_genes). Then, the data matrix is log-transformed (scanpy.pp.log1p). In the end, we selected the top 1000 genes (20–22) by the ranking variances of all samples (scanpy.pp.highly_variable_genes), which was performed variance calculation in Scanpy. More specifically, a normalized variance for each gene is computed. First, the data are standardized (i.e., z-score normalization per feature) with a regularized standard deviation. Next, the normalized variance is computed as the variance of each gene after the transformation. Genes are ranked by the normalized variance. Finally, we selected the top 1,000 genes (Supplementary Table S1) that demonstrated the highest overall variance in FPKM as the foundation for constructing RF and LightGBM models. The variance calculation and above data processing steps were all implemented in scanpy.

Construction of machine learning

Subsequently, we employed the Python framework sklearn (23) to construct the RF model using the RF program (sklearn.ensemble.RandomForestClassifier) and LightGBM program (Lightgbm.sklearn), with all parameters set to default values. The framework sklearn available online is: https://scikit-learn.org/stable/supervised_learning.html. Cross-validation was used in this study to find the optimal parameters of the classification model and help the model alleviate overfitting. This study uses fivefold cross-validation on the training dataset, and uses accuracy, precision, recall, and F1-score to evaluate the model performance, and the results are in Supplementary Table S2.

Analysis of characteristic gene

The RF and LightGBM models calculated the gene importance and identified the top 50 most important genes (24), separately (Supplementary Table S3). Furthermore, the intersection of these 50 genes was taken to obtain the feature genes. Upon constructing the aforementioned model, we obtained a set of characteristic genes. Following that, we generated expression heatmap using TBtools HeatMap illustrator program. TBtools is an integrative toolkit developed for interactive analyses of big biological data (25, 26). Survival analysis was performed using the GEPIA2 database, and GO pathway enrichment was performed using clusterProfiler R package (27, 28). Finally, we used the GeneCards database (29) to identify characteristic genes associated with occurrence of HCC (https://www.genecards.org/). The workflow diagram for this research was depicted in Figure 1.

Result

Constructing machine learning model based three distinct groups

Based on the transformative process of HCC, the data can be categorized into three groups: normal liver, precancerous lesion (including chronic hepatitis, liver cirrhosis, dysplastic nodule), and HCC (including early stage HCC and advanced HCC). We employed the RF and LightGBM algorithms of machine learning to develop a diagnostic model for the progression of HCC. Performance measure of the RF model was presented in Figure 2 and Table 1, indicating an accuracy of 0.83, precision of 0.83, recall of 0.83, and F1-score of 0.83. Similarly, performance measure of the LightGBM model indicated an accuracy of 0.96, precision of 0.96, recall of 0.96, and F1-score of 0.95.

According to the method, the models above comprised a total of 12 characteristic genes (*CLEC3B*, *RN7SL5P*, *RP11–977G19.10*, *ASPDH*, *CFP*, *CDC37L1-AS1*, *RN7SL752P*, *U3*, *IGFALS*, *MASP2*, *RN7SKP255*, *RP11–162P23.2*). Next, we utilized TBtools to generate expression heatmap for these 12 characteristic genes (Supplementary Figure S1). The characteristic genes are primarily involved in complement activation, activation of immune response, cytoplasmic vesicle lumen, complement binding, oxidoreductase activity, and other pathways ($q < 0.05$; Figure 3).

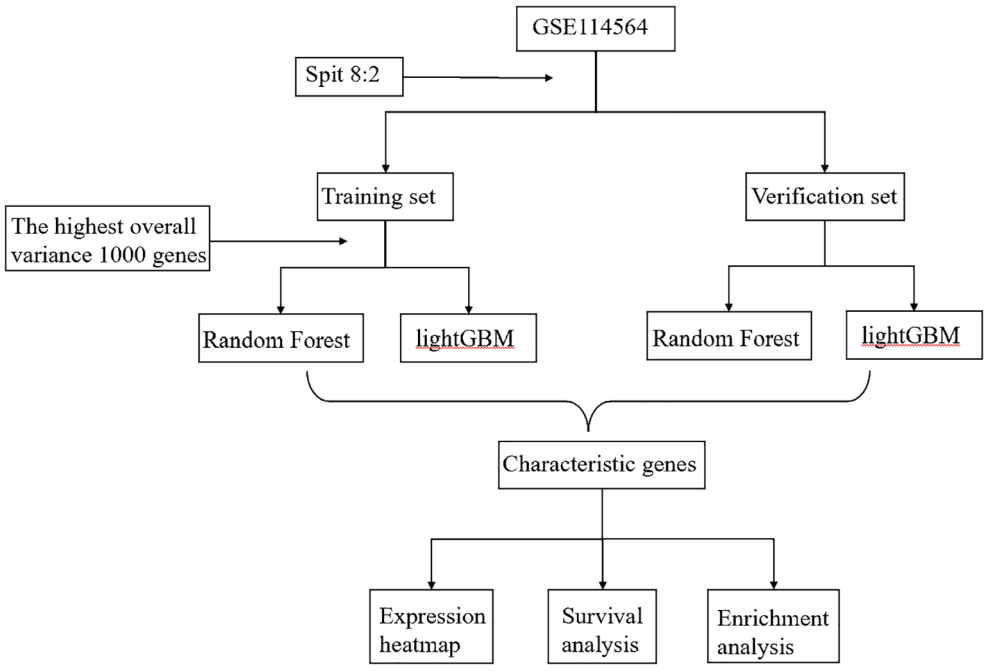

FIGURE 1
Workflow diagram in this research.

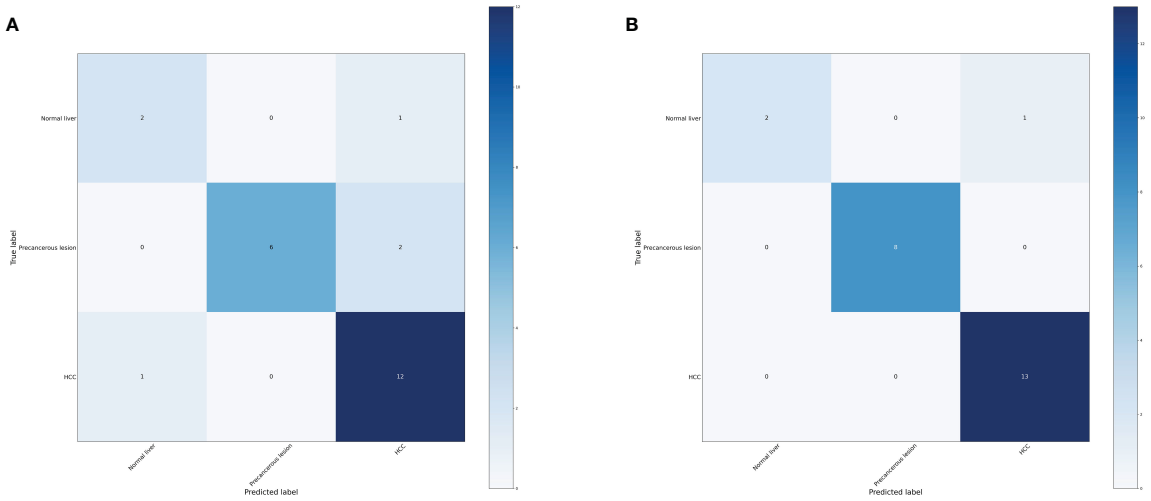

FIGURE 2
Confusion matrix of the models. **(A)** Confusion matrix of the random forest model. **(B)** Confusion matrix of the LightGBM model.

TABLE 1 Performance measure of machine learning models based three distinct groups.

Model	Accuracy	Precision	Recall	F1-score
Random forest	0.83	0.83	0.83	0.83
LightGBM	0.96	0.96	0.96	0.95

Among these genes, we found that poor prognosis was associated with low expression of *CLEC3B*, *CDC37L1-AS1*, *IGFALS*, and *MASP2* (Logrank $p < 0.05$; Figure 4). Moreover, both *CLEC3B* and *IGFALS* showed a strong association with the occurrence of HCC (Table 2) (30, 31).

Constructing machine learning model based four distinct groups

In order to further investigate the effectiveness of machine learning models in classifying early stage HCC, we categorized the data into four groups: normal liver, precancerous lesion (including chronic hepatitis, liver cirrhosis, dysplastic nodule), early stage HCC, and advanced HCC. Performance measure of the random forest model was presented in Figure 5, Table 3, indicating an accuracy of 0.83, precision of 0.83, recall of 0.83, and F1-score of 0.83. Similarly, performance measure of the LightGBM model indicated an accuracy of 0.75, precision of 0.75, recall of 0.75, and F1-score of 0.76.

According to the method, the models above comprised a total of 12 characteristic genes (*HBA2*, *RP11–977G19.10*, *AC004538.3*, *INS-IGF2*, *RNU2–63P*, *RN7SL752P*, *U3*, *VIPR1*, *MASP2*, *TDO2*, *RN7SKP255*, *RP11–162P23.2*). Furthermore, we utilized TBtools to generate expression heatmap for these 12 characteristic genes (Supplementary Figure S2). The characteristic genes are primarily enriched in pathways associated with the tryptophan metabolic process, hemoglobin complex, oxygen binding, and other pathways ($q < 0.05$; Figure 6).

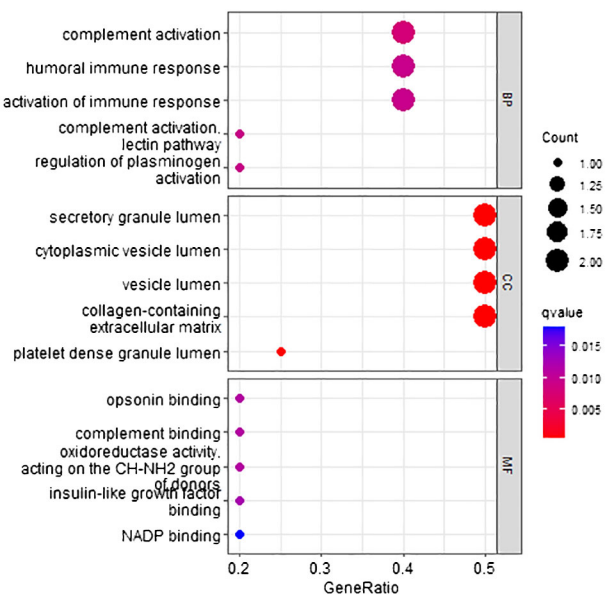

FIGURE 3
Go pathway enrichment of characteristic genes.

Regarding these genes, low expression of *AC004538.3*, *VIPR1*, and *MASP2* was associated with a poor prognosis (Logrank $p < 0.05$;

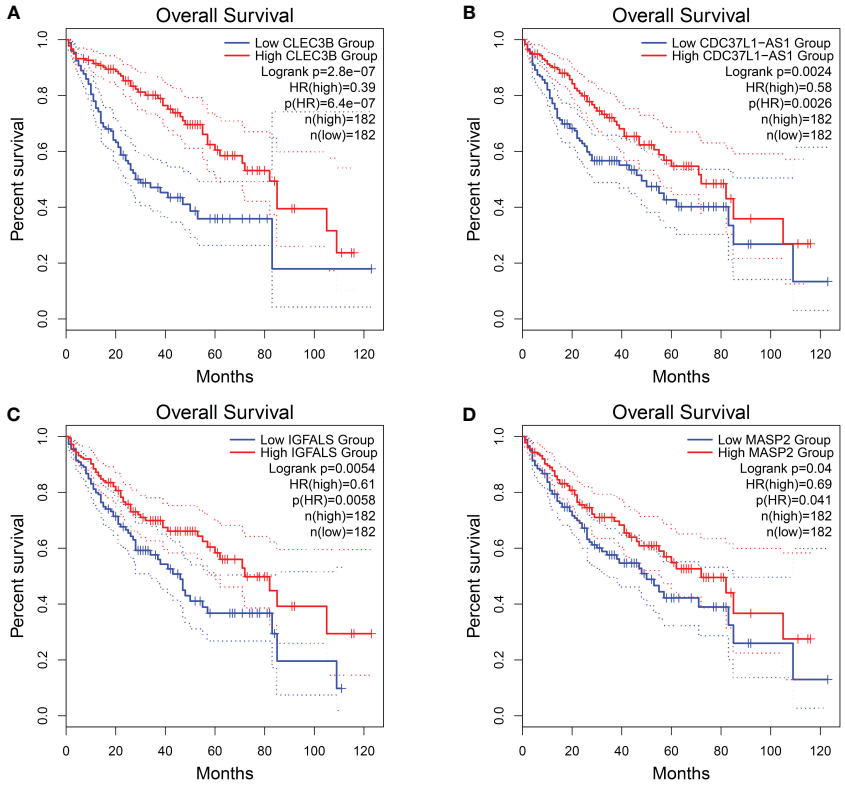

FIGURE 4
Overall survival of HCC genes in GEPIA2 database. **(A)** Overall survival of *CLEC3B*. **(B)** Overall survival of *CDC37L1-AS1*. **(C)** Overall survival of *IGFALS*. **(D)** Overall survival of *MASP2*.

Figure 7). Furthermore, *VIPR1* exhibited a strong association with the occurrence of HCC (Table 4) (32).

Constructing machine learning model based six distinct groups

We further investigated the efficacy of classifying the progression of HCC across all various stages. To achieve this, we categorized the data into six groups: normal liver, chronic hepatitis, liver cirrhosis, dysplastic nodule, early stage HCC, and advanced HCC. Performance measure of the random forest model was presented in Figure 8 and Table 5, indicating an accuracy of 0.63, precision of 0.63, recall of 0.63, and F1-score of 0.59. Similarly, performance measure of the LightGBM model indicated an accuracy of 0.71, precision of 0.71, recall of 0.71, and F1-score of 0.72.

According to the method, the models above comprised a total of 16 characteristic genes (*C1QTNF1*, *JUNB*, *CLEC3B*, *SERPINA11*, *RP11–977G19.10*, *CCNB1*, *CDC37L1-AS1*, *CFB*, *RN7SL752P*, *CCL14*, *U3*, *F12*, *ACSL4*, *MOGAT2*, *RN7SKP255*, and *TERC*). Furthermore, we utilized TBtools to generate expression heatmap for these 16 characteristic genes (Supplementary Figure S3). The characteristic genes are primarily enriched in pathways associated with regulation of plasminogen activation, positive regulation of protein processing, and other pathways ($q < 0.05$; Figure 9).

Regarding these genes, low expression of *CLEC3B*, *CDC37L1-AS1*, *CFB*, *CCL14*, and *MOGAT2* was associated with poor prognosis, while high expression of *CCNB1* and *ACSL4* was associated with a poor prognosis (Figure 10). Furthermore,

TABLE 2 *CLEC3B* and *IGFALS* reported in HCC from GeneCards database.

GeneName	Location	Function summaries	Related pathways	Report
CLEC3B	3p21.31	May be involved in the packaging of molecules destined for exocytosis.	Platelet activation, signaling and aggregation.	(30)
IGFALS	16p13.3	Encoded by this gene is a serum protein that binds insulin-like growth factors, increasing their half-life and the vascular localization.	1.Regulation of Insulin-like Growth Factor. 2.Inulin-like growth factor binding.	(31)

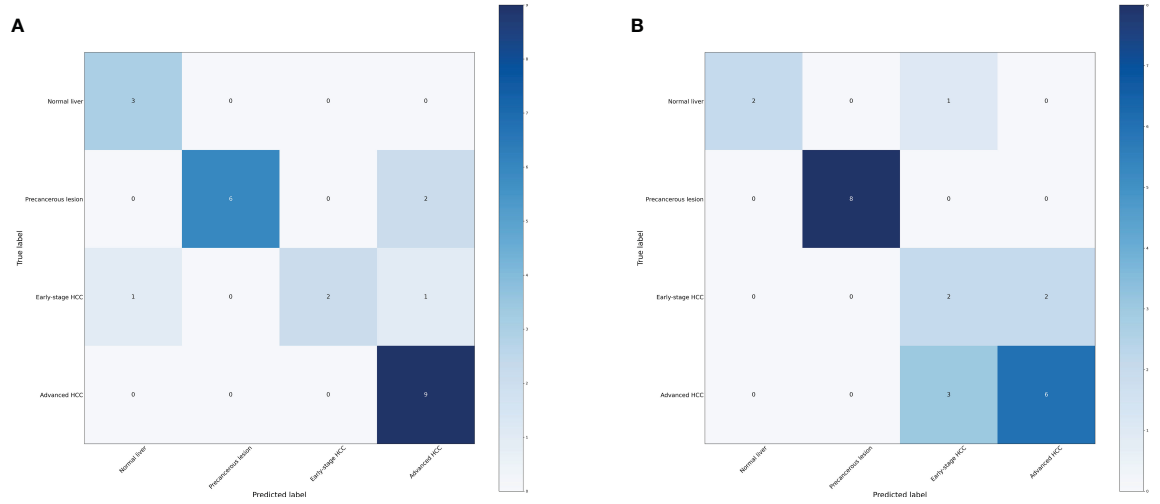

FIGURE 5
Confusion matrix of the models. **(A)** Confusion matrix of the random forest model. **(B)** Confusion matrix of the LightGBM model.

TABLE 3 Performance measure of machine learning models based four distinct groups.

Model	Accuracy	Precision	Recall	F1-score
Random forest	0.83	0.83	0.83	0.83
LightGBM	0.75	0.75	0.75	0.76

CLEC3B, *CCNB1*, *CCL14*, and *ACSL4* exhibited a strong association with the occurrence of HCC (Table 6) (30, 33–35).

Discussion

In this research, we employed machine learning algorithms, specifically random forest and LightGBM, to develop accurate diagnostic models for progression of HCC. After multiple analyses, we have identified potential diagnostic markers for the progression of HCC. Interestingly, when we categorized samples into three groups, the classification accuracy of LightGBM algorithm exceeded 0.95. Also, performance of the random forest model was slightly inferior compared to the LightGBM model. The 12 characteristic genes are primarily involved in complement activation, activation of immune response pathways. Simultaneously, among the characteristic gene *CLEC3B* generated from the model, exosomes derived from HCC with downregulated *CLEC3B* were found to promote the migration, invasion, and epithelial-mesenchymal transition of both tumor cells and endothelial cells (30). In addition, the *IGFALS*, a tumor suppressor gene, undergoes epigenetic silencing, leading to dysregulation of the IGF-II signaling in HCC (31). Our research indicated that the *CLEC3B* and *IGFALS* may be involved in the progression from normal liver to precancerous lesions to HCC, but their functions require further investigation.

Furthermore, we explored whether this model can accurately distinguish early stage HCC and assessed the potential benefits of early stage HCC diagnosis. And when the samples were categorized into four groups, the random forest model achieved a classification accuracy exceeding 0.83. Moreover, performance of the LightGBM model was slightly inferior compared to the random forest model. The 12 characteristic genes are primarily enriched in pathway associated with metabolic process. Among the characteristic gene generated from the model, loss of *VIPR1* expression in HCC

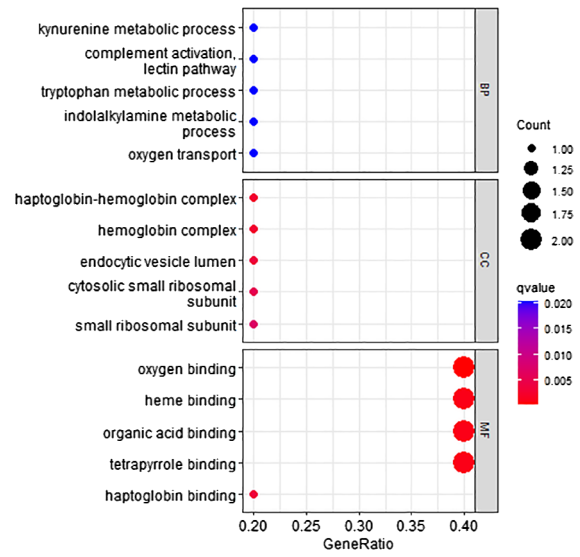

FIGURE 6
GO pathway enrichment of characteristic genes.

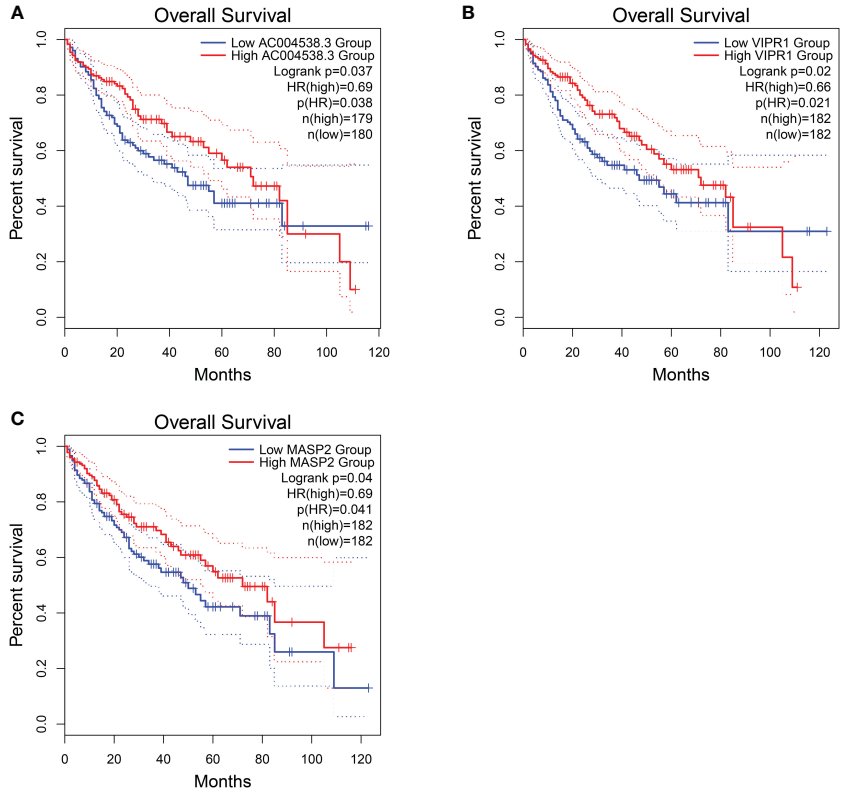

FIGURE 7
Overall survival of HCC genes in GEPIA2 database. **(A)** Overall survival of *AC004538.3*. **(B)** Overall survival of *VIPR1*. **(C)** Overall survival of *MASP2*..

TABLE 4 *VIPR1* reported in HCC from GeneCards database.

GeneName	Location	Function summaries	Related pathways	Report
VIPR1	3p22.1	This is a receptor for VIP. The activity of this receptor is mediated by G proteins which activate adenylyl cyclase.	1.Glucocorticoid receptor regulatory network. 2.GPCR downstream signal.	(32)

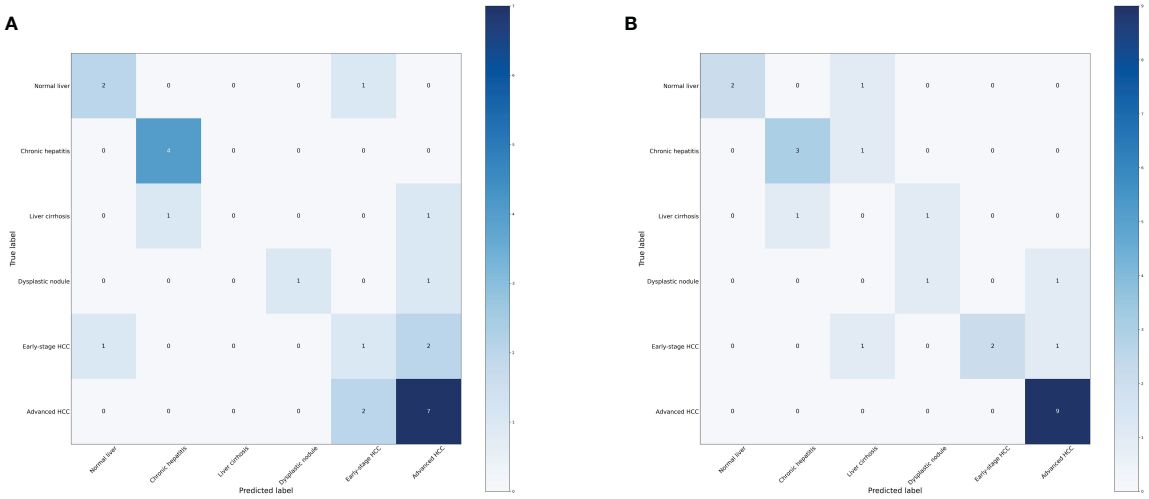

FIGURE 8
Confusion matrix of the models. **(A)** Confusion matrix of the random forest model. **(B)** Confusion matrix of the LightGBM model.

TABLE 5 Performance measure of machine learning models based six distinct groups.

Model	Accuracy	Precision	Recall	F1-score
Random forest	0.63	0.63	0.63	0.59
LightGBM	0.71	0.71	0.71	0.72

facilitated CAD phosphorylation and tumor progression, suggesting that the restoration of *VIPR1* and treatment with the *VIPR1* agonist may represent a promising approach for HCC treatment (32, 36). Our research suggested that *VIPR1* may play a role in the classification of early stage HCC and advanced HCC, but further research is needed to determine its specific function.

Moreover, when categorizing the stages of HCC into six distinct levels, the model still exhibits high diagnostic efficacy. These findings provide a solid foundation for precise treatment. The 16 characteristic genes are primarily enriched in pathway associated with positive regulation of protein processing. Among the characteristic gene generated from the model, *CCNB1* may participate in the cell cycle of HCC by regulating DNA replication, thus promoting the development of HCC (33). And, *CCL14* was a potential prognostic biomarker for determining HCC progression and was associated with immune cell infiltration in HCC (34, 37). *ACSL4* promoted the progression of HCC by stabilizing c-Myc through the ERK/FBW7/c-Myc axis (38). Our research suggested that these genes may be involved in all stages of HCC progression and serve as potential biomarkers. However, further in-depth research is needed.

In the past 20 years, sequencing technologies have continuously advanced, leading to explosive growth in available data. Artificial intelligence is often used for the characterization of sequencing data, which can enhance the ability to detect HCC tumors and provide information for disease diagnosis and staging (39).

Xie (40) utilized gene expression profiles from peripheral blood to develop an artificial neural network (ANN) model that could differentiate HCC patients from the control group with a sensitivity of 96% and specificity of 86%. Harpreet (41) utilized a large-scale transcriptomic analysis dataset containing a total of 2,316 HCC samples and 1,665 non-tumor tissue samples to identify HCC samples using machine learning, with an accuracy ranging from 93% to 98%. Although these studies have demonstrated good predictive performance, they did not further differentiate and study non-tumor tissues (pre-cancerous stages).

In addition, A single-center prospective study in the UK recruited 331 cases of liver cell carcinoma, with a control group involving only 339 patients with chronic liver disease. A logistic regression analysis model was constructed, with an AUROC of 0.97 indicating excellent predictive performance. However, the study was only validated in a cohort of patients with fatty liver disease (42). Xing (43) conducted mass spectrometry proteomics sequencing and built a random forest machine learning model that clearly distinguished between HCC and healthy individuals (sensitivity 0.975, specificity 1.000), as well as between HCC and cirrhosis (sensitivity 0.925, specificity 0.915). However, these studies did not cover all stages of liver cancer progression.

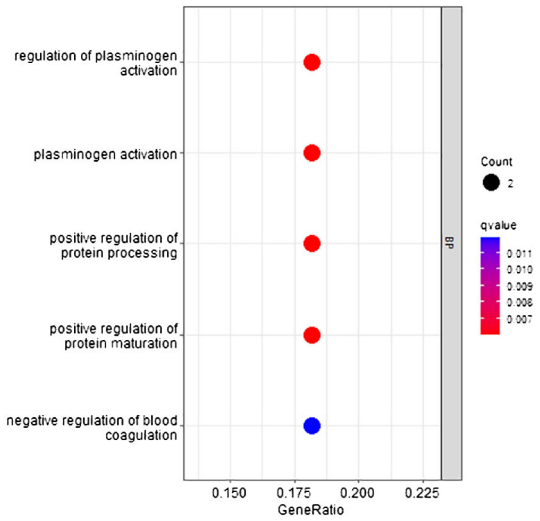

FIGURE 9
GO pathway enrichment of characteristic genes.

In our study, we comprehensively cover all stages of liver cancer development, including normal liver, chronic hepatitis, liver cirrhosis, dysplastic nodule, early stage HCC, and advanced HCC. Furthermore, we conducted detailed classifications into three categories, four categories, and six categories respectively, in order to systematically study relevant models of liver cancer progression. When we categorized three groups: normal liver, precancerous lesion (including chronic hepatitis, liver cirrhosis, dysplastic nodule) and HCC (including early stage HCC and advanced HCC), The LightGBM model exhibited outstanding performance (accuracy = 0.96, precision = 0.96, recall = 0.96, F1-score = 0.95). Surprisingly, when the progression of HCC was categorized into the most refined six stages, the diagnostic model still demonstrated high performance (accuracy = 0.71, precision = 0.71, recall = 0.71, F1 score = 0.72). In conclusion, we successfully constructed the most detailed model of HCC progression stages using machine learning methods, providing a theoretical basis for accurate diagnosis of HCC.

In summary, this research represented the pioneering construction of a diagnostic model for HCC progression through the utilization of machine learning methods. The development of liver cancer is a gradual process. Liver cancer patients undergo a process from hepatitis and liver fibrosis to abnormal nodules, ultimately developing into liver cancer. By subdividing into different stages, we can more finely assess the disease progression stage of liver cancer patients and intervene with precision medicine. We hope that targeted early intervention and treatment can prevent

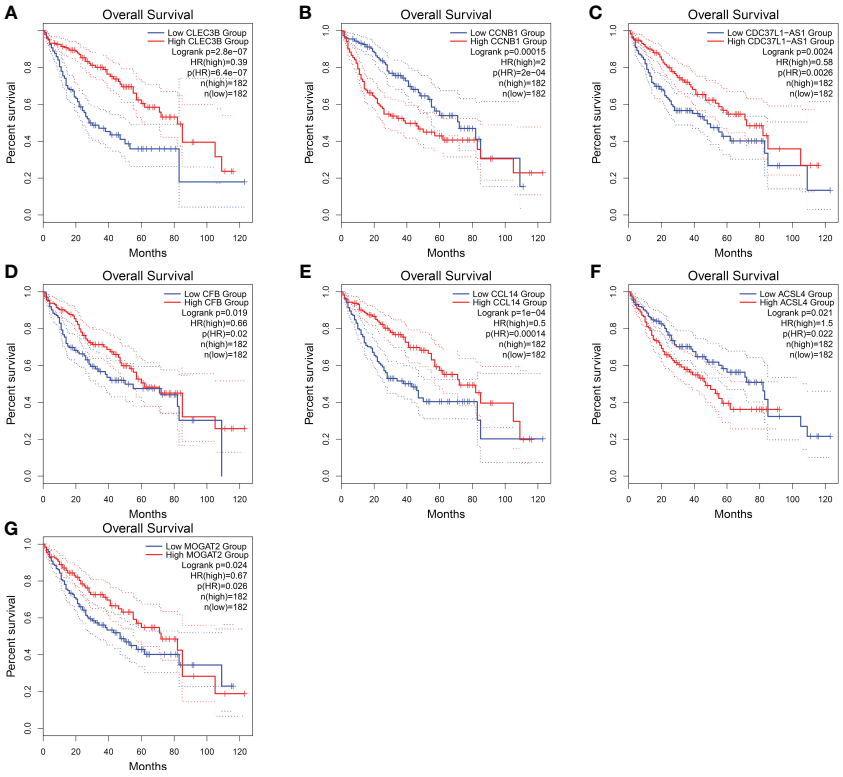

FIGURE 10
Overall survival of HCC genes in GEPIA2 database. **(A)** Overall survival of *CLEC3B*. **(B)** Overall survival of *CCNB1*. **(C)** Overall survival of *CDC37L1-AS1*. **(D)** Overall survival of *CFB*. **(E)** Overall survival of *CCL14*. **(F)** Overall survival of *ACSL4*. **(G)** Overall survival of *MOGAT2*.

TABLE 6 *CLEC3B*, *CCNB1*, *CCL14*, and *ACSL4* reported in HCC from GeneCards database.

GeneName	Location	Function summaries	Related pathways	Report
CLEC3B	3p21.31	Tetranectin binds to plasminogen and to isolated kringle 4. May be involved in the packaging of molecules destined for exocytosis.	Platelet activation, signaling and aggregation.	(30)
CCNB1	5q13.2	Essential for the control of the cell cycle at the G2/M (mitosis) transition.	1.AMPK signaling pathway. 2. Cell cycle	(33)
CCL14	17q12	This gene, chemokine (C-C motif) ligand 14, is one of several CC cytokine genes clustered.	1.MIF-mediated glucocorticoid regulation and TGF-Beta Pathway. 2.Chemokine activity.	(34)
ACSL4	Xq23	Catalyzes the conversion of long-chain fatty acids to their active form acyl-CoA for both synthesis of cellular lipids.	Fatty acid metabolism.	(35)

the progression of HCC to advanced stage in the future. Additionally, we have identified key genes associated with the progression of liver cancer. Further research on these genes will facilitate the development of effective targets for liver cancer progression. It is important to note that the HCC progression characteristic genes identified in our research still lack sufficient research concerning their impact on progression of HCC, and further exploration is warranted. Of course, it is crucial to validate effectiveness of the model using a larger sample size. Due to the reduced cost of transcriptome sequencing, increasing dataset will arise in the future. In a word, this research holds potential for clinical application due to its significance and prospect.

Data availability statement

The original contributions presented in the study are included in the article/Supplementary Material. Further inquiries can be directed to the corresponding author.

Author contributions

XJ: Data curation, Formal analysis, Writing – original draft, Writing – review & editing. RZ: Data curation, Formal analysis, Software, Writing – original draft. FJ: Data

curation, Investigation, Writing – review & editing. YY: Conceptualization, Investigation, Writing – review & editing. ZZ: Conceptualization, Supervision, Writing – original draft. JW: Conceptualization, Funding acquisition, Investigation, Writing – review & editing, Writing – original draft.

Funding

The author(s) declare financial support was received for the research, authorship, and/or publication of this article. The authors gratefully acknowledge the financial support of the Science Foundation of the Excellent Youth Scholars of Fujian Provincial Health Commission (Grant 2021ZQNZD009), Natural Science Foundation of Fujian Province (Grant 2021J01445).

Acknowledgments

The authors are grateful for the open source data from GEO.

Conflict of interest

The authors declare that the research was conducted in the absence of any commercial or financial relationships that could be construed as a potential conflict of interest.

Publisher's note

Supplementary material

The Supplementary Material for this article can be found online at: https://www.frontiersin.org/articles/10.3389/fonc.2024.1401496/full#supplementary-material

References

1. Sung H, Ferlay J, Siegel RL, Laversanne M, Soerjomataram I, Jemal A, et al. Global cancer statistics 2020: GLOBOCAN estimates of incidence and mortality worldwide for 36 cancers in 185 countries. *CA Cancer J Clin*. (2021) 71:209–49. doi: 10.3322/caac.21660

2. Bruix J, Reig M, Sherman M. Evidence-based diagnosis, staging, and treatment of patients with hepatocellular carcinoma. *Gastroenterology*. (2016) 150:835–53. doi: 10.1053/j.gastro.2015.12.041

3. Li L, Wang H. Heterogeneity of liver cancer and personalized therapy. *Cancer Lett*. (2016) 379:191–7. doi: 10.1016/j.canlet.2015.07.018

4. Chan LK, Tsui YM, Ho DW, Ng IO. Cellular heterogeneity and plasticity in liver cancer. *Semin Cancer Biol*. (2022) 82:134–49. doi: 10.1016/j.semcancer.2021.02.015

5. Villanueva A. Hepatocellular carcinoma. *N Engl J Med*. (2019) 380:1450–62. doi: 10.1056/NEJMra1713263

6. Swanson K, Wu E, Zhang A, Alizadeh AA, Zou J. From patterns to patients: Advances in clinical machine learning for cancer diagnosis, prognosis, and treatment. *Cell*. (2023) 186:1772–91. doi: 10.1016/j.cell.2023.01.035

7. Kann BH, Hosny A, Aerts H. Artificial intelligence for clinical oncology. *Cancer Cell*. (2021) 39:916–27. doi: 10.1016/j.ccell.2021.04.002

8. Zhang X, Wang Z, Tang W, Wang X, Liu R, Bao H, et al. Ultrasensitive and affordable assay for early detection of primary liver cancer using plasma cell-free DNA fragmentomics. *Hepatology*. (2022) 76:317–29. doi: 10.1002/hep.32308

9. Tang Z, Zhang F, Wang Y, Zhang C, Li X, Yin M, et al. Diagnosis of hepatocellular carcinoma based on salivary protein glycopatterns and machine learning algorithms. *Clin Chem Lab Med*. (2022) 60:1963–73. doi: 10.1515/cclm-2022–0715

10. Chen X, Ishwaran H. Random forests for genomic data analysis. *Genomics*. (2012) 99:323–9. doi: 10.1016/j.ygeno.2012.04.003

11. Sheehy J, Rutledge H, Acharya UR, Loh HW, Gururajan R, Tao X, et al. Gynecological cancer prognosis using machine learning techniques: A systematic review of the last three decades (1990–2022). *Artif Intell Med*. (2023) 139:102536. doi: 10.1016/j.artmed.2023.102536

12. Zhu J, Su Y, Liu Z, Liu B, Sun Y, Gao W, et al. Real-time biomechanical modelling of the liver using LightGBM model. *Int J Med Robot*. (2022) 18:e2433. doi: 10.1002/rcs.2433

13. Hamed EA, Salem MA, Badr NL, Tolba MF. An efficient combination of convolutional neural network and lightGBM algorithm for lung cancer histopathology classification. *Diagnostics (Basel)*. (2023) 13:2469. doi: 10.3390/diagnostics13152469

14. Penson A, Camacho N, Zheng Y, Varghese AM, Al-Ahmadie H, Razavi P, et al. Development of genome-derived tumor type prediction to inform clinical cancer care. *JAMA Oncol*. (2020) 6:84–91. doi: 10.1001/jamaoncol.2019.3985

15. Eun JW, Jang JW, Yang HD, Kim J, Kim SY, Na MJ, et al. Serum proteins, HMMR, NXPH4, PITX1 and THBS4; A panel of biomarkers for early diagnosis of hepatocellular carcinoma. *J Clin Med*. (2022) 11:2128. doi: 10.3390/jcm11082128

16. Zhao X, Li X, Lin Y, Ma R, Zhang Y, Xu D, et al. Survival prediction by Bayesian network modeling for pseudomyxoma peritonei after cytoreductive surgery plus hyperthermic intraperitoneal chemotherapy. *Cancer Med*. (2023) 12:2637–45. doi: 10.1002/cam4.5138

17. Li X, Zhao Y, Zhang D, Kuang L, Huang H, Chen W, et al. Development of an interpretable machine learning model associated with heavy metals' exposure to identify coronary heart disease among US adults via SHAP: Findings of the US NHANES from 2003 to 2018. *Chemosphere*. (2023) 311:137039. doi: 10.1016/j.chemosphere.2022.137039

18. Liu XZ, Duan M, Huang HD, Zhang Y, Xiang TY, Niu WC, et al. Predicting diabetic kidney disease for type 2 diabetes mellitus by machine learning in the real world: a multicenter retrospective study. *Front Endocrinol (Lausanne)*. (2023) 14:1184190. doi: 10.3389/fendo.2023.1184190

19. Wolf FA, Angerer P, Theis FJ. SCANPY: large-scale single-cell gene expression data analysis. *Genome Biol*. (2018) 19:15. doi: 10.1186/s13059–017-1382–0

20. Xu RH, Wei W, Krawczyk M, Wang W, Luo H, Flagg K, et al. Circulating tumour DNA methylation markers for diagnosis and prognosis of hepatocellular carcinoma. *Nat Mater*. (2017) 16:1155–61. doi: 10.1038/nmat4997

21. Eraslan G, Simon LM, Mircea M, Mueller NS, Theis FJ. Single-cell RNA-seq denoising using a deep count autoencoder. *Nat Commun*. (2019) 10:390. doi: 10.1038/s41467–018-07931–2

22. Su C, Xu Z, Shan X, Cai B, Zhao H, Zhang J. Cell-type-specific co-expression inference from single cell RNA-sequencing data. *Nat Commun*. (2023) 14:4846. doi: 10.1038/s41467–023-40503–7

23. Peng HY, Duan SJ, Pan L, Wang MY, Chen JL, Wang YC, et al. Development and validation of machine learning models for nonalcoholic fatty liver disease. *Hepatobiliary Pancreat Dis Int*. (2023) 22:615–21. doi: 10.1016/j.hbpd.2023.03.009

24. Lotfollahi M, Rybakov S, Hrovatin K, Hediyeh-Zadeh S, Talavera-López C, Misharin AV, et al. Biologically informed deep learning to query gene programs in single-cell atlases. *Nat Cell Biol*. (2023) 25:337–50. doi: 10.1038/s41556-022-01072-x

25. Chen C, Chen H, Zhang Y, Thomas HR, Frank MH, He Y, et al. TBtools: an integrative toolkit developed for interactive analyses of big biological data. *Mol Plant*. (2020) 13:1194–202. doi: 10.1016/j.molp.2020.06.009

26. Chen C, Wu Y, Li J, Wang X, Zeng Z, Xu J, et al. TBtools-II: A "one for all, all for one" bioinformatics platform for biological big-data mining. *Mol Plant*. (2023) 16:1733–42. doi: 10.1016/j.molp.2023.09.010

27. Tang Z, Kang B, Li C, Chen T, Zhang Z. GEPIA2: an enhanced web server for large-scale expression profiling and interactive analysis. *Nucleic Acids Res*. (2019) 47: W556–W60. doi: 10.1093/nar/gkz430

28. Wu T, Hu E, Xu S, Chen M, Guo P, Dai Z, et al. clusterProfiler 4.0: A universal enrichment tool for interpreting omics data. *Innovation (Camb)*. (2021) 2:100141. doi: 10.1016/j.xinn.2021.100141

29. Luo D, Fang M, Shao L, Wang J, Liang Y, Chen M, et al. The EMT-related genes GALNT3 and OAS1 are associated with immune cell infiltration and poor prognosis in lung adenocarcinoma. *Front Biosci (Landmark Ed)*. (2023) 28:271. doi: 10.31083/j.fbl2810271

30. Dai W, Wang Y, Yang T, Wang J, Wu W, Gu J. Downregulation of exosomal CLEC3B in hepatocellular carcinoma promotes metastasis and angiogenesis via AMPK and VEGF signals. *Cell Commun Signal*. (2019) 17:113. doi: 10.1186/s12964–019-0423–6

31. Neumann O, Kesselmeier M, Geffers R, Pellegrino R, Radlwimmer B, Hoffmann K, et al. Methylome analysis and integrative profiling of human HCCs identify novel protumorigenic factors. *Hepatology*. (2012) 56:1817–27. doi: 10.1002/hep.25870

32. Fu Y, Liu S, Rodrigues RM, Han Y, Guo C, Zhu Z, et al. Activation of VIPR1 suppresses hepatocellular carcinoma progression by regulating arginine and pyrimidine metabolism. *Int J Biol Sci*. (2022) 18:4341–56. doi: 10.7150/ijbs.71134

33. Rong MH, Li JD, Zhong LY, Huang YZ, Chen J, Xie LY, et al. CCNB1 promotes the development of hepatocellular carcinoma by mediating DNA replication in the cell cycle. *Exp Biol Med (Maywood)*. (2022) 247:395–408. doi: 10.1177/15353702211049149

34. Gu Y, Li X, Bi Y, Zheng Y, Wang J, Li X, et al. CCL14 is a prognostic biomarker and correlates with immune infiltrates in hepatocellular carcinoma. *Aging (Albany NY)*. (2020) 12:784–807. doi: 10.18632/aging.102656

35. Chen J, Ding C, Chen Y, Hu W, Lu Y, Wu W, et al. ACSL4 promotes hepatocellular carcinoma progression via c-Myc stability mediated by ERK/FBW7/c-Myc axis. *Oncogenesis*. (2020) 9:42. doi: 10.1038/s41389-020-0226-z

36. Lin XH, Zhang DY, Liu ZY, Tang WQ, Chen RX, Li DP, et al. lncRNA-AC079061.1/VIPR1 axis may suppress the development of hepatocellular carcinoma: a bioinformatics analysis and experimental validation. *J Transl Med*. (2022) 20:379. doi: 10.1186/s12967–022-03573–7

37. Zhu M, Xu W, Wei C, Huang J, Xu J, Zhang Y, et al. CCL14 serves as a novel prognostic factor and tumor suppressor of HCC by modulating cell cycle and promoting apoptosis. *Cell Death Dis*. (2019) 10:796. doi: 10.1038/s41419–019-1966–6

38. Chen J, Ding C, Chen Y, Hu W, Yu C, Peng C, et al. ACSL4 reprograms fatty acid metabolism in hepatocellular carcinoma via c-Myc/SREBP1 pathway. *Cancer Lett*. (2021) 502:154–65. doi: 10.1016/j.canlet.2020.12.019

39. Calderaro J, Seraphin TP, Luedde T, Simon TG. Artificial intelligence for the prevention and clinical management of hepatocellular carcinoma. *J Hepatol*. (2022) 76:1348–61. doi: 10.1016/j.jhep.2022.01.014

40. Xie H, Xue YQ, Liu P, Zhang PJ, Tian ST, Yang Z, et al. Multi-parameter gene expression profiling of peripheral blood for early detection of hepatocellular carcinoma. *World J Gastroenterol*. (2018) 24:371–8. doi: 10.3748/wjg.v24.i3.371

41. Kaur H, Dhall A, Kumar R, Raghava GPS. Identification of platform-independent diagnostic biomarker panel for hepatocellular carcinoma using large-scale transcriptomics data. *Front Genet*. (2020) 10:1306. doi: 10.3389/fgene.2019.01306

42. Johnson PJ, Pirrie SJ, Cox TF, Berhane S, Teng M, Palmer D, et al. The detection of hepatocellular carcinoma using a prospectively developed and validated model based on serological biomarkers. *Cancer Epidemiol Biomarkers Prev*. (2014) 23:144–53. doi: 10.1158/1055–9965.EPI-13–0870

43. Xing X, Cai L, Ouyang J, Wang F, Li Z, Liu M, et al. Proteomics-driven noninvasive screening of circulating serum protein panels for the early diagnosis of hepatocellular carcinoma. *Nat Commun*. (2023) 14:8392. doi: 10.1038/s41467–023-44255–2

frontiers | Frontiers in Oncology

TYPE Case Report
PUBLISHED 16 May 2024
DOI 10.3389/fonc.2024.1401882

OPEN ACCESS

EDITED BY
Rodrigo Xavier Das Neves,
National Cancer Institute (NIH), United States

REVIEWED BY
Poonam Aggarwal,
Indian Institute of Science Education and Research Mohali, India
Ivan Romic,
University Hospital Centre Zagreb, Croatia

*CORRESPONDENCE
Haibo Shao
haiboshao@aliyun.com
Yulong Tian
107564714@qq.com

RECEIVED 16 March 2024
ACCEPTED 30 April 2024
PUBLISHED 16 May 2024

CITATION
Jiang X, Aljbri A, Liu J, Shang L, Tian Y and Shao H (2024) Hepatic arterial infusion chemotherapy with implantable arterial access port for advanced-stage hepatocellular carcinoma: a case report. *Front. Oncol.* 14:1401882. doi: 10.3389/fonc.2024.1401882

Hepatic arterial infusion chemotherapy with implantable arterial access port for advanced-stage hepatocellular carcinoma: a case report

Xin Jiang, Afaf Aljbri, Jiaxuan Liu, Liqi Shang, Yulong Tian* and Haibo Shao*

Department of Interventional Radiology, The First Affiliated Hospital of China Medical University, Shenyang, Liaoning, China

Background: Hepatocellular carcinoma (HCC) is a common gastrointestinal malignancy characterized by high incidence rates and a poor prognosis. Common treatment modalities include surgery, ablation, and transarterial chemoembolization (TACE). Hepatic arterial infusion chemotherapy (HAIC) has long been used in the treatment of unresectable liver cancer. In recent years, the combination of anti-angiogenesis therapy and immune checkpoint inhibitors has shown significant advances in the treatment of middle- and advanced-stage liver cancer. This report presents a case of HCC in which sustained benefits are achieved through a combination of HAIC of infusional oxaliplatin, leucovorin, and fluorouracil (FOLFOX), targeted therapy, and immunotherapy.

Main body: A 64-year-old male patient was diagnosed with a parenchymal mass in the liver by a three-dimensional color ultrasound one month before admission, prompting consideration of liver cancer. Subsequently, computed tomography (CT) imaging performed at our hospital identified mass shadows in the right lobe of the liver and diffuse nodules throughout the liver, suggesting malignant lesions. Upon admission, the patient presented poor general health and baseline indicators. Following symptomatic treatment, the patient underwent a therapeutic regimen that combined transarterial infusion port FOLFOX-HAIC with Lenvatinib and Sintilimab. This combined treatment resulted in significant liver tumor necrosis and effectively managed the patient's condition.

Conclusion: The combined approach of using FOLFO-HAIC transarterial infusion alongside anti-angiogenesis therapy and immune checkpoint inhibitors has shown promising results that provide substantial benefits. This combined regimen has demonstrated the potential to improve treatment compliance among certain patients. Given these encouraging outcomes, further investigation into this combination therapy regimen is warranted to understand better its efficacy and potential broader applications in clinical settings.

KEYWORDS

hepatocellular carcinoma, FOLFOX-HAIC, anti-angiogenic therapy, immune checkpoint inhibitors, case report

Introduction

According to the latest global cancer data released by the WHO in 2020, primary liver cancer ranks sixth in the incidence of malignant tumors and third in mortality rate (1). The onset of liver cancer often presents subtly, and while early-stage disease can be managed by resection, liver transplantation, or ablation, a considerable proportion of patients face incurable disease and poor prognosis (2). For patients at the Barcelona Clinic, liver cancer (BCLC), stage A-B with unresectable hepatocellular carcinoma (HCC), transarterial chemoembolization (TACE) is commonly chosen as the primary treatment; however, its efficacy depends heavily on tumor size. Treatment of large HCC of Child-Pugh class A-B (10 cm) remains challenging due to unsatisfactory outcomes (3). Hepatic arterial infusion chemotherapy (HAIC), which includes oxaliplatin, leucovorin, and fluorouracil (FOLFOX), targets middle to advanced HCC and offers substantial survival benefits (4). In Japan, HAIC has preferred for people with large HCC or portal vein tumor thrombosis (PVTT), particularly for severe cases of PVTT (5). In particular, the findings of a randomized phase 3 study comparing HAIC and TACE for extensive HCC indicate that HAIC contributes to improved survival outcomes for large HCCs (6). However, the survival benefit of FOLFOX-HAIC alone remained limited.

In recent years, anti-angiogenic therapy and immune checkpoint inhibitors have effectively treated advanced HCC. Phase 3 study in 2018 revealed that Lenvatinib, a representative agent in anti-angiogenic therapy compared to Sorafenib, exhibited non-inferior OS (13.6 vs. 12.3 months) and a higher objective response rate (ORR) of 18.8% (7). In recent years, immune checkpoint inhibitors have been the focus of research in treating advanced tumors and have also made significant progress in treating HCC. Sintilimab is an anti-programmed cell death protein (PD-1) monoclonal antibody with high anti-tumor activity in HCC (8). Clinical trials and reports have increasingly demonstrated the superior effectiveness of combination therapy over monotherapy. Therefore, we report that a patient with extensive unresectable HCC who received FOLFOX-HAIC with Lenvatinib and Sintilimab through an arterial infusion port achieved a sustained survival benefit.

Case description

The patient, a 64-year-old Chinese man, presented in November 2021 with a three-month history of diarrhea, fatigue, and lower extremity symptoms. On 10 November 2021, the patient underwent a CT (CT) examination at our hospital, revealing findings of a mass shadow in the right lobe of the liver and diffuse nodules throughout the liver, suggesting malignant liver tumors. In particular, the patient had a medical history of chronic hepatitis B virus (HBV) and is currently on antiviral therapy. The patient denied any history of underlying conditions such as hypertension, diabetes, or coronary heart disease; the patient also reported no family history of infection or cancer. Before admission, the patient had not received any treatment. The chronological progression of the entire case is illustrated in Figure 1.

Diagnostic assessment

In November 2021, the patient underwent a CT examination that revealed multiple intrahepatic lesions. The maximum cross-sectional dimension of the giant mass shadow in the right liver lobe measured approximately 16.3 × 11.3 cm, accompanied by scattered nodules within the liver. These lesions demonstrated enhancement during the arterial phase of imaging, suggesting a stage B BCLC classification. The patient was then admitted for a routine examination (Table 1). The serum tumor marker test revealed a serum level of carbohydrate antigen 199 (CA199) of 70.90 U/ml, while alpha-fetoprotein (AFP) and carcinoembryonic antigen (CEA) fell within normal ranges. The indicators of liver function reflected poor liver function, and the Child-Pugh classification of liver function was B-grade. Consequently, preoperative and postoperative liver protection therapy was administered.

Based on the patient's heavy tumor load and poor liver function, FOLFOX-HAIC therapy was selected once every 21 days through the infusion port of the femoral artery after a comprehensive assessment of the patient's condition. On 23 November 2021, we performed hepatic arteriography under DSA guidance. The imaging revealed extensive lesions in the right liver lobe and multiple intrahepatic lesions supplied by both the left and right hepatic arteries, as shown in Figure 2.

To minimize postoperative adverse reactions from local chemotherapy drug infusions, we selectively embolized the gastroduodenal artery with spring coils. Subsequently, the arterial infusion port catheter was placed in the proper hepatic artery, with a lateral hole created 1 cm behind the tip to infuse the lesion in the left hepatic lobe. Finally, the artery infusion port was implanted subcutaneously 3 cm below the right groin, and liver arteriography was performed again with a 20G noninvasive needle through the artery infusion port, indicating that the catheter tip was not displaced and the catheter was unobtrusive. FOLFOX-HAIC was initiated through the femoral artery infusion port upon returning to the ward.

According to the body surface area of the patient, the specific regimen was calculated as oxaliplatin 150 mg (0–2h, 85mg/m2, 250ml/h), leucovorin 400mg (2–4h, 200mg/m2, 250ml/h), fluorouracil 3750 mg (subsequently 46–48h, 2500 mg/m2, 43 ml/h). During chemotherapy infusion, the patient had only mild liver pain related to oxaliplatin injection. On the second day after perfusion, the patient developed a fever, and relevant indicators were tested, indicating a high possibility of infection. After symptomatic treatment, the patient was discharged from the hospital and began to take 8 mg of Lenvatinib Mesylate capsule orally once a day.

In December 2021, the patient was readmitted to the hospital; the admission evaluation revealed that the patient's liver function was still poor. Symptomatic liver protection treatment was maintained before surgery. Serum CA199 had decreased to normal levels, while AFP remained within the normal range,

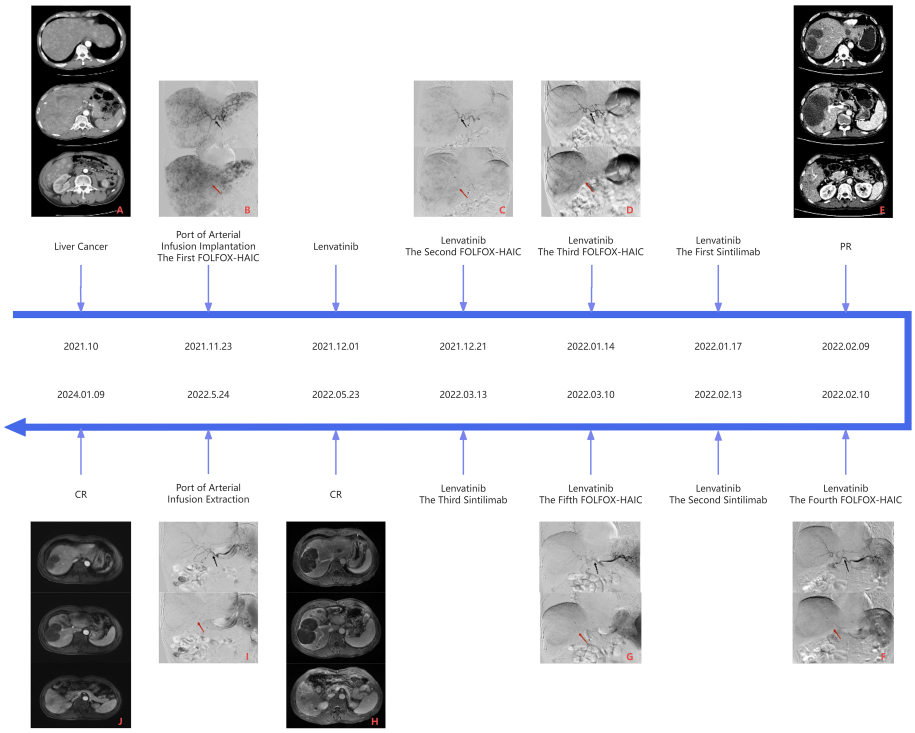

FIGURE 1
Panel **(A)** is the CT image of the liver before the first FOLFOX-HAIC, and panel B is the DSA image of the first FOLFOX-HAIC, both of which can see massive masses in the right lobe of the liver, multiple nodules in the liver, and apparent tumor staining. Panel **(E)** is the first efficacy assessment after three FOLFOX-HAIC treatments combined with Lenvatinib and Sintilimab. CT examination showed mild circular enhancement of giant tumors in the right lobe of the liver in the arterial stage, and some nodular lesions in the liver were mildly enhanced, but no new lesions were detected. Panel **(F)** is the DSA image of the fourth FOLFOX-HAIC, as shown in panel **(E)**. In contrast to panel **(B)**, the hepatic artery vessels (black arrow) become thinner, the volume of the tumor (red arrow) in the right lobe of the liver is significantly reduced, and the tumor staining is reduced considerably, which can reach partial response (PR) according to Response Evaluation Criteria in Solid Tumors (RECIST) v1.1. Panel **(H)** is the second evaluation of the efficacy after five FOLFOX-HAIC treatments combined with Lenvatinib and Sintilimab. A liver MRI examination showed fine line enhancement in the liver at the arterial stage, liquefaction necrosis in the original lesion area, and no new lesions. Panel **(I)** shows the angiography before removing the artery infusion port, where no noticeable tumor staining was observed. Compared with panel **(F)**, the blood vessels (black arrow) in the right lobe of the liver are further narrowed, and the volume of the masses (red arrow) in the right lobe of the liver is significantly slightly reduced, up to complete response (CR), and continued until the latest review.

contradicting the indication of a high tumor load in the liver. Therefore, another serum tumor marker, prothrombin induced by vitamin K absence or antagonist II (PIVKA-II), was tested, revealing a>30000.00 mAU/mL result. On 21 December 2021, liver arteriography was performed in the interventional operating room using a 20G non-damaging needle through the infusion port of the femoral artery. Based on the DSA X-ray findings, the catheter appeared well positioned without discontinuity, and multiple tumor

TABLE 1 The results of the blood test.

ITEM	The pre-treatment (2021.09)	The after treatment (2022.05)	NORMAL RANGE	UNIT
AFP	2.12	4.75	0.00-7.00	ng/mL
CEA	2.55	2.08	0.00-4.30	ng/mL
CA199	70.90	21.10	0.00-27.00	U/mL
AST	251	48	15-40	U/L
ALT	50	35	9-50	U/L
ALB	30.1	37.6	40.0-55.0	g/L
TBIL	40.6	13.4	0.0-26.0	umol/L
DBIL	29.6	3.9	0.0-8.0	umol/L
PT	12.9	13.5	11.0-13.7	s

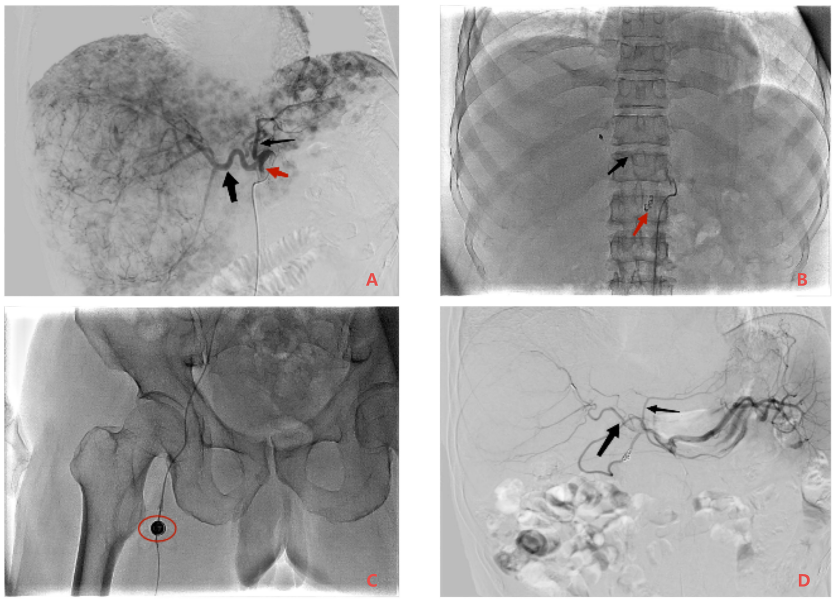

FIGURE 2
Comparison of DSA images before and after treatment and implantation of an arterial infusion port. Panel **(A)** is the image of the initial contrast. Large lesions in the right lobe of the liver and scattered lesions in the liver can be seen. Blood is supplied by the left hepatic artery (thin black arrow) and the right hepatic artery (thick black arrow), and the initial segment of the gastroduodenal artery (red arrow) can be seen. Panel **(B)** shows the position of the tip of the intrahepatic catheter at the port of arterial infusion (black arrow). In order to alleviate the adverse reactions after infusion, the gastroduodenal artery was selectively embolized with a spring ring (red arrow). Panel **(C)** shows the location and shape of the arterial infusion port (red circle). Panel **(D)** is the sixth contrast image. Compared with panel **(A)**, the left hepatic artery (thin black arrow) and the right hepatic artery (thick black arrow) were significantly thinner, and the tumor staining disappeared.

stains persisted in both the left and right lobes of the liver. However, compared to prior imaging, there was a reduction in tumor blood supply. Considering the patient's myelosuppression (severe agranulocytosis) and decreased liver function after the previous treatment, the dose of oxaliplatin was halved for the second treatment with FOLFOX-HAIC. The infusion went smoothly without adverse reactions, and the patient was discharged the next day.

In January 2022, the patient was admitted to the hospital for the third time. The preoperative examination indicated that PIVKA-II decreased significantly to 637.50 mAU/ml. Other tests were all within the normal range. On 14 January 2022, liver arteriography demonstrated persistent tumor staining but with a further reduction in blood supply. The patient underwent a third FOLFOX-HAIC treatment following the same regimen as the previous session. The infusion proceeded smoothly without adverse reactions. Due to the substantial tumor burden, discussions with the patient's family led to the decision to proceed with immunotherapy upon completion of this treatment. Before starting immunotherapy, the patient's hypothyroidism indicators and myocardial enzyme profile were average. Post-intravenous infusion of Sintilimab injection 200 mg every 21 days, there were no apparent discomforts during the infusion, and the patient was discharged the following day.

After undergoing three cycles of FOLFOX-HAIC treatment, the patient underwent an enhanced CT examination on 9th February 2022 to assess the efficacy of the treatment. As seen from the DSA images in Figures 1B–D, hepatic artery vessels (black arrow) gradually became thinner and more apparent, intrahepatic lesion staining decreased significantly, and lesion volume (red arrow) decreased significantly. Partial tumor staining was still visible in Figure 1D. As shown in Figure 1E, the liver-enhanced CT scan showed mild circular enhancement of giant masses in the right lobe and mild enhancement of some nodules in the liver during the arterial stage. Compared with the images in September 2021, the lesion scope was reduced, the enhancement was decreased significantly, and no new lesions were found. Blood tests showed that PIVKA-II again significantly decreased and dropped to an average level of 36.19mAU/mL, AFP was still within the normal range, and liver function and coagulation function were normal. It is proved that FOLFOX-HAIC treatments combined with Lenvatinib and Sintilimab are effective, and this regimen can be continued. As shown in Figures 1F, G, hepatic arteriography sessions were conducted in February and March 2022, respectively, which revealed a successive decline in tumor staining and blood supply (red arrow), with blood vessels (black arrow) supplying the tumor, becoming thinner. The preoperative evaluation indicated good liver function, absence of myelosuppression, and normalized PIVKA-II levels. Subsequently, the patient underwent the fourth and fifth cycles of FOLFOX-HAIC treatment, following the same regimen as previously administered, and the infusion process proceeded smoothly without any adverse reactions. After FOLFOX-HAIC treatment, the patient underwent immunotherapy with the same regimen as before, experiencing no apparent discomfort during infusion.

Blood tests in May 2022 indicated that PIVKA-II and AFP were in the normal range, as shown in Table 1; Figure 3, red blood cells

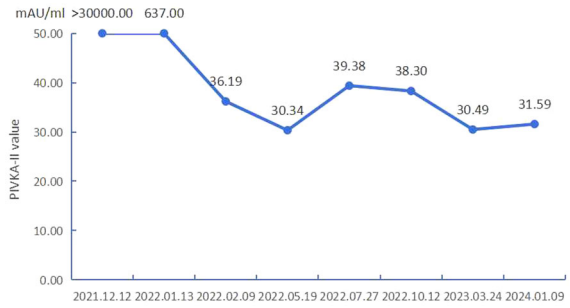

FIGURE 3
Line chart of serum PIVKA-II.

and white blood cells were in the normal range, liver function was good, and coagulation function was normal. As shown in Figure 1H, Liver-enhanced magnetic resonance imaging (MRI) showed fine line enhancement within the lesion, demonstrating a reduced lesion area compared to the CT examination conducted in February 2022. On 24 May 2022, liver arteriography indicated the disappearance of tumor staining with no emergence of new lesions, as shown in Figure 2. The patient had an excellent physical and mental condition, a regular diet and sleep, and no adverse drug reactions. After the above comprehensive assessment, the medical team determined that the patient did not require a sixth FOLFOX-HAIC treatment. Consequently, the arterial infusion port and catheter were removed, and the wound was sutured under pressure and bandaged. After a day of observation without any discomfort, the patient was discharged.

After discharge, the patient took Lenvatinib 8 mg orally once daily and received Sintilimab 200 mg intravenously every 21 days. Enhanced liver MRI evaluations in July 2022, October 2022, March 2023, and January 2024 indicated stable lesions without significant changes. Serum tests revealed good liver function with no myelosuppressive reactions.

Throughout the treatment, there was a notable decrease in liver function and a myelosuppressive reaction after the initial two FOLFOX-HAIC treatments. However, these adverse effects were mitigated and improved after receiving symptomatic treatment. Subsequent treatments showed no apparent symptoms. The patient experienced a slight increase in blood pressure after initiating Lenvatinib. There were no adverse events related to immunotherapy.

Discussion

In this report, we present the case of a patient diagnosed with unresectable HCC. The patient consented to FOLFOX-HAIC therapy, Lenvatinib targeting therapy, and Sintilimab immunotherapy after arterial infusion port implantation. Interestingly, the patient achieved a complete response after undergoing seven months of treatment, which persisted until this article's submission. Progression-free survival has been calculated at 26 months.

According to the updated 2021 Japan Society of Hepatology (JSH) consensus statement and recommendations, TACE is the primary treatment for most asymptomatic patients exhibiting single or localized multifocal HCC, provided they possess well-preserved liver function. However, for large patients with HCC with multifocal biflobular nodules, fusion nodules, and Child-Pugh grade B, HAIC has become the preferred treatment, especially for patients with severe portal vein tumor thrombosis (PVTT) (5, 9). Since the liver artery primarily supplies HCC, HAIC is the direct and continuous administration of chemotherapy drugs to the tumor via a percutaneous arterial catheter, increasing the local drug concentration of cancer, avoiding the first-pass effect, and minimizing systemic adverse reactions of drugs. Additionally, a few chemotherapy drugs subsequently enter the systemic circulation and have systemic antitumor effects. As a result, HAIC can be considered a systemic treatment method with enhanced local efficacy (10).

Moreover, He et al.'s prospective, nonrandomized study illustrated that FOLFOX-HAIC exhibits a higher Objective Response Rate (ORR) than TACE when treating large liver cancer. Specifically, HAIC based on oxaliplatin could demonstrate superior effectiveness to cisplatin-based HAIC for HCC (11). Due to single intubation, patients undergoing HAIC must remain in a supine position for more than 48 hours and cannot be turned at will. Based on the patient's history of poor compliance and treatment experience, implantable systems have been widely used in tumor perfusion therapy over the past few decades (12). We opt for FOLFOX-HAIC through a femoral artery infusion port with the patient's and their family's consent. In this case, there are two clever designs throughout the operation. One is that we created a lateral hole 1 cm behind the catheter tip, which could simultaneously inject multiple lesions of both lobes and increase the stability of the catheter. The other is implanted in the arterial infusion port in a minimally invasive way, with minor trauma and high strength. Implementing the infusion port into the artery avoids multiple punctures and catheterizations in the femoral artery, significantly reducing the time to subsequent surgery. Importantly, this method does not restrict patient activities during treatment, improving compliance with numerous long-term HAIC regimens.

In recent years, combining immune checkpoint inhibitors and anti-angiogenic agents has markedly improved the treatment of unresectable HCC. Lenvatinib was approved in 2018 as a first-line treatment for advanced HCC (7). In particular, the immune checkpoint inhibitor Sintilimab has demonstrated potent antitumor activity in various cancers (8). Anti-VEGF therapy is crucial in reducing VEGF-induced immunosuppression within tumors and their microenvironment. It can potentially increase the effectiveness of anti-PD-1 and antiprogrammed death ligand 1 (PD-L1) treatments by counteracting VEGF-mediated immunosuppression and encouraging T-cell infiltration into tumors (13). The IMbrave150 trial established the superiority of combination therapies Atezolizumab and Bevacizumab over sorafenib monotherapy. This combination exhibited a markedly high objective response rate (ORR) of 30% and unprecedented overall survival (OS) of 19.2 months compared to 13.4 months with sorafenib monotherapy ($p<0.001$) (14). Furthermore, a phase 2 clinical study highlighted the efficacy of Sintilimab in combination with Lenvatinib. It reported an ORR of 36.1% in patients with medium-advanced or locally

advanced HCC, showing a higher response rate than previously reported results from single-agent anti-PD-1 or Lenvatinib therapy. This underscores the potent antitumor activity achieved by combining Sintilimab and Lenvatinib (15).

Antiangiogenic drugs are expected to enhance the efficacy of HAIC, primarily by improving tumor vascular permeability and reducing tumor interstitial pressure. This improvement in the tumor microenvironment benefits from better distributing the chemotherapy drugs (5). A randomized Phase 3 trial was conducted among patients with advanced HCC complicated by portal vein tumor thrombosis that compared Sorafenib alone versus Sorafenib combined with FOLFOX-HAIC. The results showed that the combination therapy significantly extended overall survival (OS) (7.13 vs. 13.37 months, $p<0.001$) and exhibited a considerably higher response rate compared to the monotherapy group (51% vs. 3%, $p<0.001$) (4). Immunosuppressants demonstrate synergistic effects with HAIC, potentially inducing substantial local immune modulation within the HCC microenvironment (16). Furthermore, Lenvatinib and PD-1 inhibitors could improve chemotherapy drug delivery by promoting vascular normalization (17). In the study comparing the combined treatment of Lenvatinib, Toripalimab, and HAIC with Lenvatinib monotherapy, patients subjected to the combination therapy exhibited substantial improvements in various parameters. In particular, the combination therapy group achieved progression-free survival (PFS) of 11.1 months compared to 5.1 months for monotherapy ($p<0.001$). Similarly, overall survival (OS) improved markedly in the combination treatment group compared to monotherapy (not achieved vs 11 months, $p<0.001$). Furthermore, the combination therapy group showed higher objective response rates (ORR) according to the RECIST criteria (59.2% vs. 9.3%, $p<0.001$) and the m-RECIST criteria (67.6% vs. 16.3%, $p<0.001$). The high ORR and PFS observed in the combination treatment group might be due to synergistic antitumor effects (18).

The patient was treated with the combination of Lenvatinib after the completion of the first FOLFOX-HAIC and the combination of Sintilimab and Lenvatinib after the completion of the third FOLFOX-HAIC. According to RESIST1.1, PD was achieved after three FOLFOX-HAICs, CR was achieved after five FOLFOX-HAICs, and the arterial infusion port and catheter were easily removed. No AE related to the infusion port occurred during treatment. After combination therapy, the tumor supply vessels gradually narrowed, and the blood supply gradually decreased. All liver lesions showed necrosis, the maximum tumor volume reduced significantly, other lesions lost activity, and liver function slowly recovered. While on oral Lenvatinib, the patient experienced elevated blood pressure, which was managed with antihypertensive medication.

Moreover, there were no adverse reactions associated with immunotherapy. At the same time, throughout treatment, we also found that the patient's AFP was consistently within the normal range, but the PIVKA-II levels were extremely high. Some researchers suggest that PIVKA-II may be more beneficial than AFP in HBV-associated HCC. Increased levels of PIVKA-II were associated with larger and more aggressive tumors, intrahepatic metastases, and recurrence after treatment and were significantly correlated with tumor size ($P < 0.01$) (19, 20). In this case, the content of PIVKA-II was extremely high for the first time and decreased significantly during treatment (Figure 3). In the corresponding image data, tumor enhancement decreased significantly.

In summary, the patient completed five FOLFOX-HAIC therapies at the arterial infusion port, during which the treatment combined with Lenvatinib and Sintilimab, as well as antiviral and symptomatic treatment, significantly decreased, tumor activity disappeared, and liver function recovered, achieving a perfect therapeutic effect. However, it is still being determined which specific treatment plays a key role and whether it can achieve the same impact on other patients deserves further research. Moreover, combination therapy is expensive, the drug side effects are large, and the treatment effect varies from person to person, so more clinical studies are needed to prove the effectiveness of this treatment.

Data availability statement

The original contributions presented in the study are included in the article/supplementary material. Further inquiries can be directed to the corresponding authors.

Ethics statement

The studies involving humans were approved by The First Affiliated Hospital of China Medical University. The studies were conducted in accordance with the local legislation and institutional requirements. This article is a retrospective case report and no informed consent is required. Written informed consent was obtained from the individual(s) for the publication of any potentially identifiable images or data included in this article.

Author contributions

XJ: Conceptualization, Data curation, Investigation, Writing – original draft. HS: Data curation, Funding acquisition, Methodology, Resources, Supervision, Visualization, Writing – review & editing. YT: Data curation, Methodology, Supervision, Writing – review & editing. AA: Writing – original draft. JL: Methodology, Software, Writing – original draft. LS: Formal analysis, Software, Writing – original draft.

Funding

The author(s) declare that no financial support was received for the research, authorship, and/or publication of this article.

Conflict of interest

The authors declare that the research was conducted in the absence of any commercial or financial relationships that could be construed as a potential conflict of interest.

Publisher's note

References

1. Sung H, Ferlay J, Siegel RL, Laversanne M, Soerjomataram I, Jemal A, et al. Global cancer statistics 2020: GLOBOCAN estimates of incidence and mortality worldwide for 36 cancers in 185 countries. *CA Cancer J Clin*. (2021) 71:209–49. doi: 10.3322/caac.21660

2. Brown ZJ, Tsilimigras DI, Ruff SM, Mohseni A, Kamel IR, Cloyd JM, et al. Management of hepatocellular carcinoma: A review. *JAMA Surg*. (2023) 158:410–20. doi: 10.1001/jamasurg.2022.7989

3. Li QJ, He MK, Chen HW, Fang WQ, Zhou YM, Xu L, et al. Hepatic arterial infusion of oxaliplatin, fluorouracil, and leucovorin versus transarterial chemoembolization for large hepatocellular carcinoma: A randomized phase III trial. *J Clin Oncol*. (2022) 40:150–60. doi: 10.1200/jco.21.00608

4. He M, Li Q, Zou R, Shen J, Fang W, Tan G, et al. Sorafenib plus hepatic arterial infusion of oxaliplatin, fluorouracil, and leucovorin vs sorafenib alone for hepatocellular carcinoma with portal vein invasion: A randomized clinical trial. *JAMA Oncol*. (2019) 5:953–60. doi: 10.1001/jamaoncol.2019.0250

5. Kudo M, Kawamura Y, Hasegawa K, Tateishi R, Kariyama K, Shiina S, et al. Management of hepatocellular carcinoma in Japan: JSH consensus statements and recommendations 2021 update. *Liver Cancer*. (2021) 10:181–223. doi: 10.1159/000514174

6. Tsai WL, Sun WC, Chen WC, Chiang CL, Lin HS, Liang HL, et al. Hepatic arterial infusion chemotherapy vs transcatheter arterial embolization for patients with huge unresectable hepatocellular carcinoma. *Med (Baltimore)*. (2020) 99:e21489. doi: 10.1097/md.0000000000021489

7. Kudo M, Finn RS, Qin S, Han KH, Ikeda K, Piscaglia F, et al. Lenvatinib versus sorafenib in first-line treatment of patients with unresectable hepatocellular carcinoma: a randomised phase 3 non-inferiority trial. *Lancet*. (2018) 391:1163–73. doi: 10.1016/s0140–6736(18)30207–1

8. Ren Z, Xu J, Bai Y, Xu A, Cang S, Du C, et al. Sintilimab plus a bevacizumab biosimilar (IBI305) versus sorafenib in unresectable hepatocellular carcinoma (ORIENT-32): a randomised, open-label, phase 2–3 study. *Lancet Oncol*. (2021) 22:977–90. doi: 10.1016/s1470–2045(21)00252–7

9. Lyu N, Wang X, Li JB, Lai JF, Chen QF, Li SL, et al. Arterial chemotherapy of oxaliplatin plus fluorouracil versus sorafenib in advanced hepatocellular carcinoma: A biomolecular exploratory, randomized, phase III trial (FOHAIC-1). *J Clin Oncol*. (2022) 40:468–80. doi: 10.1200/jco.21.01963

10. Obi S, Sato S, Kawai T. Current status of hepatic arterial infusion chemotherapy. *Liver Cancer*. (2015) 4:188–99. doi: 10.1159/000367746

11. He MK, Le Y, Li QJ, Yu ZS, Li SH, Wei W, et al. Hepatic artery infusion chemotherapy using mFOLFOX versus transarterial chemoembolization for massive unresectable hepatocellular carcinoma: a prospective non-randomized study. *Chin J Cancer*. (2017) 36:83. doi: 10.1186/s40880–017-0251–2

12. Thiels CA, D'Angelica MI. Hepatic artery infusion pumps. *J Surg Oncol*. (2020) 122:70–7. doi: 10.1002/jso.25913

13. Voron T, Colussi O, Marcheteau E, Pernot S, Nizard M, Pointet AL, et al. VEGF-A modulates expression of inhibitory checkpoints on CD8+ T cells in tumors. *J Exp Med*. (2015) 212:139–48. doi: 10.1084/jem.20140559

14. Cheng AL, Qin S, Ikeda M, Galle PR, Ducreux M, Kim TY, et al. Updated efficacy and safety data from IMbrave150: Atezolizumab plus bevacizumab vs. sorafenib for unresectable hepatocellular carcinoma. *J Hepatol*. (2022) 76:862–73. doi: 10.1016/j.jhep.2021.11.030

15. Xu J, Shen J, Gu S, Zhang Y, Wu L, Wu J, et al. Camrelizumab in combination with apatinib in patients with advanced hepatocellular carcinoma (RESCUE): A nonrandomized, open-label, phase II trial. *Clin Cancer Res*. (2021) 27:1003–11. doi: 10.1158/1078–0432.Ccr-20–2571

16. Fu Y, Peng W, Zhang W, Yang Z, Hu Z, Pang Y, et al. Induction therapy with hepatic arterial infusion chemotherapy enhances the efficacy of lenvatinib and pd1 inhibitors in treating hepatocellular carcinoma patients with portal vein tumor thrombosis. *J Gastroenterol*. (2023) 58:413–24. doi: 10.1007/s00535-023-01976-x

17. Shigeta K, Datta M, Hato T, Kitahara S, Chen IX, Matsui A, et al. Dual programmed death receptor-1 and vascular endothelial growth factor receptor-2 blockade promotes vascular normalization and enhances antitumor immune responses in hepatocellular carcinoma. *Hepatology*. (2020) 71:1247–61. doi: 10.1002/hep.30889

18. He MK, Liang RB, Zhao Y, Xu YJ, Chen HW, Zhou YM, et al. Lenvatinib, toripalimab, plus hepatic arterial infusion chemotherapy versus lenvatinib alone for advanced hepatocellular carcinoma. *Ther Adv Med Oncol*. (2021) 13:17588359211002720. doi: 10.1177/17588359211002720

19. Seo SI, Kim HS, Kim WJ, Shin WG, Kim DJ, Kim KH, et al. Diagnostic value of PIVKA-II and alpha-fetoprotein in hepatitis B virus-associated hepatocellular carcinoma. *World J Gastroenterol*. (2015) 21:3928–35. doi: 10.3748/wjg.v21.i13.3928

20. Feng H, Li B, Li Z, Wei Q, Ren L. PIVKA-II serves as a potential biomarker that complements AFP for the diagnosis of hepatocellular carcinoma. *BMC Cancer*. (2021) 21:401. doi: 10.1186/s12885–021-08138–3

frontiers | Frontiers in Oncology

TYPE Original Research
PUBLISHED 16 May 2024
DOI 10.3389/fonc.2024.1398968

OPEN ACCESS

EDITED BY
Francisco Tustumi,
University of São Paulo, Brazil

REVIEWED BY
Terry Cheuk-Fung Yip,
The Chinese University of Hong Kong, Hong Kong SAR, China
Andras Perl,
Upstate Medical University, United States
Noha Kandil,
Alexandria University, Egypt

*CORRESPONDENCE
Kang Li
bjyahlk@ccmu.edu.cn
Yonghong Zhang
zhangyh@ccmu.edu.cn

RECEIVED 11 March 2024
ACCEPTED 24 April 2024
PUBLISHED 16 May 2024

CITATION
Guo D, Li J, Zhao P, Mei T, Li K and Zhang Y (2024) The hepatocellular carcinoma risk in patients with HBV-related cirrhosis: a competing risk nomogram based on a 4-year retrospective cohort study.
Front. Oncol. 14:1398968.
doi: 10.3389/fonc.2024.1398968

The hepatocellular carcinoma risk in patients with HBV-related cirrhosis: a competing risk nomogram based on a 4-year retrospective cohort study

Dandan Guo[1], Jianjun Li[1], Peng Zhao[1], Tingting Mei[1], Kang Li[2,3]* and Yonghong Zhang[1,3]*

[1]Interventional Therapy Center for Oncology, Beijing You'An Hospital, Capital Medical University, Beijing, China, [2]Biomedical Information Center, Beijing You'An Hospital, Capital Medical University, Beijing, China, [3]Beijing Research Center for Respiratory Infectious Diseases, Beijing, China

Objective: The study aimed to build and validate a competitive risk nomogram to predict the cumulative incidence of hepatocellular carcinoma (HCC) for patients with hepatitis B virus (HBV)-related cirrhosis.

Methods: A total of 1401 HBV-related cirrhosis patients were retrospectively enrolled from January 1, 2011 to December 31, 2014. Application of 20 times imputation dealt with missing data using multiple imputation by chained equations (MICE). The patients were randomly divided into a training set (n = 1017) and a validation set (n = 384) at a ratio of 3:1. A prediction study was carried out using a competing risk model, where the event of interest was HCC and the competing events were death and liver transplantation, and subdistribution hazard ratios (sHRs) with 95% CIs were reported. The multivariate competing risk model was constructed and validated.

Results: There was a negligible difference between the original database and the 20 imputed datasets. At the end of follow-up, the median follow-up time was 69.9 months (interquartile range: 43.8–86.6). There were 31.5% (442/1401) of the patients who developed HCC, with a 5-year cumulative incidence of 22.9 (95%CI, 20.8%–25.2%). The univariate and multivariate competing risk regression and construction of the nomogram were performed in 20 imputed training datasets. Age, sex, antiviral therapy history, hepatitis B e antigen, alcohol drinking history, and alpha-fetoprotein levels were included in the nomogram. The area under receiver operating characteristic curve values at 12, 24, 36, 60, and 96 months were 0.68, 0.69, 0.70, 0.68, and 0.80, and the Brier scores were 0.30, 0.25, 0.23, 0.21, and 0.20 in the validation set. According to the cumulative incidence function, the nomogram effectively screened out high-risk HCC patients from low-risk patients in the presence of competing events (Fine–Gray test $p < 0.001$).

Conclusion: The competitive risk nomogram was allowed to be used for predicting HCC risk in individual patients with liver cirrhosis, taking into account both the association between risk factors and HCC and the modifying effect of competition events on this association.

KEYWORDS

hepatocellular carcinoma (HCC), competing risk, multiple imputation, prediction, HBV-related cirrhosis

Introduction

Hepatocellular carcinoma (HCC) accounts for 85%–90% of primary liver cancer, making it the fourth most common and second deadliest cancer in China (1). Hepatitis virus infection, alcohol consumption, non-alcoholic steatohepatitis, and older age mainly lead to liver cirrhosis, which is the main risk factor of HCC (2). Most hepatitis B virus (HBV)-induced HCC patients have a background of cirrhosis in China (3). HBV infection accounts for 63.9% of cancer deaths and cases in China (4).

The current guidelines recommend a monitoring interval of 6 months (3, 5, 6) for patients with liver cirrhosis. Widely available monitoring tests include tumor markers such as alpha fetoprotein (AFP) as well as various imaging techniques including ultrasound (US), computed tomography (CT), and abdominal magnetic resonance imaging (MRI). Clinical cohort studies support a biannual HCC monitoring strategy based on ultrasound (US), which improves the clinical outcomes at a reasonable cost (7, 8). Compared to annual CT, the combination of AFP and biannual US monitoring is more sensitive in detecting HCC (9). However, the advantages of the US strongly depended on the quality of the equipment and the professional knowledge of ultrasonic instruments (10). It was more cost-effective of a clinical scoring system to screen high-HCC-risk patients with cirrhosis before the diagnostic performance of US.

There is no clinical application of the HCC scoring system only applying for patients with HBV-related cirrhosis, which comprised a huge Chinese population. Currently, many models have been reported to predict HCC risk based on different etiologies. Toronto HCC risk index (THRI) scoring system (10) and our previous research (11) were applied to assess HCC risk in patients with all-cause cirrhosis. The AASL (age, albumin, sex, and liver cirrhosis)-HCC scoring system (12), real-world risk score for hepatocellular carcinoma (RWS-HCC) (13), and Chinese University (CU)-HCC score (14) were used for the prediction of HCC risk in CHB patients, taking cirrhosis into account. However, the risk of HCC varied among patients with cirrhosis of different etiologies. It is somewhat limited that these models were applied for patients with HBV-related cirrhosis (15). We are committed to develop a HCC predictive model to provide better choices for this group of patients with HBV-related cirrhosis. Moreover, from the perspective of statistical methods, these models were established using Cox proportional risk regression and Kaplan–Meier (KM) survival curve analysis and overestimated the cumulative risk of HCC (16). KM survival curves may not capture the event of interest following the occurrence of a competing event.

Liver cirrhosis is a multistate disease model, and the mortality rate increases as the disease progresses (16). Moreover, death before HCC is non-negligible, and it should always be considered a competing risk to correctly assess the HCC risks. Herein, using a large clinical cohort of HBV-related cirrhosis patients (n = 1401) with long-term follow-up (median, 69.9 months), we aimed to assess the HCC cumulative incidence in the presence of competing events [cirrhosis-related death and liver transplantation (LT)]. We established and internally validated a competitive risk scoring system based on Fine and Gray regression to accurately predict up-to-10-year HCC risk among patients with HBV cirrhosis.

Materials and methods

Patient selection

A total of 1,401 patients with HBV-related cirrhosis who were admitted at Capital Medical University, Beijing You'An Hospital, from January 1, 2011 to December 31, 2014 were included. Patients with cirrhosis were diagnosed through imaging and histological examination based on the etiology, medical history, clinical manifestations, and complications. According to the diagnosis time of liver cirrhosis, 1,401 patients were randomly divided into a training dataset (n = 1,017) and a validation dataset (n = 384) at a ratio of 3:1. We collected demographic and baseline clinical pathological information from all patients with cirrhosis, as shown below: age, sex, medical history, blood routine examination, liver and kidney function test, coagulation markers, alpha fetoprotein (AFP), and HBV viral DNA load as described in our previous study (11).

The standard of diagnosis for cirrhosis was based on Chinese guidelines on the management of liver cirrhosis (17), and for HCC it was based on the Chinese standard for the diagnosis and treatment of primary liver cancer (18). In order to minimize inter-etiological confounding of cirrhosis, the highest known risk of HCC development was set as etiological feature according to the

standard of THRI methods (10). For the purpose of this study's analysis, patients with cirrhosis who had both chronic hepatitis B and a history of alcohol or non-alcoholic steatohepatitis were classified as chronic hepatitis B (10, 19). The inclusion criteria and the exclusion criteria were described in detail in our previous study (11), and the screening process for all patients is shown in Figure 1.

Outcomes and follow-up period

The enrolled patients were followed up at the outpatient clinic every 6 months, including medical examinations, laboratory tests, and ultrasound examinations (11). We calculated the follow-up since the date of cirrhosis diagnosis to the date of event occurrence (including HCC diagnosis, HBV cirrhosis-related death, and liver transplantation) or January 1, 2020, whichever occurred first. In this study, the HBV cirrhosis-related death and LT (shown by event 2) would hinder HCC (shown by event 1). Events 1 and 2 can be considered as competing events one for the other.

Statistical analyses

Missing data could increase bias and reduce the statistical power, and application of Multiple Imputation by Chained Equations (MICE) for 20 times could reduce this impact (20). Briefly, a simple imputation was first created, and each missing value was replaced with a mean value as a "place holder". Then, the "place holder" mean imputations of the first variable were set back to missing and then replaced with predictions (imputations) from the regression model when the first variable was the dependent variable and the other variables were independent variables. Fitting models was based on the distribution of variables, logistic regression for binary variables, linear regression for continuous variables, and Poisson model for count variables. These steps of 25 iterations for each variable that had missing values would be repeated 20 times until convergence in this study. Finally, the observed values and the 20 sets of imputed values would then constitute 20 "complete" datasets. Rubin's rules were used to pool parameter estimates, including mean deviation, regression coefficients, standard error, derive confidence intervals, and *p*-values. Multivariate imputation by MICE to handle missing values could reduce bias in the feature selection process.

Continuous variables were represented as mean ± standard deviation or median (interquartile range, IQR). The cutoff value of quantitative variables was selected by applying surv_cutpoint function as implemented in "survminer" package. The proportional subdistribution hazard ratios (sHR) were estimated by the Fine and Gray model (21). Univariate and multivariate competing risks regression analysis were performed to select risk factors with *p*-value <0.05 for constructing the final nomogram. The cumulative incidence function curve (CIF) with Fine and Gray's test was applied to evaluate the cumulative risk of primary outcome and competing risk events between the groups. A key assumption of CIF is that only one event can occur each time, and the subsequent occurrence of other event types are precluded. The cumulative incidence function for the *k*th cause is defined as $\mathrm{CIFk}(t) = \Pr(T \le t, D = k)$, which allowed for calculating the respective CIF of events of interest and competing risk events.

The nomogram predicted the 20, 40, 60, 80, and 100 months of HCC probability among cirrhosis patients. Discrimination and predictive accuracy were assessed using the area under the time-dependent receiver operator characteristic (ROC) curve (time-dependent AUC). The consistency was evaluated using a calibration curve with Brier scores and Harrell's concordance index. Basing on the established model, we predicted high-risk and low-risk groups with HCC cumulative incidence rate. CIF analysis and Fine and Gray's test were used to compare

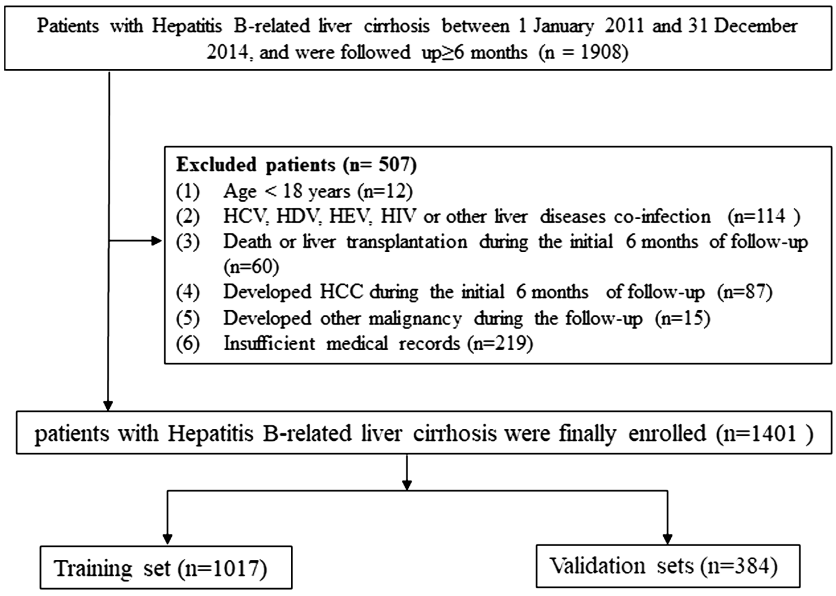

FIGURE 1
Flow chart of the enrollment in this study.

thecumulative incidence rate curves of the two groups. R (version 4.2.2) software was applied for all statistical testing and visual analysis. Extension packages, including "rms", "cmprsk," "riskRegression," "pec", and "timeROC," were also used. A *p*-value <0.05 was considered statistically significant.

Result

Multiple imputation for missing data in baseline characteristics

A total of 1,401 liver cirrhosis patients, from January 1, 2011 to December 31, 2014, who met the eligibility criteria were retrospectively enrolled. We assessed the demographic, laboratory, and clinical characteristics between the original database and the 20-times-imputation datasets (Table 1). The most missing data in

TABLE 1 Characteristics comparison of participants for the original database and 20 times multiple imputation datasets.

	Original data (missing number, value)		Pooled MI datasets
Age (years, IQR)	0	50.23 (42.52–57.21)	–
Sex (male/female)	0	998/403	–
Events (alive/HCC/death and LT)	0	821/442/138	–
Ascites (none/some/much)	0	864/482/55	–
Hepatic encephalopathy (yes/no)	0	102/1,299	–
Gastrointestinal bleeding (yes/no)	0	83/1,318	–
Hepatic failure (yes/no)	0	29/1,372	–
Antiviral therapy (yes/no)	0	809/592	–
Alcohol drinking (yes/no)	0	313/1,088	–
Alanine aminotransferase (U/L)	7 (0.49%)	39 (26.0–69.0)	39 (26–68.9)
Aspartate aminotransferase (U/L)	7 (0.49%)	44 (31.75–75)	44 (31.58–74.68)
WBC count × 10^9/L	15 (1.07%)	4.02 (2.97–5.27)	4.02 (2.97–5.27)
Neutrophil count × 10^9/L	15 (1.07%)	2.29 (1.63–3.19)	2.29 (1.63–3.19)
Lymphocyte count × 10^9/L	15 (1.07%)	1.17 (0.77–1.64)	1.18 (0.77–1.64)
Monocyte count × 10^9/L	15 (1.07%)	0.26 (0.18–0.36)	0.26 (0.18–0.36)
Hemoglobin (g/L)	15 (1.07%)	128 (108–146)	128 (108–146)
Platelet count × 10^9/L	15 (1.07%)	76.0 (52–112)	76.1 (52–112)
Total bilirubin (μmol/L)	7 (0.49%)	24.2 (16.4–38.5)	24.20 (16.42–38.30)
Direct bilirubin (μmol/L)	7 (0.49%)	5.2 (3.4–10.53)	5.2 (3.4–10.50)
Total protein (g/L)	7 (0.49%)	68.15 (61.58–73.3)	68.20 (61.60–73.29)
Albumin (g/L)	7 (0.49%)	37.45 (31.6–42.5)	37.49 (31.69–42.5)
Globulin (g/L)	7 (0.49%)	29.5 (25.8–33.6)	29.5 (25.8–33.6)
γ-GT (U/L)	8 (0.57%)	46 (27–87)	46 (27–87)
Alkaline phosphatase (U/L)	8 (0.57%)	87.0 (66–113)	86.7 (66–113)
Prealbumin (mg/L)	8 (0.57%)	101 (62–147)	101 (62–147)
Total bile acid (μmol/L)	8 (0.57%)	18.4 (7–43.45)	18.4 (7.05–43.51)
Cholinesterase (U/L)	8 (0.57%)	4,290 (2,794.25–6,453.5)	4,292.15 (2,799.15–6,449.33)
Cholesterol (mmol/L)	11 (0.79%)	3.61 (2.92–4.38)	3.61 (2.92–4.38)
Prothrombin time (s)	130 (9.28%)	13.9 (12.3–16)	13.6 (12.18–15.56)
Prothrombin time activity (%)	130 (9.28%)	73.2 (60.7–86.95)	76.73 (62.77–89.06)
International normalized ratio	130 (9.28%)	1.2 (1.07–1.37)	1.17 (1.06–1.35)
Fibrinogen (g/L)	130 (9.28%)	1.78 (1.37–2.25)	1.84 (1.44–2.33)
Thrombin time (s)	130 (9.28%)	19.3 (17.2–21.2)	19.28 (17.23–21.18)
HBsAg (IU)	3 (0.21%)	887.5 (336.85–1,560.5)	887.72 (337.49–1,562.15)
HBeAg (positive/negative)	3 (0.21%)	510/888	512/889
HBV DNA (positive/negative)	0	910/491	–
Alpha fetoprotein (ng/mL)	22 (1.57%)	4.69 (2.31–12.84)	4.69 (2.30–12.85)
Child–Pugh (A/B/C)	0	748/411/242	–
Family history of CHB (yes/no)	0	540/861	–
Family history of liver cancer (yes/no)	0	77/1,324	–

(Continued)

TABLE 1 Continued

MI, multiple imputation; IQR, interquartile range; HBsAg, hepatitis B surface antigen; HBeAg, hepatitis Be antigen; γ-GT, gamma-glutamyltransferase.
-, N.A.

clinical parameters (PT, PTA, INR, fibrinogen, and thrombin time) were 130 (9.3%). The rest of the variables had a missing proportion of less than 1.57%. The negligible difference between the original database and the 20 imputed datasets allowed for the usage of the latter for predicative research of cirrhosis patients' outcome.

Follow–up and patient outcomes

The median follow-up time was 69.9 months (IQR: 43.8–86.6). By the end of the follow-up, 80 cirrhosis patients died and 58 received LT; therefore, 138 cases were set as competitive risk events (event 2). A total of 442 patients developed HCC and were set as event of interest (event 1). The cumulative HCC incidences of 1, 3, 5, and 7 years were 1.6% (95%CI, 1.1%–2.3%), 13.3% (95%CI, 11.6%–15.2%), 22.9 (95% CI, 20.8%–25.2%), and 32.2% (95%CI, 29.6%–35.0%), respectively. The cumulative incidences of death and LT at 1, 3, 5, and 7 years were 0.3% (95%CI, 0.1%–0.7%), 2.6% (95%CI, 1.9%–3.6%), 5.0 (95%CI, 4.0%–6.3%), and 9.1% (95%CI, 7.5%–10.8%), respectively (Figure 2). The characteristics of HCC diagnosed at the end of the follow-up are summarized in Supplementary Table S1. In the HCC stage, above 60% of patients had single or small tumors or BCLC stage A, and in about 83.2% of patients metastasis did not occur.

Variable selection for predicting HCC

The univariate and multivariate competing risk regression analyses in 20 training imputed datasets were performed to select the predicting factors of HCC and estimate the respective sHRs (Table 2). Univariate analysis showed that nine variables including age, sex, antiviral therapy, alcohol drinking, family history of CHB, alanine transaminase, hepatitis B e antigen (HBeAg), hepatitis B surface antigen (HBsAg), and alpha fetoprotein (AFP) were associated with the risk of HCC. After multivariate competing risk regression analysis, six independent risk factors including age, sex, antiviral therapy history, alcohol drinking history, HBeAg, and AFP were finally identified and incorporated into the model. Cumulative incidence curve analyses of the six prognostic factors were plotted based on Fine–Gray test (Figure 3). It could be seen that the HCC risk had a statistical increase in the male group, older age (≥51 years) group, positive of HBeAg group, unacceptance of antiviral therapy group, alcohol drinking group, and high AFP level [$\log_{10}$ (AFP) ≥ 0.57) group (all Fine–Gray test, $p < 0.05$). The sHR of the prognostic factors are outlined in Table 2.

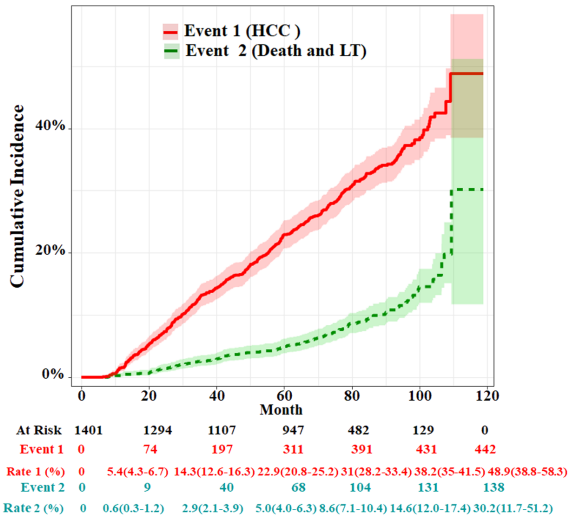

FIGURE 2
Cumulative incidence functions for HCC and competing risks event in the whole cohort. LT, liver transplantation.

Establishment and internal validation of the nomogram

The HCC competing risk nomogram was established in 20 imputed training datasets based on the following six independent predictive factors: age, sex (female or male), antiviral therapy history (yes or no), HBeAg (positive or negative), alcohol drinking history (yes or no), and $\log_{10}$ (AFP). The coefficients of competing risk nomogram are shown in Supplementary Table S2. This model could be used to calculate the probability of HCC occurrence for each cirrhosis patient—for example, a 46.36-year-old and alcohol-drinking male cirrhosis patient with 2.56 ng/mL of AFP, accepting antiviral therapy and HBeAg negative at diagnosis of cirrhosis, had a total score of about 273, and the respective 20-, 40-,60-,80-, and 100-month HCC incidences were about 4.1%, 10.5%, 16.9%, 24.1%, and 32.4% (Figure 4A).

Evaluating model overfitting was performed through bootstrap internal validation method. After 1,000 bootstrap cross-validation iterations, the adjusted C-index of the model was 0.75 (95%CI, 0.71–0.79). The time-dependent AUC was used to validate the discriminative ability of the nomogram. The time-dependent AUC values for the prediction of HCC at 12, 24, 36, 60, and 96 months in the training cohort were 0.68 (95%CI, 0.60–0.76), 0.74 (95%CI, 0.69–0.78), 0.70 (95%CI, 0.66–0.75), 0.75 (95%CI, 0.71–0.78), and 0.75 (95%CI, 0.70–0.80), respectively (Figure 4B). The adjusted Brier scores of the calibration curve for the model at 12, 24, 36, 60, and 96 months were 0.34 (95%CI, 0.31–0.36), 0.29 (95%CI, 0.27–0.32), 0.26 (95%CI, 0.24–0.28), 0.22 (95%CI, 0.20–0.23), and 0.20 (95%CI, 0.19–0.21) (Figure 4C), respectively. Similarly, the time-dependent AUC values were assessed in the validation cohort at 12, 24, 36, 60, and 96 months, which were 0.68 (95%CI, 0.52–0.83), 0.69 (95%CI, 0.60–0.78), 0.70 (95%CI, 0.62–0.78), 0.68 (95%CI, 0.60–0.75), and 0.80 (95%CI, 0.73–0.87), respectively (Figure 4D), and the adjusted Brier scores were 0.30 (95%CI, 0.25–0.34), 0.25 (95% CI, 0.22–0.29), 0.23 (95%CI, 0.20–0.26), 0.21 (95%CI, 0.18–0.24), and 0.20 (95%CI, 0.19–0.22) (Figure 4E).

Performance of the competitive risk nomogram

In order to further evaluate the discriminative ability of the HCC competitive risk prediction nomogram, the risk score of each

TABLE 2 Univariate and multivariate Fine–Gray competing risk regression analyses in the training set (pooled MI datasets).

	Univariate analysis		Multivariate analysis	
	sHR (95%CI)	*p*-value	sHR (95%CI)	*p*-value
Age (years)	1.02 (1.01–1.03)	1.30e-07	1.04 (1.03–1.04)	7.09e-13
Sex (female vs. male)	0.77 (0.71–1.01)	0.033	0.58 (0.46–0.75)	2.31e-04
Antiviral therapy history (yes/no)	0.43 (0.36–0.52)	1.12e-13	0.46 (0.38–0.56)	7.35e-11
Alcohol drinking history	1.37 (1.16–1.64)	0.0025	1.43 (1.15–1.78)	7.30e-03
Family history of CHB (yes vs. no)	1.39 (1.16–1.67)	0.0026	1.33 (1.09–1.62)	0.175
Family history of liver cancer (yes vs. no)	1.78 (1.27–2.53)	0.057		
Alanine aminotransferase (U/L), ≥40 vs. <40	1.34 (1.14–1.58)	0.015	1.09 (0.89–1.34)	0.48
Aspartate aminotransferase (U/L), ≥40 vs. <40	1.18 (0.99–1.39)	0.11		
Total bilirubin (μmol/L), ≥50.8 vs. <50.8	0.71 (0.57–0.89)	0.097		
Direct bilirubin (μmol/L), ≥10.7 vs. <10.7	0.78 (0.65–0.95)	0.33		
HBeAg (positive/negative)	1.69 (1.44–1.98)	5.95e-08	1.52 (1.24–1.86)	7.78e-04
$\log_{10}$ (HBsAg), (IU)	1.29 (1.16–1.44)	1.51e-04	0.99 (0.88–1.12)	0.98
Total protein (g/L), ≥65 vs. <65	1.07 (0.91–1.25)	0.50		
Albumin (g/L), ≥40 vs. <40	1.89 (0.71–5.02)	0.28		
γ-GT (U/L), ≥50 vs. <50	1.00 (0.99–1.01)	0.128		
Alkaline phosphatase (U/L), ≥125 vs. <125	1.14 (0.96–1.38)	0.21		
Hemoglobin (g/L), ≥130 vs. <130	1.31 (1.12–1.54)	0.051		
International normalized ratio	0.85 (1.65–1.13)	0.37		
Fibrinogen (g/L)	1.11 (0.99–1.233)	0.13		
MLR, ≥0.44 vs. <0.44	0.84 (0.70–1.00)	0.112		
NLR, ≥1.56 vs. <1.56	0.85 (0.71–1.03)	0.18		
PLR, ≥53.5 vs. <53.5	0.83 (0.69–1.00)	0.109		
$\log_{10}$ (AFP), (ng/mL)	1.47 (1.30–1.65)	1.5e-07	1.49 (1.27–1.55)	1.44e-05

sHR, subdistribution hazard ratios; MI, multiple imputation; IQR, interquartile range; HBsAg, hepatitis B surface antigen; HBeAg, hepatitis Be antigen; γ-GT, gamma-glutamyltransferase; MLR, monocyte-to-lymphocyte ratio; NLR, neutrophil-to-lymphocyte ratio; PLR, platelet-to-lymphocyte ratio; AFP, alpha fetoprotein.

cirrhosis patient was calculated. The low-risk group (score <1.67) and high-risk group (score ≥1.67) were created based on the cutoff value of the risk score, which was selected by applying surv_cutpoint function implemented in "survminer" software. Patients in the training and validation cohorts were stratified based on their risk scores of HCC in the presence of competing events. The cumulative incidence curves of HCC and competitive risk event in the two groups were drawn (Figure 5). The respective incidences had significant differences in the low-risk and high-risk groups both in the two cohorts ($p < 0.001$). For the training cohort, the cumulative 20-, 40- 60-, 80-, and 100-month incidences of HCC were 11.2 (95%CI, 8.2–13.6), 26.0 (95%CI, 21.6–30.6), 42.1 (95%CI, 36.9–47.1), 53.0 (95%CI, 47.2–58.5), and 63.2 (95%CI, 55.7–69.8) in the high-risk group and 2.4 (95%CI, 1.4–3.8), 7.7 (95%CI, 5.8–10.0), 13.0 (95%CI, 10.5–15.8), 19.4 (95%CI, 16.2–22.90), and 26.3 (95% CI, 22.0–30.8) in the low-risk group ($p < 0.001$) (Figure 5A). The cumulative 20-, 40- 60-, 80-, and 100-month incidences of HCC were 8.6 (95%CI, 4.8–13.7), 23.2 (95%CI, 16.7–30.62), 32.7 (95%CI, 25.3–40.3), 43.3 (95%CI, 34.5–51.9), and 60.6 (95%CI, 45.0–73.1) in the high-risk group and 2.2 (95%CI, 0.8–4.8), 8.4 (95%CI, 5.3–12.5), 13.8 (95%CI, 9.7–18.7), 20.8 (95%CI, 15.5–26.8), and 26.0 (95%CI, 19.4–33.2) in the validation cohort (Figure 5B). In addition, patients with a higher HCC risk did not have a higher risk of death and LT.

Meanwhile, we compare our model with four other existing risk scores whose parameters all included HBV infection and cirrhosis. Toronto HCC risk index (THRI) scoring system, our previous You'an model (11), the AASL (age, albumin, sex and liver cirrhosis)-HCC scoring system, and real-world risk score for hepatocellular carcinoma (RWS-HCC) were allowed to apply our data. The result of time-dependent AUC of our model and other four models showed that our model has best discriminatory power (Figure 6).

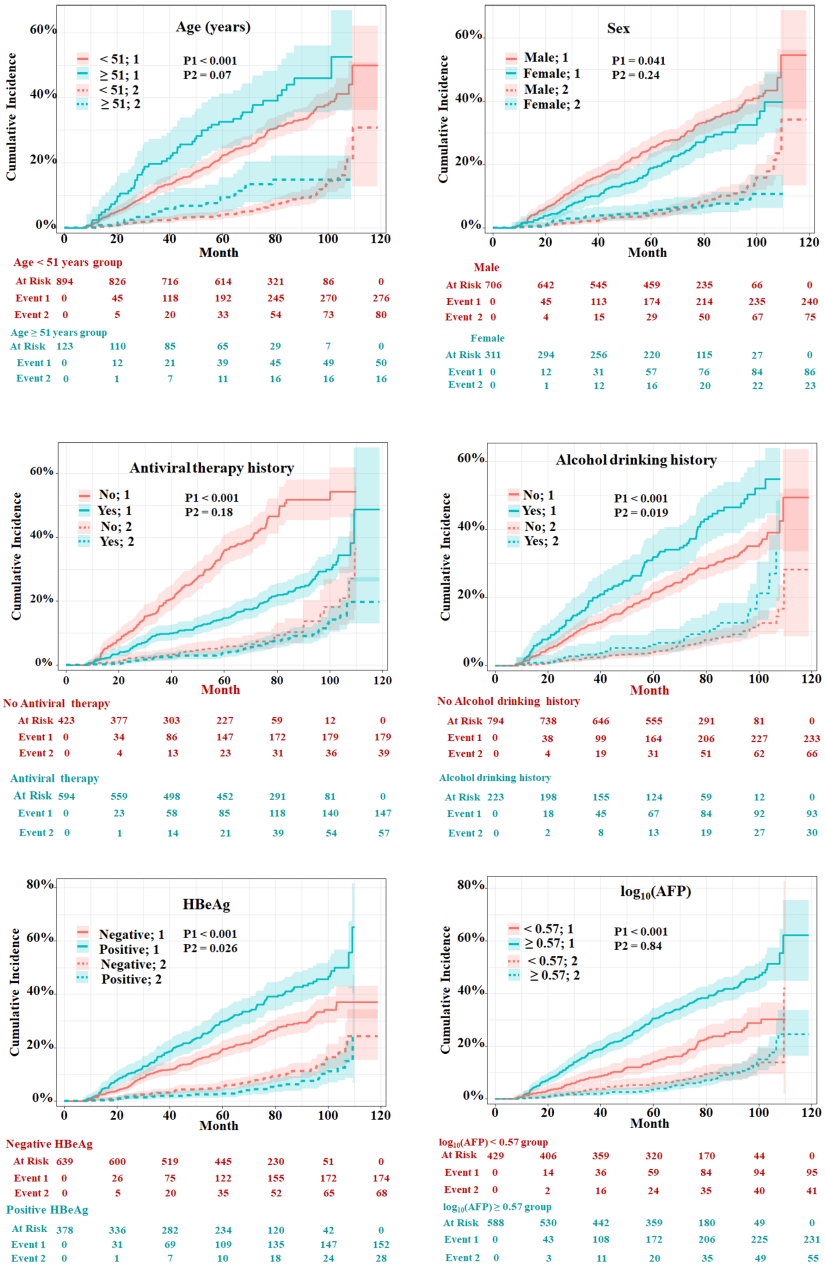

FIGURE 3
Evaluation of cumulative incidence rate for HCC of predictive risk factors in patients with HBV-related cirrhosis of the training cohort. "1" represents the outcome as HCC; "2" represents the outcome as competing risks (cirrhosis-related death and liver transplantation). The *p*-values were determined using Fine–Gray test.

Discussion

Early screening of HCC is strongly recommended for HCC surveillance in high-risk HBV cirrhosis patients. The individualized risk of HCC varies with different etiologies of cirrhosis. In this study, we conducted a long-term follow-up (median, 69.9 months) of a large clinical cohort of patients with HBV-related cirrhosis and provided important data on the incidence rate of HCC. The establishment and validation of a competing risk model to predict the 10-year cumulative incidence of HCC in patients with HBV-related cirrhosis were pursued. During the follow-up of 0–10 years, the cumulative incidence rate of HCC in the high-risk group was significantly higher than that in the low-risk group.

The fact that the etiology of liver cirrhosis is a key determinant of HCC risk (10) indicates that there are specific risk factors for HCC in patients with HBV-related cirrhosis. After adjusting for other risk factors, the relative risk of HCC for HBsAg-positive patients alone was 9.6 (95%CI, 6.0–15.2 compared to negative patients, while the relative risk of HCC for HBsAg and HBeAg-positive patients was 60.2 (95%CI, 35.5–102.1). Positive HBeAg usually indicated active replication of HBV in hepatocytes and was an increased risk factor for HCC in CHB patients (22). In fact, liver

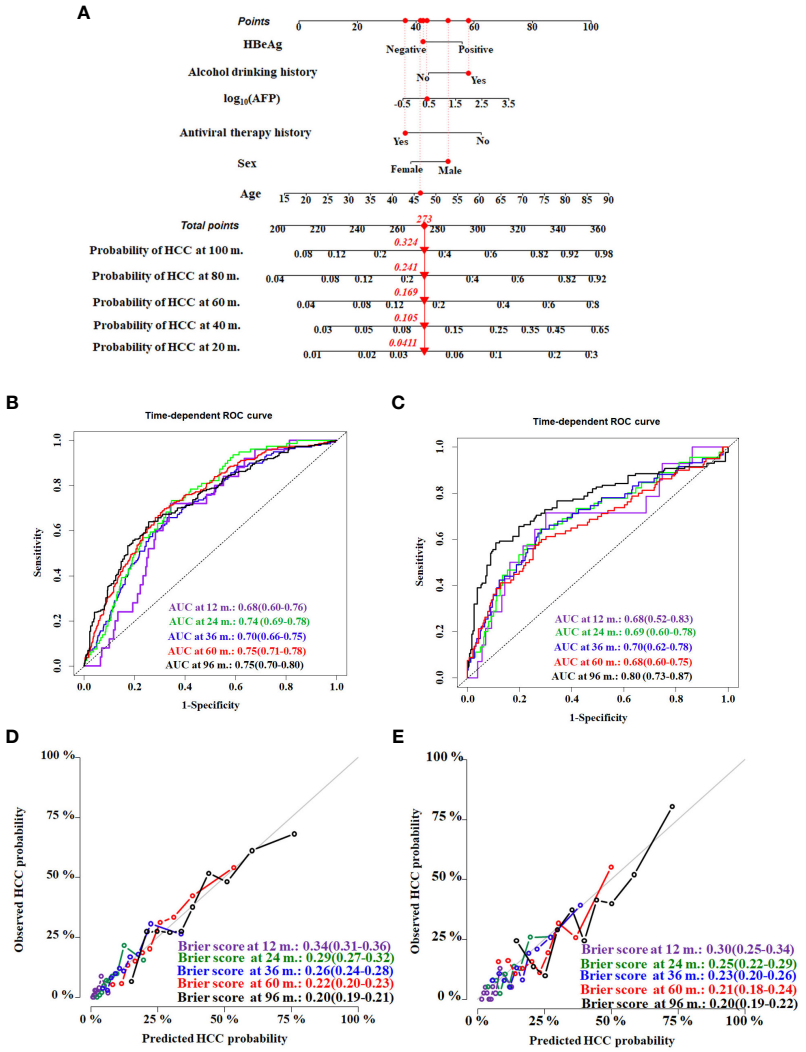

FIGURE 4
Construction and validation of the HCC competing risk nomogram for predicting the probability in HBV-related cirrhosis patients. **(A)** HCC competing risk nomogram. Time-dependent ROC curves by nomogram for HCC occurrence probability at 12, 24, 36, 60, and 96 months in the training cohort **(B)** and the validation cohort **(C)**. Calibration curves of nomogram in terms of agreement between predicted and actual HCC occurrence probability at 12, 24, 36, 60, and 96 months in the training cohort **(D)** and the validation cohort **(E)**. AUC, area under receiver operating characteristic curve.

cirrhosis patients who clear HBeAg and inhibit HBV DNA could significantly reduce the risk of HCC (23). In this study, positive HBeAg is also an increased risk factor for HCC among cirrhosis patients. It is currently clear that antiviral therapy reduces the HCC risk in CHB patients with or without cirrhosis.

Liver cirrhosis is a typical multistate model of disease progression (24); its clinical states mostly include compensated and decompensated cirrhosis and advanced decompensated state (16). The mortality rate varies in different states. In untreated patients with decompensated state, death occur in approximately 30% in 1 to 2 years after the index bleeding. Ascites is associated with a 5-year mortality of about 50% in decompensated patients (25). Overt hepatic encephalopathy and/or jaundice are associated with a 5-year survival of about 20% in advanced cirrhosis (26, 27). Renal function impairment (28), liver dysfunction, and bacterial infections (29) are associated with organ failures and high mortality in advanced cirrhosis. Competing events (cirrhosis related-death and LT) are frequent in liver cirrhosis. Death should always be considered a competing risk for assessing the incidence of HCC event in the course of the disease. If a competing event is treated as considered data, the probability of an event is overestimated using the Kaplan–Meier method (30–33). Competing risk analysis is based on the CIF to predict the probability of any event occurring first, resulting in a desirable total probability from zero to one (or the sum of probabilities for each event) (16). Meantime, because of the occurrence of competing events precluding the occurrence of event of interest, its probability does not necessarily approach unity in the end (34).

In this study, we applied Fine–Gray models and CIF to assess the risk factor and cumulative incidence of HCC in the presence of competing risks. The risk factors, i.e., alcohol drinking (yes or no) and HBeAg (positive or negative) at diagnosis of cirrhosis, were

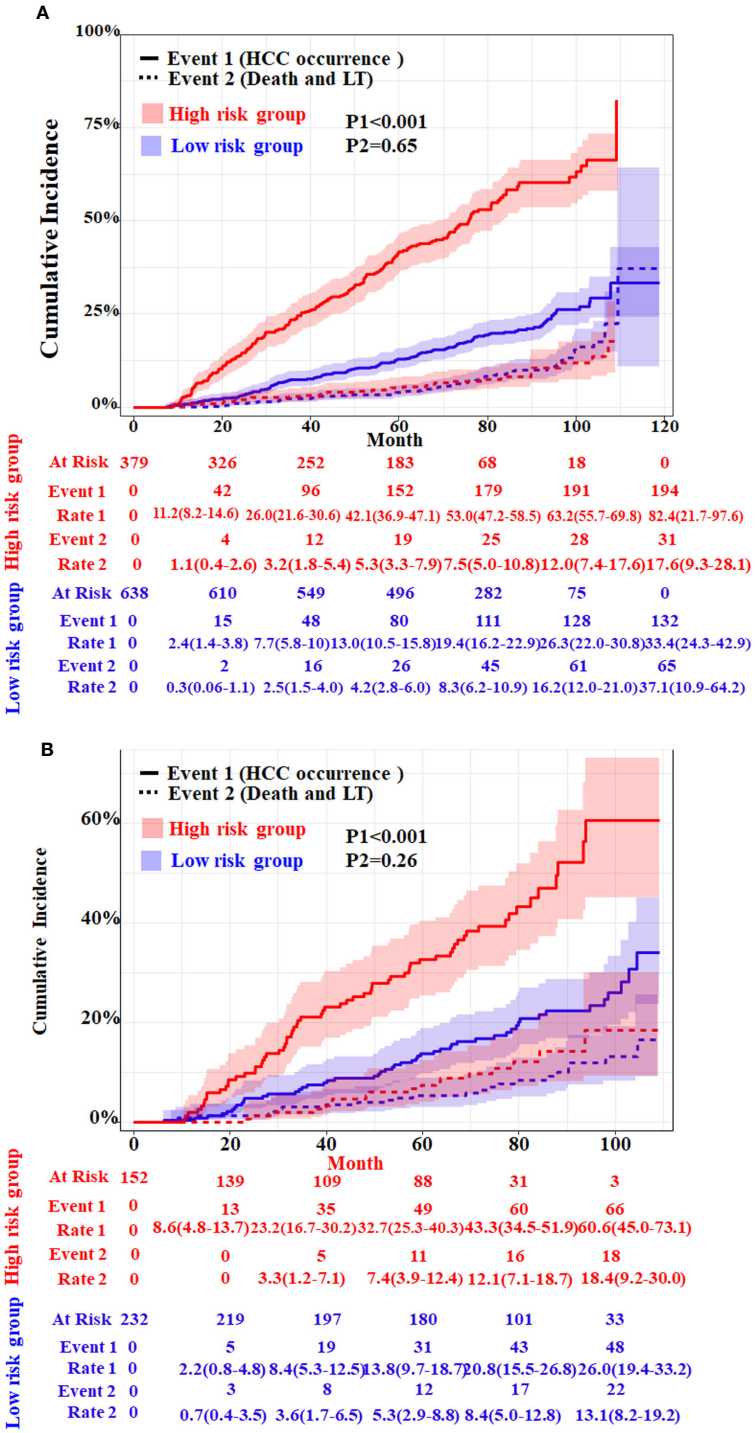

FIGURE 5
Cumulative incidence with 95%CI of HCC and competing risks event in the low- and high-risk groups of HBV-related cirrhosis patients in the training cohort **(A)** and the validation cohort **(B)**. LT, liver transplantation. The *p*-values were determined using Fine–Gray test.

significantly correlated with HCC (both $p < 0.001$). Meanwhile, they also were slightly associated with competing events (both $p < 0.05$). The other four predictive factors, $\log_{10}$(AFP), age, sex (female or male), and antiviral therapy (yes or no), were all significantly associated with HCC (both $p < 0.05$). However, they did not show an association with competing events (both $p > 0.05$). The cumulative risk incidence of HCC and competing events were both evaluated simultaneously using these variables. Meanwhile, our model was allowed to be used for predicting HCC risk in individual patients with liver cirrhosis, taking into account both the association between risk factors and HCC and the modifying effect of competition events on this association.

This study also had limitations. Firstly, due to the retrospective nature, selection bias is inevitable, and further external validation is

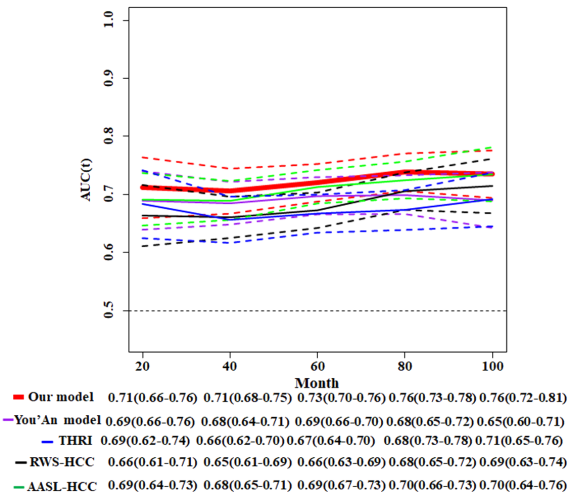

FIGURE 6
Comparison of time-dependent AUCs with 95%CIs for the competitive risk nomogram and other four HCC models. THRI, Toronto HCC risk index scoring system; You'An model, our previous research (11); AASL-HCC, age, albumin, sex and liver cirrhosis-HCC scoring system; RWS-HCC, real-world risk score for hepatocellular carcinoma.

needed to increase the extrapolation of the model. Secondly, risk factors from common laboratory tests in hospitals were fully analyzed in this study. Transaldolase and aldolase B regulated the reprogramming of pentose phosphate pathway to have a deep effect on hepatocellular carcinogenesis (35–37). Thus, the novel metabolic markers should be comprehensively evaluated as risk variables that might improve predictive performance. Thirdly, potential interactions between risk factors need to be explored to evaluate the effects on outcomes.

Conclusions

In the present study, we provided a systematic estimation of HCC in HBV-related liver cirrhosis patients using a retrospective cohort followed up for more than 10 years. Moreover, we established and validated a competing risk nomogram to predict the HCC risk, which might be a convenient and predictive tool for HCC screening.

Data availability statement

The original contributions presented in the study are included in the article/Supplementary Material. Further inquiries can be directed to the corresponding authors.

Ethics statement

The studies involving humans were approved by Ethics Committee of the Beijing You'An Hospital. The studies were conducted in accordance with the local legislation and institutional requirements. The ethics committee/institutional review board waived the requirement of written informed consent for participation from the participants or the participants' legal guardians/next of kin because this article is a retrospective study. Therefore, the institutional waived the requirement to obtain distinct written informed consent from the patients.

Author contributions

DG: Conceptualization, Data curation, Formal Analysis, Methodology, Supervision, Writing – original draft, Writing – review & editing. JL: Conceptualization, Data curation, Writing – review & editing. PZ: Conceptualization, Data curation, Writing – review & editing. TM: Formal Analysis, Methodology, Writing – review & editing. KL: Conceptualization, Writing – review & editing. YZ: Conceptualization, Data curation, Project administration, Writing – review & editing.

Funding

The author(s) declare financial support was received for the research, authorship, and/or publication of this article. This study was funded by a grant Beijing research center for respiratory infectious diseases project (BJRID2024–007), the Beijing You'An Hospital (BJYAYY-YN2023–10) and Construction of research-oriented wards in Beijing municipality.

Conflict of interest

The authors declare that the research was conducted in the absence of any commercial or financial relationships that could be construed as a potential conflict of interest.

Publisher's note

All claims expressed in this article are solely those of the authors and do not necessarily represent those of their affiliated organizations, or those of the publisher, the editors and the reviewers. Any product that may be evaluated in this article, or claim that may be made by its manufacturer, is not guaranteed or endorsed by the publisher.

Supplementary material

The Supplementary Material for this article can be found online at: https://www.frontiersin.org/articles/10.3389/fonc.2024.1398968/full#supplementary-material

References

1. Xie DY, Ren ZG, Zhou J, Fan J, Gao Q. 2019 Chinese clinical guidelines for the management of hepatocellular carcinoma: updates and insights. *Hepatobiliary Surg Nutr*. (2020) 9:452–63. doi: 10.21037/hbsn

2. Man L, Qun WZ, Lu Z, Hao Z, Wu LD, Geng ZM. Burden of cirrhosis and other chronic liver diseases caused by specific etiologies in China, 1990–2016: findings from the global burden of disease study 2016. *BioMed Environ Sci*. (2020) - 33:1–10. doi: 10.3967/bes2020.001

3. Yan YP, Su HX, Ji ZH, Shao ZJ, Pu ZS. Epidemiology of hepatitis B virus infection in China: current status and challenges. *J Clin Transl Hepatol*. (2014) 2:15–22. doi: 10.14218/JCTH

4. Omata M, Cheng AL, Kokudo N, Kudo M, Lee JM, Jia J, et al. Asia-Pacific clinical practice guidelines on the management of hepatocellular carcinoma: a 2017 update. *Hepatol Int*. (2017) 11:317–70. doi: 10.1007/s12072-017-9799-9

5. EASL-EORTC clinical practice guidelines: management of hepatocellular carcinoma. *J Hepatol*. (2012) 56:908–43. doi: 10.1016/j.jhep.2011.12.001

6. Marrero JA, Kulik LM, Sirlin CB, Zhu AX, Finn RS, Abecassis MM, et al. Diagnosis, staging, and management of hepatocellular carcinoma: 2018 practice guidance by the american association for the study of liver diseases. *Hepatology*. (2018) 68:723–50. doi: 10.1002/hep.29913

7. Trinchet JC, Chaffaut C, Bourcier V, Degos F, Henrion J, Fontaine H, et al. Ultrasonographic surveillance of hepatocellular carcinoma in cirrhosis: a randomized trial comparing 3- and 6-month periodicities. *Hepatology*. (2011) 54:1987–97. doi: 10.1002/hep.24545

8. Andersson KL, Salomon JA, Goldie SJ, Chung RT. Cost effectiveness of alternative surveillance strategies for hepatocellular carcinoma in patients with cirrhosis. *Clin Gastroenterol Hepatol*. (2008) 6:1418–24. doi: 10.1016/j.cgh.2008.08.005

9. Pocha C, Dieperink E, McMaken KA, Knott A, Thuras P, Ho SB. Surveillance for hepatocellular cancer with ultrasonography vs. computed tomography – a randomised study. *Aliment Pharmacol Ther*. (2013) 38:303–12. doi: 10.1111/apt.2013.38.issue-3

10. Sharma SA, Kowgier M, Hansen BE, Brouwer WP, Maan R, Wong D, et al. Toronto HCC risk index: A validated scoring system to predict 10-year risk of HCC in patients with cirrhosis. *J Hepatol*. (2018) 68:92–9. doi: 10.1016/j.jhep.2017.07.033

11. Wang Q, Guo D, Gao W, Yuan C, Li J, Zhang Y, et al. Individual surveillance by competing risk model for patients with hepatocellular carcinoma occurrence in all-cause cirrhosis. *J Cancer Res Clin Oncol*. (2023) 149:13403–16. doi: 10.1007/s00432-023-04911-y

12. Yu JH, Suh YJ, Jin YJ, Heo NY, Jang JW, You CR, et al. Prediction model for hepatocellular carcinoma risk in treatment-naive chronic hepatitis B patients receiving entecavir/tenofovir. *Eur J Gastroenterol Hepatol*. (2019) 31:865–72. doi: 10.1097/MEG.0000000000001357

13. Poh Z, Shen L, Yang HI, Seto WK, Wong VW, Lin CY, et al. Real-world risk score for hepatocellular carcinoma (RWS-HCC): a clinically practical risk predictor for HCC in chronic hepatitis B. *Gut*. (2016) 65:887–8. doi: 10.1136/gutjnl-2015-310818

14. Wong VW, Chan SL, Mo F, Chan TC, Loong HH, Wong GL, et al. Clinical scoring system to predict hepatocellular carcinoma in chronic hepatitis B carriers. *J Clin Oncol*. (2010) 28:1660–5. doi: 10.1200/JCO.2009.26.2675

15. Heimbach JK, Kulik LM, Finn RS, Sirlin CB, Abecassis MM, Roberts LR, et al. AASLD guidelines for the treatment of hepatocellular carcinoma. *Hepatology*. (2018) 67(1):358–80. doi: 10.1002/hep.29086

16. D'Amico G, Morabito A, D'Amico M, Pasta L, Malizia G, Rebora P, et al. Clinical states of cirrhosis and competing risks. *J Hepatol*. (2018) 68:563–76. doi: 10.1016/j.jhep.2017.10.020

17. Chinese Society of Hepatology. Chinese guidelines on the management of liver cirrhosis. *Zhonghua Gan Zang Bing Za Zhi*. (2019) 27:846–65. doi: 10.3760/cma.j.issn.1007-3418.2019.11.008

18. General Office of National Health Commission. Standard for diagnosis and treatment of primary liver cancer (2022 edition). *J Clin Hepatol*. (2022) 38:288–303. doi: 10.3969/j.issn.1001-5256.2022.02.009

19. Åström H, Ndegwa N, Hagström H. External validation of the Toronto hepatocellular carcinoma risk index in a Swedish population. *JHEP Rep*. (2021) 3:100343. doi: 10.1016/j.jhepr.2021.100343

20. van Buuren S, Groothuis-Oudshoorn K. mice: multivariate imputation by chained equations in R. *J Stat Software*. (2011) 45:1–67. doi: 10.18637/jss.v045.i03

21. Fine JP, Gray RJ. A proportional hazards model for the subdistribution of a competing risk. *J Am Stat Assoc*. (1999) 94:496–509. doi: 10.1080/01621459.1999.10474144

22. Yang H-I, Lu S-N, Liaw Y-F, You S-L, Sun C-A, Wang L-Y, et al. Hepatitis B e antigen and the risk of hepatocellular carcinoma. *N Engl J Med*. (2002) 347:168–74. doi: 10.1056/NEJMoa013215

23. Fattovich G, Stroffolini T, Zagni I, Donato F. Hepatocellular carcinoma in cirrhosis: Incidence and risk factors. *Gastroenterology*. (2004) 127:S35–50. doi: 10.1053/j.gastro.2004.09.014

24. Jepsen P, Vilstrup H, Andersen PK. The clinical course of cirrhosis: The importance of multistate models and competing risks analysis. *Hepatology*. (2015) 62:292–302. doi: 10.1002/hep.27598

25. Planas R, Montoliu S, Ballesté B, Rivera M, Miquel M, Masnou H, et al. Natural history of patients hospitalized for management of cirrhotic ascites. *Clin Gastroenterol Hepatol*. (2006) 4:1385–94,94.e1. doi: 10.1016/j.cgh.2006.08.007

26. D'Amico G, Pasta L, Morabito A, D'Amico M, Caltagirone M, Malizia G, et al. Competing risks and prognostic stages of cirrhosis: a 25-year inception cohort study of 494 patients. *Aliment Pharmacol Ther*. (2014) 39:1180–93. doi: 10.1111/apt.12721

27. Jepsen P, Ott P, Andersen PK, Sørensen HT, Vilstrup H. Clinical course of alcoholic liver cirrhosis: A Danish population-based cohort study. *Hepatology*. (2010) 51:1675–82. doi: 10.1002/hep.23500

28. Fagundes C, Barreto R, Guevara M, Garcia E, Solà E, Rodríguez E, et al. A modified acute kidney injury classification for diagnosis and risk stratification of impairment of kidney function in cirrhosis. *J Hepatol*. (2013) 59:474–81. doi: 10.1016/j.jhep.2013.04.036

29. Wiest R, Lawson M, Geuking M. Pathological bacterial translocation in liver cirrhosis. *J Hepatology*. (2014) 60:197–209. doi: 10.1016/j.jhep.2013.07.044

30. Yang J, Pan Z, He Y, Zhao F, Feng X, Liu Q, et al. Competing-risks model for predicting the prognosis of penile cancer based on the SEER database. *Cancer Med*. (2019) 8:7881–9. doi: 10.1002/cam4.2649

31. Tullio A, Magli A, Moretti E, Valent F. Why we should take care of the competing risk bias in survival analysis: A phase II trial on the toxicity profile of radiotherapy for prostate cancer. *Rep Pract Oncol Radiother*. (2019) 24:511–9. doi: 10.1016/j.rpor.2019.08.001

32. Saleh RR, Nadler MB, Desnoyers A, Rodin DL, Abdel-Qadir H, Amir E. Influence of competing risks on estimates of recurrence risk and breast cancer-specific mortality in analyses of the early breast cancer trialists collaborative group. *Sci Rep*. (2020) 10:4091. doi: 10.1038/s41598-020-61093-0

33. Nie ZQ, Ou YQ, Qu YJ, Yuan HY, Liu XQ. [A new perspective of survival data on clinical epidemiology: introduction of competitive risk model]. *Zhonghua liuxingbingxue zazhi*. (2017) 38:1127–31. doi: 10.3760/cma.j.issn.0254-6450.2017.08.026

34. Austin PC, Lee DS, Fine JP. Introduction to the analysis of survival data in the presence of competing risks. *Circulation*. (2016) 133:601–9. doi: 10.1161/CIRCULATIONAHA.115.017719

35. Oaks Z, Patel A, Huang N, Choudhary G, Winans T, Faludi T, et al. Cytosolic aldose metabolism contributes to progression from cirrhosis to hepatocarcinogenesis. *Nat Metab*. (2023) 5:41–60. doi: 10.1038/s42255-022-00711-9

36. Winans T, Oaks Z, Choudhary G, Patel A, Huang N, Faludi T, et al. mTOR-dependent loss of PON1 secretion and antiphospholipid autoantibody production underlie autoimmunity-mediated cirrhosis in transaldolase deficiency. *J Autoimmun*. (2023) 140:103112. doi: 10.1016/j.jaut.2023.103112

37. Li M, He X, Guo W, Yu H, Zhang S, Wang N, et al. Aldolase B suppresses hepatocellular carcinogenesis by inhibiting G6PD and pentose phosphate pathways. *Nat Cancer*. (2020) 1:735–47. doi: 10.1038/s43018-020-0086-7

frontiers | Frontiers in Oncology

TYPE Original Research
PUBLISHED 17 May 2024
DOI 10.3389/fonc.2024.1391486

OPEN ACCESS

EDITED BY
Francisco Tustumi,
University of São Paulo, Brazil

REVIEWED BY
Antonella Argentiero,
National Cancer Institute Foundation (IRCCS), Italy
Zheng Liu,
Virginia Commonwealth University, United States

*CORRESPONDENCE
Jinghai Song
jhaisong2003@126.com
Xuefei Li
xuefei.li@siat.ac.cn

†These authors have contributed equally to this work

RECEIVED 25 February 2024
ACCEPTED 06 May 2024
PUBLISHED 17 May 2024

CITATION
Tan T, Hu H, Zhang W, Cui J, Lu Z, Li X and Song J (2024) Novel immune classification based on machine learning of pathological images predicts early recurrence of hepatocellular carcinoma.
Front. Oncol. 14:1391486.
doi: 10.3389/fonc.2024.1391486

Novel immune classification based on machine learning of pathological images predicts early recurrence of hepatocellular carcinoma

Tianhua Tan[1†], Huijuan Hu[2†], Wei Zhang[3], Ju Cui[4], Zhenhua Lu[5], Xuefei Li[2*] and Jinghai Song[1*]

[1]Department of General Surgery, Beijing Hospital, National Center of Gerontology, Institute of Geriatric Medicine, Chinese Academy of Medical Sciences & Peking Union Medical College, Beijing, China, [2]Key Laboratory of Quantitative Synthetic Biology, Shenzhen Institute of Synthetic Biology, Shenzhen Institutes of Advanced Technology, Chinese Academy of Sciences, Shenzhen, Guangdong, China, [3]Department of Pathology, Beijing Hospital, National Center of Gerontology, Institute of Geriatric Medicine, Chinese Academy of Medical Sciences, Beijing, China, [4]The Key Laboratory of Geriatrics, Beijing Hospital, National Center of Gerontology, Institute of Geriatric Medicine, Chinese Academy of Medical Sciences, Beijing, China, [5]Key Laboratory of Carcinogenesis and Translational Research (Ministry of Education), Department of Gastrointestinal Cancer Center, Ward I, Peking University Cancer Hospital & Institute, Beijing, China

Introduction: Immune infiltration within the tumor microenvironment (TME) plays a significant role in the onset and progression of hepatocellular carcinoma (HCC). Machine learning applied to pathological images offers a practical means to explore the TME at the cellular level. Our former research employed a transfer learning procedure to adapt a convolutional neural network (CNN) model for cell recognition, which could recognize tumor cells, lymphocytes, and stromal cells autonomously and accurately within the images. This study introduces a novel immune classification system based on the modified CNN model.

Method: Patients with HCC from both Beijing Hospital and The Cancer Genome Atlas (TCGA) database were included in this study. Additionally, least absolute shrinkage and selection operator (LASSO) analyses, along with logistic regression, were utilized to develop a prognostic model. We proposed an immune classification based on the percentage of lymphocytes, with a threshold set at the median lymphocyte percentage.

Result: Patients were categorized into high or low infiltration subtypes based on whether their lymphocyte percentages were above or below the median, respectively. Patients with different immune infiltration subtypes exhibited varying clinical features and distinct TME characteristics. The low-infiltration subtype showed a higher incidence of hypertension and fatty liver, more advanced tumor stages, downregulated immune-related genes, and higher infiltration of immunosuppressive cells. A reliable prognostic model for predicting early recurrence of HCC based on clinical features and immune classification was established. The area under the curve (AUC) of the receiver operating characteristic (ROC) curves was 0.918 and 0.814 for the training and test sets, respectively.

Discussion: In conclusion, we proposed a novel immune classification system based on cell information extracted from pathological slices, provides a novel tool for prognostic evaluation in HCC.

KEYWORDS

hepatocellular carcinoma, pathological images, tumor microenvironment, early recurrence, prognostic model

1 Introduction

Liver cancer ranks as the fourth most common cause of cancer-related deaths and the sixth most frequently diagnosed cancer globally, with its highest incidence in East Asia and Africa and a rising occurrence worldwide (1). Hepatocellular carcinoma (HCC) stands as a predominant form of primary liver cancer, encompassing 75–85% of all cases (2). Patients diagnosed with early-stage HCC derive benefit from hepatic resection or transplantation, boasting a 5-year survival rate of 70%. Nonetheless, HCC exhibits a notable intrahepatic recurrence rate, with recurrence within 2 years affecting 50–70% of patients, signifying a poor prognosis (3). Recent advancements in systemic therapies have further enhanced overall survival rates (4, 5). A combination strategy of anti-angiogenesis agents with immunotherapy, bevacizumab plus atezolizumab, has been approved as the first-line treatment for patients with unresectable HCC, other anti-angiogenesis agents including regorafenib and cabozantinib have been proven to improve overall survival (OS) as second-line treatment (6). The various systemic therapies pose a new challenge for surgeons and oncologists in terms of selecting optimal personalized treatment strategies, and the study of the immune microenvironment of HCC provides evidence for addressing this challenge.

Previous studies have revealed that early recurrence of HCC is associated with both clinical and tumor traits, such as male gender, high levels of bilirubin and alpha-fetoprotein (AFP), tumor size, and microvascular invasion. Prediction models have been established based on these traits (7, 8). Advances in genomics and transcriptomics have further unveiled correlations between the tumor microenvironment (TME) and early recurrence at the molecular level (9, 10), while radiomics offers a different perspective on tumor traits (11). In addition to clinical characteristics and multiomics, pathological images also contain abundant information that has been insufficiently explored. HCC consists of a mixture of cell types, including malignant hepatocytes, immune cells, and stromal cells. Pathological images of HCC are commonly used to classify and grade tumors based on the degree of differentiation, satellite nodules, microvascular invasion, and other histological features. However, recognizing and annotating the types of individual cells in these images, and exploring the interactions among them, may provide more comprehensive information.

Lymphocytes constitute most immune cells in HCC, and studies indicate that abundant lymphocyte infiltration in HCC is associated with a better prognosis (12). Previous studies of lymphocyte infiltration primarily relied on the technique of genomics and transcriptomics, which required complicated examination and additional cost. Our previous study employed image processing techniques and adapted a convolutional neural network (CNN) initially designed for lung cancer to establish a novel cell recognition model suitable for patients with HCC (13), which classified cells autonomously and accurately in pathological images into three types: tumor cells, lymphocytes, and stromal cells (14). The cell recognition model provides a more efficient and available method to evaluate lymphocyte infiltration in the HCC landscape, reducing both time and financial cost.

Patients from the Beijing Hospital and the Liver Hepatocellular Carcinoma (LIHC) cohort in The Cancer Genome Atlas (TCGA) database were included. Given the crucial role of lymphocytes in tumor elimination and evasion, we categorized patients into high and low immune infiltration groups based on lymphocyte levels (15). Furthermore, we analyzed differences in clinical features, prognosis, and TME between these subtypes. We observed distinct disease-free survival (DFS) among different subtypes in both the Beijing Hospital and TCGA cohorts. To predict potential early recurrence of HCC (defined as DFS less than 1 year) (16), we developed a novel prognostic model based on clinical features and immune subtypes. Additionally, we created a nomogram to aid in clinical decision-making.

Our study primarily focused on individual cells within pathological images of HCC and proposed a novel immune subtype based on lymphocyte levels. These findings could offer new insights into the pathology of HCC and contribute to personalized post-operative treatment strategies.

2 Methods

2.1 Data collection and preprocessing

We examined patients who underwent surgical resection or liver transplantation between 2013 and 2019 at Beijing Hospital. Patients included in this study had to meet the following criteria: (a) be at least 18 years old; (b) have a pathological diagnosis of HCC; (c) not receive any preoperative treatment; (d) have no history of prior malignancy, autoimmune disease, or immune deficiency disease;

and (e) provide well-preserved formalin-fixed paraffin-embedded (FFPE) slides with hematoxylin-eosin (H&E) staining. Patients with incomplete clinical information were excluded. Ultimately, 64 patients were included in the study.

To analyze the TME of HCC and validate the prognostic model, pathological images, clinical information, and RNA-sequencing data were retrieved from the TCGA-LIHC database via Genomic Data Commons (http://gdc.cancer.gov/). Data preprocessing was conducted to enhance the quality of data and ensure the reliability of further analysis. The gene expression RNAseq data were normalized, duplicated values and missing values were eliminated. Patients without complete survival data or pathological images were excluded. Finally, 198 patients were included.

2.2 Pathologic images processing pipeline

Our prior study proposed a reliable and effective pathological images processing pipeline (14). Each image was digitally captured at 40× magnification and labeled as a region of interest (ROI), defined as the major malignant region, using the ImageScope annotation tool. Subsequently, we randomly sampled 20 patches within each ROI and calculated the number of tumor cells, lymphocytes and stromal cells within these patches.

2.3 Immune infiltration classification

To categorize tumors into distinct immune phenotypes, we initially determined the percentage of lymphocytes and the ratio of lymphocytes to tumor cells in each image. Subsequently, we conducted a test for normality to identify the parameter with the least dispersion, selected based on the interquartile range (IQR), for further analysis (15). Patients were then stratified into two subtypes based on immune infiltration levels: high and low. This categorization was determined using the median lymphocyte percentage as the threshold. Finally, we compared clinical features and prognosis between these two subtypes.

2.4 Functional enrichment analysis

We identified differentially expressed genes (DEGs) among various subtypes using the DESeq2 R package, employing criteria of a base mean > 10, log2 Fold Change > 1, and adjusted P value < 0.05 (17). Subsequently, we conducted Gene Ontology (GO) functional pathway enrichment analysis using the clusterProfiler R package, with significance determined at a P value < 0.05 (18). Furthermore, we obtained HALLMARK- and KEGG-related gene datasets from the Gene Set Enrichment Analysis (GSEA) official website. We then performed GSEA utilizing the GSEA algorithm (19) and Gene Set Variation Analysis (GSVA) employing the GSVA R package (20).

2.5 Evaluation of immune features

The ESTIMATE (Estimation of STromal and Immune cells in Malignant Tumor tissues using expression data) analysis was performed to assess the level of immune infiltration, utilizing the estimate R package (21). Additionally, Cell type Identification By Estimating Relative Subsets Of RNA Transcripts (CIBERSORT) analysis was employed to determine the relative abundance of 22 different immune cell types within the tumor tissue (22). Furthermore, Tumor Immune Dysfunction and Exclusion (TIDE) analysis was carried out to evaluate the potential for tumor immune escape, utilizing the TIDE website (http://tide.dfci.harvard.edu/) (23).

2.6 Prognostic model establishment and validation

To further investigate the prognostic value of immune classification, we categorized patients into two groups: a good prognosis group and a poor prognosis group, defined as having a DFS > 1 year (16). From the Beijing Hospital cohort, we collected 55 variables comprising clinical and pathological features. We then developed Receiver Operating Characteristic (ROC) curves for each variable using the pROC R package and extracted the Area Under the Curve (AUC) for evaluation (24). Variables with an AUC exceeding 0.6 were selected, and Least Absolute Shrinkage and Selection Operator (LASSO) analysis was employed to reduce the number of variables in the risk model using the Glmnet R package (25). A 20-fold cross-validation was conducted to identify the optimal lambda value. "Lambda.1se" was utilized to determine the minimum number of independent variables required for a well-performing model. Subsequently, we employed the Beijing Hospital cohort as the training set and 58 patients from the TCGA-LIHC database, who provided complete clinical information, as the test set. Logistic regression was then applied to establish a prognostic model, and ROC curves were generated for both the training and test sets. Finally, a nomogram was constructed based on the prognostic model.

2.7 Statistical analysis

OS was defined as the period between the day of pathological diagnosis and the day of death, while DFS was defined as the duration between the day of pathological diagnosis and the occurrence of tumor recurrence, metastasis, or death. Patients who remained free of recurrence were censored at the final follow-up. Survival analysis was conducted using Kaplan–Meier (K-M) analysis employing the Survival and Survminer R packages. Categorical and non-normally distributed measurement variables were compared using the Wilcoxon test, whereas normally distributed measurement variables were compared using the t-test. All statistical analyses were performed using R software (version 4.1.3).

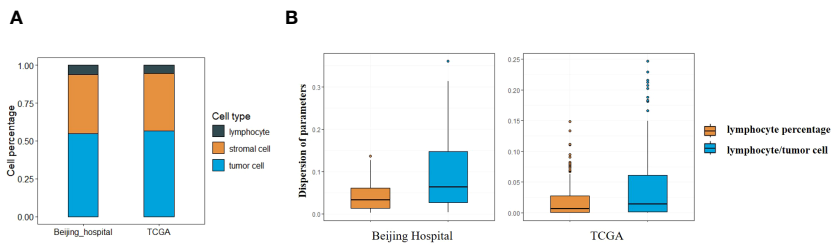

FIGURE 1
(A) Percentage of different types of cells in Beijing Hospital and TCGA cohorts. **(B)** Central tendency for lymphocyte percentage and lymphocyte/tumor cell ratio.

3 Results

3.1 Cell type recognition and immune subtype classification

Our prior research had developed an adapted CNN model to recognize cells autonomously and accurately in pathological images of patients with HCC, with classification accuracies of 95.7%, 92.3%, and 77.6% for tumor cells, lymphocytes, and stromal cells, respectively (14).

The adapted CNN model was utilized in this study, applied to both the Beijing Hospital and the TCGA cohort. Analysis of cell type percentages revealed no significant disparities between the two cohorts (Figure 1A). Lymphocyts, stromal cells and tumor cells account for 6.26%, 38.76% and 70.52% in the Beijing Hospital cohort, and 5.56%, 37.70% and 66.44% in the TCGA cohort respectively.

Lymphocyte percentage and lymphocyte/tumor cell ratio were computed as potential parameters for further analyses, the parameter with a lower degree of dispersion serves as the basis for subsequent grouping. Both parameters constituted non-normally distributed continuous variables, with the dispersion of lymphocyte percentage being less pronounced (IQR 0.07 vs. 0.14 in the Beijing cohort, 0.04 vs. 0.09 in the TCGA cohort, as depicted in Figure 1B), so that the lymphocyte percentage was selected as the parameter for stratification (26). Images with lymphocyte percentages above or below the median were categorized as having high or low immune infiltration (median = 0.039 in the Beijing cohort, median = 0.011 in the TCGA cohort). Lymphocyte percentages falling 1.5 times below Q1 or exceeding 1.5 times above Q3 were identified as outliers, 2 outliers in Beijing cohort and 14 outliers in TCGA cohort were excluded.

3.2 Patients in different immune subtypes presented variant clinical features and prognosis

We categorized the patients into high- and low-immune cell infiltration subtypes based on the threshold described above. For patients in the Beijing Hospital cohort, we collected data on 17 parameters, including epidemiological factors, indicators of liver function, medical history, tumor stage, and pathohistological

TABLE 1 Clinical and pathological characteristics of patients in the 2 subtypes*.

Characteristic	Low infiltration (n = 35)	High infiltration (n = 29)	P value
Male	29 (82.8)	23 (79.3)	0.968
Age, Mean ± SD, **years**	61.94 ± 14.97	57.17 ± 12.21	0.165
Alb*, Median (Q1, Q3), **g/L**	40 (39.5, 41)	41 (40, 43)	0.101
TB*, Median (Q1,Q3), **μmol/L**	12 (8.7, 15.15)	11.5 (9.3, 14.1)	0.914
PT*, Mean ± SD, **s**	11.47 ± 1.11	11.39 ± 0.94	0.770
AFP* (≥400 ng/ml)	12 (34.2)	3 (10.3)	0.051
Diabetes	11 (31.4)	3 (10.3)	0.084
Hypertension	18 (51.4)	5 (17.2)	0.010
Alcohol	11 (31.4)	8 (27.6)	0.952
Hepatitis	26 (74.3)	24 (82.8)	0.608
Liver cirrhosis	24 (68.6)	21 (72.4)	0.952
Fatty liver	9 (25.7)	1 (3.4)	0.017
MVI*			0.389
M0	20 (57.1)	20 (69.0)	
M1	10 (28.6)	4 (13.8)	
M2	5 (14.3)	5 (17.2)	
Tumor size, Median (Q1,Q3), **cm**	5.0 (3.5, 9.5)	4.5 (2.5, 7.0)	0.048
Vascular invasion, n (%)	8 (22.9)	4 (13.8)	0.546
Satellite nodules, n (%)	12 (34.3)	3 (10.3)	0.051
TNM Stage, n (%)			0.050
Stage 1	16 (45.7)	20 (69.0)	
Stage 2	15 (42.9)	5 (17.2)	
Stage 3	2 (5.7)	4 (13.8)	
Stage 4	2 (5.7)	0 (0)	

*Values are numbers of patients (percentages) unless otherwise indicated; Alb for albumin; TB for total bilirubin; PT for prothrombin time; AFP for alpha-fetoprotein; MVI for microvascular invasion, M0 means no MVI, M1 means less than 5 MVI occurred within 1 cm from the tumor, M2 means more than 5 MVI or MVI occurred 1 cm away from the tumor.

features of the tumor, and compared the two subtypes (refer to Table 1). The low-infiltration subtype exhibited a higher incidence of hypertension (51.4% vs. 17.2%, p = 0.010) and fatty liver (25.7% vs. 3.4%, p = 0.017), and displayed a larger tumor diameter (median 5.0 vs 4.5, p = 0.048). Additionally, the low-infiltration subtype demonstrated a higher incidence of satellite nodules, elevated AFP levels, and a more advanced TNM stage, but showed no statistical significance. These findings suggest that lower immune infiltration may be associated with a history of metabolic syndrome and may promote tumor progression.

We further performed K-M analysis on both the Beijing Hospital and TCGA cohorts to assess the prognostic value of immune classification. In the Beijing Hospital cohort, patients with the high-infiltration subtype exhibited a favorable prognosis in terms of DFS (p=0.013), but no significant difference was observed in OS (Figures 2A, B). In the TCGA cohort, the high infiltration subtype demonstrated a favorable prognosis in both OS and DFS (Figures 2C, D, p=0.012 for OS, p=0.026 for DFS).

3.3 Different immune subtypes present a distinct TME

RNA sequencing data were gathered from the TCGA-LIHC database. We identified the DEGs between the two subtypes using the DESeq2 R package and annotated genes associated with immune pathways according to the KEGG database (Figures 3A, B). The analysis revealed that most of the immune-related genes were down-regulated in the low infiltration subtype. To delve deeper into the discrepancies in cellular function between the subtypes, we performed functional enrichment analyses utilizing the GO, GSEA, and GSVA methodologies (Figures 3C, D, E). The top 10 pathways enriched in the GO analysis (sorted by qvaule, increased) were all linked to immune function. Meanwhile, the top two pathways enriched in the GSEA analysis (ranked by absolute NES, decreased) were the chemokine and cytokine signaling pathways. The extent of immune infiltration was quantified using ESTIMATE analysis, and the estimated immune and stromal scores were compared between the two subtypes using the Wilcoxon test (Figure 3F). The high-infiltration subtype exhibited higher scores, indicating a greater degree of immune cell infiltration in the TME. Subsequently, CIBERSORT analysis was performed to assess immune cell abundance in the two subtypes (Figure 3G). The findings revealed that the low-infiltration subtype manifested a higher level of type 2 macrophages (M2), monocytes, and resting natural killer (NK) cells, suggesting a propensity towards immune suppression. Finally, TIDE analysis was employed to evaluate the potential for tumor escape, indicating no significant difference between the two subtypes (Figure 3H).

3.4 Establishment and validation of the prognostic model based on immune subtypes and clinical features

Patients with a DFS shorter or longer than 1 year were classified into poor or good prognosis groups. A total of 55 variables, including clinical and pathological features, were collected from the patients in the Beijing Hospital cohort. ROC curves were developed for each variable to evaluate their predictive value, and variables with an AUC

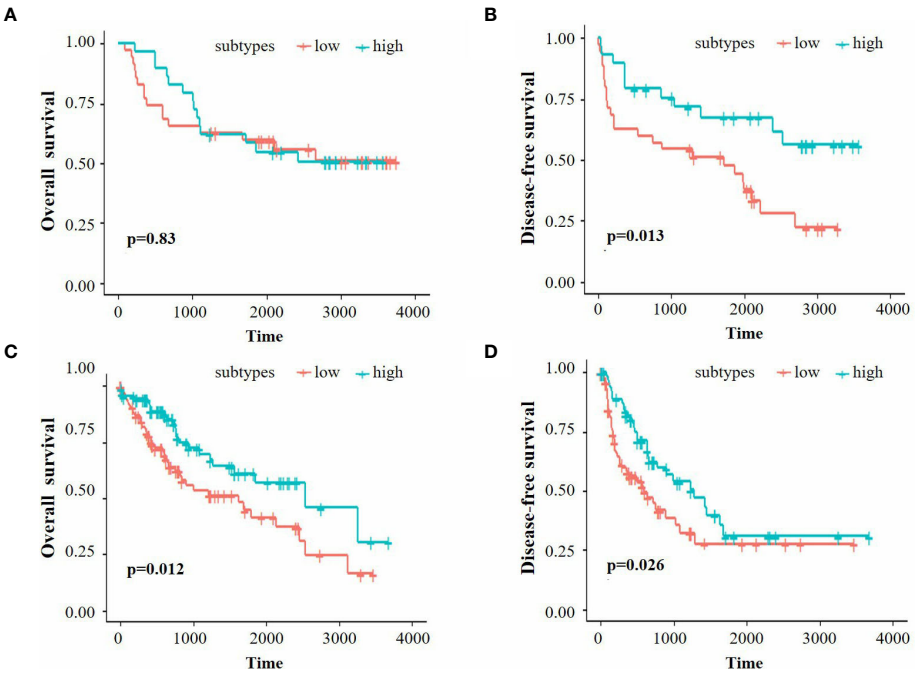

FIGURE 2
(A, B) K-M survival analysis of OS and DFS for the Beijing Hospital cohort. **(C, D)** K-M survival analysis of OS and DFS for the TCGA cohort.

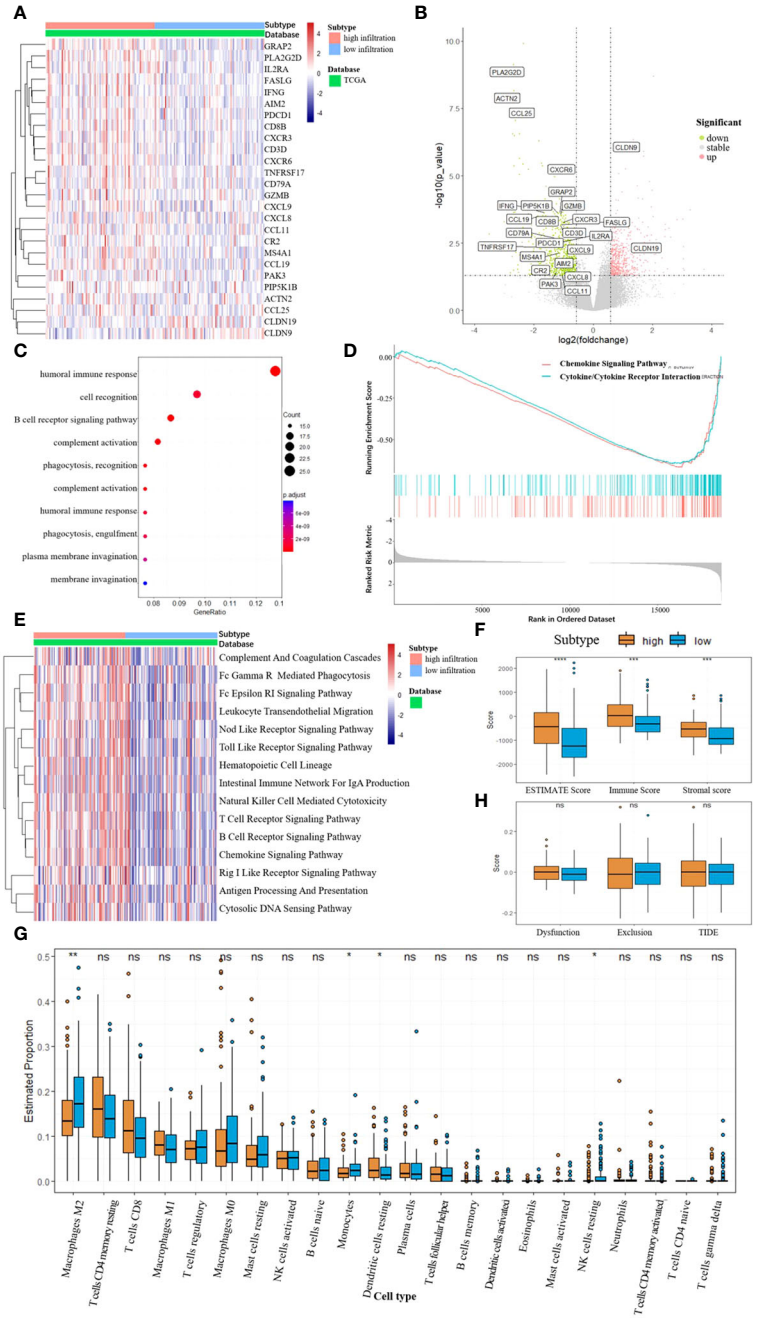

FIGURE 3
(A, B) Differentially expressed genes between the two subtypes, DEGs related to immune pathways were annotated. **(C)** GO enrichment, biological process (BP). **(D)** Top 2 pathway enriched in GSEA analysis. **(E)** GSVA enrichment according to the KEGG database. **(F)** ESTIMATE scores between the two subtypes, *** p<0.001, **** p<0.0001. **(G)** Abundance of different immune cells between the two subtypes, * p<0.05, ** p<0.01, NS for not significant. **(H)** TIDE scores between the two subtypes, NS for not significant.

greater than 0.6 were listed (Figure 4A). The immune classification ranked 8 (AUC = 0.67), while other variables with high rankings were mostly tumor features, such as TNM stage, microvascular invasion (MVI), and serum AFP level, which were consistent with previous findings (7, 8). To develop a prognostic model for patient outcomes, we used all patients from the Beijing Hospital cohort as the training set and 58 patients from the TCGA cohort with complete clinical information as the test set. We performed LASSO analysis and cross-validation to reduce the number of variables and determine the minimum number of variables needed for a model with favorable performance (Figure 4B). Finally, five variables were included in the logistic regression analysis: immune classification, age, AFP level, vascular invasion, and TNM stage, and a nomogram was developed (Figure 4C). ROC curves were generated for both the training and test sets, with AUCs of 0.918 and 0.814, respectively (Figure 4D).

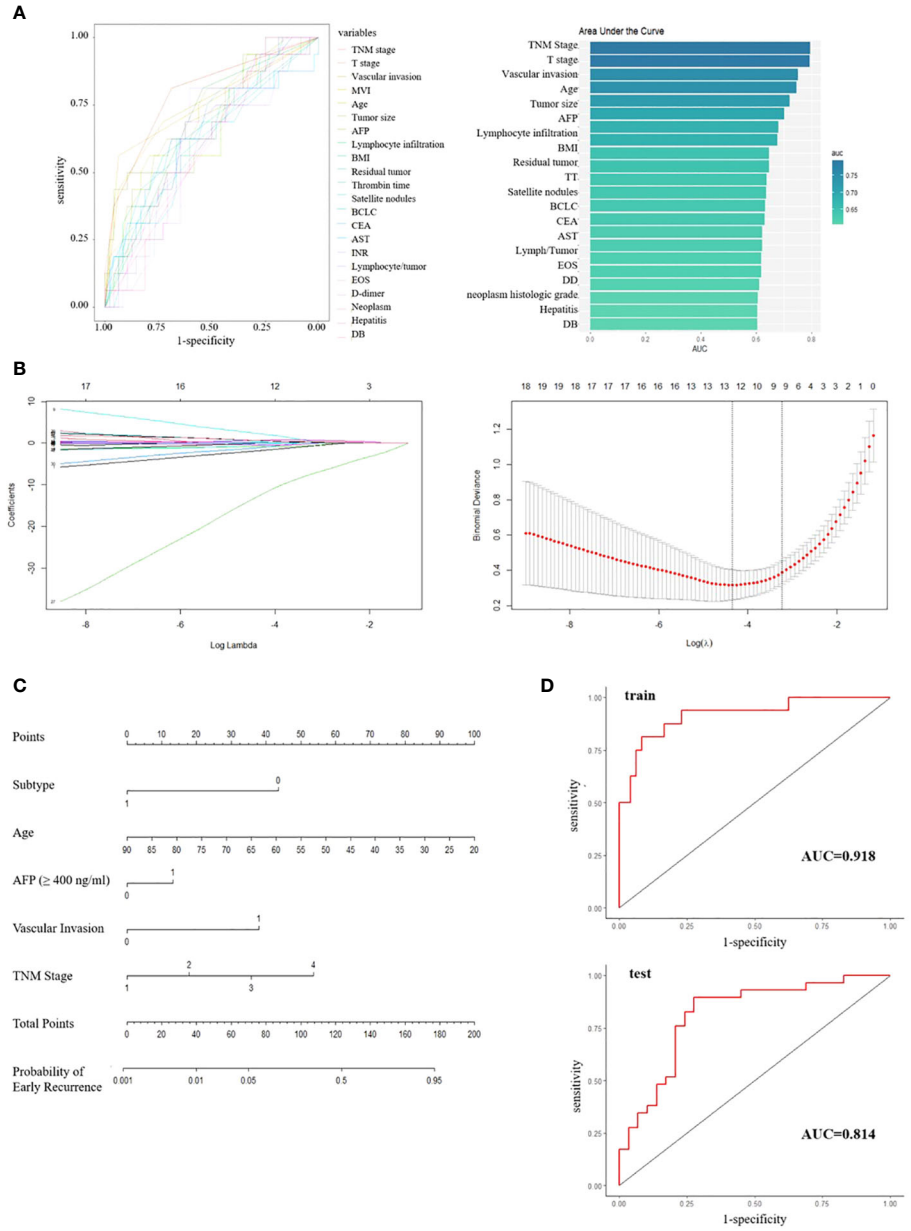

FIGURE 4
(A) ROC curves and ranked AUC of clinical and pathological features. **(B)** LASSO regression and cross-validation for variable selection. **(C)** Nomogram for predicting early recurrence; Subtype, 0/1 means low/high infiltration subtype; AFP, 0/1 means the level of AFP less than 400 ng/ml or not; Vascular invasion, 0/1 means no/any type of vascular invasion; TNM stage, 1/2/3/4 means stage I/II/III/IV respectively. **(D)** ROC curves for training set and test set.

4 Discussion

Benefiting from advanced genomics and transcriptomics technologies, the TME of HCC has been extensively explored in recent years. This exploration has revealed impressive immune heterogeneity, fueling the development of immune therapies for HCC, such as PD1/PDL1 inhibitors. Apart from immune heterogeneity, spatial heterogeneity also significantly influences tumor progression and metastasis (27). While studies on spatial heterogeneity have primarily focused on the gene or molecular level using techniques like single-cell RNA sequencing and spatial transcriptomics (28, 29). Examining the spatial distribution of different cell types within the TME could offer a novel perspective.

Pathological images serve as the gold standard for tumor diagnosis, containing vast amounts of information that warrant further investigation. Traditional pathological research methods, such as immunohistochemistry and fluorescence *in situ* hybridization, operate at the molecular level and often require additional experiments. Hence, a method that directly extracts cellular information from H&E-stained pathological images could prove more efficient. The primary challenge lies in accurately and efficiently recognizing and classifying cells within these images. Previous studies

on lung cancer have successfully developed reliable deep-learning models capable of identifying different cell types in pathological images of lung adenocarcinoma and non-small cell lung cancer (30–32). However, such models have seen limited application in HCC (33). Our previous study proposed an effective pathological image processing pipeline and adapted a CNN model to classify the cells in the pathological images of patients with HCC.

Based on the modified CNN model, we have proposed a novel immune classification based on the percentage of lymphocytes in the images. We hypothesize that this novel immune classification holds potential prognostic value. Upon dividing patients into high and low immune infiltration groups, we observed that the low-infiltration subtype exhibited a higher incidence of hypertension and fatty liver. This suggests that metabolic disturbances may impact immune infiltration in the TME. Further analysis of RNA sequencing data from the TCGA dataset confirmed the reasonability and reliability of our novel immune classification system. The next objective of our study was to establish a prognostic model based on this novel immune classification. We utilized the Beijing Hospital cohort as the training set and the TCGA cohort as the test set. Patients were divided into poor/good prognosis groups according to DFS. We conducted LASSO analysis and logistic regression on 55 variables and developed a nomogram for prognosis prediction. The AUC of the ROC curves was 0.918 and 0.814 for the training set and the test set, respectively. The variables included in the nomogram were immune classification, age, AFP level, TNM stage, and vascular invasion status. Except for immune classification, all other variables were available in the process of HCC treatment. Our modified CNN model also facilitated the determination of immune classification. With this nomogram, we can conveniently evaluate the risk of early recurrence in patients diagnosed with HCC who undergo surgical resection or liver transplantation. For patients at high risk of early recurrence, more intensive follow-up and a more proactive postoperative treatment strategy are warranted.

This study is a single-center retrospective study, and only 64 patients were included in the Beijing Hospital cohort, which inevitably limits the reliability of its results and the prognostic value of the proposed model. The utilization of lymphocyte percentage as the sole parameter for immune classification appears insufficient. To address these limitations, a multi-center prospective study design is necessary, along with more comprehensive investigations exploring the spatial relationships among various cell types. Furthermore, the predictive value of our novel immune classification in response to various immunotherapy strategies merits further exploration. Our future research efforts will be focused on addressing these challenges.

An unexpected finding of this study was the observation that patients with different immune infiltration subtypes exhibited distinct histories of metabolic syndrome. This discovery underscores the importance of investigating the correlation and interaction between metabolic and immune pathways in the TME, a topic that warrants further exploration.

Overall, our study proposed a novel immune classification system based on a reliable cell recognition model and demonstrated favorable prognostic value. The novel prognostic model and nomogram, developed from clinical features and immune classification, could serve as practical tools for evaluating the risk of early recurrence in patients with HCC. Moreover, they could provide reliable suggestions for postoperative clinical decision-making.

Data availability statement

The raw data supporting the conclusions of this article will be made available by the authors, without undue reservation.

Ethics statement

The studies involving humans were approved by Ethics committee, Beijing Hospital. The studies were conducted in accordance with the local legislation and institutional requirements. The human samples used in this study were acquired from a by-product of routine care or industry. Written informed consent for participation was not required from the participants or the participants' legal guardians/next of kin in accordance with the national legislation and institutional requirements.

Author contributions

TT: Data curation, Formal analysis, Investigation, Methodology, Project administration, Visualization, Writing – original draft, Writing – review & editing. HH: Investigation, Methodology, Project administration, Resources, Software, Writing – review & editing. WZ: Funding acquisition, Writing – review & editing. JC: Conceptualization, Data curation, Methodology, Supervision, Validation, Writing – review & editing. ZL: Writing – review & editing. XL: Conceptualization, Supervision, Validation, Writing – review & editing. JS: Conceptualization, Funding acquisition, Resources, Supervision, Validation, Writing – review & editing.

Funding

The author(s) declare that financial support was received for the research, authorship, and/or publication of this article. This work was supported by National High Level Hospital Clinical Research Funding (BJ-2023-083 and BJ-2022-144).

Conflict of interest

The authors declare the research was conducted in the absence of any commercial or financial relationships that could be construed as a potential conflict of interest.

Publisher's note

References

1. Sung H, Ferlay J, Siegel RL, Laversanne M, Soerjomataram I, Jemal A, et al. Global cancer statistics 2020: globocan estimates of incidence and mortality worldwide for 36 cancers in 185 countries. *CA Cancer J Clin*. (2021) 71:209–49. doi: 10.3322/caac.21660

2. Singal AG, Lampertico P, Nahon P. Epidemiology and surveillance for hepatocellular carcinoma: new trends. *J Hepatol*. (2020) 72:250–61. doi: 10.1016/j.jhep.2019.08.025

3. Zhou SL, Zhou ZJ, Song CL, Xin HY, Hu ZQ, Luo CB, et al. Whole-genome sequencing reveals the evolutionary trajectory of hbv-related hepatocellular carcinoma early recurrence. *Signal transduction targeted Ther*. (2022) 7:24. doi: 10.1038/s41392-021-00838-3

4. Hepatocellular carcinoma. *Nat Rev Dis Primers*. (2021) 7:7. doi: 10.1038/s41572-021-00245-6

5. Villanueva A. Hepatocellular carcinoma. *New Engl J Med*. (2019) 380:1450–62. doi: 10.1056/NEJMra1713263

6. Solimando AG, Susca N, Argentiero A, Brunetti O, Leone P, De Re V, et al. Second-line treatments for advanced hepatocellular carcinoma: A systematic review and bayesian network meta-analysis. *Clin Exp Med*. (2022) 22:65–74. doi: 10.1007/s10238-021-00727-7

7. Chan AWH, Zhong J, Berhane S, Toyoda H, Cucchetti A, Shi K, et al. Development of pre and post-operative models to predict early recurrence of hepatocellular carcinoma after surgical resection. *J Hepatol*. (2018) 69:1284–93. doi: 10.1016/j.jhep.2018.08.027

8. Zheng J, Kuk D, Gönen M, Balachandran VP, Kingham TP, Allen PJ, et al. Actual 10-year survivors after resection of hepatocellular carcinoma. *Ann Surg Oncol*. (2017) 24:1358–66. doi: 10.1245/s10434-016-5713-2

9. Calderaro J, Couchy G, Imbeaud S, Amaddeo G, Letouzé E, Blanc JF, et al. Histological subtypes of hepatocellular carcinoma are related to gene mutations and molecular tumour classification. *J Hepatol*. (2017) 67:727–38. doi: 10.1016/j.jhep.2017.05.014

10. Iizuka N, Oka M, Yamada-Okabe H, Nishida M, Maeda Y, Mori N, et al. Oligonucleotide microarray for prediction of early intrahepatic recurrence of hepatocellular carcinoma after curative resection. *Lancet (London England)*. (2003) 361:923–9. doi: 10.1016/s0140-6736(03)12775-4

11. Kim S, Shin J, Kim DY, Choi GH, Kim MJ, Choi JY. Radiomics on gadoxetic acid-enhanced magnetic resonance imaging for prediction of postoperative early and late recurrence of single hepatocellular carcinoma. *Clin Cancer research: an Off J Am Assoc Cancer Res*. (2019) 25:3847–55. doi: 10.1158/1078-0432.Ccr-18-2861

12. Zhang K, Yuan E. Combined analysis of bulk and single-cell rna sequencing reveals novel natural killer cell-related prognostic biomarkers for predicting immunotherapeutic response in hepatocellular carcinoma. *Front Immunol*. (2023) 14:1142126. doi: 10.3389/fimmu.2023.1142126

13. Wang S, Wang T, Yang L, Yang DM, Fujimoto J, Yi F, et al. Convpath: A software tool for lung adenocarcinoma digital pathological image analysis aided by a convolutional neural network. *EBioMedicine*. (2019) 50:103–10. doi: 10.1016/j.ebiom.2019.10.033

14. Hu H, Tan T, Liu Y, Liang W, Zhang W, Cui J, et al. Deep learning-based spatial feature extraction for prognostic prediction of hepatocellular carcinoma from pathological images. *bioRxiv*. (2024). doi: 10.1101/2024.02.10.579571

15. Sia D, Jiao Y, Martinez-Quetglas I, Kuchuk O, Villacorta-Martin C, Castro de Moura M, et al. Identification of an immune-specific class of hepatocellular carcinoma, based on molecular features. *Gastroenterology*. (2017) 153:812–26. doi: 10.1053/j.gastro.2017.06.007

16. Sun Y, Wu L, Zhong Y, Zhou K, Hou Y, Wang Z, et al. Single-cell landscape of the ecosystem in early-relapse hepatocellular carcinoma. *Cell*. (2021) 184:404–21.e16. doi: 10.1016/j.cell.2020.11.041

17. Love MI, Huber W, Anders S. Moderated estimation of fold change and dispersion for rna-seq data with deseq2. *Genome Biol*. (2014) 15:550. doi: 10.1186/s13059-014-0550-8

18. Ashburner M, Ball CA, Blake JA, Botstein D, Butler H, Cherry JM, et al. Gene ontology: tool for the unification of biology. The gene ontology consortium. *Nat Genet*. (2000) 25:25–9. doi: 10.1038/75556

19. Subramanian A, Tamayo P, Mootha VK, Mukherjee S, Ebert BL, Gillette MA, et al. Gene set enrichment analysis: A knowledge-based approach for interpreting genome-wide expression profiles. *Proc Natl Acad Sci United States America*. (2005) 102:15545–50. doi: 10.1073/pnas.0506580102

20. Hänzelmann S, Castelo R, Guinney J. Gsva: gene set variation analysis for microarray and rna-seq data. *BMC Bioinf*. (2013) 14:7. doi: 10.1186/1471-2105-14-7

21. Yoshihara K, Shahmoradgoli M, Martínez E, Vegesna R, Kim H, Torres-Garcia W, et al. Inferring tumour purity and stromal and immune cell admixture from expression data. *Nat Commun*. (2013) 4:2612. doi: 10.1038/ncomms3612

22. Newman AM, Liu CL, Green MR, Gentles AJ, Feng W, Xu Y, et al. Robust enumeration of cell subsets from tissue expression profiles. *Nat Methods*. (2015) 12:453–7. doi: 10.1038/nmeth.3337

23. Fu J, Li K, Zhang W, Wan C, Zhang J, Jiang P, et al. Large-scale public data reuse to model immunotherapy response and resistance. *Genome Med*. (2020) 12:21. doi: 10.1186/s13073-020-0721-z

24. Robin X, Turck N, Hainard A, Tiberti N, Lisacek F, Sanchez JC, et al. Proc: an open-source package for R and S+ to analyze and compare roc curves. *BMC Bioinf*. (2011) 12:77. doi: 10.1186/1471-2105-12-77

25. Tibshirani R, Hastie T, Friedman J. Regularized paths for generalized linear models via coordinate descent. *Journal of statistical software*. (2010) 33(1):1–22. doi: 10.1163/ej.9789004178922.i-328.7

26. Montironi C, Castet F, Haber PK, Pinyol R, Torres-Martin M, Torrens L, et al. Inflamed and non-inflamed classes of hcc: A revised immunogenomic classification. *Gut*. (2023) 72:129–40. doi: 10.1136/gutjnl-2021-325918

27. Saviano A, Henderson NC, Baumert TF. Single-cell genomics and spatial transcriptomics: discovery of novel cell states and cellular interactions in liver physiology and disease biology. *J Hepatol*. (2020) 73:1219–30. doi: 10.1016/j.jhep.2020.06.004

28. Sun YF, Wu L, Liu SP, Jiang MM, Hu B, Zhou KQ, et al. Dissecting spatial heterogeneity and the immune-evasion mechanism of ctcs by single-cell rna-seq in hepatocellular carcinoma. *Nat Commun*. (2021) 12:4091. doi: 10.1038/s41467-021-24386-0

29. Wu Y, Yang S, Ma J, Chen Z, Song G, Rao D, et al. Spatiotemporal immune landscape of colorectal cancer liver metastasis at single-cell level. *Cancer Discovery*. (2022) 12:134–53. doi: 10.1158/2159-8290.CD-21-0316

30. AbdulJabbar K, Raza SEA, Rosenthal R, Jamal-Hanjani M, Veeriah S, Akarca A, et al. Geospatial immune variability illuminates differential evolution of lung adenocarcinoma. *Nat Med*. (2020) 26(7):1054–62. doi: 10.1038/s41591-020-0900-x

31. Coudray N, Ocampo PS, Sakellaropoulos T, Narula N, Snuderl M, Fenyo D, et al. Classification and mutation prediction from non-small cell lung cancer histopathology images using deep learning. *Nat Med*. (2018) 24:1559–67. doi: 10.1038/s41591-018-0177-5

32. Wang S, Rong R, Yang DM, Fujimoto J, Yan S, Cai L, et al. Computational staining of pathology images to study the tumor microenvironment in lung cancer. *Cancer research*. (2020) 80(10):2056–66. doi: 10.1158/0008-5472.can-19-1629

33. Shi J-Y, Wang X, Ding G-Y, Dong Z, Han J, Guan Z, et al. Exploring prognostic indicators in the pathological images of hepatocellular carcinoma based on deep learning. *Gut*. (2020) 70(5):951–61. doi: 10.1136/gutjnl-2020-320930

frontiers | Frontiers in Oncology

TYPE Original Research
PUBLISHED 21 May 2024
DOI 10.3389/fonc.2024.1408584

OPEN ACCESS

EDITED BY
Francisco Tustumi,
University of São Paulo, Brazil

REVIEWED BY
Tamer A. Addissouky,
University of Menoufia, Egypt
Hongyu Lin,
Xiamen University, China
Julia Maroto García,
Clínica Universidad de Navarra, Spain

*CORRESPONDENCE
Bowen Yao
ybwsplendid@xjtufh.edu.cn

†These authors have contributed equally to this work

RECEIVED 28 March 2024
ACCEPTED 07 May 2024
PUBLISHED 21 May 2024

CITATION
Li Y, Wang H, Ren D, Li J, Mu Z, Li C, He Y, Zhang J, Fan R, Yin J, Su J, He Y and Yao B (2024) Interleukin-41: a novel serum marker for the diagnosis of alpha-fetoprotein-negative hepatocellular carcinoma. *Front. Oncol.* 14:1408584. doi: 10.3389/fonc.2024.1408584

Interleukin-41: a novel serum marker for the diagnosis of alpha-fetoprotein-negative hepatocellular carcinoma

Yazhao Li[1†], Haoyu Wang[2†], Danfeng Ren[3], Jingyu Li[2], Zihan Mu[2], Chaoyi Li[2], Yongchao He[2], Jiayi Zhang[2], Rui Fan[2], Jiayuan Yin[2], Jiaojiao Su[2], Yinli He[4] and Bowen Yao[5*]

[1]Center for Translational Medicine, The First Affiliated Hospital of Xi'an Jiaotong University, Xi'an, China, [2]Zonglian College, Xi'an Jiaotong University Health Science Center, Xi'an, China, [3]Department of Communicable Disease, The First Affiliated Hospital of Xi'an Jiaotong University, Xi'an, China, [4]Biobank, The First Affiliated Hospital of Xi'an Jiaotong University, Xi'an, China, [5]Department of Hepatobiliary Surgery, The First Affiliated Hospital of Xi'an Jiaotong University, Xi'an, China

Background: For the lack of effective serum markers for hepatocellular carcinoma(HCC) diagnosis, it is difficult to detect liver cancer and identify its recurrence early.

Methods: Databases were used to analyze the genes potentially associated with alpha-fetoprotein(AFP). ELISA assay was used to detect the serum IL-41 in HCC, liver metastases, hepatitis, and healthy people. Immunohistochemical staining was used to analyze the relative quantification of IL-41 in HCC and paracancer tissues. Various survival curves were plotted according to clinical pathological data and helped us draw the ROC curve of IL-41 diagnosis of HCC.

Results: The serum expression of IL-41 was highest in AFP negative HCC patients and significantly higher than that in AFP positive HCC and metastatic cancer patients. There was a significant negative correlation between elevated serum IL-41 and AFP(<1500ng/ml). The clinicopathological features suggested that the serum IL-41 level was significantly correlated with capsule invasion, low differentiation and AFP. High serum expression of IL-41 suggests poorer survival and earlier recurrence after resection, and IL-41 upregulated in patients with early recurrence and death. The expression of IL-41 was higher in HCC tissues of patients with multiple tumors or microvascular invasion. The ROC curve showed that serum IL-41 had a sensitivity of 90.17 for HCC and a sensitivity of 96.63 for AFP-negative HCC, while the specificity was higher than 61%.

Conclusion: IL-41 in serum and tissue suggests poor prognosis and postoperative recurrence in HCC patients and could be a new serum diagnostic marker for AFP negative patients.

KEYWORDS

IL41, METRNL, hepatocellular carcinoma, AFP, serum biomarker

Introduction

Hepatocellular carcinoma (HCC) incidence in China is high (1), with about 50% of global cases originating from China (2). At present, HCC is the fourth common malignancy and second cause of death in China, posing a serious threat to people's life and health (3). The etiology of HCC is complex and diverse and has been shown to be associated with cirrhosis, viral hepatitis, alcohol consumption, and fatty liver (4). In particular, chronic hepatitis B virus-related cirrhosis was reported as the primary risk factor for HCC development in China (5). HCC progression is a multifactorial, multistep process driven by epithelial-mesenchymal transition (6), the tumor microenvironment (7), cancer stem cells (8), and aging (9). Due to the rapid progression and poor prognosis of HCC, postoperative recurrence remains a major challenge in the clinical management of the disease. Surgery is currently the main treatment approach for HCC (10), but the 5-year postoperative recurrence rate is close to 70% (11). In addition, micrometastases are often difficult to detect by imaging after surgery, resulting in delayed treatment for many patients (12). Therefore, there is an urgent need to identify novel diagnostic markers and therapeutic targets for HCC.

Alpha fetoprotein (AFP) is the most widely used serological marker for HCC worldwide. Its application stems from the discovery that some HCC secretes high levels of AFP (13). In addition, an AFP concentration of 400 ng/mL was recommended as the threshold for auxiliary diagnosis in the 2001 and 2017 Chinese HCC diagnostic staging criteria (14). However, some HCC patients with AFP levels below the diagnostic threshold (e.g., AFP-negative patients) can only rely on imaging for the detection of postoperative recurrence, which often leads to delayed diagnosis and treatment (15). Therefore, novel sensitive markers are needed for identifying AFP-negative HCC patients. Although the combined use of AFP and several serological markers such as DCP, AFP-L3, and PIVKA-II (16) have been shown to improve HCC detection rate, the specificity and sensitivity of these markers are inadequate to provide early HCC diagnosis. Furthermore, efforts in finding serum diagnostic markers for HCC have lessened in recent years, and the serum markers tested in combination with AFP thus far have not resulted in much improvement in sensitivity and specificity. For example, DCP has a 51.7% sensitivity and 86.7% specificity for HCC, while DCP combined with AFP has a 78.3% sensitivity for HCC (17). Large cohort clinical studies conducted at different centers suggest that diagnostic models are superior to serum markers for HCC diagnosis, but their widespread application in the real world is constrained by the incorporation of complex indicators and high detection cost. Another example is the classical liver cancer histological marker HSP90, which has been confirmed to be associated with cancer occurrence. However, since HSP90 is highly expressed in various cancers, such as salivary gland and breast cancers, it is not a specific diagnostic marker for HCC (18).

Interleukin (IL)-41, also known as meteroin-like protein (METRNL), is a newly discovered immunomodulatory cytokine or adipokine expressed in a wide range of cells and tissues (19, 20), most prominently in human subcutaneous white adipose tissue (21). IL-41 has been reported to antagonize insulin resistance (22), and its expression is upregulated by factors such as inflammation, exercise, and cold exposure (23). In addition, IL-41 plays a key anti-inflammatory role in several inflammatory diseases such as psoriatic arthritis and inflammatory bowel disease (24–26). IL-41 can regulate cytokine levels through macrophages and is involved in the modulation of inflammatory responses in a mouse model of sepsis (27, 28). However, the role and mechanism of IL-41 in cancer are currently unclear. This study suggests for the first time that IL-41 is a novel marker for HCC detection and may play an important role in predicting the prognosis and treatment response of HCC.

Methods

Patients and clinicopathological features

Among the 176 HCC patients included in this study, 88 were AFP-positive and 85 were AFP-negative. Additionally, 18 CRC patients with liver metastases, 15 patients with acute AFP-positive hepatitis, and 19 healthy controls were also included. All patients received treatment at the First Affiliated Hospital of Xi'an Jiaotong University between 2018 and 2021. The study was approved by the Ethics Committee of Xi'an Jiaotong University, and tissue and serum samples were collected in accordance with medical research ethics. Patient information, including gender, age, tumor size, tumor number, tumor stage, tumor differentiation, capsule integrity, microvascular invasion, and tumor recurrence, were obtained from the electronic medical records of the First Affiliated Hospital of Xi'an Jiaotong University. All study participants included in the data analysis were followed for at least three years up until February 14, 2024. Prognostic survival was assessed using overall survival (OS), recurrence-free survival (RFS), progression-free survival (PFS), and time to tumor recurrence (TTR). OS is defined as the time from HCC diagnosis to death of any cause. RFS is the time from tumor diagnosis to either tumor recurrence or tumor-related death, whichever occurs earlier. PFS refers to the time from randomization to either tumor progression or death of any cause, whichever occurs earlier. TTR is defined as the time from tumor diagnosis to tumor recurrence. A total of 162 patients were included in the analysis, excluding those who had incomplete pathological data or were lost to follow-up, and were divided into the high IL-41 expression (≥ 65.853 pg/mL, median serum expression of IL41) group and low IL-41 expression (< 65.853 pg/mL) group to assess differences in OS,

Abbreviations: IL-41, interleukin 41; AFP, alpha-fetoprotein; HBV, hepatitis-b-virus; DCP, des-gamma-carboxy prothrombin, AFP-L3, AFP Lens culinaris agglutinin-reactive fraction of AFP; HSP90, heat shock protein 90; OS, overall survival; RFS, recurrence-free survival; PFS, progression-free survival; TTR, time to disease recurrence; ELISA, enzyme-linked immunosorbent assay; AST, alanine aminotransferase; ALT, alanine aminase; TBIL, total bilirubin; DBIL, direct bilirubin; TP, total protein; ALB, albumin; PLT, platelet; PT, prothrombin time; APTT, activated partial prothrombin time; IHC, Immunohistochemistry; TCGA, The Cancer Genome Atlas; GEO, Gene Expression Omnibus; PIVKA2, vitamin K deficiency or antagonist 2; GP73, Golgi protein73; MVI, Microvascular invasion; OD, Optical Density.

PFS, RFS, and TTR. AFP is considered negative when diagnosing liver cancer with an AFP of less than 20ng/ml. The correlation between serum IL-41 expression and various liver function markers, including serum alanine aminotransferase (AST), alanine aminase (ALT), total bilirubin (TBIL), direct bilirubin (DBIL), total protein (TP), albumin (ALB), platelet (PLT), hepatitis B virus surface antigen (HBsAg), as well as prothrombin time (PT) and activated partial prothrombin time (APTT), was analyzed.

ELISA

Serum concentration of human IL-41 was measured using the Human Interleukin-41 (IL-41) Quantitative Assay Kit (RX100486). Briefly, high-affinity microplate was coated with anti-human IL-41 monoclonal antibody, incubated with diluted serum samples (1:5) and standards, washed, incubated with biotinylated anti-hIL-41 detection antibody, washed, incubated with horseradish peroxidase-labeled streptavidin (streptavidin-HRP), washed, and incubated with the chromogenic substrate TMB. The reaction was terminated by the addition of a stop solution, and absorbance at 450 nm was measured using a microplate reader. The standard curve was generated by plotting the concentrations of the standards on the x-axis (6 standards plus one blank, totaling 7 concentration points) and the corresponding OD values on the y-axis, followed by a four-parameter Logistic curve fitting. IL-41 concentrations in the serum samples were determined by the sample OD values using the standard curve.

Immunohistochemistry

Tissue IL-41 expression levels in HCC patients and healthy controls were quantified by IHC. Briefly, formalin-fixed, paraffin-embedded tissues were cut into 2 μm thick sections, cleared by xylene, dehydrated in ethanol gradient, dewaxed in water, washed with distilled water, incubated with 3% H_2O_2 at room temperature for 10 min to quench endogenous peroxidase, and washed with PBS 3 times at 5 min each wash. Antigen retrieval was performed using preheated sodium citrate-EDTA solution, and the tissue sections were then blocked with 5% BSA solution at 37°C for 30 min. After tapping off the solution, the tissue sections were incubated with drops of diluted primary antibody (Immunoway, METRL rabbit pAb, YT7556) at 4°C overnight, washed 3 times in PBS (5 min per wash), incubated with biotinylated goat anti-rabbit IgG (BASTER, Wuhan, China) at 37°C for 30 min, washed 3 times in PBS (5 min per wash), incubated with streptavidin-biotin complex at 37°C for 30min, washed 3 times in PBS (5 min per wash), and stained with DAB. After rinsing thoroughly under tap water, the tissue sections were counterstained with hematoxylin and mounted with neutral gum and water-soluble sealant.

The degree of positive IHC staining is influenced by antigen content, distribution, labeling method, and sensitivity. The average gray value (staining intensity) and percentage of positive area (staining area) were quantified by ImageJ and scored as highly positive (3 points), moderately positive (2 points), weakly positive (1 point), and negative (0 point). The total score of IHC is the sum of the percentage of positive area multiplied by the corresponding scores.

Receiver operating characteristic curve analysis

The ROC curve is generated by plotting the true positive rates of cutoff values on the y-axis against their false positive rates on the x-axis. The diagnostic accuracy of IL-41 in HCC was compared to that of existing pathology criteria. The curves of subjects were plotted, and the area under the curve (AUC) was determined.

Statistical analysis

Measurement data are compared using the chi-square test or Fisher's exact test. Factors showing statistical significance were analyzed by one-way ANOVA, logistic regression, and multivariate analyses to determine their correlations with IL-41 level, tumor recurrence and clinicopathological features of patients. Count data were compared using the Student's *t*-test, and correlation between IL-41 and AFP was determined by the Spearman's rank correlation coefficient. Survival of patients with different IL-41 expression levels was estimated by the Kaplan-Meier plot. All data analyses were performed in IBM SPSS v.28.0, and data were visualized using GraphPad Prism 7.0. A P <0.05 was considered statistically significant.

Results

IL-41 is highly expressed in the serum of AFP-negative HCC patients

We have previously screened the The Cancer Genome Atlas (TCGA) and Gene Expression Omnibus(GEO) databases and identified IL-41 as a potential gene associated with serum AFP expression in HCC patients. Although the TCGA dataset showed no significant difference between the relative tissue expression of IL-41 and AFP in HCC patients (Supplementary Figure S1A), we gradually observed a trend of increased negative correlation after narrowing the distribution range of AFP (data not shown). In order to assess the performance of IL-41 as a potential serum biomarker, we first measured the level of serum IL-41 expression in HCC patients before surgery (HCC was pathologically confirmed after resection), CRC patients with liver metastases (confirmed after colon or rectal cancer surgery), and healthy controls who underwent physical examination at our hospital around the same time period. ELISA showed that serum IL-41 expression was significantly higher in AFP-negative HCC patients than in AFP-positive HCC patients, CRC patients with liver metastases, and healthy controls ($P < 0.01$; Figure 1A). In addition, we found a GEO dataset showing a significant negative correlation between tissue IL-41 expression and serum AFP expression in relapsed HCC patients

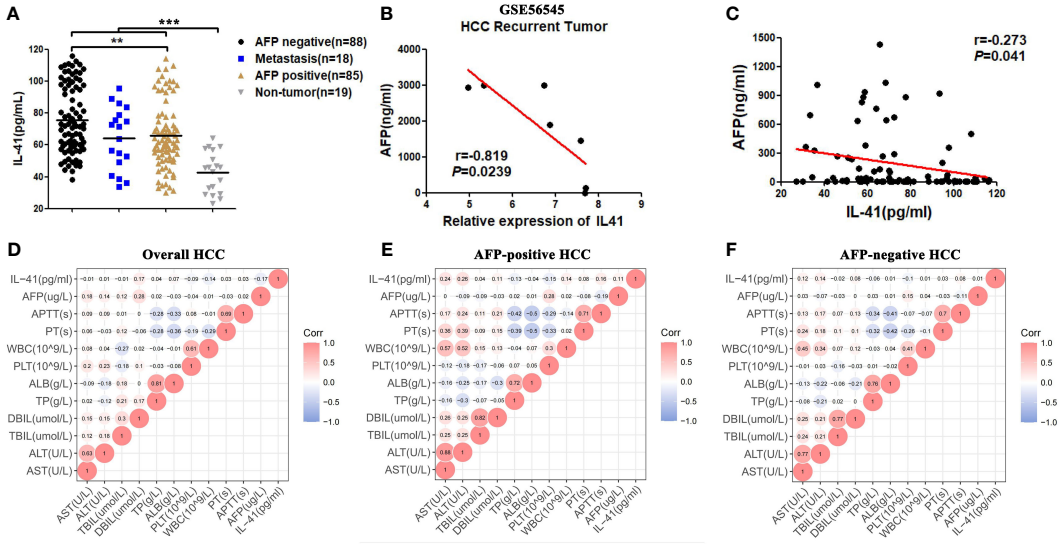

FIGURE 1
(A) The expression level of IL41 in serum of AFP negative, AFP positive HCC patients, liver metastatic cancer patients and healthy people(pg/ml) (**P<0.01, ***P<0.001); **(B)** Correlation between serum AFP(ng/ml) and tissue IL41 mRNA relative expression in patients with recurrence HCC in GSE56545 dataset (P<0.05); **(C)** Based on the data analysis of our center, serum IL41 of HCC patients with AFP no more than 1500ng/ml was significantly negatively correlated with AFP(P<0.05); **(D)** The serum indicators of all HCC patients included IL41, AST, ALT, TBIL, DBIL, TP, ALB, PT, APTT, AFP, WBC and PLT correlation heat map; **(E)** The serum indexes of AFP positive HCC patients included IL41, AST, ALT, TBIL, DBIL, TP, ALB, PT, APTT, AFP, WBC and PLT correlation heat map; **(F)** The serum markers of AFP negative HCC patients included correlation heat maps of IL41, AST, ALT, TBIL, DBIL, TP, ALB, PT, APTT, AFP, WBC and PLT.

(Figure 1B) but not in relapse-free HCC patients (Supplementary Figure S1B). Next, we analyzed the correlation between the serum expression levels of AFP and IL-41 using data from a single-center study and found no significant correlation between the two markers, which was likely attributed to the large variance in AFP values. As a result, we continued to narrow the range of AFP values and discovered that serum IL-41 level was negatively correlated with AFP level when the latter was less than or equal to 1500 ng/mL (Figure 1C). Taken together, these results demonstrated that IL-41 may be a novel marker for HCC patients with low AFP expression.

Considering the prevalence of liver cancer secondary to hepatitis and cirrhosis in China, we sought to determine the correlation between IL-41 level and serum indicators of liver function and systemic inflammatory response. Our data revealed that IL-41 was not correlated with liver function indicators in all HCC patients (Figure 1D). To test the diagnostic sensitivity and specificity of IL-41, we also examined the serum expression level of IL-41 in patients with acute hepatitis (including sera of patients with HBV, HCV, and autoimmune hepatitis) who were positive for AFP. We found that serum IL-41 level varied greatly among patients with acute hepatitis and was comparable among the different groups of patients (Supplementary Figure S1C). Analysis of sera from AFP-negative and AFP-positive HCC patients demonstrated that serum IL-41 level was positively correlated with ALT and AST levels in AFP-positive HCC patients (Figures 1D–F, Supplementary Figures S1D, E) but not in AFP-negative HCC patients. Collectively, these data indicate that serum IL-41 level is significantly higher in HCC patients than in healthy individuals, and higher in AFP-negative than in AFP-positive HCC patients. In addition, serum IL-41 expression is not correlated with common liver function indicators in AFP-negative HCC patients.

IL-41 is significantly upregulated in HCC tissues

We next analyzed the relative expression of IL-41 in 22 pairs of HCC and adjacent tissues using the HPA database and by performing IHC staining of single-center tissue samples. Our results showed that HCC tissues were stained positive for IL-41 whereas intrahepatic cholangiocarcinoma (ICC) tissues were mostly negative for IL-41 (Figure 2A, ICC data not shown). IHC scoring of 12 pairs of tissue from AFP-positive (6 pairs) and AFP-negative (6 pairs) patients revealed higher IL-41 expression in HCC tissues (all patients or AFP negative or positive patients) than in paracancerous tissues (Figures 2B–E). Furthermore, we found that serum IL-41 expression was also positively correlated with tissue IL-41 expression in HCC (Figure 2F).

High serum IL-41 expression is correlated with tumor recurrence and poor prognosis

To further evaluate the diagnostic performance of IL-41, we analyzed the correlation between IL-41 expression and the various clinicopathological features of HCC patients. Our findings showed that serum IL-41 expression was significantly correlated with micro-vascular invasion(MVI), poorly differentiated cancer cells, and high preoperative AFP (Table 1). We further analyzed correlations

10.3389/fonc.2024.1408584

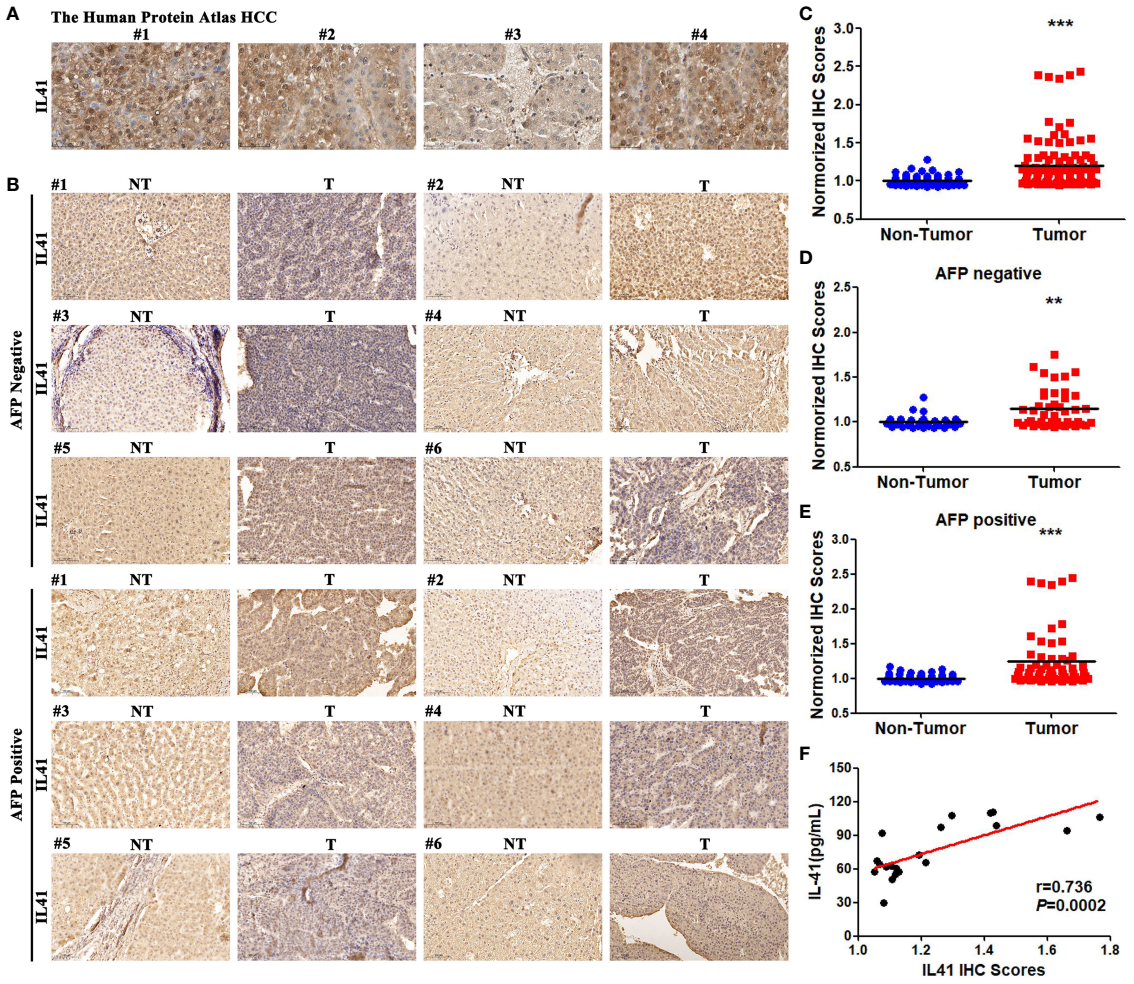

FIGURE 2
(A) IHC results of IL41 in Human Protein Atlas in HCC tissues; **(B)** IHC results of IL41 of 22 pairs of HCC analyzed by our center and 6 pairs of AFP positive and AFP negative HCC patients selected from corresponding paracancer tissues; **(C)** IL41 was significantly higher in HCC tissues than in paracancer tissues in all HCC patients (***P<0.001); **(D)** IL41 in HCC patients with negative AFP was significantly higher than that in paracancer tissues (**P<0.01). **(E)** IL41 in HCC patients with positive AFP was significantly higher than that in paracancer tissues (***P<0.001). **(F)** The expression of IL41 in 22 HCC tissues was significantly positively correlated with the serum IL14 level (P<0.01).

between clinicopathologic characteristics and survival or recurrence of hepatocellular carcinoma patients. Tables listed factors such as serum AFP and IL-41 expression, and MVI had strong correlation between survival and recurrence (Supplementary Tables S1-S3). However, only AFP could be the sole risk for HCC patients survival (Supplementary Table S4). Besides, IL-41 could be one of the HCC recurrence and early recurrence predictors after resections (Tables 2, 3). Moreover, we examined the OS, PFS, RFS, and postoperative recurrence of HCC patients with high and low IL-41 expression as well as HCC patients who were positive or negative for AFP. We found that OS was shorter in all HCC patients with high IL-41 expression and AFP-positive HCC patients (Figures 3A, B) but was similar between AFP-negative HCC patients with high or low IL-41 expression (Figure 3C). In addition, PFS was not significantly different among all HCC patients (Figure 3D) but was shorter in AFP-negative or -positive HCC patients with high serum IL-41 levels (Figures 3E, F). Since the patients included in this study had undergone resection for HCC, we also analyzed important indicators of post-resection outcomes, including RFS and TTR. RFS analysis showed that post-resection recurrence rate was higher in all HCC patients and AFP-positive HCC patients with high serum IL-41 expression (Figures 3G, H), but comparable between AFP-negative HCC patients with high or low IL-41 expression (Figure 3I). Interestingly, while there was no significant difference in TTR between the high and low IL-41 expression groups (Figure 3J), TTR was shorter in both the AFP-positive and AFP-negative subgroups with high IL-41 expression (Figures 3K, L). In summary, high expression of IL-41 is associated with poor differentiation, AFP, and suggests poor prognosis and post-resection recurrence. More importantly, we found that the serum IL-41 level was lower in patients with late recurrence (2 years after resection) than in patients with early recurrence and death (Figures 3M–O). These findings suggest that IL-41 expression may be a reliable predictor for tumor progression and survival outcomes in HCC patients.

TABLE 1 Correlation between the clinicopathologic characteristics and IL41 serum expression in hepatocellular carcinoma.

Clincopathological Features	Cases (n=162)	IL41 Serum Expression		*P* value
		IL41 ^{high} (n=81)	IL41^{low} (n=81)	
Narrow Surgical Edge (≤0.5cm)				
Yes	65	37	28	0.149
No	97	44	53	
Capsule Invasion				
Yes	52	27	25	0.736
No	110	54	56	
HBV Infection				
Yes	146	74	72	0.598
No	16	7	9	
Serum AFP before Resection (ng/ml)				
AFP positive	78	31	47	**0.012**
AFP negative	84	50	34	
Tumor Diameter(cm)				
≥ 5	52	31	21	0.092
< 5	110	50	60	
Tumor number				
≥ 2	18	12	6	0.134
< 2	144	69	75	
Age				
≥ 65	53	29	24	0.503
< 65	109	52	57	
Gender				
Male	113	60	53	0.231
Female	49	21	28	
MVI				
M0	47	4	43	**<0.001**
M1 or M2	115	77	38	
Edmondson-Steiner grading				
I+II	112	46	66	**0.001**
III+IV	50	35	15	

Bold font statistically significant.

The expression of IL-41 indicated malignant progression of HCC

Since serum IL-41 expression is positively correlated with faster tumor progression and poor prognosis as well as tissue IL-41 expression, we also examined the relationship between tissue IL-41 expression and clinicopathological features. We measured IL-41 expression in HCC tissues of patients with no recurrence, early recurrence, late recurrence, and death after tumor resection. We found that IHC score was the lowest for patients without recurrence and highest for those who died, while the IHC score of patients with early recurrence was between those with late recurrence and death (Figure 4A). This suggests that there is a trend of worsened outcomes as the level of tissue IL-41 expression increased. Further

TABLE 2 Univariate and multivariate cox hazard analysis of clinical features for HCC recurrence.

Clincopathological Features	Univariate analysis		*P* value	Multivariate analysis		*P* value
	HR	95 CI		HR	95 CI	
IL41(high)	2.787	1.440-5.398	**0.002**	1.858	1.389-3.889	**0.043**
MVI(M1/M2)	7.973	2.943-21.602	**<0.001**	7.173	2.305-22.322	**0.001**
Edmondson-Steiner grading(poor)	1.871	0.948-3.695	0.071	1.231	0.577-2.626	0.592
Narrow Surgical Edge	2.274	1.184-4.365	**0.014**	2.490	1.209-5.127	**0.013**

Bold font statistically significant.
CI, confidence interval; HR, Hazard ratio.

analyses of tissue IL-41 expression and tumor number, tumor size, and microvascular invasion in the 22 HCC patients revealed that patients with multiple metastases and microvascular invasion had significantly higher tissue IL-41 expression level (Figures 4B, C). On the other hand, tumor size (tumor size ≥5 cm or <5cm) was not associated with tissue IL-41 expression (data not shown). In general, these findings indicate that high tissue IL-41 expression is associated with malignant pathological features and adverse tumor outcomes following surgical resection. We posit that postoperative detection of IL-41 expression not only aids in HCC diagnosis but also serves as a predictor for postoperative recurrence and mortality. Additionally, it can potentially act as a warning signal for more frequent follow-up and early preventive treatment in these patients.

IL-41 can be used as a new serum diagnostic marker for HCC

As described above, we analyzed the serum expression of IL-41 in 170 HCC patients, 18 patients with liver metastases (colon cancer liver metastasis), 15 patients with acute hepatitis, and 19 healthy controls. ROC curve analysis indicated that the IL-41 cutoff for HCC diagnosis was 46.87 pg/mL, and its diagnostic sensitivity and specificity were 90.17% and 61.08%, respectively (Figure 5A). It should be noted that the diagnostic sensitivity and specificity of IL-41 were 96.63% and 68.42% in AFP-negative HCC patients, respectively. The sensitivity of IL-41 for HCC diagnosis exceeds that of any single serological marker currently available. In order to further verify the reliability of IL-41, we expanded our cohort to include obese patients and liver cancer patients diagnosed with HCC by imaging but not confirmed by pathology. However, due to the limited number of AFP-negative patients in this expanded cohort, we found that serum IL-41 expression was higher than the diagnostic cutoff (46.87) in five newly added patients but lower in 2 patients with hepatic hemangioma (not shown), resulting in a diagnostic accuracy of 100% among these newly added liver cancer patients (Figure 5B). In summary, IL-41 is a promising sensitive serum marker for HCC diagnosis worthy of further research and application.

Discussion

In the present study, we identified IL-41 as a potential diagnostic biomarker through database screening and verified its expression in clinical samples. Our data showed that high IL-41 expression was associated with early postoperative recurrence and poor prognosis in AFP-negative HCC patients. In addition, serum IL-41 expression was significantly higher in AFP-negative HCC patients than in AFP-positive HCC patients, colorectal cancer (CRC) patients with liver metastases, and healthy control. Furthermore, IL-41 expression in HCC tissues was higher in patients with early post-resection recurrence and death and was potentially associated with multiple metastases and microvascular invasion. Subsequent ROC curves and supplementation of additional patient sera confirmed the high sensitivity of IL-41 in the diagnosis of HCC, especially in AFP negative HCC patients. Taken together, our findings demonstrate that serum and tissue IL-41 expression is a promising new diagnostic marker for AFP-negative HCC.

HCC is a life-threatening and recurrent disease that impacts over a million patients worldwide every year (1), and its prevalence has been steadily rising in China due to the increasing rate of hepatitis B virus infection, making China a high-risk region for hepatitis and liver cancer (2). The discovery of new and reliable diagnostic and therapeutic targets for HCC is key to defeating liver cancer. Although AFP (3), PIVKA2 (4), GP73 (5), and other proteins have been identified as biomarkers for liver cancer diagnosis and treatment, there is currently no reliable tumor marker for patients with AFP-negative HCC. In this study, we retrospectively analyzed the clinical

TABLE 3 Univariate and multivariate cox hazard analysis of clinical features for early HCC recurrence.

Clincopathological Features	Univariate analysis		*P* value	Multivariate analysis		*P* value
	HR	95 CI		HR	95 CI	
IL41(high)	0.19	0.053-0.681	**0.011**	5.250	1.467-18.784	**0.011**

Bold font statistically significant.
Abbreviations: CI, confidence interval; HR, Hazard ratio.

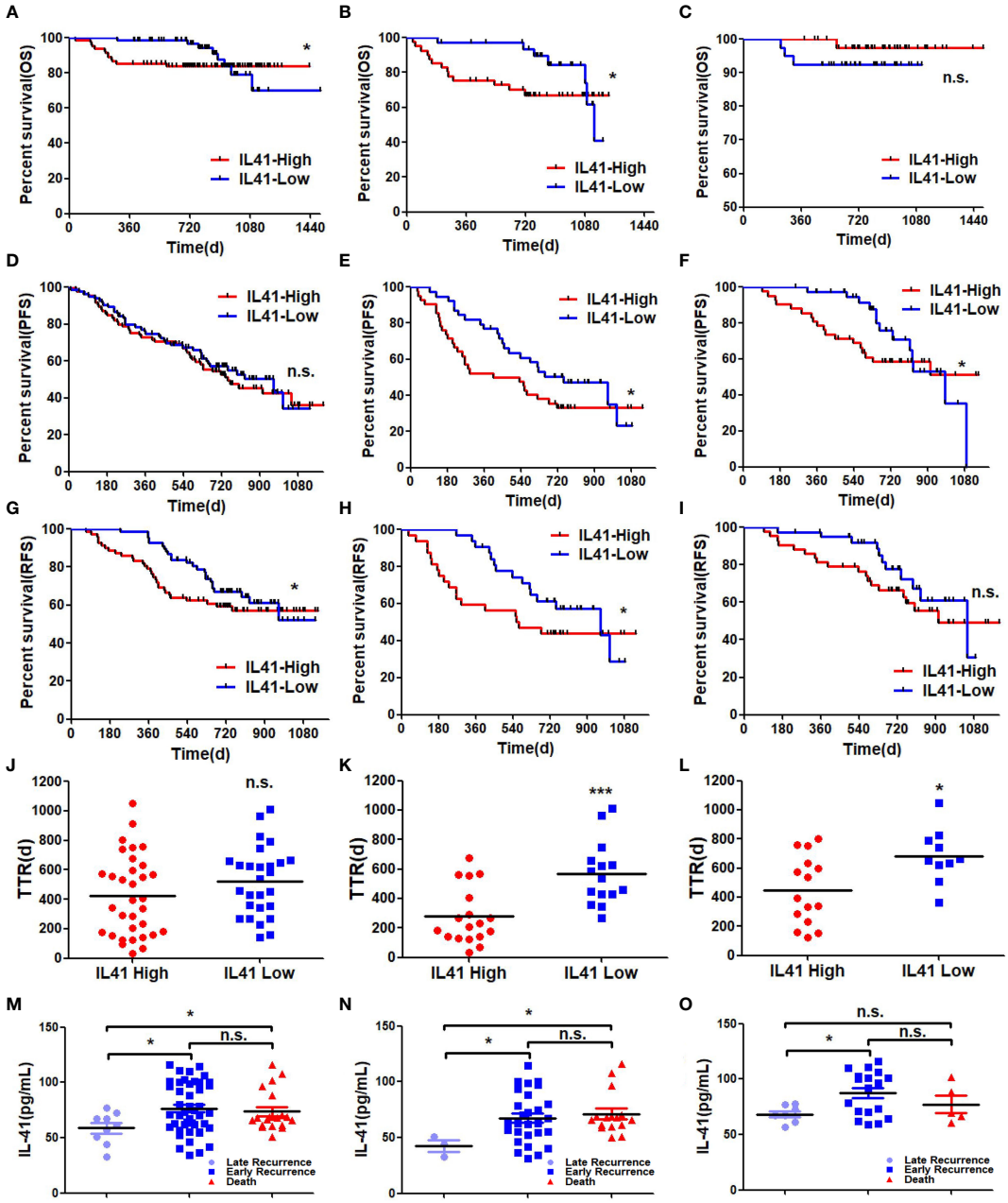

FIGURE 3
(A) OS of all HCC patients associated with high and low expression of IL41 (*P<0.05); **(B)** OS in AP-positive HCC patients associated with high and low expression of IL41 (*P<0.05); **(C)** OSin HCC patients with negative AFP associated with high and low expression of IL41 (n.s. no significance); **(D)** PFS (n.s, no significance) of all HCC patients associated with high and low expression of IL41; **(E)** PFS of AFP-positive HCC patients with high and low expression of IL41 (*P<0.05); **(F)** High and low expression of IL41 were associated with AFP negative PFS in HCC patients (*P<0.05); **(G)** RFS of all HCC patients associated with high and low expression of IL41 (*P<0.05); **(H)** RFS of AP-positive HCC patients associated with high and low expression of IL41 (*P<0.05); **(I)** RFS in HCC patients with negative AFP associated with high and low expression of IL41 (n.s. no significance); **(J)** TTR of all HCC patients associated with high and low expression of IL41 (n.s. no significance); **(K)** TTR of AP-positive HCC patients associated with high and low expression of IL41 (***P<0.001); **(L)** TTR of HCC patients with negative AFP associated with high and low expression of IL41 (*P<0.05); **(M)** The expression level of serum IL41 in HCC patients with late recurrence, early recurrence and death (*P<0.05, n.s. no significance); **(N)** The expression level of IL41 in serum of AFP positive HCC patients with late recurrence, early recurrence and death (*P<0.05, n.s. no significance); **(O)** Serum IL41 expression levels in AFP-negative HCC patients with late recurrence, early recurrence, and death (*P<0.05, n.s, no significance).

data of 176 HCC patients and identified IL-41 as a potential marker that negatively correlates with AFP expression using the TCGA the GEO databases and the biobank data of our center. The excellent diagnostic sensitivity of IL-41 (90.17%) indicates that it is the best serum marker thus far for HCC diagnosis, and the first and most sensitive (96.63%) marker for AFP-negative HCC. However, it is undeniable that IL-41 has limited specificity for HCC diagnosis, which may be attributed to the complex functions of the cytokine.

IL-41, also known as METRNL, is a novel secreted immunomodulatory protein highly expressed in barrier tissues,

10.3389/fonc.2024.1408584

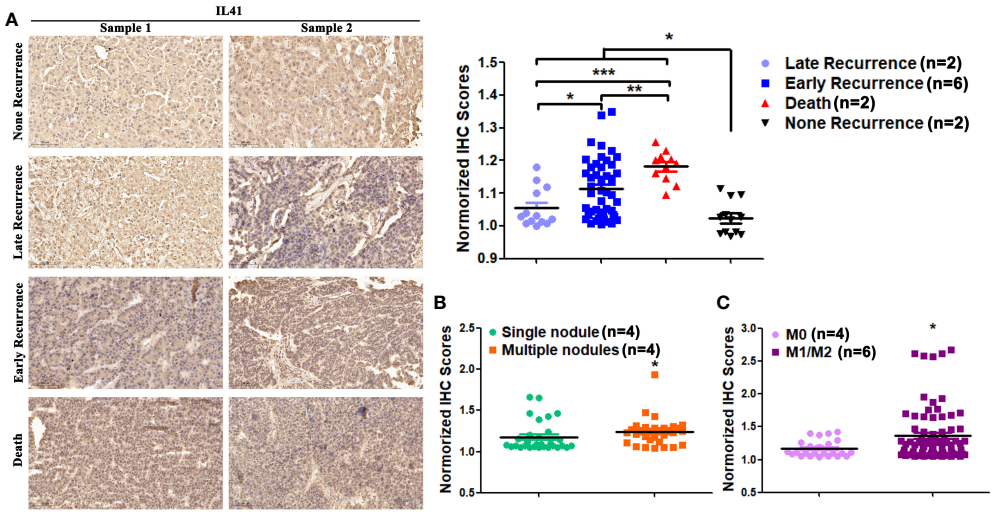

FIGURE 4
(A) The expression level of IL41 in tumor tissues of HCC patients with no recurrence, late recurrence, early recurrence and death (*P<0.05); **(B)** The expression level of IL41 in tumor tissues of patients with single and multiple HCC (*P<0.05, **P<0.01, ***P<0.001); **(C)** The expression level of IL41 in tumor tissues of HCC patients without microvascular invasion (M0) and with microvascular invasion (M1/2) (*P<0.05).

especially white adipose tissue (6, 7). This cytokine was first reported in 2004 (8) and its expression has been shown to be upregulated by factors such as inflammation (9), exercise, and cold exposure. The function of IL-41 is complex and diverse. It can act as a neurotrophic factor for neurons, neuroblasts, and spiral ganglion neurons (10), attenuate lipid-induced inflammation, alleviate insulin resistance, and lead to increased energy consumption and improved glucose tolerance in mice by inducing the browning of

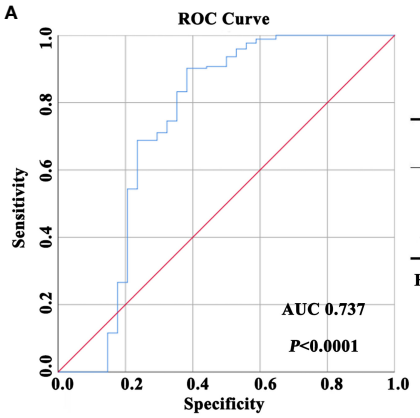

Group	Sensitivity(%)	Specificity(%)
Overall HCC	90.17	61.08
AFP-negative HCC	96.63	68.42

HCC IL41≥46.8708pg/ml

B

Patient	Diagnosis	IL41(pg/ml)	AFP(ng/ml)
#1	HCC	52.84	6.12
#2	Recurrence HCC	73.35	6.43
#3	HCC	59.12	3.44
#4	Recurrence HCC	55.08	5.40
#5	HCC	61.22	1.76

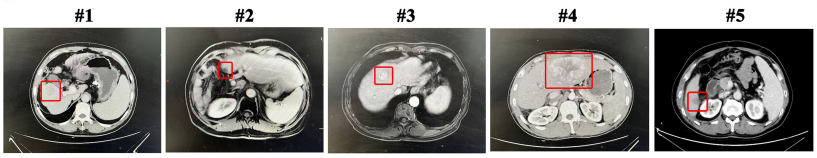

FIGURE 5
(A) ROC curve, sensitivity and specificity of IL41 in the diagnosis of HCC; **(B)** According to the diagnostic criteria in **(A)**, the diagnostic accuracy of serum IL41 in the diagnosis of HCC in 5 newly added AFP-negative HCC patients was 100% (HCC lesions marked in the red box below).

white fat (11). The role of IL-41 in inflammatory response is a key focus of current research. IL-41 has been reported to be significantly upregulated in inflammatory bowel disease, sepsis, psoriatic arthritis, and other inflammatory diseases, and plays a protective role in local tissues (12–14). Therefore, IL-41 is a potential diagnostic marker and therapeutic target for a wide range of immune diseases and may impact the progression of liver cancer. The 15 newly added hepatitis patients were active hepatitis patients with elevated AFP expression, and we found that serum IL-41 expression significantly varied among hepatitis patients. On the other hand, serum IL-41 expression was positively correlated with ALT and AST levels in AFP-positive liver cancer patients. Therefore, liver inflammation and acute liver damage caused by active hepatitis can potentially lead to inaccurate diagnosis by IL-41. Similar to the need of excluding active hepatitis, pregnancy, and reproductive system tumors when diagnosing liver cancer with AFP, active hepatitis and acute liver damage should also be excluded for IL-41-based liver cancer diagnosis. In addition, the serum levels of IL-41 in patients with autoimmune diseases, allergies, and infectious diseases such as chronic obstructive pulmonary disease in elderly patients with liver cancer, other types of viral hepatitis, and very rare liver cancer with liver abscess, should also be investigated to determine the effects of these conditions on IL-41 expression. We are currently measuring the serum level of IL-41 in obese patients and additional multicenter liver cancer patients to obtain a more scientific and accurate diagnostic cutoff for IL-41 in liver cancer.

We must note that the correlation analysis results of IL-41 and AFP are partly contradictory and the mRNA level of IL-41 in the TCGA database is significantly lower than that in normal liver tissues. During our search for diagnostic markers, we originally planned to look for extracellular proteins that are significantly negatively associated with AFP level but were constrained by the limited datasets that also examined serum AFP expression levels. Nevertheless, we still identified the GSE56545 dataset and found that the serum AFP expression was significantly negatively correlated with tissue IL-41 level in HCC patients who relapsed after resection. However, our analyses of the TCGA dataset and single-center data showed no correlation between serum AFP level and serum or tissue IL-41 expression. Considering the large variance in AFP expression, data with greater than 10,000 or even 100,000 ng/mL seriously affected the significance of the correlation. It is worth mentioning that the negative correlation between serum AFP and serum IL-41 increased as AFP decreased. In fact, when AFP was ≤ 1500ng/mL, AFP was negatively correlated with serum IL-41 expression. Furthermore, the IL-41 mRNA level in the TCGA dataset was lower or similar in HCC tissues compared with normal tissues, which resulted in no difference in serum or tissue IL-41 protein expression. Since proteins are responsible for mediating functions and there are various mechanisms of transcriptional modifications that can affect protein function and stability, the presence or absence of differences in mRNA expression is unlikely to affect the role of IL-41 protein in the diagnosis and treatment of HCC.

Similarly, the important diagnostic role of IL-41 is evidenced in the poor prognosis of HCC patients. Analyses of OS, PFS, RFS, and TTR of HCC patients with high and low IL-41 expression revealed that high serum IL-41 expression was associated with poor prognosis and post-resection recurrence in HCC patients. IHC analysis also indicated that high tissue IL-41 expression is associated with early recurrence, death, multiple metastases, and microvascular invasion after HCC resection. However, the source of IL-41 and the molecular mechanisms by which IL-41 overexpression promotes malignant progression of liver cancer are still unknown. Therefore, further studies are warranted to answer these questions. Our supplementary data hinted that IL-41 is associated with various immune cells, most strongly with macrophages. We used CD68 to locate macrophages in HCC tissues and stain the markers of M2 macrophages in order to explore whether macrophages and other cells in the tumor microenvironment are involved in the high expression of IL-41 and the malignant progression of HCC. Our team plans to send to HCC tissues with significantly high and low expression of IL-41, as well as transcriptome sequencing of HCC cell lines with overexpression and knockdown of IL-41, to search for potential downstream pathways and targets of IL-41.

In summary, IL-41 is a promising novel serum marker for HCC diagnosis and a potential predictor for poor prognosis and malignant progression of HCC. This marker is the cornerstone that paves the way for the development of further diagnostic markers and therapeutic targets for AFP-negative liver cancer patients.

Data availability statement

The datasets presented in this study can be found in online repositories. The names of the repository/repositories and accession number(s) can be found in the article/Supplementary Material.

Ethics statement

The studies involving humans were approved by the Ethics Committee of Xi'an Jiaotong University. The studies were conducted in accordance with the local legislation and institutional requirements. Written informed consent for participation in this study was provided by the participants' legal guardians/next of kin. Written informed consent was obtained from the individual(s) for the publication of any potentially identifiable images or data included in this article.

Author contributions

BY: Data curation, Funding acquisition, Investigation, Resources, Supervision, Writing – review & editing. YL: Funding acquisition, Data curation, Investigation, Resources, Writing – original draft, Writing – review & editing. HW: Investigation, Methodology, Software, Writing – original draft. DR: Investigation, Resources, Data curation, Writing – original draft. JL: Investigation, Methodology, Resources, Writing – original draft. ZM: Investigation, Methodology, Writing – original draft. CL: Investigation, Methodology, Writing – original draft. YoH:

Investigation, Software, Writing – original draft. JZ: Investigation, Software, Writing – original draft. RF: Methodology, Writing – original draft. JY: Methodology, Software, Writing – original draft. JS: Methodology, Writing – original draft. YiH: Resources, Writing – original draft.

Funding

The author(s) declare financial support was received for the research, authorship, and/or publication of this article. This study was supported by Hospital Research and Development Fund of the First Affiliated Hospital of Xi'an Jiaotong University (2021QN-04), Research and Development Program Fund of Shaanxi Province (2023-JC-YB-680), National Natural Science Foundation of China (82303460), Hospital Research and Development Fund of the First Affiliated Hospital of Xi'an Jiaotong University (2022QN-30), Research and Development Program Fund of Shaanxi Province (2024JC-YBQN-0897).

Acknowledgments

These biological samples are banked by the Biobank of First Affiliated Hospital. of Xi'an Jiaotong University.

Conflict of interest

The authors declare that the research was conducted in the absence of any commercial or financial relationships that could be construed as a potential conflict of interest.

Publisher's note

Supplementary material

The Supplementary Material for this article can be found online at: https://www.frontiersin.org/articles/10.3389/fonc.2024.1408584/full#supplementary-material

SUPPLEMENTARY FIGURE 1
(A) There was no significant correlation between serum AFP of HCC patients and tissue IL41 mRNA in TCGA database; **(B)** There was no correlation between the relative expression of IL41 mRNA in non-recurrent HCC tissues and serum AFP in GSE56545 dataset; **(C)** There were 15 new patients with acute hepatitis and the expression of IL41 in different groups was analyzed. There was no significant difference in serum IL41 between hepatitis patients and other groups; (***P*<0.01,****P*<0.001), n.s.: no signifcance. **(D)** There was a significant positive correlation between serum IL41 and ALT in AFP positive HCC patients(*P*<0.05). **(E)** There was a significant positive correlation between serum IL41 and AST in AFP positive HCC patients (*P*<0.05). **(F)** IL41(METRNL) in the TCGA database was positively correlated with multiple immune cell infiltrations (****P*<0.001).

SUPPLEMENTARY FIGURE 2
(A) The OS of HCC patients with high or low expression of IL41 presented in the TCGA database (*P*<0.05); **(B)** The OS of HCC patients with high or low IL41 expression combined with hepatitis B was shown in TCGA database(*P*<0.05); **(C)** The OS of HCC patients with high or low IL41 expression combined with non-alcoholic hepatitis was shown in the TCGA database (*P*<0.05); **(D)** OS of HCC patients with positive or negative AFP in our center (****P*<0.001).

References

1. Yao B, Li Y, Chen T, Niu Y, Wang Y, Yang Y, et al. Hypoxia-induced cofilin 1 promotes hepatocellular carcinoma progression by regulating the PLD1/AKT pathway. *Clin Transl Med*. (2021) 11:e366. doi: 10.1002/ctm2.366

2. Yao B, Lu Y, Li Y, Bai Y, Wei X, Yang Y, et al. BCLAF1-induced HIF-1α accumulation under normoxia enhances PD-L1 treatment resistances via BCLAF1-CUL3 complex. *Cancer Immunol Immunother*. (2023) 72:4279–92. doi: 10.1007/s00262–023-03563–8

3. Yao B, Li Y, Niu Y, Wang L, Chen T, Guo C, et al. Hypoxia-induced miR-3677–3p promotes the proliferation, migration and invasion of hepatocellular carcinoma cells by suppressing SIRT5. *J Cell Mol Med*. (2020) 24:8718–31. doi: 10.1111/jcmm.15503

4. Kim E, Viatour P. Hepatocellular carcinoma: old friends and new tricks. *Exp Mol Med*. (2020) 52:1898–907. doi: 10.1038/s12276–020-00527–1

5. Yeh SH, Li CL, Lin YY, Ho MC, Wang YC, Tseng ST, et al. Hepatitis B virus DNA integration drives carcinogenesis and provides a new biomarker for HBV-related HCC. *Cell Mol Gastroenterol Hepatol*. (2023) 15:921–9. doi: 10.1016/j.jcmgh.2023.01.001

6. Du D, Liu C, Qin M, Zhang X, Xi T, Yuan S, et al. Metabolic dysregulation and emerging therapeutical targets for hepatocellular carcinoma. *Acta Pharm Sin B*. (2022) 12:558–80. doi: 10.1016/j.apsb.2021.09.019

7. Llovet JM, Castet F, Heikenwalder M, Maini MK, Mazzaferro V, Pinato DJ, et al. Immunotherapies for hepatocellular carcinoma. *Nat Rev Clin Oncol*. (2022) 19:151–72. doi: 10.1038/s41571–021-00573–2

8. Cheng K, Cai N, Zhu J, Yang X, Liang H, Zhang W. Tumor-associated macrophages in liver cancer: From mechanisms to therapy. *Cancer Commun (Lond)*. (2022) 42:1112–40. doi: 10.1002/cac2.12345

9. Shin SW, Ahn KS, Kim SW, Kim TS, Kim YH, Kang KJ. Liver resection versus local ablation therapies for hepatocellular carcinoma within the milan criteria: A systematic review and meta-analysis. *Ann Surg*. (2021) 273:656–66. doi: 10.1097/SLA.0000000000004350

10. Vitale A, Cabibbo G, Iavarone M, Viganò L, Pinato DJ, Ponziani FR, et al. HCC Special Interest Group of the Italian Association for the Study of the Liver. Personalised management of patients with hepatocellular carcinoma: a multiparametric therapeutic hierarchy concept. *Lancet Oncol*. (2023) 24:e312–22. doi: 10.1016/S1470–2045(23)00186–9

11. Gong C, Wang H, Liu P, Guo T. Impact of intraoperative vascular occlusion during liver surgery on long-term outcomes: A systematic review and meta-analysis. *Int J Surg*. (2017) 44:110–6. doi: 10.1016/j.ijsu.2017.06.050

12. Minami Y, Nishida N, Kudo M. Therapeutic response assessment of RFA for HCC: contrast-enhanced US, CT and MRI. *World J Gastroenterol*. (2014) 20:4160–6. doi: 10.3748/wjg.v20.i15.4160

13. Sherman M. Alphafetoprotein: an obituary. *J Hepatol*. (2001) 34:603–5. doi: 10.1016/s0168–8278(01)00025–3

14. Norman JS, Li PJ, Kotwani P, Shui AM, Yao F, Mehta N. AFP-L3 and DCP strongly predict early hepatocellular carcinoma recurrence after liver transplantation. *J Hepatol*. (2023) 79:1469–77. doi: 10.1016/j.jhep.2023.08.020

15. Singh S, Hoque S, Zekry A, Sowmya A. Radiological diagnosis of chronic liver disease and hepatocellular carcinoma: A review. *J Med Syst*. (2023) 47:73. doi: 10.1007/s10916–023-01968–7

16. Tayob N, Kanwal F, Alsarraj A, Hernaez R, El-Serag HB. The performance of AFP, AFP-3, DCP as biomarkers for detection of hepatocellular carcinoma (HCC): A phase 3 biomarker study in the United States. *Clin Gastroenterol Hepatol*. (2023) 21:415–423.e4. doi: 10.1016/j.cgh.2022.01.047

17. Sumi A, Akiba J, Ogasawara S, Nakayama M, Nomura Y, Yasumoto M, et al. Des-γ-carboxyprothrombin (DCP) and NX-DCP expressions and their relationship

with clinicopathological features in hepatocellular carcinoma. *PloS One*. (2015) 10: e0118452. doi: 10.1371/journal.pone.0118452

18. Wang S, Zhou L, Ji N, Sun C, Sun L, Sun J, et al. Targeting ACYP1-mediated glycolysis reverses lenvatinib resistance and restricts hepatocellular carcinoma progression. *Drug Resist Update*. (2023) 69:100976. doi: 10.1016/j.drup.2023.100976

19. Onuora S. Novel cytokine, IL-41, linked with PsA. *Nat Rev Rheumatol*. (2019) 15:636. doi: 10.1038/s41584–019-0314–7

20. Bridgewood C, Russell T, Weedon H, Baboolal T, Watad A, Sharif K, et al. The novel cytokine Metrnl/IL-41 is elevated in Psoriatic Arthritis synovium and inducible from both entheseal and synovial fibroblasts. *Clin Immunol*. (2019) 208:108253. doi: 10.1016/j.clim.2019.108253

21. Li ZY, Zheng SL, Wang P, Xu TY, Guan YF, Zhang YJ, et al. Subfatin is a novel adipokine and unlike Meteorin in adipose and brain expression. *CNS Neurosci Ther*. (2014) 20:344–54. doi: 10.1111/cns.12219

22. Li ZY, Song J, Zheng SL, Fan MB, Guan YF, Qu Y, et al. Adipocyte metrnl antagonizes insulin resistance through PPARγ Signaling. *Diabetes*. (2015) 64:4011–22. doi: 10.2337/db15–0274

23. Rao RR, Long JZ, White JP, Svensson KJ, Lou J, Lokurkar I, et al. Meteorin-like is a hormone that regulates immune-adipose interactions to increase beige fat thermogenesis. *Cell*. (2014) 157:1279–91. doi: 10.1016/j.cell.2014.03.065

24. Zhang SL, Li ZY, Wang DS, Xu TY, Fan MB, Cheng MH, et al. Aggravated ulcerative colitis caused by intestinal Metrnl deficiency is associated with reduced autophagy in epithelial cells. *Acta Pharmacol Sin B*. (2020) 41:763–70. doi: 10.1038/s41401–019-0343–4

25. Ushach I, Arrevillaga-Boni G, Heller GN, Pone E, Hernandez-Ruiz M, Catalan-Dibene J, et al. Meteorin-like/meteorin-β Is a novel immunoregulatory cytokine associated with inflammation. *J Immunol*. (2018) 201:3669–76. doi: 10.4049/jimmunol.1800435

26. Nishino J, Yamashita K, Hashiguchi H, Fujii H, Shimazaki T, Hamada H. Meteorin: a secreted protein that regulates glial cell differentiation and promotes axonal extension. *EMBO J*. (2004) 23:1998–2008. doi: 10.1038/sj.emboj.7600202

27. Cen T, Mai Y, Jin J, Huang M, Li M, Wang S, et al. Interleukin-41 diminishes cigarette smoke-induced lung inflammation in mice. *Int Immunopharmacol*. (2023) 124:110794. doi: 10.1016/j.intimp.2023.110794

28. Zuo L, Ge S, Ge Y, Li J, Zhu B, Zhang Z, et al. The adipokine metrnl ameliorates chronic colitis in IL-10-/- mice by attenuating mesenteric adipose tissue lesions during spontaneous colitis. *J Crohns Colitis*. (2019) 13:931–41. doi: 10.1093/ecco-jcc/jjz001

frontiers | Frontiers in Oncology

TYPE Review
PUBLISHED 21 May 2024
DOI 10.3389/fonc.2024.1404683

OPEN ACCESS

EDITED BY
Rongxin Zhang,
Guangdong Pharmaceutical University, China

REVIEWED BY
Alejandro Serrablo,
Hospital Universitario Miguel Servet, Spain
Eric Toshiyuki Nakamura,
University of São Paulo, Brazil

*CORRESPONDENCE
Francisco Tustumi
franciscotustumi@gmail.com

RECEIVED 21 March 2024
ACCEPTED 03 May 2024
PUBLISHED 21 May 2024

CITATION
Andraus W, Ochoa G, de Martino RB, Pinheiro RSN, Santos VR, Lopes LD, Arantes Júnior RM, Waisberg DR, Santana AC, Tustumi F and D'Albuquerque LAC (2024) The role of living donor liver transplantation in treating intrahepatic cholangiocarcinoma. *Front. Oncol.* 14:1404683. doi: 10.3389/fonc.2024.1404683

The role of living donor liver transplantation in treating intrahepatic cholangiocarcinoma

Wellington Andraus, Gabriela Ochoa, Rodrigo Bronze de Martino, Rafael Soares Nunes Pinheiro, Vinicius Rocha Santos, Liliana Ducatti Lopes, Rubens Macedo Arantes Júnior, Daniel Reis Waisberg, Alexandre Chagas Santana, Francisco Tustumi* and Luiz Augusto Carneiro D'Albuquerque

Department of Gastroenterology, Transplantation Unit, Universidade de São Paulo, São Paulo, Brazil

Introduction: Intrahepatic cholangiocarcinoma (iCC) is the liver's second most common neoplasm. Until now, surgery is the only curative option, but only 35% of the cases are considered resectable at the diagnosis, with a post-resection survival of around 30%. Advancements in surgical techniques and perioperative care related to liver transplantation (LT) have facilitated the expansion of indications for hepatic neoplasms.

Method: This study is a comprehensive review of the global experience in living donor LT (LDLT) for treating iCC and describes our first case of LDLT for an unresectable iCC.

Results: While exploring LT for intrahepatic cholangiocarcinoma dates to the 1990s, the initial outcomes were discouraging, marked by poor survival and high recurrence rates. Nevertheless, contemporary perspectives underscore a reinvigorated emphasis on extending the frontiers of LT indications within the context of the "oncologic era." The insights gleaned from examining explants, wherein incidental iCC was categorized as hepatocellular carcinoma in the preoperative period, have demonstrated comparable survival rates to small hepatocellular carcinoma. These findings substantiate the potential viability of LT as a curative alternative for iCC. Another investigated scenario pertains to "unresectable tumors with favorable biological behavior," LT presents a theoretical advantage by providing free margins without the concern of a small future liver remnant. The constraint of organ shortage persists, particularly in nations with low donation rates. LDLT emerges as a viable and secure alternative for treating iCC.

Conclusion: LDLT is an excellent option for augmenting the graft pool, particularly in carefully selected patients.

KEYWORDS

cholangiocarcinoma, liver transplantation, living donors, hepatectomy, liver neoplasms

Introduction

Cancer is considered a contraindication to transplant for most organs. However, liver transplantation can be a curative strategy for some malignancies. The expansion of indications in the new era of oncologic transplantation was made possible due to the improvement of the perioperative outcomes and postoperative treatment and the long experience in treating hepatocellular carcinoma (HCC) (1).

HCC is an accepted indication for transplantation. However, tumor size and standardized multidisciplinary treatment protocols are necessary to ensure optimal patient outcomes. On the other hand, cholangiocarcinoma (CC) is still a controversial indication worldwide (2).

CC is a highly lethal epithelial cell malignancy along the biliary tree and within the hepatic parenchyma. The CCAs are divided into three subtypes depending on their anatomical location: intrahepatic (iCC), hilar (hCC), and distal (dCC). CC is the second most common primary hepatic malignancy, after HCC, comprising approximately 15% of all primary liver tumors and 3% of gastrointestinal cancers. Despite its rarity, the incidence (0.3–6 per 100,000 inhabitants per year) and mortality (1–6 per 100,000 inhabitants per year globally) of CC have witnessed a discernible surge worldwide over recent decades, constituting a global health challenge (3). The prognosis for this malignancy remains bleak, with a 5-year survival rate ranging from 7 to 20% and a notable risk for tumor recurrence after resection. Surgery is the treatment of choice for early-stage tumors, regardless of the anatomical type. However, only 35% of the patients are eligible for surgical treatment, and there is a high rate of postoperative recurrence (4).

The iCC subgroup represents 10–20% of all CC and arises above the second-order bile ducts. The prognosis is usually dismal, with a reported 5-year overall survival of 10% to 35%. However, the prognosis is strictly related to stage and molecular profiles (5). The recommended treatment for advanced stages is chemotherapy combined with immunotherapy, with a median overall survival of less than one year (6, 7).

Liver transplantation (LT) offers a theoretical advantage to allowing surgical radicality. LT avoids the risk of the liver's future small remanent and cures the underlying liver disease in cases of cirrhosis. The initial international experience with LT for iCC in the 1990s, particularly in advanced cases, yielded suboptimal outcomes marked by compromised survival rates and heightened morbidity (8). Currently, emphasis has shifted towards meticulous candidate selection, considering factors such as tumor size and biological behavior to identify individuals who are more likely to benefit from LT (9–11).

Due to organ shortage and increasing organ demand in most countries worldwide, the allocation of liver grafts is always meticulously analyzed and discussed before any expansion of transplant indications in cases of deceased donor LT. In 2022, Brazil achieved a donation rate of 16.5 per million population (pmp), surpassing certain neighboring countries but still trailing behind nations with more robust organ donation rates, such as Spain and the USA, which boast 46 and 44 pmp per year, respectively (12). In this context, living donor liver transplantation (LDLT) is an excellent option in regions where the allocation system does not allow a real opportunity to get an organ on the waiting list. In countries with low donation rates, such as Latin America, the LDLT represents a good solution for oncological indications in LT.

While LT has become one of the main treatment alternatives for hCC, LT is still not universally accepted for iCC (13). We presented a comprehensive review of the international experience with LTLT for iCC and reported our first case of LTLT for iCC (14, 15).

Initial experience

In the '90s and the beginning of 2000, during the expansion of the indications of LT, a few cases of unresectable liver malignancies were treated with LT. However, the oncologic results were poor, with a high recurrence rate and a low overall survival. Goldstein et al. reported 17 patients with cholangiocarcinoma submitted to LT in 1993. Three of them were excluded due to premature mortality. Among the remaining 14 patients, 11 experienced recurrences during the follow-up, and within one year, seven succumbed to disease progression. The 1-year survival rate within this series was 53%, with a corresponding disease-free survival rate of 40% (16). In 2000, Meyer et al. reported 207 cases of LT for unresectable CC or cholangiohepatoma. The survival of 1, 2, and 5-year were 72, 48, and 23%. Fifty-one percent of patients presented a recurrence of their tumors after transplantation, and 84% of recurrences occurred within two years of transplantation (17).

LT in incidental lesions of iCC in the explant or HCC misdiagnosis

Regarding HCC, the LT is the best treatment to cure cases under biological and size selection criteria, with an excellent overall survival at five years, reaching 80%. Consequently, in the contemporary landscape, HCC is one of the main indications for LT worldwide, serving as a cornerstone in oncologic transplantation support. Since it is unnecessary to perform a biopsy for suspected tumors, a small percentage of misdiagnosed lesions had been included for transplant over time. Sapisochin et al. published in 2011 the analysis of 14 explant specimens from 302 patients (4.6%) who underwent LT intentionally for HCC that showed mixed HCC-CC or iCC, with 10 falling into the latter category. After a median follow-up period of 32 months, 8 of the 14 patients (57%) suffered from tumor recurrence, and the median disease-free survival time was eight months (18). In 2014, the same author advocated incorporating a size criterion, following a Spanish-matched cohort multicenter study comparing 27 iCC with 54 HCC. Patients with uninodular tumors of 2 cm or smaller in the study group had similar 1-, 3-, and 5-year survival rates with the HCC control group (92%, 83%, 62% *vs.* 100%, 80%, 80%; $P = 0.4$). In contrast, patients with multinodular or uninodular tumors larger than 2 cm had worse 1-, 3-, and 5-year survival rates than their controls (80%, 66%, and 61% *vs.* 99%, 96%, and 90%; $P < 0.001$) (19).

In 2016, the iCC International Consortium introduced the term "very early iCC," denoting single tumors with a size of 2 cm or smaller. Their findings revealed compelling survival rates for this category, with percentages of 93%, 84%, and 65% at 1, 3, and 5 years, respectively. In contrast, the advanced iCC group, characterized by a single tumor larger than 2 cm or multifocal disease, exhibited survival rates of 79%, 50%, and 45% at the respective time intervals (20).

The discovery of incidental iCC lesions in LT explants and their subsequent analysis has rekindled interest in using LT as a viable treatment modality for this disease.

LT for unresectable advanced iCC

Currently, unresectable intrahepatic tumors are usually treated with systemic chemotherapy. The regimen with gemcitabine and cisplatin yields an overall survival rate of only 18.9 months and a progression-free survival duration of 11.1 months (21).

In recent years, significant advances have been achieved in understanding iCC. The new distinction between small and large duct tumors, coupled with identifying mutations and associated risk factors for each subtype, seems to be the key to advancement in treatment. This nuanced distinction holds promise for refining the selection of cases based on their biological behavior and, eventually, enabling the identification of candidates for LT in the context of unresectable tumors, with the ultimate goal of achieving curative outcomes (22–24).

The experience with pCC showed that neoadjuvant therapy followed by LT results in a long-term survival advantage in patients without disease progression (13). For iCC the first case series of neoadjuvant treatment was reported by Hong at all in 2011. In their published experience, encompassing 25 transplanted patients with iCC, they detailed that nine of these individuals underwent neoadjuvant and adjuvant therapy. When comparing patients who received combined neoadjuvant and adjuvant therapy to those who received no therapy or only adjuvant treatment, a discernible advantage in terms of survival emerged for the group that underwent both treatments (47% *vs.* 20% *vs.* 33%, respectively; P = 0.03) (25).

Lunsford et al. reported that 12 patients underwent evaluation for potential LT and were diagnosed with unresectable iCC in 2018. These individuals underwent an extensive neoadjuvant protocol involving gemcitabine-based chemotherapy and, in some cases, a subsequent second or third-line regimen. At the time of publication, six of the patients had undergone transplantation. The survival rates at 1, 3, and 5 years were 100%, 83.3%, and 83.3%, respectively. However, during the follow-up period, disease recurrence occurred in three patients, constituting a recurrence rate of 50% (26).

Certainly, neoadjuvant therapies play a crucial role in reducing the likelihood of recurrence and serve as a valuable assessment tool for evaluating the favorable biological behavior of tumors. Moreover, they contribute to the selective identification of patients who stand to benefit from liver transplantation as a viable treatment strategy for tumors.

LDLT for iCC

The limited availability of donor organs in comparison to the growing demand has intensified concerns about the allocation of grafts, mainly when used for innovative indications, especially in the context of cancer. This concern is further exacerbated by the potential for disease recurrence and associated mortality, prompting careful consideration of resource allocation in these circumstances.

In most countries, the shortage of organs due to a low rate of donations and the dropout in the waiting list of patients with current indications does not allow the expansion of LT to treat new conditions. Like most nations, Brazil has adopted the Model for End-Stage Liver Disease (MELD) score allocation system. This system grants exception points for specific criteria in HCC cases. However, it does not permit the inclusion of patients with other primary malignant liver neoplasms, thereby limiting the chances for individuals with iCC to be added to the waiting list (27).

In this context, LDLT stands as a safety-assured strategy for the global expansion of liver transplantation. LDLT has become an effective treatment option to overcome the deceased donor organ shortage and an excellent alternative to treat selected oncologic cases (28).

The LDLT for HCC has been widely used, especially in oriental countries. For instance, Kyushu University reported 90 cases of LT in 2017, employing expanded criteria based on size and des-γ-carboxy prothrombin levels in HCC, utilizing living donor grafts. This cohort's 5-year overall patient survival rate was an impressive 89%. Similarly, the pilot study conducted by the Barcelona Clinic Liver Group 2018 utilized extended criteria, incorporating factors such as size, number, and downstaging as selection criteria. The study, comprising 22 patients with a follow-up duration of 81 months, reported survival rates of 95.5%, 86.4%, 80.2%, and 66.8% at 1, 3, 5, and 10 years, respectively. These findings underscore the success of LDLT in managing HCC and the potential applicability of expanded criteria in diverse clinical settings (29, 30).

The LDLT strategy offers a valuable solution for iCC, avoiding the long waiting list. This strategy proves beneficial not only in early iCC accompanied by underlying cirrhosis but also in advanced stages exhibiting a favorable response post-neoadjuvant therapy. The expeditious nature of this approach is crucial, considering the observed higher dropout rates in iCC patients.

While the literature on this topic remains limited, our review revealed eight articles documenting cases of LDLT for iCC. Among them, five specifically addressed living donors as a primary focus, while three presented a more comprehensive series encompassing cases of LDLT. Notably, only two reports featured more than two cases. The most extensive series was published by Sierra et al., focusing on LT outcomes for primary sclerosing cholangitis. Within this series, 55 out of 805 LDLT cases culminated in an iCC diagnosis, with an overall survival rate for LDLT recipients reaching 81.9%. Intriguingly, multivariate analysis identified concurrent cholangiocarcinoma as a significant predictor of mortality (HR: 2.07; 95% CI: 1.71–2.50; p < 0.001) (31). The

second largest series was published in 2020 by Bhatti et al., who analyzed the experience in LDLT for cholangiocarcinoma in cases with early stages of the disease and incidental diagnoses. Their study revealed a three-year survival rate of 63% (32). We resume the cases series in Table 1, including our first reported case (33–37).

A multicentric single-arm clinical trial (NCT04195503) is currently underway to validate LT's efficacy for stable advanced iCC. This prospective investigation aims to provide conclusive evidence for the therapeutic effectiveness of LT in this context, a crucial step as these findings have not been prospectively verified to date. Of course, one inclusion criterion in this trial is the availability of a compatible living donor (39).

The first case reported of LDLT for ICC unresectable in Brazil

A 36-year-old female patient with no previous medical history presented with upper right abdominal pain. The investigation revealed a multinodular tumor in the liver, characterized by an extensive central tumor affecting the cava vein (Figure 1). The CA 19.9 level exceeded 6900 U/mL. A percutaneous biopsy was conducted, confirming the presence of iCC. A multidisciplinary committee deliberated on the unresectable case and opted for systemic therapy using gemcitabine and cisplatin.

There was no significant response after three cycles of systemic chemotherapy. Subsequently, the treatment strategy was altered to intra-arterial chemotherapy with oxaliplatin and gemcitabine, and she underwent a total of eight cycles. CA19.9 exhibited a significant decrease, reaching 216 U/mL, and the tumoral volume was reduced by 20%. Subsequently, she entered a maintenance phase of treatment with intravenous cisplatin and gemcitabine.

Due to the excellent response to intra-arterial treatment, the multidisciplinary board reevaluated the treatment strategy. Despite the positive outcome, the tumor remained unresectable, and LT was considered. The national allocation system in Brazil does not permit the inclusion of iCC in the waiting list. Consequently, the LDLT was an attractive alternative.

A right hepatic lobe LDLT was performed. The donor was his husband. An open surgery was performed. The right hepatectomy was performed, excluding the middle hepatic vein (the vein remained for the donor).

The total liver volume was 1881 cm^3, and the right lobe volume was 1006 cm^3. The volume of the remnant liver (left lobe + caudate lobe) was 875 cm^3 (46.5%). The donor had normal biliary tree anatomy, with one duct after bifurcation to the right lobe. The right hepatic artery originated from the superior mesenteric artery. The donor had a large right hepatic vein, and the middle hepatic vein drained mostly the left lobe.

The graft weight was 922g, and the ratio graft weight/recipient weight was 1.41%. After reperfusion, the graft showed no congested or ischemic areas.

Given the complexity of the lesion and the invasion of the cava vein, a veno-venous bypass was executed, and the cava vein underwent resection and reconstruction using an iliac graft (Figure 2).

The donor and recipient had an uneventful postoperative course. Pathological analysis of the explant revealed a moderately differentiated, multinodular intrahepatic cholangiocarcinoma, with 30% viable neoplasm and no involvement of the six examined lymph nodes. After 24 months of follow-up, the patient remains alive with no signs of recurrence.

Discussion

The field of oncologic transplantation has expanded globally, particularly with the extension of indications for primary liver cancer. Initially, the eligibility for transplantation in HCC was confined to the "Milan Criteria," which selected cases based on size and number (40). Patients meeting the Milan criteria were confirmed as suitable candidates for liver transplantation, leading to an overall survival rate exceeding 70% in five years (41). Currently, it is known that patients who successfully undergo downstage therapy exhibit comparable survival rates to those initially meeting the Milan criteria (42). Other scores incorporating biological indicators and dynamic measures of responsiveness to

TABLE 1 Summary of the articles evaluating living donor liver transplantation (LDLT) for intrahepatic cholangiocarcinoma (iCC).

Authors	Year	Number	Staged	Setting	Follow-up (months)	Recurrence
Takatsuki et al. (33)	2001	1	early	incidental	30	0
Jonas et al. (34)	2005	2	advanced	unresectable	46, 35	2
Sotiropoulos et al. (35)	2008	1	advanced	unresectable	21	1
Lunsford et al.* (26)	2018	2	advanced	unresectable	36	1
Hafeez Bhatti et al. (32)	2020	9	early	incidental	36	not informed
De Martin et al. (36)	2020	1	early	incidental	48	not informed
Rauchfuß et al. (37)	2020	2	advanced	unresectable	23, 17	0
Sierra et al.** (31)	2023	55	not reported	not reported	not specificated	not informed
Bednarsch et al. (38)	2024	1	advanced	unresectable	18	no
Andraus et al***	2024	1	advanced	unresectable	23	no

*Domino's transplant, **patients with primary sclerosing cholangitis, ***in edition for publication.

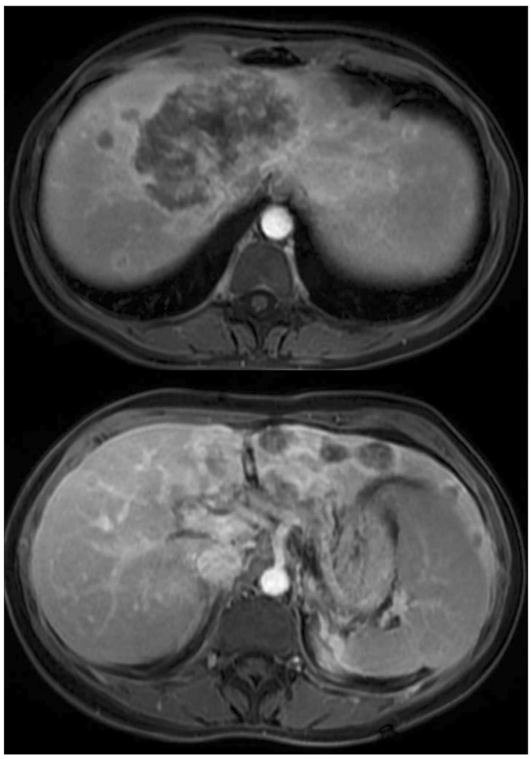

FIGURE 1
Magnetic resonance imaging showed a multinodular lesion with a predominantly tumor in the central liver with cava vein invasion.

pre-transplant locoregional therapy and waiting time have been established.

Furthermore, there is mounting evidence indicating that tumor load is just one among numerous variables affecting post-LT outcomes. Recently proposed pre-LT selection criteria have evolved to encompass markers of tumor biology, such as alpha-fetoprotein (AFP) and responsiveness to locoregional treatments. The Working Group Report from the ILTS Transplant Oncology Consensus Conference in 2020 underscored that the selection process should consider tumor biology (including AFP), tumor size, number of tumors, probability of survival, transplant benefit, organ availability, waiting list composition, and allocation priorities (43).

The expansion of LT indications for iCC follows the same steps as HCC. Prior to the 1990s, the concept of biological behavior was unfamiliar, and suboptimal outcomes were attributed to the need for more refined selection criteria. Today, including HCC cases beyond the Milan criteria is widely accepted, particularly in patients exhibiting favorable biological behavior. In the context of iCC, over the last decade, size criteria have been explored, especially for incidental lesions found in LT explants from patients with cirrhosis. It is acknowledged that early-staged lesions of iCC yield comparable oncologic outcomes to early cases of HCC after LT (44). Nevertheless, confining LT indications to early lesions might be overly restrictive. Drawing from the insights gained in the evolution of HCC transplantation, there is a growing perspective that the emphasis should shift toward identifying cases of liver malignancy with favorable biological behavior. This approach could allow for

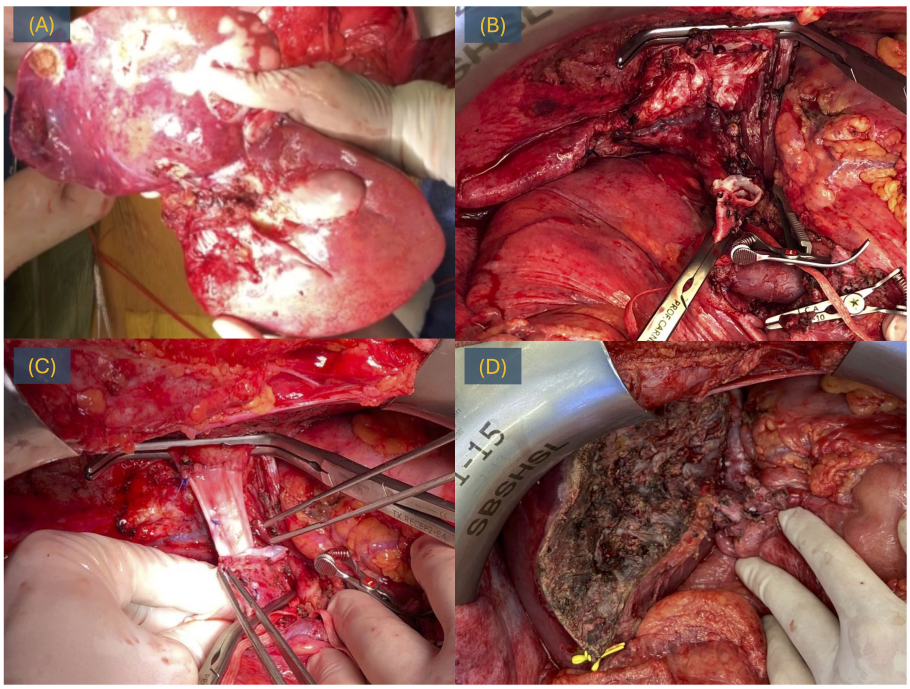

FIGURE 2
LDLT for iCC, surgery. **(A)** Explant with the tumor. **(B)** Post-hepatectomy time with a cava vein resected. **(C)** Reconstruction of the cava vein with iliac graft. **(D)** Hepatic transection.

LT as a viable treatment option, irrespective of size and number considerations.

LT in the treatment of iCC is still being defined. Recent publications have proposed highly stringent selection criteria for LT in these patients (18, 19). However, regarding LDLT, the selection process has become even more intricate. Although the risk for the donor must be considered, LDLT offers the advantage of mitigating the impact of an additional indication for LT on the waiting list, presenting itself as a viable option in these non-standard indications.

The 5th edition of the World Health Organization Classification of Tumors, published in 2019, emphasizes the subclassification of iCC based on small and large ducts (45). The small duct type typically manifests in the periphery of the liver and tends to form mass lesions. This subtype shares etiologic and imaging features with HCC, which exhibits better biological behavior (46, 47). Some centers are currently conducting investigations, and certain histological features may contribute to achieving improved outcomes for liver resection or LT in the context of this disease (48, 49).

Certain authors have demonstrated positive outcomes in iCC with LT in patients who responded to neoadjuvant therapy (25, 26). While dropout rates during the waiting period were notable, the tumor's post-therapy behavior emerged as a crucial parameter for selecting the most suitable candidates for the procedure. In this context, it would be inappropriate to categorically contraindicate LT for all patients with unresectable iCC without considering specific features of the disease, particularly the favorable response observed after neoadjuvant therapy.

The international experience of LT in cases of iCC remains limited to a few centers and is primarily documented in retrospective studies. Only two centers, UCLA and Houston Methodist-MD Anderson, have published prospective findings involving standardized neoadjuvant procedures in patients with preoperatively confirmed iCC (26). Given the current landscape, reaching definitive conclusions about which patients would benefit most from LT for iCC is challenging, but it is clear that the results are promising. Recognizing the significance of international collaboration, contributions to prospective clinical trials encompassing both early and advanced stages of iCC become crucial. Currently, three ongoing trials are actively seeking patients with iCC for LT, two in Canada and one in Norway. These trials recruit individuals with early-staged and unresectable iCC, underscoring the global effort to advance our understanding of LT as a treatment option for this challenging condition (39, 50, 51).

The ideal strategy for expanding LT for iCC would involve using deceased donors (52). Unfortunately, many countries' low donation rates, particularly Latin America, pose significant challenges. This limited supply of organs fails to meet the demands for traditional indications and hinders the allocation of grafts for new oncological indications like iCC (15, 16). The LDLT is a historical safety strategy for HCC treatment, and now it is being explored for other liver malignancies. Given the rarity of iCC, the selection criteria and the availability of living donors pose additional restrictive factors. Consequently, reports of LDLT for iCC are scarce. Our review identified just eight authors with a short series. Notably, our additional case represents the first report of an LDLT to treat iCC in Latin America. In this instance, we successfully treated a patient with an unresectable advanced tumor compromising the cava vein but with an excellent response to neoadjuvant treatment. In a disease stage where options for potential cure were limited, LDLT with cava resection emerged as the only viable option, and the procedure was highly successful, with no signs of recurrence observed after 24 months of follow-up. This case highlights the effectiveness of selecting candidates based on biological behavior, irrespective of the size and number of tumors.

Currently, there is still a shortage of pieces of evidence in the field of LDLT for iCC. While the favorable outcome of the case we presented is encouraging, it is not sufficient to recommend this therapeutic approach broadly, but rather in carefully selected cases. The challenges related to patient selection, the variability among studies, and the relatively short follow-up period are critical factors that could affect the general applicability of our findings. Despite these limitations, the insights gained from our study provide valuable contributions to the growing body of LDLT for iCC, highlighting its potential as a curative option in selected patients.

Final comments

There is growing evidence that certain iCC cases may benefit from LT. The key to the success of this approach is a meticulous selection process that identifies patients with the potential for curative treatment. Living donor liver transplantation emerges as a contemporary alternative to broaden the application of LT, particularly in regions facing organ shortages.

Author contributions

WA: Supervision, Writing – original draft, Writing – review & editing. GO: Data curation, Writing – original draft, Writing – review & editing. RM: Validation, Writing – original draft, Writing – review & editing. RP: Visualization, Writing – original draft, Writing – review & editing. VS: Methodology, Writing – original draft, Writing – review & editing. LL: Investigation, Writing – original draft, Writing – review & editing. RA: Project administration, Writing – original draft, Writing – review & editing. DW: Visualization, Writing – original draft, Writing – review & editing. AS: Formal analysis, Writing – original draft, Writing – review & editing. FT: Conceptualization, Writing – original draft, Writing – review & editing. LC: Supervision, Writing – original draft, Writing – review & editing.

Funding

The author(s) declare that no financial support was received for the research, authorship, and/or publication of this article.

Conflict of interest

The authors declare that the research was conducted in the absence of any commercial or financial relationships that could be construed as a potential conflict of interest.

Publisher's note

References

1. Panayotova G, Lunsford KE, Latt NL, Paterno F, Guarrera JV, Pyrsopoulos N. Expanding indications for liver transplantation in the era of liver transplant oncology. *World J Gastrointest Surg*. (2021) 13:392–405. doi: 10.4240/wjgs.v13.i5.392

2. Kubal C, Mihaylov P, Holden J. Oncologic indications of liver transplantation and deceased donor liver allocation in the United States. *Curr Opin Organ Transplantation*. (2021) 26:168–75. doi: 10.1097/MOT.0000000000000866

3. Altekruse SF, Petrick JL, Rolin AI, Cuccinelli JE, Zou Z, Tatalovich Z, et al. Geographic variation of intrahepatic cholangiocarcinoma, extrahepatic cholangiocarcinoma, and hepatocellular carcinoma in the United States. *PloS One*. (2015) 10:e0120574. doi: 10.1371/journal.pone.0120574

4. Brindley PJ, Bachini M, Ilyas SI, Khan SA, Loukas A, Sirica AE, et al. Cholangiocarcinoma. *Nat Rev Dis primers*. (2021) 7:65. doi: 10.1038/s41572-021-00300-2

5. Andraus W, Tustumi F, de Meira Junior JD, Pinheiro RSN, Waisberg DR, Lopes LD, et al. Molecular profile of intrahepatic cholangiocarcinoma. *Int J Mol Sci*. (2023) 25:461. doi: 10.3390/ijms25010461

6. Spolverato G, Vitale A, Cucchetti A, Popescu I, Marques HP, Aldrighetti L, et al. Can hepatic resection provide a long-term cure for patients with intrahepatic cholangiocarcinoma? *Cancer*. (2015) 121:3998–4006. doi: 10.1002/cncr.29619

7. Mazzaferro V, Gorgen A, Roayaie S, Droz Dit Busset M, Sapisochin G. Liver resection and transplantation for intrahepatic cholangiocarcinoma. *J Hepatol*. (2020) 72:364–77. doi: 10.1016/j.jhep.2019.11.020

8. O'Grady JG, Polson RJ, Rolles K, Calne RY, Williams R. Liver transplantation for Malignant disease. *Results 93 consecutive patients. Ann Surg*. (1988) 207:373–9. doi: 10.1097/00000658–198804000–00002

9. Sapisochin G, Facciuto M, Rubbia-Brandt L, Marti J, Mehta N, Yao FY, et al. Liver transplantation for "very early" intrahepatic cholangiocarcinoma: International retrospective study supporting a prospective assessment. *Hepatology*. (2016) 64:1178–88. doi: 10.1002/hep.28744

10. Sapisochin G, de Lope CR, Gastaca M, de Urbina JO, López-Andujar R, Palacios F, et al. Intrahepatic cholangiocarcinoma or mixed hepatocellular-cholangiocarcinoma in patients undergoing liver transplantation: a Spanish matched cohort multicenter study. *Ann Surg*. (2014) 259:944–52. doi: 10.1097/SLA.0000000000000494

11. Kodali S, Saharia A, Ghobrial RM. Liver transplantation and intrahepatic cholangiocarcinoma: time to go forward again? *Curr Opin Organ Transplant*. (2022) 27:320–8. doi: 10.1097/MOT.0000000000000983

12. Gómez MP, Irazábal MM Jr., Manyalich M. International registry in organ donation and transplantation (IRODAT)–2019 worldwide data. *Transplantation*. (2020) 104:S272. doi: 10.1097/01.tp.0000699864.69759.d7

13. Andraus W, Tustumi F, Santana AC, Pinheiro RSN, Waisberg DR, Lopes LD, et al. Liver transplantation as an alternative for the treatment of perihilar cholangiocarcinoma: a critical review. *Hepatobiliary Pancreat Dis Int*. (2024) 23 (2):139–45. doi: 10.1016/j.hbpd.2024.01.003

14. Salvalaggio PR, Seda Neto J, Alves JA, Fonseca EA, Carneiro de Albuquerque L, Andraus W, et al. Consensus, dilemmas, and challenges in living donor liver transplantation in Latin America. *Transplantation*. (2016) 100:1161–4. doi: 10.1097/TP.0000000000001180

15. Andraus W. Barriers and limitations to access to liver transplantation in Latin America. *Clin Liver Dis (Hoboken)*. (2019) 13:36–8. doi: 10.1002/cld.763

16. Goldstein RM, Stone M, Tillery GW, Senzer N, Levy M, Husberg BS, et al. Is liver transplantation indicated for cholangiocarcinoma? *Am J Surg*. (1993) 166:768–71; discussion 771–2. doi: 10.1016/s0002–9610(05)80696–8

17. Meyer CG, Penn I, James L. Liver transplantation for cholangiocarcinoma: results in 207 patients. *Transplantation*. (2000) 69:1633–7. doi: 10.1097/00007890–200004270–00019

18. Sapisochin G, Fidelman N, Roberts JP, Yao FY. Mixed hepatocellular cholangiocarcinoma and intrahepatic cholangiocarcinoma in patients undergoing transplantation for hepatocellular carcinoma. *Liver Transpl*. (2011) 17:934–42. doi: 10.1002/lt.22307

19. Sapisochin G, de Lope CR, Gastaca M, de Urbina JO, López-Andujar R, Palacios F, et al. Intrahepatic cholangiocarcinoma or mixed hepatocellular-cholangiocarcinoma in patients undergoing liver transplantation: a Spanish matched cohort multicenter study. *Ann Surg*. (2014) 259:944–52. doi: 10.1097/SLA.0000000000000494

20. Sapisochin G, Facciuto M, Rubbia-Brandt L. Liver transplantation for 'very early' intrahepatic cholangiocarcinoma: International retrospective study supporting a prospective assessment. *Hepatology*. (2016) 64:1178–1188. doi: 10.1002/hep.28744

21. Lamarca A, Ross P, Wasan HS, Hubner RA, McNamara MG, Lopes A, et al. Advanced intrahepatic cholangiocarcinoma: post hoc analysis of the ABC-01, -02, and -03 clinical trials. *J Natl Cancer Inst*. (2020) 112:200–10. doi: 10.1093/jnci/djz071

22. Banales JM, Marin JJG, Lamarca A, Rodrigues PM, Khan SA, Roberts LR, et al. Cholangiocarcinoma 2020: the next horizon in mechanisms and management. *Nat Rev Gastroenterol Hepatol*. (2020) 17:557–88. doi: 10.1038/s41575-020-0310-z

23. Ilyas SI, Affo S, Goyal L, Lamarca A, Sapisochin G, Yang JD, et al. Cholangiocarcinoma—novel biological insights and therapeutic strategies. *Nat Rev Clin Oncol*. (2023) 20:470–86. doi: 10.1038/s41571-023-00770-1

24. Mazzaferro V, Gorgen A, Roayaie S, Droz Dit Busset M, Sapisochin G. Liver resection and transplantation for intrahepatic cholangiocarcinoma. *J Hepatol*. (2020) 72:364–77. doi: 10.1016/j.jhep.2019.11.020

25. Hong JC, Jones CM, Duffy JP, Petrowsky H, Farmer DG, French S, et al. Comparative analysis of resection and liver transplantation for intrahepatic and hilar cholangiocarcinoma: a 24-year experience in a single center. *Arch Surg*. (2011) 146:683–9. doi: 10.1001/archsurg.2011.116

26. Lunsford KE, Javle M, Heyne K, Shroff RT, Abdel-Wahab R, Gupta N, et al. Liver transplantation for locally advanced intrahepatic cholangiocarcinoma treated with neoadjuvant therapy: a prospective case-series. *Lancet Gastroenterol Hepatol*. (2018) 3:337–48. doi: 10.1016/S2468–1253(18)30045–1

27. Andraus W. Liver transplantation in Brazil: the urgent need of A new allocation system for the exceptions in meld score. *Arq Gastroenterol*. (2020) 57:1–2. doi: 10.1590/S0004–2803.202000000–01

28. Goldaracena N, Barbas AS. Living donor liver transplantation. *Curr Opin Organ Transplant*. (2019) 24:131–7. doi: 10.1097/MOT.0000000000000610

29. Uchiyama H, Itoh S, Yoshizumi T, Ikegami T, Harimoto N, Soejima Y, et al. Living donor liver transplantation for hepatocellular carcinoma: results of prospective patient selection by Kyushu University Criteria in 7 years. *HPB (Oxford)*. (2017) 19:1082–90. doi: 10.1016/j.hpb.2017.08.004

30. Llovet JM, Pavel M, Rimola J, Diaz MA, Colmenero J, Saavedra-Perez D, et al. Pilot study of living donor liver transplantation for patients with hepatocellular carcinoma exceeding Milan Criteria (Barcelona Clinic Liver Cancer extended criteria). *Liver Transpl*. (2018) 24:369–79. doi: 10.1002/lt.24977

31. Sierra L, Barba R, Ferrigno B, Goyes D, Diaz W, Patwardhan VR, et al. Living-donor liver transplant and improved post-transplant survival in patients with primary sclerosing cholangitis. *J Clin Med*. (2023) 12:2807. doi: 10.3390/jcm12082807

32. Hafeez Bhatti AB, Tahir R, Qureshi NR, Mamoon N, Khan NY, Zia HH. Living donor liver transplantation for intra hepatic cholangiocarcinoma. *Ann Med Surg (Lond)*. (2020) 57:82–4. doi: 10.1016/j.amsu.2020.07.028

33. Takatsuki M, Uemoto S, Inomata Y, Egawa H, Kiuchi T, Hayashi M, et al. Living-donor liver transplantation for Caroli's disease with intrahepatic adenocarcinoma. *J Hepatobiliary Pancreat Surg*. (2001) 8:284–6. doi: 10.1007/s005340170030

34. Jonas S, Mittler J, Pascher A, Theruvath T, Thelen A, Klupp J, et al. Extended indications in living-donor liver transplantation: bile duct cancer. *Transplantation*. (2005) 80:S101–4. doi: 10.1097/01.tp.0000187106.29908.2b

35. Sotiropoulos GC, Kaiser GM, Lang H, Molmenti EP, Beckebaum S, Fouzas I, et al. Liver transplantation as a primary indication for intrahepatic cholangiocarcinoma: a single-center experience. *Transplant Proc*. (2008) 40:3194–5. doi: 10.1016/j.transproceed.2008.08.053

36. De Martin E, Rayar M, Golse N, Dupeux M, Gelli M, Gnemmi V, et al. Analysis of liver resection versus liver transplantation on outcome of small intrahepatic cholangiocarcinoma and combined hepatocellular-cholangiocarcinoma in the setting of cirrhosis. *Liver Transpl*. (2020) 26:785–98. doi: 10.1002/lt.25737

37. Rauchfuß F, Ali-Deeb A, Rohland O, Dondorf F, Ardelt M, Settmacher U. Living donor liver transplantation for intrahepatic cholangiocarcinoma. *Curr Oncol*. (2022) 29:1932–8. doi: 10.3390/curroncol29030157

38. Bednarsch J, Lang SA, Heise D, Strnad P, Neumann UP, Ulmer TF. Laparoscopic Living donor liver transplantation in irresectable intrahepatic cholangiocarcinoma in primary sclerosing cholangitis associated liver cirrhosis. *Z Gastroenterol*. (2024) 62:50–5. doi: 10.1055/a-2221–6126

39. Sapisochin G. Liver transplant for stable, advanced intrahepatic cholangiocarcinoma. *ClinicalTrials.gov [Internet]*. Bethesda (MD): National Library of Medicine (US). Available at: https://clinicaltrials.gov/study/NCT04195503. [cited 2024 May 08].

40. Mazzaferro V, Regalia E, Doci R, Andreola S, Pulvirenti A, Bozzetti F, et al. Liver transplantation for the treatment of small hepatocellular carcinomas in patients with cirrhosis. *N Engl J Med*. (1996) 334:693–9. doi: 10.1056/NEJM199603143341104

41. Sapisochin G, Bruix J. Liver transplantation for hepatocellular carcinoma: outcomes and novel surgical approaches. *Nat Rev Gastroenterol Hepatol*. (2017) 14:203–17. doi: 10.1038/nrgastro.2016.193

42. Tabrizian P, Holzner ML, Mehta N, Halazun K, Agopian VG, Yao F, et al. Ten-year outcomes of liver transplant and downstaging for hepatocellular carcinoma. *JAMA Surg*. (2022) 157:779–88. doi: 10.1001/jamasurg.2022.2800

43. Mehta N, Bhangui P, Yao FY, Mazzaferro V, Toso C, Akamatsu N, et al. Liver transplantation for hepatocellular carcinoma. Working group report from the ILTS transplant oncology consensus conference. *Transplantation*. (2020) 104:1136–42. doi: 10.1097/TP.0000000000003174

44. Alvaro D, Gores GJ, Walicki J, Hassan C, Sapisochin G, Komuta M, et al. EASL-ILCA Clinical Practice Guidelines on the management of intrahepatic cholangiocarcinoma. *J hepatology*. (2023) 79:181–208. doi: 10.1016/j.jhep.2023.03.010

45. Gonzalez RS, Raza A, Propst R, Adeyi O, Bateman J, Sopha SC, et al. Recent advances in digestive tract tumors: updates from the 5th edition of the world health organization "Blue book". *Arch Pathol Lab Med*. (2021) 145:607–26. doi: 10.5858/arpa.2020-0047-RA

46. Ruff SM, Dillhoff M. Review of IDH mutations and potential therapies for intrahepatic cholangiocarcinoma. *Hepatoma Res*. (2023) 9:37. doi: 10.20517/2394–5079.2023.51

47. Kendall T, Verheij J, Gaudio E, Evert M, Guido M, Goeppert B, et al. Anatomical, histomorphological and molecular classification of cholangiocarcinoma. *Liver Int*. (2019) 39 Suppl 1:7–18. doi: 10.1111/liv.14093

48. Mauro E, Ferrer-Fàbrega J, Sauri T, Soler A, Cobo A, Burrel M, et al. New challenges in the management of cholangiocarcinoma: the role of liver transplantation, locoregional therapies, and systemic therapy. *Cancers*. (2023) 15:1244. doi: 10.3390/cancers15041244

49. Calderon Novoa F, Ardiles V, Pekolj J, Mattera J, de Santibañes M. Liver transplantation for intrahepatic cholangiocarcinoma: a narrative review of the latest advances. *HepatomaRes*. (2023) 9:33. doi: 10.20517/2394–5079.2023.36

50. Sapisochin G, Bruix J. Liver transplantation for early intrahepatic cholangiocarcinoma (LT for iCCA). *ClinicalTrials.gov [Internet]*. Bethesda (MD): National Library of Medicine (US). Available at: https://clinicaltrials.gov/study/NCT02878473. [cited 2024 May 08].

51. Smedman M, Yaqub S. Liver transplantation for non-resectable intrahepatic cholangiocarcinoma: a prospective exploratory trial (TESLA Trial). *ClinicalTrials.gov [Internet]*. Bethesda (MD): National Library of Medicine (US). Available at: https://clinicaltrials.gov/study/NCT04556214. [cited 2024 May 08].

52. Sotiropoulos GC, Kaiser GM, Lang H, Molmenti EP, Beckebaum S, Fouzas I, et al. Liver transplantation as a primary indication for intrahepatic cholangiocarcinoma: a single-center experience. *Transplant Proc*. (2008) 40:3194–5. doi: 10.1016/j.transproceed.2008.08.053

frontiers | Frontiers in Oncology

TYPE Original Research
PUBLISHED 24 May 2024
DOI 10.3389/fonc.2024.1395740

OPEN ACCESS

EDITED BY
Francisco Tustumi,
University of São Paulo, Brazil

REVIEWED BY
Wei Wang,
First Affiliated Hospital of Wannan Medical College, China
Chong Wen,
Southwest Jiaotong University, China
Wenying Qiao,
Capital Medical University, China
Hongwei Cheng,
University of Macau, China

*CORRESPONDENCE
Yixin Lin
linyixin_phd@126.com
Geng Liu
liu2geng6@163.com
Bei Li
libei@scu.edu.cn

RECEIVED 04 March 2024
ACCEPTED 06 May 2024
PUBLISHED 24 May 2024

CITATION
Tian Y, Wang Y, Wen N, Lin Y, Liu G and Li B (2024) Development and validation of nomogram to predict overall survival and disease-free survival after surgical resection in elderly patients with hepatocellular carcinoma. *Front. Oncol.* 14:1395740. doi: 10.3389/fonc.2024.1395740

Development and validation of nomogram to predict overall survival and disease-free survival after surgical resection in elderly patients with hepatocellular carcinoma

Yuan Tian[1,2], Yaoqun Wang[1,2], Ningyuan Wen[1,2], Yixin Lin[1,2*], Geng Liu[1,2*] and Bei Li[1,2*]

[1]Division of Biliary Surgery, Department of General Surgery, West China Hospital, Sichuan University, Chengdu, China, [2]Research Center for Biliary Diseases, West China Hospital, Sichuan University, Chengdu, China

Background: Hepatocellular carcinoma (HCC) is one of the common causes of tumor death in elderly patients. However, there is a lack of individualized prognostic predictors for elderly patients with HCC after surgery.

Method: We retrospectively analyzed HCC patients over 65 years old who underwent hepatectomy from 2015 to 2018, and randomly divided them into training cohort and validation cohort in a ratio of 3:1. Univariate Cox regression was used to screen the risk factors related to prognosis. Prognostic variables were further selected by least absolute shrinkage and selection operator regression model (LASSO) and multivariate Cox regression to identify the predictors of overall survival (OS) and disease-free survival (DFS). These indicators were then used to construct a predictive nomogram. The receiver operating characteristic curve (ROC curve), calibration curve, consistency index (C-index) and decision analysis curve (DCA) were used to test the predictive value of these independent prognostic indicators.

Result: A total of 188 elderly HCC patients who underwent hepatectomy were enrolled in this study. The independent prognostic indicators of OS included albumin (ALB), cancer embolus, blood loss, viral hepatitis B, total bilirubin (TB), microvascular invasion, overweight, and major resection. The independent prognostic indicators of DFS included major resection, ALB, microvascular invasion, laparoscopic surgery, blood loss, TB, and pleural effusion. In the training cohort, the ROC curve showed that the predictive values of these indicators for OS and DFS were 0.827 and 0.739, respectively, while in the validation cohort, they were 0.798 and 0.694. The calibration curve nomogram exhibited good prediction for 1-year, 2-year, and 3-year OS and DFS. Moreover, the nomogram models exhibited superior performance compared to the T-staging suggested by C-index and DCA.

Conclusion: The nomogram established in this study demonstrate commendable predictive efficacy for OS and DFS in elderly patients with HCC after hepatectomy. Core Tip: The purpose of this retrospective study is to screen the risk factors of survival and recurrence in elderly patients with HCC after hepatectomy. The nomogram included cancer embolus, viral hepatitis B, overweight, major resection, ALB, microvascular invasion, laparoscopic surgery, blood loss, TB, and pleural effusion as predictors. The calibration curve of this nomogram was good, indicating credible predictive value and clinical feasibility.

KEYWORDS

prognosis, recurrence, nomogram, hepatocellular carcinoma, elderly

1 Introduction

Primary hepatic cancer is a common malignant tumor of the digestive system, more than 90% of which is hepatocellular carcinoma (HCC). It is the sixth-highest incidence of malignant tumors in the world, accounting for 8.3% of cancer-related deaths worldwide, and is the third most frequent cause of cancer-related death (1). As one of the most populous countries with the largest number of hepatitis B patients in the world, the new cases of HCC in China account for 45% of the new cases in the world every year, and this proportion is also unceasingly growing (2). Therefore, HCC is still a major global health problem to be solved.

In recent years, the aging of the population has become a global problem, which has caused people's concern that it will increase the morbidity of cancer. Clinical research has already confirmed that aging is an established risk factor for HCC (3). Research related to aging shows that cell and tissue aging caused by DNA damage, epigenetic changes, oxidative stress, and mitochondrial dysfunction will also increase the risk of malignant tumors (4). According to statistics, about 80% of HCC cases are elderly patients (5). Given the increase in life expectancy and the aging of the population around the world, it is expected that the number of elderly HCC patients may continue to rise.

At present, hepatectomy, liver transplantation, or radiofrequency ablation has become a recognized surgical treatment for HCC. As far as hepatectomy is concerned, the methods of surgery have developed from wedge-shaped resection or conventional hepatectomy to minimally invasive and precise hepatectomy (6). The concept of Enhanced Recovery After Surgery (ERAS) put forward in recent years emphasizes the integration of preoperative individualized disease assessment, surgical plan formulation, and perioperative rehabilitation treatment to minimize surgical trauma, protect remaining liver function, and strive for the best rehabilitation effect (7).

Although liver resection, the most commonly used surgical modality, has shown good results in elderly patients (8, 9), it is still a complex procedure (10). At the same time, due to the decline of physical function and underlying health conditions, elderly patients have a higher probability of severe postoperative complications, which leads to poor prognosis (11). Therefore, for such elderly patients, there may be large differences in prognosis due to individual conditions. However, there is no individualized prognostic prediction model for elderly HCC patients after liver resection.

This study aims to retrospectively analyze the relationship between perioperative indicators and tumor prognosis in elderly patients. Consequently, the objective is to propose an individualized prognosis prediction scheme for elderly HCC patients after surgery.

2 Materials and methods

2.1 Patient characteristics

We collected clinical and follow-up data of elderly patients > 65 years of age who underwent radical hepatectomy for HCC at West China Hospital of Sichuan University (Chengdu, Sichuan Province, China) from January 2015 to September 2018. The preoperative diagnosis of HCC was performed according to the criteria of the American Association for the Study of Liver Diseases (AASLD) (12). The absolute contraindications for liver resection are American Society of Anesthesiologists (ASA) grade >= III, ascites, extrahepatic metastasis, unresectable large vessel tumor invasion, or future residual liver <40%-50% (13). The inclusion criteria were as follows:(1) Patients aged >= 65 years (male or female); (2) Primary hepatocellular carcinoma was confirmed by postoperative pathological examination; (3) The years of diagnosis were 2015–2018; (4) Without the absolute contraindications for liver resection;

Abbreviations: AFP, Alpha Fetoprotein; ALB, Albumin; ALT, Alanine Aminotransferase; ASA, American Society of Anesthesiologists; AST, Aspartate Aminotransferase; AUC, Area Under the Curve; BMI, Body mass index; COPD, Chronic Obstructive Pulmonary Disease; DFS, Disease-Free Survival; DCA, decision curve analysis; HBV, Hepatitis B Virus; HCC, Hepatocellular carcinoma; HCV, Hepatitis C Virus; ICGR15, Indocyanine green retention rate at 15 minutes; LASSO, Least Absolute Shrinkage and Selection Operator regression model; OS, Overall Survival; PLT, Platelet; ROC, Receiver Operating Characteristic Curve; TB, Total Bilirubin; WBC, White Blood Count.

(5) no preoperative anticancer treatments. The exclusion criteria were as follows: (1) Patients aged < 65 years; (2) Intrahepatic cholangiocarcinoma or mixed-type HCC was confirmed by postoperative pathological examination; (3) Patients have absolute contraindications for liver resection; (4) Severe dysfunction of vital organs; (5) History of any other malignancy.

2.2 Data collection

For the included patients, we collected the basic information of the patients at the time of admission in the medical records, including age, sex, overweight (BMI>24), viral hepatitis B, liver cirrhosis, abdominal surgery history, hypertension, diabetes, chronic obstructive pulmonary disease (COPD), tumor size (cm), tumor numbers (single or multiply), tumor location (VII/VIII/IVa or not), alpha-fetoprotein (AFP, ng/L), indocyanine green retention rate at 15 minutes (ICGR15, %), TB (mmol/L), ALB (g/L), aspartate aminotransferase (AST, IU/L), alanine aminotransferase (ALT, IU/L), platelet (PLT, IU/L), white blood count (WBC, 10^9/L).

In addition, we also collected the data of patients undergoing surgical treatment, postoperative pathological data, and postoperative complications in the medical records. The information includes ASA(I~IV), surgical type(laparoscopic or open), major resection, blood loss(ml), intraoperative transfusion, total pringle time(min), margin distance(mm), cancer embolus, microvascular invasion, capsular invasion, microsatellite nodules, poor differentiation, necrosis (0~4), fibrosis (0~4), overall complications, major complications, liver-specific complications, liver failure, hemorrhage, ascites, biliary leakage, general complications, respiratory complications, respiratory infection, wound infection, pleural effusion, atelectasis respiratory insufficiency, Clavien-Dindo Grade(I~IV) and hospital stay.

All patients were followed up every 1 month for the first 3 months after discharge and every 3 months thereafter. The median follow-up time was 34.5 months. The primary endpoints of the study were overall survival (OS) and disease-free survival (DFS), and the secondary endpoint was complication rate. DFS was defined from the end of surgery to death or recurrence; OS was defined from the end of surgery to death.

2.3 Statistical analysis

All patients were randomly assigned into training cohort and validation cohort in a ratio of 3:1. For descriptive statistics of patient clinical characteristics data, the statistical description median [interquartile range (IQR)] was used for continuous variables, and frequency (%) was used for categorical variables. Univariate Cox regression was used to screen the risk factors related to prognosis. Prognostic variables were further selected by least absolute shrinkage and selection operator regression model (LASSO) and multivariate Cox regression to identify the predictors of overall survival (OS) and disease-free survival (DFS). Proportional hazards assumption was used to assessed the Cox regression models. These indicators were then used to construct a predictive nomogram.

A series of validation methods were used to validate the accuracy and discrimination of the nomogram, including AUC, calibration curve and consistency index (C-index). In order to explore clinical application value of the model, decision analysis curve (DCA) was used to calculate net benefit under different thresholds. At the same time, we divided all patients into low-risk and high-risk groups based on each patient's nomogram score. Log-rank test and Kaplan-Meier (K-M) curve were used to compare survival differences among patients in different groups.

All data analyses were performed using R 4.1.1. and SPSS 25.0. All tests were two-sided, and a $P<0.05$ was considered statistically significant.

3 Result

3.1 Baseline characteristics

A total of 188 elderly HCC patients who underwent hepatectomy were included in this study, as shown in Figure 1. Of these patients, males accounted for 77.66% and the median age was 69 (66,72) years. Among them, 40.43% of the patients were overweight (BMI>24). 39.36% and 41.49% of the patients had a history of hepatitis B and liver cirrhosis respectively. 29.26% of the patients had abdominal surgery history. In terms of common chronic diseases in the elderly, hypertension accounted for 34.57%, diabetes accounted for 17.55%, and COPD accounted for only 3.19% (Table 1).

The median tumor size of patients was 5.65cm (4.00,7.00). The tumors of 72.87% of the patients were single lesions, and the tumors of 51.06% of the patients were located in the posterosuperior

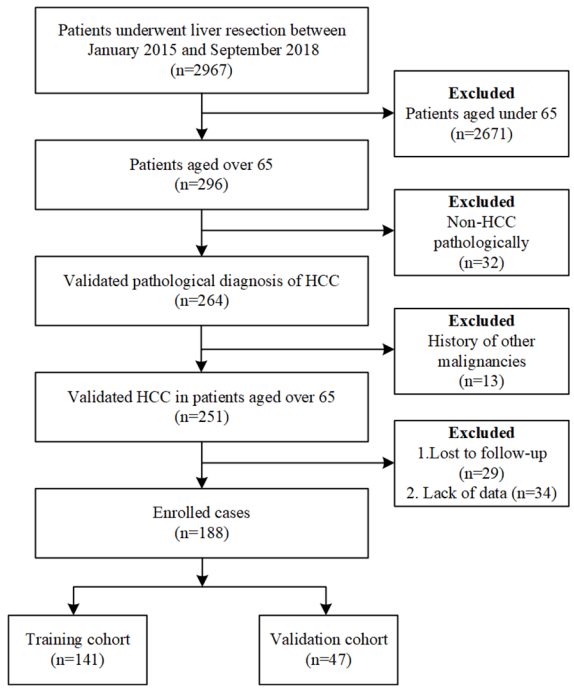

FIGURE 1
Flow chart of included and excluded patients in the study.

TABLE 1 Characteristics of 188 elderly patients with hepatocellular carcinoma.

Variables	All (N=188)	Training cohort (N=141)	Validation cohort (N=47)	P
Age (years)	69 (66,72)	69 (66, 72)	70 (67, 74)	0.689
Sex (Male%)	146 (77.66%)	108 (76.60%)	38 (80.85%)	0.544
Overweight (BMI>24)	76 (40.43%)	58 (41.13%)	18 (38.30%)	0.731
Viral hepatitis B	74 (39.36%)	53 (37.59%)	21 (44.68%)	0.389
Liver cirrhosis	78 (41.49%)	55 (39.00%)	23 (48.94%)	0.232
Abdominal surgery history	55 (29.26%)	44 (31.21%)	11 (23.40%)	0.309
Hypertension	65 (34.57%)	46 (32.62%)	19 (40.43%)	0.330
Diabetes	33 (17.55%)	22 (15.60%)	11 (23.40%)	0.223
COPD	6 (3.19%)	4 (2.83%)	2 (4.26%)	0.632
Tumor size (cm)	5.65 (4.00, 7.00)	5.50 (4.00, 7.50)	6.00 (4.00, 7.00)	0.915
Tumor numbers (single)	137 (72.87%)	105 (74.47%)	32 (68.09%)	0.394
Tumor location (VII/VIII/IVa)	96 (51.06%)	71 (50.35%)	25 (53.19%)	0.736
AFP (ng/L)	8.23 (3.77, 132.10)	8.03 (3.59, 133.35)	8.28 (4.41, 132.1)	0.736
ICGR15 (%)	6.90 (4.03, 10.50)	6.90 (3.58, 10.50)	7.40 (4.40, 10.50)	0.804
TB (mmol/L)	14.25 (10.53, 18.45)	14.40 (10.65, 18.10)	13.50 (9.60, 19.80)	0.517
ALB (g/L)	41.50 (37.75, 44.45)	41.30 (37.65, 44.30)	42.40 (37.90, 44.50)	0.631
AST (IU/L)	35.00 (25.00, 52.00)	36.00 (26.00, 53.00)	32.00 (24.00, 51.00)	0.278
ALT (IU/L)	31.50 (19.00, 48.75)	33.00 (19.00, 52.00)	31.00 (19.00, 47.00)	0.743
PLT (IU/L)	126.00(86.25,172.00)	122.00 (84.50, 169.50)	144.00 (98.00, 175.00)	0.141
WBC (10^9/L)	5.60 (4.17, 7.09)	5.45 (4.09, 6.96)	5.98 (4.33, 7.50)	0.328

segments (VII/VIII/IVa) (Table 1). Part of the blood routine, blood biochemical, and serum tumor marker data of the patients are shown in Table 1. All data were collected at the time of admission. Table 2 shows the surgical, pathological, and postoperative information of 188 patients.

In the training cohort, 46 patients died, while in the validation cohort, 15 patients died. The 1-year and 3-year OS of the training cohort was 83.7% and 72.3% of that of the validation cohort, respectively, and the OS of the validation cohort was 85.1% and 74.5%, respectively.

3.2 Univariate Cox regression analysis of OS and DFS

In order to initially determine the factors related to the OS and DFS of the elderly patients, univariate Cox regression analysis was performed. The results showed that ALB, viral hepatitis B, TB, PLT, cancer embolus, capsular invasion, major resection, microvascular invasion, blood loss, and overweight (BMI>24) were significantly related to the OS of the patients (Table 3). ALB, major resection,

TABLE 2 Surgical, pathological and postoperative information of 188 patients.

Variables	All (N=188)	Training cohort (N=141)	Validation cohort (N=47)	P
ASA				0.770
I	13 (6.91%)	10 (7.09%)	3 (6.38%)	
II	139 (73.94%)	103 (73.05%)	36 (76.60%)	
III	35 (18.62%)	27 (19.15%)	8 (17.02%)	
IV	1 (0.53%)	1 (0.71%)	0 (0.00%)	
Surgical type (Laparoscopic: open)	91:97	70:71	21:26	0.555

(Continued)

TABLE 2 Continued

Variables	All (N=188)	Training cohort (N=141)	Validation cohort (N=47)	P
Major resection	13 (6.91%)	9 (6.38%)	4 (8.51%)	0.868
Blood loss (ml)	300 (150, 400)	300 (150, 400)	300 (200, 400)	0.737
Intraoperative transfusion	21 (11.17%)	14 (9.92%)	7 (14.89%)	0.349
Total pringle time (min)	30 (13, 45)	32 (15, 45)	22 (0, 45)	0.431
Margin distance (mm)	10 (2, 10)	10 (2, 10)	10 (2, 10)	0.538
Cancer embolus	6 (3.19%)	3 (2.13%)	3 (6.38%)	0.338
Microvascular invasion	63 (33.51%)	46 (32.62%)	17 (36.17%)	0.656
Capsular invasion	116 (61.70%)	90 (63.83%)	26 (61.70%)	0.299
Microsatellite nodules	37 (19.68%)	25 (17.73%)	12 (25.53%)	0.244
Poor differentiation	110 (58.51%)	85 (60.28%)	25 (53.19%)	0.393
Necrosis				0.277
0	0 (0.00%)	0 (0.00%)	0 (0.00%)	
1	33 (17.55%)	21 (14.89%)	12 (25.53%)	
2	94 (50.00%)	73 (51.77%)	21 (44.68%)	
3	54 (28.72%)	42 (29.79%)	12 (25.53%)	
4	7 (3.72%)	5 (3.55%)	2 (4.26%)	
Fibrosis				0.102
0	0 (0.00%)	0 (0%)	0 (0.00%)	
1	20 (10.64%)	9 (6.38%)	11 (23.40%)	
2	43 (22.87%)	34 (24.11%)	9 (19.15%)	
3	54 (28.72%)	43 (30.50%)	11 (23.40%)	
4	71 (37.77%)	55 (39.01%)	16 (34.04%)	
Overall complications	149 (79.26%)	111 (78.72%)	38 (80.85%)	0.755
Major complications	5 (2.66%)	3 (2.13%)	2 (4.26%)	0.749
Liver-specific complications	127 (67.55%)	94 (66.67%)	33 (70.21%)	0.653
Liver failure	3 (1.60%)	2 (1.42%)	1 (2.13%)	0.737
Hemorrhage	3 (1.60%)	3 (2.13%)	0 (0.00%)	0.737
Ascites	123 (65.43%)	91 (64.53%)	32 (68.09%)	0.658
Biliary leakage	2 (1.06%)	1 (0.71%)	1 (2.13%)	0.439
General complications	15 (7.98%)	12 (8.51%)	3 (6.38%)	0.877
Respiratory complications	19 (10.11%)	14 (9.92%)	5 (10.64%)	1.000
Respiratory infection	5 (2.66%)	3 (2.13%)	2 (4.26%)	0.794
Wound infection	3 (1.60%)	3 (2.13%)	0 (0.00%)	0.574
Pleural effusion	12 (6.38%)	8 (5.67%)	4 (8.51%)	1.000
Atelectasis	3 (1.60%)	3 (2.13%)	0 (0.00%)	0.574
Respiratory insufficiency	1 (0.53%)	1 (0.71%)	0 (0.00%)	1.000
Clavien-Dindo Grade				0.697
I	123 (65.43%)	92 (65.25%)	31 (65.96%)	

(Continued)

TABLE 2 Continued

Variables	All (N=188)	Training cohort (N=141)	Validation cohort (N=47)	P
II	21 (11.17%)	16 (11.35%)	5 (10.64%)	
IIIA	0 (0.00%)	0 (0.00%)	0 (0.00%)	
IIIB	2 (1.06%)	1 (0.71%)	1 (2.13%)	
IV	3 (1.60%)	2 (1.42%)	1 (2.13%)	
Hospital stay (days)	7 (5, 8)	7 (5, 8.5)	7 (6, 8)	0.743

TABLE 3 Univariate Cox regression analysis of OS and DFS in 141 elderly patients with hepatocellular carcinoma after operation.

Variables	HR (95% CI)	P value
OS		
ALB (g/L)	0.01(0.002~0.04)	<0.001
Viral hepatitis B	3.19(1.76~5.79)	<0.001
TB (mmol/L)	2.34(1.49~3.69)	<0.001
PLT (IU/L)	0.47(0.30~0.74)	0.001
Cancer embolus	5.19(1.59~16.97)	0.006
Capsular invasion	2.47(1.22~4.99)	0.011
Major resection	2.98(1.16~7.61)	0.023
Microvascular invasion	1.97(1.09~3.56)	0.026
Blood loss (ml)	1.30(1.02~1.66)	0.035
Overweight (BMI>24)	1.87(1.04~3.38)	0.037
Total pringle time (min)	0.90(0.80~1.01)	0.083
Hospital stay (days)	1.51(0.92~2.48)	0.099
Pleural effusion	2.16(0.76~6.14)	0.149
Hypertension	1.53(0.84~2.78)	0.162
DFS		
ALB (g/L)	0.05(0.01~0.22)	<0.001
Major resection	3.73(1.66~8.37)	0.001
Capsular invasion	2.16(1.24~3.75)	0.006
TB (mmol/L)	1.63(1.11~2.38)	0.012
Pleural effusion	2.08(1.18~6.65)	0.019
Microvascular invasion	1.65(1.01~2.72)	0.046
PLT (IU/L)	0.69(0.47~1.00)	0.050
Cancer embolus	2.84(0.88~9.09)	0.079
Viral hepatitis B	1.53(0.94~2.51)	0.090
Blood loss (ml)	1.18(0.97~1.44)	0.095
ASA	0.46(0.19~1.16)	0.100
Hospital stay (days)	1.39(0.93~2.08)	0.113
Laparoscopic surgery	0.70(0.43~1.13)	0.146
Respiratory complications	1.73(0.82~3.63)	0.148

capsular invasion, TB, pleural effusion, microvascular invasion, and PLT were significantly related to the DFS of the patients (Table 3).

3.3 LASSO regression analysis of OS and DFS

The LASSO regression analysis was used to reduce high-dimensional data (14). The features with a P value <0.2 in the univariate Cox regression analysis of OS and DFS were included in the LASSO. The cross-validation was used to determine the most appropriate λ value as optimal parameters (Figure 2). The results for OS yield a λ value of 12, and the results for DFS yield a λ value of 13. Indicating that 12 features associated with OS and 13 features associated with DFS included in LASSO were important.

3.4 Multivariate Cox regression analysis of OS and DFS

Significant variables output by LASSO regression analysis were included in multivariate Cox regression analysis. The results of multivariate Cox regression analysis showed that ALB, cancer embolus, blood loss, viral hepatitis B, TB, microvascular invasion, overweight (BMI>24), and major resection were independent risk factors for OS in elderly patients (Table 4). Major resection, ALB, microvascular invasion, laparoscopic surgery, blood loss, TB, and pleural effusion were independent risk factors for DFS in elderly patients (Table 4). The proportional hazards assumption was evaluated and found reasonable for each variable (Table S1).

3.5 Establishment of the nomogram and accuracy evaluation

The following factors were used to construct the nomogram (Figures 3, 4). 1-, 2-, and 3-year OS and DFS in elderly patients were predicted by the nomogram. We used ROC curves to verify the predictive value of these independent prognostic factors. As shown in Figures 3 and 4, the area under the curve (AUC value) of the eight independent prognostic factors for the prediction of OS was 0.827. The AUC value of 6 independent prognostic factors for the prediction of DFS was 0.739. In the validation cohort, the AUC values were 0.798 and 0.694, respectively. This suggests that these

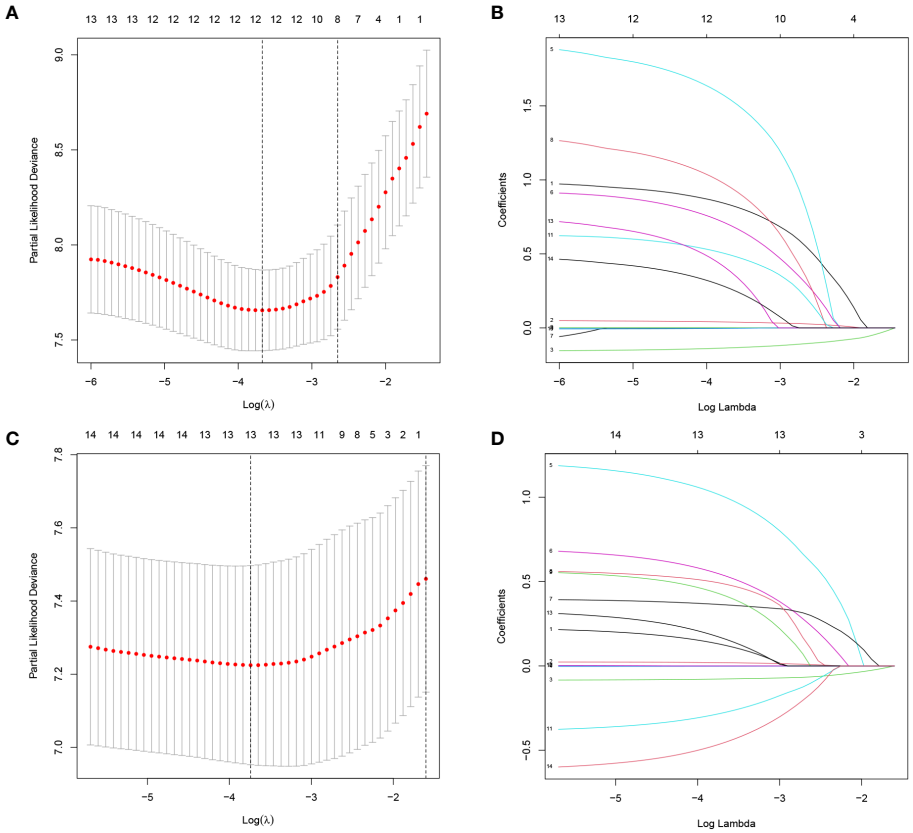

FIGURE 2
Screening of variables based on Lasso regression. **(A)** OS, **(C)** DFS: The selection process of the optimum value of the parameter λ in the Lasso regression model by cross-validation method. **(B)** OS, **(D)** DFS: The variation characteristics of the coefficient of variables.

TABLE 4 Multivariate Cox regression analysis of OS and DFS in elderly patients with hepatocellular carcinoma after operation.

Variables	HR (95% CI)	P value
OS		
ALB (g/L)	0.85(0.79~0.91)	<0.001
Cancer embolus	9.03(2.45~33.27)	<0.001
Blood loss (ml)	1.01(1.00~1.02)	<0.001
Viral hepatitis B	2.86(1.52~5.40)	0.001
TB (mmol/L)	1.05(1.01~1.09)	0.007
Microvascular invasion	2.49(1.25~4.96)	0.009
Overweight (BMI>24)	2.27(1.17~4.41)	0.016
Major resection	3.36(1.17~9.67)	0.024
DFS		
Major resection	4.56(1.92~10.81)	<0.001
ALB (g/L)	0.91(0.86~0.96)	0.001
Microvascular invasion	2.02(1.17~3.47)	0.012
Laparoscopic surgery	0.54(0.32~0.89)	0.016
Blood loss (ml)	1.01(1.00~1.02)	0.020
TB (mmol/L)	1.03(1.00~1.06)	0.039
Pleural effusion	2.68(1.02~7.04)	0.046

factors have good predictive value for OS and DFS. Subsequently, calibration curves were depicted, and the results showed that the predicted values of the prediction models were generally consistent with the actual observed values (Figures 3, 4).

3.6 Clinical application of the nomogram

The predictive value of the constructed nomogram was compared with the 8th edition American Joint Committee on Cancer (AJCC) T-staging system in terms of clinical practicability. The results are shown in Figure 5. In the training cohort, the C-index of the nomogram for OS and DFS was 0.825 and 0.699, respectively, which was significantly higher than that of the T-staging (OS: 0.590; DFS: 0.537). Similarly, in the validation cohort, the C-index of the nomogram for OS (0.914) and DFS (0.761) was also significantly higher than that of the T-staging (OS: 0.613; DFS: 0.621). Additionally, DCA suggested that the nomogram had better predictive power than the T-staging (Figure 6). Overall, the nomogram models exhibited superior performance compared to the T-staging.

All patients were assigned to the high-risk group or the low-risk group based on their nomogram scores. In both the training and validation cohorts, patients in the low-risk group exhibited significantly higher survival rates and lower recurrence rates than those in the high-risk group (Figure 7).

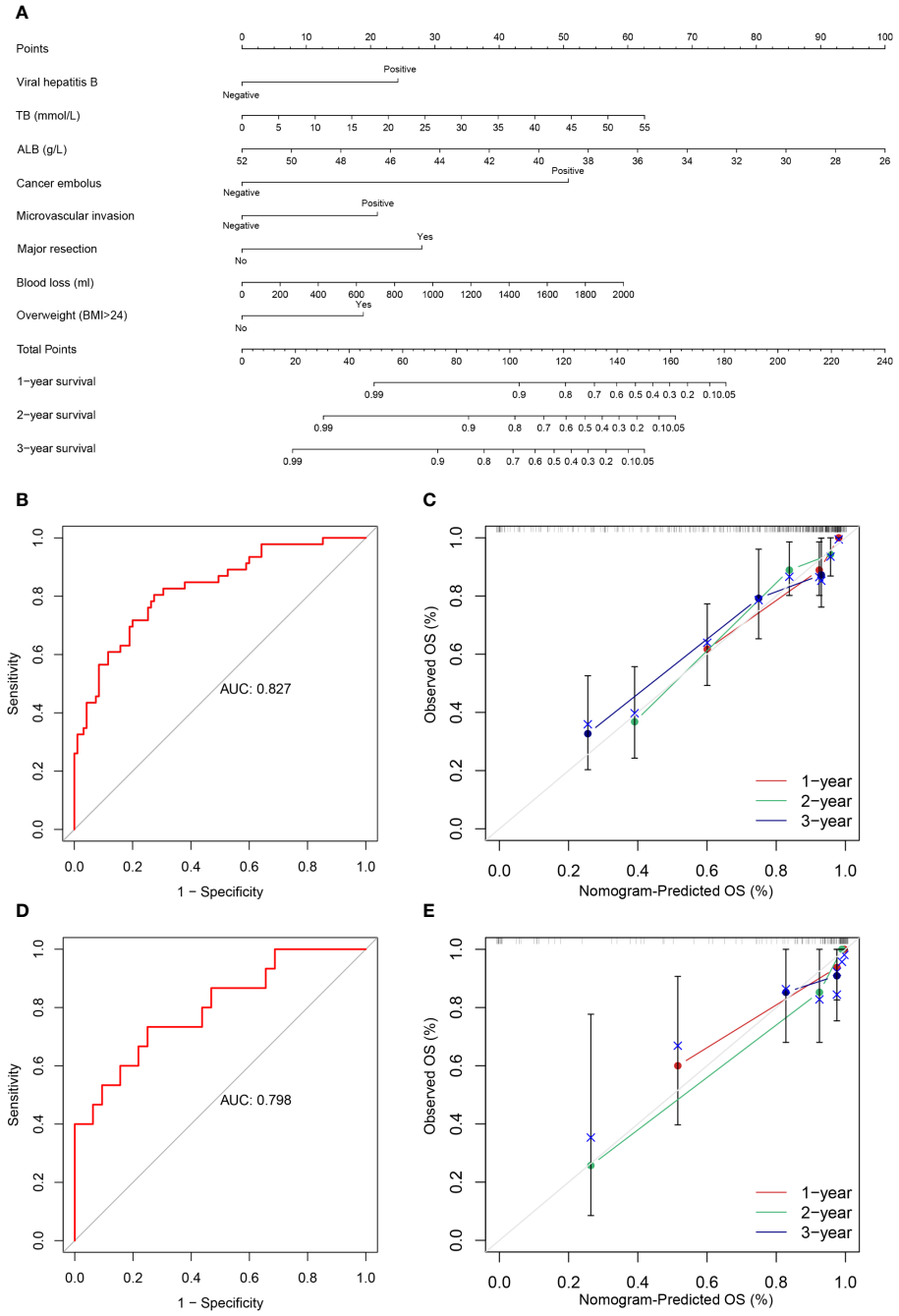

FIGURE 3
(A) Nomogram prediction model and prediction OS curve; **(B)** AUC for predicting OS in training cohort; **(C)** Calibration curves of 1-, 2-, and 3-year OS in training cohort; **(D)** AUC for predicting OS in validation cohort; **(E)** Calibration curves of 1-, 2-, and 3-year OS in the validation cohort.

4 Discussion

4.1 The significance of nomogram

At present, the prognosis prediction model of malignant tumor patients has been widely used. In recent years, the nomogram related to HCC has been gradually developed, which has played a very active role in the diagnosis, treatment, and prognosis prediction of HCC. For example, Li et al. constructed a nomogram to predict the risk of liver nodule malignant transformation into HCC, which is helpful for the early diagnosis of HCC (15). Lin et al. established a simplified model to help guide decisions about prophylactic transarterial chemoembolization after hepatectomy for patients with HCC (16). Wang et al. developed a nomogram to predict recurrence in patients with early-stage HCC (17). However, the prognosis of HCC patients is closely related to age. In addition, the incidence of HCC is highest in the elderly population, whose postoperative prognostic factors are different from other age groups. For example, the underlying health conditions of elderly patients and the higher incidence of postoperative complications will affect the prognosis of patients.

10.3389/fonc.2024.1395740

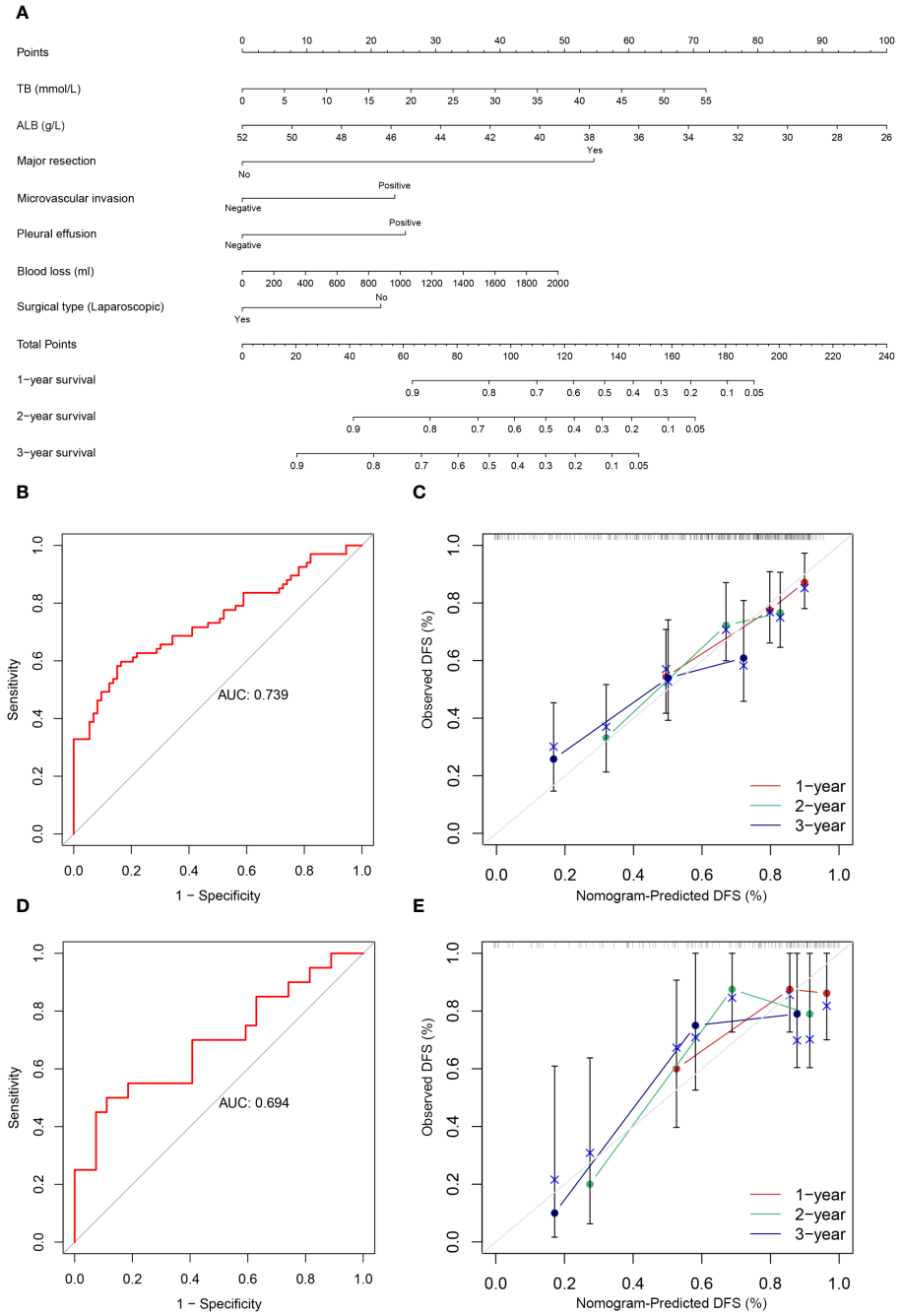

FIGURE 4
(A) Nomogram prediction model and prediction DFS curve; **(B)** AUC for predicting DFS in training cohort; **(C)** Calibration curves of 1-, 2-, and 3-year DFS in training cohort; **(D)** AUC for predicting DFS in validation cohort; **(E)** Calibration curves of 1-, 2-, and 3-year DFS in the validation cohort.

Currently, there is still a lack of predictive models for recurrence and survival after liver resection in elderly patients, so we constructed a nomogram to predict the prognosis of such elderly patients.

Unlike earlier prognostic indicators such as BCLC and Child–Pugh grade (18), the nomogram we developed calculates the survival rate and recurrence rate for each patient rather than simply categorizing patients into different risk groups. This approach reduces the impact of heterogeneity, thereby aiding clinicians in making individualized treatment decisions for elderly HCC patients and establishing a foundation for managing high-risk patients in clinical practice.

4.2 Summary of main risk factors

Our study collected the clinical information of elderly HCC patients over 65 years old who underwent liver resection in our hospital. After univariate analysis, LASSO regression analysis, and

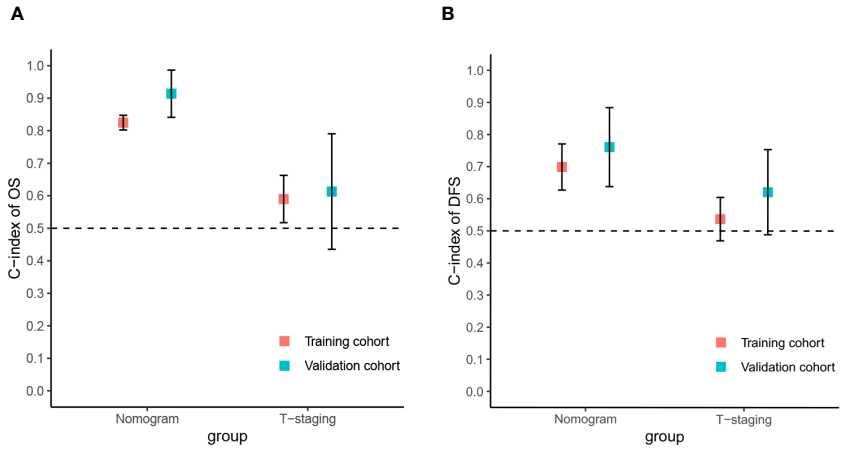

FIGURE 5
The C-index of the nomograms and T-staging. **(A)** The C-index of the OS nomogram and T-staging; **(B)** The C-index of the DFS nomogram and T-staging.

multivariate Cox analysis, it was found that ALB, cancer embolus, blood loss, viral hepatitis B, TB, microvascular invasion, overweight (BMI>24), and major resection were closely related to the OS of this group of people. Major resection, ALB, microvascular invasion, laparoscopic surgery, blood loss, TB, and pleural effusion are closely related to the DFS of this group. Among them, ALB, blood loss, TB, microvascular invasion, and major resection are related to both DFS and OS. Previous studies have shown that these factors are associated with the prognosis of HCC.

4.2.1 Discussion of risk factors associated with basic characteristics

Many previous studies have shown that a serum ALB level of <35g/L is a risk factor for prognosis of HCC. As for the mechanism, ALB has been shown to inhibit HCC growth, migration and invasion (19, 20). In a recent investigation by Zeng et al. (21), focusing on young patients with HCC, it was elucidated that a lower ALB level correlated with increased recurrence after liver resection. ALB and TB are important parameters to access liver functional estimation in the Child-Pugh score. But in recent years, more and more studies have used the Albumin-Bilirubin (ALBI) grade to evaluate the liver reserve function and prognosis prediction ability of HCC patients (22–24). Our study discovered that ALB and TB levels affect the prognosis of elderly HCC patients as independent predictive factors, which is consistent with previous studies.

For elderly patients, there is still insufficient evidence of whether overweight increases the risk of poor prognosis after liver resection. Currently, there is only limited evidence that obesity itself does not

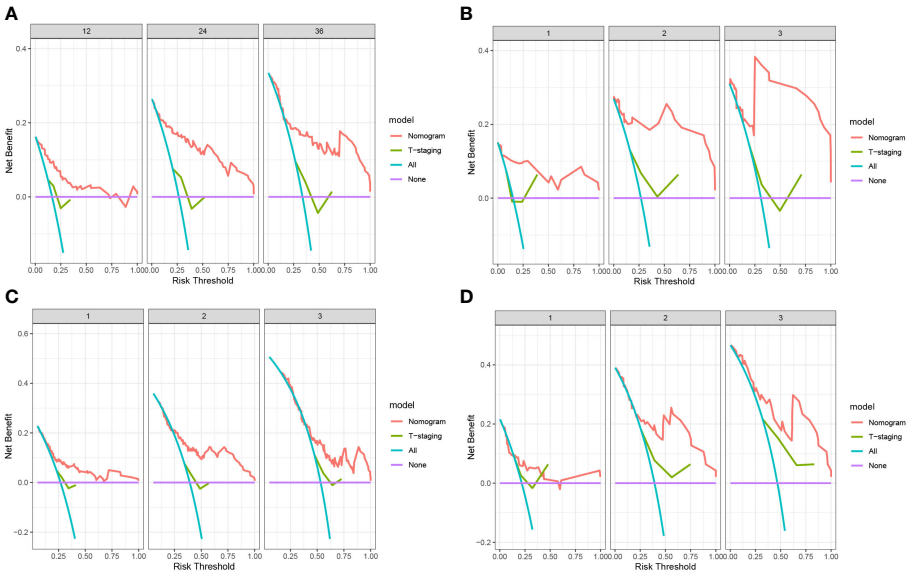

FIGURE 6
(A) DCA of OS in training cohort; **(B)** DCA of OS in validation cohort; **(C)** DCA of DFS in training cohort; **(D)** DCA of DFS in validation cohort.

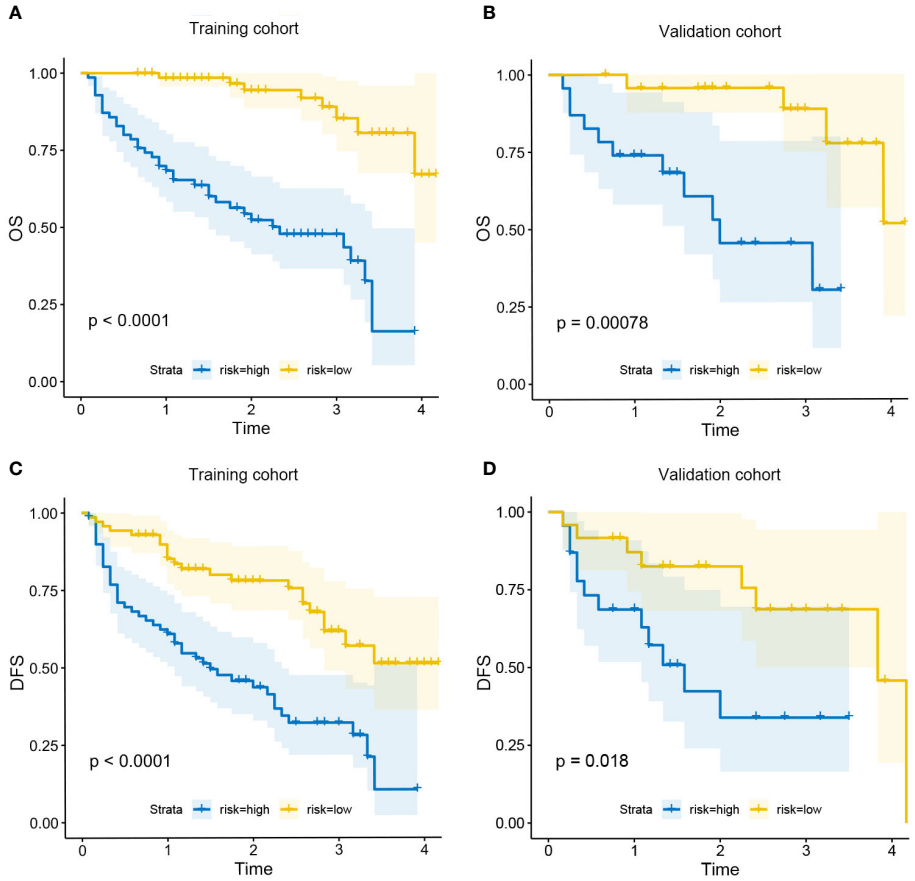

FIGURE 7
Kaplan-Meier curves for OS in the low-risk and high-risk groups in training cohort **(A)** and validation cohort **(B)**; Kaplan-Meier curves for DFS in the low-risk and high-risk groups in training cohort **(C)** and validation cohort **(D)**.

affect the prognosis of postoperative patients with HCV-related HCC (25). Another study shows that overweight and obese patients with cirrhosis have an increased morbidity rate after hepatectomy (26). However, we found that being overweight may be a risk factor for OS in elderly HCC patients undergoing hepatectomy.

HBV has long been considered an independent risk factor associated with poor prognosis in HCC. High HBV replication rate and related non-resolving inflammation are major risk factors of postoperative recurrence, and antiviral treatment can effectively prolong postoperative survival (27). But our study only found that HBV was associated with OS in elderly patients, not with DFS.

4.2.2 Discussion of risk factors associated with surgical resection

The effect of whether to perform major hepatectomy on prognosis is still controversial. On the one hand, extended liver resection can benefit those patients with large and locally advanced HCC (28), but at the same time, it will increase the burden on the residual liver and increase the risk of liver failure (29). However, we found that major resection is a risk factor in older patients.

Suh et al. (30) revealed that intraoperative blood loss ≥ 700 mL were risk factors for tumor recurrence after surgical resection for HCC, consistent with the findings of our study. Large-volume blood loss may impede the immune reaction against tumor cells and induce hypoxic ischemia, thereby increasing the likelihood of tumor recurrence (31).

As for the choice of surgical method, many studies recommend laparoscopic surgery for elderly patients (32). Our study further confirmed that laparoscopic surgery is sufficiently safe, has no significant impact on OS, and can reduce the risk of recurrence. On the one hand, laparoscopic resection is significantly associated with less blood loss, wider resection margins, shorter hospital stays, and lower morbidity (33). On the other hand, smaller tumors are more inclined to be eligible for laparoscopic resection. Challenges persist in laparoscopic approaches, particularly with lesions located in the posterosuperior segments, large and recurrent tumors, and in cases of advanced cirrhosis (34).

4.2.3 Discussion of risk factors associated with pathological characteristics

As is known to us, tumor embolism is seen most commonly in metastatic renal cell carcinoma; hepatocellular carcinoma; and carcinomas of the breast, stomach, and prostate (35). For tumor embolism caused by HCC, studies have shown that it is associated with poor prognosis of HCC (36, 37). This is also consistent with our conclusion. For microvascular invasion, it is also an established

risk factor for HCC (38), which not only can affect OS but also DFS for elderly HCC patients, due to its association with microscopic residual metastatic disease after resection (39). Microvascular invasion and tumor embolism are associated with circulating tumor cells (CTCs). CTCs are independent significant risk factors for HCC recurrence and can be identified as biomarkers for diagnosis, prognostication, and therapeutic monitoring.

4.2.4 Discussion of risk factors associated with postoperative complications

Previous studies have shown that complications after hepatectomy in HCC patients will affect their prognosis (40). For the elderly, their reserve capacity is low, and many comorbidities, such as cardiovascular disease, diabetes, and respiratory system disease, etc., make postoperative rehabilitation and treatment difficult (32, 41). Therefore, the incidence of postoperative complications is higher than that of patients in other age groups. Our data showed that postoperative pleural effusion was an independent risk factor for DFS. Due to the limited number of patients with various complications in our included patients, we did not find that the occurrence of other postoperative complications was related to the prognosis of the patients.

4.3 Strengths and limitations

Overall, the clinical features we used to construct the nomogram after statistical screening were reported in previous studies. It is suggested that these factors may be related to the OS and DFS of patients. However, in terms of these clinical features, no studies have systematically analyzed them in elderly HCC patients undergoing hepatectomy and determined their impact on prognosis. We initially confirmed the validity of the nomogram for OS and DFS prediction in elderly HCC patients who underwent hepatectomy, and found that it exhibited superior predictive power compared to T-staging, as suggested by DCA. This nomogram can effectively identify patients at high risk of death and recurrence. Therefore, the model we developed is an intuitive clinical tool with good predictive performance, assisting physicians in making rational treatment decisions for elderly HCC patients.

However, this study still has some limitations. First of all, we constructed the nomogram based on the clinical data of West China Hospital of Sichuan University. This does not necessarily represent other countries and regions. Secondly, as a retrospective analysis, this study inevitably has information bias and selection bias, which may affect the conclusion to a certain extent. Third, the nomogram we constructed has only been internally verified, and more clinical data and multi-center studies are still needed for external verification to further prove the effectiveness of the nomogram.

5 Conclusion

We have built and internally validated a nomogram to identify the risk factors of overall survival and recurrence in elderly HCC patients who underwent hepatectomy. Although the nomograms have exhibited better prediction for OS and DFS, further multi-center studies and external verification are still needed.

Data availability statement

The original contributions presented in the study are included in the article/Supplementary Material. Further inquiries can be directed to the corresponding authors.

Ethics statement

The studies involving humans were approved by Biomedical Ethics Review Committee of West China Hospital of Sichuan University. The studies were conducted in accordance with the local legislation and institutional requirements. The ethics committee/institutional review board waived the requirement of written informed consent for participation from the participants or the participants' legal guardians/next of kin because 1.The medical records used in this study were obtained from previous clinical records. 2.In this study, the risk to patients is no greater than the minimum risk. 3.Exemption from informed consent will not have adverse effects on the rights and health of the subjects. 4.The privacy and personal identity information of the subjects are protected. 5.This study does not utilize medical records that patients have explicitly refused to use in the past. 6.This study does not involve personal privacy and commercial interests.

Author contributions

YT: Data curation, Methodology, Validation, Writing – original draft. YW: Formal analysis, Investigation, Resources, Visualization, Writing – original draft. NW: Investigation, Methodology, Software, Visualization, Writing – original draft. YL: Data curation, Resources, Supervision, Writing – review & editing. GL: Project administration, Resources, Software, Writing – review & editing. BL: Conceptualization, Funding acquisition, Resources, Supervision, Writing – review & editing.

Funding

The author(s) declare financial support was received for the research, authorship, and/or publication of this article. This work was supported by National Natural Science Foundation of China (Grant No.82002578); Sichuan Science and Technology Program (Grant No.2022YSF0060, Grant No.2022YSF0114, Grant No.2022NSFSC0680, Grant No. 2023YFS0094); 1·3·5 project for disciplines of excellence–Clinical Research Incubation Project, West China Hospital, Sichuan University (20HXFH021); 1·3·5 project for disciplines of excellence, West China Hospital, Sichuan University (ZYJC21049).

Conflict of interest

The authors declare that the research was conducted in the absence of any commercial or financial relationships that could be construed as a potential conflict of interest.

Publisher's note

All claims expressed in this article are solely those of the authors and do not necessarily represent those of their affiliated organizations, or those of the publisher, the editors and the reviewers. Any product that may be evaluated in this article, or claim that may be made by its manufacturer, is not guaranteed or endorsed by the publisher.

Supplementary material

The Supplementary Material for this article can be found online at: https://www.frontiersin.org/articles/10.3389/fonc.2024.1395740/full#supplementary-material

References

1. Sung H, Ferlay J, Siegel RL, Laversanne M, Soerjomataram I, Jemal A, et al. Global cancer statistics 2020: GLOBOCAN estimates of incidence and mortality worldwide for 36 cancers in 185 countries. *CA Cancer J Clin*. (2021) 71:209–49. doi: 10.3322/caac.21660

2. Chen W, Zheng R, Baade PD, Zhang S, Zeng H, Bray F, et al. Cancer statistics in China, 2015. *CA Cancer J Clin*. (2016) 66:115–32. doi: 10.3322/caac.21338

3. Bosch FX, Ribes J, Cléries R, Díaz M. Epidemiology of hepatocellular carcinoma. *Clin Liver Dis*. (2005) 9:191–211. doi: 10.1016/j.cld.2004.12.009

4. Campisi J. Aging, cellular senescence, and cancer. *Annu Rev Physiol*. (2013) 75:685–705. doi: 10.1146/annurev-physiol-030212-183653

5. Macias RIR, Monte MJ, Serrano MA, González-Santiago JM, Martín-Arribas I, Simão AL, et al. Impact of aging on primary liver cancer: epidemiology, pathogenesis and therapeutics. *Aging (Albany NY)*. (2021) 13:23416–34. doi: 10.18632/aging.v13i19

6. Lv A, Li Y, Qian HG, Qiu H, Hao CY. Precise navigation of the surgical plane with intraoperative real-time virtual sonography and 3D simulation in liver resection. *J Gastrointest Surg*. (2018) 22:1814–8. doi: 10.1007/s11605-018-3872-0

7. Niu X, Liu J, Feng Z, Zhang T, Su T, Han W. Short-term efficacy of precise hepatectomy and traditional hepatectomy for primary liver cancer: a systematic review and meta-analysis. *J Gastrointest Oncol*. (2021) 12:3022–32. doi: 10.21037/jgo

8. Kishida N, Hibi T, Itano O, Okabayashi K, Shinoda M, Kitago M, et al. Validation of hepatectomy for elderly patients with hepatocellular carcinoma. *Ann Surg Oncol*. (2015) 22:3094–101. doi: 10.1245/s10434-014-4350-x

9. Oishi K, Itamoto T, Kohashi T, Matsugu Y, Nakahara H, Kitamoto M. Safety of hepatectomy for elderly patients with hepatocellular carcinoma. *World J Gastroenterol*. (2014) 20:15028–36. doi: 10.3748/wjg.v20.i41.15028

10. Wu FH, Shen CH, Luo SC, Hwang JI, Chao WS, Yeh HZ, et al. Liver resection for hepatocellular carcinoma in oldest old patients. *World J Surg Oncol*. (2019) 17:1. doi: 10.1186/s12957-018-1541-0

11. Inoue Y, Tanaka R, Fujii K, Kawaguchi N, Ishii M, Masubuchi S, et al. Surgical outcome and hepatic regeneration after hepatic resection for hepatocellular carcinoma in elderly patients. *Dig Surg*. (2019) 36:289–301. doi: 10.1159/000488327

12. Marrero JA, Kulik LM, Sirlin CB, Zhu AX, Finn RS, Abecassis MM, et al. Diagnosis, staging, and management of hepatocellular carcinoma: 2018 practice guidance by the American association for the study of liver diseases. *Hepatology*. (2018) 68:723e50. doi: 10.1002/hep.29913

13. Altekruse SF, McGlynn KA, Dickie LA, Kleiner DE. Hepatocellular carcinoma confirmation, treatment, and survival in surveillance, epidemiology, and end results registries, 1992–2008. *Hepatology*. (2012) 55:476e82. doi: 10.1002/hep.24710

14. Tibshirani R. Regression shrinkage and selection via the Lasso. *J R Stat Soc Ser B Methodol*. (1996) 58:267–88. doi: 10.1111/j.2517-6161.1996.tb02080.x

15. Li J, Xu Y, Liu H, Guo B, Guo X, Li Y, et al. Construction and validation of NSMC-ASIL, a predictive model for risk assessment of Malignant hepatic nodules. *Am J Cancer Res*. (2022) 12:5315–24.

16. Lin N, Wang L, Huang Q, Zhou W, Liu X, Liu J. A simplified model for prophylactic transarterial chemoembolization after resection for patients with hepatocellular carcinoma. *PloS One*. (2022) 17:e0276627. doi: 10.1371/journal.pone.0276627

17. Wang Q, Qiao W, Zhang H, Liu B, Li J, Zang C, et al. Nomogram established on account of Lasso-Cox regression for predicting recurrence in patients with early-stage hepatocellular carcinoma. *Front Immunol*. (2022) 13:1019638. doi: 10.3389/fimmu.2022.1019638

18. Reig M, Forner A, Rimola J, Ferrer-Fàbrega J, Burrel M, Garcia-Criado Á, et al. BCLC strategy for prognosis prediction and treatment recommendation: The 2022 update. *J Hepatology*. (2022) 76:681–93. doi: 10.1016/j.jhep.2021.11.018

19. Bağırsakçı E, Şahin E, Atabey N, Erdal E, Guerra V, Carr BI. Role of albumin in growth inhibition in hepatocellular carcinoma. *Oncology*. (2017) 93:136–42. doi: 10.1159/000471807

20. Fu X, Yang Y, Zhang D. Molecular mechanism of albumin in suppressing invasion and metastasis of hepatocellular carcinoma. *Liver Int*. (2022) 42:696–709. doi: 10.1111/liv.15115

21. Zeng J, Lin K, Liu H, Huang Y, Guo P, Zeng Y, et al. Prognosis factors of young patients undergoing curative resection for hepatitis B virus-related hepatocellular carcinoma: A multicenter study. *Cancer Manag Res*. (2020) 12:6597–606. doi: 10.2147/CMAR.S261368

22. Zhao S, Wang M, Yang Z, Tan K, Zheng D, Du X, et al. Comparison between Child-Pugh score and Albumin-Bilirubin grade in the prognosis of patients with HCC after liver resection using time-dependent ROC. *Ann Transl Med*. (2020) 8:539. doi: 10.21037/atm

23. Liao J, Liu J, Li C, Fan J, Wang Z. Albumin-bilirubin grade as a prognostic factor of hepatocellular carcinoma after treatment with orthotopic liver transplantation. *Transl Cancer Res*. (2019) 8:1457–65. doi: 10.21037/tcr

24. Wang Z, Fan Q, Wang M, Wang E, Li H, Liu L. Comparison between Child-Pugh Score and albumin-bilirubin grade in patients treated with the combination therapy of transarterial chemoembolization and sorafenib for hepatocellular carcinoma. *Ann Transl Med*. (2020) 8:537. doi: 10.21037/atm

25. Nishikawa H, Arimoto A, Wakasa T, Kita R, Kimura T, Osaki Y. The relation between obesity and survival after surgical resection of hepatitis C virus-related hepatocellular carcinoma. *Gastroenterol Res Pract*. (2013) 2013:430438. doi: 10.1155/2013/430438

26. Tanaka S, Iimuro Y, Hirano T, Hai S, Suzumura K, Nakamura I, et al. Safety of hepatic resection for hepatocellular carcinoma in obese patients with cirrhosis. *Surg Today*. (2013) 43:1290–7. doi: 10.1007/s00595-013-0706-2

27. Du Y, Han X, Ding YB, Yin JH, Cao GW. Prediction and prophylaxis of hepatocellular carcinoma occurrence and postoperative recurrence in chronic hepatitis B virus-infected subjects. *World J Gastroenterol*. (2016) 22:6565–72. doi: 10.3748/wjg.v22.i29.6565

28. Pamecha V, Sasturkar SV, Sinha PK, Mahansaria SS, Bharathy KGS, Kumar S, et al. Major liver resection for large and locally advanced hepatocellular carcinoma. *Indian J Surg*. (2017) 79:326–31. doi: 10.1007/s12262-016-1545-3

29. Wang J, Zhang Z, Shang D, Li J, Liu C, Yu P, et al. Noninvasively assessed portal hypertension grade predicts post-hepatectomy liver failure in patients with hepatocellCarcinoma: A multicenter study. *Front Oncol*. (2022) 12:934870. doi: 10.3389/fonc.2022.934870

30. Suh SW, Lee SE, Choi YS. Influence of intraoperative blood loss on tumor recurrence after surgical resection in hepatocellular carcinoma. *J Pers Med*. (2023) 13:1115. doi: 10.3390/jpm13071115

31. Nakanishi K, Kanda M, Kodera Y. Long-lasting discussion: Adverse effects of intraoperative blood loss and allogeneic transfusion on prognosis of patients with gastric cancer. *World J Gastroenterol*. (2019) 25:2743–51. doi: 10.3748/wjg.v25.i22.2743

32. Wang S, Ye G, Wang J, Xu S, Ye Q, Ye H. Laparoscopic versus open liver resection for hepatocellular carcinoma in elderly patients: A systematic review and meta-analysis of propensity score-matched studies. *Front Oncol*. (2022) 12:939877. doi: 10.3389/fonc.2022.939877

33. Sotiropoulos GC, Prodromidou A, Kostakis ID, Machairas N. Meta-analysis of laparoscopic vs open liver resection for hepatocellular carcinoma. *Updates Surg*. (2017) 69:291–311. doi: 10.1007/s13304-017-0421-4

34. Berardi G, Muttillo EM, Colasanti M, Mariano G, Meniconi RL, Ferretti S, et al. Challenging scenarios and debated indications for laparoscopic liver resections for hepatocellular carcinoma. *Cancers (Basel)*. (2023) 15:1493. doi: 10.3390/cancers15051493

35. Silva CIS, Müller NL. Online case 45. In: Silva CIS, Müller NL, editors. *Teaching files in radiology, the teaching files: chest*. W.B. Saunders (2010). p. 90–1. doi: 10.1016/B978-1-4160-6110-6.10045-9

36. Zhou Z, Qi L, Mo Q, Liu Y, Zhou X, Zhou Z, et al. Effect of surgical margin on postoperative prognosis in patients with solitary hepatocellular carcinoma: A propensity score matching analysis. *J Cancer*. (2021) 12:4455–62. doi: 10.7150/jca.57896

37. Ou H, Huang Y, Xiang L, Chen Z, Fang Y, Lin Y, et al. Circulating tumor cell phenotype indicates poor survival and recurrence after surgery for hepatocellular carcinoma. *Dig Dis Sci*. (2018) 63:2373–80. doi: 10.1007/s10620-018-5124-2

38. Xu L, Li L, Wang P, Zhang M, Zhang Y, Hao X, et al. Novel prognostic nomograms for hepatocellular carcinoma patients with microvascular invasion: experience from a single center. *Gut Liver*. (2019) 13:669–82. doi: 10.5009/gnl18489

39. Erstad DJ, Tanabe KK. Prognostic and therapeutic implications of microvascular invasion in hepatocellular carcinoma. *Ann Surg Oncol*. (2019) 26:1474–93. doi: 10.1245/s10434-019-07227-9

40. Harimoto N, Shirabe K, Ikegami T, Yoshizumi T, Maeda T, Kajiyama K, et al. Postoperative complications are predictive of poor prognosis in hepatocellular carcinoma. *J Surg Res*. (2015) 199:470–7. doi: 10.1016/j.jss.2015.06.012

41. Santambrogio R, Barabino M, Scifo G, Costa M, Giovenzana M, Opocher E. Effect of age (over 75 years) on postoperative complications and survival in patients undergoing hepatic resection for hepatocellular carcinoma. *J Gastrointest Surg*. (2017) 21:657–65. doi: 10.1007/s11605-016-3354-1

Frontiers in Oncology

Advances knowledge of carcinogenesis and tumor progression for better treatment and management

The third most-cited oncology journal, which highlights research in carcinogenesis and tumor progression, bridging the gap between basic research and applications to imrpove diagnosis, therapeutics and management strategies.

Discover the latest Research Topics

See more →

Frontiers

Avenue du Tribunal-Fédéral 34
1005 Lausanne, Switzerland
frontiersin.org

Contact us

+41 (0)21 510 17 00
frontiersin.org/about/contact